2014

DEVELOPMENT OF CEMENTITIOUS MATERIALS FOR ADHESION TYPE APPLICATIONS COMPRISING CALCIUM SULFOALUMINATE (CSA) CEMENT AND LATEX POLYMER

Joshua V. Brien
University of Kentucky, vanbrien@yahoo.com

STUDENT AGREEMENT:

I represent that my thesis or dissertation and abstract are my original work. Proper attribution has been given to all outside sources. I understand that I am solely responsible for obtaining any needed copyright permissions. I have obtained and attached hereto needed written permission statement(s) from the owner(s) of each third-party copyrighted matter to be included in my work, allowing electronic distribution (if such use is not permitted by the fair use doctrine).

I hereby grant to The University of Kentucky and its agents the irrevocable, non-exclusive, and royalty-free license to archive and make accessible my work in whole or in part in all forms of media, now or hereafter known. I agree that the document mentioned above may be made available immediately for worldwide access unless a preapproved embargo applies. I retain all other ownership rights to the copyright of my work. I also retain the right to use in future works (such as articles or books) all or part of my work. I understand that I am free to register the copyright to my work.

REVIEW, APPROVAL AND ACCEPTANCE

The document mentioned above has been reviewed and accepted by the student's advisor, on behalf of the advisory committee, and by the Director of Graduate Studies (DGS), on behalf of the program; we verify that this is the final, approved version of the student's dissertation including all changes required by the advisory committee. The undersigned agree to abide by the statements above.

Joshua V. Brien, Student

Dr. Kamyar C. Mahboub, Major Professor

Dr. Y.T. Wang, Director of Graduate Studies

DEVELOPMENT OF CEMENTITIOUS MATERIALS FOR ADHESION TYPE APPLICATIONS COMPRISING CALCIUM SULFOALUMINATE (CSA) CEMENT AND LATEX POLYMER

DISSERTATION

A dissertation submitted in partial fulfillment of the requirements for the degree of Doctor of Philosophy in the College of Engineering at the University of Kentucky

By
Joshua V Brien
Lexington, Kentucky

Director: Dr. Kamyar C Mahboub, Associate Dean for Outreach and External Partnerships, Lawson Professor of Civil Engineering, Department of Civil Engineering, University of Kentucky
Lexington, Kentucky

2013

ABSTRACT OF DISSERTATION

DEVELOPMENT OF CEMENTITIOUS MATERIALS FOR ADHESION TYPE APPLICATIONS COMPRISING CALCIUM SULFOALUMINATE (CSA) CEMENT AND LATEX POLYMER

The objective of this research was to develop high performing polymer modified calcium sulfoaluminate (CSA) cement materials for use in applications requiring superior adhesion characteristics. Little information is available describing interactions of CSA cement containing minor phase tri-calcium aluminate (C_3A) with commonly used admixtures. Given the scarcity of information, a basic approach for developing cementitious materials was followed. The basic approach consisted of four tasks: cement design, admixture design, polymer design and testing developed materials. The iterative, time consuming process is necessary for understanding the influence of specific constituent components on overall system behavior. Results from the cement design task suggest calcium sulfate type influences microstructural characteristics and strength development for materials based upon the experimental CSA cement. Results from the admixture design task suggest lithium carbonate and tartaric acid are effective accelerating and retarding admixtures for hydration reactions including reactants yeelimite, calcium sulfate and water. Results from the polymer design task suggest vinyl acetate / ethylene (VAE) dispersible polymer powders (DPP) are compatible with systems containing the experimental CSA cement and other commonly used admixtures. Additionally, results from the polymer design task highlight a method for specifying the ductile behavior of materials containing the experimental CSA cement as majority hydraulic binding agent. Finally, results from the testing of developed materials task suggests adhesion performance for materials containing the experimental CSA cement can be influenced by adjusting the ratio of polymer to hydraulic binding agent in material formulations. Polymer modified CSA cement mortars demonstrated bond strength resulting in substrate failure when cast over porous concrete substrates. Developed mortars demonstrated consistent bonding performance when applied to non-porous substrate materials, metal and glass. Select polymer modified mortars displayed adhesion bond performance such that the glass substrate materials fractured during pull off testing.

Joshua V Brien
Student Signature

08May2014
Date

KEYWORDS: calcium sulfoaluminate (CSA) cement; vinyl acetate/ethylene dispersible polymer powder; adhesion; porous substrate; non-porous substrate

DEVELOPMENT OF CEMENTITIOUS MATERIALS FOR ADHESION TYPE APPLICATIONS COMPRISING CALCIUM SULFOALUMINATE (CSA) CEMENT AND LATEX POLYMER

By
Joshua V Brien
Lexington, Kentucky

_____ Dr. Kamyar C Mahboub _____
Director:

_____ Dr. Y.T. (Ed) Wang _____
Director of Graduate Studies:

_____08May2014_____
Date

TABLE OF CONTENTS

LISTING OF TABLES

LISTING OF FIGURES

Chapter 1: Introductory Remarks

INTRODUCTION

In 2005, the American Association of State Highway Transportation Officials (AASHTO) organization published a document entitled *Grand Challenges, A Strategic Plan for Bridge Engineering*. The document addresses six total grand challenges for future bridge construction: extending service life, optimizing structural systems, accelerating bridge construction, advancing the AASHTO specifications, monitoring bridge condition and contributing to national policy (Mertz et al, 2005). In regards to extending service life, optimizing structural systems and accelerating bridge construction, AASHTO clearly supports more widespread implementation of somewhat recently developed high performance materials –the family of ultra high performance concrete materials. When speaking of bridge decks and girders, AASHTO suggests wider implementation of ultra high performance concrete (UHPC) as a viable means for extending service life, optimizing structural systems and accelerating bridge construction (Mertz et al, 2005).

UHPC is a result of the "minimum defect" concept for creating materials with a minimum amount of defects such as micro-cracks and interconnected pore spaces in order to more closely approach the potential ultimate strength of the components and enhance durability (Vande Voort et al., 2008). Two lines of research have been pursued in developing minimum defect materials --macro-defect free (MDF) and densified small particle or densified system with ultra fine particles (DSP) (Vande Voort et al., 2008). Development of UHPC stemmed from the DSP approach (Vande Voort et al., 2008). DSP concretes contain high amounts of superplasticizer and silica fume or other finely ground materials. DSP concretes must either use extremely hard coarse aggregates or eliminate coarse aggregate entirely to prevent the coarse aggregates from being the weakest component of the mix (Vande Voort et al., 2008). Several types of UHPC have been developed in different countries by different manufacturers with the primary difference being the amount and type of fibers incorporated into product formulations (Vande Voort et al., 2008). In addition to numerous other organizations, both the US Army Corps of Engineers and the Federal Highway Administration have published a number of UHPC related reports (Graybeal, 2010, Graybeal, 2009, Oneil et al, 2004, Cargile et al, 2002).

Within the cementitious materials industry, the author expects widespread introduction of DSP or other "minimum defect" materials as structural components to increase demand for patch and repair materials with excellent adhesion characteristics. One primary reason for such an expectation revolves around bonding mechanisms for cementitious materials. In general, the presence of surface defects increases the likelihood for developing acceptable bond strengths between cementitious materials and substrate materials as the presence of surface defects increases the total available area for which mechanical bonding mechanisms may act.

Substrate porosity is often listed as one of the most important factors when assessing adhesion characteristics for cementitious materials. Adhesion mechanisms for cementitious materials applied over various substrates are theorized to behave in similar fashion to the known behavior of cement paste and lightweight aggregate. Lightweight aggregate is often more porous than traditional stone aggregate (Chandra et al, 2003). For lightweight aggregate, a portion of the paste bleed water moves into the aggregate's pore structure resulting in an overall decrease of the cement paste / aggregate interfacial zone (Chandra et al, 2003). As with lightweight aggregate, cementitious substrate materials should allow movement of bleed water from the freshly applied cementitious material into the existing capillary pore structure of the substrate. The author theorizes materials diffusing with the bleed water will set and harden in the substrate capillary pore network thus forming a bonding mechanism for the adjacent materials. This cement paste bleed water / existing capillary pore structure bonding mechanism may see a decrease in effectiveness for dense MDF materials possessing less total area of capillary pores at the bonding interface. UHPC's dense microstructure and decreased overall void space is expected to create challenges for bonding contemporary cementitious materials to such MDF substrate materials. In this respect, contemporary cementitious materials refers to material formulations that do not include specialty chemicals for improving adhesion performance.

Latex polymers are a large family of materials commonly used as building blocks for adhesives and paints, so to speak. These materials are available in either solid or liquid form. These materials have been used to improve the properties of cementitious systems for decades (Chandra et al, 1994, Ohama 1995). Latex polymers in the form of dispersible polymer powders are examined in this study. Dispersible polymer powders are becoming increasingly popular when compared with liquid polymer dispersions for reasons such as

improved dispersing behavior in cementitious systems, improved handling for batch mixing operations and improved storage capability on the job site as dispersible polymer powders are not susceptible to freeze damage.

Dispersible polymer powders are known to improve the adhesion performance of cementitious materials (Chandra et al, 1994, Ohama 1995). Dispersible polymer powder has the ability to form both physical and chemical bonds with various substrate materials. In cementitious materials design, a number of possibilities exist for various interactions within either the newly applied mortar or the substrate depending upon the composition of the respective constituent materials. Such possibilities are succinctly described with the following quotation:

> The bonds in the cementitious composite systems are the outcome of the combination of different mechanisms, such as van der Waal's forces, hydrogen bonds and possibly chemical bonds. The nature of these mechanisms varies from system to system depending upon the chemical nature of the raw materials, etc." (Chandra et al. 2003)

Such interactions as mentioned in the quotation are very difficult to quantify. In an effort to further understand the influences of polymer type on adhesion behavior of the tested mortars, this study evaluated the adhesion bond strength of each polymer modified mortar to substrate materials with unique characteristics --concrete, wood, glass and metal.

OBJECTIVE

The objective of this research was to develop high performing polymer modified calcium sulfoaluminate (CSA) cement materials for use in applications requiring superior adhesion characteristics. The materials are high performing for three reasons. The developed materials demonstrate rapid strength development, acceptable adhesion characteristics to non-porous substrate materials and perhaps the most interesting aspect is the developed materials also present the possibility for improvements in ductile behavior with increases in total polymer content.

SUMMARY OF APPROACH

Developing cementitious materials for specific applications from scratch is an iterative, time consuming process. Figure 1.1 represents a flowchart of experimental activities for the presented research. On a macro level, the experimental process should be viewed as behaving in step-wise fashion with left to right convention. The entire experimental process began with cement design and analysis and ended with analysis of experimental materials designed for use in applications where adhesion performance is paramount. On a micro level, the experimental process allowed for each specific task to run concurrently. For lack of better terminology, the entire process should be viewed as a continuously progressing feedback loop utilizing significant sets of analysis from each task for decision making. Interpretation of data from the analysis tasks inevitably provided experimental direction through an iterative process eventually resulting in development of experimental materials. The outcome was development of a few cement mortar formulations demonstrating rapid strength development, good adhesion to non-porous substrates and improved ductility when compared with traditional cementitious materials.

EXPERIMENTAL FLOW CHART

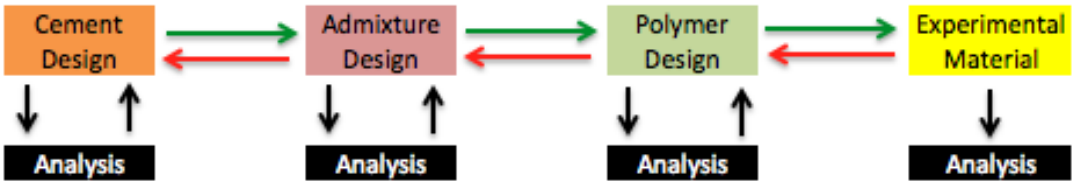

Figure 1.1: Experimental flow chart

OUTLINE OF THE REPORT

This report is divided into seven chapters. Chapters 1 and 2 consist of an introduction along with a rather in depth discussion of the influence of curing conditions on CSA cement pastes and mortars. Information displayed in Chapter 2 is included at various points throughout the document in an effort to explain observed strength behaviors. Chapter 3 serves as the basis for understanding relationships between microstructural characteristics and strength development within CSA cement materials. Chapter 4 discusses the influence of various admixtures on the performance characteristics of CSA

cement pastes and mortars. Chapter 5 discusses the influence of latex polymer addition on mechanical property performance behavior of CSA cement mortars. Chapter 6 discusses the adhesion characteristics of the developed polymer modified CSA cement mortars. Chapter 7 presents succinct concluding remarks along with a number of thoughts pertaining to future research endeavors on the subject of polymer modified CSA cement materials.

SIGNIFICANCE OF THE RESEARCH

The information provided in Chapter 2 is significant as it displays the influence of relative humidity on hydration characteristics of calcium sulfoaluminate (CSA) cement containing minor phase tri-calcium aluminate (C_3A) in the presence of different types of calcium sulfate. The information displayed in Chapter 2 is of further significance as it illustrates latex polymer as a viable means for mitigating ettringite decomposition behavior in CSA cement materials cured at constant low humidity.

The information provided in Chapter 3 is significant as it correlates mechanical property performance behavior to microstructural characteristics for CSA cement materials containing different types of calcium sulfate.

The information provided in Chapter 4 is of less significance as the use of accelerating and retarding admixtures in ettringite forming systems is well documented.

The information provided in Chapter 5 is significant as it demonstrates material compatibility between vinyl acetate / ethylene (VAE) based dispersible polymer powders (DPP) and CSA cement. Furthermore, the information displayed in Chapter 5 illustrates a novel concept for varying polymer / cement (p/c) ratio within cementitious materials as a means for significantly improving ductile behavior by increasing the concentration of tough, flexible polymer film per specific volume of material microstructure.

The information provided in Chapter 6 is significant as it illustrates the improved adhesion performance of polymer modified CSA cement mortars when compared with non-polymer modified CSA cement mortars. Furthermore, the study presents remarkable adhesion performance of polymer modified mortars to non-porous substrate materials with a notable illustration being a polymer modified CSA cement mortar demonstrating bond strength to glass substrate materials sufficient to create failure of the glass substrates during pull-off testing.

1 References:

- Cargile, J.D., Oneil, E.F., Neeley, B.D., 2002, Very High Strength Concretes for Use in Blast and Penetration Resistant Structures, US Army Corps of Engineers Engineer Research and Development Center, AMPTIAC Quarterly Volume 6, Number 4
- Chandra, S., Berntsson, L., 2003, Lightweight Aggregate Concrete, Science, Technology and Applications, Building Materials Series ISBN 0-8155-1486-7
- Chandra, S., Ohama, Y., 1994, Polymers in Concrete, CRC Press, ISBN 0-8493-4815-3
- Graybeal, B., 2010, Behavior of Field Cast Ultra High Performance Concrete Bridge Deck Connections Under Cyclic and Static Structural Loading, November 2010, FHWA-HRT-11-023
- Graybeal, B., 2010, FHWA-HRT-11-022, Field Cast UHPC Connections for Modular Bridge Deck Components, November 2010, FHWA-HRT-11-022
- Graybeal, B., 2009, FHWA-HRT-09-069, Structural Behavior of a 2nd Generation UHPC Pi-Girder, October 2009, FHWA-HRT-09-069
- Mertz, D., Rehm, K., Beal, D., 2005, Grand Challenges: A Strategic Plan for Bridge Engineering, AASHTO Highway Subcommittee on Bridges and Structures, June 2005
- Ohama, Y., 1995, Handbook of Polymer-Modified Concrete and Mortars, Noyes Publications, ISBN 0-8155-1358-8
- Oneil, E.F., Cummins, T.K., Durst, B.P., Kinnebrew, P.G., Boone, R.N., 2004, Development of Very High Strength and High Performance Concrete Materials for Improvement of Barriers Against Blast and Projectile Penetration, US Army Corps of Engineers, US Army Engineer Research and Development Center
- Vande Voort, T., Suleiman, M., Sritharan, S., 2008, Design and Performance Verification of Ultra-High Performance Concrete Piles for Deep Foundations, Iowa Highway Research Board, Iowa Department of Transportation, IHRB Project TR-558

CHAPTER 2: Influence of Curing Conditions on CSA Cement Pastes

Dry mix mortar products are typically formulated for specific purposes. Production of dry mix mortar products entails accessing, metering, blending and packaging a number of previously packaged components. Several of the presented experiments assess the influence of specific mass amounts of gypsum and anhydrite on system behavior, even though gypsum and anhydrite differ in both chemical composition and formula weight. From a production perspective, it is likely either gypsum or anhydrite will at least once be mistaken for the other if both are indeed delivered to the production facility in packages of equal mass, with an example being 25kg bags. The experimental results contribute to the body of knowledge necessary for producing durable materials with the experimental calcium sulfoalumiante (CSA) cement containing minor phase tri-calcium aluminate (C_3A).

CSA cements are often utilized for creating specialized materials which benefit in some fashion from ettringite formation. Numerous authors suggest additional long term studies are necessary before implementing CSA cement materials on a broad scale. More research is necessary as CSA cements are available with a wide range of constituent components which increase the likelihood for creating different reaction scenarios when hydrated in the presence of commonly used admixtures. Chapter 2 represents the first step in an iterative process for designing cementitious materials from scratch when little information is available describing interactions of the experimental hydraulic binder with other components. Chapter 2 consists of a rather detailed study assessing the influence of relative humidity on the hydration characteristics of polymer modified and non-polymer modified calcium sulfoaluminate (CSA) cement pastes ultimately highlighting differences in behaviors for small samples with large available surface area when compared with total sample volume. The presented information is not well known and considered relevant for both industrial and academic stakeholders alike. From an applications type perspective, the presented behavioral differences should be considered when utilizing the experimental CSA cement as a component in dry mix mortar products to be applied in different climates.

Influence of Relative Humidity on the Hydration Characteristics of CSA Cement Pastes

INTRODUCTION

The present study assesses the microstructural behavior of a calcium sulfoaluminate (CSA) cement containing minor phase tri-calcium aluminate (C_3A) cured at humidity extremes. The analyzed CSA cement is somewhat unique as it offers two potential hydration mechanisms for ettringite formation. Cement nomenclature is utilized in various instances throughout this document. In cement nomenclature, C = CaO, S = SiO_2, A = Al_2O_3, $\underline{S}$ = SO_3, $\underline{C}$ = CO_2 and H = H_2O.

Cement clinkers possessing a majority of $C_4A_3\underline{S}$ in combination with calcium sulfate are often referred to as CSA cements. $C_4A_3\underline{S}$ is chemical shorthand nomenclature synonymous with "Klein's Compound" or "Yeelimite". Third Cement Series (TCS) technology practiced mainly in China is based on clinkers containing 60 to 70 percent $C_4A_3\underline{S}$ content (Gartner et al, 2004). TCS series cements can be used in a wide variety of applications depending on their different phase compositions and on the amount of gypsum or anhydrite interground to make the final cement (Gartner et al, 2004).

Cement clinkers containing a majority $C_4A_3\underline{S}$ have been used in combination with ordinary portland cement (OPC) for development of Type K expansive cements since the 1940s (Kalousek, 1973). The use of CSA cements as stand alone hydraulic binding agents is limited to the past few decades. Much remains to be learned about the hydration characteristics of CSA cements over the long term.

Literature reports the hydration behavior of CSA cement systems together with the formed phase assemblages are highly dependent upon amount and type of constituent materials (Winnefeld and Lothenbach, 2013, Winnefeld and Barlag, 2010, Winnefeld and Lothenbach, 2010,). It is well known that in the presence of sufficient calcium sulfate and water, CSA cements hydrate to form ettringite. The mineral name ettringite refers to the calcium trisulphoaluminate hydrate ($C_6A\underline{S}_3H_{32}$) found in several hydrated construction cements (Grounds et al, 1988). Several potential reaction schemes exist for yeelimite hydrating to form ettringite, monosulfate and aluminum hydroxide --of which three are listed below utilizing cement chemistry nomenclature (Winnefeld and Lothenbach, 2013, Gastaldi et al, 2009):

$$C_4A_3\bar{S} + 2C\bar{S} + 38H \rightarrow C_6A\bar{S}_3H_{32} + 2AH_3 \quad (1)$$

$$C_4A_3\bar{S} + 2C\bar{S}H_2 + 34H \rightarrow C_6A\bar{S}_3H_{32} + 2AH_3 \quad (2)$$

$$C_4A_3\bar{S} + 18H \rightarrow C_4A\bar{S}H_{12} + 2AH_3 \quad (3)$$

Reaction 1 displays yeelimite, anhydrite and water hydrating to form ettringite and aluminum hydroxide. Reaction 2 displays yeelimite, gypsum and water hydrating to form ettringite and aluminum hydroxide. Reaction 3 displays yeelimite, and water hydrating to form monosulfate and aluminum hydroxide.

In addition to forming ettringite, a number of other hydrated phase assemblages are possible with CSA cement systems, such as either amorphous or crystalline aluminum hydroxide and perhaps monosulfate depending upon the ratio of yeelimite to calcium sulfate (Winnefeld and Lothenbach, 2013). With regard to potential hydration products, as calcium sulfate addition increases, the quantity of monosulfate decreases while the quantity of ettringite increases, where ettringite reaches its maximum at a molar ratio of yeelimite to calcium sulfate of 1:2 (Winnefeld and Lothenbach, 2013). Once the molar ratio of yeelimite to calcium sulfate of 1:2 is surpassed, monosulfate is no longer present while an excess of gypsum normally occurs (Winnefeld and Lothenbach, 2013). Figure 2.1 provides a phase diagram for determining theoretical hydration products based upon the concentrations of constituent materials, of which calcium sulfate is perhaps one of the most influential.

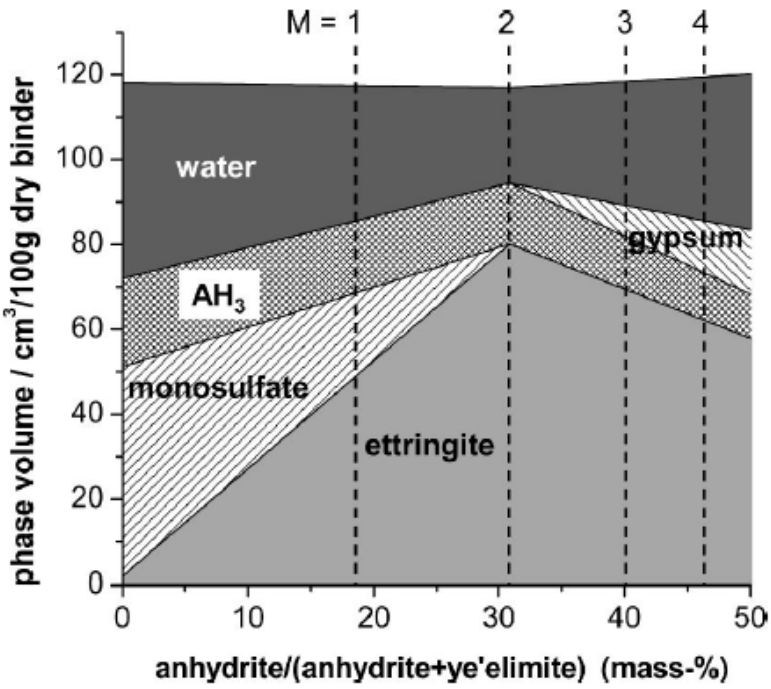

Fig. 1 Calculated phase diagram of the thermodynamic stable hydrate assemblages of the system ye'elimite - calcium sulfate - water using a water/solid ratio of 1 at 20℃. M=molar ratio of calcium sulfate to ye'elimite. Adapted from [8].

Figure 2.1: Calculated phase diagram of the thermodynamic stable hydrate assemblages of the system yeelimite – calcium sulfate – water using a water/solid ratio of 1 at 20°C. M=molar ratio of calcium sulfate to yeelimite. This figure is taken from Winnefeld and Lothenbach (2013), with permission of Dr Frank Winnefeld.

As previously mentioned, calcium sulfate concentration, type and particle size distribution influences the conversion rates associated with hydration reactions for CSA cement materials. Physical and chemical properties of calcium sulfate products may vary depending upon production processes. Calcium sulfate products can be produced through mining and subsequently processing the naturally occurring mineral; or, calcium sulfate products may be synthesized through reaction of a calcium salt with either sulfuric acid or sulfur dioxide (Patnaik, 2003). Natural gypsum is generally found to contain both dihydrate ($CaSO_4 \cdot 2H_2O$) and anhydrous ($CaSO_4$) forms of calcium sulfate (Patnaik, 2003). Naturally occurring gypsum may also contain a number of impurities, not limited to clay, silica, limestone and magnesium carbonate (Patnaik, 2003). The dihydrate, gypsum, can be dehydrated to form either anhydrite or hemihydrate (Patnaik, 2003). Naturally occurring gypsum may be processed where the rock is crushed to size as required and calcined

(Patnaik, 2003). Calcination usually takes place in a steel cylindrical vessel under hot air flow at temperatures between 100 to 125°C (Patnaik, 2003). Soluble anhydrite may be produced by further heating the calcined material at temperatures between 200 to 220°C, and may be obtained in either fine powder or granule form (Patnaik, 2003). Soluble anhydrite is synonymous with gamma-$CaSO_4$, γ-$CaSO_4$ (Taylor, 1997). Insoluble anhydrite may be produced in similar fashion where the calcination takes place over longer periods of time (Patnaik, 2003). Temperature controls and rate of heating are crucial factors during manufacture of various forms of calcium sulfate (Patnaik, 2003). A number of chemical reactions may also be utilized to produce synthetic calcium sulfate products. A few examples of such reactions are listed below utilizing standard chemistry nomenclature (Patnaik, 2003):

$$Ca_3(PO_4)_2 + 3H_2SO_4 + 6H_2O \rightarrow 3CaSO_4{\cdot}2H_2O + 2H_3PO_4 \quad (4)$$

$$Ca(OH)_2 + H_2SO_4 \rightarrow CaSO_4{\cdot}2H_2O \quad (5)$$

$$Ca(OH)_2 + SO_4 \rightarrow CaSO_4 + 2H_2O \quad (6)$$

$$2CaSO_3 + O_2 \rightarrow 2CaSO_4 \quad (7)$$

Table 2.1 lists thermodynamic data for both gypsum and anhydrite under conditions of standard ambient temperature and pressure, 298K and 1 atm, unless otherwise noted.

Table 2.1: THERMODYNAMIC PROPERTIES OF CALCIUM SULFATE			
Property	Gypsum ($CaSO_4 \cdot 2H_2O$)	Anhydrite ($CaSO_4$)	Source
Gibbs Free Energy of Formation (ΔG_f)	-429.6 (kcal/mol)	-315.93 (kcal/mol)	Patnaik, 2003
Enthalpy of Formation (ΔH_f)	-483.42 (kcal/mol)	-342.76 (kcal/mol)	Patnaik, 2003
Entropy (S^o)	46.4 cal/(degree*mol)	25.5 cal/(degree*mol)	Patnaik, 2003
Solubility Product Constant (K_{sp})	3.14×10^{-5}	4.93×10^{-5}	Lide, 1997
Solubility (25°C)	0.208 (g/100g solution)	0.63 (g/100g solution)	Perry, 1995
Solubility (100°C)	0.1619 (g/100g solution)	0.151 (g/100g solution)	Perry, 1995

Table 2.1: Thermodynamic data from various sources for both gypsum and anhydrite at standard ambient temperature and pressure unless otherwise noted

Thermodynamic principles are often utilized to either evaluate or predict outcomes associated with cementitious hydration reactions, as hydration is fundamentally a dissolution-precipitation process (Scrivener and Nonat, 2011). Entropy is a measure of a system's disorder. The Third Law of Thermodynamics states that the entropy of a perfectly crystalline substance is zero at T=0K, a temperature of absolute zero (Atkins, 1997). According to the Third Law, S(0)=0 for all perfectly crystalline materials (Atkins, 1997). Therefore, the absolute entropy of a substance is calculated by extending the measurement of heat capacities down to absolute zero, or as close to absolute zero as possible, and determining the area under the curve where the y-axis is represented by heat capacity divided by temperature and the x-axis represents temperature, up to the temperature of interest (Atkins, 1997). The difference in entropy between the products and the reactants in their standard states is called the standard reaction entropy (Atkins, 1997). Simple reactions at standard temperature and pressure are considered spontaneous so long as the entropy of reaction is positive (Atkins, 1997). However, when making determinations with regard to reaction spontaneity, it is imperative to consider the entropy of both the system

and the surroundings (Atkins, 1997). The Gibbs energy serves as a "generating function" for the other thermodynamic properties, and implicitly represents "complete" property information (Smith et al, 1996). The value associated with Gibbs energy gives the maximum amount of non-expansion work that can be extracted from a system that is undergoing a change at constant temperature and pressure (Atkins, 1997). Non-Expansive work is considered any work other than that arising from the expansion of the system (Atkins, 1997).

Given a "perfect world" scenario, excluding common ion effects and other thermodynamic complexities associated with hydrating cementitious systems, the data in Table 2.1 may be interpreted as follows: anhydrite is more soluble when compared with gypsum at 25°C; whereas, gypsum is slightly more soluble when compared with anhydrite at 100°C. The solubility product constant, which provides a means of inference pertaining to dissolution behavior for solutes at specific combinations of temperature and pressure, suggests anhydrite is more readily soluble when compared with gypsum at 25°C and 1atm. Additionally, the K_{sp} values suggest gypsum will precipitate out of solution before anhydrite at 25°C and 1atm. Furthermore, Taylor, (1997), states at ordinary temperatures, the metastable solubility of calcium sulfate hemihydrate or soluble anhydrite is considerably higher than the solubility of gypsum, which is thus precipitated upon mixing any of the former materials with water (Taylor, 1997). The entropy values in Table 2.1 suggest soluble anhydrite will spontaneously react to a hydrous form, either hemihydrate or gypsum, when exposed to water, which agrees with observations reported in literature (Taylor, 1997). The Gibbs Free Energy values suggest gypsum is the preferred state in nature. Additionally, the Gibbs Free Energy values suggest gypsum is capable of delivering more non-expansive work on the surrounding system when compared with anhydrite.

In the "real world", including common ion effects and other thermodynamic complexities inherent to hydrating cementitious systems, it is well known that calcium sulfate / water systems are quite complex (Christensen et al, 2008, Taylor, 1997, Blount, 1973, Hardie, 1967). An extensive literature review suggests such complex calcium sulfate / water solution behavior contributes to different rates of ettringite formation for CSA cement based materials containing different amounts and types of calcium sulfate (Pelletier et al, 2010, Winnefeld and Barlag 2010, Winnefeld and Lothenbach, 2010, Pourchet et al, 2009, Sahu et al, 1991, Majling et al, 1985). Furthermore, the temperature rise typically associated with hydrating cementitious systems adds a further degree of complexity as it is

well known that both anhydrite and gypsum display different solubility behaviors in water solutions at different temperatures (Taylor, 1997, Hardie, 1967). Table 2.2 provides data sourced from a chart presented by Hardie, (1967), describing the solubility of both gypsum and anhydrite in water solutions at various temperatures and atmospheric pressure. The information displayed in Table 2.2 suggests gypsum solubility remains in somewhat of a narrow range over the temperature interval from 10 to 70°C; whereas, anhydrite solubility seems to decrease significantly with increasing temperature. The data displayed in Table 2.2 is similar to calcium sulfate solubility information provided by Perry and Green, (1997) and Taylor, (1997). The anhydrite solubility information displayed in Table 2.2 is significantly less than the value listed in Table 1 from Perry, (1995), for 25°C; and, the anhydrite solubility data derived from Table 2.2 will be less than the solubility information from Perry, (1995), if it were to be extrapolated to 100°C. Nevertheless, it is important to note physical properties, with an example being particle size distribution, can significantly influence dissolution behavior of the various anhydrites.

Table 2.2: SOLUBILITY DATA FOR CALCIUM SULFATE							
Temperature (°C)	10	20	30	40	50	60	70
Gypsum Solubility (g/100g H_2O)	0.19	0.195	0.21	0.21	0.205	0.2	0.195
Anhydrite Solubility (g/100g H_2O)	0.3	0.295	0.275	0.25	0.21	0.18	0.15

Table 2.2: Solubility data for solutes gypsum and anhydrite in solution with water as a solvent sourced from a chart displayed in Hardie (1967)

As an illustration of two anhydrites with different solution behavior, Majling et al, (1985), investigated the influence of anhydrite activity on the hydration of calcium sulfoaluminate cement clinker (Majling et al, 1985). The experiment utilized two anhydrites with different activities according to specific surface area, temperature of calcination and the dissolution rate in water. Majling et al, (1985), prepared the anhydrites through calcination of gypsum at 800°C and 1300°C with Blaine surfaces of 630m^2/kg and 390m^2/kg, respectively. Cement paste samples were prepared such that all variables were

constant with the only difference being the type of incorporated anhydrite (Majling et al, 1985). The results indicated the CSA cement paste containing the anhydrite produced with calcination temperature of 800°C and Blaine surface of 630m²/kg displayed accelerated hydration reactions and strength development when compared with the CSA cement paste containing the lower activity anhydrite (Majling et al, 1985). Additionally, the CSA cement paste containing the higher activity anhydrite yielded the greatest concentrations of ettringite during the early hours of hydration when compared with the CSA cement paste incorporating the lower activity anhydrite (Majling et al, 1985).

Sahu et al, (1991), investigated the hydration behavior of sulphoaluminate belite cement in the presence of various calcium sulfates. The investigators synthesized a sulfoaluminate belite cement clinker with main phases C_2S, $C_4A_3\$$ and C_4AF from limestone, fly ash and gypsum (Sahu et al, 1991). The hydration of this CSA cement was studied in the presence of different calcium sulfates, where the different calcium sulfates consist of anhydrites calcined at temperatures of 750°C and 1200°C, hemihydrate and gypsum (Sahu et al, 1991). The experimental hydrating systems differed only in the amount and type of incorporated calcium sulfate, while all other system parameters remained constant (Sahu et al, 1991). The investigators report samples containing either gypsum or hemihydrate displayed accelerated reaction mechanisms and greater concentrations of ettringite during early hydration when compared with samples containing anhydrite (Sahu et al, 1991).

Winnefeld and Barlag, (2010), investigated the influence of calcium sulfates with different reactivities, gypsum and anhydrite, on the hydration kinetics and hydration phase assemblages of the main hydraulic phase, yeelimite through the use of isothermal conduction calorimetry, thermogravimetric analysis, x-ray diffraction analysis and thermodynamic modeling (Winnefeld and Barlag, 2010). The anhydrite was prepared by heating calcium sulfate dihydrate in a laboratory furnace at 700°C for two hours (Winnefeld and Barlag, 2010). The investigators state anhydrite formed under those conditions exhibits much slower dissolution kinetics than calcium sulfate dihydrate (Winnefeld and Barlag, 2010). The investigators found the hydration of pure calcium sulfoaluminate, without added calcium sulfate, exhibited very slow hydration kinetics during the first 10 hours (Winnefeld and Barlag, 2010). The investigators state the hydration of calcium sulfoaluminate can be accelerated by the addition of calcium sulfate, where gypsum was reported to yield accelerated hydration mechanisms leading to greater amounts of ettringite being formed in the early hours when compared with samples incorporating

anhydrite (Winnefeld and Barlag, 2010). Furthermore, the investigators found that the amount and type of incorporated calcium sulfate influences the ratio between hydration products such as ettringite, monosulfate and amorphous aluminum hydroxide (Winnefeld and Barlag, 2010).

Winnefled and Lothenbach, (2010), investigated the hydration behavior of two calcium sulfoaluminate cements containing different types of calcium sulfate (Winnefeld and Lothenbach, 2010). The first CSA cement ,CSA-1, was produced in the laboratory by blending 78% of a commercial CSA clinker (density 2.78g/cm^3, Blaine surface area 4860 cm^2/g) with 22% of calcium sulfate dihydrate (Fluka); whereas, the second CSA cement, CSA-2 (density 2.84 g/cm^3, Blaine surface area 4630 cm^2/g) was used as provided by the manufacturer where it had already been dosed with anhydrite (Winnefeld and Lothenbach, 2010). The investigators report the two types of calcium sulfate incorporated with CSA-1 and CSA-2 behave differently, where analysis of the pore solution shows that CSA-1 is saturated with respect to gypsum until the gypsum is depleted after 16 hours of hydration; whereas, the anhydrite in CSA-2 is undersaturated beyond one hour of hydration due to its slower dissolution kinetics (Winnefeld and Lothenbach, 2010).

The CSA cement inherent to this study is all the more interesting as it contains minor phase tri-calcium aluminate (C_3A), thus providing numerous additional potential hydration reactions for ettringite and monosfulfatre formation depending upon amount and type of constituent materials. Reactions 8, 9 and 10 below list three of several possible reaction scenarios utilizing cement chemistry nomenclature (Romain et al, 2013, Pourchet et al, 2009):

$$C_3A + 3C\bar{S} + 32H \rightarrow C_6A\bar{S}_3H_{32} \quad (8)$$

$$C_3A + 3C\bar{S}H_2 + 26H \rightarrow C_6A\bar{S}_3H_{32} \quad (9)$$

$$C_3A + C\bar{S} + 12H \rightarrow C_4A\bar{S}H_{12} \quad (10)$$

Reaction 8 lists tri-calcium aluminate plus anhydrite and water to form ettringite; whereas, reaction 9 lists tri-calcium aluminate plus gypsum and water to form ettringite (Pourchet et al, 2009). Reaction 10 lists tri-calcium aluminate plus anhydrite and water to form monosulfate. A literature review suggests calcium sulfate concentration and type also

influences hydration mechanisms associated with tri-calcium aluminate (Pourchet et al, 2009, Silva and Monteiro, 2007, Meredith et al, 2004). For CSA cements containing accessory phases, C-S-H, $C_2A\bar{S}H_8$ or calcium aluminate hydrates, mainly CAH_{10} or C_4AH_{13} can be formed in addition to the primary phases ettringite, monosulfoaluminate and aluminum hydroxide during hydration (Pelletier-Chaignat et al, 2012).

When compared with other hydrated cement phases, the chemical structure of ettringite possesses an abundance of water (Glasser and Zhang, 2001). Therefore, CSA cements tend to have high chemical water demands (CWD) and are known for somewhat rapid desiccating behavior during hydration due to ettringite formation (Glasser and Zhang, 2001). Little is known about the influence of curing conditions on the long term behavior of hydrating CSA cement materials. As new types of cement are becoming increasingly popular for substituting the use of ordinary portland cement (OPC) in various applications, it is becoming increasingly important to develop a complete understanding of the hydration characteristics associated with these newer cements (Schneider and Nonat, 2011, Scrivener et al, 2011).

Cements based on sulfoaluminates are already successful and are attractive from the point of view of their special quick-setting and hardening properties (Lawrence, 1998). However, the sulfoaluminate based cements require further assessment regarding long term durability and strength (Lawrence, 1998). It is well known that ettringite has relatively low resistance to CO_2 attack (Lawrence, 1998, Sherman et al, 1995, Sato et al, 1992). When cured in a controlled environment designed to accelerate carbonation behavior of cementitious materials, CSA cement materials experienced greater degrees of carbonation and strength loss when compared with OPC materials (Jewell et al, 2009, Sherman et al, 1995). Lea's Cement and Concrete, Fourth Edition, reports a system based upon $C_4A_3\bar{S}$ incorporating $C_5S_2\bar{S}$ rather than β-C_2S was found to show very high early and late strengths; however, strength loss occurred at ordinary humidity levels because carbonation led to decomposition of ettringite (Lawrence, 1998). Additionally, a similar system based upon $C_4A_3\bar{S}$ incorporating $C_5S_2\bar{S}$ rather than β-C_2S exposed to accelerated carbonation conditions for 28 days ultimately yielded a decrease in strength to about 67 percent of the initial value while the quantity of ettringite present fell from 47.9 to 18.5 percent (Lawrence, 1998). Literature also reports ettringite is subject to decomposition through dehydration mechanisms (Zhou et al, 2004, Zhou et al, 2001, Skoblinskaya, 1975). Zhang et al, (2005), report concrete specimens based upon CSA cement removed from field

service after many years of service display nearly no signs of decomposition resulting from carbonation mechanisms. Additionally, Glasser and Zhang, (2001), report the high early strengths of CSA mortars and concretes do not appear to degrade with time in normal service (Glasser and Zhang, 2001). They further report the principle matrix phase, ettringite, is stable relative to AFm in the thermodynamic sense; therefore, conversion type reactions known to occur in high aluminate cements when metastable hydroxyl AFm converts to hydrogarnet, C_3AH_6, do not readily occur in hydrating CSA cements as sufficient sulfate is typically added to avoid forming much AFm phase (Glasser and Zhang, 2001). Last, with perhaps the most important remark pertaining to experimental results in this study, Taylor, (1997), reports that carbonation behavior in laboratory experiments might be extreme given large available surface area to volume ratios inherent to laboratory type samples when compared with field type applications, which are much larger in scale.

Latex polymer addition is an effective means for reducing carbonation behavior in OPC based systems (Ohama, 1995, Chandra et al, 1994). Essentially, the underlying mechanism consists of tough, flexible polymer film occupying existing pore structures thereby reducing diffusion rates of materials throughout the material's microstructure. Slowing the rate of diffusion for substances, with one example being carbon dioxide, into the material microstructure ultimately reduces the concentration of these materials within the microstructure thereby influencing the rates of chemical reactions resulting from the presence of said diffusing materials within the material microstructure.

Latex polymers are available in the form of dispersible polymer powders. During production of vinyl acetate / ethylene (VAE) dispersible polymer powders (DPP), anti-caking agents are added, typically in a range from eight to 15 percent by total dry mass. Examples of popular anti-caking agents should not be limited to various forms of calcium carbonate and kaolin clay. Literature reports such mass percentages of calcium carbonate may influence hydration mechanisms associated with CSA cement materials (Winnefeld and Lothenbach, 2013, Chaignat et al, 2012). For example, a cement paste containing 20g CSA cement clinker, 6g anhydrite, 4g VAE DPP with 12% anti-caking agent demonstrates approximate molar ratios of calcium carbonate / yeelimite and calcium sulfate / yeelimite of 0.146 and 1.35, respectively. The approximate mass percentage of calcium carbonate / (calcium carbonate + yeelimite + anhydrite + polymer) = 1.6%. The same CSA cement paste possesses an approximate mass percentage of anhydrite / (anhydrite + yeelimite) of 23.1%.

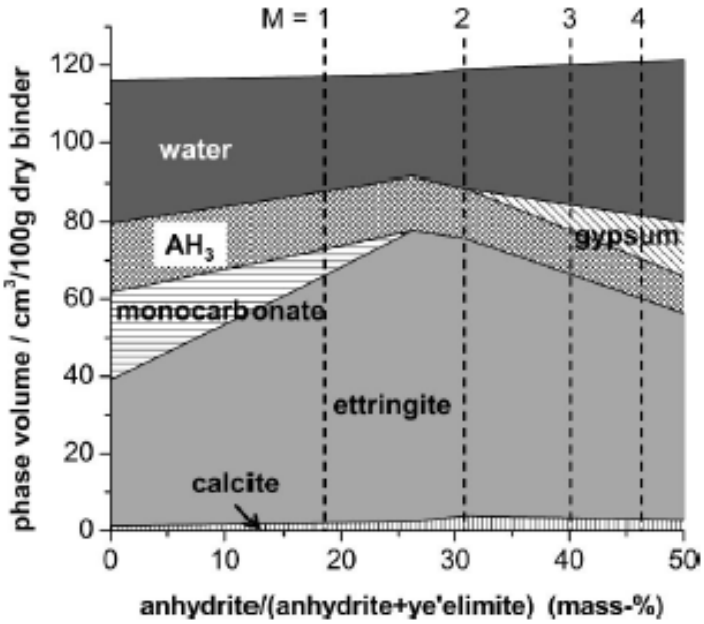

Fig. 4 Calculated phase diagram of the thermodynamic stable hydrate assemblages of the system ye'elimite - calcium carbonate - calcium sulfate - water at 20℃ and a water/binder ratio of 1. A 1 : 1 molar ratio (86 : 14 by mass) of ye'elimite to calcite was used. M=molar ratio of calcium sulfate to ye'elimite

Figure 2.2: Calculated phase diagram of the thermodynamic stable hydrate assemblages of the system yeelimite – calcium carbonate - calcium sulfate – water using a water/solid ratio of 1 at 20°C. M=molar ratio of calcium sulfate to yeelimite. This figure is taken from Winnefeld and Lothenbach (2013), with permission of Dr Frank Winnefeld.

The molar and mass ratios for the example polymer modified CSA cement paste together with the information displayed in Figure 2.2 suggests small percentages of monocarbonate may be expected together with the other hydrated phase assemblages. Utilizing the same molar and mass ratios for the example polymer modified CSA cement paste together with the information displayed in Figure 2.3 also provides justification for the emergence of monocarbonate as a potential hydration phase. Monocarbonate, sometimes referred to as calcium monocarboaluminate, which is more accurately designated as tetra calcium monocarboaluminate 11-hydrate, $3CaO{\cdot}Al_2O_3{\cdot}CaCO_3{\cdot}11H_2O$ ($C_4A\bar{C}H_{11}$ utilizing cement nomenclature), represents an AFm type hydrated phase (Gabrovsek, et al, 2008).

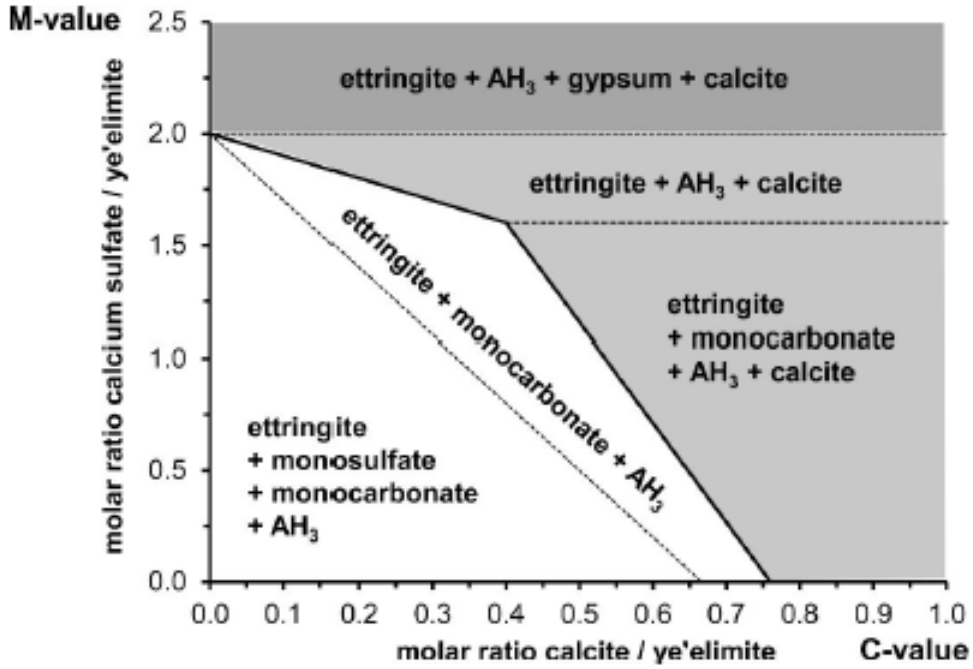

Fig. 5 Calculated stable phase assemblages in the system ye'elimite-calcium sulfate-calcium carbonate-water at 20℃ and a water/binder ratio of 1. In the light grey area excess calcite is present, in the dark grey area excess calcite and gypsum are present

Figure 2.3: Calculated stable phase assemblages in the system yeelimite – calcium carbonate - calcium sulfate – water at 20°C and a water / binder ratio of 1. In the light grey area excess calcite is present, while in the darg grey area ecess calcite and gypsum are present. This figure is taken from Winnefeld and Lothenbach (2013), with permission of Dr Frank Winnefeld.

The information presented in Figure 2.3 illustrates scenarios where primary hydration phases may vary depending upon the amounts of constituent materials yeelimite, calcium carbonate and calcium sulfate. The presence of calcite in CSA cements utilizing anhydrite as a sole source of calcium sulfate presents a scenario such that a portion of monosulfate formed during early hydration may subsequently convert to monocarbonate during later ages of hydration through consumption of calcite (Pelletier-Chaignat et al, 2012). Furthermore, the use of limestone filler with CSA cement is advantageous from a number of perspectives, with examples being accelerating hydration at early ages, significantly improving long term strength behavior and stabilizing the formed ettringite (Pelletier-Chaignat et al, 2012).

Although the thermodynamic concepts surrounding CSA cement hydration in the presence of different types of calcium sulfate are well documented, little information is available describing the microstructural characteristics of hydrated CSA cements containing minor phase C_3A in the presence of different types of calcium sulfate. Little information exists describing morphology and behavior of ettringite crystals formed through hydration of CSA cement containing minor phase C_3A in the presence of different types of calcium sulfate. Little information is available describing the hydration behavior of CSA cements containing different types and amounts of calcium sulfate when cured at humidity extremes. Little information is available describing the influence of latex polymer on microstructural behavior of hydrated CSA cement materials. The present study examines CSA cement pastes containing different types and amounts of calcium sulfate, as well as two mix designs containing latex polymer, when cured at ambient laboratory temperature of 23°C and both 50% and 100% relative humidity for extended periods of time.

MATERIALS

Cement

CSA cement containing tri-calcium aluminate (C_3A) was utilized in this study. XRD analysis provides the following listing of constituent materials:

Yeelimite >> Tri-Calcium Aluminate > Belite > Anhydrite (trace quantity)

Anhydrite

Calcium sulfate anhydrite for this study was sourced from Allied Custom Gypsum. This anhydrite has a variable particle size, typically with approximately 50% passing three microns while having a top size of approximately 10% retained on a 45 micron sieve with the remainder being a continuous distribution down to dust.

Gypsum

Terra Alba gypsum was sourced from US Gypsum (USG) with particle size within the range of 12 to 15 microns. (USG TDS)

VAE Dispersible Polymer Powder

Two VAE dispersible polymer powders were sourced from leading industrial suppliers. FX2311 is a VAE dispersible polymer powder with T_g = 20°C, and 5044N is a VAE dispersible polymer powder with T_g = -7°C.

Experimental Program

This study provides a detailed phase analysis for CSA cement pastes cured at extreme humidity conditions. The study included thermogravimetric analysis (TGA/SDT) and powder X-Ray diffraction (XRD).

Powder X-ray Diffraction (XRD)

X-Ray diffraction is a powerful technique which allows crystalline phases to be identified in cementitious systems (Chowaniec, 2012). Each crystalline phase has a unique X-Ray diffraction pattern determined by the spacing of the crystallographic planes described by Bragg's law (Chowaniec, 2012). X-Ray diffraction does not readily identify poorly crystalline or amorphous materials. The experimental results do not utilize quantitative Rietveld analysis.

For XRD analysis, cement pastes were cured in small, plastic calorimeter containers without lids in a humidity chamber controlled at 50% relative humidity and ambient laboratory temperature of 23°C. For each mix design, all test specimens were taken from the same hydrating CSA cement paste sample. Cement paste test specimens were ground to a fine powder using a mortar and pestle. The samples were washed with acetone to remove water in an effort to mitigate the hydration reaction. After washing with acetone, the samples were thoroughly dried in an oven at 45°C for an hour. Powder X-ray diffraction (XRD) analyses were performed with a Philips X'Pert diffractometer (model PW3040-PRO) operating at 45 kV and 40 mA. The samples were dry mounted in aluminum holders and scanned at 8-60° 2θ with Cu K-α radiation.

TGA/SDT

All TGA/SDT sample specimens were prepared with the same procedures as the XRD specimens; that is, after curing they were ground, washed with acetone and dried at 45°C. TGA analyses utilized one cycle with a temperature ramp rate of 20°C per minute through a final cycle temperature 800°C. TGA analysis was performed with a SDT 600 from

TA Instruments. Some limitations of TGA analysis relate to overlapping phase decomposition ranges which sometimes create difficulties for exact phase identification and quantification (Chowaniec, 2012). For the experimental results, the option was chosen such that the instrument software transformed the original mass loss curve into the derivative form with units of percent mass per degree Celsius. Some researchers prefer to report the derivative form of mass loss, as the weight loss effects are more visible in derivative form (Chowaniec, 2012).

Cement Pastes

Five CSA cement paste mix designs were analyzed after curing at 50% and 100% relative humidity. These mix designs are displayed in Table 2.3. Each mix design had constant mass amounts of CSA cement, calcium sulfate and water. The water / cementitious materials ratio for each mix design was 0.31. The low water / cementitious materials ratio provided very interesting results which illustrate the relationship between microstructural behavior and relative humidity for the analyzed CSA cement pastes.

For preparing the cement pastes, individual components were weighed and placed in a plastic calorimeter container. After all components were added, the container was sealed and shaken vigorously by hand for approximately 10 seconds, which is an efficient method for simulating blending action associated with ribbon blenders commonly utilized with industrial dry mix mortar manufacturing processes. After mixing the dry components, water was added, and the paste was then mixed to homogenous consistency by hand with a spatula. After mixing, each container was placed in its respective curing chamber, either the curing cabinet at 50% relative humidity and 23^{o}C or the curing room at 100% relative humidity and 23^{o}C. The lids were not placed on the little plastic calorimeter containers containing the cement paste samples during the entire curing regimen.

Table 2.3: CSA CEMENT PASTE FORMULATIONS FOR ANALYTICAL STUDY										
Sample	CC1	CC2	CC3	CC4	CC5	CC6	CC7	CC8	CC9	CC10
Relative Humidity	100%	100%	100%	100%	100%	50%	50%	50%	50%	50%
Temperature	23°C	23°C	23°C	23°C	23°C	23°C	23°C	23°C	23°C	23°C
Materials	mass (g)	mass (g)	mass (g)	mass (g)	mass (g)	mass (g)	mass (g)	mass (g)	mass (g)	mass (g)
CSA Cement	20	20	20	20	20	20	20	20	20	20
Anhydrite		6	3	6	6	6	6		6	3
Gypsum	6		3					6		3
VAE T_g = -7°C					4				4	
VAE T_g = 20°C				4		4				
Total Mass	26	26	26	30	30	30	26	26	30	26
Deionized Water	8	8	8	8	8	8	8	8	8	8

Table 2.3: CSA cement paste formulations for analytical study

2.1 Anhydrite as a source of calcium sulfate

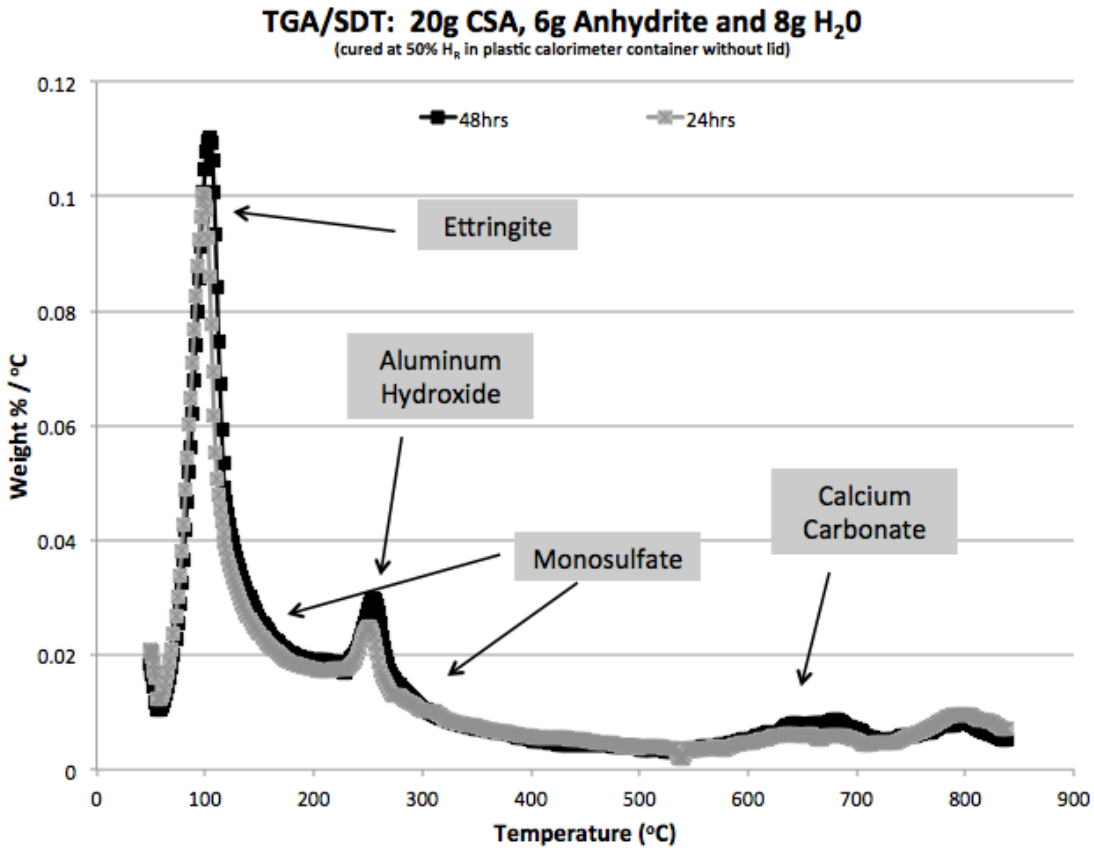

Figure 2.1.1: TGA/SDT analysis of CSA cement paste 7 containing solely anhydrite in Table 2.3 after hydrating for periods of 24 hours and 48 hours at 50% relative humidity and 23°C

Figure 2.1.1 displays TGA/SDT analysis of CSA cement paste 7 containing solely anhydrite in Table 2.3 after hydrating for periods of 24 hours and 48 hours at 50% relative humidity and 23°C. The peaks near 120°C suggest the concentration of ettringite increases with increases in hydration time for the first two days. The peaks near 250°C suggest the concentration of aluminum hydroxide also progressively increases during the first two days of hydration. In the early hours of hydration, it is possible that the dissolution kinetics of anhydrite are slow enough such that the system is under saturated with respect to calcium sulfate leading to formation of monosulfate with peaks near 190°C (Winnefeld and Lothenbach, 2010). Given a molar ratio of yeelimite to calcium sulfate of 0.74 for the cement paste containing solely anhydrite, ettringite is expected to be the majority hydration phase formed during the early portion of hydration, which agrees with the curves displayed in Figure 2.1.1. The peak designations for Figure 2.1.1 are in agreement with literature

describing the water associated with ettringite decomposition near 120°C, monosuflate decomposition near 190°C and aluminum hydroxide decomposition in the vicinity of 250°C (Winnefeld and Lothenbach 2010, Winnefeld and Barlag, 2010, Sherman et al, 1995, Sato et al, 1992, Sato, 1985). .

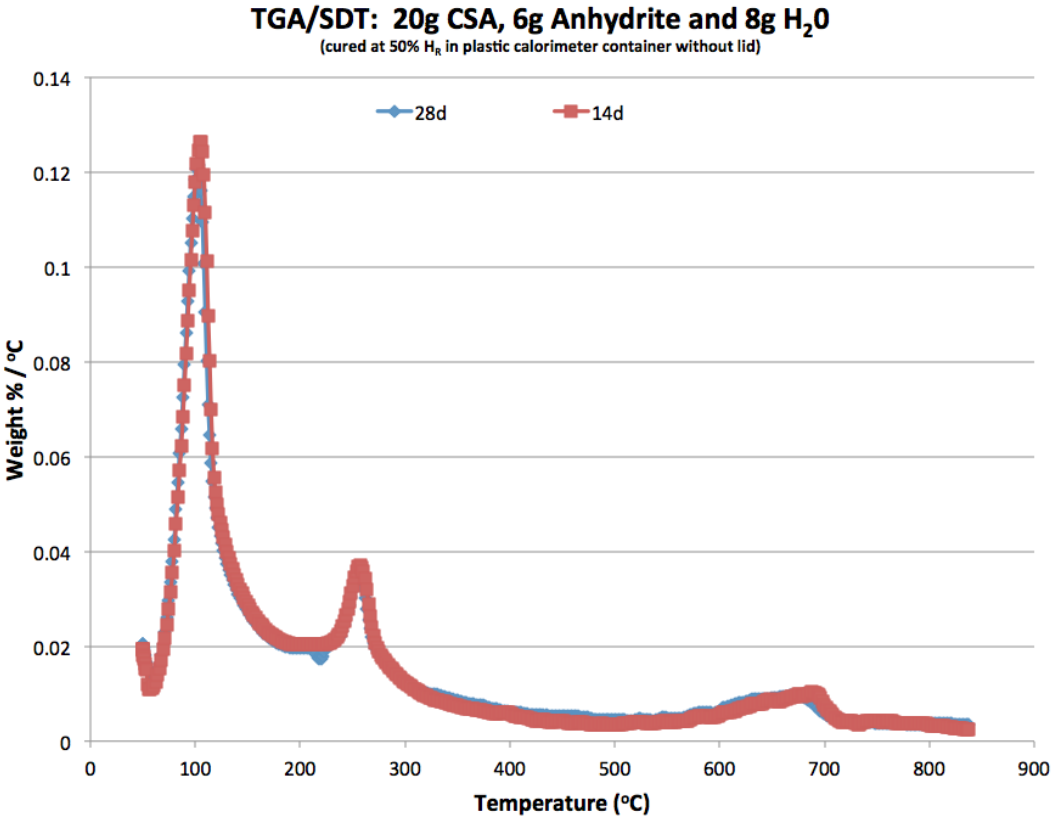

Figure 2.1.2: TGA/SDT analysis of CSA cement paste 7 containing solely anhydrite in Table 2.3 after curing for periods of 14 days and 28 days at 50% relative humidity and 23°C

Figure 2.1.2 displays TGA/SDT analysis of CSA cement paste 7 containing solely anhydrite in Table 2.3 after curing for periods of 14 days and 28 days at 50% relative humidity and 23°C. The peaks near 120°C suggest the ettringite concentration is no longer increasing with increases in hydration time after 14 days of hydration, as the peaks are similar in both amplitude and breadth for hydration periods of 14 and 28 days. There seems to be no apparent change in aluminum hydroxide concentration for curing periods of 14 days and 28 days.

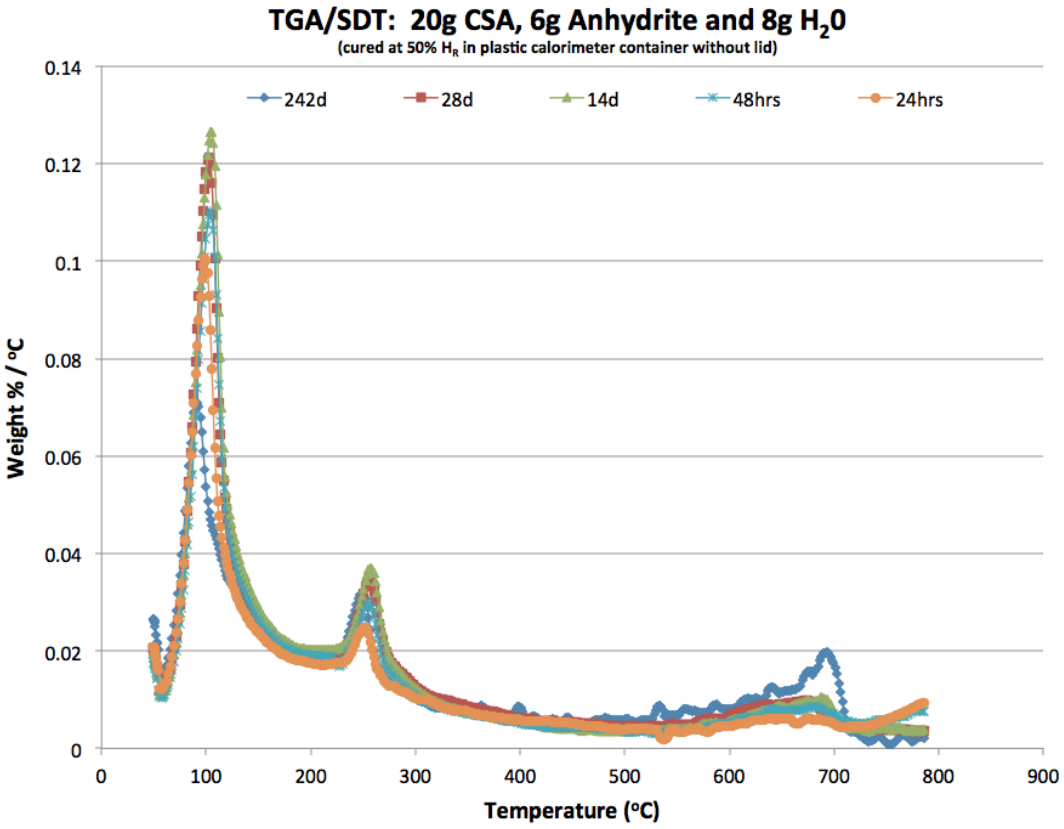

Figure 2.1.3: TGA/SDT analysis of CSA cement paste 7 containing solely anhydrite in Table 2.3 after curing for periods of 24 hours, 48 hours, seven days, 14 days, 28 days and 242 days at 50% relative humidity and 23°C

Figure 2.1.3 displays TGA/SDT analysis of CSA cement paste 7 containing solely anhydrite in Table 2.3 after curing for periods of 24 hours, 48 hours, 7 days, 14 days, 28 days and 242 days at 50% relative humidity and 23°C. Note that the concentration of ettringite increases for hydration periods of 24 hours through 14 days, then the concentration of ettringite reaches an apparent peak at 14 days , where after 14 days the concentration remains relatively constant for some period of time before subsequently decreasing for the remainder of the hydration period –some 242 days of hydration at constant 50% relative humidity and 23°C. The concentration of aluminum hydroxide represented by the peak and curve near 250°C increases through 14 days and remains relatively constant throughout the remainder of the experiment. Given the range of potential constituent materials comprising commercially available CSA cements and their potential to influence hydration behavior, the experimental aluminum hydroxide behavior is similar to that reported by Winnefeld and Lothenbach, (2010), where two diagrams

depicting modeled phase volume versus time for two hydrating CSA cements containing different types of calcium sulfate are displayed such that the phase volume of aluminum hydroxide gradually increases with hydration time throughout the 1000 hour life of each model (Winnefeld and Lothenbach, 2010).

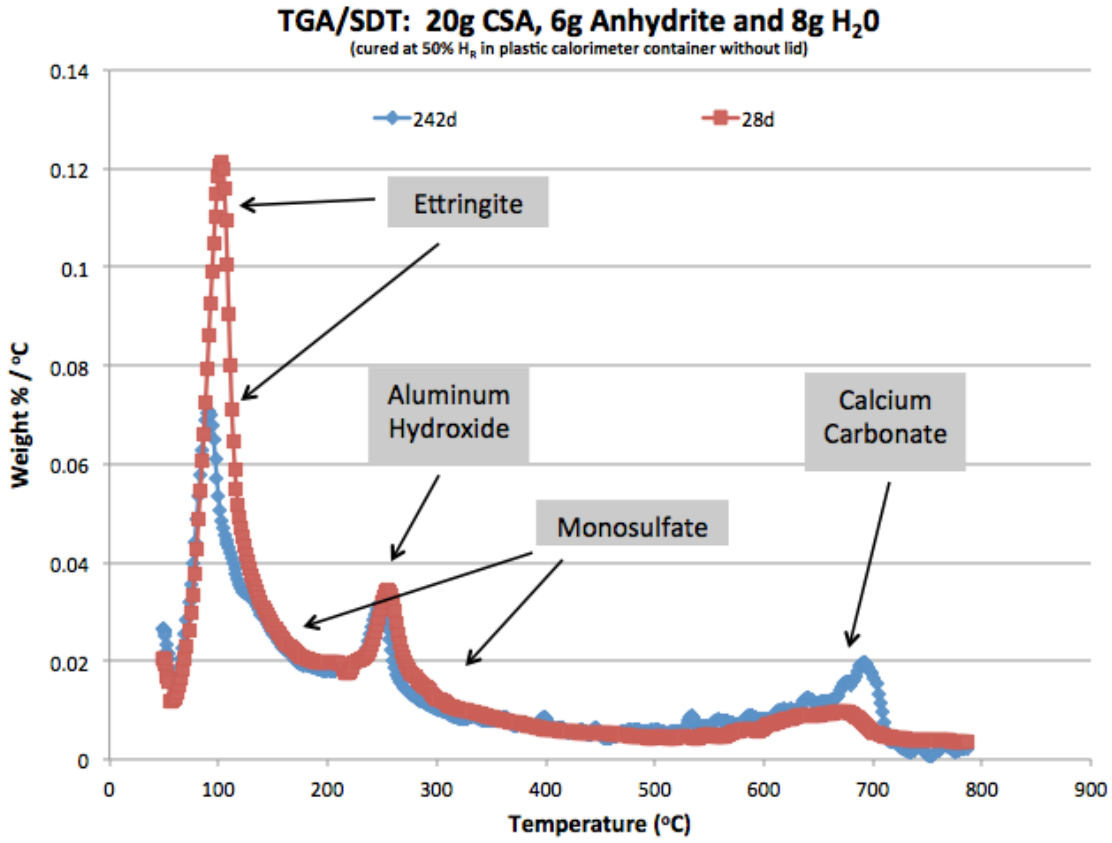

Figure 2.1.4: TGA/SDT analysis of CSA cement paste 7 containing solely anhydrite in Table 2.3 after curing for periods of 28 days and 242 days at 50% relative humidity and 23°C

Figure 2.1.4 displays TGA/SDT analysis of CSA cement paste 7 containing solely anhydrite in Table 2.3 after curing for periods of 28 days and 242 days at 50% relative humidity and 23°C. As with other TGA/SDT related figures, the peak near 120°C represents the concentration of ettringite which seems to decrease between 28 days and 242 days of hydration. The aluminum hydroxide peak near 250°C in Figure 2.1.4 seems to remain somewhat constant while the calcium carbonate peak near 700°C seems to increase slightly after 242 days of hydration. The decrease in ettringite concentration coupled with the increase in calcium carbonate concentration suggests ettringite decomposition is taking

place between 28 days and 242 days of hydration at constant 50% relative humidity and ambient laboratory temperature of 23°C (Sato et al, 1992, Skoblinskaya et al, 1975). It is unlikely ettringite converted to monosulfate during this period. For hydrating CSA cements, literature reports ettringite content reaches its maximum at a molar ratio of yeelimite to calcium sulfate of 1:2, and beyond that ratio, monosulfate is no longer present, but instead an excess of calcium sulfate occurs (Winnefeld and Lothenbach, 2013). The molar ratio of yeelimite to anhydrite for the CSA cement paste containing solely anhydrite in Table 2.3 is 0.74; therefore, ettringite is not expected to transition to formation of monosulfate at later ages, while the existence of excess calcium sulfate is expected. The following quote from Glasser and Zhang, (2001), describes similar behavior for hydrating CSA cements possessing lower water / cement ratios:

> We first envisaged that in a water-deficient environment, i.e., in the regime developed in formulations having less than the calculated CWD, AFm might simply form at the expense of the more water-rich AFt phase. But, experimentally, enhanced AFm formation is not observed in a variety of exposures, including both laboratory specimens and commercial concretes exposed to weathering for 10-15 years. Sufficient ettringite forms to consume all free water and thereafter ettringite continues to coexist with unhydrated clinker. (Glasser and Zhang, 2001)

Taylor (1997), suggests carbonation type behavior is more severe in laboratory type samples with greater available surface area when compared with total volume. It is likely the small sample size further contributes to the potential for ettringite to decompose when cured at constant 50% relative humidity and 23°C.

Table 2.1.1: LISTING OF MATERIALS FROM XRD ANALYSES FOR HYDRATING CSA CEMENT PASTE	
24 hours	Yeelimite > Anhydrite > Brownmillerite, $Ca_3Al_2O_6$ > alpha Ca_2SiO_4, Ettringite, Belite
21 days	Yeelimite > Anhydrite >> Brownmillerite, $Ca_3Al_2O_6$ > Ettringite, Belite, alpha-Ca_2SiO_4
28 days	Yeelimite > Anhydrite >> Brownmillerite, $Ca_3Al_2O_6$ > Ettringite, Belite, alpha-Ca_2SiO_4
242 days	Yeelimite > Anhydrite >> Ettringite, $Ca_3Al_2O_6$ > Gamma Ca_2SiO_4, Belite

Table 2.1.1: Interpretations of XRD diffractograms for the cement paste containing anhydrite in Table 2.3 when cured at 23°C and 50% relative humidity

Table 2.1.1 displays XRD results for the cement paste containing anhydrite in Table 2.3 when cured at 23°C and 50% relative humidity. As displayed, ettringite is present after 24 hours of hydration and reactants yeelimite and anhydrite are in the highest concentrations, which, given the low experimental water / cement ratio, is consistent with CSA cement hydration with anhydrite as the only source of calcium sulfate described in literature (Winnefeld and Lothenbach, 2013, Winnefeld and Lothenbach, 2010). Alpha-Ca_2SiO_4, alpha calcium silicate, is a mineral commonly associated with slags which is known to be metastable at low temperatures (Tossavainen, et al, 2007). XRD does not detect aluminum hydroxide; however, the presence of aluminum hydroxide should not be ruled out as its morphology may either be amorphous or microcrystalline, thus making it difficult to detect with XRD (Pelletier et al, 2010, Winnefeld and Barlag, 2010, Winnefeld and Lothenbach, 2010). Additionally, XRD does not detect monosulfate as its morphology is likely amorphous making it difficult to detect (Pelletier et al, 2010, Winnefeld and Barlag, 2010, Winnefeld and Lothenbach, 2010).

Between 21 days and 28 days of hydration, essentially no significant differences exist for microstructural constituent materials. This is expected, as ettringite has a high chemical water demand and is known for introducing rapid desiccating type behavior during formation (Glasser et al, 2001). Given water is a limiting reagent for hydrating materials possessing a low water/cement ratio, the majority of free water was likely chemically bound during ettringite formation by 21 days of hydration at constant 50% relative humidity and 23°C. After hydrating for 242 days, the material composition of the cement paste sample changed as brownmillerite and alpha-Ca_2SiO_4 are no longer detected while ettringite continues to display a minor concentration relative to other materials.

At 242 days, Gamma-Ca_2SiO_4, gamma calcium silicate, emerges. Gamma calcium silicate is described as one of the most common minerals associated with slags, as it is known to be stable at low temperatures (Tossavainen, et al, 2007). The relationship between ettringite and belite in Table 2.1.1 at later ages is interesting. During hydration of CSA cements, belite is typically a slower reacting constituent known for continued hydration at longer ages (Glasser and Zhang, 2001). As a stand alone binder, belite is reported to have experienced less than 20% of its hydration potential up to seven to 10 days after initial hydration (Scrivener and Nonat, 2011). For the CSA cement paste represented in Table 2.1.1, the author theorizes the concentration of ettringite increased relative to that of belite between 28 and 242 days, as additional belite was likely consumed

during continued hydration, perhaps reacting further to form amorphous phases not easily detected by XRD. It is important to note quantitative Rietveld analysis was not utilized to arrive at the determinations displayed in Table 2.1.1.

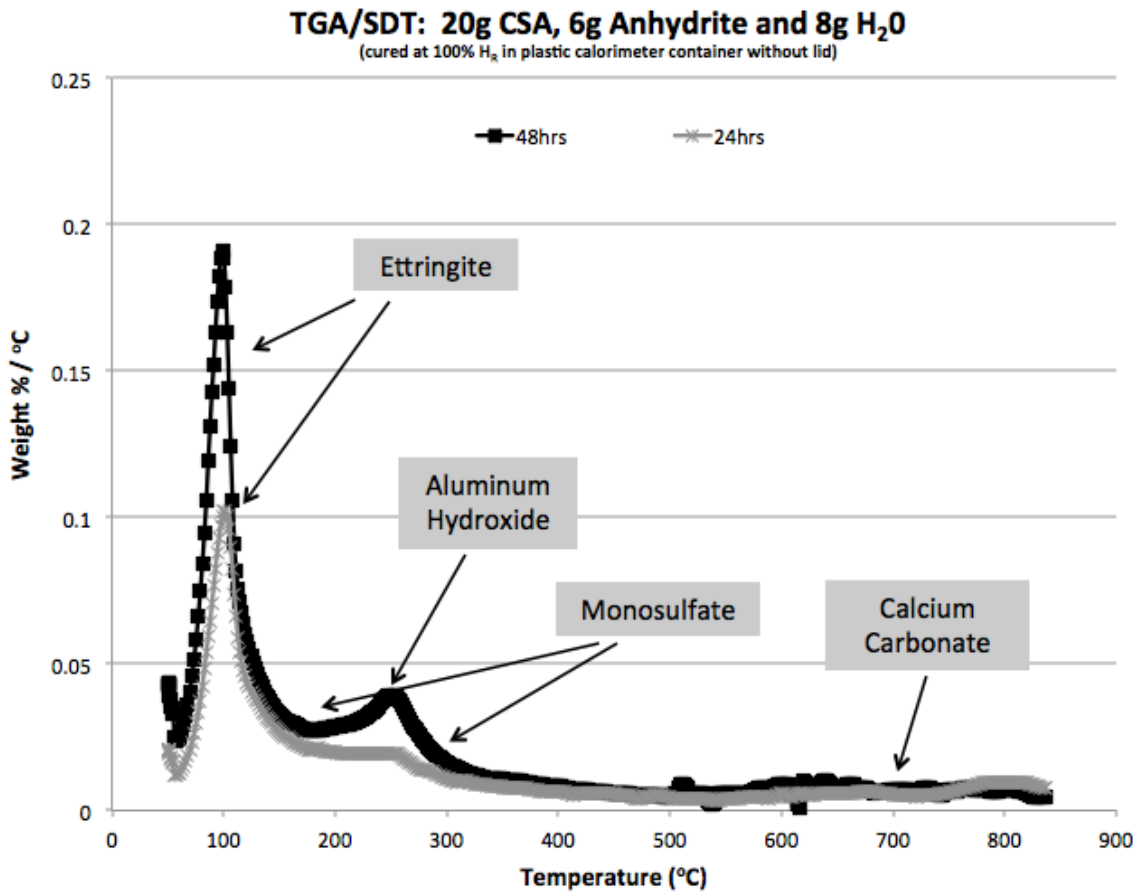

Figure 2.1.5: TGA/SDT analysis of CSA cement paste 2 containing solely anhydrite in Table 2.3 after hydrating for periods of 24 hours and 48 hours at 100% relative humidity and 23°C

Figure 2.1.5 displays TGA/SDT analysis of CSA cement paste 2 containing solely anhydrite in Table 2.3 after hydrating for periods of 24 hours and 48 hours at 100% relative humidity and 23°C. The peaks near 120°C suggest the concentration of ettringite increases with increases in hydration time during the early stages of hydration. The peaks near 250°C suggest the concentration of aluminum hydroxide increases with increases in hydration time. The portion of the curve near 190°C suggests the monosulfate concentration increased between 24 hours and 48 hours of hydration at 100% relative humidity. The peak designations for Figure 2.1.5 are in agreement with literature describing the water

associated with ettringite decomposition near 120°C, monosulfate decomposition near 190°C and aluminum hydroxide decomposition in the vicinity of 250°C (Winnefeld and Lothenbach 2010, Winnefeld and Barlag, 2010, Sherman et al, 1995, Sato et al, 1992, Sato, 1985). It is quite interesting to note the change in ettringite concentration at 48 hours for the like samples displayed in Figures 2.1.1 and 2.1.5 cured at humidity extremes of constant 50% relative humidity and constant 100% relative humidity, respectively. This information highlights the influence of self-desiccation on CSA cement hydration for materials possessing low water / cement ratios. For the pastes cured at constant 50% relative humidity in Figure 2.1.1, ettringite formation apparently ceased once the available water had been consumed by the hydration reactions. For the case of Figure 2.1.5, the 100% humidity environment mitigated the influence of evaporative processes on the hydration reactions, while the environment might also create the possibility for additional water to migrate into the microstructure during this early stage of hydration.

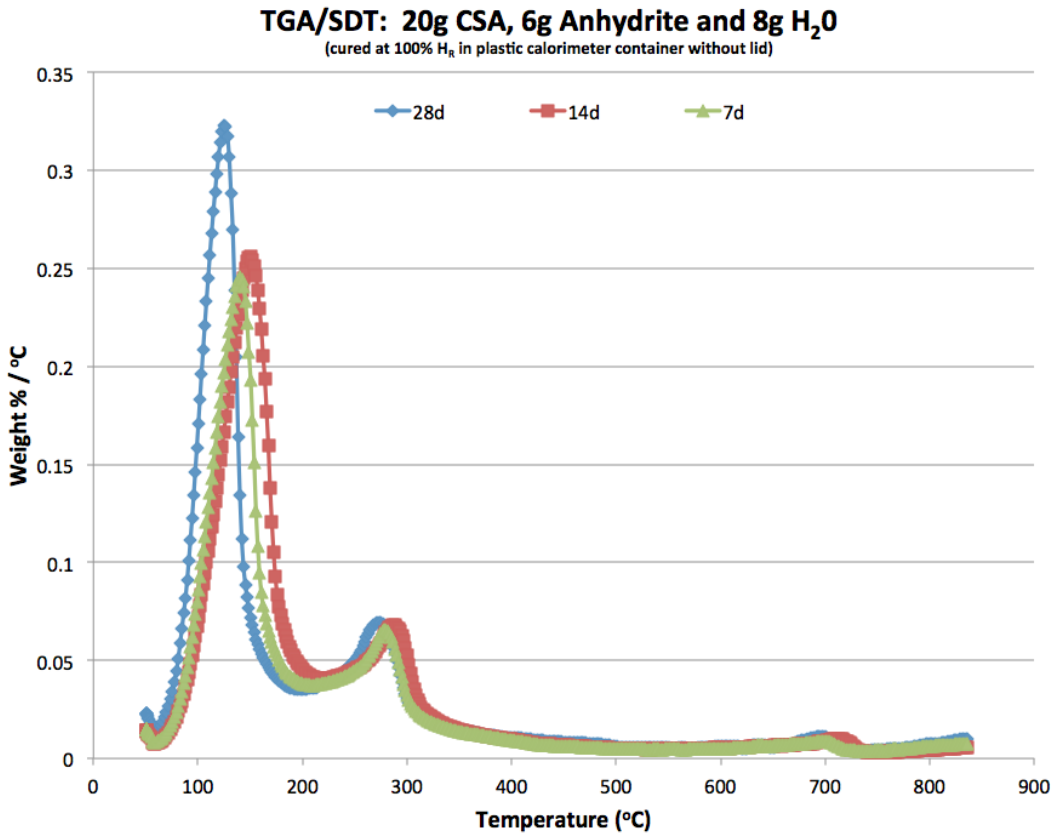

Figure 2.1.6: TGA/SDT analysis of CSA cement paste 2 containing solely anhydrite in Table 2.3 after curing for periods of seven days, 14 days and 28 days at 100% relative humidity and 23°C

Figure 2.1.6 displays TGA/SDT analysis of CSA cement paste 2 containing solely anhydrite in Table 2.3 after curing for periods of 7 days, 14 days and 28 days at 100% relative humidity and 23°C. As with Figure 2.1.5, the peaks near 120°C display the concentration of ettringite increasing with increasing hydration time through 28 days. There seems to be no apparent change in aluminum hydroxide concentration for curing periods of 7 days, 14 days and 28 days. Once again, comparing the information displayed in Figure 2.1.6 with Figure 2.1.2 highlights the self-desiccating nature of CSA cements possessing low water / cement ratios when cured in low humidity environments. After 28 days of hydration, the ettringite concentration for the sample displayed in Figure 2.1.6 cured at 100% relative humidity displays a value nearly 3x the amplitude of the curve associated with the like sample displayed in Figure 2.1.2.

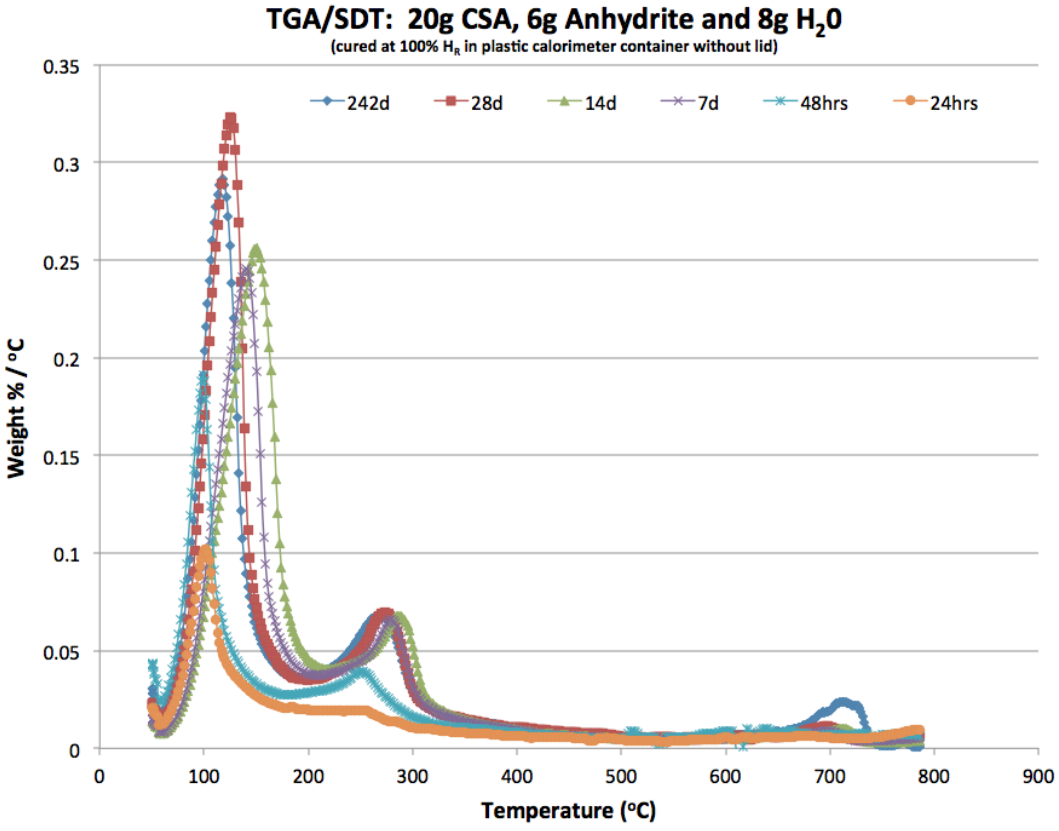

Figure 2.1.7: TGA/SDT analysis of CSA cement paste 2 containing solely anhydrite in Table 2.3 after curing for periods of 24 hours, 48 hours, seven days, 14 days, 28 days and 242 days at 100% relative humidity and 23°C

Figure 2.1.7 displays TGA/SDT analysis of CSA cement paste 2 containing solely anhydrite in Table 2.3 after curing for periods of 24 hours, 48 hours, 7 days, 14 days, 28 days and 242 days at 100% relative humidity and 23°C. As seen in Figure 2.1.7, the ettringite concentration seems to constantly increase through 28 days of hydration before showing a slight decrease from 28 days to 242 days of hydration at constant 100% relative humidity and 23°C. It is interesting to note the increase in the calcium carbonate peak near 700°C which suggests ettringite decomposition between 28 days and 242 days of hydration at 100% relative humidity via carbonation (Sato et al, 1995). The portion of the curve near the aluminum hydroxide peak seems to increase from 24 hours to 7 days, then the aluminum hydroxide peak remains relatively constant from 7 days through 242 days hydration.

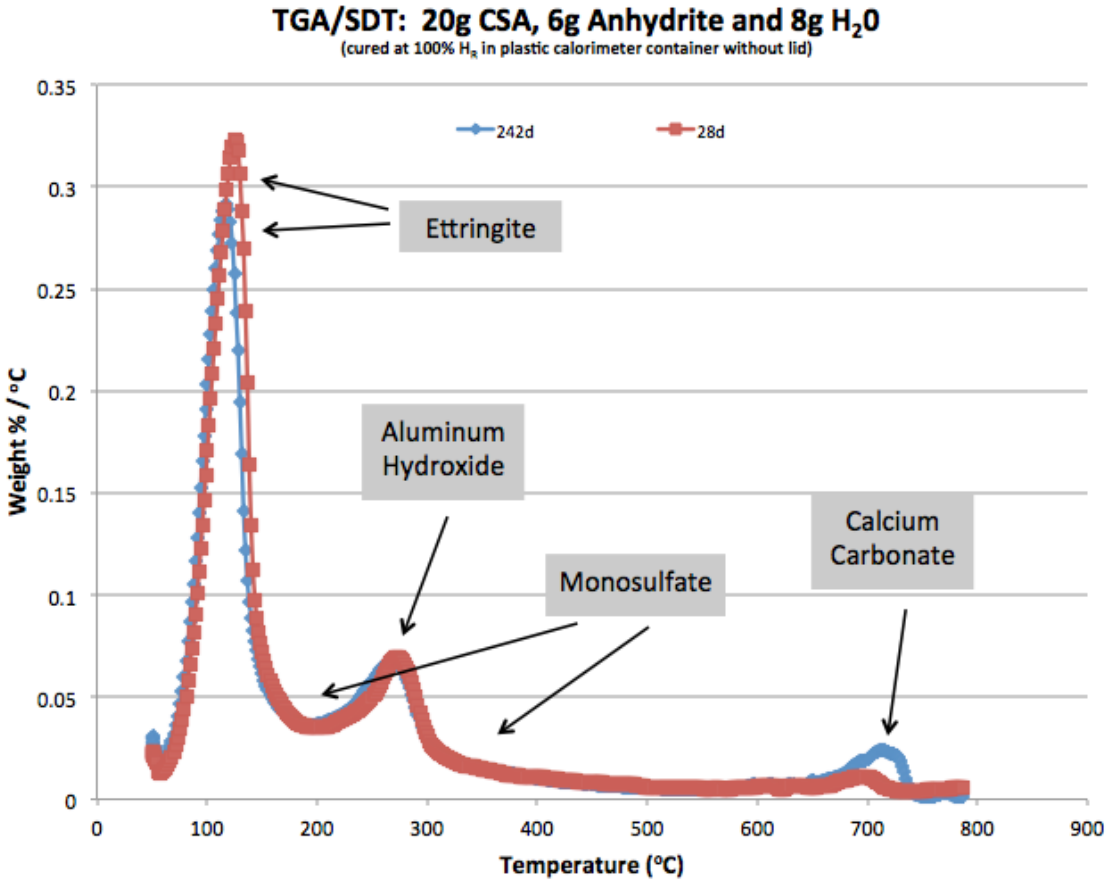

Figure 2.1.8: TGA/SDT analysis of CSA cement paste 2 containing solely anhydrite in Table 2.3 after curing for periods of 28 days and 242 days at 100% relative humidity and 23°C

As previously mentioned, Figure 2.1.8 displays TGA/SDT analysis of CSA cement paste 2 containing solely anhydrite in Table 2.3 after curing for periods of 28 days and 242 days at 100% relative humidity and 23°C with a slight decrease in ettringite concentration from 28 days to 242 days. The slight increase in the calcium carbonate peak at 700°C suggests ettringite decomposition between 28 days and 242 days hydration at 100% relative humidity and 23°C. In this 100% relative humidity environment, such ettringite decomposition is likely a result of carbonation type processes, which may be severe in the small samples with large available surface area when compared with total volume (Taylor, 1997).

Table 2.1.2: LISTING OF MATERIALS FROM XRD ANALYSES FOR HYDRATING CSA CEMENT PASTE	
24 hours	Yeelimite > Anhydrite > $Ca_3Al_2O_6$, Brownmillerite, Ettringite > alpha Ca_2SiO_4, Belite
21 days	Yeelimite, Anhydrite > Ettringite, alpha Ca_2SiO_4, $Ca_3Al_2O_6$, Brownmillerite > Belite
28 days	Yeelimite, Anhydrite > Ettringite > $Ca_3Al_2O_6$, Brownmillerite > alpha Ca_2SiO_4, Belite, Hannebachite
242 days	Ettringite, Yeelimite, Anhydrite > Brownmillerite, $Ca_3Al_2O_6$, > Belite, Calcite, $Ca_4Al_6O_{13}*3H_2O$, Gamma Ca_2SiO_4, Fluorite

Table 2.1.2: Interpretations of XRD diffractograms for the cement paste containing anhydrite in Table 2.3 cured at 23°C and 100% relative humidity.

Table 2.1.2 displays XRD characterizations for the cement paste sample containing anhydrite as a sole source of calcium sulfate when cured at 23°C and 100% relative humidity. The displayed XRD analyses support the corresponding thermogravimetric analyses displayed in Figures 2.1.5 through 2.1.8. After 24 hours of hydration, ettringite is present and reactants yeelimite and anhydrite are in the highest concentrations. This is indicative of hydration reactions proceeding as expected. XRD does not detect aluminum hydroxide; however, the presence of aluminum hydroxide should not be ruled out as its morphology may either be amorphous or microcrystalline, thus making it difficult to detect with XRD (Pelletier et al, 2010, Winnefeld and Barlag, 2010, Winnefeld and Lothenbach, 2010). Additionally, XRD does not detect monosulfate as its morphology is also likely

amorphous, thus making it difficult to detect (Pelletier et al, 2010, Winnefeld and Barlag, 2010, Winnefeld and Lothenbach, 2010).

At 21 days, the ettringite concentration has increased relative to other constituent materials for the CSA cement paste sample containing solely anhydrite as a source of calcium sulfate when cured at 100% H_R and 23°C when compared with results for the like sample cured at 50% H_R and 23°C displayed in Table 2.1.1.

At 28 days, the ettringite concentration is also greater relative to other materials for the sample hydrated at 100% when compared with the like sample hydrated at 50% H_R. Given the 100% humidity environment, water is no longer a limiting reagent, and the hydration reactions can proceed until another limiting factor is encountered. Additionally, the presence of hannebachite further validates the TGA/SDT trends displayed in Figures 2.1.7 and 2.1.8 as yeelimite and anhydrite may conceivably undergo continued hydration to form ettringite at 100% relative humidity while previously developed ettringite simultaneously decomposes.

At 242 days, the ettringite concentration is considerably greater relative to other materials for the sample hydrated at 100% H_R when compared with the like sample hydrated at 50% H_R. As with the 28 day results, the presence of calcite and the calcium aluminate hydrates further validates the TGA/SDT trends as yeelimite and anhydrite may conceivably undergo continued hydration to form ettringite at 100% relative humidity while previously developed ettringite simultaneously decomposes via carbonation processes as described by Sato et al, (1992). Additionally, the likelihood of continued hydration occurring in the small laboratory type samples is increased due to large available surface area when compared with total volume.

2.2: Gypsum as a source of calcium sulfate

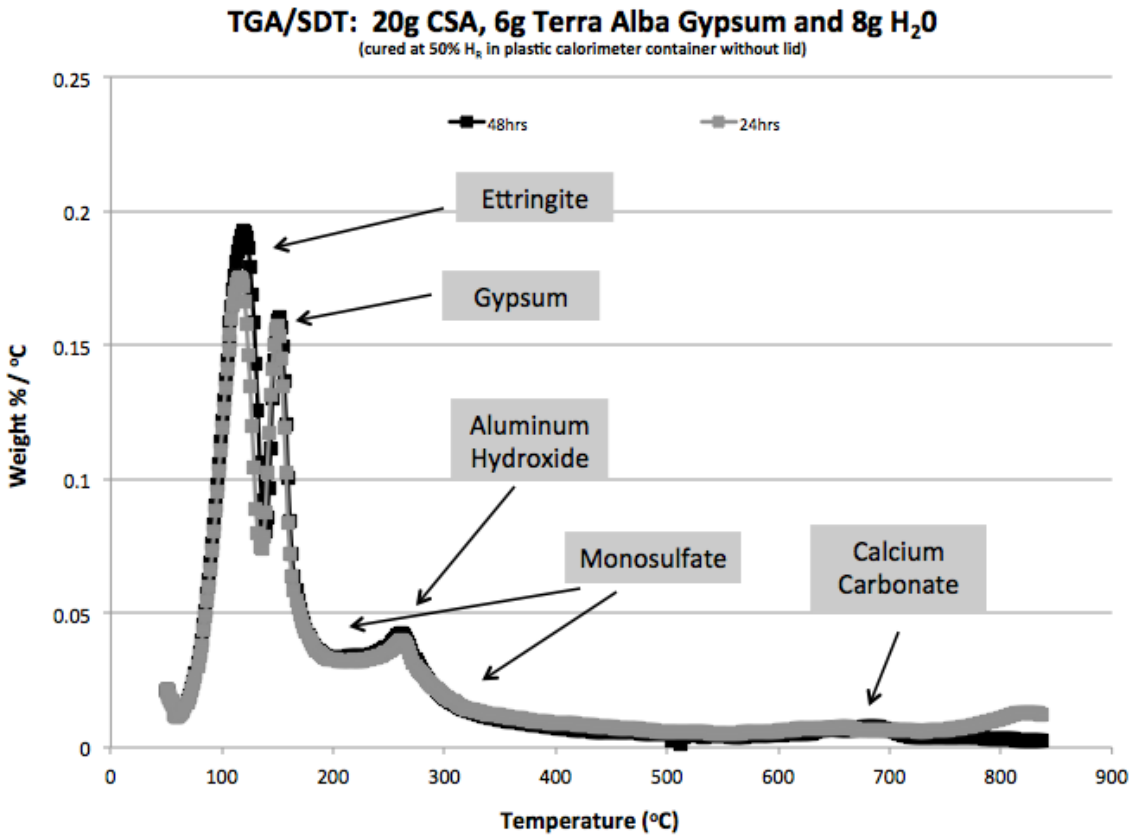

Figure 2.2.1: TGA/SDT analysis of CSA cement paste 8 containing solely gypsum in Table 2.3 after hydrating for periods of 24 hours and 48 hours at 50% relative humidity and 23°C

Figure 2.2.1 displays TGA/SDT analysis of CSA cement paste 8 containing solely gypsum in Table 2.3 after hydrating for periods of 24 hours and 48 hours at 50% relative humidity and 23°C. The peaks near 120°C represent the concentration of ettringite as being quite similar after hydrating for 24 hours and 48 hours, respectively. The peaks near 150°C represent the concentrations of gypsum as also being similar for each sample, which agrees with literature (Yu et al, 2010). The portion of the curve near 170 to 190°C represents monosulfate (Winnefeld and Barlag, 2010). The apparent ratios of ettringite to monosulfate, as represented by the respective portions of each curve, are in agreement with literature describing the composition of hydrating CSA cement pastes with similar molar ratios of yeelimite to gypsum (Winnefeld and Barlag, 2010). The molar ratio of yeelimite to gypsum is 0.88 for the CSA cement paste sample containing gypsum as a source of calcium

sulfate in Table 2.3. The peaks near 250°C represent the concentrations of aluminum hydroxide as being approximately equal for each sample as well. The peak designations for Figure 2.2.1 are in agreement with literature describing the water associated with ettringite near 120°C, thermal decomposition of gypsum near 150°C, thermal decomposition of monosulfate near 190°C and aluminum hydroxide decomposition in the vicinity of 250°C (Winnefeld and Lothenbach 2013, Winnefeld and Lothenbach, 2010, Winnefeld and Barlag, 2010, Sherman et al, 1995, Sato et al, 1992, Sato, 1985).

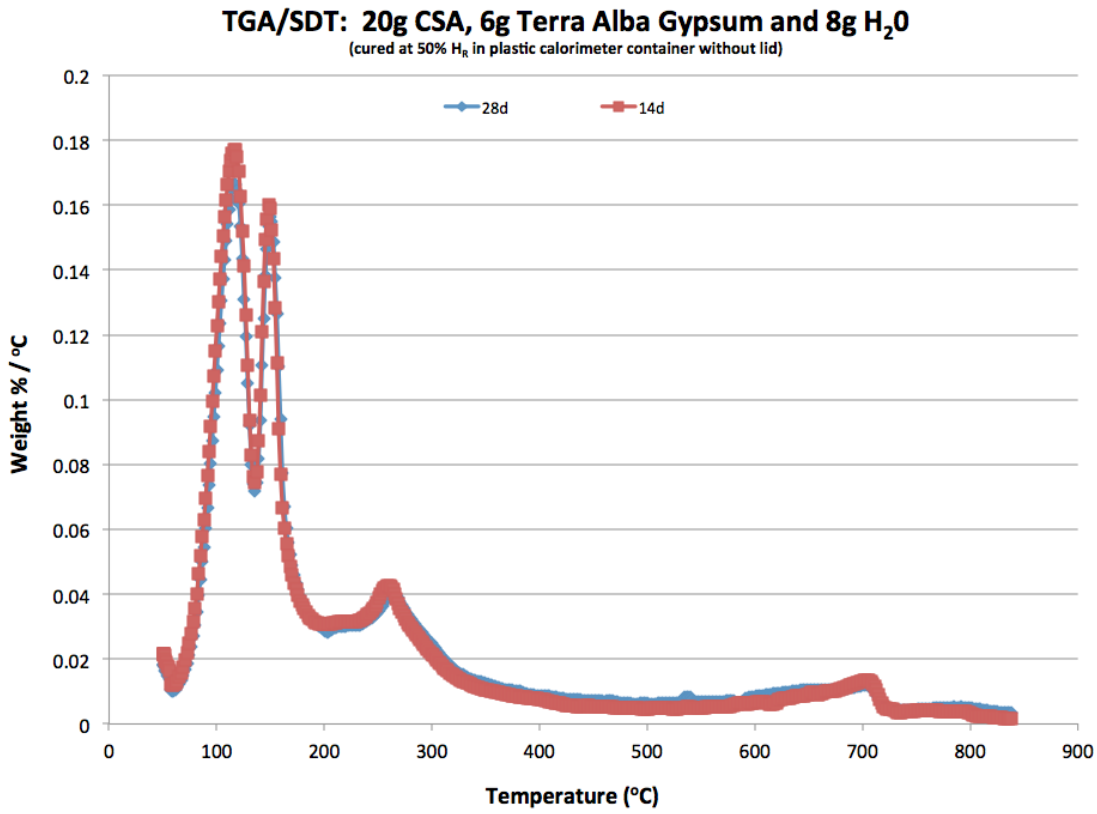

Figure 2.2.2: TGA/SDT analysis of CSA cement paste 8 containing solely gypsum in Table 2.3 after hydrating for periods of 14 days and 28 days at 50% relative humidity and 23°C

Figure 2.2.2 displays TGA/SDT analysis of CSA cement paste 8 containing solely gypsum in Table 2.3 after hydrating for periods of 14 days and 28 days at 50% relative humidity and 23°C. The peaks near 120°C represent the concentrations of ettringite as being relatively equal for each sample. The peaks near 150°C represent the concentrations

of gypsum as being relatively equal for each sample. The peaks near 250°C represent the concentrations of aluminum hydroxide as being similar for each sample.

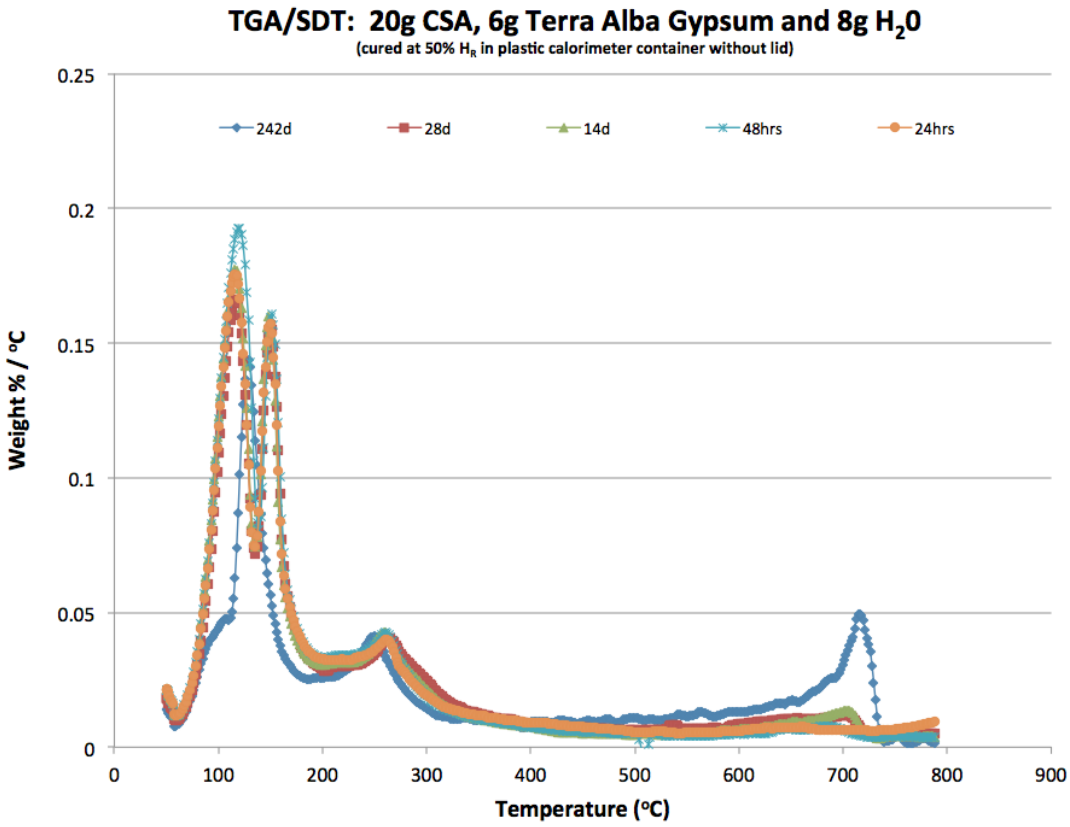

Figure 2.2.3: TGA/SDT analysis of CSA cement paste 8 containing solely gypsum in Table 2.3 after hydrating for periods of 24 hours, 48 hours, 14 days, 28 days and 242 days at 50% relative humidity and 23°C

Figure 2.2.3 displays TGA/SDT analysis of CSA cement paste 8 containing solely gypsum in Table 2.3 after hydrating for periods of 24 hours, 48 hours, 14 days, 28 days and 242 days at 50% relative humidity and 23°C. The peaks near 120°C suggest the concentrations of ettringite increase through 48 hours before showing a slight decrease through 28 days. After 28 days of hydration, the ettringite concentration decreased significantly. The peaks near 150°C represent the concentrations of gypsum being within a controlled range for all samples through 28 days of hydration. The curve for 242 days of hydration shows the concentrations of ettringite and gypsum decrease while that of calcium carbonate increased when compared with early age samples. Furthermore, there is an

apparent shift in the curve near 130°C, where the shift potentially represents a different morphology, likely gypsum or monosulfate. Sato et al, (1992), report that ettringite decomposes via carbonation under dry conditions to form gypsum and calcium carbonate, where the calcium carbonate was found to be vaterite in the initial stage, followed by aragonite as the predominant phase in a later stage (Sato et al, 1992).

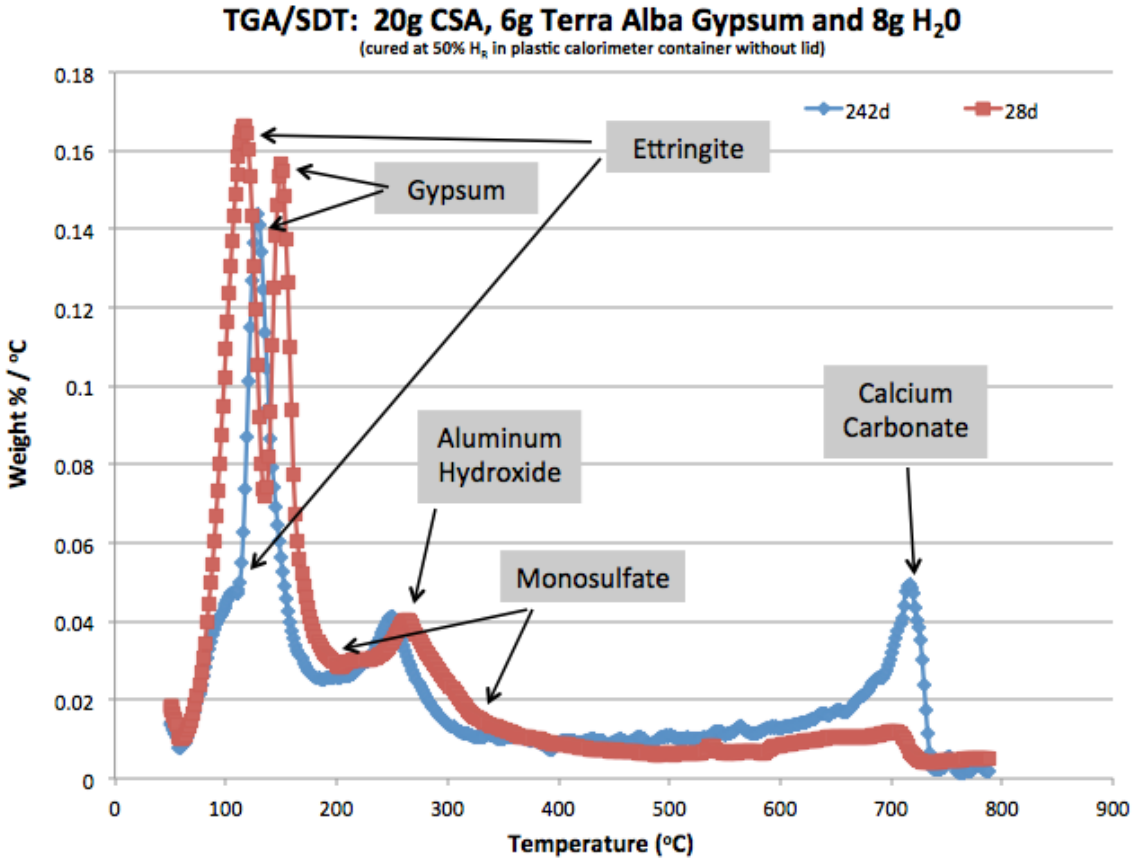

Figure 2.2.4: TGA/SDT analysis of CSA cement paste 8 containing solely gypsum in Table 2.3 after hydrating for periods of 28 days and 242 days at 50% relative humidity and 23°C

Figure 2.2.4 displays TGA/SDT analysis of CSA cement paste 8 containing solely gypsum in Table 2.3 after hydrating for periods of 28 days and 242 days at 50% relative humidity and 23°C. The curve for 242 days of hydration shows the ettringite concentration being less than that of the early age sample. Near 700°C, the curves suggest the calcium carbonate concentration increased between 28 days and 242 days of hydration. The information displayed in Figure 2.2.4 suggests ettringite is decomposing, possibly as a result

of carbonation processes as described by Sato et al, (1992), or possibly as a result of dehydration processes as explained by Skoblinskaya et al, (1975) or perhaps by both.

Table 2.2.1: LISTING OF MATERIALS FROM XRD ANALYSES FOR HYDRATING CSA CEMENT PASTE	
24 hours	Yeelimite >> $Ca_3Al_2O_6$, Gypsum, Ettringite > alpha Ca_2SiO_4 > Belite
21 days	Yeelimite >> Gypsum, $Ca_3Al_2O_6$, > Ettringite, Belite, alpha Ca_2SiO_4, Anhydrite
28 days	Yeelimite > Gypsum, $Ca_3Al_2O_6$, > alpha Ca_2SiO_4, Anhydrite, Ettringite, Belite
242 days	Yeelimite, Gypsum >> $Ca_3Al_2O_6$, > Ettringite, Belite, Wairakite, alpha Ca_2SiO_4, gamma Ca_2SiO_4 > Anhydrite

Table 2.2.1: Interpretations of XRD diffractograms for the cement paste containing gypsum cured at 23°C and 50% relative humidity.

Table 2.2.1 displays XRD information for the hydrating CSA cement paste containing gypsum as a sole source of calcium sulfate in Table 2.3 when cured at 23°C and constant 50% relative humidity. After 24 hours of hydration, yeelimite displays the greatest concentration relative to other constituent materials while the concentration of ettringite is similar to that of gypsum. For the first 24 hours of hydration, the information displayed in Table 2.2.1 agrees with literature describing hydrated phase assemblages for a CSA cement paste with similar molar ratio of yeelimite to calcium sulfate (Winnefeld and Barlag, 2010). Additionally, XRD does not detect aluminum hydroxide; however, the presence of aluminum hydroxide should not be ruled out as its morphology may either be amorphous or microcrystalline, thus making it difficult to detect with XRD (Pelletier et al, 2010, Winnefeld and Barlag, 2010, Winnefeld and Lothenbach, 2010). Similarly, XRD does not detect monosulfate as its morphology is likely amorphous making it difficult to detect (Pelletier et al, 2010, Winnefeld and Barlag, 2010, Winnefeld and Lothenbach, 2010).

After 21 days of hydration, changes are apparent in the microstructure of the CSA cement paste containing gypsum as a source of calcium sulfate when compared with the early age sample. At 21 days, the concentration of ettringite has decreased relative to other materials, while the concentration of gypsum seems to have increased relative to other constituent materials. Additionally, anhydrite has emerged as a constituent material with a

minor concentration at 21 days. Ettringite is reported to decompose to calcium sulfate, calcium carbonate and aluminum hydroxide (Sato et al, 1992). Given, an increase in the concentration of gypsum relative to other materials, a decrease in the concentration of ettringite relative to other materials and the emergence of anhydrite as a new minor phase suggests ettringite decomposition is occurring in the CSA cement paste sample containing gypsum as the sole source of calcium suflate after curing for 21 days at constant 50% relative humidity.

The relative concentrations of phases displayed for both the 28 and 242 day samples in Table 2.2.1 provide further evidence for occurrence of processes associated with ettringite decomposition within the microstructure of the CSA cement paste containing gypsum as the sole source of calcium sulfate when cured at constant low humidity for greater than 28 days. According to the information displayed in Table 2.2.1, gypsum continually increases in concentration relative to other materials versus time. Processes associated with ettringite decomposition potentially deliver additional gypsum, calcium carbonate and perhaps amorphous aluminum hydroxide to the system and provide plausible scenarios for explaining both the increase in gypsum concentration and decrease in ettringite concentration relative to other constituent materials over the course of the experiment.

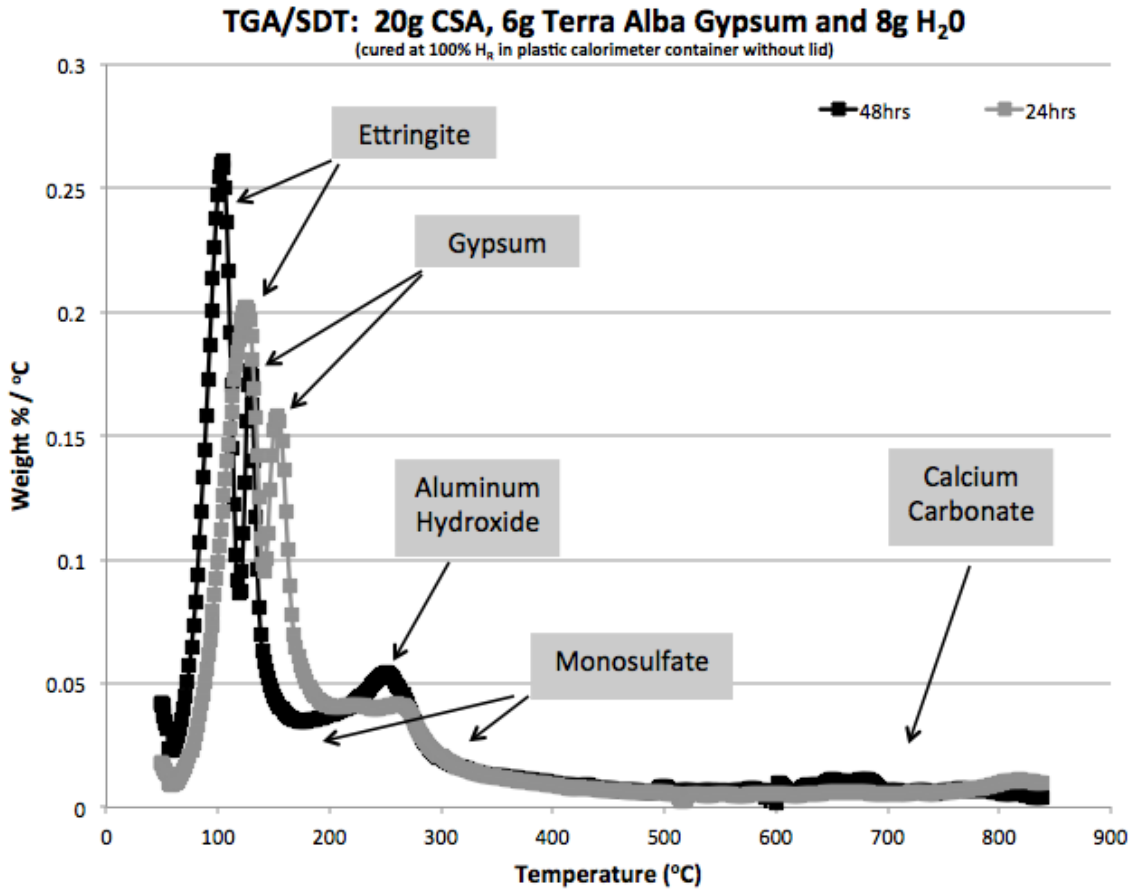

Figure 2.2.5: TGA/SDT analysis of CSA cement paste 1 containing solely gypsum in Table 2.3 after hydrating for periods of 24 hours and 48 hours at 100% relative humidity and 23°C

Figure 2.2.5 displays TGA/SDT analysis of CSA cement paste 1 containing solely gypsum in Table 2.3 after hydrating for periods of 24 hours and 48 hours at 100% relative humidity and 23°C. The peaks near 120°C represent the concentration of ettringite as increasing with increases in hydration time. The peaks near 150°C suggest the concentration of gypsum slightly increased for the later age sample. The portion of each curve between 150°C and 200°C suggest the concentration of monosulfate decreased between 24 and 48 hours of hydration at 100% relative humidity. The peaks near 250°C represent the concentrations of aluminum hydroxide as increasing with increases in hydration time. It is quite interesting to note the increased concentrations of ettringite for like samples cured at 100% relative humidity displayed in Figure 2.2.5 when compared with identical samples cured at 50% relative humidity displayed in Figure 2.2.1. Such

differences illustrate the rapid self-desiccating nature of ettringite formation in CSA cement materials possessing low water / cement ratios cured in low humidity environments.

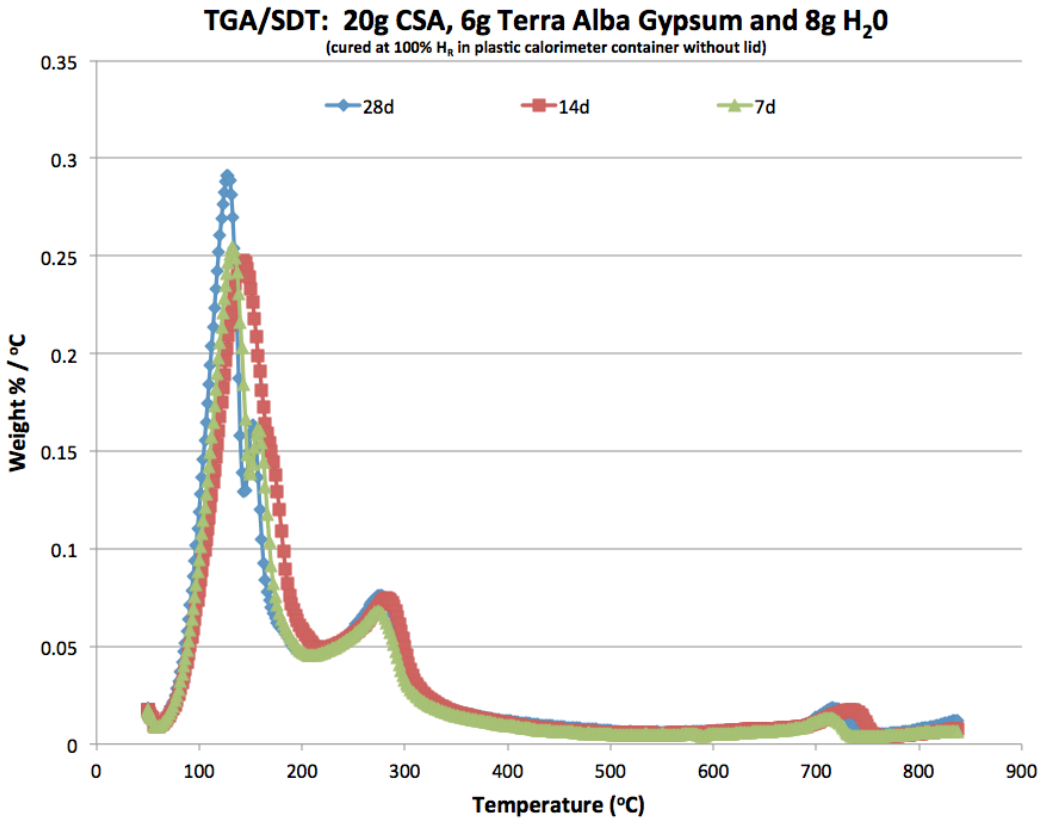

Figure 2.2.6: TGA/SDT analysis of CSA cement paste 1 containing solely gypsum in Table 2.3 after hydrating for periods of 7 days, 14 days and 28 days at 100% relative humidity and 23°C

Figure 2.2.6 displays TGA/SDT analysis of CSA cement paste 1 containing solely gypsum in Table 2.3 after hydrating for periods of 7 days, 14 days and 28 days at 100% relative humidity and 23°C. The concentrations of ettringite continually increase with increases in hydration time. The peaks near 150°C suggest the gypsum concentrations display a slight decrease for the displayed samples. The peaks near 250°C suggest the aluminum hydroxide concentrations remain somewhat constant for the displayed samples.

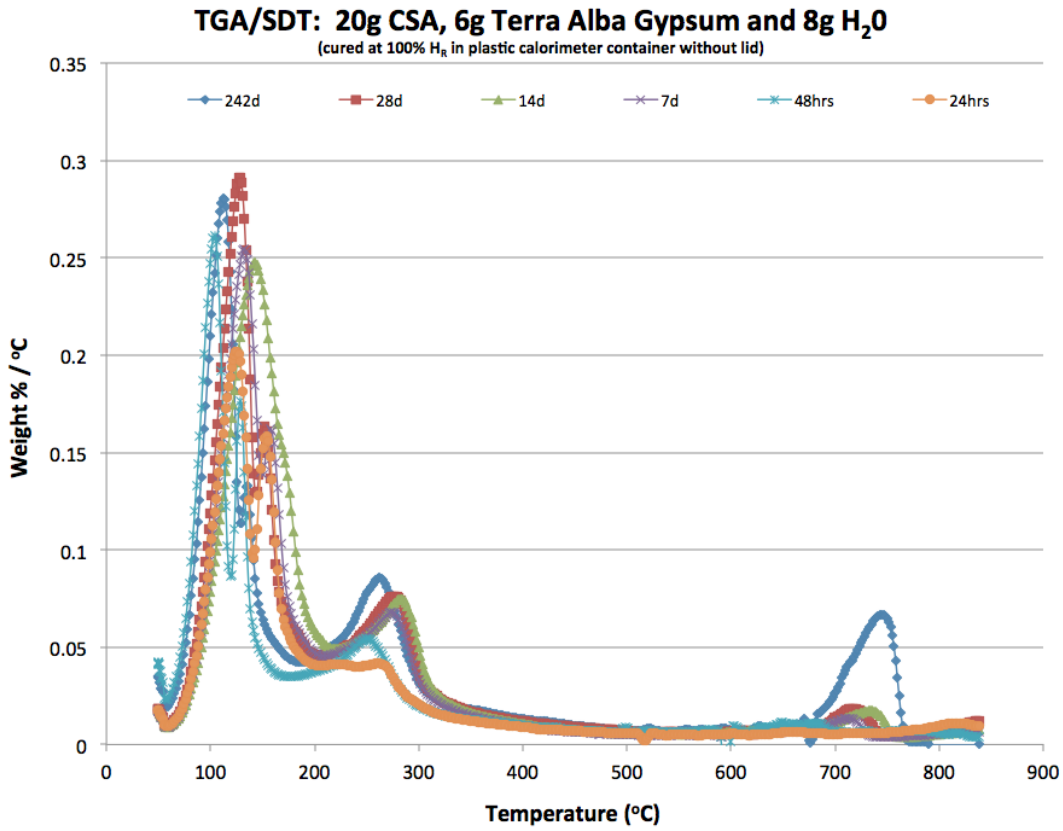

Figure 2.2.7: TGA/SDT analysis of CSA cement paste 1 containing solely gypsum in Table 2.3 after hydrating for periods of 24 hours, 48 hours, 7 days, 14 days, 28 days and 242 days at 100% relative humidity and 23°C

Figure 2.2.7 displays TGA/SDT analysis of CSA cement paste 1 containing solely gypsum in Table 2.3 after hydrating for periods of 24 hours, 48 hours, 7 days, 14 days, 28 days and 242 days at 100% relative humidity and 23°C. The concentration of ettringite increased through 28 days of hydration and subsequently decreased between 28 days and 242 days of hydration. The portion of the curves between 150°C and 200°C suggest monosulfate concentration remains relatively constant throughout the duration of the experiment. The peaks near 250°C suggest the aluminum hydroxide concentration increases slightly between 28 days and 242 days hydration at 100% H_R and 23°C. The peak near 700°C suggests the calcium carbonate concentration appears to increase between 28 days and 242 days hydration at 100% H_R and 23°C. Such an increase in calcium carbonate concentration coupled with a slight decrease in ettringite concentration suggests ettringite decomposition via carbonation for the cement paste containing solely gypsum cured at constant 100% relative humidity and 23°C. It is unlikely ettringite decomposition is due to dehydration for these samples cured at constant 100% relative humidity and 23°C.

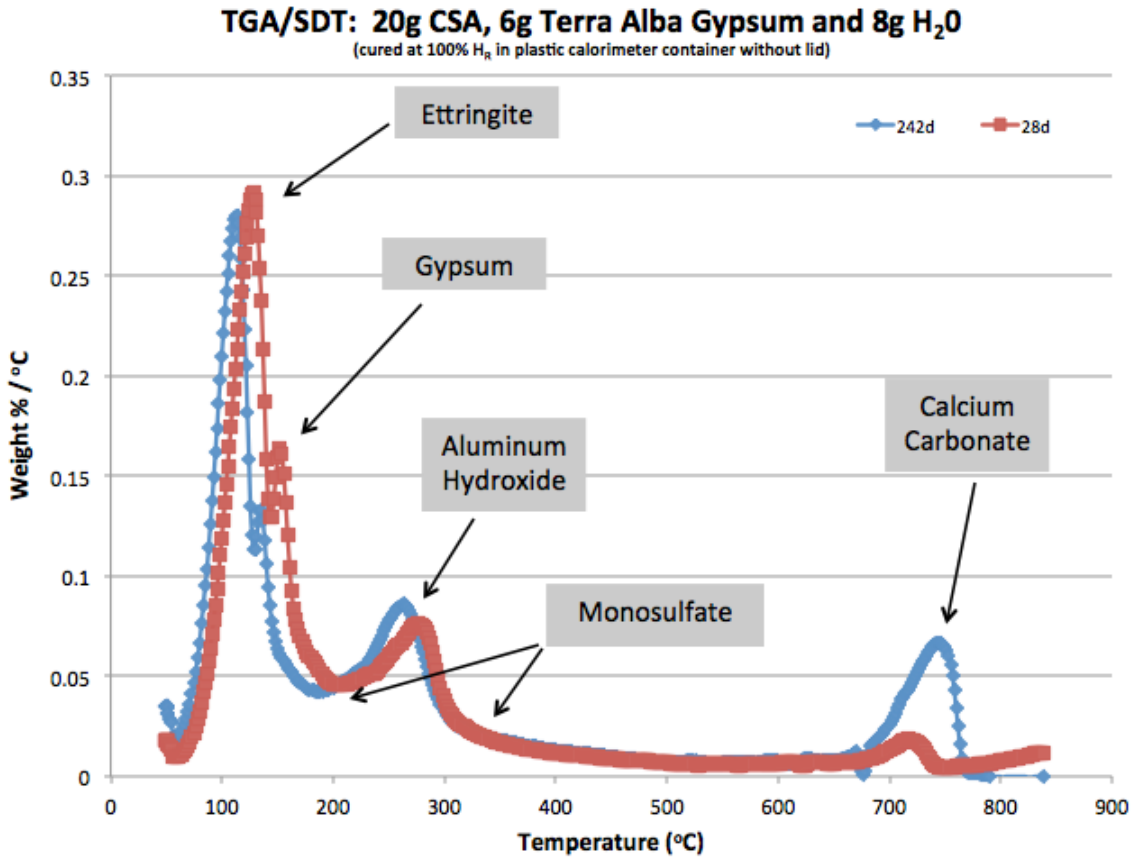

Figure 2.2.8: TGA/SDT analysis of CSA cement paste 1 containing solely gypsum in Table 2.3 after hydrating for periods of 28 days and 242 days at 100% relative humidity and 23°C

Figure 2.2.8 displays TGA/SDT analysis of CSA cement paste 1 containing solely gypsum in Table 2.3 after hydrating for periods of 28 days and 242 days at 100% relative humidity and 23°C. The peaks near 120°C display a slight decrease in ettringite concentration for the sample cured for 242 days when compared with the sample cured for 28 days. The peaks near 250°C suggest the aluminum hydroxide concentration appears to increase slightly between 28 days and 242 days hydration at 100% H_R and 23°C. The peak near 700°C suggests the calcium carbonate concentration appears to increase somewhat significantly between 28 days and 242 days hydration at 100% H_R and 23°C. Such an increase in calcium carbonate concentration coupled with a slight decrease in ettringite concentration suggests ettringite decomposition via carbonation for the cement paste containing solely gypsum cured at constant 100% relative humidity and 23°C.

Table 2.2.2: LISTING OF MATERIALS FROM XRD ANALYSES FOR HYDRATING CSA CEMENT PASTE	
24 hours	Yeelimite >> Ettringite, Gypsum, $Ca_3Al_2O_6$, > alpha Ca_2SiO_4 > Belite, Anhydrite
21 days	Yeelimite >> Ettringite, Gypsum, $Ca_3Al_2O_6$, > alpha Ca_2SiO_4 > Belite, Anhydrite
28 days	Yeelimite > $Ca_3Al_2O_6$, Ettringite, alpha Ca_2SiO_4 > Gypsum, Brownmillerite, Belite, Anhydrite > Calcite
242 days	Ettringite > Gypsum, Yeelimite > $Ca_3Al_2O_6$, Anhydrite > $Ca_4Al_6O_{13}$*$3H_2O$, Wairakite, Belite, Calcite

Table 2.2.2: Interpretations of XRD diffractograms for the cement paste containing gypsum cured at 23°C and 100% relative humidity.

Table 2.2.2 displays XRD information for the hydrating CSA cement paste containing gypsum as a sole source of calcium sulfate in Table 2.3 when cured at 23°C and constant 100% relative humidity. After 24 hours of hydration, yeelimite displays the greatest concentration relative to other constituent materials while the concentration of ettringite is similar to that of gypsum. For the first 24 hours of hydration, the information displayed in Table 2.2.2 supports the TGA/SDT information displayed in Figure 2.2.5 as the concentration of ettringite is greater than that of gypsum for the CSA cement paste containing gypsum as a sole source of calcium suflate after hydrating for 24 hours at 100% relative humidity. Additionally, XRD does not detect aluminum hydroxide; however, the presence of aluminum hydroxide should not be ruled out as its morphology may either be amorphous or microcrystalline, thus making it difficult to detect with XRD (Pelletier et al, 2010, Winnefeld and Barlag, 2010, Winnefeld and Lothenbach, 2010). Likewise, XRD does not detect monosulfate as its morphology is also likely amorphous, making it difficult to detect (Pelletier et al, 2010, Winnefeld and Barlag, 2010, Winnefeld and Lothenbach, 2010).

After 21 days of hydration, no changes are apparent in the microstructure of the CSA cement paste containing gypsum as a source of calcium sulfate when compared with the early age sample. Therefore, the information displayed in Table 2.2.2 supports the TGA/SDT information displayed in Figure 2.2.6.

` After 28 days of hydration, the relative concentrations of phases displayed for the CSA cement paste sample containing solely gypsum as a source of calcium sulfate cured at

100% relative humidity suggests continued hydration is taking place. Such continued explains the increase in ettringite concentration relative to yeelimite when compared with samples representing earlier hydration periods. Given the 100% humidity environment, water is no longer a limiting reagent, hydration reactions can proceed until another limiting factor is encountered. Furthermore, the emergence of calcite together with the relative concentrations of both gypsum and anhydrite suggest ettringite decomposition is occurring via carbonation type processes as described by Sato et al, (1992). In wet systems, ettringite decomposes to gypsum (Sato et al, 1992). It is conceivable that continued hydration reactions occur yielding additional ettringite while carbonation type processes decompose existing ettringite inevitably creating additional amounts of gypsum, calcium carbonate and aluminum hydroxide.

After 242 days of hydration, ettringite displays the greatest concentration of constituent materials, gypsum has increased in concentration relative to early age samples and yeelimite has decreased in concentration for the CSA cement paste sample containing solely gypsum as a source of calcium sulfate when cured at 100% relative humidity. Such behavior suggests continued hydration is taking place, which explains the increase in ettringite concentration relative to yeelimite when compared with samples for earlier hydration periods. Furthermore, as with the 28 day sample, the continued presence of calcite together with the relative concentrations of both gypsum and anhydrite suggests ettringite decomposition is continually occurring via carbonation type processes as described by Sato et al, (1992). The emergence of the zeolite, wairakite, together with $Ca_4Al_6O_{13}*3H_2O$ are interesting, as these materials are not present in the microstructure of the like material cured at constant 50% relative humidity.

2.3: 50 weight % gypsum and 50 weight % anhydrite as a source of calcium sulfate

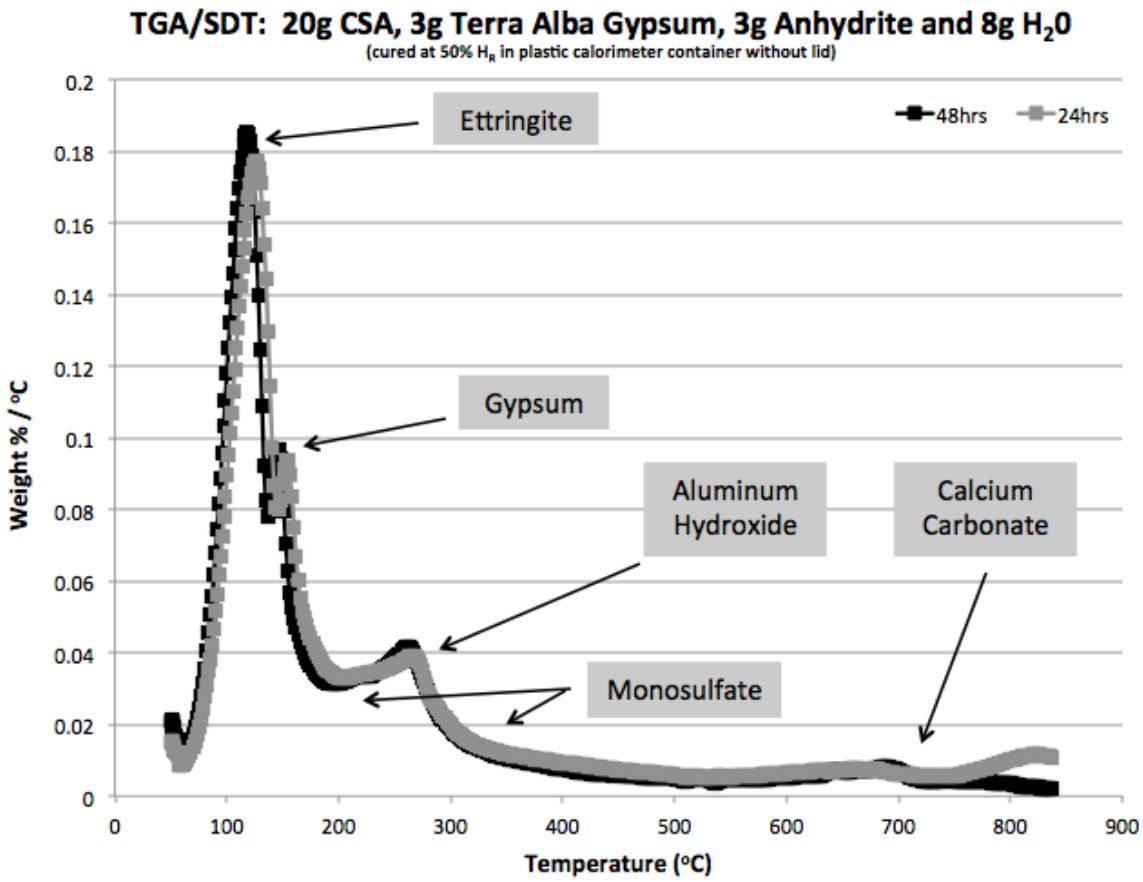

Figure 2.3.1: TGA/SDT analysis of CSA cement paste 10 containing 50 weight % gypsum and 50 weight % anhydrite in Table 2.3 after hydrating for periods of 24 hours and 48 hours at 50% relative humidity and 23°C

Figure 2.3.1 displays TGA/SDT analysis of CSA cement paste 10 containing 50 weight % gypsum and 50 weight % anhydrite in Table 2.3 after hydrating for periods of 24 hours and 48 hours at 50% relative humidity and 23°C. The peaks near 120°C represent the concentration of ettringite as being relatively equal after hydrating for both 24 hours and 48 hours, respectively. The peaks near 150°C represent both sample concentrations of gypsum as being similar. The portion of the curve between 150°C and 200°C suggests a small quantity of monosulfate has been produced relative to ettringite, which is consistent with literature given the experimental molar ratio of yeelimite to calcium sulfate of 0.84

(Winnefeld and Lothenback, 2013). The peaks near 250°C suggest the concentrations of aluminum hydroxide are approximately equal. The peak designations for Figure 2.3.1 are in agreement with literature describing the water associated with ettringite decomposition near 120°C, monosulfate decomposition between 150°C and 200°C, gypsum decomposition near 150°C and aluminum hydroxide decomposition in the vicinity of 250°C (Winnefeld and Barlag, 2010, Winnefeld and Lothenbach, 2010, Sherman et al, 1995, Sato et al, 1992).

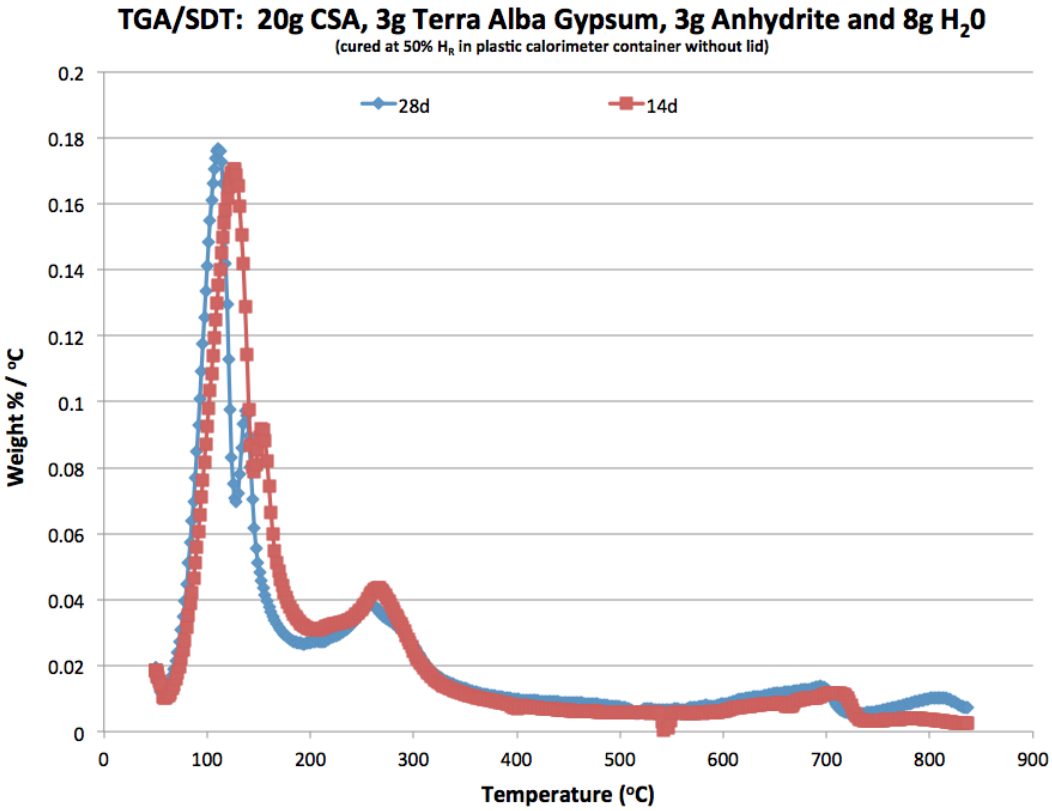

Figure 2.3.2: TGA/SDT analysis of CSA cement paste 10 containing 50 weight % gypsum and 50 weight % anhydrite in Table 2.3 after hydrating for periods of 14 days and 28 days at 50% relative humidity and 23°C

Figure 2.3.2 displays TGA/SDT analysis of CSA cement paste 10 containing 50 weight % gypsum and 50 weight % anhydrite in Table 2.3 after hydrating for periods of 14 days and 28 days at 50% relative humidity and 23°C. The peaks near 120°C represent the concentration of ettringite as being similar after hydrating for both 14 days and 28 days, respectively. The peaks near 150°C represent the concentrations of gypsum as being approximately equal for the sample associated with each hydration period. The portion of the curve between 150 and 200°C suggests the concentrations of monosulfate are similar

for hydration periods of 14 and 28 days. The peaks near 250°C represent the concentrations of aluminum hydroxide as being similar for both hydration periods.

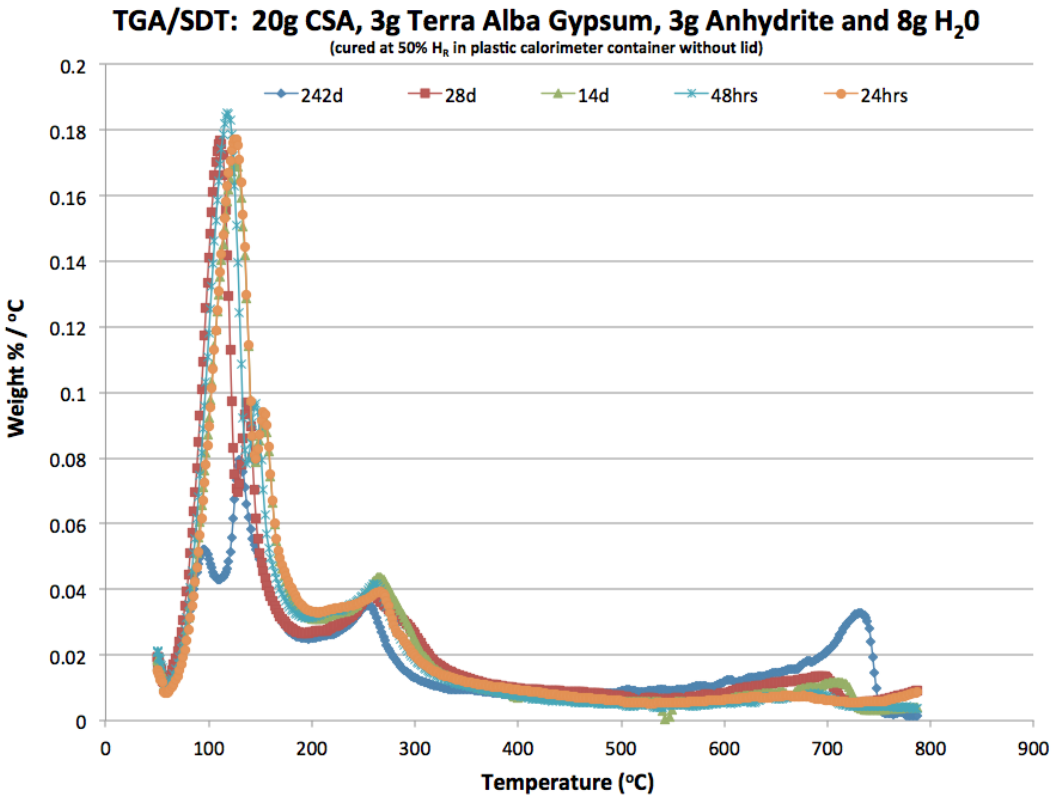

Figure 2.3.3: TGA/SDT analysis of CSA cement paste 10 containing 50 weight % gypsum and 50 weight % anhydrite in Table 2.3 after hydrating for periods of 24 hours, 48 hours, 14 days, 28 days and 242 days at 50% relative humidity and 23°C

Figure 2.3.3 displays TGA/SDT analysis of CSA cement paste 10 containing 50 weight % gypsum and 50 weight % anhydrite in Table 2.3 after hydrating for periods of 24 hours, 48 hours, 14 days, 28 days and 242 days at 50% relative humidity and 23°C. The ettringite concentration remains relatively constant through 28 days before decreasing significantly from 28 days to 242 days. The calcium carbonate concentration increases significantly from 28 days to 242 days. This likely suggests ettringite decomposition by mechanisms associated with either carbonation or dehydration.

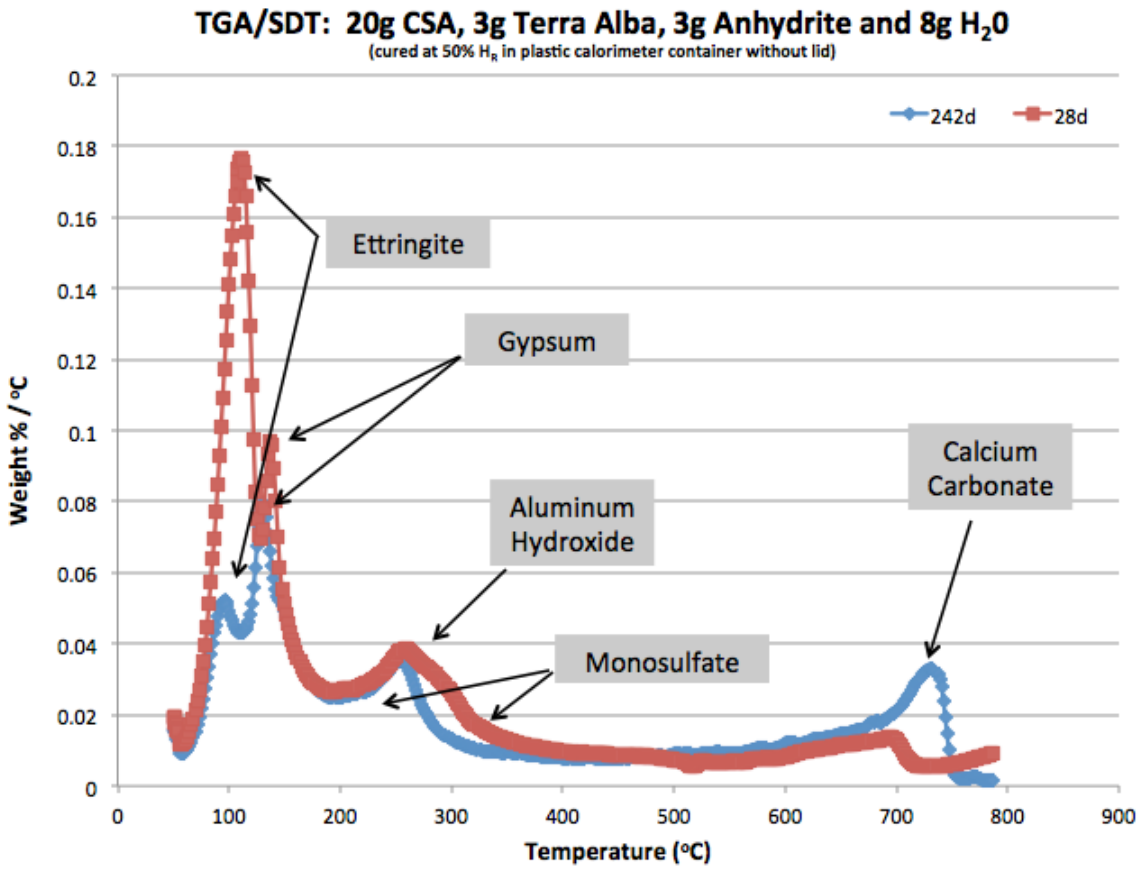

Figure 2.3.4: TGA/SDT analysis of CSA cement paste 10 containing 50 weight % gypsum and 50 weight % anhydrite in Table 2.3 after hydrating for periods of 28 days and 242 days at 50% relative humidity and 23°C

Figure 2.3.4 displays TGA/SDT analysis of CSA cement paste 10 containing 50 weight % gypsum and 50 weight % anhydrite in Table 2.3 after hydrating for periods of 28 days and 242 days at 50% relative humidity and 23°C. The peaks near 120°C suggest the ettringite concentration is greater after hydrating for 28 days at 50% H_R and 23°C with the ettringite concentration decreasing after hydrating for 242 days at 50% H_R and 23°C. The peaks near 150°C suggest the gypsum concentration seems to remain constant after hydrating for both 28 and 242 days at 50% H_R and 23°C. The portion of the curve between 150°C and 200°C suggests the concentrations of monosulfate remain relatively constant for the respective hydration periods. The peaks near 700°C suggest calcium carbonate concentration increases between 28 days and 242 days of hydration at 50% H_R and 23°C potentially suggesting the occurrence of ettringite decomposition.

Table 2.3.1: LISTING OF MATERIALS FROM XRD ANALYSES FOR HYDRATING CSA CEMENT PASTE	
24 hours	Yeelimite > Anhydrite > $Ca_3Al_2O_6$, Ettringite > Belite, alpha Ca_2SiO_4, Gypsum
21 days	Yeelimite > Anhydrite > Brownmillerite, $Ca_3Al_2O_6$ > Ettringite, alpha Ca_2SiO_4 > Belite, Gypsum
28 days	Yeelimite > Anhydrite > Brownmillerite, $Ca_3Al_2O_6$, Ettringite > alpha Ca_2SiO_4, Belite, Gypsum
249 days	Yeelimite > Anhydrite > Gypsum > $Ca_3Al_2O_6$ > Ettringite, Wairakite, Belite, alpha Ca_2SiO_4

Table 2.3.1: Interpretations of XRD diffractograms for the cement paste containing 50 weigth % anhydrite and 50 weight % gypsum in Table 2.3 cured at 23°C and 50% relative humidity

Table 2.3.1 displays XRD characterizations for the cement paste sample containing 50 weight % anhydrite and 50 weigth % gypsum cured at 23°C and 50% relative humidity. It is important to note that quantitative Rietveld analysis was not utilized to arrive at the results displayed in Table 2.3.1. Overall, the information displayed in Table 2.3.1 supports the information presented in Figure 2.3.1 through Figure 2.3.4.

After hydrating for 24 hours, ettringite is present and reactants yeelimite and anhydrite display the greatest concentration of materials. Additionally, the concentration of gypsum is significantly less than the concentration of anhydrite suggesting gypsum is consumed at a more rapid rate during early hydration when compared with anhydrite, which agrees with literature (Pelletier, et al, 2010). XRD does not detect aluminum hydroxide; however, the presence of aluminum hydroxide should not be ruled out as its morphology may be either amorphous or microcrystalline; thus, making it difficult to detect with XRD (Pelletier et al, 2010, Winnefeld and Barlag, 2010, Winnefeld and Lothenbach, 2010). Similarly, XRD does not detect monosulfate as its morphology is likely amorphous also making it difficult to detect (Pelletier et al, 2010, Winnefeld and Barlag, 2010, Winnefeld and Lothenbach, 2010).

After hydrating for 21 days, ettringite continues to display a minor concentration relative to other materials while reactants yeelimite and anhydrite show the greatest material concentrations with concentration of yeelimite being greater than concentration of anhydrite.

After hydrating for 28 days, XRD interpretation indicates the concentration of ettringite has increased relative to yeelimite, anhydrite, belite and gypsum. Continued

hydration of yeelimite and calcium sulfate, likely gypsum, provides one explanation for the shift in ettringite concentration relative to other materials.

After hydrating for 249 days, the material composition of the cement paste sample changed considerably as the concentration of gypsum increased relative to other materials while the concentration of ettringite decreased relative to other materials. Such a change in gypsum concentration relative to other materials suggests decomposition of ettringite occurred between 28 days and 249 days of hydration at 23°C and 50% relative humidity. Ettringite decomposition is described as yielding gypsum, aluminum hydroxide and potentially monosulfate under dry conditions (Sato et al, 1992). Given that both aluminum hydroxide and monosulfate are difficult to detect with XRD, the increased concentration of gypsum relative to other materials is significant and suggests some mechanisms, whether they be associated with either carbonation or dehydration processes, are resulting in decomposition of ettringite.

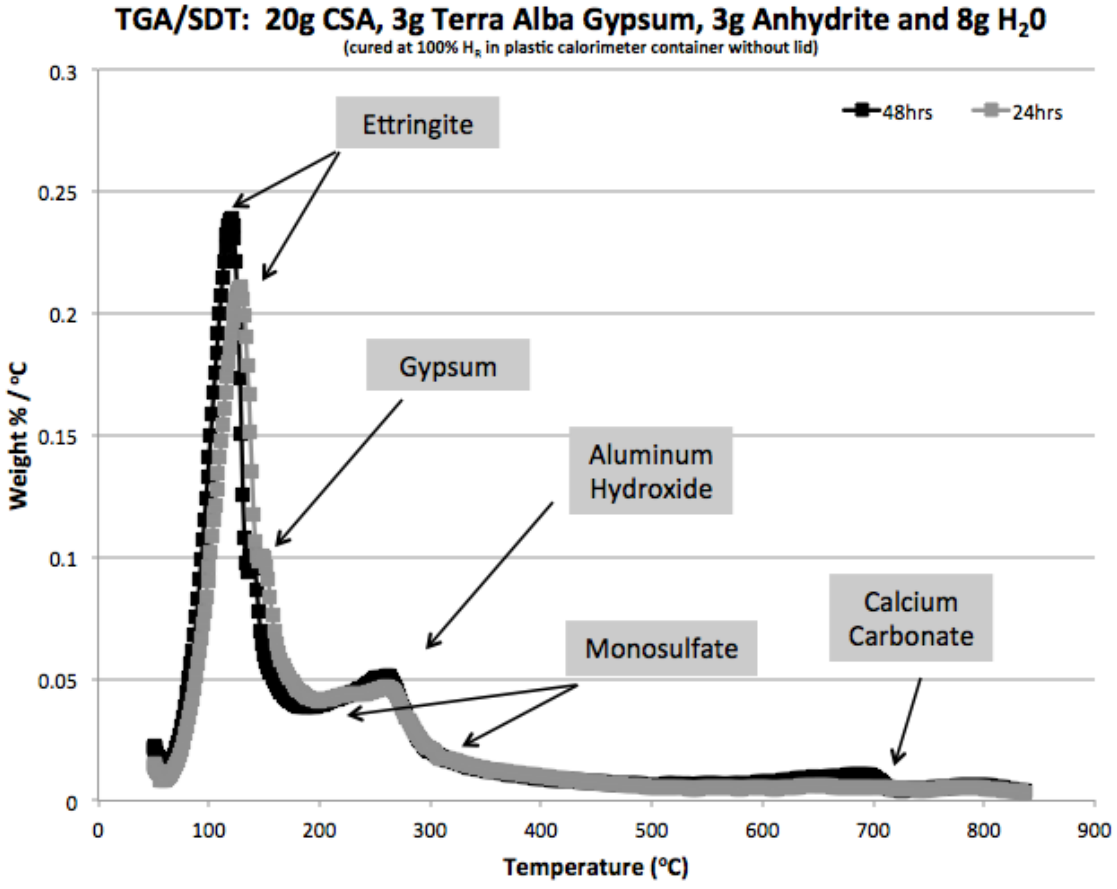

Figure 2.3.5: TGA/SDT analysis of CSA cement paste 3 containing 50 weight % gypsum and 50 weight % anhydrite in Table 2.3 after hydrating for periods of 24 hours and 48 hours at 100% relative humidity and 23°C

Figure 2.3.5 displays TGA/SDT analysis of CSA cement paste 3 containing 50 weight % gypsum and 50 weight % anhydrite in Table 2.3 after hydrating for periods of 24 hours and 48 hours at 100% relative humidity and 23°C. The peaks near 120°C represent the concentration of ettringite as being slightly greater for the later age sample. The peaks near 150°C represent the concentrations of gypsum as being similar for both samples. The portion of the curve between 150°C and 200°C suggests the concentrations of monosulfate are similar for each sample. The peaks near 250°C represent the concentrations of aluminum hydroxide as being approximately equal for both samples. It is quite interesting to note the increased concentrations of ettringite for like samples cured at 100% relative humidity displayed in Figure 2.3.5 compared with identical samples cured at 50% relative humidity displayed in Figure 2.3.1. Such differences illustrate the rapid self-desiccating nature of ettringite formation in CSA cement materials possessing low water / cement ratios while cured in low humidity environments.

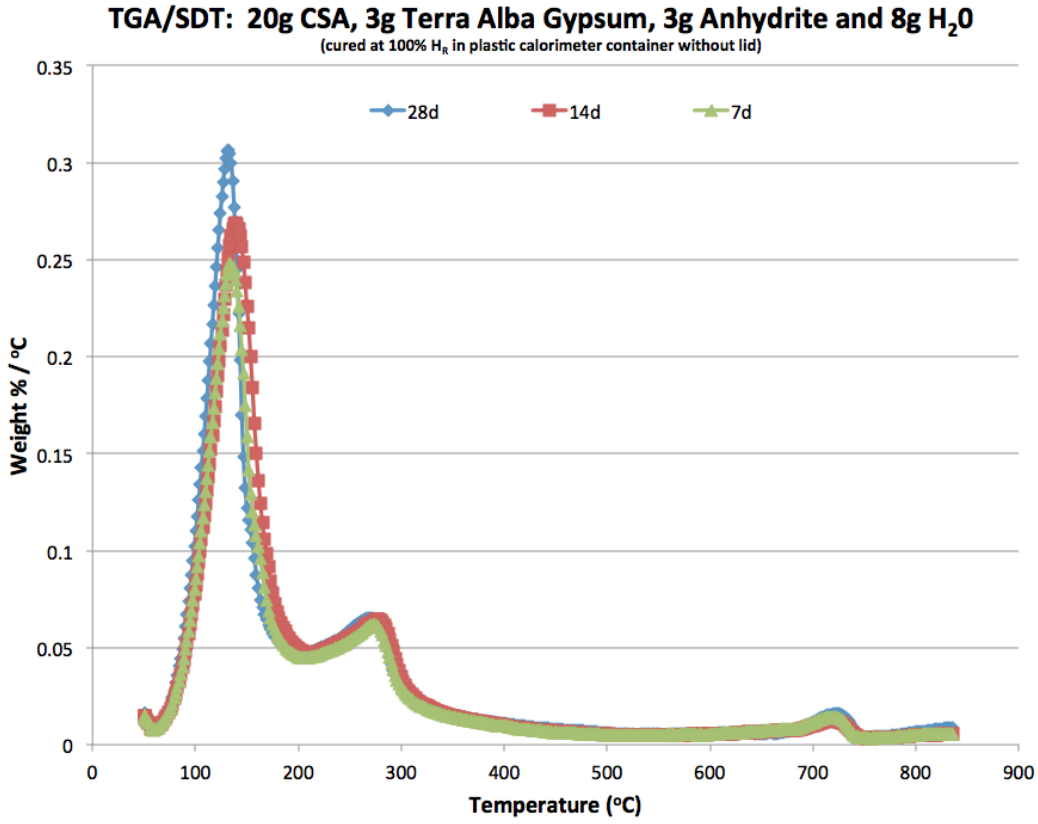

Figure 2.3.6: TGA/SDT analysis of CSA cement paste 3 containing 50 weight % gypsum and 50 weight % anhydrite in Table 2.3 after hydrating for periods of seven days, 14 days and 28 days at 100% relative humidity and 23°C

Figure 2.3.6 displays TGA/SDT analysis of CSA cement paste 3 containing 50 weight % gypsum and 50 weight % anhydrite in Table 2.3 after hydrating for periods of 7 days, 14 days and 28 days at 100% relative humidity and 23°C. The overall trend for ettringite concentration increases with increases in hydration time. It is quite interesting to note the peaks near 150°C have disappeared suggesting that gypsum has been consumed somewhere between 48 hours and 7 days of curing at constant 100% relative humidity and 23°C. The portion of the curve between 150°C and 200°C representing monosulfate remains constant for hydration periods of 7, 14 and 28 days suggesting ettringite is the primary hydration product for the CSA cement paste containing half anhydrite and half gypsum as a combined source of calcium sulfate possessing a molar ratio of yeelimite to calcium sulfate of 0.84, which agrees with literature (Winnefeld and Lothenback, 2013, Winnefeld and Lothenbach, 2010, Winnefeld and Barlag, 2010). The peaks near 250°C suggest the aluminum hydroxide concentrations remain somewhat constant for the displayed hydration periods.

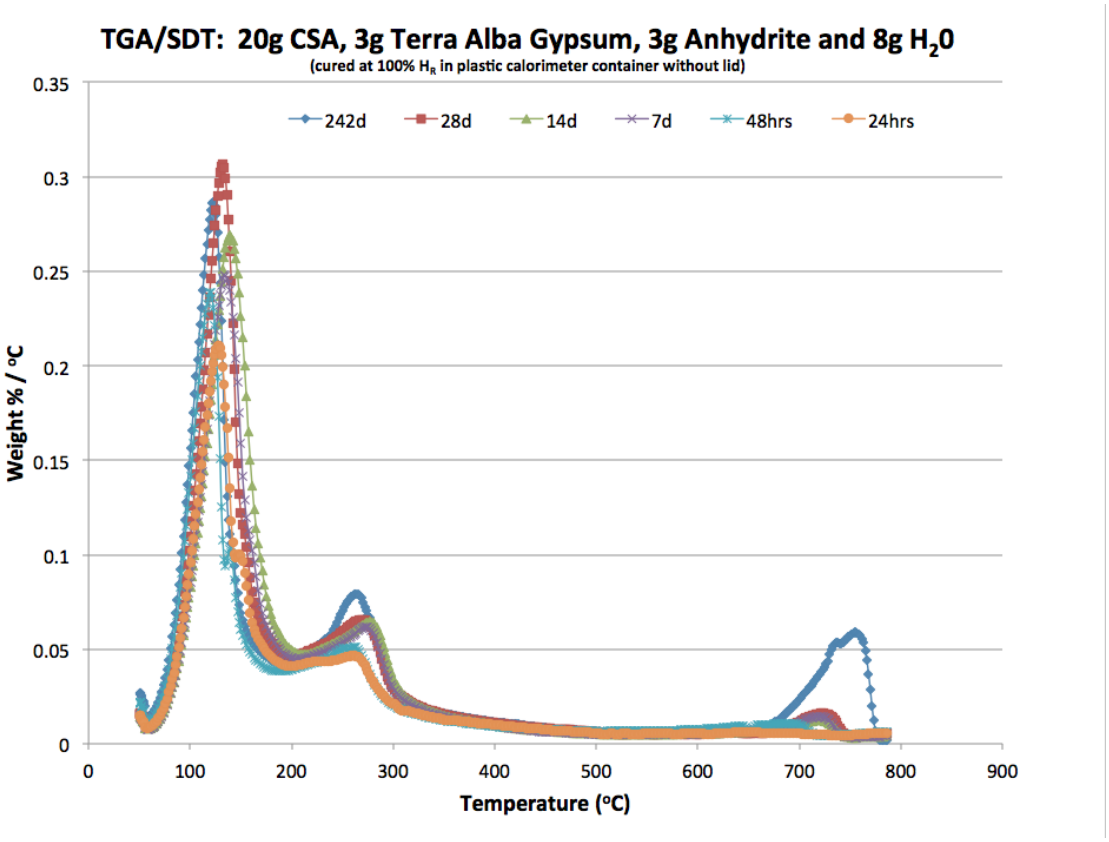

Figure 2.3.7: TGA/SDT analysis of CSA cement paste 3 containing 50 weight % gypsum and 50 weight % anhydrite in Table 2.3 after hydrating for periods of 24 hours, 48 hours, 7 days, 14 days, 28 days and 242 days at 100% relative humidity and 23°C

Figure 2.3.7 displays TGA/SDT analysis of CSA cement paste 3 containing 50 weight % gypsum and 50 weight % anhydrite in Table 2.3 after hydrating for periods of 24 hours, 48 hours, 7 days, 14 days, 28 days and 242 days at 100% relative humidity and 23°C. The curves suggest the concentration of ettringite increases through 28 days of hydration and subsequently remains relatively constant between 28 days and 242 days of hydration. The portion of the curves between 150°C and 200°C suggest the concentrations of monosulfate remain relatively constant throughout the duration of the experiment. The peaks near 250°C suggest the aluminum hydroxide concentration appears to increase slightly between 28 days and 242 days hydration at 100% H_R and 23°C. The peak near 700°C suggests the calcium carbonate concentration appears to increase between 28 days and 242 days hydration at 100% H_R and 23°C. Such an increase in calcium carbonate concentration coupled with a slight decrease in ettringite concentration suggests ettringite decomposition via carbonation for the cement paste containing solely gypsum cured at constant 100% relative humidity and 23°C. It is unlikely the ettringite decomposition is due to dehydration, as these samples were cured at constant 100% relative humidity and 23°C.

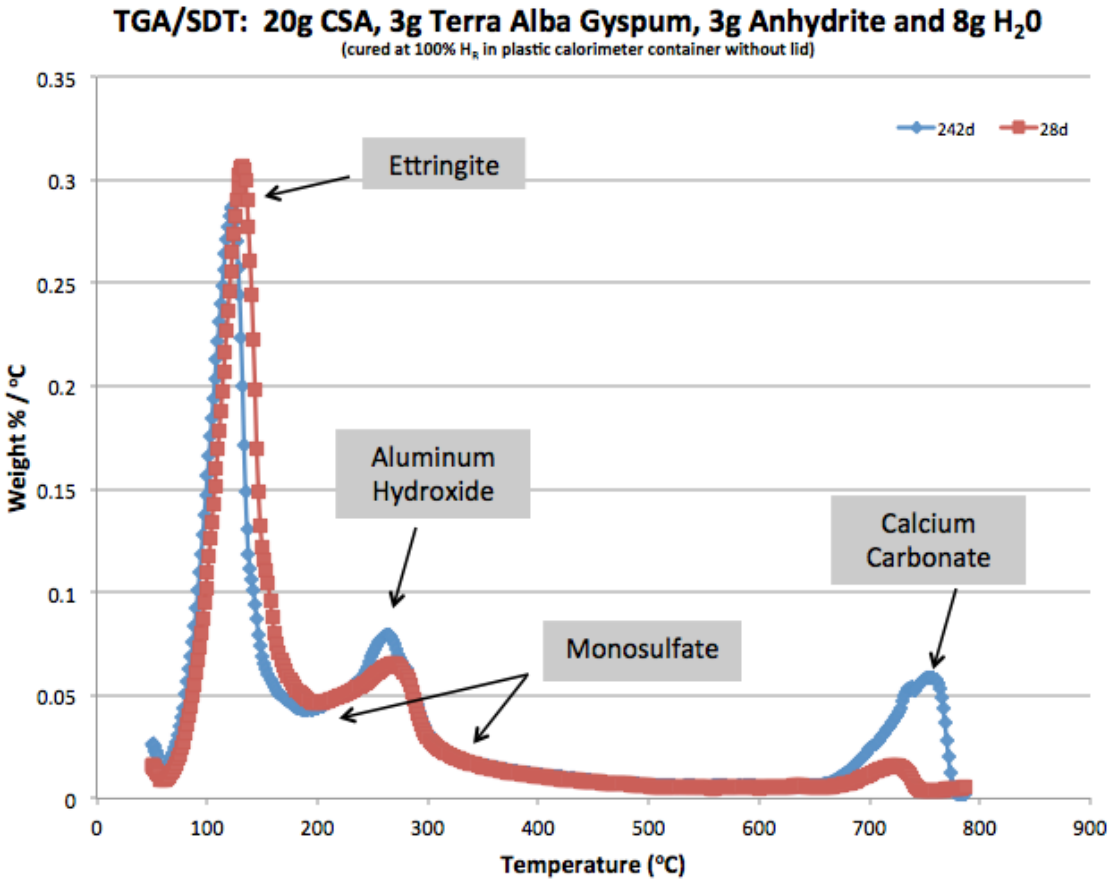

Figure 2.3.8: TGA/SDT analysis of CSA cement paste 3 containing 50 weight % gypsum and 50 weight % anhydrite in Table 2.3 after hydrating for periods of 28 days and 242 days at 100% relative humidity and 23°C

Figure 2.3.8 displays TGA/SDT analysis of CSA cement paste 3 containing 50 weight % gypsum and 50 weight % anhydrite in Table 2.3 after hydrating for periods of 28 days and 242 days at 100% relative humidity and 23°C. As seen in Figure 2.3.8, the peaks near 120°C display a slight decrease in ettringite concentration between hydration periods of 28 days and 242 days, respectively. Figure 2.3.8 displays a slight increase in aluminum hydroxide concentration for the sample cured for 242 days. In addition, Figure 2.3.8 displays an increase in calcium carbonate concentration for the sample cured for 242 days when compared with the sample cured for 28 days. The slight decrease in ettringite concentration together with the increase in calcium carbonate concentration suggests ettringite decomposition is related to carbonation type mechanisms for the hydration period between 28 days and 242 days at constant 100% relative humidity and 23°C.

Table 2.3.2: LISTING OF MATERIALS FROM XRD ANALYSES FOR HYDRATING CSA CEMENT PASTE	
24 hours	Yeelimite > Anhydrite > Ettringite, $Ca_3Al_2O_6$, > alpha Ca_2SiO_4, Belite > Gypsum
21 days	Yeelimite > Anhydrite, Ettringite > $Ca_3Al_2O_6$, alpha Ca_2SiO_4, Brownmillerite > Belite > Gypsum
28 days	Yeelimite > Anhydrite, Ettringite > $Ca_3Al_2O_6$, alpha Ca_2SiO_4, Brownmillerite > Belite > Gypsum
242 days	Ettringite >Yeelimite > Anhydrite > Brownmillerite, alpha Ca_2SiO_4, $Ca_3Al_2O_6$, Calcite > Wairakite, Belite, Gypsum

Table 2.3.2: Interpretations of XRD diffractograms for the cement paste containing 50 weight % anhydrite and 50 weight % gypsum in Table 2.3 cured at 23°C and 100% relative humidity

Table 2.3.2 displays XRD characterizations for the cement paste sample containing 50 weight % anhydrite and 50 weigth % gypsum as a combined source of calcium sulfate when cured at 23°C and 100% relative humidity for the duration of the experiment. As with other XRD related information, it is important to note that quantitative Rietveld analysis was not utilized to arrive at the results displayed in Table 2.3.2. Overall, the information displayed in Table 2.3.2 supports the information presented in Figures 2.3.5 through 2.3.8. However, the later age TGA/SDT curves suggest gypsum has been completely consumed; whereas, XRD identifies gypsum as being present as a minor concentration in relation to other constituent materials throughout the course of the experiment.

After 24 hours of hydration at 100% relative humidity, ettringite is present and reactants yeelimite and anhydrite display the greatest concentration of materials. As with the like sample cured at constant 50% relative humidity, XRD indicates consumption of gypsum was preferred when compared with anhydrite during early hydration. The thermodynamic properties and behaviors associated with common ions in solution reported for the various forms of calcium sulfate support the experimental findings (Scrivener and Nonat, 2011, Taylor 1997, Perry and Green, 1997, Smith et al, 1996). XRD does not detect aluminum hydroxide; however, the presence of aluminum hydroxide should not be ruled out as its morphology may be either amorphous or microcrystalline; thus, making it difficult to detect with XRD (Pelletier et al, 2010, Winnefeld and Barlag, 2010, Winnefeld and Lothenbach, 2010). Similarly, XRD does not detect monosulfate as its

morphology is likely amorphous also making it difficult to detect (Pelletier et al, 2010, Winnefeld and Barlag, 2010, Winnefeld and Lothenbach, 2010).

After hydrating for 21 days, concentration of ettringite has increased relative to other constituent materials, while the reactant yeelimite maintains the greatest concentration among the various constituents. Given the 100% humidity environment, water is no longer a limiting reagent, and the hydration reactions can proceed until another limiting factor is encountered. Essentially no significant differences exist for microstructural constituent materials between 21 days and 28 days of hydration.

After hydrating for 242 days, the material composition of the cement paste sample changed considerably as the concentration of ettringite significantly increased in relation to other constituent materials. Such an increase in ettringite concentration strongly suggests continuation of hydration reactions between 28 days and 242 days of hydration at 23^{o}C and 100% relative humidity, which is quite conceivable as all reactants were available. Additionally, the presence of calcite at 242 days suggests previously formed ettringite decomposed to gypsum and calcium carbonate while new ettringite was being formed from continued hydration.

2.4: Anhydrite as a source of calcium sulfate with VAE dispersible polymer powder with T_g = -7°C

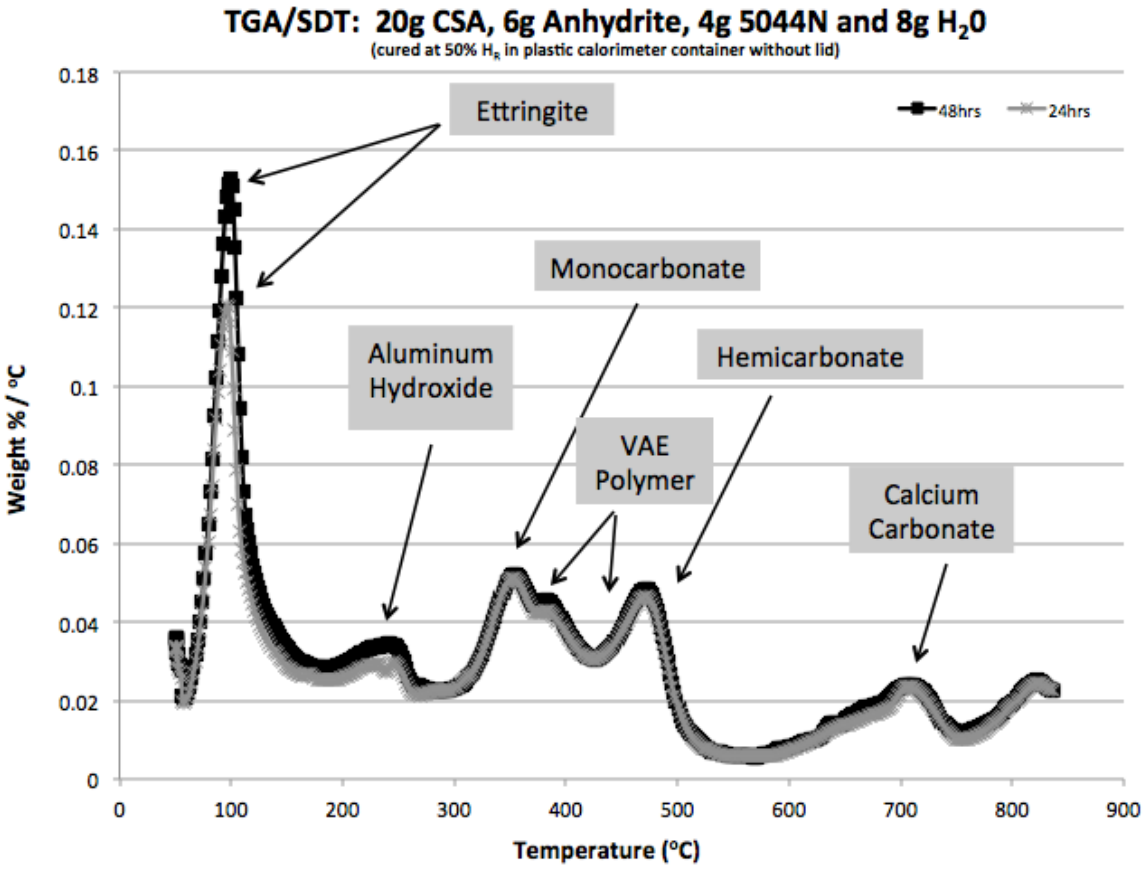

Figure 2.4.1: TGA/SDT analysis of CSA cement paste 9 containing anhydrite and VAE dispersible polymer powder with T_g = -7°C in Table 2.3 after hydrating for periods of 24 hours and 48 hours at 50% relative humidity and 23°C

Figure 2.4.1 displays TGA/SDT analysis of CSA cement paste 9 containing anhydrite and VAE dispersible polymer powder with T_g = -7°C in Table 2.3 after hydrating for periods of 24 hours and 48 hours at 50% relative humidity and 23°C. The peaks near 120°C suggest the concentration of ettringite increases with increases in hydration time. The portions of the curve between 300°C and 350°C together with the range from 450°C to 500°C are theorized to be associated with either hemicarbonate or perhaps monocarbonate for this CSA cement paste incorporating vinyl acetate / ethylene dispersible polymer powder (VAE DPP) which is known to contain approximately 12% calcium carbonate by total dry mass.

Literature is not so clear of the timing associated with the emergence of monocarbonate in various cementitious systems, including those containing yeelimite, calcium sulfate and calcium carbonate, as the emergence of such hydrated assemblages is quite dependent on amount and type of calcium sulfate and other associated admixtures (Winnefeld and Lothenbach, 2013, Pelletier-Changnat et al, 2012, Chowaniec, 2012, Gameiro et al, 2012, Gabrovsek et al, 2008). The peaks near 250°C and 300°C are theorized to be representative of aluminum hydroxide concentration (Candela et al., 1986, Sato, 1985). Aluminum hydroxide is often referred to as either hydrargillite (γ-$Al(OH)_3$) or bayerite (α-$Al(OH_3)$. Additionally, both hydrargillite and bayerite can be further classified as types I and II with different shape thermal decomposition curves, each with peaks between 200°C and 300°C (Sato, 1985). Some of the peaks from 300 to 500°C may represent the polymer concentration. Literature reports VAE polymers usually decompose by a two step mechanism, with the loss of acetic acid during the first step (300-350°C), resulting in the formation of unsaturated polyenes, while the second decomposition step involves random chain scission of the remaining material, forming unsaturated vapor species (~430°C), such as butene and ethylene (Hull et al, 2003). Similarly, Maurin et al, (1991), report the heating of vinyl acetate / ethylene copolymers results in a two step thermal decomposition in the ranges from 360 to 450°C and 450 to 550°C (Maurin et al, 1991).

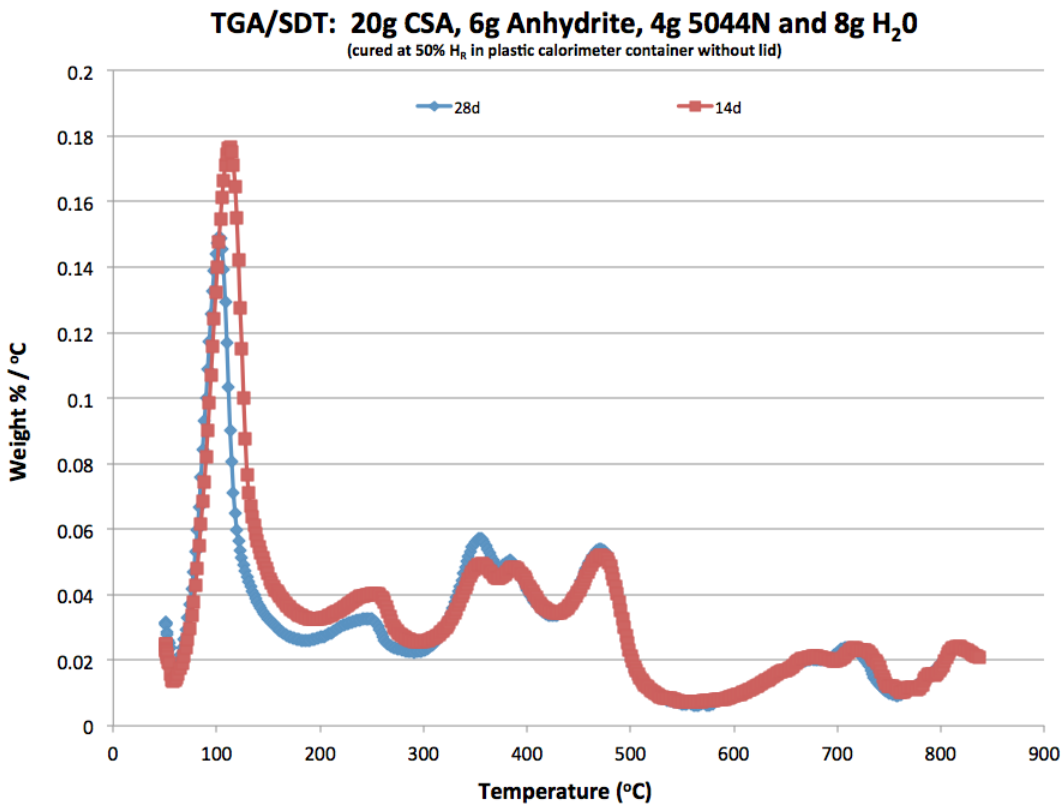

Figure 2.4.2: TGA/SDT analysis of CSA cement paste 9 containing anhydrite and VAE dispersible polymer powder with T_g = -7°C in Table 2.3 after hydrating for periods of 14 days and 28 days at 50% relative humidity and 23°C

Figure 2.4.2 displays TGA/SDT analysis of CSA cement paste 9 containing anhydrite and VAE dispersible polymer powder with T_g = -7°C in Table 2.3 after hydrating for periods of 14 days and 28 days at 50% relative humidity and 23°C. The peaks near 120°C suggest the concentration of ettringite decreased between 14 days and 28 days of hydration. The peaks near 250°C represent the aluminum hydroxide concentrations as being approximately equal for both samples. As previously mentioned, the peaks from 300 to 500°C represent the polymer concentration through a two stage decomposition process with the first stage taking place in the interval from 300 to 350°C and the second stage taking place in the interval from 350 to 500°C (Hull et al, 2003). Additionally, the peak near 450°C likely represents hemicarbonate as described by literature (Winnefeld and Lothenbach, 2013, Chowaniec, 2012).

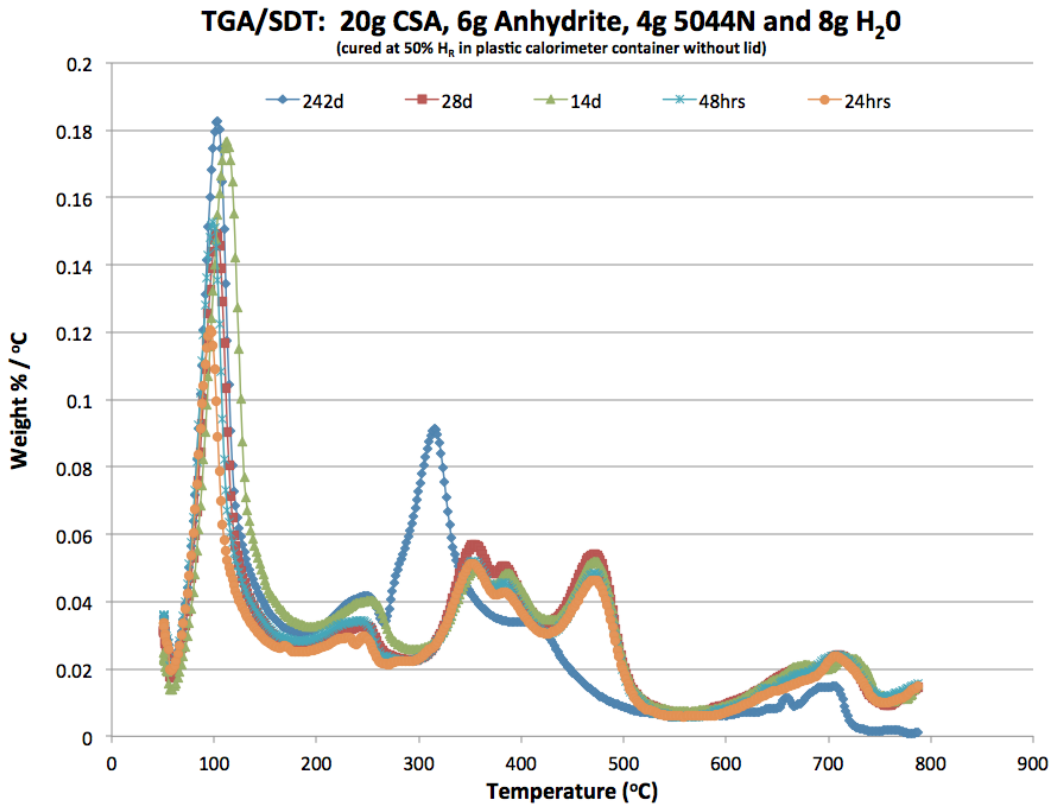

Figure 2.4.3: TGA/SDT analysis of CSA cement paste 9 containing anhydrite and VAE dispersible polymer powder with T_g = -7°C in Table 2.3 after hydrating for periods of 24 hours, 48 hours, 14 days, 28 days and 242 days at 50% relative humidity and 23°C

Figure 2.4.3 displays TGA/SDT analysis of CSA cement paste 9 containing anhydrite and VAE dispersible polymer powder with T_g = -7°C in Table 2.3 after hydrating for periods of 24 hours, 48 hours, 14 days, 28 days and 242 days at 50% relative humidity and 23°C. The interesting aspects of Figure 2.4.3 are the differences in peaks between 200 and 700°C for early and later age samples. The peaks located near 120°C represent the aggregate ettringite concentration as continually increasing for the duration of the experiment. There is no significant decrease in ettringite concentration from 28 days to 242 days of hydration at constant 50% relative humidity and 23°C. The other changes are discussed in the following paragraphs.

A new peak seems to have emerged near 300°C for the polymer modified CSA cement paste containing anhydrite as a source of calcium sulfate displayed in Table 2.3 after hydrating for 242 days at constant 50% relative humidity and 23°C. Before labeling this peak, it is important to note VAE DPP includes anti-caking agents added during production, often in the range of 10 to 15 percent by mass of the final product. Examples of typical anti-

caking agents are calcium carbonate and kaolin clay. Winnefeld and Lothenbach, (2013), report the ternary system, yeelimite, calcium sulfate, calcium carbonate has potential to form either hemicarbonate or monocarbonate in addition to the primary hydration assemblages ettringite, monosulfate and aluminum hydroxide (Winnefeld and Lothenbach, 2013). Furthermore, the authors suggest hemi-carbonate may initially form and coexist for some period of time, likely due to slow formation kinetics of moncarbonate as observed in ordinary portland cement, before reacting with yeelimite and calcite to form either ettringite or monocarbonate (Winnefeld and Lothenbach, 2013). Additionally, literature reports for CSA cements containing accessory phases, C-S-H, $C_2A\bar{S}H_8$ or calcium aluminate hydrates, mainly CAH_{10} or C_4AH_{13}, can be formed in addition to the aforementioned primary hydration assemblages (Pelletier-Chaignat et al, 2012). Before labeling the new late age peak at 300°C, consideration should also be given to reports stating for CSA cement containing belite as a constituent, belite reacts slower than yeelimite forming stratlingite at later ages (Romain et al, 2013). It is well known metastable aluminate hydrates, with examples being CAH_{10},C_4AH_{13} or $C_2A\bar{S}H_8$ may convert to C_3AH_6, hydrogarnet, at later ages (Taylor, 1997). Literature reports thermal decomposition characteristics of monocarbonate, gamma aluminum hydroxide and hydrogarnet possessing similar peaks near 300°C (Chowaniec, 2012, Gameiro et al, 2012, Gabrovsek et al, 2008, Scrivener and Capmas, 1998, Taylor, 1997). The size of the new peak at 300°C is also important for purposes of determination, as it displays a significant concentration relative to other materials. Given this information, the author theorizes the new peak near 300°C is associated with monocarbonate. The theory is further supported by the peaks near 450°C for the early age samples, likely hemicarbonate, which are not visible with analysis of the later age sample. The presence of hemicarbonate at early ages of hydration suggests the polymer modified CSA cement paste containing minor amounts of calcium carbonate hydrated to form ettringite, aluminum hydroxide, hemicarbonate and possibly monosulfate during the early ages, where the hemicarbonate converted to monocarbonate at later ages, which agrees with literature (Winnefeld and Lothenbach, 2013). In further support, Chowaniec, (2012), displays thermogravimetric analysis (TGA) charts for decomposition of both hemicarbonate and monocarbonate where the peak near 450°C is noted as a means for differentiating hemicarbonate from monocarbonate, as the peak does not appear during thermogravimetric analysis of monocarbonate.

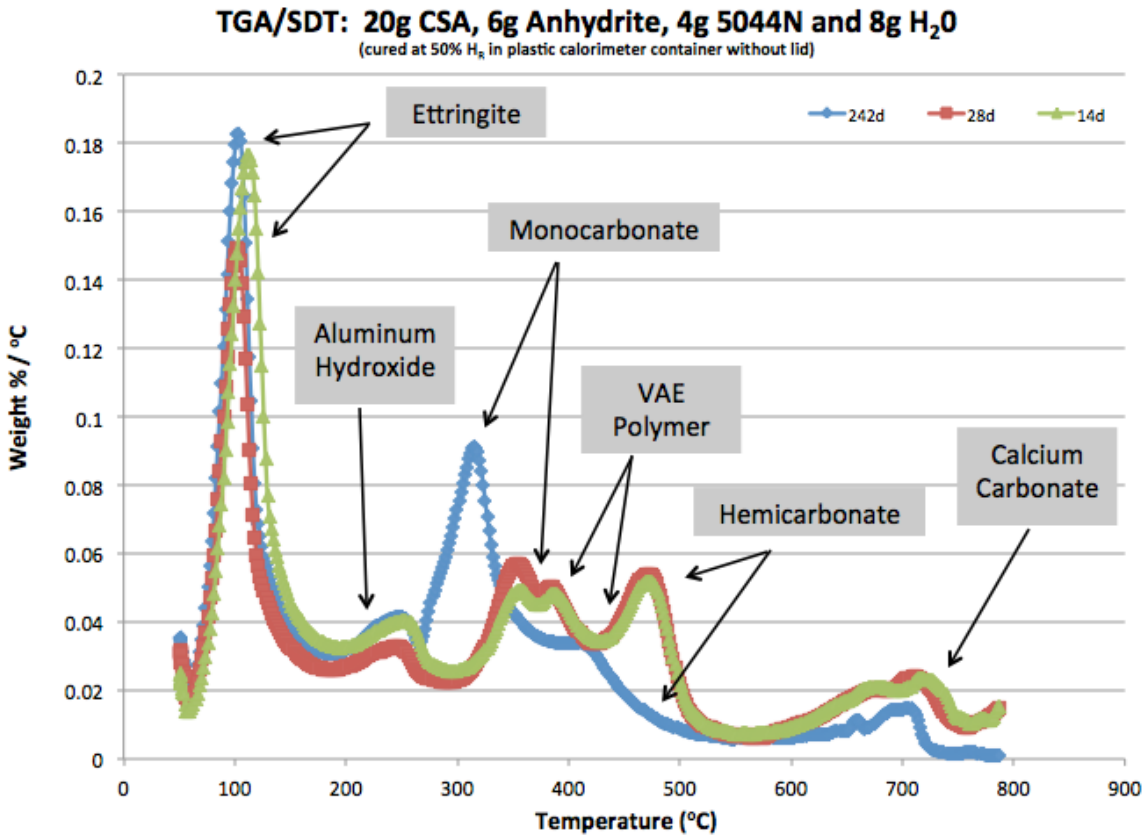

Figure 2.4.4: TGA/SDT analysis of CSA cement paste 9 containing anhydrite and VAE dispersible polymer powder with T_g = -7°C in Table 2.3 after hydrating for periods of 14 days, 28 days and 242 days at 50% relative humidity and 23°C

Figure 2.4.4 displays TGA/SDT analysis of CSA cement paste 9 containing anhydrite and VAE dispersible polymer powder with T_g = -7°C in Table 2.3 after hydrating for periods of 14 days, 28 days and 242 days at 50% relative humidity and 23°C. It is quite interesting to note the ettringite concentration seems to decrease from 14 days to 28 days while subsequently increasing from 28 days to 242 days of hydration. One potential explanation is the author had a broken wrist that hindered sample collection which required breaking chunks off of the larger CSA cement paste sample with a hammer; so, the thought of a more exposed sample, which is easier to gather with a broken wrist, is plausible. For example, a few surface chunks were chipped off the sample and ground with mortar and pestle for the 28 days sample. Nevertheless, it is also interesting to note the ettringite concentration is within the same range for the samples cured for 14 days and 242 days at constant 50% relative humidity.

Table 2.4.1: LISTING OF MATERIALS FROM XRD ANALYSES FOR HYDRATING CSA CEMENT PASTE	
24 hours	Yeelimite > Anhydrite > $Ca_3Al_2O_6$, Ettringite, alpha Ca_2SiO_4 > Belite
21 days	Yeelimite > Anhydrite > Brownmillerite, Ettringite, $Ca_3Al_2O_6$, alpha Ca_2SiO_4, Belite > trace of calcite
28 days	Yeelimite > Anhydrite > Brownmillerite, $Ca_3Al_2O_6$, Ettringite, alpha Ca_2SiO_4, Belite > trace of calcite
242 days	Yeelimite > Anhydrite > Ettringite > Brownmillerite, $Ca_3Al_2O_6$

Table 2.4.1: Interpretations of XRD diffractograms for the cement paste containing anhydrite and VAE DPP with T_g = -7°C cured at 23°C and 50% relative humidity.

Table 2.4.1 displays XRD characterizations for the cement paste sample containing anhydrite and VAE DPP with T_g = -7°C cured at 23°C and 50% relative humidity. The information displayed in Table 2.4.1 supports the information displayed in Figures 2.4.1 through 2.4.4. That is, after 24 hours of hydration, ettringite is present and reactants yeelimite and anhydrite display the greatest concentration of materials. After hydrating for 21 days, ettringite continues to display a minor concentration relative to other materials while reactants yeelimite and anhydrite show the greatest material concentrations with concentration of yeelimite being greater than the concentration of anhydrite. Essentially no significant differences exist for microstructural constituent materials between 21 days and 28 days of hydration. After hydrating for 242 days, the material composition of the cement paste sample changed somewhat as alpha Ca_2SiO_4, belite and a trace of calcite were consumed and ultimately disappeared from the characterization. Neither hemicarbonate nor monocarbonate were detected by XRD analysis. The author theorizes the yeelimite – calcium carbonate – calcium sulfate system hydrated to first form ettringite, aluminum hydroxide and hemicarbonate, with the hemicarbonate subsequently converting to monocarbonate at later ages. The disappearance of calcite at later ages supports the theory. Additionally, belite likely hydrated to form AFm type phases between 28 days and 242 days of hydration.

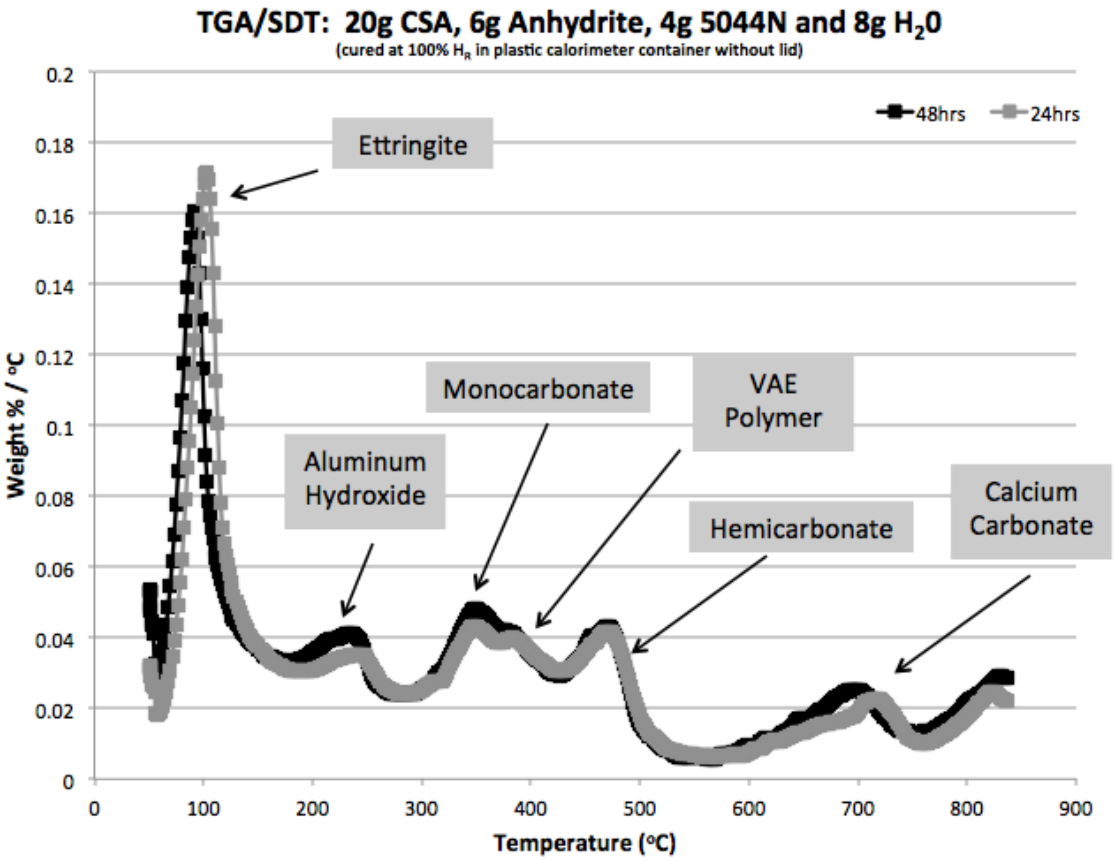

Figure 2.4.5: TGA/SDT analysis of CSA cement paste 5 containing anhydrite and VAE dispersible polymer powder with T_g = -7°C in Table 2.3 after hydrating for periods of 24 hours and 48 hours at 100% relative humidity and 23°C

Figure 2.4.5 displays TGA/SDT analysis of CSA cement paste 5 containing anhydrite and VAE dispersible polymer powder with T_g = -7°C in Table 2.3 after hydrating for periods of 24 hours and 48 hours at 100% relative humidity and 23°C. The peaks near 120°C suggest the concentration of ettringite increases with increases in hydration time. The portion of the curve between 150°C and 200°C is theorized to be associated with either hemicarbonate or perhaps monocarbonate for this CSA cement paste incorporating VAE DPP which is known to contain approximately 12% calcium carbonate by total dry mass. Literature is not so clear of the timing associated with the emergence of monocarbonate in various cementitious systems, including those containing yeelimite, calcium sulfate and calcium carbonate, as the emergence of such hydrated assemblages is quite dependent on amount and type of calcium sulfate and other associated admixtures (Winnefeld and Lothenbach, 2013, Pelletier-Changnat et al, 2012, Chowaniec, 2012, Gameiro et al, 2012, Gabrovsek et al, 2008). The peaks near 250°C and 300°C are theorized to be representative

of aluminum hydroxide concentration (Candela et al., 1986, Sato, 1985). Aluminum hydroxide is often referred to as either hydrargillite (γ-$Al(OH)_3$) or bayerite (α-$Al(OH_3)$. Additionally, both hydrargillite and bayerite can be further classified as types I and II with different shape thermal decomposition curves, each with peaks between 200°C and 300°C (Sato, 1985). Some of the peaks from 300 to 500°C represent the polymer concentration. VAE polymers usually decompose by a two step mechanism, with the loss of acetic acid during the first step (300-350°C), resulting in the formation of unsaturated polyenes, while the second decomposition step involves random chain scission of the remaining material, forming unsaturated vapor species (~430°C), such as butene and ethylene (Hull et al, 2003). Similarly, Maurin et al, (1991), report the heating of vinyl acetate / ethylene copolymers results in a two step thermal decomposition in the ranges from 360 to 450°C and 450 to 550°C (Maurin et al, 1991). Additionally, the peaks near 450°C likely represent hemicarbonate as described by literature (Winnefeld and Lothenbach, 2013, Chowaniec, 2012).

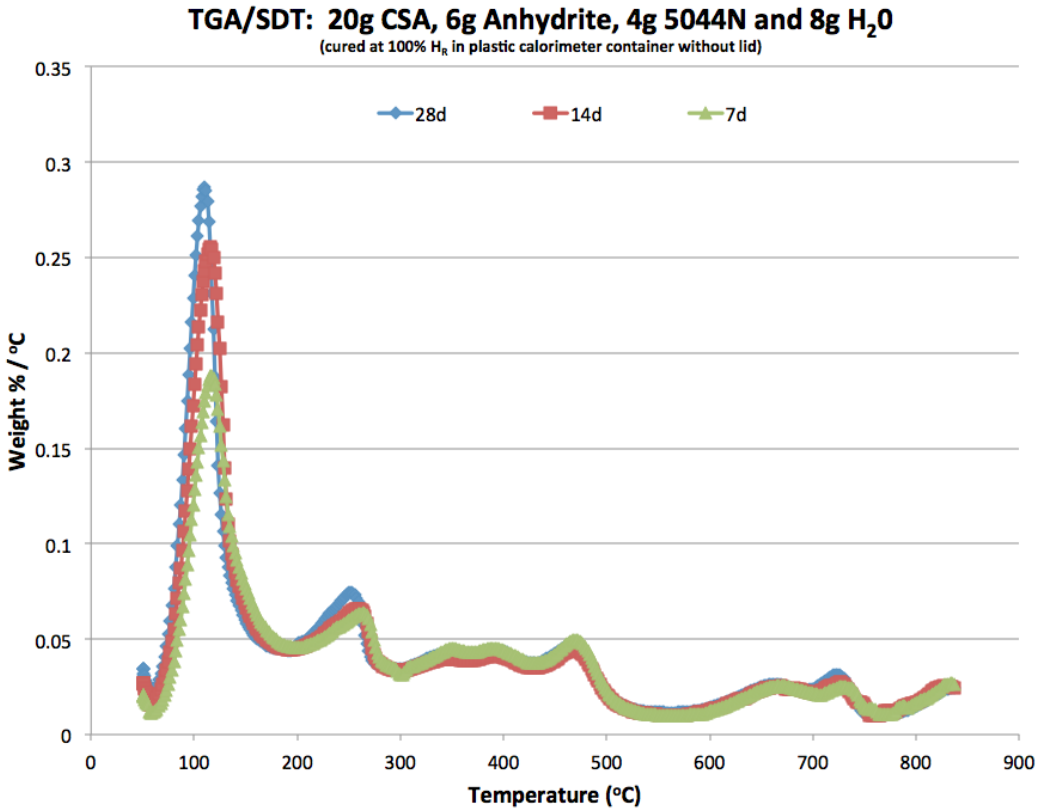

Figure 2.4.6: TGA/SDT analysis of CSA cement paste 5 containing anhydrite and VAE dispersible polymer powder with T_g = -7°C in Table 2.3 after hydrating for periods of seven days, 14 days and 28 days at 100% relative humidity and 23°C

Figure 2.4.6 displays TGA/SDT analysis of CSA cement paste 5 containing anhydrite and VAE dispersible polymer powder with T_g = -7°C in Table 2.3 after hydrating for periods of seven days, 14 days and 28 days at 100% relative humidity and 23°C. The peaks near 120°C suggest concentrations of ettringite continually increase for hydration periods of 7 days, 14 days and 28 days, respectively. The peaks near 250°C suggest a slight increase in aluminum hydroxide concentration between 14 days and 28 days of hydration.

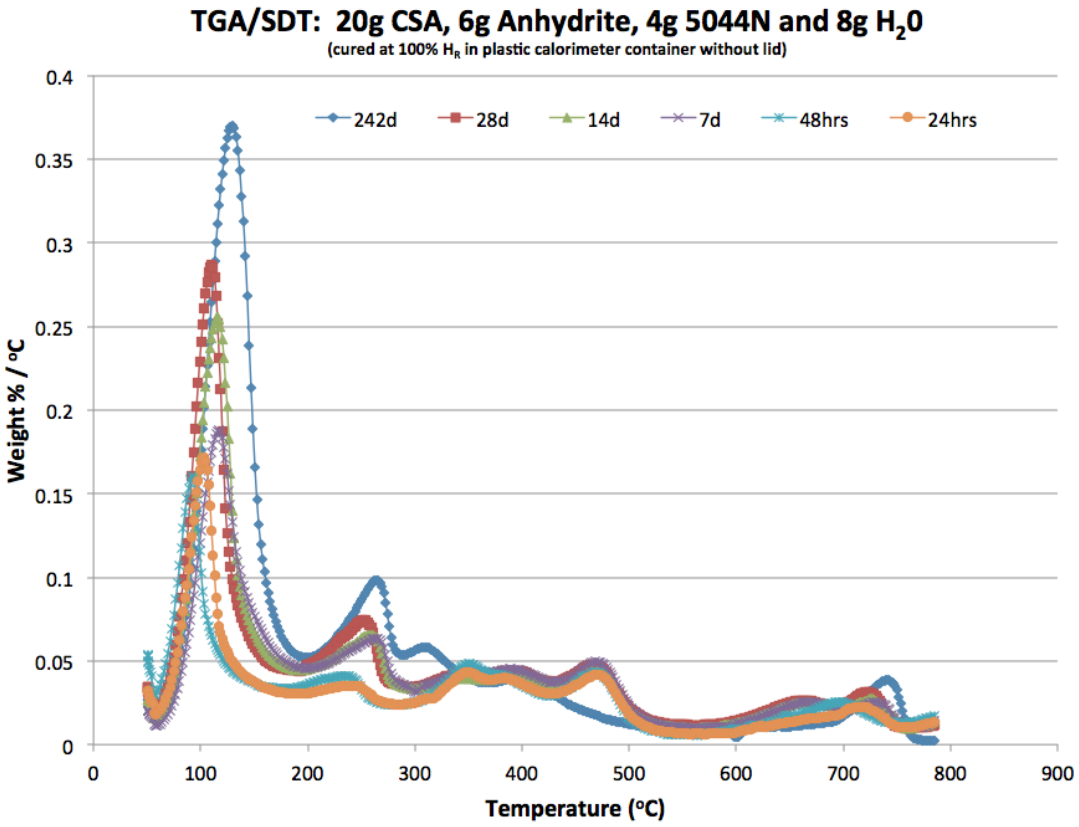

Figure 2.4.7: TGA/SDT analysis of CSA cement paste 5 containing anhydrite and VAE dispersible polymer powder with T_g = -7°C in Table 2.3 after hydrating for periods of 24 hours, 48 hours, 7 days, 14 days, 28 days and 242 days at 100% relative humidity and 23°C

Figure 2.4.7 displays TGA/SDT analysis of CSA cement paste 5 containing anhydrite and VAE dispersible polymer powder with T_g = -7°C in Table 2.3 after hydrating for periods of 24 hours, 48 hours, 7 days, 14 days, 28 days and 242 days at 100% relative humidity and 23°C. The peaks near 120°C display an overall increasing trend of ettringite concentration versus time. The ettringite concentration for polymer modified CSA cement paste 5 in Table 2.3 after hydrating for 242 days at constant 100% relative humidity and 23°C appears to be

some 2x the magnitude associated with the ettringite concentration displayed in Figure 2.4.4 for an identical polymer modified CSA cement paste cured at constant 50% relative humidity and 23°C. Such a comparison strongly suggests yeelimite and anhydrite continue hydration to form ettringite in polymer modified CSA cement materials so long as all primary reactant materials are available in sufficient quantity. Additionally, the peak near 450°C, likely associated with hemicarbonate, decreases while the peak near 300°C theorized to be monocarbonate increases between 28 and 242 days of hydration at 100% relative humidity.

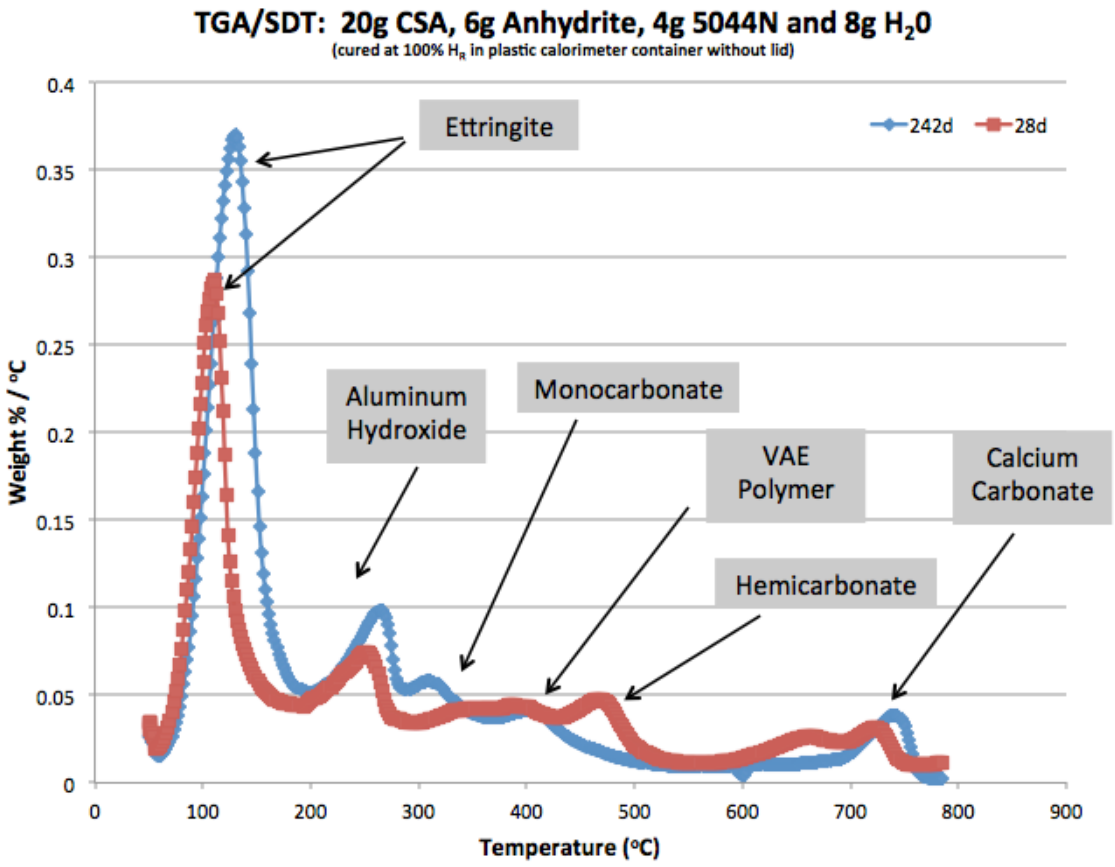

Figure 2.4.8: TGA/SDT analysis of CSA cement paste 5 containing anhydrite and VAE dispersible polymer powder with T_g = -7°C in Table 2.3 after hydrating for periods of 28 days and 242 days at 100% relative humidity and 23°C

Figure 2.4.8 displays TGA/SDT analysis of CSA cement paste 5 containing anhydrite and VAE dispersible polymer powder with T_g = -7°C in Table 2.3 after hydrating for periods of 28 days and 242 days at 100% relative humidity and 23°C. Noteworthy in Figure 2.4.8 is the significant decrease in ettringite concentration near 120°C, the significant increase in

aluminum hydroxide concentration near 250°C and the decrease in hemicarbonate near 450°C coupled with the increase in monocarbonate near 300°C.

Table 2.4.2: LISTING OF MATERIALS FROM XRD ANALYSES FOR HYDRATING CSA CEMENT PASTE	
24 hours	Yeelimite > Anhydrite > Brownmillerite, Ettringite, $Ca_3Al_2O_6$, alpha Ca_2SiO_4 > Belite
21 days	Anhydrite, Yeelimite, Ettringite > $Ca_3Al_2O_6$, alpha Ca_2SiO_4 > Belite > trace of lime
28 days	Anhydrite, Yeelimite, Ettringite > alpha Ca_2SiO_4, $Ca_3Al_2O_6$ > Belite
242 days	Ettringite >> Anhydrite > $Ca_3Al_2O_6$ > Lime, Yeelimite, Belite

Table 2.4.2: Interpretations of XRD diffractograms for the cement paste containing anhydrite and VAE DPP with T_g = -7°C cured at 23°C and 100% relative humidity

Table 2.4.2 lists XRD interpretations for the polymer modified CSA cement paste displayed in Table 2.3 when cured at constant 100% relative humidity and 23°C. The results listed in Table 2.4.2 support those displayed in Figures 2.4.5 through 2.4.8. After 24 hours of hydration, ettringite is present and the concentration of ettringite is less than both yeelimite and anhydrite, which is plausible for a polymer modified CSA cement paste microstructure after 24 hours of hydration. After 21 days of hydration at 100% relative humidity, the concentration of ettringite seems to be nearly equivalent to the concentrations of both yeelimite and anhydrite, suggesting continued hydration given water is no longer a limiting reagent. No apparent differences are noted between 21 days and 28 days of hydration. After 242 days of hydration, the concentration of yeelimite has been significantly reduced when compared with other constituent materials suggesting the small samples continue to hydrate so long as all reactants are available. Furthermore, the presence of calcite suggests ettringite decomposition potentially via carbonation at some point between 28 days and 242 days of hydration as no calcite was detected in the sample hydrated for 28 days at constant 100% relative humidity.

2.5: Anhydrite as a source of calcium sulfate with VAE dispersible polymer powder with T_g = 20°C

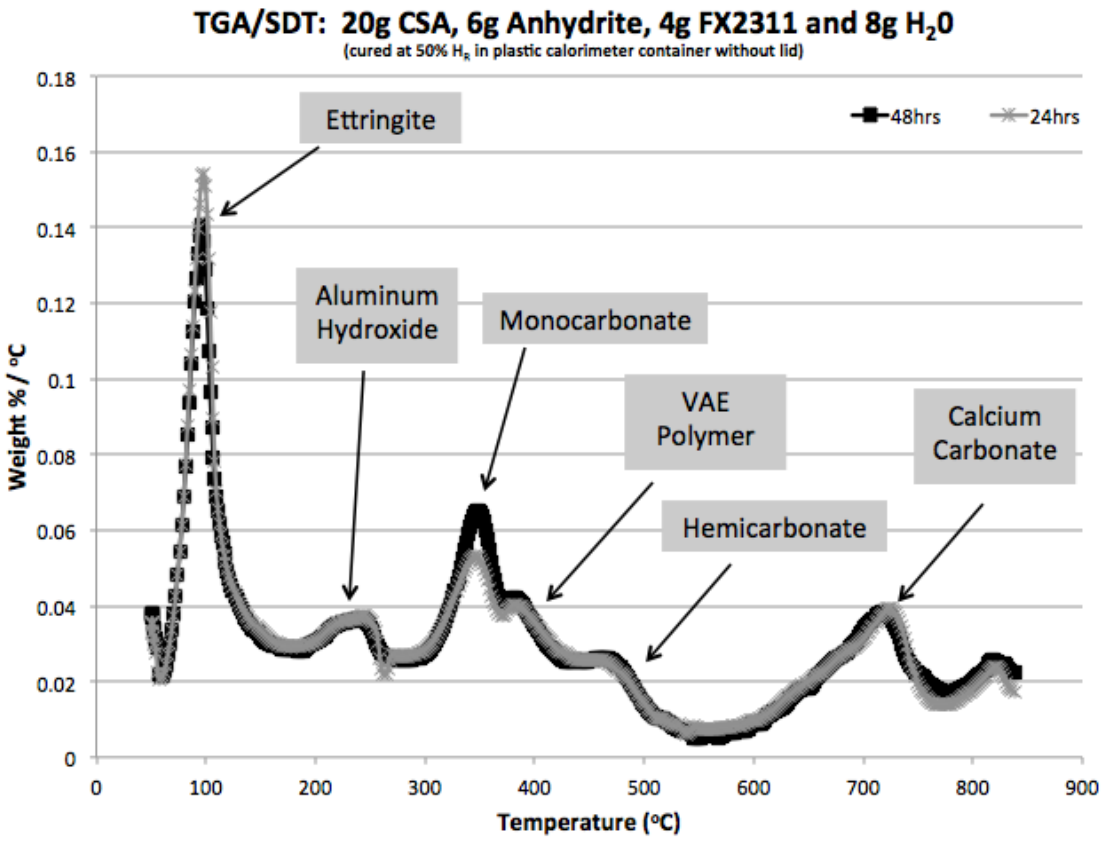

Figure 2.5.1: TGA/SDT analysis of CSA cement paste 6 containing anhydrite and VAE dispersible polymer powder with T_g = 20°C in Table 2.3 after hydrating for periods of 24 hours and 48 hours at 50% relative humidity and 23°C

Figure 2.5.1 displays TGA/SDT analysis of CSA cement paste 6 containing anhydrite and VAE dispersible polymer powder with T_g = 20°C in Table 2.3 after hydrating for periods of 24 hours and 48 hours at 50% relative humidity and 23°C. The peaks near 120°C suggest the concentration of ettringite is similar for each sample. The portion of the curve between 150°C and 200°C is theorized to be associated with either hemicarbonate or perhaps monocarbonate for this CSA cement paste incorporating VAE DPP, which includes anti-caking agents. Literature is not so clear of the timing associated with the emergence of monocarbonate in various cementitious systems, including those containing yeelimite, calcium sulfate and calcium carbonate, as the emergence of such hydrated assemblages is

quite dependent on amount and type of calcium sulfate and other associated admixtures (Winnefeld and Lothenbach, 2013, Pelletier-Changnat et al, 2012, Chowaniec, 2012, Gameiro et al, 2012, Gabrovsek et al, 2008). The peaks near 250°C and 300°C are theorized to be representative of aluminum hydroxide (Candela et al., 1986, Sato, 1985). Aluminum hydroxide is often referred to as either hydrargillite (γ-$Al(OH)_3$) or bayerite (α-$Al(OH_3)$). Additionally, both hydrargillite and bayerite can be further classified as types I and II with different shape thermal decomposition curves, each with peaks between 200°C and 300°C (Sato, 1985). Some of the peaks from 300 to 500°C represent the polymer concentration. VAE polymers usually decompose by a two step mechanism, with the loss of acetic acid during the first step (300-350°C), resulting in the formation of unsaturated polyenes, while the second decomposition step involves random chain scission of the remaining material, forming unsaturated vapor species (~430°C), such as butene and ethylene (Hull et al, 2003). Additionally, the peaks near 450°C likely represent hemicarbonate as described by literature (Winnefeld and Lothenbach, 2013, Chowaniec, 2012).

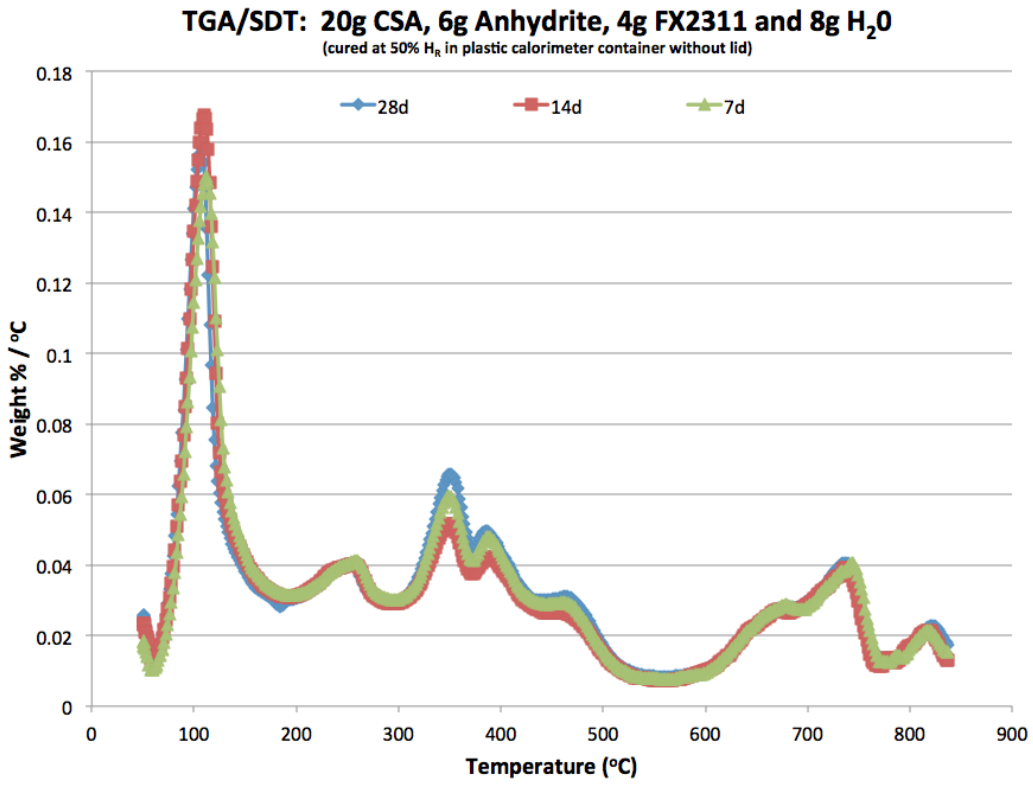

Figure 2.5.2: TGA/SDT analysis of CSA cement paste 6 containing anhydrite and VAE dispersible polymer powder with T_g = 20°C in Table 2.3 after hydrating for periods of 7 days, 14 days and 28 days at 50% relative humidity and 23°C

Figure 2.5.2 displays TGA/SDT analysis of CSA cement paste 6 containing anhydrite and VAE dispersible polymer powder with T_g = 20°C in Table 2.3 after hydrating for periods of 7 days, 14 days and 28 days at 50% relative humidity and 23°C. The peaks near 120°C suggest the ettringite concentration remains similar for hydration periods of 7 days, 14 days and 28 days, respectively.

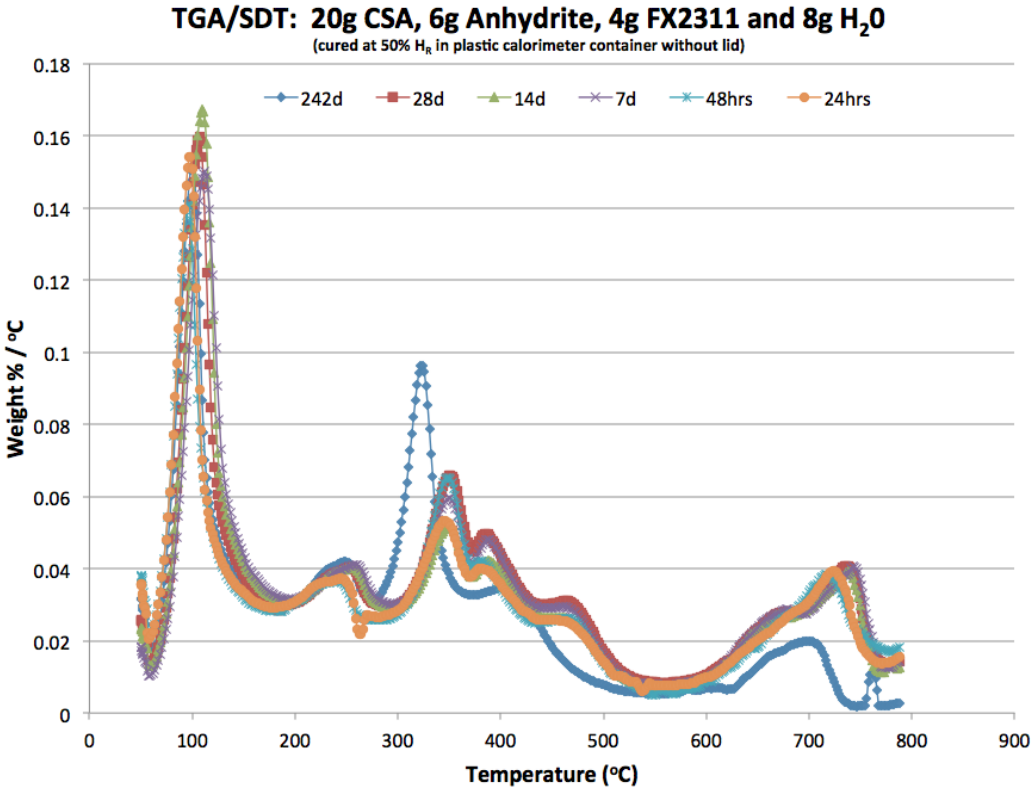

Figure 2.5.3: TGA/SDT analysis of CSA cement paste 6 containing anhydrite and VAE dispersible polymer powder with T_g = 20°C in Table 2.3 after hydrating for periods of 24 hours, 48 hours, 7 days, 14 days, 28 days and 242 days at 50% relative humidity and 23°C

Figure 2.5.3 displays TGA/SDT analysis of CSA cement paste 6 containing anhydrite and VAE dispersible polymer powder with T_g = 20°C in Table 2.3 after hydrating for periods of 24 hours, 48 hours, 7 days, 14 days, 28 days and 242 days at 50% relative humidity and 23°C. The interesting aspects of Figure 2.5.3 are the somewhat constant concentrations of ettringite, the increase in aluminum hydroxide concentration and the apparent decrease in calcium carbonate content. The peaks near 120°C suggest the concentration of ettringite

remains relatively constant for hydration periods ranging from 24 hours to 242 days. The peaks near 250°C and 300°C suggest the concentration of aluminum hydroxide increased.

Similar to behavior of the CSA cement paste sample containing VAE DPP with glass transition temperature of -7°C, a new peak seems to have emerged near 300°C for the polymer modified CSA cement paste containing VAE DPP with glass transition temperature of 20°C, also containing anhydrite as a source of calcium sulfate as displayed in Table 2.3 after hydrating for 242 days at constant 50% relative humidity and 23°C. Before labeling this peak, it is important to note that VAE DPP includes anti-caking agents added during production, often in the range of 10 to 15 percent by mass of the final product. Examples of typical anti-caking agents are calcium carbonate and kaolin clay. Winnefeld and Lothenbach, (2013), report the ternary system, yeelimite, calcium sulfate, calcium carbonate has potential to form either hemicarbonate or monocarbonate in addition to the primary hydration assemblages ettringite, monosulfate and aluminum hydroxide (Winnefeld and Lothenbach, 2013). Furthermore, the authors suggest hemi-carbonate may initially form and coexist for some period of time, likely due to slow formation kinetics of moncarbonate as observed in ordinary portland cement, before reacting with yeelimite and calcite to form either ettringite or monocarbonate (Winnefeld and Lothenbach, 2013). Additionally, literature reports for CSA cements containing accessory phases, C-S-H, $C_2A\bar{S}H_8$ or calcium aluminate hydrates, mainly CAH_{10} or C_4AH_{13}, can be formed in addition to the aforementioned primary hydration assemblages (Pelletier-Chaignat et al, 2012). Before labeling the new late age peak at 300°C, consideration should also be given to reports stating for CSA cement containing belite as a constituent, belite reacts slower than yeelimite forming stratlingite at later ages (Romain et al, 2013). It is well known metastable aluminate hydrates, with examples being CAH_{10}, C_4AH_{13} or $C_2A\bar{S}H_8$ may convert to C_3AH_6, hydrogarnet, at later ages (Taylor, 1997). Literature reports thermal decomposition characteristics of monocarbonate, gamma aluminum hydroxide and hydrogarnet possessing similar peaks near 300°C (Chowaniec, 2012, Gameiro et al, 2012, Gabrovsek et al, 2008, Scrivener and Capmas, 1998, Taylor, 1997). The size of the new peak at 300°C is also important for purposes of determination, as it displays a significant concentration relative to other materials. Given this information, the author theorizes the new peak near 300°C is associated with monocarbonate. The theory is further supported by the peaks near 450°C for the early age samples, likely representing hemicarbonate, which are not visible with analysis of the later age sample. The presence of hemicarbonate at early ages of hydration

suggests the polymer modified CSA cement paste containing minor amounts of calcium carbonate hydrated to form ettringite, aluminum hydroxide, hemicarbonate and possibly monosulfate during the early ages, where the hemicarbonate converted to monocarbonate at later ages, which agrees with literature (Winnefeld and Lothenbach, 2013). In further support, Chowaniec, (2012), displays thermogravimetric analysis (TGA) charts for decomposition of both hemicarbonate and monocarbonate where the peak near 450°C is noted as a means for differentiating hemicarbonate from monocarbonate, as the peak does not appear during TGA analysis of monocarbonate. Additionally, the relatively constant concentrations of ettringite throughout the duration of all analyses together with the either constant or decreasing concentrations of calcium carbonate suggest latex polymer addition as an effective means for mitigating ettringite decomposition in the tested CSA cement pastes.

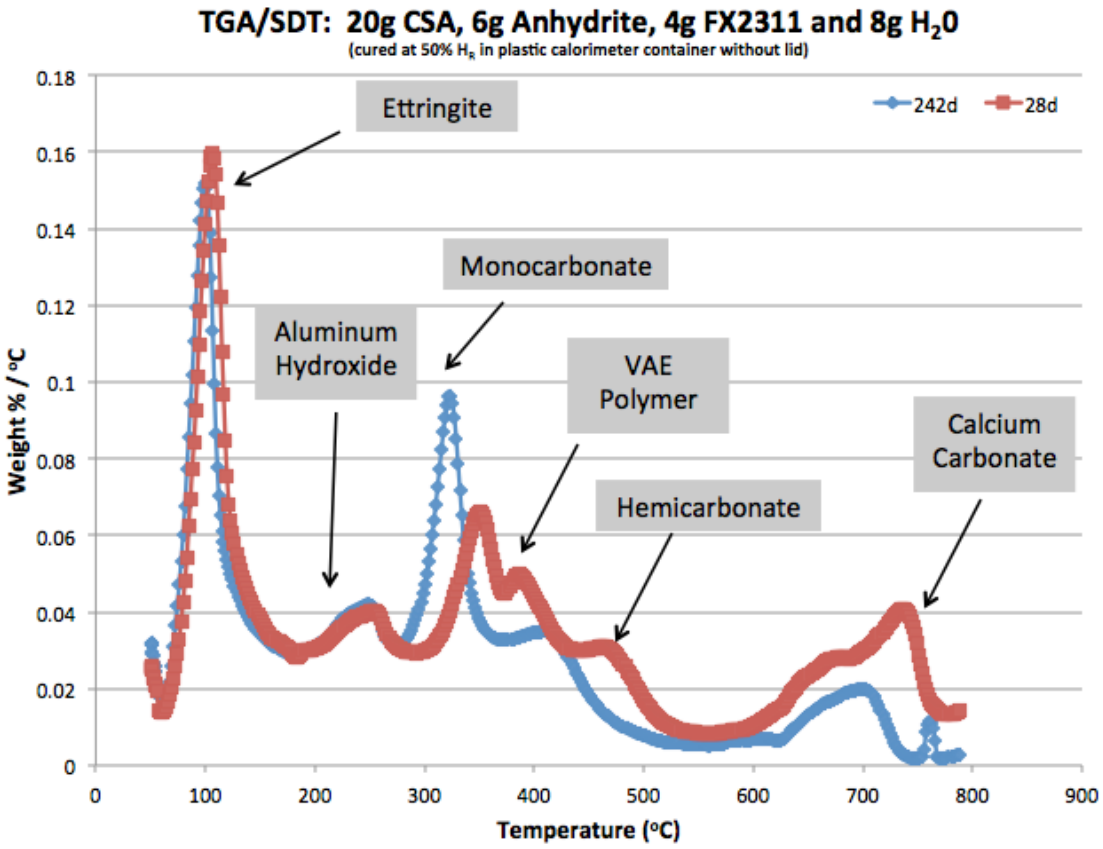

Figure 2.5.4: TGA/SDT analysis of CSA cement paste 6 containing anhydrite and VAE dispersible polymer powder with T_g = 20°C in Table 2.3 after hydrating for periods of 28 days and 242 days at 50% relative humidity and 23°C

Figure 2.5.4 displays TGA/SDT analysis of CSA cement paste 6 containing anhydrite and VAE dispersible polymer powder with T_g = 20°C in Table 2.3 after hydrating for periods of 28 days and 242 days at 50% relative humidity and 23°C. As previously mentioned, the peaks near 120°C represent a somewhat constant concentration of ettringite for both samples, while the peaks between 700 and 800°C are theorized to represent a decrease in calcium carbonate content, further supporting the theory associated with the conversion of hemicarbonate to monocarbonate at later ages.

Table 2.5.1: LISTING OF MATERIALS FROM XRD ANALYSES FOR HYDRATING CSA CEMENT PASTE	
24 hours	Yeelimite > Anhydrite > $Ca_3Al_2O_6$, Ettringite, Brownmillerite > alpha Ca_2SiO_4 > Belite
21 days	Yeelimite > Anhydrite > Brownmillerite , Ettringite, $Ca_3Al_2O_6$ > Belite, alpha Ca_2SiO_4
28 days	Yeelimite > Anhydrite >> Brownmillerite , Ettringite, $Ca_3Al_2O_6$ > Belite, alpha Ca_2SiO_4
242 days	Yeelimite > Anhydrite > Ettringite > $Ca_3Al_2O_6$ > Belite

Table 2.5.1: Interpretations of XRD diffractograms for the cement paste containing solely anhydrite and VAE DPP with T_g = 20°C cured at 23°C and 50% relative humidity

Table 2.5.1 displays XRD characterizations for the cement paste sample containing anhydrite and VAE DPP with T_g = 20°C cured at 23°C and 50% relative humidity. The information displayed in Table 2.5.1 supports the information displayed in Figures 2.5.1 through 2.5.4. As with other XRD interpretations, it is important to note that quantitative Rietveld analysis was not utilized to arrive at the results displayed in Table 2.5.1. After 24 hours of hydration, ettringite is present while reactants yeelimite and anhydrite display the greatest concentration of constituent materials. After hydrating for 21 days, ettringite continues to display a minor concentration relative to other materials while reactants yeelimite and anhydrite show the greatest material concentrations with concentration of yeelimite being greater than concentration of anhydrite. Essentially no significant differences exist for microstructural constituent materials between 21 days and 28 days of hydration. After hydrating for 242 days, the material composition of the cement paste

sample changed somewhat as both Brownmillerite and alpha Ca_2SiO_4 disappear from the characterization, as they were likely consumed with occurrence of later age hydration mechanisms.

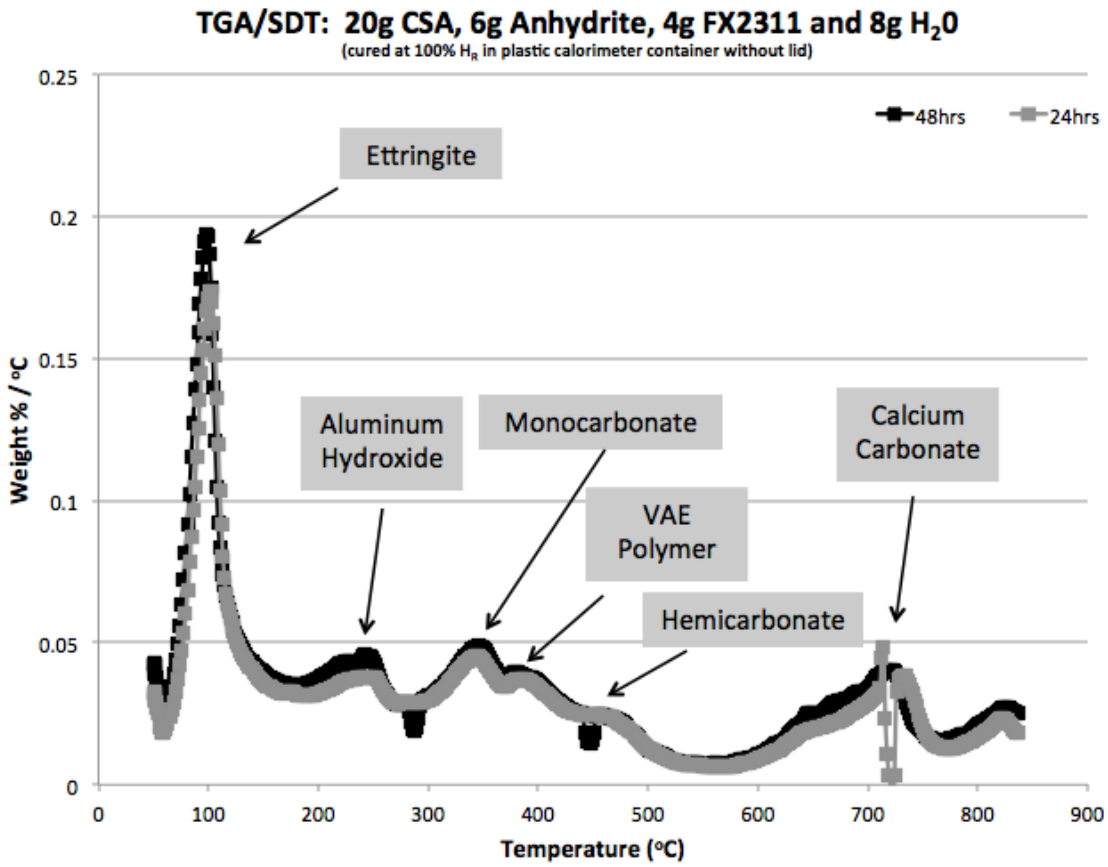

Figure 2.5.5: TGA/SDT analysis of CSA cement paste 4 containing anhydrite and VAE dispersible polymer powder with T_g = 20°C in Table 2.3 after hydrating for periods of 24 hours and 48 hours at 100% relative humidity and 23°C

Figure 2.5.5 displays TGA/SDT analysis of CSA cement paste 4 containing anhydrite and VAE dispersible polymer powder with T_g = 20°C in Table 2.3 after hydrating for periods of 24 hours and 48 hours at 100% relative humidity and 23°C. The peaks near 120°C suggest the concentration of ettringite increases with increases in hydration time. The portion of the curve between 150°C and 200°C is theorized to be associated with either hemicarbonate or perhaps monocarbonate for this CSA cement paste incorporating VAE DPP which includes anti-caking agents. The peaks near 250°C and 300°C are theorized to be representative of aluminum hydroxide concentration (Candela et al., 1986, Sato, 1985). Aluminum hydroxide is often referred to as either hydrargillite (γ-$Al(OH)_3$) or bayerite (α-

$Al(OH_3)$. Additionally, both hydrargillite and bayerite can be further classified as types I and II with different shape thermal decomposition curves, each with peaks between 200°C and 300°C (Sato, 1985). Some of the peaks from 300 to 500°C represent the polymer concentration. VAE polymers usually decompose by a two step mechanism, with the loss of acetic acid during the first step (300-350°C), resulting in the formation of unsaturated polyenes, while the second decomposition step involves random chain scission of the remaining material, forming unsaturated vapor species (~430°C), such as butene and ethylene (Hull et al, 2003). Additionally, the peaks near 450°C likely represent hemicarbonate as described by literature (Winnefeld and Lothenbach, 2013, Chowaniec, 2012).

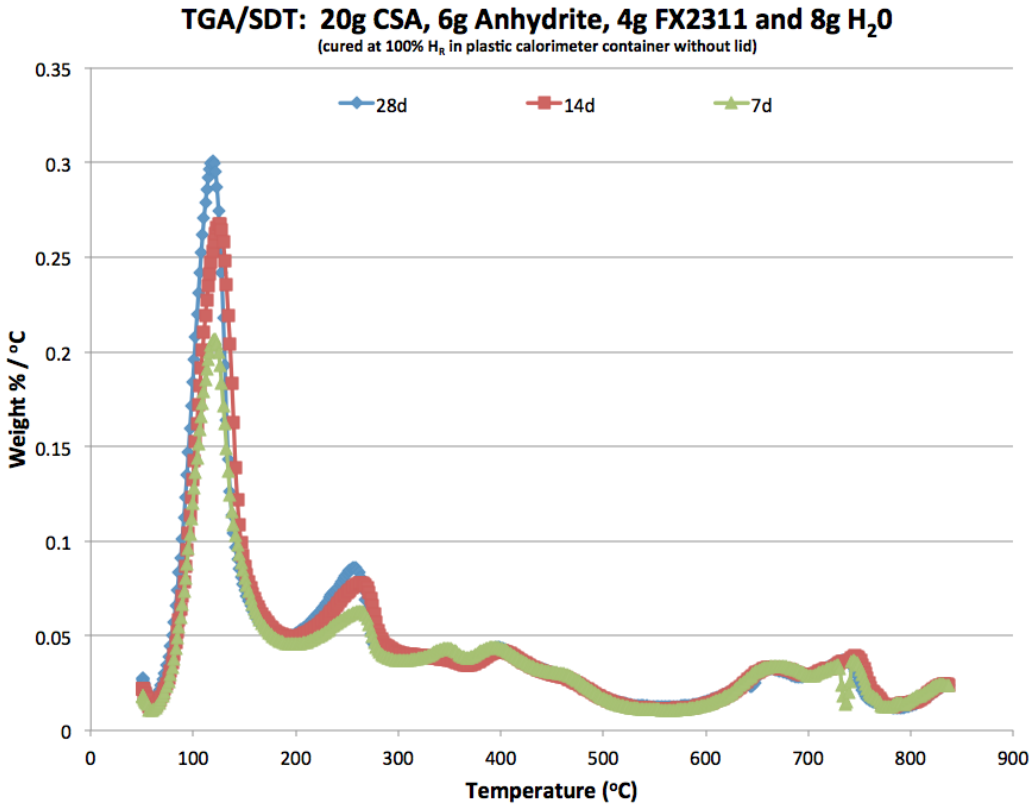

Figure 2.5.6: TGA/SDT analysis of CSA cement paste 4 containing anhydrite and VAE dispersible polymer powder with T_g = 20°C in Table 2.3 after hydrating for periods of 7 days, 14 days and 28 days at 100% relative humidity and 23°C

Figure 2.5.6 displays TGA/SDT analysis of CSA cement paste 4 containing anhydrite and VAE dispersible polymer powder with T_g = 20°C in Table 2.3 after hydrating for periods of 7 days, 14 days and 28 days at 100% relative humidity and 23°C. The important aspect of Figure 2.5.6 is the continually increasing concentration of ettringite for samples hydrated at

100% relative humidity in comparison to like samples cured at constant 50% relative humidity. Additionally, the peaks near 250°C suggest slight increases in aluminum hydroxide concentrations for hydration periods of 7 days, 14 days and 28 days. Again, holding temperature constant, concentrations of hydrated phases for CSA cement samples cured at 100% relative humidity seem to be much greater in magnitude when compared with like samples cured at 50% relative humidity.

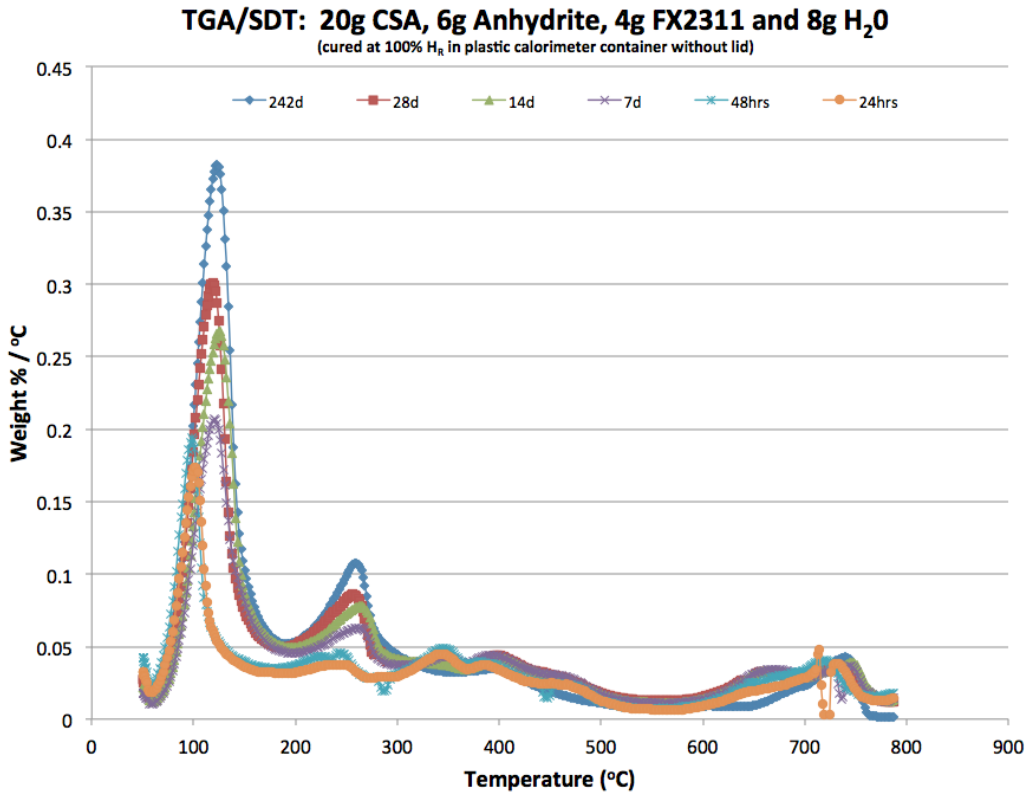

Figure 2.5.7: TGA/SDT analysis of CSA cement paste 4 containing anhydrite and VAE dispersible polymer powder with T_g = 20°C in Table 2.3 after hydrating for periods of 24 hours, 48 hours, 7 days, 14 days, 28 days and 242 days at 100% relative humidity and 23°C

Figure 2.5.7 displays TGA/SDT analysis of CSA cement paste 4 containing anhydrite and VAE dispersible polymer powder with T_g = 20°C in Table 2.3 after hydrating for periods of 24 hours, 48 hours, 7 days, 14 days, 28 days and 242 days at 100% relative humidity and 23°C. Figure 2.5.7 was included to clearly illustrate the increases in both ettringite and aluminum hydroxide concentations for CSA cement paste CC4 cured at constant 100% relative humidity when compared with the like sample, CC6, cured at constant 50% relative humidity.

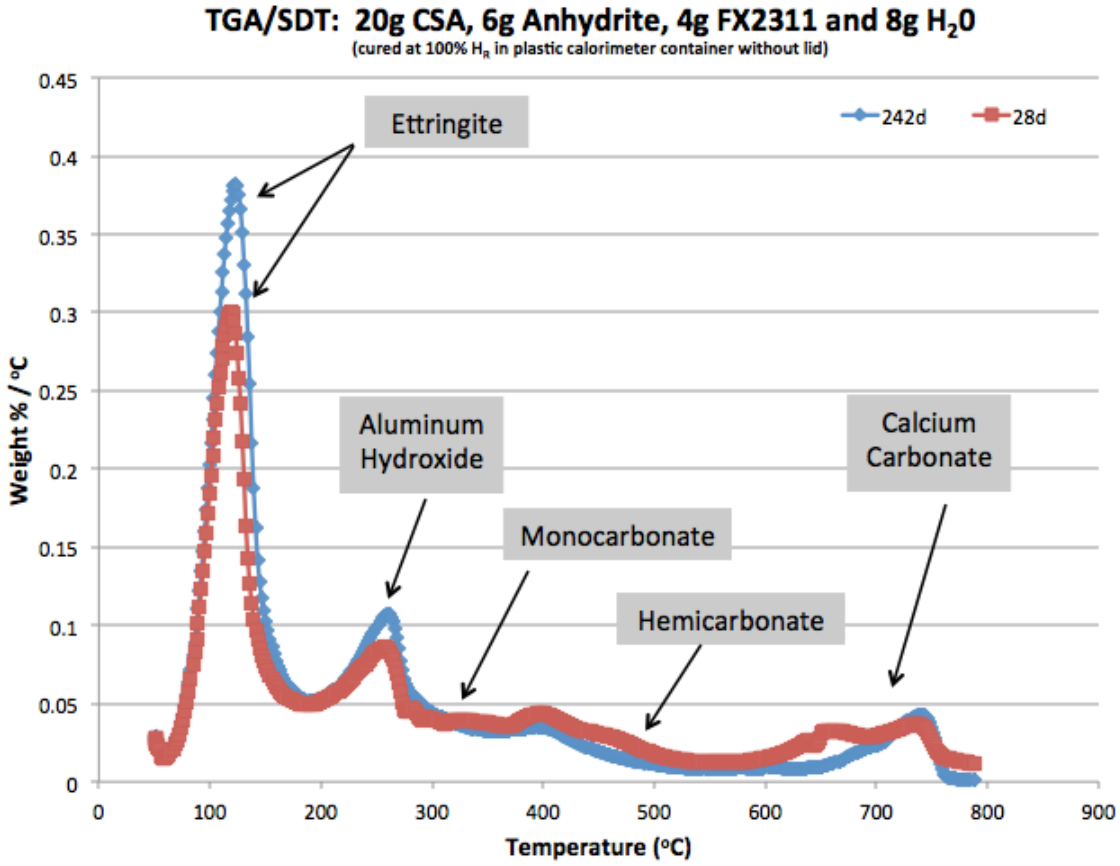

Figure 2.5.8: TGA/SDT analysis of CSA cement paste CC4 containing anhydrite and VAE dispersible polymer powder with T_g = 20°C in Table 2.3 after hydrating for periods of 28 days and 242 days at 100% relative humidity and 23°C

Figure 2.5.8 displays TGA/SDT analysis of CSA cement paste CC4 containing anhydrite and VAE dispersible polymer powder with T_g = 20°C in Table 2.3 after hydrating for periods of 28 days and 242 days at 100% relative humidity and 23°C. The peaks near 120°C suggest the ettringite concentrations continually increase for hydration periods of 28 days and 242 days, respectively. As previously discussed, the peaks near 250°C represent a significant increase in aluminum hydroxide concentration for hydration periods of 28 days and 242 days, respectively. It is interesting to note there is no emergence of a later age peak near 300°C for this polymer modified sample cured at 100% relative humidity when compared with the like polymer modified sample cured at 50% relative humidity. It is possible that the hemicarbonate reacted with yeelimite and calcite to form ettringie as explained in

literature (Winnefeld and Lothenbach, 2013). The increase in concentration of ettringite supports this theory.

Table 2.5.2: LISTING OF MATERIALS FROM XRD ANALYSES FOR HYDRATING CSA CEMENT PASTE	
24 hours	Yeelimite > Anhydrite > Ettringite, Brownmillerite, $Ca_3Al_2O_6$, alpha Ca_2SiO_4 > Belite
21 days	Ettringite, Anhydrite > Yeelimite, alpha Ca_2SiO_4, $Ca_3Al_2O_6$, > Belite, Lime?
28 days	Ettringite, Anhydrite > Yeelimite, alpha Ca_2SiO_4, $Ca_3Al_2O_6$, > Belite, Lime?
242 days	Ettringite >> Anhydrite > alpha Ca_2SiO_4, $Ca_3Al_2O_6$, > Calcite, Belite

Table 2.5.2: Interpretations of XRD diffractograms for the cement paste containing solely anhydrite and VAE DPP with T_g = 20°C cured at 23°C and 100% relative humidity

Table 2.5.2 lists XRD interpretations for the polymer modified CSA cement paste displayed in Table 2.3 when cured at constant 100% relative humidity and 23°C. The information displayed in Figure 2.5.2 further supports the information displayed in Figures 2.5.5 through 2.5.8. After hydrating for 24 hours, ettringite is present and the concentrations yeelimite and anhydrite are the greatest relative to other constituent materials, which is plausible for a polymer modified CSA cement paste microstructure after 24 hours of hydration. The microstructure changed between 24 hours and 21 days hydration at 100% H_R and 23°C, as the concentration of ettringite surpassed that of yeelimite and other constituents. No apparent differences are noted for constituent materials ultimately comprising the microstructure of the polymer modified CSA cement paste sample between 21 days and 28 days of hydration. After 242 days of hydration at 100% relative humidity, the yeelimite appears to have completely been consumed, which is in contrast to the behavior of the like sample cured at constant 50% relative humidity. Such behavior suggests the reaction of yeelimite, anhydrite and water continues toward completion in a 100% humidity environment until some limiting factor is reached for the small samples possessing large surface area when compared with total volume. Furthermore, the presence of calcite at later ages suggests ettringite decomposition via

carbonation at some point between 28 days and 242 days of hydration as no calcite was detected in the sample hydrated for 28 days at constant 100% relative humidity.

SUMMARY

In summary, the presented calcium sulfoaluminate (CSA) cement paste study indicates microstructural behavior for this cement containing minor phase tri-calcium aluminate is influenced by relative humidity, polymer addition and type of calcium sulfate included in the mix design. Although it is well known that relative humidity influences hydration behavior of ordinary portland cement (OPC) based systems, little is known about the influence of relative humidity on hydrating systems containing the experimental CSA cement. Therefore, these findings are quite important for developing packaged materials incorporating this particular cement, as microstructural behavior ultimately influences observations on strength gain, strength loss and dimensional stability.

CSA cement paste containing solely anhydrite displayed different concentrations of hydrated materials for like samples cured at constant 50% relative humidity and constant 100% relative humidity. Noteworthy is that each sample experienced a decrease in ettringite concentration from 28 days to 242 days of hydration. Each sample experienced an increased in calcium carbonate concentration with the later age sample perhaps as a result of ettringite decomposition.

CSA cement paste containing solely gypsum displayed different concentrations of hydrated materials for like samples cured at constant 50% relative humidity and constant 100% relative humidity. Noteworthy is that each sample experienced a decrease in ettringite concentration from 28 days to 242 days of hydration. Each sample experienced an increase in calcium carbonate concentration with the later age sample perhaps as a result of ettringite decomposition.

CSA cement paste containing half anhydrite and half gypsum as a source of calcium sulfate displayed different concentrations of hydrated materials for like samples cured at constant 50% relative humidity and constant 100% relative humidity. Noteworthy is that each sample experienced a decrease in ettringite concentration from 28 days to 242 days of hydration. Each sample experienced an increase in calcium carbonate concentration with the later age sample perhaps as a result of ettringite decomposition.

CSA cement paste containing anhydrite and vinyl acetate / ethylene (VAE) dispersible polymer powder (DPP) with T_g = -7°C displayed different concentrations of hydrated materials for like samples cured at constant 50% relative humidity and constant 100% relative humidity. Noteworthy is that the samples did not experience a significant decrease in ettringite concentration suggesting latex polymer addition as an effective means for mitigating ettringite decomposition in cementitious materials. Additionally, it is theorized the presence of calcium carbonate led to small concentrations of hemicarbonate being produced at early ages before subsequently converting to monocarbonate at later ages.

CSA cement paste containing anhydrite and VAE polymer with T_g = 20°C displayed different concentrations of hydrated materials for like samples cured at constant 50% relative humidity and constant 100% relative humidity. Noteworthy is that the samples did not experience a significant decrease in ettringite concentration suggesting latex polymer addition as an effective means for mitigating ettringite decomposition in cementitious materials. Furthermore, the sample cured at 50% relative humidity displayed hemicarbonate being present at early ages before subsequently converting to monocarbonate; whereas, the sample cured at 100% relative humidity displayed hemicarbonate being present at early ages before decreasing in quantity, perhaps converting to ettringite at later ages. No monocarbonate was recognized as being present in the later age sample cured at 100% relative humidity for the polymer modified cement paste incorporating VAE DPP with glass transition temperature of 20°C.

2 REFERENCES:

- Atkins, P., 1997, The Elements of Physical Chemistry, Oxford University Press, ISBN 0-7167-3077-4
- Blount, C., 1973, Gypsum-Anhydrite Equilibria in Systems CaSO4-H2O and CaCO4-NaCL-H2O, American Mineralogist, Volume 58, pages 323-333, 1973
- Candela, L., Perlmutter, D., 1986, Pore Structure and Kinetics of Thermal Decomposition of $Al(OH)_3$, AIChe Journal, September 1986, Vol. 32, No. 9
- Chandra, S., Ohama, Y., 1994, Polymers in Concrete, CRC Press, ISBN 0-8493-4815-3
- Chowaniec, O., 2012, Limeston Addition in Cement, Thesis Number 5335, EPFL, Ecole Polytechnique Federale de Lausanne, www.epfl.ch
- Christensen, A., Olesen, M., Cerenius, Y., Jensen, T., 2008, Formation and Transformation of Five Different Phases in the CaSO4-H2O System: Crystal Structure of the Subhydrate beta-CaSO4*0.5H2O and Soluble Anhydrite CaSO4, Chem. Mater. 2008, 20, 2124-2132, 2008 American Chemical Society
- Gabrovsek, R., Vuk, T., Kaucic, V., 2008, The Preparation and Thermal Behavior of Calcium Monocarboaluminate, Acta Chim Slov, 2008, 55, 942-950
- Gameiro, A., Silva, A., Veiga, M., Velosa, A., 2012, Lime-Metakaoling Hydration Products: A Microscopy Analysis, Materials and Technology 46 (2012) 2, 145-148
- Garnter, E., 2004, Industrially Interesting Approaches to "low-CO_2" Cements, Cement and Concrete Research 34 (2004) 1489-1498
- Gastaldi, D., Fulvio, C., Boccaleri, E.,2009, Ettringite and calcium sulfoaluminate cement: investigation of water content by near-infrared spectroscopy, Journal of Material Science, 44: 5788-5794, 2009
- Glasser, F., Zhang, L., 2001, High-performance cement matrices based on calcium sulfo-aluminate-belite compositions, Cement and Concrete Research 31 (2001) 1881-1886
- Grounds, T., Midgley, H., Nowell, D., 1988, Carbonation of Ettringite by Atmospheric Carbon Dioxide, Thermochimica Acta, 135 (1988) 347-352
- Hardie, L., 1967, The Gypsum-Anhydrite Equilibrium at One Atmosphere Pressure, The American Mineralogist, Volume 52, January-February, 1967

- Hull, T., Price, D., Liu, Y., Wills, C., Brady, J., 2003, An investigation into the decomposition and burning behaviour of Ethylene-vinyl acetate copolymer nanocomposite materials, Polymer Degradation and Stability 82 (2003) 365-371
- Jewell, R., Rathbone, R., Robl, T., Henke, K., 2009, Fabrication and Testing of CSAB Cements in Mortar and Concrete that Utilize Circulating Fluidized Bed Combustion Byproducts, 2009 World of Coal Ash (WOCA) Conference, 4-7May2009, Lexington, KY, USA, http://www.flyash.info
- Kalousek, G.L., 1973, Klein's Symposium on Expansive Cement Concretes, ACI Special Publication, SP-38, Library of Congress Catalog Number 73-77948
- Lawrence, C.D., Hewlett, P., 1998, Production of Low Energy Cements, Chapter 9, Lea's Chemistry of Cement and Concrete, 4th Edition, Arnold, John Wiley and Sons, New York, New York, ISBN 0-340-56589-6
- Lide, D.R., 1997, CRC Handbook of Chemistry and Physics, 78th Edition, CRC Press, New York, New York, Boca Raton, FL, ISBN 0-07-016197-6
- Majling, J., Znasik, P., Gabrisova, A., Svetik, S., 1985, The Influence of Anhydrite Activity upon the Hydration of Calcium Sulphoaluminate Cement Clinker, Thermochimica Acta, 92 (1985) 349-352, Elsevier Science Publishers B.V., Amsterdam
- Maurin, M., Dittert, L., Hussain, A., 1991, Thermogravimetric analysis of ethylene-vinyl acetate copolymers with Fourier transform infrared analysis of the pyrolysis products, Thermochimica Acta, 186 (1991) 97-102
- Meredith, P., Donald, A., Meller, N., Hall, C., 2004, Tricalcium aluminate hydration: microstructural observations by in-situ electron microscopy, Jounal of Materials Science 39 (2004) 997-1005
- Ohama, Y., 1995, Handbook of Polymer-Modified Concrete and Mortars, Noyes Publications, ISBN 0-8155-1358-8
- Patnaik, P., 2003, Handbook of Inorganic Chemicals, The McGraw Hill Companies, ISBN 0-07-049439-8
- Pelletier-Chaignet, L., Winnefeld, F., Lothenbach, B., Muller, C., 2012, Beneficial use of limestone filler with calcium sulphoaluminate cement, Construction and Building Materials 26 (2012) 619-627

- Pelletier, L., Winnefeld, F., Lothenbach, B., 2010, The ternary system Portland cement – calcium sulphoaluminate clinker – anhydrite: Hydration mechanism and mortar properties, Cement and Concrete Composites, 32 (2010) 497-507
- Perry, D., 1995, Handbook of Inorganic Compounds, CRC Press, New York, New York, Boca Raton, FL, ISBN 0-8493-8671-3
- Perry, R., Green, D., 1997, Perry's Chemical Engineers Handbook, 7th Edition, McGraw Hill, ISBN 0-07-049841-5
- Pourchet, S., Regnaud, L., Perez, J., Nonat, A., 2009, Early C3A hydration in the presence of different kinds of calcium sulfate, Cement and Concrete Research 39 (2009) 989-996
- Romain, T., Winnefeld, F., Mechling, J., Lecomte, A., Roux, A., LeRolland, B., 2013, Composition and Thermodynamic Modeling of Calcium Sulfoaluminate Cement and Ordinary Portland Cement Blends, Proceedings of the First International Conference on Sulphoaluminate Cement, Materials and Engineering Technology, Wuhan University of Technology, Wuhan, China, 23-25Oct2013
- Sahu, S., Havlica, J., Tomkova, V., Majling, J., 1991, Hydration Behaviour of Sulphoaluminate Belite Cement in the Presence of Various Calcium Sulphates, Thermochimica Acta, 175 (1991) 45-52, Elsevier Science Publications B.V., Amsterdam
- Sato, T., 1985, Thermal Decomposition of Aluminum Hydroxides to Aluminas, Thermochimica Acta, 88 (1985) 69-84
- Sato, K., Takebe, T., Nishikawa, T., Suzuki, K., Ito, S., 1992, Decomposition of Synthesized Ettringite by Carbonation, Cement and Concrete Research 22 (1992) 6-14
- Schneider, M., Romer, M., Tschudin, M., Bolio, H., 2011, Sustainable cement production –present and future, Cement and Concrete Research 41 (2011) 642-650
- Scrivener, K., Capmas, A., 1998, Calcium Aluminate Cements, Chapter 13, Lea's Chemistry of Cement and Concrete, 4th Edition, Arnold, John Wiley and Sons, New York, New York, ISBN 0-340-56589-6
- Scrivener, K., Nonat, A., 2011, Hydration of cementitious materials, present and future, Cement and Concrete Research 41 (2011) 651-665

- Sherman, N., Beretka, J., Santoro, L., Valenti, G., 1995, Long-Term Behaviour of Hydraulic Binders Based on Calcium Sulfoaluminate and Calcium Sulfosilicate, Cement and Concrete Research, Vol. 25, No. 1, pp. 113-126
- Silva, D., Monteiro, P., 2007, Early Formation of Ettringite in Tricalcium Aluminate – Calcium Hydroxide – Gypsum Dispersions, Journal of American Ceramic Society 90(2) 614-617
- Skoblinskaya, N., Krasilnikov, K., 1975, Changes in Crystal Structure of Ettringite on Dehydration 1, Cement and Concrete Research, Vol. 5, pp. 381-394, 1975
- Skoblinskaya, N., Krasilnikov, K., Nikitina, L., Varlamov, V., 1975, Changes in Crystal Structure of Ettringite on Dehydration 2, Cement and Concrete Research, Vol. 5, pp. 419-432, 1975
- Smith, J., Van Ness, H., Abbott, M., 1996, Introduction to Chemical Engineering Thermodynamics, The McGraw Hill Companies, New York, New York, St Louis, MO, ISBN 0-07-0529239-X
- Taylor, H., 1997, Cement Chemistry, Second Edition, Thomas Telford Publishing, 1997, ISBN 0 7277 2592 0
- Tossavainen, M., Engstrom, F., Yang, Q., Nourreddine, M., Lidstrom, M., Bjorkman, B., 2007, Characteristics of Steel Slag Under Different Cooling Conditions, Waste Management (2007), Vol 27, p 1335-1344
- Winnefeld, F., Barlag, S., 2010, Calorimetric and thermogravimetric study on the influence of calcium sulfate on the hydration of yeelimite, Journal of Thermal Analysis and Calorimetry (2010) 101:949-957
- Winnefeld, F., Lothenbach, B., 2013, Thermodynamic modeling of hydration of calcium sulfoaluminate cements blended with mineral additions, Proceedings of the First International Conference on Sulphoaluminate Cement, Materials and Engineering Technology, Wuhan University of Technology, Wuhan, China, 23-25Oct2013
- Winnefeld, F., Lothenbach, B., 2010, Hydration of calcium sulfoaluminate cements – Experimental findings and thermodynamic modeling, Cement and Concrete Research 40 (2010) 1239-1247
- Yu, Q.L., Brouwers, H.J.H., 2010, Gypsum: an investigation of microstructure and mechanical properties, Department of Architecture, Building and Planning,

Eindhoven University of Technology, the Netherlands, 8th fib PhD Symposium in Kgs. Lyngby, Denmark, June 20-23, 2010

- Zhang, L., Glasser, F., 2005, Investigation of the microstructure and carbonation of CSA based concretes removed from service, Cement and Concrete Research 35 (2005) 2252-2260
- Zhou, Q., Glasser, F., 2001, Thermal stability and decomposition mechanisms of ettringite at <120°C, Cement and Concrete Research 31 (2001) 1333-1339
- Zhou, Q., Lachowski, E., Glasser, F., 2004, Metaettringite, a decomposition product of ettringite, Cement and Concrete Research 34 (2004) 703-710

Chapter 3: Observations on Mechanical Property Performance of CSA Cement Mortars

The information presented in Chapter 3 further explores the cement design task in the iterative process associated with developing dry mix mortar materials when little information is available describing interactions of the experimental cement with other constituent materials. Chapter 3 expands upon the information presented in Chapter 2 by linking mechanical property behavior to microstructural behavior for CSA cement mortars. The first part discusses the influence of relative humidity on direct tensile strength of CSA cement mortars. The second part highlights the influence of calcium sulfate type on strength behavior of CSA cement mortars. The second part also introduces a potential mechanism for observed strength loss in the laboratory samples possessing high surface area / total volume ratios. The findings associated with Chapter 3 illustrate the importance of choosing an appropriate calcium sulfate for delivering desired performance characteristics when developing formulations including this specific CSA cement containing minor phase tri-calcium aluminate.

3.1 Influence of Curing Environment on Direct Tensile Strength of CSA Cement Mortar

INTRODUCTION

The chemical water demand (CWD) for complete hydration of CSA cement clinker is high when compared with OPC (Glasser and Zhang, 2001, Zhang et al, 2005). Given the high CWD for CSA cement systems, mixes made with lower water/cement (w/c) ratios are likely to retain much unhydrated clinker (Glasser and Zhang, 2001). Literature is scarce detailing the influence of curing environment on unhydrated clinker in CSA cement mortar systems. A lack of literature also exists regarding the influence of different types of calcium sulfate on microstructural development and related behavioral characteristics within CSA cement systems. Obtaining a thorough understanding of the influence of different types of calcium sulfate on microstructural development within CSA cement systems is of paramount importance for embracing these materials as viable substitutes for ordinary portland cement (OPC). This study provides insight for both the influence of different types of

calcium sulfate on the behavior of CSA cement systems and the influence of curing environment on unhydrated clinker in CSA cement systems.

MATERIALS

Cement

CSA cement containing C_3A, tri-calcium aluminate, was utilized in this study. XRD analysis provides the following listing of constituent materials:

Yeelimite >> C_3A > Belite > Anhydrite (trace quantity)

Anhydrite

Calcium sulfate anhydrite for this study was sourced from Allied Custom Gypsum. This anhydrite has a variable particle size, typically with approximately 50% passing three microns while having a top size of approximately 10% retained on a 45 micron sieve with the remainder being a continuous distribution down to dust.

Gypsum

Terra Alba gypsum was sourced from US Gypsum (USG) with particle size within the range of 12 to 15 microns. (USG TDS)

Aggregate

American Society for Testing and Materials (ASTM) finely graded sand from Ottawa Illinois was used in all formulations. A coarser, 20/30 sand, was also used in all formulations.

Experimental Program

This study involved both hydration analysis for CSA cement pastes and direct tensile strength analysis for CSA cement mortar. The hydration analysis included thermogravimetric analysis (TGA/SDT) and powder X-Ray diffraction (XRD). Direct tensile strength testing was performed according to ASTM C307, Standard Test Method for Tensile Strength of Chemical Resistant Mortars, Grouts and Monolithic Surfaces. Mortars were cured on the bench top in molds covered with plastic for 24 hours before being placed in

each humidity environment. Cement pastes were placed directly in each humidity environment after preparation.

Powder X-ray Diffraction (XRD)

Cement pastes were cured in small, plastic calorimeter containers without lids in a humidity chamber controlled at 50% relative humidity and ambient laboratory temperature of 23°C. For each mix design, all test specimens were taken from the same hydrating CSA cement paste sample. Cement paste test specimens were ground to a fine powder using a mortar and pestle. The samples were washed with acetone to remove water in an effort to mitigate the hydration reaction. After washing with acetone, the samples were thoroughly dried in an oven at 45°C for an hour. Powder X-ray diffraction (XRD) analyses were performed with a Philips X'Pert diffractometer (model PW3040-PRO) operating at 45 kV and 40 mA. The samples were dry mounted in aluminum holders and scanned at 8-60° 2θ with Cu K-α radiation.

Thermogravimetric Analysis (TGA/SDT)

All TGA/SDT sample specimens were prepared with the same procedures as the XRD specimens; that is, after curing they were ground, washed with acetone and dried at 45°C. TGA analyses utilized one cycle with a temperature ramp rate of 20°C per minute through a final cycle temperature 800°C. TGA analysis was performed with a SDT 600 from TA Instruments.

Mortars

Two CSA cement based mortar mix designs were analyzed. These mix designs are displayed in Table 3.1.1. Each mix design had constant mass amounts of CSA cement, calcium sulfate, sand and water. The water / cementitious materials ratio for each mix design was 0.33. The low water / cementitious materials ratio resulted in very interesting results which illustrate the relationship between direct tensile strength and developments within the microstructure for these specific CSA cement mortars. Each mix design used different types of calcium sulfate. One mix design contained solely anhydrite. The second mix design contained 50 weight % anhydrite ($CaSO_4$) and 50 weight % gypsum ($CaSO_4 \bullet 2H_2O$).

For preparing the dry mix mortars, individual mortar components were weighed and placed into a plastic mixing bag. After all components were added, the bag was sealed and shaken vigorously by hand for approximately ninety seconds. This type of mixing is an industry proven simulation for blending operations in the manufacturing of dry mix mortar products containing minute quantities of additives such as accelerators and retarders. Table 3.1.1 lists the mortar formulations.

Experimental specimens were cast according to ASTM C307. Three test specimens were cast for each test series. During the first 24 hours of curing, each test specimen remained in the mold covered with plastic on the work bench, i.e., identical curing conditions for all samples for the first 24 hours of hydration. After this initial curing period, test specimens were removed from their molds and placed in the appropriate curing area. Samples cured at 50% relative humidity were placed in a cabinet with a constant temperature of 23°C and constant relative humidity. Samples cured at 100% relative humidity were placed in a misting room which consistently remains at 23°C and a constant 100% relative humidity.

Table 3.1.1: CSA CEMENT MORTAR FORMULATIONS FOR CURING CONDITIONS COMPARISONS				
Curing Conditions	50% H_R	100% H_R	50% H_R	100% H_R
Description	"160g Anh"	"160g Anh"	"80g Anh/80g Gyp"	"80g Anh/80g Gyp"
Materials	mass (g)	mass (g)	mass (g)	mass (g)
CSA Cement	500	500	500	500
Anhydrite	160	160	80	80
Gypsum (Terra Alba)	0	0	80	80
Graded Sand	1375	1375	1375	1375
20-30 Sand	125	125	125	125
Tartaric Acid	2	2	2	2
Total Mass	2162	2162	2162	2162
DI Water	220	220	220	220

Table 3.1.1: CSA cement mortar mix designs cured at either 50% relative humidity or 100% relative humidity

RESULTS

Figure 3.1.1 displays direct tensile strength data according to ASTM C307 for the CSA cement mortars displayed in Table 3.1.1. As seen in the figure, the formulation containing solely anhydrite displayed seven day direct tensile strength values of 493psi (3.4 MPa) and 528psi (3.6 MPa) for samples cured at 50% and 100% relative humidity, respectively. The formulation containing solely anhydrite displayed 28 day direct tensile strength values of 633psi (4.4MPa) and 748psi (5.2MPa) for samples cured at 50% and 100% relative humidity, respectively. In like fashion, the sample containing 50 weight % gypsum and 50 weight % anhydrite displayed seven day direct tensile strength values of 483psi (3.3MPa) and 664psi (4.6MPa) for samples cured at 50% and 100% relative humidity, respectively. Finally, the sample containing 50 weight % gypsum and 50 weight % anhydrite displayed 28 day direct tensile strength values of 597psi (4.1MPa) and 809psi (5.6MPa) for samples cured at 50% and 100% relative humidity, respectively.

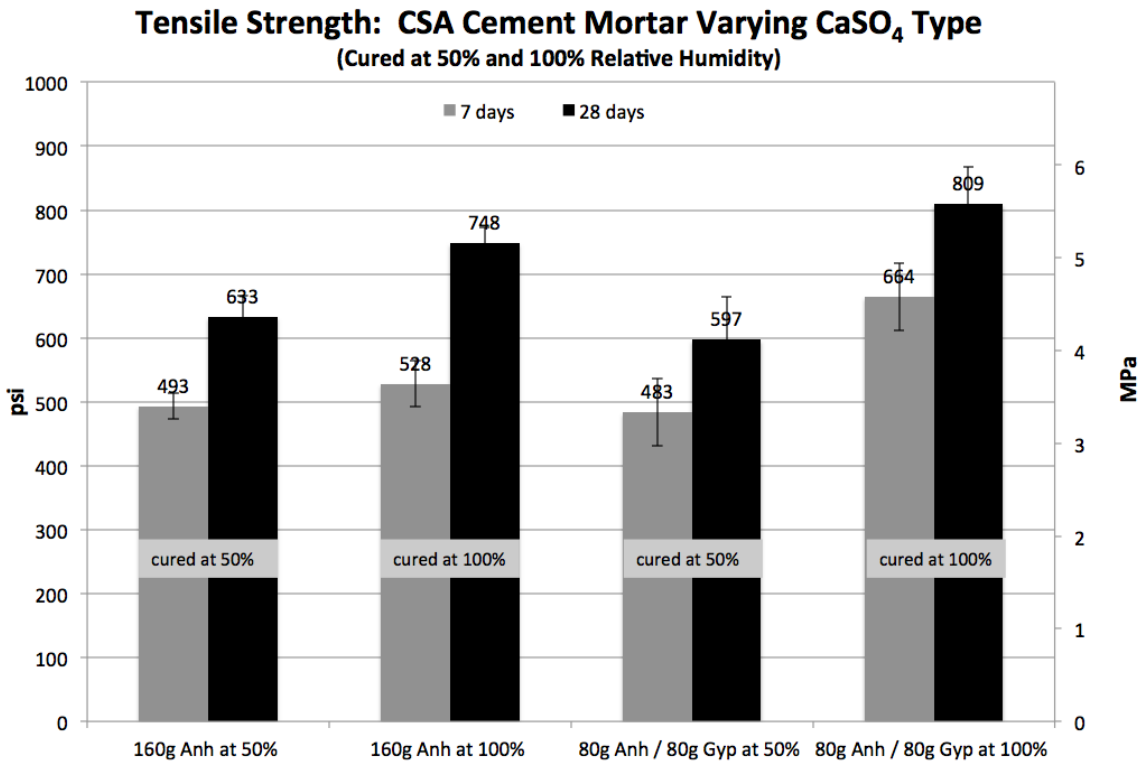

Figure 3.1.1: Direct tensile strength for CSA cement mortars listed in Table 3.1.1 cured at 50% and 100% relative humidity for 7 days or 28 days (3 dog bones each)

Table 3.1.2 displays the aforementioned data along with a percent difference calculation for each set of samples cured under different conditions. The percent difference calculation is as follows:

% difference = ((sample at 100% H_R – sample at 50% H_R) / sample at 50% H_R)*100

It is interesting to note the percent difference values in Table 3.1.2 with respect to samples containing solely anhydrite and samples containing 50 weight % gypsum and 50 weight % anhydrite as sources of calcium sulfate for each CSA cement mortar mix design listed in Table 3.1.1. The samples containing anhydrite display a 7.1% difference in direct tensile strength for samples cured for seven days at 100% relative humidity versus samples cured for seven days at 50% relative humidity. Likewise, the samples containing solely anhydrite display a 18.2% difference in direct tensile strength for samples cured for 28 days at 100% relative humidity versus samples cured for 28 days at 50% relative humidity. When looking at samples containing 50 weight % gypsum and 50 weight % anhydrite, these samples showed a 37.5% difference and a 35.5% difference for samples cured for seven days and 28 days at 50% relative humidity and 100% relative humidity, respectively.

Table 3.1.2: DIRECT TENSILE STRENGTH INFORMATION FOR CURING CONDITIONS COMPARISONS

Descriptions	7d 160g Anh	28d 160g Anh	7d 80g Anh / 80g Gyp	28d 80g Anh / 80g Gyp
Units of Measure/ Curing Conditions	psi	Psi	Psi	Psi
100% H_R	528	748	664	809
50% H_R	493	633	483	597
% Difference (Direct Tensile Strength)	7.1%	18.2%	37.5%	35.5%

Table 3.1.2: Direct tensile strength data at both 50% and 100% relative humidity for formulations listed in Table 3.1.1 and Figure 3.1.1 suggesting microstructural differences contributing to percent difference behavior for the two mix designs being analyzed

When observing the percent differences for the tested samples, it is very important to note that all CSA cement mortar samples were cured in their respective molds covered in plastic for 24 hours before being placed in either the curing cabinet at ambient laboratory temperature and 50% H_R or the misting room at ambient laboratory temperature and 100% H_R. In essence, the microstructures for all samples from each mortar mix design formed under identical conditions --when cured at ambient laboratory temperature in their respective molds covered in plastic. After 24 hours of curing in identical conditions, the samples were placed in significantly different environments, let us call these different environments "humidity extremes". The experimental results suggest the microstructures for mortars containing solely anhydrite behaved differently from the microstructures for mortars containing 50 weight % anhydrite and 50 weight % gypsum when cured at "humidity extremes".

DISCUSSION

Table 3.1.3 lists information on pastes that were hydrated for seven or 28 days at 23°C and at 50% or 100% relative humidity. This discussion utilizes TGA/SDT, XRD and scanning electron microscopy (SEM) analyses of each cement paste listed in Table 3.1.3 to develop rationales for the results presented in Figure 3.1.1 and Table 3.1.2. The discussion focuses on ettringite formation versus time.

Table 3.1.3: CSA CEMENT PASTE FORMULATIONS FOR ANALYTICAL ANALYSIS		
Cement Paste Information	Sample 1	Sample 2
Materials	mass (g)	mass (g)
CSA Cement	20	20
Anhydrite	6	3
Gypsum	0	3
Total Mass	26	26
Deionized Water	8	8

Table 3.1.3: CSA cement paste constituent components by mass for both TGA/SDT and XRD analysis

Figure 3.1.2 illustrates the TGA/SDT results for the cement paste containing only anhydrite after seven days and 28 days of curing 23°C and 50% relative humidity. The peaks located near 120°C represent the presence of ettringite after hydrating for periods of

seven days and 28 days, respectively. This ettringite designation agrees with literature (Sherman et al, 1995, Sato et al, 1992). The portion of the curves between 150°C and 200°C represent monosulfate (Winnefeld and Lothenbach, 2013, Winnefeld and Lothenbach, 2010). The smaller peaks around 250°C may represent aluminum hydroxide.

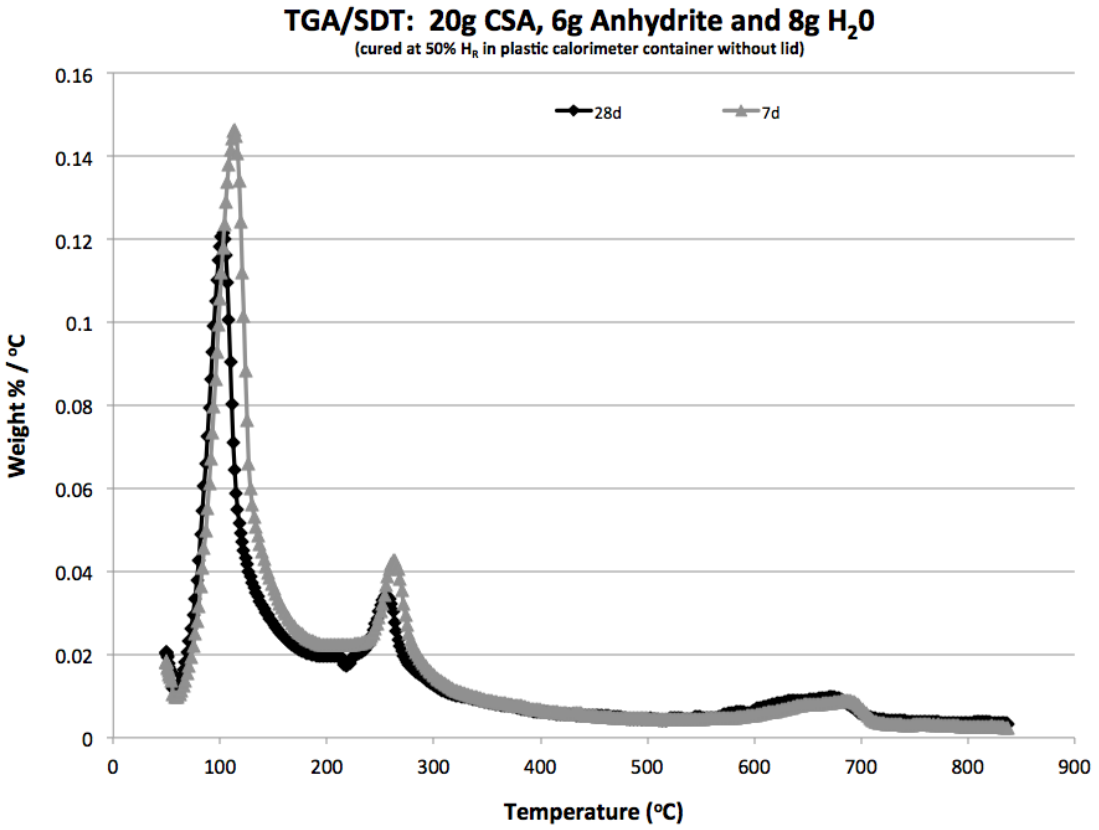

Figure 3.1.2: TGA/SDT analysis for CSA cement paste containing only anhydrite in Table 3.1.2 after curing for seven or 28 days at 50% relative humidity

Figure 3.1.3 is illustrates the TGA/SDT results for the cement paste containing only anhydrite after seven days and 28 days of curing at 23°C and 100% relative humidity. According to the data presented in Table 3.1.4, the peaks located near 120°C represent the presence of ettringite after hydrating for periods of seven days and 28 days, respectively. This ettringite designation agrees with literature (Sherman et al, 1995, Sato et al, 1992). The portion of the curves between 150°C and 200°C represent monosulfate (Winnefeld and Lothenbach, 2013, Winnefeld and Lothenbach, 2010). As with Figure 3.1.3, the smaller peaks around 250°C represent aluminum hydroxide.

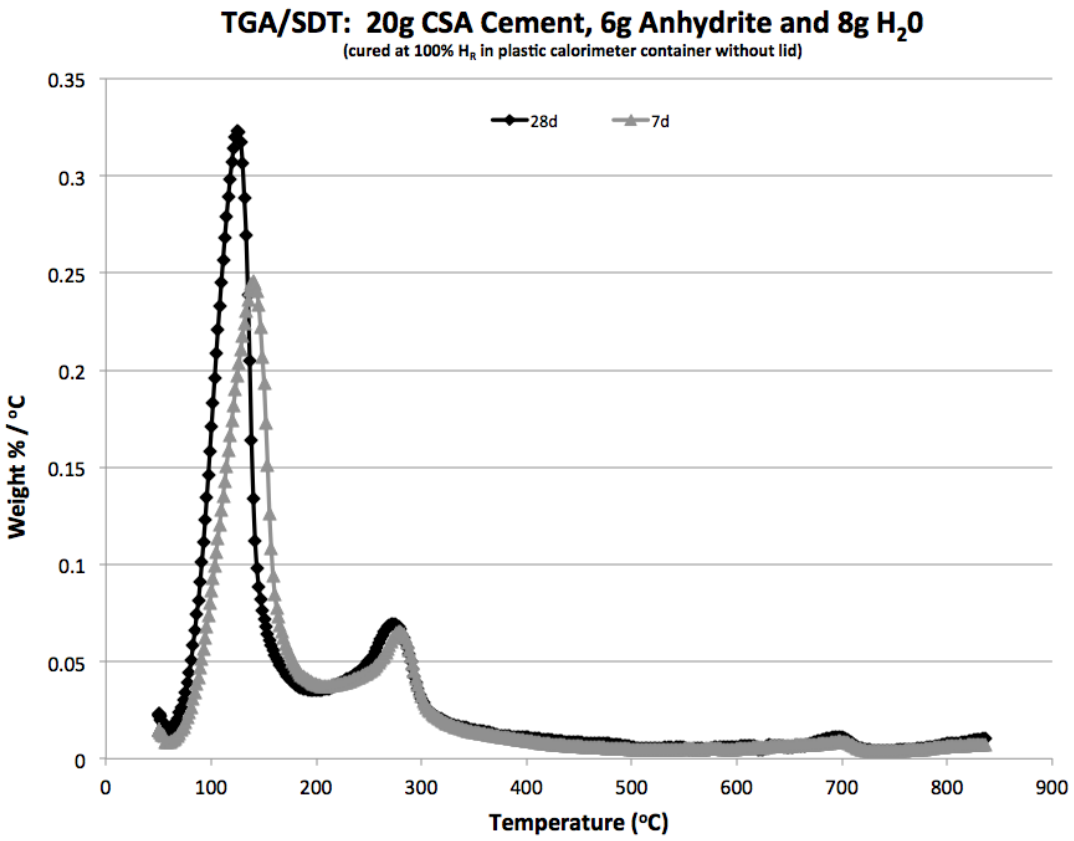

Figure 3.1.3: TGA/SDT analysis for CSA cement paste containing only anhydrite as shown in Table 3.1.2 after curing for seven or 28 days at 100% relative humidity

Table 3.1.4: XRD Interpretations for CSA Cement Paste Containing Anhydrite (28 days hydration at 23°C with different relative humidity)	
50% relative humidity	Yeelimite > Anhydrite >> Brownmillerite, $Ca_3Al_2O_6$ > Ettringite, Belite, alpha-Ca_2SiO_4
100% relative humidity	Yeelimite, Anhydrite > Ettringite > $Ca_3Al_2O_6$, Brownmillerite > alpha Ca_2SiO_4, Belite, Hannebachite

Table 3.1.4: XRD interpretations for CSA cement pastes containing anhydrite as a sourced of calcium sulfate when cured at 23°C and either constant 50% or 100% relative humidity

Table 3.1.4 displays XRD interpretations for the CSA cement paste containing only anhydrite as a source of calcium sulfate after curing for 28 days at either 50% relative

humidity or 100% relative humidity. The XRD interpretations support the information presented in both Figures 3.1.2 and 3.1.3, suggesting that the CSA cement paste cured for 28 days at 100% relative humidity displays a greater concentration of ettringite relative to other constituent materials when compared with the CSA cement paste cured for 28 days at 50% relative humidity. It is theorized the sample cured at 100% relative humidity experienced greater degrees of hydration at later ages which resulted in increased tensile strength behavior when compared with the like sample cured at constant 50% relative humidity.

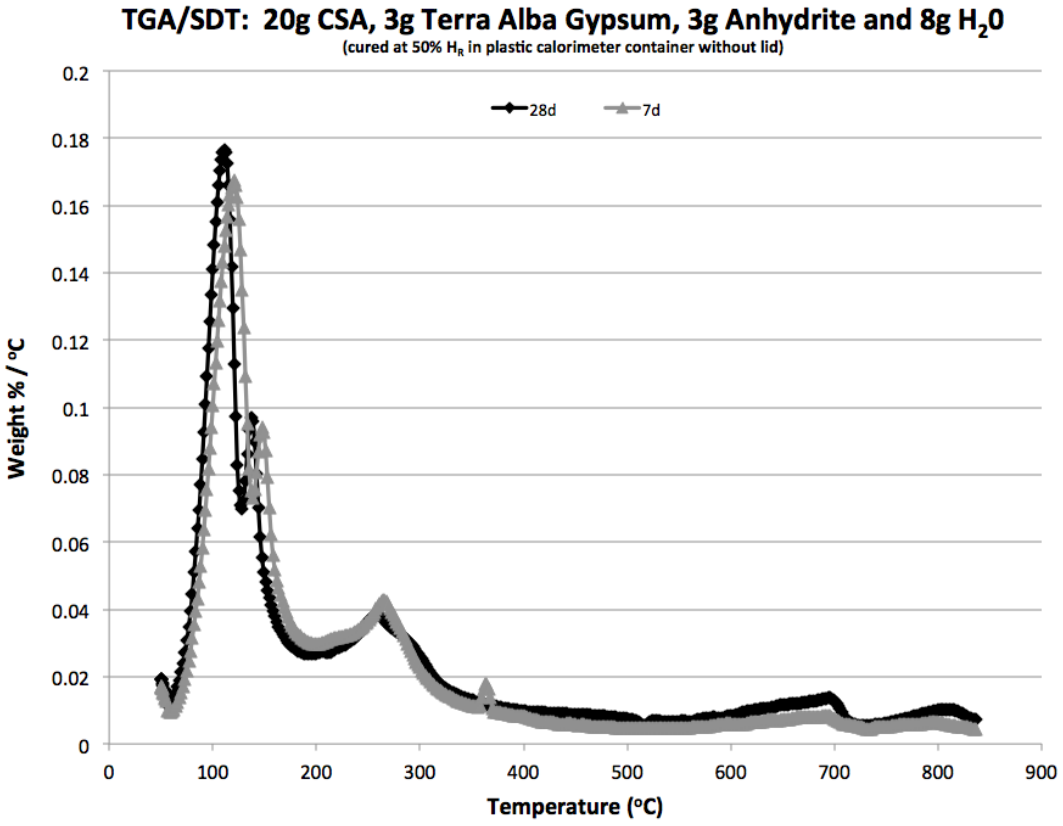

Figure 3.1.4: TGA/SDT analysis for CSA cement paste containing 50 weight % gypsum and 50 weight % anhydrite in Table 3.1.2 after curing for seven or 28 days at 50% relative humidity

Figure 3.1.4 illustrates the TGA/SDT results for the cement paste containing 50 weight % gypsum and 50 weight % anhydrite after seven days and 28 days of curing at 23°C and 50% relative humidity. The peaks located near 120°C represent the concentration of ettringite, which agrees with literature (Sherman et al, 1995, Sato et al, 1992). The peaks near 150°C represent the concentration of gypsum for each hydration period (Winnefeld and Lothenbach, 2010). The smaller peaks around 250°C are theorized to represent aluminum hydroxide.

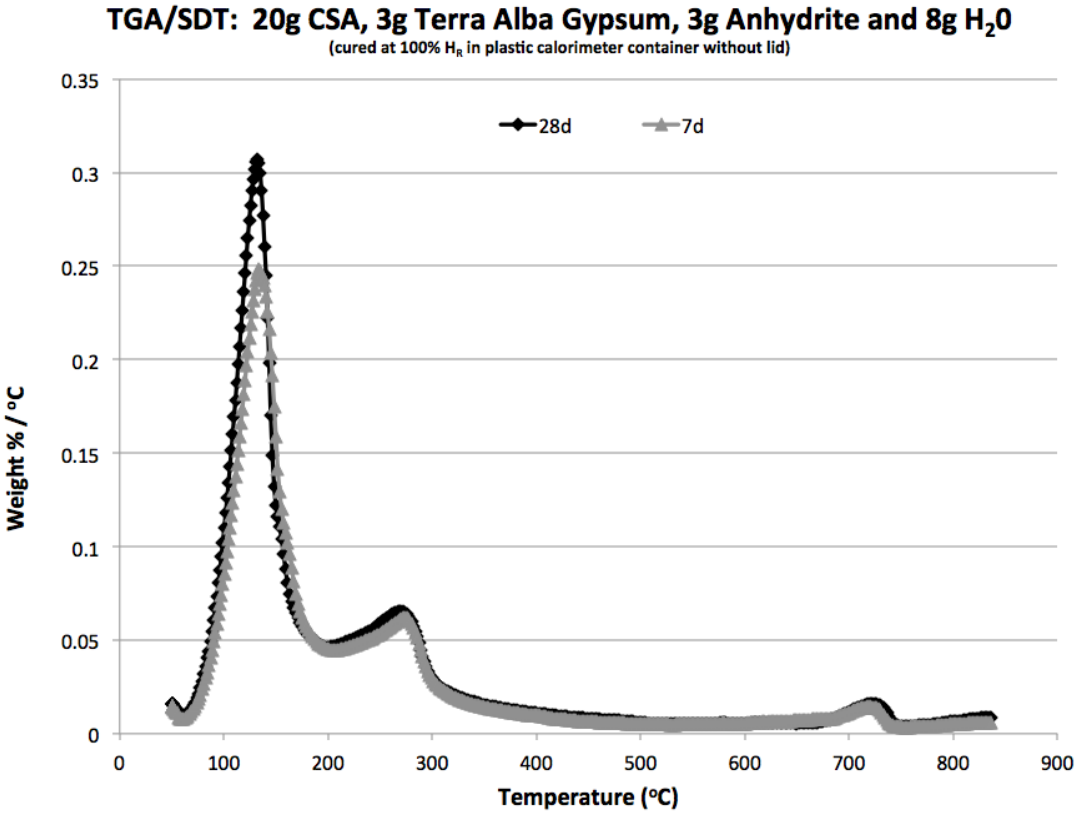

Figure 3.1.5: TGA/SDT analysis for CSA cement paste containing 50 weight % gypsum and 50 weight % anhydrite in Table 3.1.2 after curing for seven or 28 days at 100% relative humidity

Figure 3.1.5 illustrates the TGA/SDT results for the cement paste containing 50 weight % gypsum and 50 weight % anhydrite after seven days and 28 days of curing at 23°C and 100% relative humidity. The peaks located near 120°C represent the concentration of ettringite after hydrating for periods of seven days and 28 days, respectively. This ettringite designation agrees with literature (Sherman et al, 1995, Sato et al, 1992). It is interesting to

note the gypsum peak is not so distinct for the sample cured at 100% relative humidity, which suggests gypsum has been consumed to a greater extent after 7 days of hydration at 100% relative humidity when compared with the like sample cured at 50% relative humidity. As with Figure 3.1.4, the smaller peaks around 250°C are theorized to represent aluminum hydroxide.

Table 3.1.5: XRD Interpretations for CSA Cement Paste Containing 50% Anhydrite and 50% Gypsum as a Combined Source of Calcium Sulfate (28 days hydration at 23°C with different relative humidity)	
50% relative humidity	Yeelimite > Anhydrite > Brownmillerite, $Ca_3Al_2O_6$, Ettringite > alpha Ca_2SiO_4, Belite, Gypsum
100% relative humidity	Yeelimite > Anhydrite, Ettringite > $Ca_3Al_2O_6$, alpha Ca_2SiO_4, Brownmillerite > Belite > Gypsum

Table 3.1.5: XRD interpretations for CSA cement pastes containing 50 weight % anhydrite and 50 weight % gypsum as a combined sourced of calcium sulfate when cured at 23°C and either constant 50% or 100% relative humidity

Table 3.1.5 displays XRD interpretations for the CSA cement paste containing 50 weight % gypsum and 50 weight % anhydrite after curing for 28 days at 50% relative humidity and 100% relative humidity, respectively. The XRD results support the information presented in Figures 3.1.4 and 3.1.5. Table 3.1.5 suggests that the CSA cement paste cured for 28 days at 100% relative humidity displays a greater concentration of ettringite when compared with the CSA cement paste cured for 28 days at 50% relative humidity. The differences in concentrations of constituent materials displayed with both the TGA and XRD results suggest tensile strength behavior is a function of microstructural characteristics.

Furthermore, such experimental results suggest un-hydrated clinker will resume hydration when exposed to proper environments. Hydration reactions are complex and may contain several sets of rate limiting criteria. Different environments may offer unique conditions, with examples being high sulfate content, high calcium content or high humidity, which replenish specific limiting reagents resulting in continuation of chemical reactions. It is theorized water was the limiting reactant for samples cured at 50% relative humidity in

this study. With time, the samples cured at high humidity experienced greater degrees of hydration when compared with the samples cured at 50% relative humidity.

Although quite limited in scope, the experimental results suggest further research may indeed contribute to further understanding the hydration kinetics of CSA cement when exposed to water for extended periods of time throughout the life of the CSA cement material. Such research may indeed allow future generations to "do more with less" if optimum curing regimens can be identified such that higher conversion rates are achieved for desired hydration reactions.

CONCLUSIONS

This study suggests CSA cement microstructural behavior is influenced by the amount and type of added calcium sulfate. This study suggests:

- Mortar mix design containing only anhydrite showed very little difference in direct tensile strength after curing for seven days at both 50% and 100% relative humidity
- Mortar mix design containing only anhydrite displayed a greater direct tensile strength after curing at 100% relative humidity for 28 days when compared with same mortar cured at 50% relative humidity for 28 days
- Mortar mix design containing 50 weight % gypsum and 50 weight % anhydrite displayed greater direct tensile strengths when cured at 100% relative humidity for both seven and 28 days when compared with same mortar cured at 50% relative humidity for both seven and 28 days
- TGA/SDT and XRD analyses suggest that the concentrations of ettringite are greater for all cement pastes cured at 100% relative humidity when compared with identical cement pastes cured at 50% relative humidity
- Both direct tensile strength analysis and analytical analyses suggest un-hydrated clinker in low water to cement ratio CSA materials will react to a certain extent when cured at 100% relative humidity for an extended period of time

3.2 Observations of Strength Loss in CSA Cement Mortars

INTRODUCTION

Calcium sulfoalumiante (CSA) cements hydrate in the presence of calcium sulfate to form ettringite. It is known that ettringite has relatively low resistance to CO_2 attack (Sherman et al, 1995, Sato et al, 1992, Skoblinskaya, N, 1975). When cured in a controlled environment designed to accelerate carbonation behavior of cementitious materials, CSA cement materials experienced greater degrees of carbonation and strength loss when compared with OPC materials (Jewell et al, 2009, Sherman et al, 1995).

An interesting perspective regarding carbonation type findings in general is that contamination by atmospheric CO_2 (carbonation) can probably be more serious in laboratory studies than in practical concrete mixes of lower surface to volume ratio (Taylor 1997). Zhang and Glasser, (2005), report on two CSA cement concretes being removed from service after several years of service in very good condition showing little signs of carbonation. One sample was taken from a normal strength crane column while the other sample was taken from a high strength concrete pile (Zhang and Glasser, 2005). The crane column sample was cored in 1997, wrapped in plastic except for one end, and stored at normal ambient temperature until examination in 2001 (Zhang and Glasser, 2005). The high strength concrete pile sample was cut off in 1993 and transported to Beijing where it was stored outside in the elements until examined in 2001 (Zhang and Glasser, 2005). It would be helpful to know the relative humidity for the indoor storage environment for the crane column sample. According to a climate web site, the average annual relative humidity for Beijing is 56.5% on a monthly basis with a range of 46% in April to 74% in August (http://www.beijing.climatetemp.info).

> "Because it is so central to the formation and property development of cementitious systems it is critical to understand the underlying mechanisms in order to progress; particularly on the most burning challenge facing the world today –the need to continually lower environmental impact, to do more with less" (Scrivener et al, 2011).

At early ages, properly formulated systems based upon CSA cement often demonstrate impressive mechanical property behavior when compared with OPC systems. The concept of "achieving more with less" via substituting a percentage of CSA cement for

OPC cements in specific applications is viable. However, more research is necessary regarding the long term performance of CSA cement systems in extreme environments.

This study presents destructive mechanical property testing results for CSA cement mortars cured at ambient laboratory temperature and constant 50% relative humidity. On a grand scale, this environment is somewhat extreme due to such a constant low humidity. However, according to historical data provided by the National Weather Service, such low atmospheric moisture content is plausible for specific environments, with examples being either Phoenix or Tucson, Arizona. The study assesses both compressive strength behavior and direct tensile strength behavior. Direct tensile strength testing was included to highlight any changes in strength characteristics resulting from changes in microstructural characteristics. Tensile type testing seeks out the weakest link, as it appears to give a more accurate indication of the concrete deterioration than measurements of compressive strength (Chandra et al, 2003). Cement pastes samples were analyzed by TGA/SDT and XRD in an effort to correlate mechanical property behavior with microstructural behavior.

MATERIALS

Cement

CSA cement containing C_3A, tri-calcium aluminate, was utilized in this study. XRD analysis provides the following listing of constituent materials:

Yeelimite >> C_3A > Belite > Anhydrite (trace quantity)

Anhydrite

Calcium sulfate anhydrite for this study was sourced from Allied Custom Gypsum. This anhydrite has a variable particle size, typically with approximately 50% passing three microns while having a top size of approximately 10% retained on a 45 micron sieve with the remainder being a continuous distribution down to dust.

Gypsum

Terra Alba gypsum was sourced from US Gypsum (USG) with particle size within the range of 12 to 15 microns. (USG TDS)

Aggregate

ASTM finely graded sand from Ottawa Illinois was used in all formulations. A coarser, 20/30 sand, was also used in all formulations.

Experimental Program

This study involved both hydration analysis for CSA cement pastes and mechanical strength analysis for CSA cement mortar. The hydration analysis included thermogravimetric analysis (TGA/SDT) and powder X-Ray diffraction (XRD). Direct tensile strength testing was performed according to ASTM C307, Standard Test Method for Tensile Strength of Chemical Resistant Mortars, Grouts and Monolithic Surfaces. Compressive strength testing was performed according to ASTM C109, Standard Test Method for Compressive Strength of Hydraulic Cement Mortar using standard cubes. All samples were cured at ambient laboratory temperature and 50% relative humidity.

Powder X-ray Diffraction (XRD)

Cement pastes were cured in small, plastic calorimeter containers without lids in a humidity chamber controlled at 50% relative humidity and ambient laboratory temperature of 23^{o}C. For each mix design, all test specimens were taken from the same hydrating CSA cement paste sample. Cement paste test specimens were ground to a fine powder using a mortar and pestle. The samples were washed with acetone to remove water in an effort to mitigate the hydration reaction. After washing with acetone, the samples were thoroughly dried in an oven at 45^{o}C for an hour. Powder X-ray diffraction (XRD) analyses were performed with a Philips X'Pert diffractometer (model PW3040-PRO) operating at 45 kV and 40 mA. The samples were dry mounted in aluminum holders and scanned at 8-60^{o} 2θ with Cu K-α radiation.

TGA/SDT

All TGA/SDT sample specimens were prepared with the same procedures as the XRD specimens; that is, after curing they were ground, washed with acetone and dried at 45^{o}C. TGA analyses utilized one cycle with a temperature ramp rate of 20^{o}C per minute through a final cycle temperature 800^{o}C. TGA analysis was performed with a SDT 600 from TA Instruments.

Mortars

Three CSA cement based mortar mix designs were analyzed for direct tensile strength. These mix designs are displayed in Table 3.2.1. Each mix design had constant mass amounts of CSA cement, calcium sulfate and sand. Two mix designs possessed identical water / cementitious materials ratios while one mix design possessed a slightly higher water / cementitious materials ratio. The water / cementitious materials ratio for the two mix designs containing anhydrite was 0.33. The water / cementitious materials ratio for the mix design containing gypsum was 0.35. These low water / cementitious materials ratios resulted in very interesting results which illustrate the relationship between direct tensile strength and developments within the microstructure for these specific CSA cement mortars. Each mix design differed in type of specific calcium sulfate comprising the constant mass amount of calcium sulfate. One mix design contained solely anhydrite. The second mix design contained 50 weight % anhydrite and 50 weight % gypsum. The third mix design solely contained gypsum.

The mortar containing solely gypsum was also analyzed for compressive strength testing along with another mortar containing 50 weight % gypsum and 50 weigth % anhydrite. The sample containing 50 weight % gypsum and 50 weight % anhydrite for compressive strength testing contained double the amount of calcium sulfate when compared with the mortar tested for direct tensile strength displayed in Table 3.2.1. Mortar formulations for compressive strength testing are displayed in Table 3.2.2.

For preparing the dry mix mortars, individual mortar components were weighed and placed into a plastic mixing bag. After all components were added, the bag was sealed and shaken vigorously by hand for approximately ninety seconds. This type of mixing is an industry proven simulation for blending operations manufacturing dry mix mortar products containing minute quantities of additives such as accelerators and retarders.

Experimental specimens were cast according to both ASTM C307 and ASTM C109. Three test specimens were cast for each test series. During the first 24 hours of curing, each test specimen remained in the mold covered with plastic. After this initial curing period, test specimens were removed from their molds and either tested or placed in a chamber at ambient laboratory temperature and 50% relative humidity until time for testing.

Table 3.2.1: CSA CEMENT MORTAR FORMULATIONS FOR TENSILE STRENGTH TESTING			
Cement Mortar Data (ASTM C307)	Solely Anhydrite	50% Anhydrite / 50% Gypsum	Solely Gypsum
Materials	Mass (g)	Mass (g)	Mass (g)
CSA Cement	500	500	500
Anhydrite	160	80	0
Gypsum	0	80	160
Coarse Sand	125	125	125
Graded Sand	1375	1375	1375
DI Water	220	220	230

Table 3.2.1: CSA cement mortar constituent components by mass for ASTM C307 direct tensile strength testing

Table 3.2.2: CSA CEMENT MORTAR FORMULATIONS FOR COMPRESSIVE STRENGTH TESTING		
Cement Mortar Data (ASTM C109)	50% Anhydrite / 50% Gypsum	Solely Gypsum
Materials	Mass (g)	Mass (g)
CSA Cement	500	500
Anhydrite	160	0
Gypsum	160	160
Coarse Sand	125	125
Graded Sand	1375	1375
DI Water	240	230

Table 3.2.2: CSA cement mortar constituent components by mass for ASTM C109 compressive strength testing

Cement Pastes

Table 3.2.3: CSA CEMENT PASTE FORMULATIONS FOR ANALYTICAL ANALYSIS			
Cement Paste Data	Sample 1	Sample 2	Sample 3
Materials	Mass (g)	Mass (g)	Mass (g)
CSA Cement	20	20	20
Anhydrite	6	3	0
Gypsum	0	3	6
Total Mass	26	26	26
DI Water	8	8	8

Table 3.2.3: CSA cement paste constituent components by mass for both TGA/SDT and XRD analysis

RESULTS

Figure 3.2.1 displays direct tensile strength values for the mix design containing solely anhydrite as a source of calcium sulfate. For the tested samples, which were cured at 50% relative humidity and 23^{o}C, the strength development trend increased from the point of initial hydration up through some period between 28 days and 56 days of hydration. Such an increase in strength performance is likely a result of continued hydration reactions. Microstructure characteristics are further discussed in the coming pages. As illustrated in Figure 3.2.1, the direct tensile strength results for 24 hours, 48 hours, 7 days and 28 days are 275psi (1.9MPa), 488psi (3.4MPa), 493psi (3.4MPa) and 633psi (4.4MPa), respectively. Whereas, the direct tensile strength results for 28 days, 56 days and 109 days are 633psi (4.4MPa), 567psi (3.9MPa) and 539psi (3.7MPa), respectively. The period from initial hydration through 28 days is clearly a period of increasing direct tensile strength; whereas, the period from 28 days through 109 days of hydration is clearly a period of decreasing direct tensile strength. Statistical analysis information is available in the appendices. Additionally, Appendix B contains linear regression polynomial fit plots and associated information. The author theorizes the fitted quadratic equation is not a good predictor of strength behavior for the CSA cement mortar containing anhydrite as a source of calcium sulfate within the range of data; therefore, the plot is displayed in the appendix.

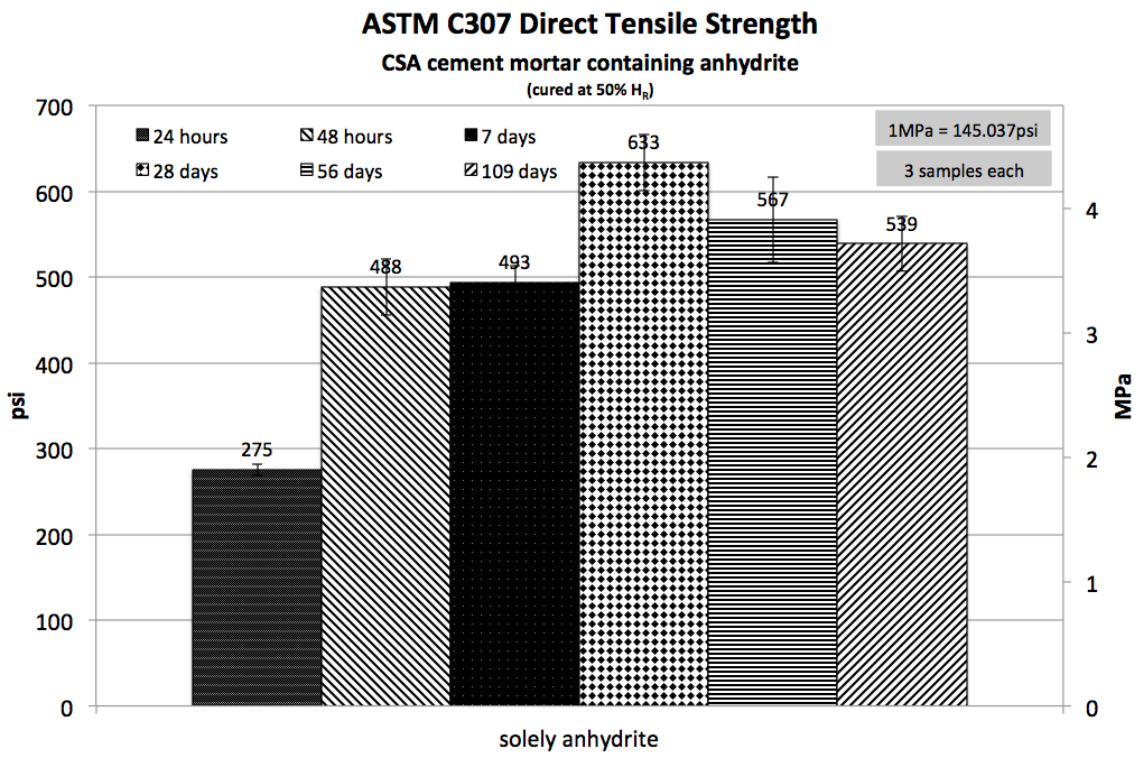

Figure 3.2.1: Direct tensile strength for CSA cement mortar containing anhydrite as a source of calcium sulfate cured at ambient temperature and constant 50% relative humidity

Figure 3.2.2 displays direct tensile strength values for the mix design containing 50 weight % anhydrite and 50 weight % gypsum as a combined source of calcium sulfate. For the tested samples, which were cured at 50% relative humidity and 23°C, the strength development trend increased from the point of initial hydration up through some period between 28 days and 56 days of hydration. The author theorizes such changes in strength behavior are related to microstructural characteristics which are influenced by chemical reactions. Microstructural characteristics are further discussed in subsequent pages. As illustrated in Figure 3.2.2, the direct tensile strength results for 24 hours, 48 hours, 7 days and 28 days are 387psi (2.7MPa), 492psi (3.4MPa), 491psi (3.4MPa) and 597psi (4.1MPa), respectively. Whereas, the direct tensile strength results for 28 days and 56 days are 597psi (4.1MPa) and 313psi (2.2MPa), respectively. The period from initial hydration through 28 days is clearly a period of increasing direct tensile strength; whereas, the period from 28 days through 56 days of hydration is clearly a period of decreasing direct tensile strength. Statistical analysis information for the data set is available in the appendices. Additionally, Appendix B contains linear regression polynomial fit plots and associated information. The fitted quadratic equation for tensile strength versus time behavior of the

CSA cement mortar containing 50% by weight anhydrite and 50% by weight gypsum is significant. However, the fit is not great. The author theorizes increasing both testing frequency and sample size for future experiments will improve the validity of regression analysis exercises.

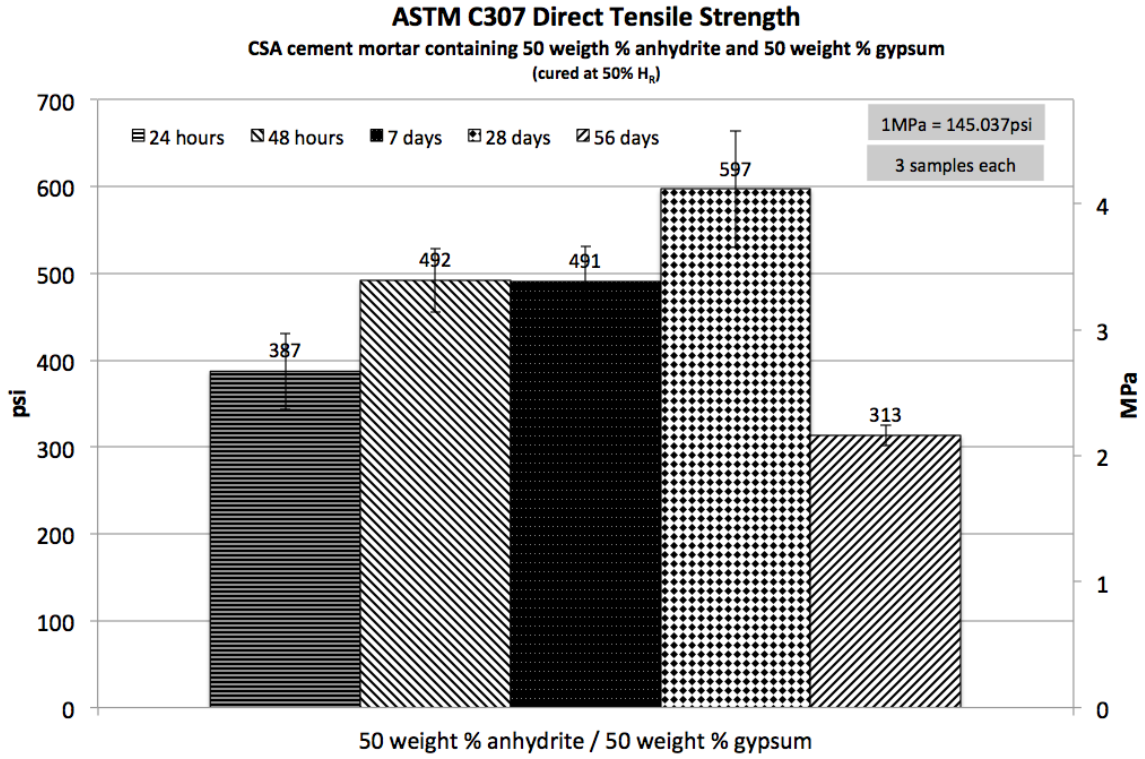

Figure 3.2.2: Direct tensile strength for CSA cement mortar containing half gypsum and half anhydrite as a source of calcium sulfate cured at ambient temperature and constant 50% relative humidity

Figure 3.2.3 displays direct tensile strength values for the mix design containing solely gypsum as a source of calcium sulfate. For the tested samples, which were cured at 50% relative humidity and 23°C, the strength development trend increased from the point of initial hydration up through some period between 7 days and 28 days of hydration. As illustrated in Figure 3.2.3, the direct tensile strength results for 24 hours, 48 hours and 7 days are 346psi (2.4MPa), 371psi (2.6MPa) and 463psi (3.2MPa), respectively. Whereas, the direct tensile strength results for 7 days and 28 days are 463psi (3.2MPa) and 343psi (2.4MPa), respectively. The period from initial hydration through 7 days is clearly a period of increasing direct tensile strength; whereas, the period from 7 days through 28 days of hydration is clearly a period of decreasing direct tensile strength. It is theorized decreases

in strength are related to ettringite decomposition, which is further discussed in subsequent pages. The appendices contain statistical analysis information for the presented data. Appendix B contains regression analysis curve fit information. The fitted quadratic equation does not present an ideal model for describing tensile strength behavior versus time for the CSA cement mortar containing gypsum as a source of calcium sulfate. For this reason, the regression analysis exercise was included as an appendix.

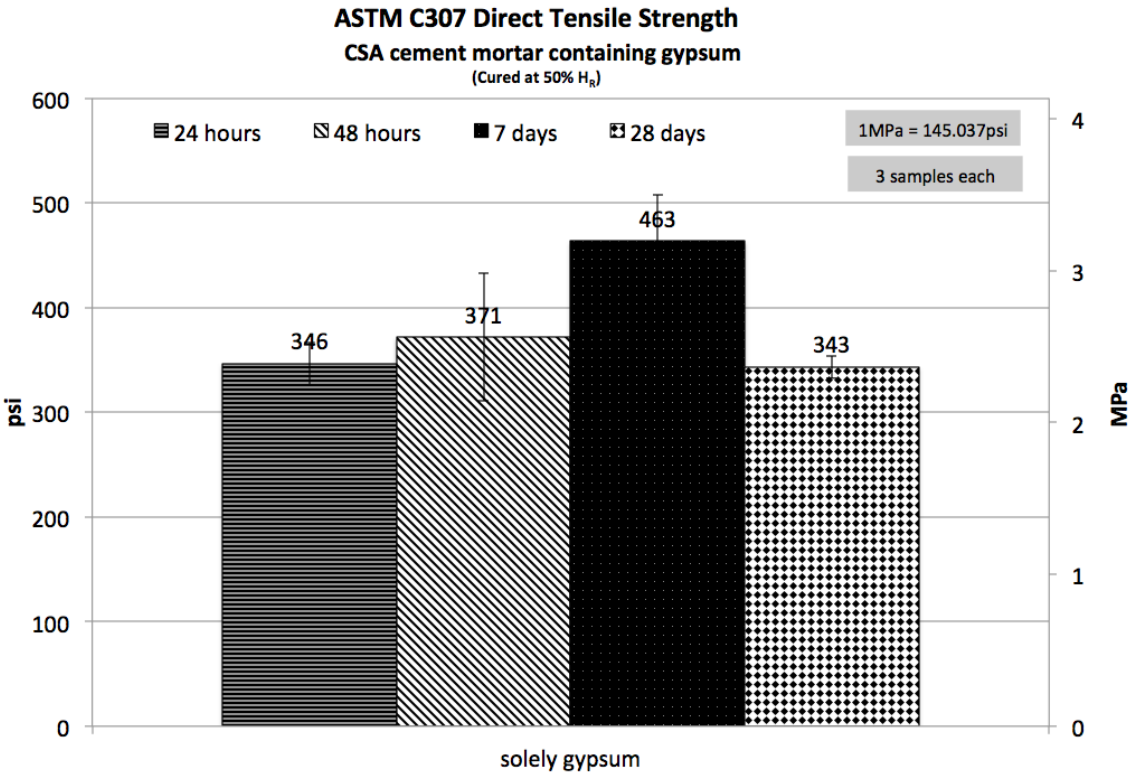

Figure 3.2.3: Direct tensile strength for CSA cement mortar containing half gypsum and half anhydrite as a source of calcium sulfate cured at ambient temperature and constant 50% relative humidity

Figure 3.2.4 displays compressive strength values for the mix design containing 50 weight % anhydrite and 50 weight % gypsum displayed in Table 3.2.2. For the tested samples, which were cured at 50% relative humidity and 23°C, the strength development trend increased from the point of initial hydration up through some period between 461 days and 537 days of hydration. As illustrated in Figure 3.2.4, the compressive strength results for 24 hours, 48 hours, 7 days and 461 days are 6,092psi (42MPa), 9,572psi (66MPa), 12,183psi (84MPa) and 12,473psi (86MPa), respectively. Whereas, the compressive strength results for 461 days and 537 days are 12,473psi (86MPa) and

10,153psi (70MPa), respectively. The period from initial hydration through 461 days is clearly a period of increasing compressive strength; whereas, the period from 461 days through 537 days of hydration is clearly a period of decreasing compressive strength. The appendices contain statistical analysis information. Appendix B presents an exercise in curve fitting utilizing linear regression techniques. The fitted quadratic equation for describing compressive strength behavior versus time for the CSA cement mortar containing half anhydrite and half gypsum by mass as a combined source of calcium sulfate does not accurately represent strength behavior for the range of data. Therefore, the exercise is presented in the appendix.

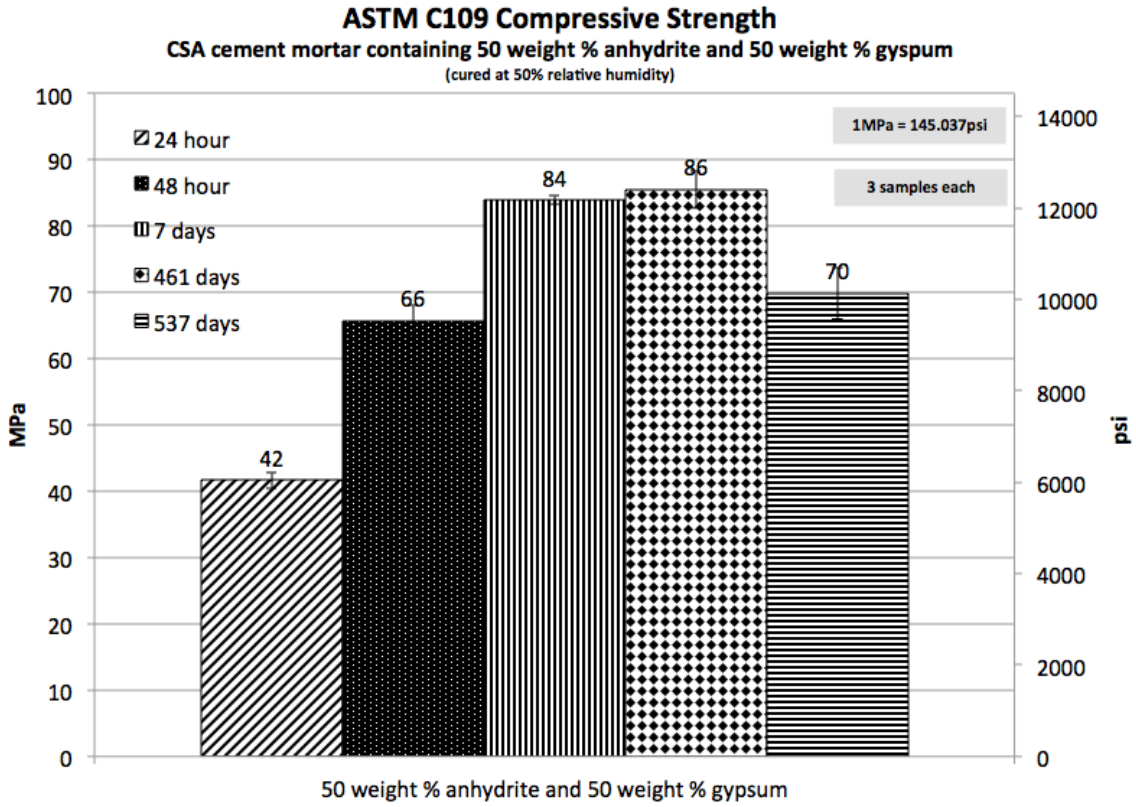

Figure 3.2.4: Compressive strength for CSA cement mortar containing half gypsum and half anhydrite displayed in Table 3.2.2 cured at ambient temperature and constant 50% relative humidity

Figure 3.2.5 displays compressive strength values for the mix design containing solely gypsum displayed in Table 3.2.2. For the tested samples, which were cured at 50% relative humidity and 23°C, the strength development trend increased from the point of

initial hydration up through some period between 7 days and 460 days of hydration. As illustrated in Figure 3.2.5, compressive strength results for 24 hours, 48 hours and 7 days are 6,092psi (42MPa), 9,717psi (67MPa) and 11,748psi (81MPa); respectively, whereas, the compressive strength results for 7 days, 460 days and 537 days are 11,748psi (81MPa), 9,572psi (66MPa) and 6,818psi (47MPa), respectively. The period from initial hydration through 7 days is clearly a period of increasing compressive strength; whereas, the period from 7 days through 537 days of hydration is clearly a period of decreasing compressive strength. The appendices contain statistical analysis information. Appendix B presents and exercise in curve fitting utilizing regression analysis; however, the fitted equation is not perceived as a good model for describing strength behavior versus time. Therefore, the exercise is presented in the appendix.

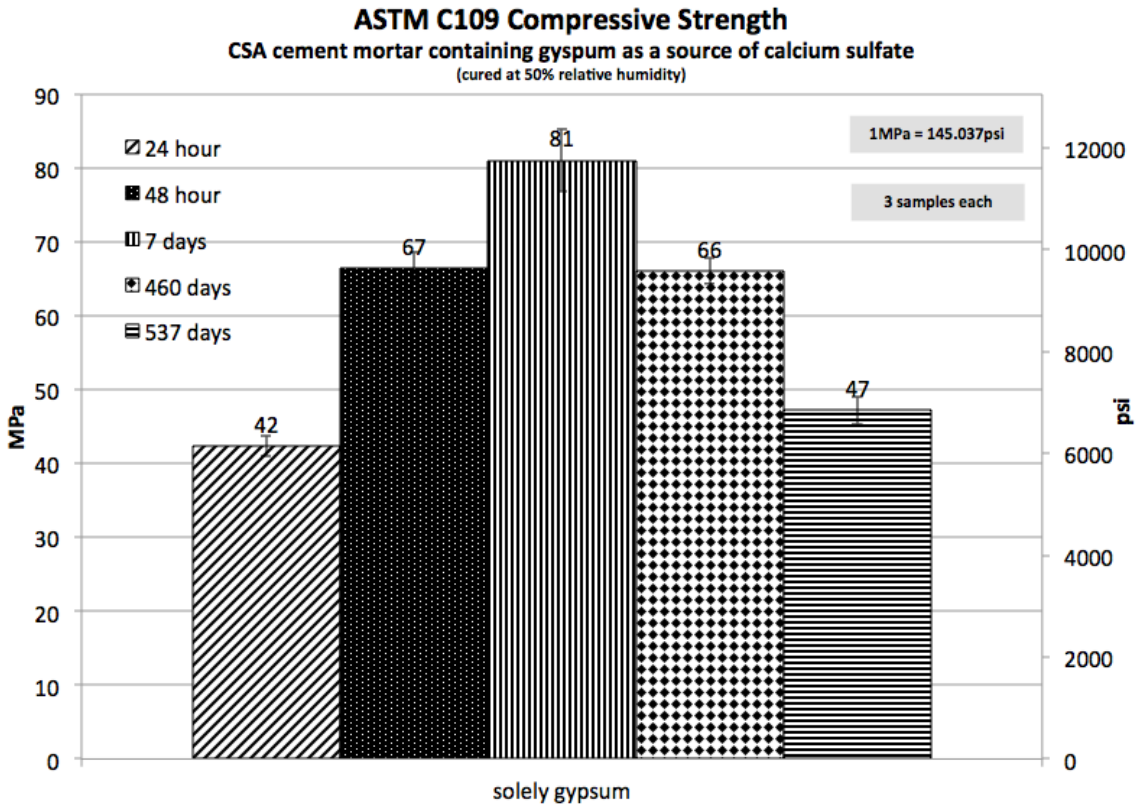

Figure 3.2.5: Compressive strength for CSA cement mortar containing solely gypsum displayed in Table 3.2.2 cured at ambient temperature and constant 50% relative humidity

DISCUSSION

Depending upon both the rate of formation and composition of the microstructure, calcium sulfoaluminate (CSA) cements can be employed as shrinkage resistant, self-stressing and high early strength cements, (Beretka et al, 1996). Such a range of application areas stems from selection of various constituent materials which ultimately hydrate to yield ettringite crystals with differing morphology (Beretka et al, 1996). It is well known both amount and type of incorporated calcium sulfate influences both rate of formation and composition of microstructure for CSA cement based materials (Winnefeld and Lothenbach, 2013, Winnefeld and Lothenbach, 2010, Beretka et al, 1996). Although extensive studies have been conducted on systems containing CSA cement, there is still a lack of firm relationships between microstructural features of ettringite-generating systems and their technical properties (Telesca et al, 2013). Although the information presented with this study does not allow for firm correlations to be drawn between microstructural characteristics and mechanical property performance, it does identify statistically significant strength loss behavior which should be utilized for further research endeavors. It is the author's opinion the old adage "the more you learn, the less you know" seems to readily apply to ettringite behavior.

Ettringite has a possible disadvantage in that it may decompose under extremes of normal, ambient conditions (Zhou and Glasser, 2001). Lea's Cement and Concrete, Fourth Edition, reports a system based upon $C_4A_3\overline{S}$ incorporating $C_5S_2\overline{S}$ rather than β-C_2S was found to show very high early and late strengths; however, strength loss occurred at ordinary humidity levels because carbonation led to decomposition of ettringite (Lawrence, 1998). Additionally, a similar system based upon $C_4A_3\overline{S}$ incorporating $C_5S_2\overline{S}$ rather than β-C_2S exposed to accelerated carbonation conditions for 28 days ultimately yielded a decrease in strength to about 67 percent of the initial value while the quantity of ettringite present fell from 47.9 to 18.5 percent (Lawrence, 1998).

The mechanism and reaction kinetics of ettringite decomposition and reconstitution are not well known (Zhou and Glasser, 2001). The principle decomposition products of ettringite are calcium sulfate dihydrate (gypsum), calcium carbonate and aluminum hydroxide (Grounds et al, 1988). Others describe ettringite decomposition products as $C_4A_3\overline{S}$, $CaSO_4$ and CaO, in agreement with reports cited in Lea (Zhou and Glasser, 2001). Furthermore, it has been suggested that ettringite decomposes to calcite, gypsum and

alumina gel by carbonation as follows, utilizing standard general chemistry nomenclature (Sato et al, 1992):

$$3CaO*Al_2O_3*3CaSO_4*32H_2O + 3CO_2 \rightarrow 3CaCO_3 + 3(CaSO_4{\cdot}2H_2O) + Al_2O_3{\cdot}xH_2O + (26\text{-}x)H_2O$$

Water is especially important to ettringite stability because of the high water content of the solid, which has the constitution, $3CaO{\cdot}Al_2O_3{\cdot}3CaSO_4{\cdot}30 + xH_2O$, where *x* is in the range of 0 to 2 (Zhou et al, 2001)."

A four stage process for water loss from ettringite is described as follows (Skoblinskaya et al, 1975):

- Water present in the channels will withdraw first thus reducing the total number of water molecules down to 30
- Second, the water molecules from the Ca polyhedra of the columns should withdraw, namely those which are at the additional apices of the trigonal prisms. These 12 being out, the number of water molecules is now reduced to 18
- Water molecules at the main vertices of the trigonal prisms will be displaced from their previous positions in the column and that will change somewhat the conditions of their interaction with SO_4 groups. Therefore a part of the bonds between the columns will be strained between loss of water molecules within the range from 18 to 6
- Finally, one should expect the withdrawal of the OH group from the Ca and Al polyhedral that will decrease n from 6 to 0…In this case the greatest reduction in strength for each column and for bonds between the columns can be expected. It may be accompanied by appearance of longitudinal and transverse cracks in the crystals as well as by their disintegration

Table 3.2.4 displays mass loss data for all ASTM C109 compressive strength cubes. The mass value corresponding to each cube was recorded both upon initial removal from the mold and immediately before testing. The CSA cement mortar cubes containing half gypsum and half anhydrite experienced mass loss of 1.7g and 7g after curing for 7 days and 537 days, respectively. The CSA cement mortar cubes containing solely gypsum experienced mass loss of 1.8g and 8.2g after curing for 7 days and 537 days, respectively.

Table 3.2.4: CSA CEMENT MORTAR CUBE MASS LOSS INFORMATION		
	cube mass loss: 50% anhydrite / 50% gypsum	cube mass loss: solely gypsum
7 day average for 3 cubes (g)	1.7	1.8
standard deviation	0.3	0.1
537 day average for 3 cubes (g)	7.0	8.2
standard deviation	0.6	0.4

Table 3.2.4: Average mass loss values for compressive strength testing of mortar cubes corresponding to formulations displayed in Table 3.2.2 after being cured at ambient laboratory temperature and 50% relative humidity for each specified interval (3 cubes each)

The compressive strength behavior displayed in Figures 3.2.4 and 3.2.5 together with the mass loss information displayed in Table 3.2.4 seems to correspond to the ettringite decomposition through dehydration mechanisms described by Skoblinskaya et al, (1975). The rationale presented by Zhou et al, (2004), for ettringite decomposition to metaettringite might also be utilized for describing the observed behaviors. The remaining paragraphs utilize both TGA/SDT analysis and XRD analysis to discuss the observed direct tensile strength trends.

Figure 3.2.6 displays TGA/SDT analysis for cement paste 1, containing solely anhydrite, in Table 3.2.3 after hydrating for 28 days and 242 days at 50% relative humidity and 23^{o}C. The peaks near 120^{o}C represent the concentration of ettringite in each sample. Such a designation for ettringite is in agreement with literature (Clark et al, 2006, Sherman et al, 1995). Figure 3.2.1 shows the CSA cement mortar corresponding to cement paste 1 in Table 3.2.3 beginning to show a decreasing direct tensile strength trend between 28 days and 56 days of hydration. The results listed in both Figure 3.2.1 and Figure 3.2.6 suggest a relationship exists between direct tensile strength and ettringite concentration. Although the experimental results suggest observed tensile strength losses correlate to processes associated with ettringite decomposition, the study was not designed to yield data sufficient for quantifying the observed behaviors.

The peaks located near 700^{o}C in Figure 3.2.6 represent calcium carbonate. It is interesting to note the increase in calcium carbonate concentration for cement paste 1 in

Table 3.2.3 after hydrating for both 28 days and 242 days at 50% relative humidity and 23°C.

Such an increase in calcium carbonate concentration at such a late stage in the hydration cycle suggests occurrence of ettringite decomposition type processes (Sherman et al, 1995, Sato et al, 1992).

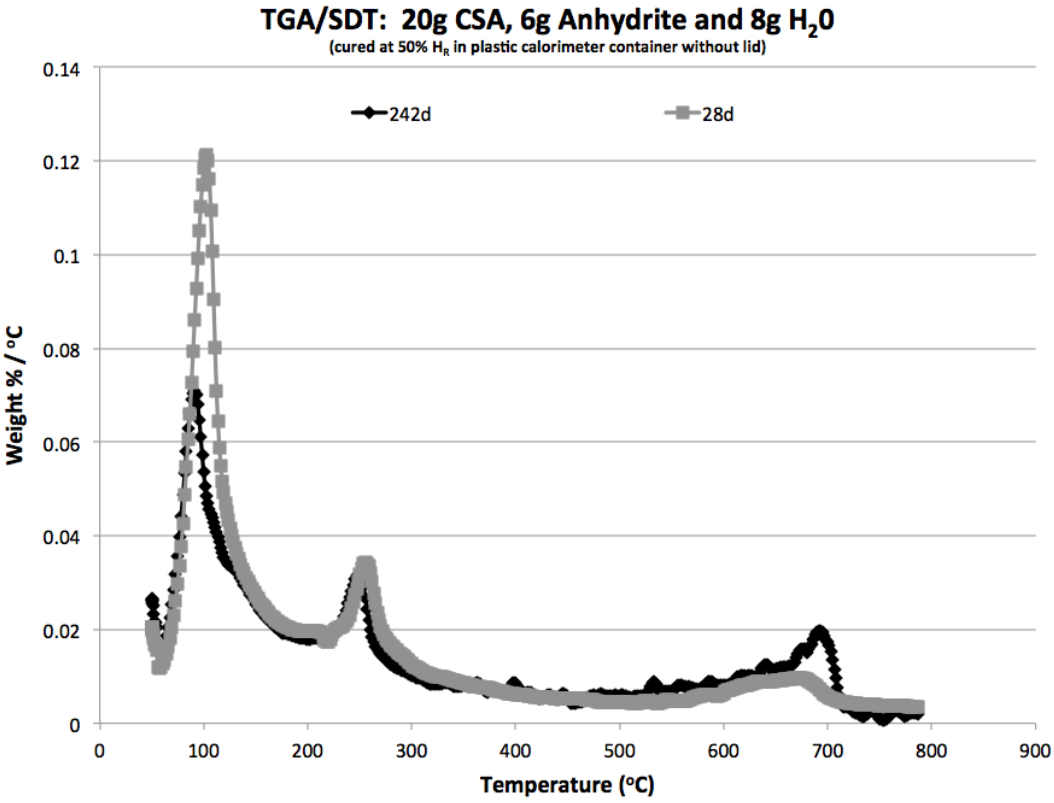

Figure 3.2.6: TGA/SDT analysis for CSA cement mortar containing solely anhydrite as a source of calcium sulfate

Interpretation of XRD analysis for sample 1 in Table 3.2.3 after curing for 242 days at 50% relative humidity yields the following characterization of constituent materials:

Yeelimite > Anhydrite >> Ettringite, $Ca_3Al_2O_6$ > Gamma Ca_2SiO_4, Belite

The concentration of ettringite in the XRD characterization relative to other constituent materials supports the TGA/SDT results displayed in Figure 3.2.6. The analytical results suggest the CSA cement mortar containing solely anhydrite is experiencing a decrease in ettringite concentration versus time. A decrease in ettringite concentration must create

changes in the microstructure for the CSA cement mortar. Such microstructural changes could very well explain the decreasing direct tensile strength trend displayed in Figure 3.2.1. For example, Skoblinskya et al, (1975), describe ettringite decomposition processes resulting in cracking of components comprising the material microstructure together with subsequent strength loss.

Figure 3.2.7 displays TGA/SDT analysis for cement paste 2, containing 50 weight % gypsum and 50 weight % anhydrite, in Table 3.2.3 after hydrating for 28 days and 242 days at 50% relative humidity and 23°C. As with Figure 3.2.6, the peak near 120°C represents the concentration of ettringite for each sample. This peak designation for ettringite agrees with literature (Clark et al, 2006 and Sherman et al, 1995). The second peak in Figure 3.2.7 near 150°C is theorized to represent gypsum. Figure 3.2.3 shows the CSA cement mortar corresponding to cement paste 2 in Table 3.2.3 beginning to show a decreasing direct tensile strength trend between 28 days and 56 days of hydration. Both the mechanical property and analytical results suggest a relationship exists between direct tensile strength and ettringite concentration. As previously mentioned, the author theorizes processes associated with ettringite decomposition create changes within the material microstructure resulting in subsequent strength loss.

As before, the peaks located near 700°C in Figure 3.2.7 represent calcium carbonate. It is interesting to note the increase in calcium carbonate concentration for cement paste 2 in Table 3.2.3 after hydrating for both 28 days and 242 days at 50% relative humidity and 23°C. As with all other presented trends, this data suggests ettringite decomposition is occurring, where the driving force is theorized to be associated with processes related to either carbonation or dehydration. Furthermore, processes theorized as being associated with ettringite decomposition inevitably alter the relationships amongst microstructural components potentially resulting in strength loss.

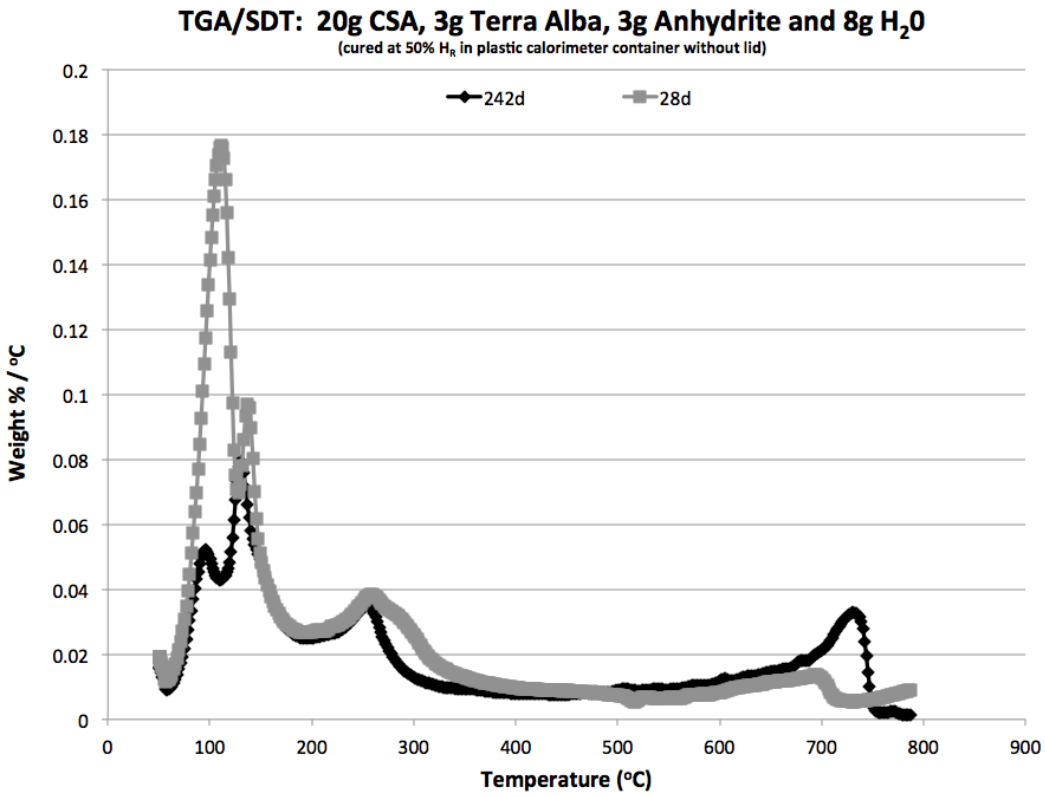

Figure 3.2.7: TGA/SDT analysis for CSA cement mortar with the source of calcium sulfate comprising 50 weight % anhydrite and 50 weight % gypsum

XRD analysis for sample 2 in Table 3.2.3 after curing for 249 days at 50% relative humidity yields the following characterization:

Yeelimite > Anhydrite > Gypsum > $Ca_3Al_2O_6$ > Ettringite, Wairakite, Belite, alpha Ca_2SiO_4

The concentration of ettringite in the XRD characterization relative to other constituent materials supports the TGA/SDT results displayed in Figure 3.2.7. The cement paste behavior displayed in Figures 3.2.6 and 3.2.7 suggests the CSA cement mortar containing 50 weight % anhydrite and 50 weight % gypsum is experiencing a decrease in ettringite concentration versus time. As with the other samples, a decrease in ettringite concentration must create changes in the microstructure for the CSA cement mortar. Such microstructural changes could very well explain the decreasing direct tensile strength trend displayed in Figure 3.2.2.

Figure 3.2.8 displays TGA/SDT analysis for cement paste 3, containing solely gypsum as a source of calcium sulfate, in Table 3.2.3 after hydrating for 28 days and 242 days at 50% relative humidity and 23°C. As with the other TGA/SDT results, the peak near 120°C represents the concentration of ettringite for each sample. The peak at approximately 150°C is theorized to be gypsum. Figure 3.2.3 shows the CSA cement mortar corresponding to cement paste 3 in Table 3.2.3 beginning to show a decreasing direct tensile strength trend between 7 days and 28 days of hydration. The results listed in both Figure 3.2.8 and Figure 3.2.9 suggest a relationship exists between direct tensile strength and ettringite concentration; however, more data is needed to quantify the relationship.

The peaks located near 700°C in Figure 3.2.9 represent calcium carbonate. It is interesting to note the increase in calcium carbonate concentration for cement paste 3 in Table 3.2.2 after hydrating for both 28 days and 242 days at 50% relative humidity and 23°C. In similar fashion to other present trends, this data suggests ettringite decomposition (Sherman et al, 1995, Sato et al, 1992). The author ponders dehydration as potentially the correct mechanism for ettringite decomposition in this low humidity environment.

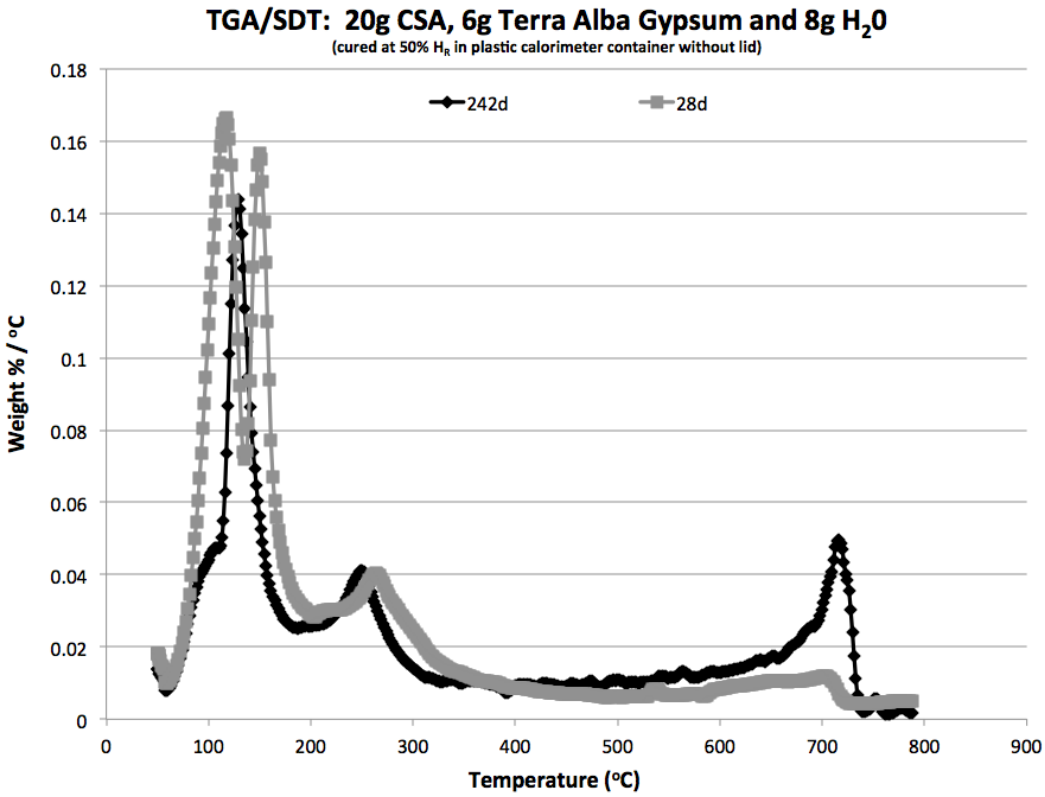

Figure 3.2.8: TGA/SDT analysis for CSA cement mortar containing solely gypsum as a source of calcium sulfate

XRD analysis for sample 3 in Table 3.2.3 after curing for 249 days at 50% relative humidity yields the following characterization:

Yeelimite, Gypsum >> $Ca_3Al_2O_6$ > Ettringite, Belite, Wairakite, Alpha Ca_2SiO_4?, Gamma Ca_2SiO_4 > Anhydrite

The concentration of ettringite in the XRD characterization relative to other constituent materials supports the TGA/SDT results displayed in Figure 3.2.8. As with all other presented information, the cement paste behavior suggests the CSA cement mortar containing solely gypsum is experiencing a decrease in ettringite concentration versus time. This and all other data suggests dehydration to be a potential mechanism for ettringite decomposition and related strength loss for the tested CSA cement mortars.

CONCLUSIONS

In conclusion, the results presented in this study further muddy the waters, so to speak, in regard to understanding the long term strength behavior of calcium sulfoaluminate (CSA) cement systems cured at low humidity for extended periods of time. The statement from Taylor (1997), that carbonation behavior of cementitious systems may be overstated in laboratory conditions given higher exposed surface area / total volume ratios for the tested samples may indeed be applicable to the presented results. Or, perhaps such a statement can also be extrapolated to the case of ettringite decomposition through dehydration, as sample size will certainly influence the heat and mass transfer processes necessary for desiccation.

. The results of this study were largely unexpected. The study presents observations pertaining to relationships between mechanical property performance and microstructural characteristics. However, given time constraints, the author was not afforded the opportunity to further study the presented observations. Nevertheless, the experimental results demonstrate statistically significant strength loss for four CSA cement mortars cured at ambient laboratory temperature and constant 50% relative humidity for various mechanical property testing scenarios. Furthermore, the results presented in this study suggest that onset of both strength loss and theorized ettringite decomposition are influenced by both amount and type of calcium sulfate incorporated into specific

formulations. The water / cement (w/c) ratio for all mortars was low. However, the w/c for a gypsum containing mortar was higher than w/c for the anhydrite containing mortars, even excluding the chemically bound water inherent to gypsum. It is quite interesting to note that this gypsum containing mortar with the highest w/c ratio experienced the earliest onset of strength loss when compared with the other mortars.

The experimental results suggest CSA cement mortars seemingly continue to lose strength when cured at constant low humidity for extended periods of time. Therefore, the presented results raise questions regarding which mechanical property performance values to utilize during design of reinforced concrete structures based upon CSA cement. Do materials manufactured with CSA cement continually lose strength when cured at constant low humidity, and thus render themselves unsuitable for structural type applications in low humidity environments? Or, do materials based upon CSA cement demonstrate some sort of peak strength behavior while eventually reaching some asymptotic strength value with time, thus defining their suitability for use in structural applications in low humidity environments?

The presented long term mechanical property performance information for CSA cement mortars cured at constant low humidity is indeed significant. It appears that ettringite decomposition through dehydration type processes is the contributing cause for both observed strength loss and microstructural changes within the tested CSA cement based materials.

The information presented in this study highlights the need for additional testing of materials comprising CSA cement when cured at constant low humidity.

3 REFERENCES:

- Beretka, J., Marroccoli, M., Sherman, N., Valenti, G., 1996, The Influence of C4A3S Content and W/S Ratio on the Performance of Calcium Sulfoaluminate Based Cements, Cement and Concrete Research, Vol. 26, No. 11, pp 1673-1681, 1996
- Chandra, S., Berntsson, L., 2003, Lightweight Aggregate Concrete, Science, Technology and Applications, Building Materials Series ISBN 0-8155-1486-7
- Clark, S., Colas, B., Kunz, M., Speziale, S., Monteiro, P., 2006, Effect of pressure on the crystal structure of ettringite, Cement and Concrete Research 38 (2008) 19-26
- Glasser, F., Zhang, L., 2001, High-performance cement matrices based on calcium sulfo-aluminate-belite compositions, Cement and Concrete Research 31 (2001) 1881-1886
- Grounds, T., Midgley, H., Nowell, D., 1988, Carbonation of Ettringite by Atmospheric Carbon Dioxide, Thermochimica Acta, 135 (1988) 347-352
- Jewell, R., Rathbone, R., Robl, T., Henke, K., 2009, Fabrication and Testing of CSAB Cements in Mortar and Concrete that Utilize Circulating Fluidized Bed Combustion Byproducts, 2009 World of Coal Ash (WOCA) Conference, 4-7May2009, Lexington, KY, USA, http://www.flyash.info
- Lawrence, C.D., Hewlett, P., 1998, Production of Low Energy Cements, Chapter 9, Lea's Chemistry of Cement and Concrete, 4th Edition, Arnold, John Wiley and Sons, New
- NOAA, National Weather Service, www.noaa.gov, relative humidity = www.erh.noaa.gov/er/gyx/climo/avgrh.html
- Sato, K., Takebe, T., 1992, Decomposition of Synthesized Ettringite by Carbonation, Cement and Concrete Research 22 (1992) 6-14
- Scrivener, K., Nonat, A., 2011, Hydration of cementitious materials, present and future, Cement and Concrete Research 41 (2011) 651-665
- Sherman, N., Beretka, J., Santoro, L., Valenti, G., 1995, Long-Term Behaviour of Hydraulic Binders Based on Calcium Sulfoaluminate and Calcium Sulfosilicate, Cement and Concrete Research, Vol. 25, No. 1, pp. 113-126
- Skoblinskaya, N., Krasilnikov, K., 1975, Changes in Crystal Structure of Ettringite on Dehydration 1, Cement and Concrete Research, Vol. 5, pp. 381-394, 1975

- Skoblinskaya, N., Krasilnikov, K., Nikitina, L., Varlamov, V., 1975, Changes in Crystal Structure of Ettringite on Dehydration 2, Cement and Concrete Research, Vol. 5, pp. 419-432, 1975
- Taylor, H., 1997, Cement Chemistry, Second Edition, Thomas Telford Publishing, 1997, ISBN 0 7277 2592 0
- Telesca, A.,.Marroccoli, M., Tomasulo, M., Valenti, G., Allevi, S., Marchi, M., 2013, Microstructural Features and Technical Properties of Calcium Sulfoaluminate Based Cements, Proceedings of The First International Conference on Sulphoaluminate Cement: Materials and Engineering Technology, Wuhan, China, October, 2013
- Winnefeld, F., Barlag, S., 2010, Calorimetric and thermogravimetric study on the influence of calcium sulfate on the hydration of yeelimite, Journal of Thermal Analysis and Calorimetry (2010) 101:949-957
- Winnefeld, F., Lothenbach, B., 2013, Thermodynamic modeling of hydration of calcium sulfoaluminate cements blended with mineral additions, Proceedings of the First International Conference on Sulphoaluminate Cement, Materials and Engineering Technology, Wuhan University of Technology, Wuhan, China, 23-25Oct2013
- Winnefeld, F., Lothenbach, B., 2010, Hydration of calcium sulfoaluminate cements – Experimental findings and thermodynamic modeling, Cement and Concrete Research 40 (2010) 1239-1247
- World Business Council for Sustainable Development, http://www.wbcsd.org
- Zhang, L., Glasser, F., 2005, Investigation of the microstructure and carbonation of CSA based concretes removed from service, Cement and Concrete Research 35 (2005) 2252-2260
- Zhou, Q., Glasser, F., 2001, Thermal stability and decomposition mechanisms of ettringite at <120^{o}C, Cement and Concrete Research 31 (2001) 1333-1339
- Zhou, Q., Lachowski, E., Glasser, F., 2004, Metaettringite, a decomposition product of ettringite, Cement and Concrete Research 34 (2004) 703-710

Chapter 4: Influence of Admixtures on CSA Cement Mortars

Chapter 4 presents information pertaining to yet another very important step in the iterative process associated with developing dry mix mortar materials when little literature is available describing interactions of various constituent components. The primary deliverable for such a step in the research process is to ascertain whether specific admixtures are indeed compatible with the experimental CSA cement. The first study examines the influence of tartaric acid on the early age behavior of rapid setting systems based on CSA cement. The second portion presents information pertaining to the influence of lithium carbonate, hydroxyethylmethyl cellulose (HEMC) and superplasticizer on mechanical property performance behavior of CSA cement materials.

4.1 Use of Tartaric Acid as a Retarding Agent for CSA Cement Hydration

INTRODUCTION

The hydration of cementitious systems is obviously far more complex than the sum of the hydration reactions of the individual materials (Bishop et al, 2006). Furthermore, there are still many unanswered questions on the kinetics and thermodynamics of early age cement hydration (Xu and Stark, 2005). Additionally, inclusion of additives such as accelerators and retarders, tends to change hydration processes and conditions within the developing microstructure (Xu and Stark, 2005). If sufficient literature is not available describing interactions of specific hydraulic binders with various constituent materials, prudence dictates the materials be evaluated for compatibility. Little information is available describing the interactions of calcium sulfoaluminate (CSA) cement containing minor phase tri-calcium aluminate in the presence of commonly used accelerating or retarding admixtures, with examples being lithium carbonate and tartaric acid, respectively. Lithium carbonate and tartaric acid are commonly utilized with ettringite forming systems (Anderberg and Wadso, 2010, Baumann et al, 2007).

Accelerators cause very rapid hydration in the first few minutes after mixing, where such rapid setting often makes sample preparation difficult (Xu and Stark, 2005). Therefore, it is sometimes necessary to include retarding mixtures in an effort to increase the working life of the hydrating system. Tartaric acid was included to delay onset of

hydration reactions for the developed rapid setting mortars. Tartaric acid is a chelating agent conveniently described with the following quotes: "a typical chelating unit forms a strong six membered ring with a metal ion. For example, tartaric acid contains this grouping and thus is a strong retarder. The retarding effect is related to the molecules ability to chelate at more than one site (Chandra et al, 1994)." It is well known that CSA cement hydrates to form ettringite (Marraccoli et al, 2010, Gastaldi et al, 2009). Tartaric acid has been labeled as "the most effective retarder for shutting down ettringite formation" (Bishop et al., 2006).

MATERIALS

Cement

Calcium sulfoaluminate cement (CSA) containing tri-calcium aluminate (C_3A) was utilized in this experiment.

Anhydrite

Calcium sulfate anhydrite for this experiment was sourced from Allied Custom Gypsum.

Aggregate

ASTM finely graded sand from Ottawa Illinois was used in all formulations. A coarser, 20/30 sand, was also utilized in all formulations.

Tartaric Acid

Reagent grade tartaric acid sourced from Fischer Scientific was utilized in this experiment.

Lithium Carbonate

Reagent grade lithium carbonate sourced from Fischer Scientific was utilized in this experiment.

Mortars

Three mortar formulations were created with differing amounts of tartaric acid by mass – 0.12%, 0.17% and 0.26%. Cement mass remained constant across all formulations. Lithium carbonate mass remained constant across all formulations. Aggregate mass remained constant across all formulations. A water / cement ratio of 0.31 was used for all cement pastes and mortars. Individual mortar components were weighed and placed into a

plastic mixing bag. After all components were added, the bag was sealed and shaken vigorously by hand for approximately ninety seconds. This type of mixing is an industry proven simulation for blending operations manufacturing dry mix mortar products containing minute quantities of additives such as accelerators and retarders. Table 4.1.2 lists mortar formulations analyzed in this experiment.

Table 4.1.1: CSA CEMENT PASTE FORMULATIONS FOR CALORIMETER ANALYSIS			
Cement Paste Data	Sample 1	Sample 2	Sample 3
Materials	mass(g)	mass(g)	mass(g)
CSA Cement	20	20	20
Anhydrite	6	6	6
Tartaric Acid	0.05	0.1	0.15
Total Mass	26.05	26.1	26.15
DI Water	8	8	8

Table 4.1.1: CSA cement paste formulations for calorimeter analysis

Table 4.1.2: CSA CEMENT MORTAR FORMULATIONS FOR COMPRESSIVE STRENGTH TESTING			
Cement Mortar Data	RT1	RT2	RT3
Materials	Percentage (%)	Percentage (%)	Percentage (%)
CSA Cement	23.11	23.1	23.08
Anhydrite	7.4	7.39	7.38
Lithium Carbonate	0.05	0.05	0.05
Graded Sand	63.55	63.52	63.46
23-30 Sand	5.78	5.77	5.77
Tartaric Acid	0.12	0.17	0.26
Total %	100	100	100

Table 4.1.2: CSA cement mortar mix designs for compressive strength testing

Table 4.1.3: CSA CEMENT PASTE FORMULATIONS FOR TGA/SDT ANALYSIS			
Cement Paste Data	RT1	RT2	RT3
Materials	mass (g)	mass (g)	mass (g)
CSA Cement	20	20	20
Anhydrite	6	6	6
Lithium Carbonate	0.05	0.05	0.05
Tartaric Acid	0.1	0.15	0.23
Total Mass	26.15	26.2	26.28
DI Water	8	8	8

Table 4.1.3: CSA cement paste formulations for TGA/SDT analysis

EXPERIMENTAL PROGRAM

For this study, an isothermal calorimeter was used to measure hydration characteristics of three CSA cement pastes. The pastes differ only in percent mass of tartaric acid – 0.12%, 0.17% and 0.26%. CSA cement mortars with similar constituent compositions were created for early age compressive strength evaluation. The mortar mix designs differ from the calorimeter cement paste analysis as the mortar mix designs contain lithium carbonate.

Calorimeter Analysis

CSA cement paste formulations listed in Table 4.1.1 were prepared for calorimeter analysis. An isothermal calorimeter was used to acquire data illustrating hydration characteristics for the cement pastes being studied. This is an eight channel calorimeter specifically designed for cementitious materials analyses.

Sample preparation techniques required cement paste constituent materials to be individually weighed and placed into a small, plastic calorimeter container. After addition of individual dry constituent materials, the lid was placed on the small, plastic calorimeter container, and the dry components were thoroughly mixed by vigorously shaking the container for approximately thirty seconds. After mixing, the container lid was removed and an exact mass of deionized was added to the calorimeter container. A spatula was used

to provide hand type mixing in an effort to bring the dry constituent materials and deionized water into paste form, thus creating individual cement pastes. After each paste was formed, the plastic calorimeter container lid was securely sealed and the item was placed in its corresponding channel in the calorimeter jacket block for hydration analysis.

Compressive Strength Test

Mortar cube specimens were cast in accordance to ASTM C109, Standard Test Method for Compressive Strength of Hydraulic Cement Mortars. Three mortar cubes were cast for each mix design. The cubes were tested after three hours of curing on the bench top in brass molds while covered with plastic.

Thermogravimetric Analysis (TGA)

Cement paste samples were prepared for TGA analysis according to the formulations listed in Table 4.1.3. Cement paste samples were cured in a small, plastic calorimeter container with a lid at ambient laboratory temperature. Sample specimens were taken from each calorimeter container after each CSA cement paste had hydrated for a period of three hours. Cement paste sample specimens were ground to a fine powder using a mortar and pestle. The samples were washed with acetone after being finely ground. The samples were placed in an oven at 45^{o}C for an hour after washing with acetone. TGA analysis was conducted using a SDT 600 from TA Instruments while using one cycle with a temperature ramp rate of 20^{o}C per minute through a final cycle temperature 800^{o}C.

Test Results and Discussion

Test Results

Figure 4.1.1 displays calorimeter trends for energy released during the first 200,000 seconds (55.6hrs) of CSA cement paste hydration. Figure 4.1.1 presents observations regarding the testing of one sample for each formulation. The results presented in Figure 4.1.1 are not statistically significant results given only one sample was analyzed for each formulation. Mass amounts of cement paste constituent materials shown in Figure 4.1.1 can be viewed in Table 4.1.1. Trend lines in Figure 4.1.1 represent total energy released during the exothermic hydration reaction. Typically, trend line regions with steeper slopes

represent more rapid rates of hydration as more energy is released per unit time during the hydration reaction.

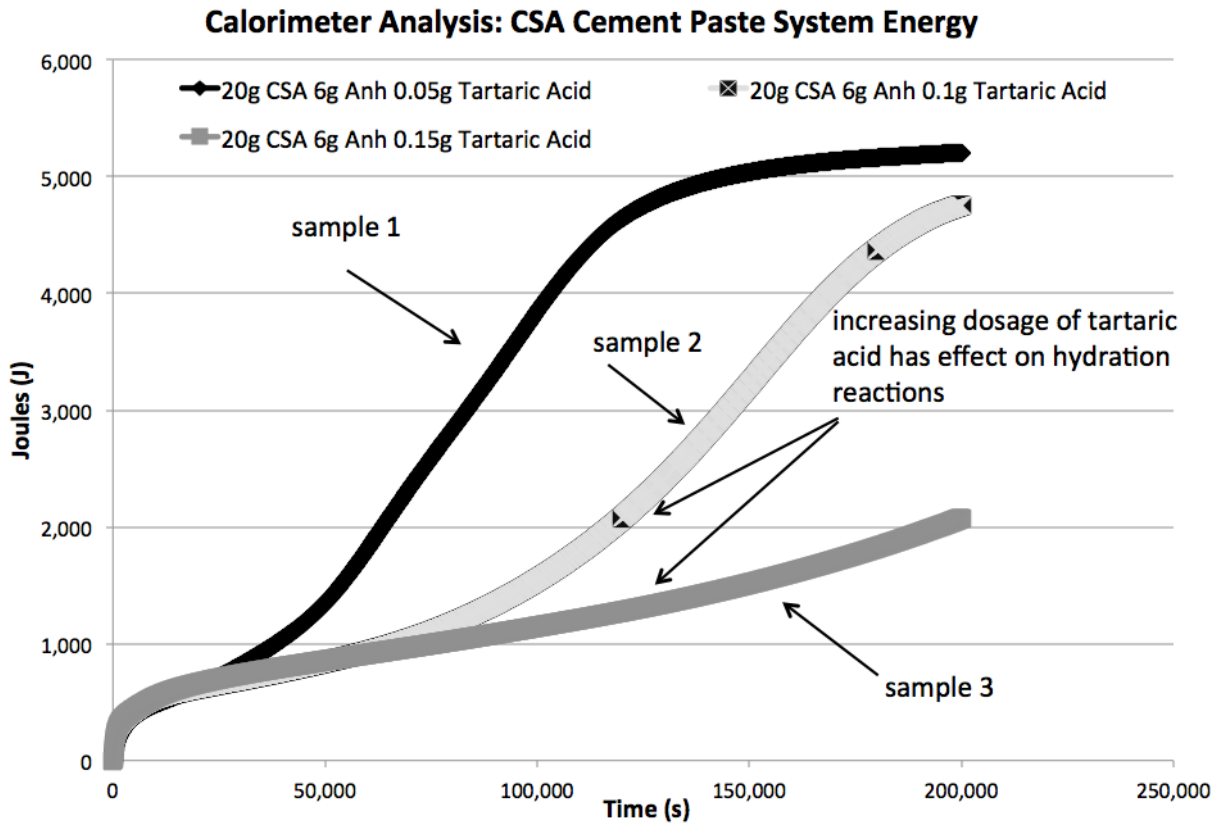

Figure 4.1.1: Calorimeter data for cement pastes listed in Table 4.1.1 illustrating total liberated energy for hydration reaction of CSA cement pastes containing 0.12%, 0.17% and 0.26% tartaric acid with w/c = 0.31.

The trend line for sample 1 containing 0.12% (0.05g) tartaric acid (black line) shows hydration accelerates around 50,000s (13.8hrs) and begins to slow at 160,000s (44.4hrs) after liberating 5000J of energy.

The trend line for sample 2 containing 0.17% (0.1g) tartaric acid (gray line) shows hydration accelerates around 97,000s (26.9hrs) and begins to slow at 200,000s (55.6hrs) after liberating more than 4500J of energy.

The trend line for sample 3 containing 0.26% (0.15g) tartaric acid (dark gray line) shows hydration beginning to accelerate around 200,000s (55.6hrs). The experiment was stopped at 200,000s due to unforeseen circumstances.

Figure 4.1.2 lists three hour compressive strength values for CSA cement mortar mix designs listed in Table 4.1.2. These mortars contain 0.12%, 0.17% and 0.26% tartaric acid while having a constant water to cement ratio w/c = 0.31. Formulation RT1 contained 0.12% tartaric acid and yielded a three-hour compressive strength of 15.26MPa (2,213psi). Formulation RT2 contained 0.17% tartaric acid and yielded a three-hour compressive strength of 5.88MPa (852psi). Formulation RT3 contained 0.26% tartaric acid and yielded a three-hour compressive strength of 2.79MPa (404psi).

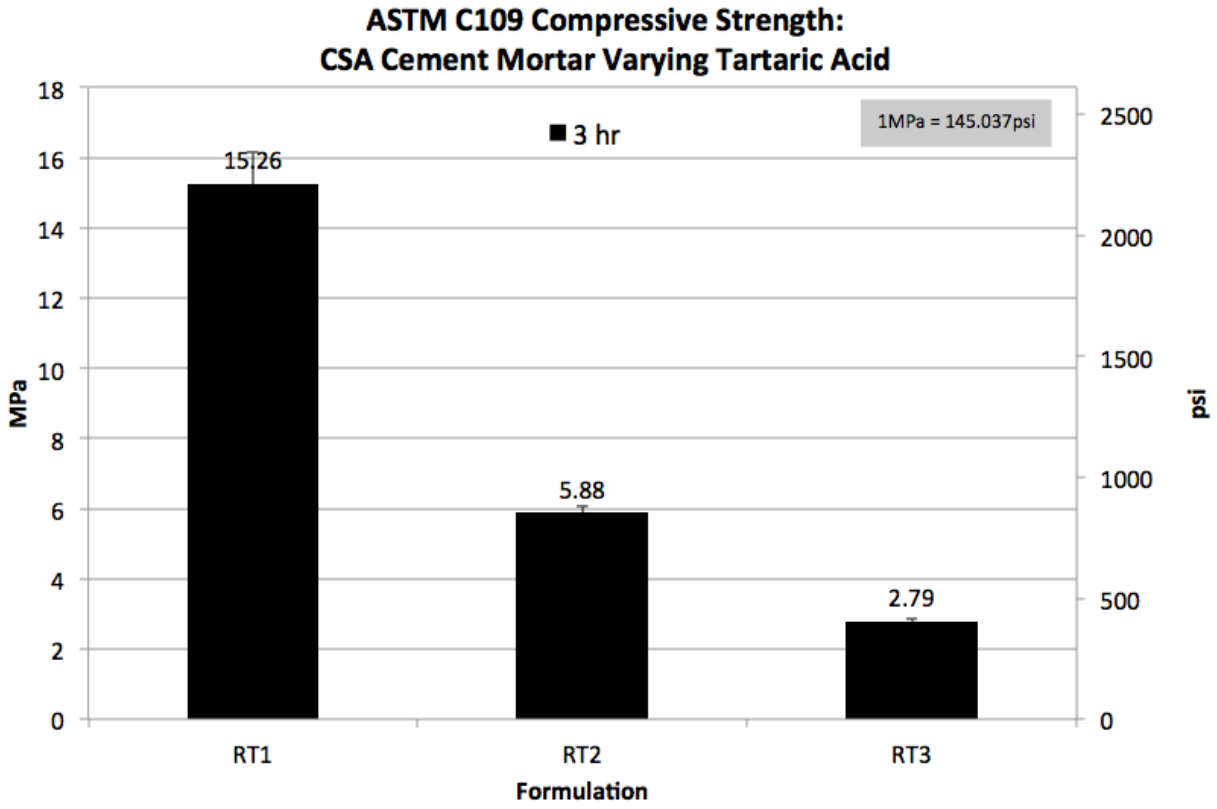

Figure 4.1.2: Three hour compressive strength evaluation for CSA cement mortars listed in Table 4.1.2. (3 cubes each)

Figure 4.1.3 illustrates trend lines resulting from TGA analysis for the CSA cement paste mix designs listed in Table 4.1.3. The CSA cement paste mix designs listed in Table 4.1.3 correspond to the CSA cement mortars listed in Table 4.1.2. Both the CSA cement mortar information listed in Figure 4.1.2 and the CSA cement paste information listed in Figure 4.1.3 represent "accelerated" hydration systems. The mix designs listed in both Table 4.1.2 and Table 4.1.3 contain lithium carbonate. Lithium carbonate was included in CSA cement paste mix designs for TGA analysis in an effort to gain an understanding of

ettringite formation and its relation to compressive strength during the first three hours of hydration.

The observations presented in Figure 4.1.3 support the compressive strength data displayed in Figure 4.1.2. Although the observations are based on one sample, such observations might be utilized for design of future experiments with specific task of correlating the relationship between microstructural constituents and material behavior. The peaks near 120°C represent the concentrations of ettringite present in each sample. Cement paste sample RT1 contains the greatest concentration of ettringite after three hours hydration. Cement paste RT2 contains an ettringite concentration less than RT1 and greater than RT3. Cement paste RT3 contains the least concentration of ettringite after three hours hydration. Decreasing concentrations of ettringite present in CSA cement paste samples RT1, RT2 and RT3 explain the decreasing strength trend displayed in Figure 4.1.2 for CSA cement mortar mix designs RT1, RT2 and RT3 displayed in Table 4.1.2.

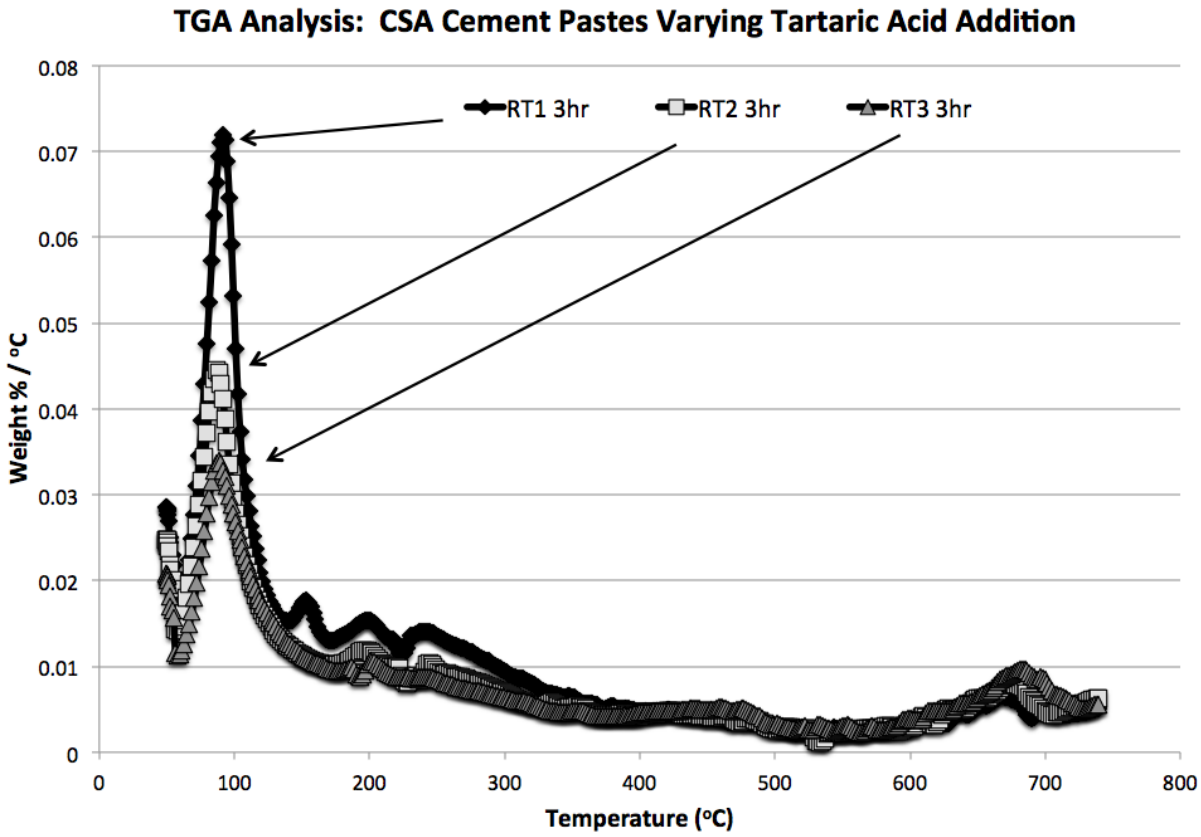

Figure 4.1.3: Thermogravimetric analysis (TGA) results illustrating differences in ettringite concentrations for CSA cement paste formulations listed in Table 4.1.3 after hydrating for three hours in a sealed plastic calorimeter container.

DISCUSSION

The results presented in both Figure 4.1.1 and Figure 4.1.2 correlate well with each other. Onset of hydration occurred first for the cement paste corresponding to mortar mix design RT1, which is the mix design containing the least amount of tartaric acid. It stands to reason that the mortar formulation containing the least amount of tartaric acid retarding agent would be the first to undergo hydration thus yielding the greatest three-hour compressive strength values. This is further supported by the TGA trend line displayed in Figure 4.1.3 which suggests sample RT1 contains the greatest concentration of ettringite after three hours of hydration. The cement paste corresponding to mortar mix design RT2, which contains the second highest dose of tartaric acid, experienced onset of hydration after the cement paste associated with RT1 and before the cement paste associated with RT3. Again, it stands to reason that the mix design containing the second highest amount of tartaric acid retarding agent would be the second to undergo onset of hydration while also possessing the second highest three hour compressive strength values. This is further supported by the TGA trend line displayed in Figure 4.1.3 which suggests sample RT2 contains the second highest concentration of ettringite after three hours of hydration. The cement paste corresponding to mortar mix design RT3 was the last cement paste to experience onset of hydration. This observation follows the convention of the other tested materials such that the mix design with the greatest amount of tartaric acid retarding agent was the last to experience onset of hydration while its corresponding mortar mix design RT3 demonstrated the lowest compressive strength values after hydrating for three hours. This is further supported by the TGA trend line displayed in Figure 4.1.3 which suggests sample RT3 contains the smallest concentration of ettringite after three hours of hydration.

CONCLUSION

In conclusion, the results presented in this study suggest tartaric acid to be an effective retarding agent for calcium sulfoaluminate (CSA) cement. The analyzed cement pastes illustrated in Figure 4.1.1 do not contain the accelerating admixture lithium carbonate. The analyzed mortars do contain the accelerating admixture lithium carbonate. Certainly, if lithium carbonate had been included in the cement paste compositions listed in Table 4.1.1, the results displayed in Figure 4.1.1 would differ from the reported data. Lithium carbonate was omitted from the calorimeter cement paste study in an effort to truly understand the retarding potential of tartaric acid when combined with CSA cement. If

lithium carbonate had not been included in the mortar study mix designs, the author theorizes the mortar cubes would have been far too weak for testing after a curing period of three hours. Nevertheless, the experimental results from both the calorimeter paste study, the TGA paste study and the mortar study demonstrate the effectiveness of tartaric acid as a retarding agent for CSA cement systems which may or may not include accelerating admixtures.

As previously inferred, both calorimeter data and compressive strength data suggest that increasing the constituent percentage of tartaric acid in mix designs increases the time required for onset of hydration resulting in an overall decrease of early age compressive strength for corresponding CSA cement mortar cubes.

(i) Mortar mix design RT1 and its corresponding, non-accelerated cement paste contained the least amount of tartaric acid. The calorimeter cement paste associated with mortar mix design RT1 experienced onset of hydration after approximately 50,000 seconds (14 hours). The accelerated TGA cement paste corresponding to RT1 contained the greatest concentration of ettringite after three hours hydration while RT1 mortar cubes demonstrated the greatest three hour average compressive strength value of 15.26MPa (2,213psi).

(ii) Mortar mix design RT2 and its corresponding, non-accelerated cement paste contained the second highest amount of tartaric acid. The calorimeter cement paste associated with mortar mix design RT2 experienced onset of hydration after approximately 97,000 seconds (27 hours). The accelerated TGA cement paste corresponding to RT2 contained the second largest concentration of ettringite after three hours hydration while RT2 mortar cubes demonstrated a three hour average compressive strength value of 5.88MPa (852psi), which was the second greatest reported strength.

(iii) Mortar mix design RT3 and its corresponding, non-accelerated cement paste contained the greatest amount of tartaric acid. The calorimeter cement paste associated with mortar mix design RT3 experienced onset of hydration after approximately 200,000 seconds (55.5 hours). The accelerated TGA cement paste corresponding to RT3 contained the lowest concentration of ettringite after three hours hydration while RT3 mortar cubes demonstrated a three hour average compressive strength value of 2.79MPa (404psi), which was the lowest reported strength value.

4.2 Influence of Lithium Carbonate, HEMC and superplasticizer on 28 day strength

The purpose of this study was to assess the influence of lithium carbonate, HEMC and superplasticizer on strength development in CSA cement mortars. These materials comprise a tool kit for altering the rheology characteristics of cementitious systems. Literature is scarce describing combinations of these materials with such unique CSA cement containing minor phase tri-calcium aluminate. Given the scarcity of literature, it was necessary to test various combinations of these materials throughout the design process in an effort to understand factors most critical to strength development.

Lithium carbonate is well known for accelerating hydration reactions associated with ettringite formation (Pera et al, 2004, Scrivener et al, 1998, Taylor, 1997). Lithium carbonate was included to accelerate CSA cement hydration reactions for development of the rapid setting mortars.

Hydroxyethyl methyl cellulose (HEMC) is a commonly used viscosity modifier for cementitious systems. One common use for HEMC is oil well cementing (Bensted 1998). One objective of cement viscosity modification is to maintain a uniform distribution of water throughout the cement microstructure during the hydration process (Bensted 1998). Cementitious materials applied in well bores can sometimes be exposed to high pressure, inclusion of HEMC in mix designs allows water to remain within the hydrating cement matrix as opposed to the water being driven from the cement matrix by pressure effects. The author theorizes these water retention characteristics inherent to HEMC will improve hydration characteristics for otherwise rapidly desiccating CSA cements.

MATERIALS

Cement

CSA cement containing C_3A, tri-calcium aluminate, was utilized in this study. XRD analysis provides the following listing of constituent materials:

Yeelimite >> C_3A > Belite > Anhydrite (trace quantity)

Anhydrite

Calcium sulfate anhydrite for this study was sourced from Allied Custom Gypsum. This anhydrite has a variable particle size, typically with approximately 50% passing three microns while having a top size of approximately 10% retained on a 45 micron sieve with the remainder being a continuous distribution down to dust.

HEMC

Hydroxyethyl methyl cellulose (HEMC) polymeric material with medium viscosity was utilized in various experiments.

Superplasticizer

Spray dried powders of modified polycarboxylic ether were utilized in this study.

Lithium Carbonate

Reagent grade lithium carbonate sourced from Fisher Scientific was included in all applicable mortar mix designs.

EXPERIMENTAL PROGRAM

For this experimental work, an isothermal calorimeter was used to measure hydration characteristics of two CSA cement pastes, one that contains lithium carbonate and one that does not contain lithium carbonate. CSA cement mortars with similar constituent compositions were cast for compressive strength analysis following ASTM C109 after curing for 1hr, 6hr, 24hr, 48hr, 7d and 28d at 50% relative humidity and 23^{o}C.

CSA cement mortars containing HEMC were evaluated. One series of tests assessed the influence of water / cement ratio on direct tensile strength behavior of CSA cement containing constant amounts of HEMC after curing for 7 days at ambient laboratory temperature of 23^{o}C and constant 50% relative humidity. One series of tests assessed the influence of lithium carbonate addition on compressive strength of CSA cement mortars containing constant amounts of HEMC after curing for 28 days at ambient laboratory temperature of 23^{o}C and 50% relative humidity.

The simplest of CSA cement mortars containing anhydrite as a source of calcium sulfate were tested to assess the influence of lithium carbonate concentration on both

compressive and tensile strength behavior after curing for 28 days at ambient laboratory temperature of 23°C and 50% relative humidity. One additional series of mortars was subsequently evaluated to assess the influence of superplasticizer addition on both compressive and direct tensile strength behavior of these simple mortars containing anhydrite and lithium carbonate.

Calorimeter Analysis

CSA cement paste formulations listed in Table 4.2.1 were prepared for calorimeter analysis. An isothermal calorimeter was used to acquire data illustrating hydration characteristics for the cement pastes being studied. This is an eight channel calorimeter specifically designed for cementitious materials analysis.

Sample preparation techniques required cement paste constituent materials to be individually weighed and placed into a small, plastic calorimeter container. After addition of individual dry constituent materials, the lid was placed on the small, plastic calorimeter container, and the dry components were thoroughly mixed by vigorously shaking the container for approximately thirty seconds. After mixing, the container lid was removed and an exact mass of deionized water was added to the calorimeter container. A spatula was used to provide hand type mixing in an effort to bring the dry constituent materials and deionized water into paste form, thus creating individual cement pastes. After each paste was formed, the plastic calorimeter container lid was securely sealed and the item was placed in its corresponding channel in the calorimeter jacket block for hydration analysis.

Compressive Strength Test

Mortar cube specimens were cast in accordance to ASTM C109, Standard Test Method for Compressive Strength of Hydraulic Cement Mortars. Three mortar cubes were cast for each mix design. The cubes were tested after curing at constant 50% relative humidity and 23°C.

Direct Tensile Strength Test

Mortar dog bone specimens were cast in accordance to ASTM C307, Standard Test Method for Tensile Strength of Chemical Resistant Mortars, Grouts and Monolithic Surfaces. Three samples were cast for each mix design. The samples were tested after curing at constant 50% relative humidity and 23°C with an Instron 600DX universal testing machine

equipped with special grips for accommodating dog bone samples associated with test method ASTM C307.

RESULTS AND DISCUSSION

Table 4.2.1 lists CSA cement paste formulations for the calorimeter analysis displayed in Figure 4.2.1. The CSA cement pastes in Table 4.2.1 differ in concentration of lithium carbonate. Lithium carbonate is a commonly used accelerating agent for improving early age strength performance in ettringite forming systems. It is well known that small concentrations of lithium carbonate have a profound influence on hydration characteristics of ettringite forming systems (Pera et al, 2004, Scrivener et al, 1998, Taylor, 1997). It is also known that lithium carbonate addition sometimes decreases later age strength performance for ettringite forming systems. Nevertheless, lithium carbonate serves as a wonderful tool for adjusting hydration characteristics of mortars containing CSA cement with minor phase tri-calcium aluminate.

Table 4.2.1: CSA CEMENT PASTE FORMULATIONS FOR CALORIMETER ANALYSIS		
Constituent Materials (mass)	Control	Lithium Carbonate
CSA Cement (g)	20	20
Anhydrite (g)	6	6
Lithium Carbonate (g)	0	0.1
Water	8	8

Table 4.2.1: CSA cement paste formulations with and without lithium carbonate for calorimeter analysis

As seen in Figure 4.2.1, the CSA cement paste containing lithium carbonate liberated a tremendous amount of energy within the first few hours of hydration when compared with the control CSA cement mortar. Such differences in early age energy release for hydration reactions correlate to ettringite formation and subsequent strength gain as displayed in Figure 4.2.2.

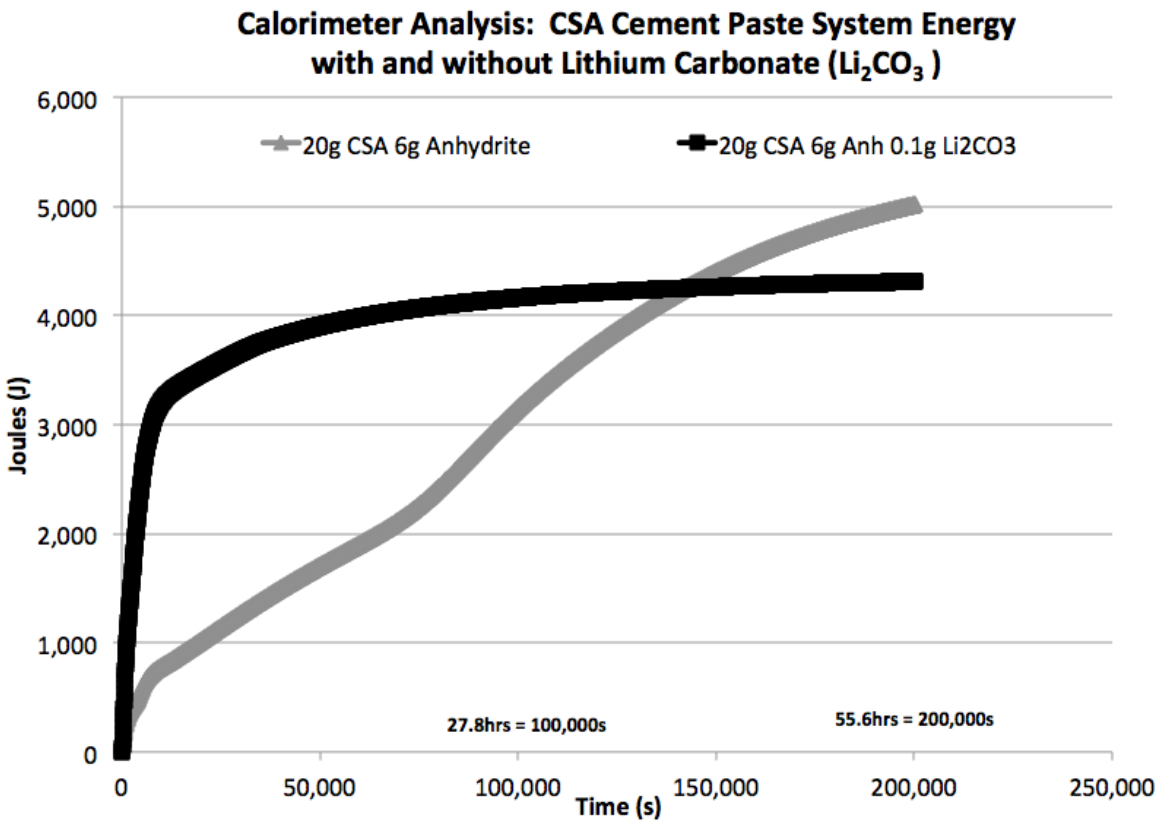

Figure 4.2.1: Calorimeter analysis displaying total joules liberated versus time for hydration of CSA cement paste with and without lithium carbonate

Table 4.2.2 displays CSA cement mortar formulations which are more or less representative of the CSA cement pastes listed in Table 4.1.1. The only difference is that the mortar containing lithium carbonate also contains HEMC. HEMC alone can attribute to some decreases in overall strength behavior when compared with materials not containing HEMC. However, the early age strength behavior of the CSA cement mortar containing both HEMC and lithium carbonate clearly illustrates the information displayed in Figure 4.2.1 which supports the notion of accelerated hydration reactions resulting in increases in strength gain during the early hours of hydration. It is important to note the calorimeter results presented in Figure 4.2.1 are based on one sample, thus the results are considered an observation, not a statistically significant event. Nevertheless, such results might be utilized for design of future experiments with specific purpose of correlating the influence of microstructural constituent components to strength behavior for materials based upon the experimental CSA cement.

Table 4.2.2: CSA CEMENT MORTAR FORMULATIONS FOR MECHANICAL PROPERTY COMPARISONS		
Constituent Materials (mass)	Control	Lithium Carbonate
CSA Cement (g)	500	500
Anhydrite (g)	160	160
Fine Sand (g)	1375	1375
Coarse Sand (g)	125	125
Lithium Carbonate (g)	0	1
HEMC	0	2
Sodium Citrate (g)	2.5	2.5
Water	210	210

Table 4.2.2: CSA cement mortar formulations with and without lithium carbonate for mechanical property comparisons

Figure 4.2.2 shows compressive strength data for a control mortar containing 160g anhydrite and a mortar which contains 160g anhydrite along with 1g lithium carbonate. The data suggests that addition of small amounts of lithium carbonate can significantly contribute to early strength gains in CSA cement mortars. For example, 24 hour mortar cube compressive strength for the control is 18.8MPa (2,730psi) while 24hr mortar cube compressive strength for formulation containing HEMC and lithium carbonate is 42.2MPa (6,121psi). Lithium carbonate's effect on CSA cement mortar hydration can clearly be seen as the one hour mortar cube compressive strength for the mortar containing lithium carbonate is 20.4MPa (2,956psi) –a value slightly greater than the 24hr mortar cube compressive strength of the control sample. The data also suggest that lithium carbonate accelerates early strength development while compromising strength at later ages. It is quite interesting to note that 28 day mortar cube compressive strength for the control mortar is 89.4MPa (12,961psi) while 28 day mortar cube compressive strength for the accelerated mortar is 63.4MPa (9,199psi).

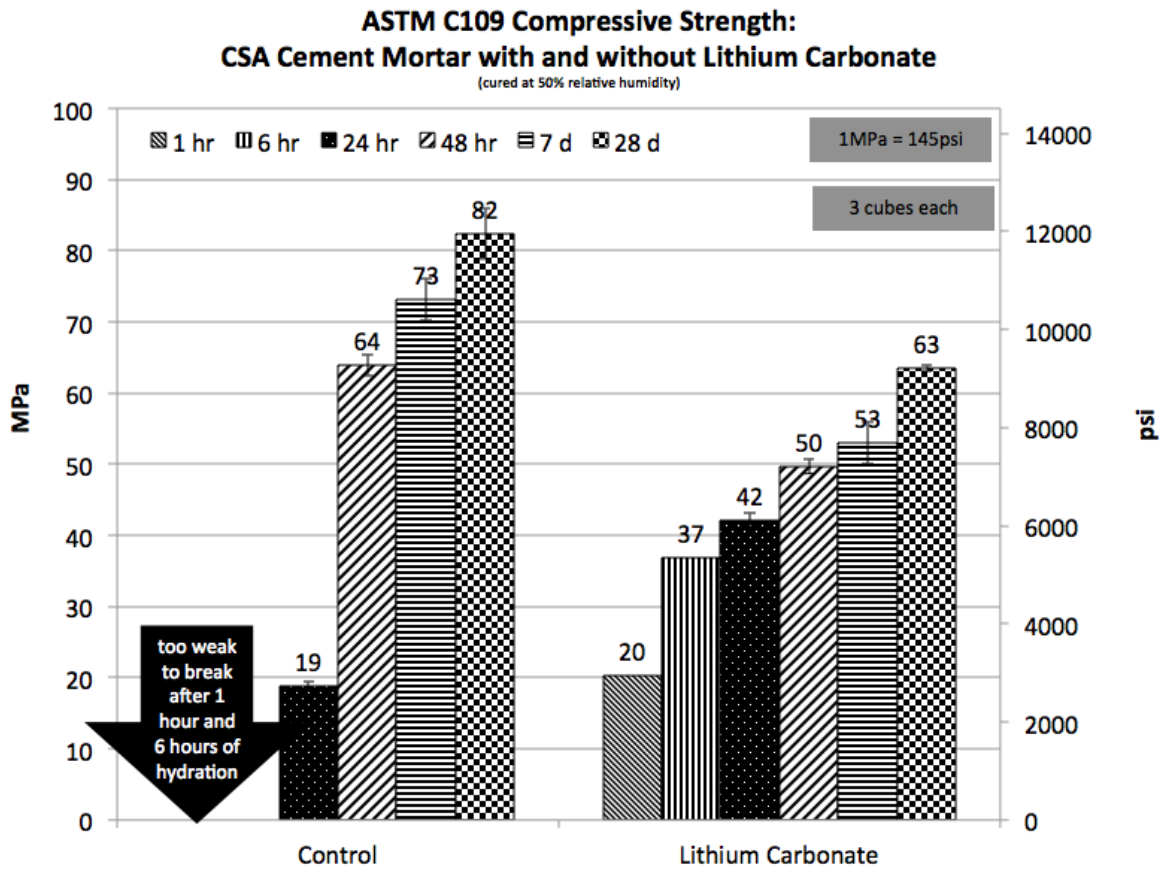

Figure 4.2.2: Compressive strength comaparison for CSA cement mortar with and without lithium carbonate cured at constant 50% relative humidity and 23°C (3 cubes each)

Although CSA cements require a high water / cement ratio of 0.6 for complete hydration, CSA cements tend to undergo self-desiccation, as a low water / cement ratio of 0.3-0.45 is typically used (Juenger et al, 2011). HEMC is a rheology modifier theorized to improve the hydration characteristics of CSA cement by retaining a greater concentration of water within the microstructure during hydration. Traditionally, a very minute amount of HEMC relative to other constituent materials is sufficient to provide a marked change in rheology. Table 4.2.3 lists CSA cement mortar formulations containing HEMC while varying water / cement (w/c) ratio. The water / cement ratios listed in Table 4.2.3 were chosen as the workability of the resulting mortars was suitable for casting samples. In the author's opinion, w/c below 0.32 would be too dry while w/c above 0.35 would be too loose for casting samples.

Table 4.2.3: CSA CEMENT MORTAR FORMULATIONS FOR DIRECT TENSILE STRENGTH ANALYSIS			
Constituent Materials (mass)	w/c = 0.32	w/c = 0.33	w/c = 0.35
CSA Cement (g)	500	500	500
Anhydrite (g)	160	160	160
Fine Sand (g)	1375	1375	1375
Coarse Sand (g)	125	125	125
HEMC (g)	2	2	2
Tartaric Acid (g)	2	2	2
Water	210	220	230

Table 4.2.3: CSA cement mortar formulations containing HEMC varying water demand for direct tensile strength analysis

Figure 4.2.3 displays average direct tensile strength values for the CSA cement mortar formulations displayed in Table 4.2.3 after curing for 7 days at ambient laboratory temperature and 50% relative humidity. Direct tensile strength values for mortars containing w/c = 0.32, w/c = 0.33 and w/c = 0.35 are 618psi (4.3MPa), 492psi (3.4MPa) and 347psi (2.4MPa), respectively.

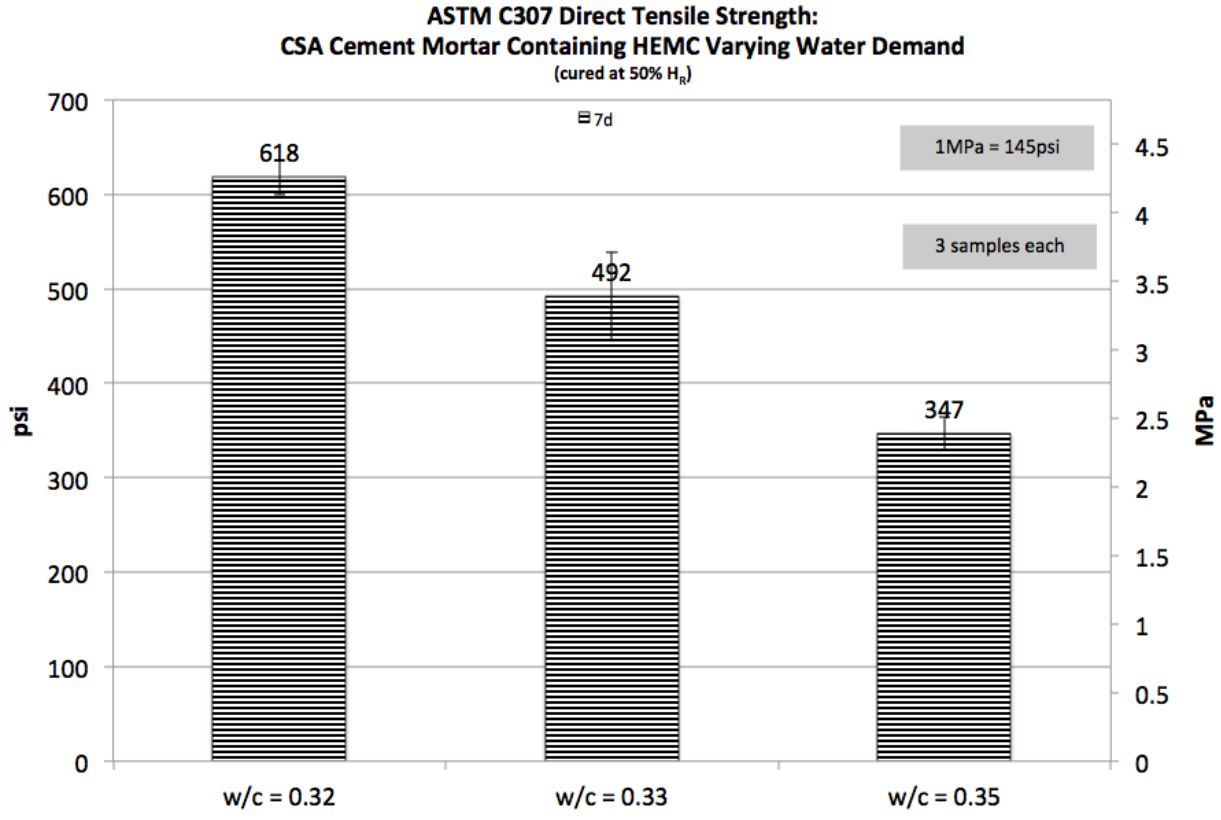

Figure 4.2.3: Direct tensile strength comparison for CSA cement mortar containing HEMC varying water demand (water / cement ratio)

Table 4.2.4 displays CSA cement mortar formulations containing HEMC while varying mass amounts of lithium carbonate. This series of tests was included to assess the influence of lithium carbonate on 28 day strength behavior of CSA cement containing HEMC.

Table 4.2.4: CSA CEMENT MORTAR FORMULATIONS FOR MECHANICAL PROPERTY COMPARISONS			
Constituent Materials (mass)	2g HEMC	2g HEMC + 1g Lithium Carbonate	2g HEMC + 1.5g Lithium Carbonate
CSA Cement (g)	500	500	500
Anhydrite (g)	160	160	160
Fine Sand (g)	1375	1375	1375
Coarse Sand (g)	125	125	125
Lithium Carbonate (g)	0	1	1.5
HEMC (g)	2	2	2
Sodium Citrate (g)	2.5	2.5	2.5
Water	210	210	210

Table 4.2.4: CSA cement mortar formulations containing HEMC with and without lithium carbonate for mechanical property comparisons

Figure 4.2.4 displays average compressive strength values for the CSA cement mortars displayed in Table 4.2.4 after curing for 28 days at constant 50% relative humidity and 23^{o}C. Average compressive strength values for the mortar containing 2g HEMC, the mortar containing 2g HEMC plus 1g lithium carbonate and the mortar containing 2g HEMC plus 1.5g lithium carbonate are 77MPa (11,167psi), 63MPa (9,137psi) and 58MPa (8,412psi), respectively.

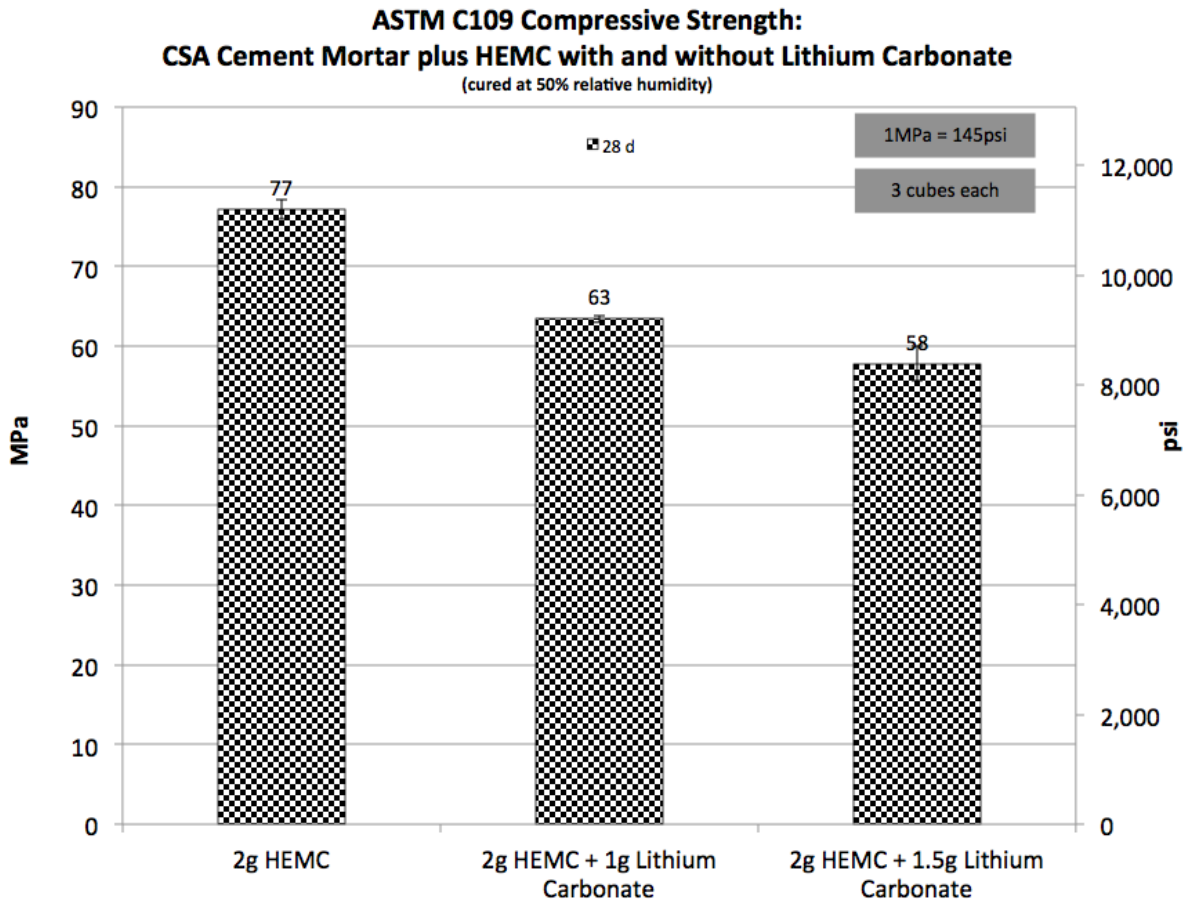

Figure 4.2.4: Compressive strength comparison for CSA cement mortar containing HEMC with and without lithium carbonate cured at constant 50% relative humidity and 23°C (3 cubes each)

Table 4.2.5 displays a very simple set of CSA cement mortar formulations containing anhydrite as a source of calcium sulfate while varying the mass amount of lithium carbonate. The results of this study further illustrate the influence of lithium carbonate on strength behavior within systems containing a majority CSA cement.

Table 4.2.5: CSA CEMENT MORTAR FORMULATIONS FOR MECHANICAL PROPERTY COMPARISONS		
Constituent Materials (mass)	1g Lithium Carbonate	2g Lithium Carbonate
CSA Cement (g)	500	500
Anhydrite (g)	160	160
Fine Sand (g)	1375	1375
Coarse Sand (g)	125	125
Lithium Carbonate (g)	1	2
Tartaric Acid (g)	2	2
Water	220	220

Table 4.2.5: CSA cement mortar formulations varying lithium carbonate for mechanical property comparisons

Figure 4.2.5 displays average compressive strength values of 6,502psi (44.8MPa) and 4,999psi (34.5MPa) for CSA cement mortars containing 1g and 2g of lithium carbonate, respectively. Although the additional lithium carbonate may give the mortar a boost in initial performance, it is important to note the presented long term strength behavior trends for design considerations.

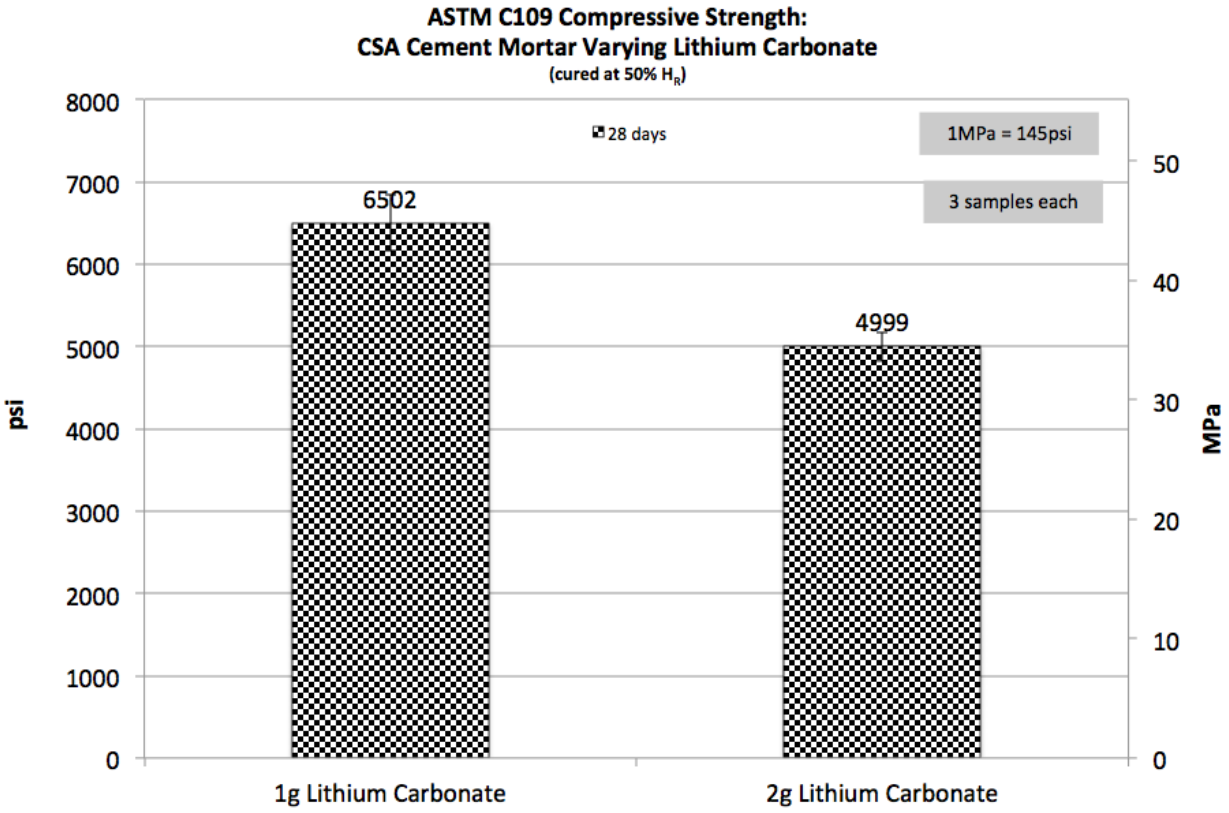

Figure 4.2.5: Compressive strength comparison for CSA cement mortar containing anhydrite as a source of calcium sulfate while varying mass amount of lithium carbonate

Figure 4.2.6 displays average direct tensile strength values of 320psi (2.2MPa) and 350psi (2.4MPa) for CSA cement mortars containing 1g and 2g of lithium carbonate, respectively. It appears that there is no significant change in direct tensile strength behavior for the CSA cement mortars.

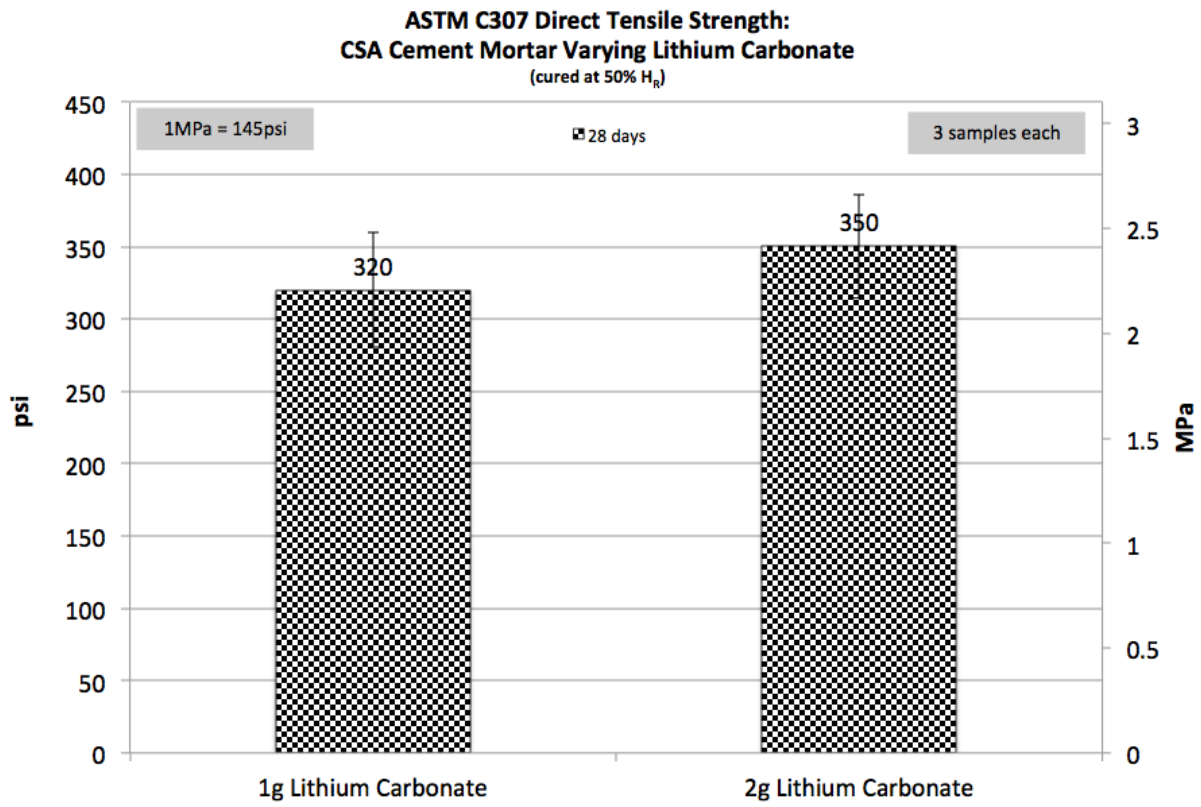

Figure 4.2.6: Direct tensile strength comparison for CSA cement mortar containing anhydrite as a source of calcium sulfate while varying mass amount of lithium carbonate

Table 4.2.6 displays CSA cement mortars containing lithium carbonate with and without superplasticizer. This set of experiments illustrates the influence of superplasticizer on 28 day strength behavior of CSA cement containing minor phase tri-calcium aluminate.

Table 4.2.6: CSA CEMENT MORTAR FORMULATIONS FOR MECHANICAL PROPERTY COMPARISONS		
Constituent Materials (mass)	1g Lithium Carbonate	1g Lithium Carbonate + 1g Superplasticizer
CSA Cement (g)	500	500
Anhydrite (g)	160	160
Fine Sand (g)	1375	1375
Coarse Sand (g)	125	125
Lithium Carbonate (g)	1	1
Tartaric Acid (g)	2	2
Superplasticizer (g)	0	1
Water	220	220

Table 4.2.6: CSA cement mortar formulations with and without superplasticizer for mechanical property comparisons

Figure 4.2.7 displays average compressive strength values of 6,502psi (44.8MPa) and 7,585psi (52.3MPa) for CSA cement mortars containing lithium carbonate and a combination of lithium carbonate and superplasticizer, respectively.

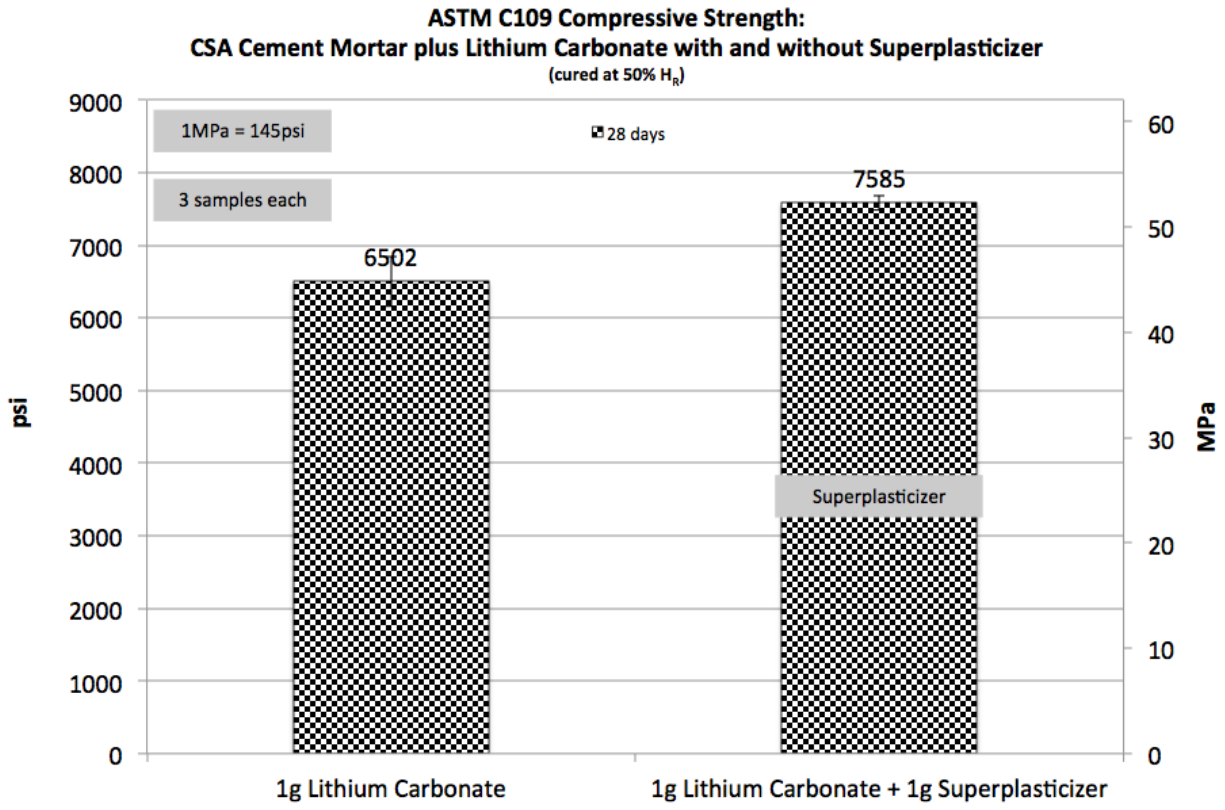

Figure 4.2.7: Compressive strength comaparison for CSA cement mortar containing lithium carbonate with and without superplasticizer cured at constant 50% relative humidity and 23°C (3 cubes each)

Figure 4.2.8 displays average direct tensile strength values of 320psi (2.2MPa) and 427psi (2.9MPa) for CSA cement mortars containing lithium carbonate and a combination of lithium carbonate and superplasticizer, respectively.

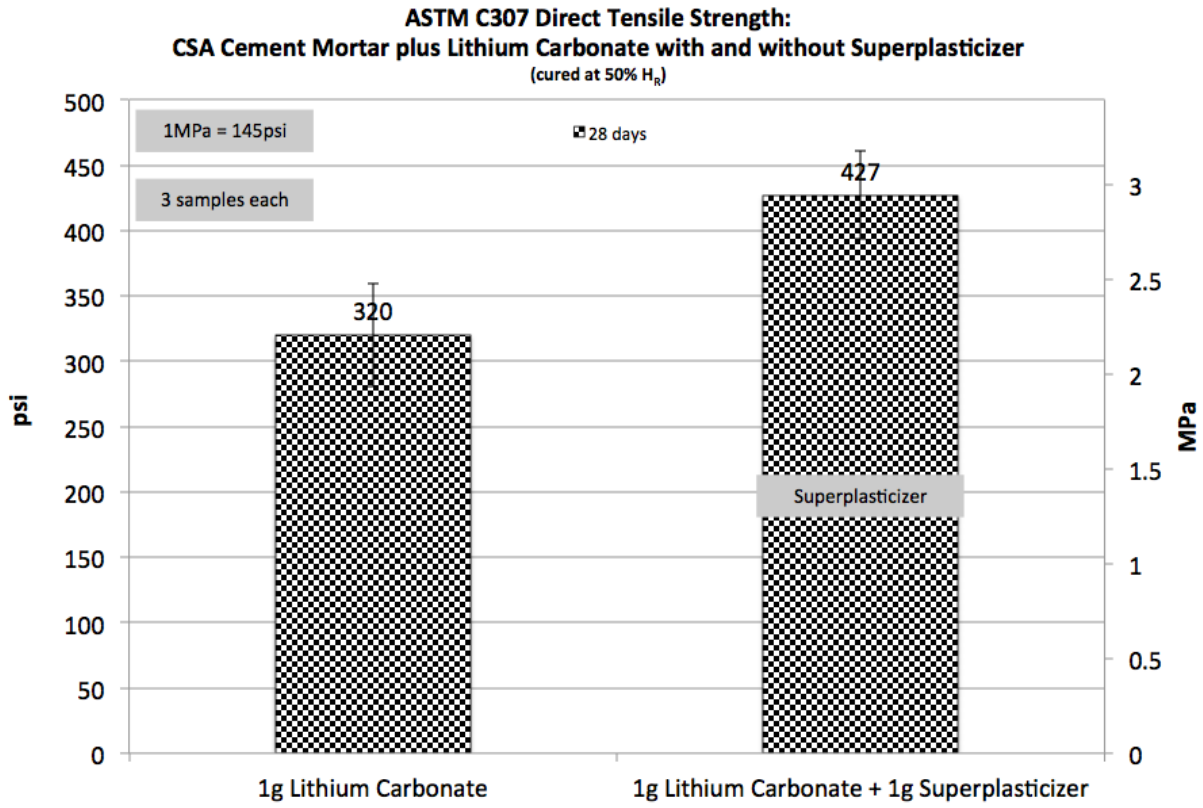

Figure 4.2.8: Direct tensile strength comaparison for CSA cement mortar containing lithium carbonate with and without superplasticizer cured at constant 50% relative humidity and 23°C (3 samples each)

Table 4.2.7 displays CSA cement mortars containing superplasticizer while varying the mass amount of lithium carboante. This set of experiments illustrates the influence of various combinations of lithium carbonate and superplasticizer on 28 day strength behavior of CSA cement containing minor phase tri-calcium aluminate.

Table 4.2.7: CSA CEMENT MORTAR FORMULATIONS FOR MECHANICAL PROPERTY COMPARISONS		
Constituent Materials (mass)	1g Lithium Carbonate + 1g Superplasticizer	2g Lithium Carbonate + 1g Superplasticizer
CSA Cement (g)	500	500
Anhydrite (g)	160	160
Fine Sand (g)	1375	1375
Coarse Sand (g)	125	125
Lithium Carbonate (g)	1	2
Tartaric Acid (g)	2	2
Superplasticizer (g)	1	1
Water	220	220

Table 4.2.7: CSA cement mortar formulations with and without superplasticizer for mechanical property comparisons

Figure 4.2.9 displays average compressive strength values of 7,585psi (52.3MPa) and 5,623psi (38.8MPa) for CSA cement mortars containing 1g lithium carbonate plus 1g superplasticizer and a CSA cement mortar containing 2g lithium carbonate plus 1g superplasticizer, respectively.

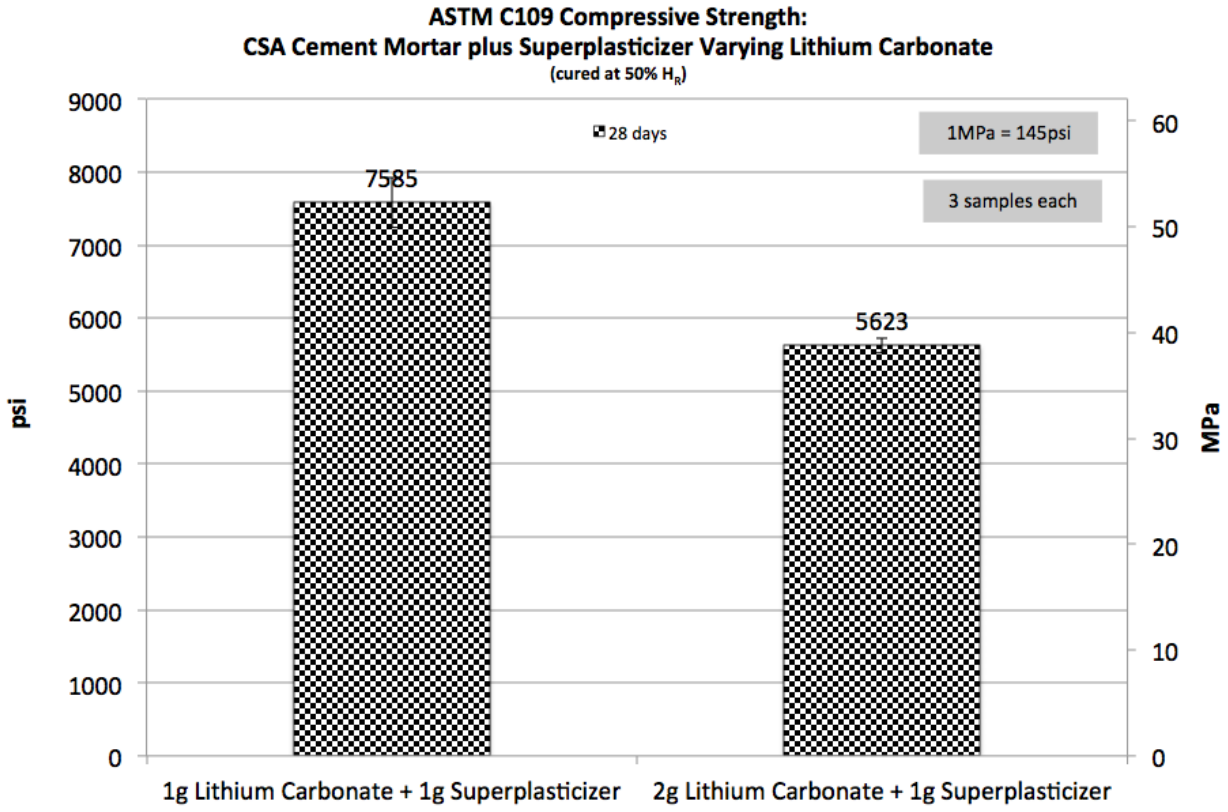

Figure 4.2.9: Compressive strength comaparison for CSA cement mortar containing superplasticizer while varying lithium carbonate cured at constant 50% relative humidity and 23°C (3 samples each)

Figure 4.2.10 displays average direct tensile strength values of 427psi (2.9MPa) and 349psi (2.4MPa) for CSA cement mortars containing 1g lithium carbonate plus 1g superplasticizer and a CSA cement mortar containing 2g lithium carbonate plus 1g superplasticizer, respectively.

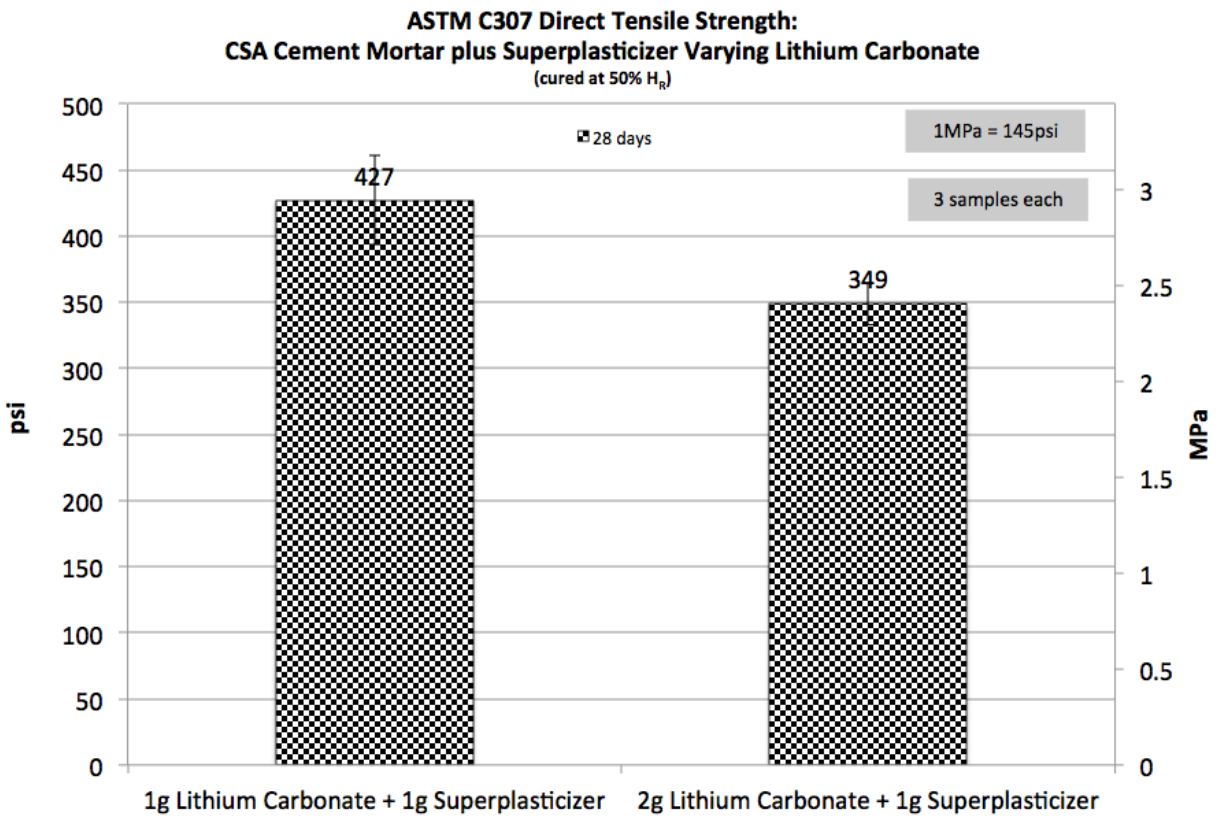

Figure 4.2.10: Direct tensile strength comaparison for CSA cement mortar containing superplasticizer while varying lithium carbonate cured at constant 50% relative humidity and 23°C (3 samples each)

REMARKS

For the purposes of developing cementitious materials for specific applications, it is important to note small concentrations of specific materials sometimes result in significant changes in behavior. It is often necessary to perform iterative testing schemes in an effort to truly understand the influence of individual components on microstructure behavior and subsequent strength development, that is, unless an abundance of literature exists on the topic.

An abundance of such literature was not available for assessing the influence of commonly used admixtures on strength behavior of calcium sulfoalumiante (CSA) cement containing minor phase tri-calcium aluminate. The previously presented experiments were conducted to obtain this information.

Lithium carbonate addition to CSA cement mortar significantly improved early age strength development while sometimes compromising strength performance at later ages. Lithium carbonate is viewed as an excellent tool for adjusting the hydration characteristics of CSA cement mortars.

Hydroxyethyl methyl cellulose (HEMC) is a rheology modifier capable of imparting a number of improvement characteristics to hydrating materials. In this case, HEMC was utilized to increase the concentration of water per specific volume of material microstructure throughout the wet state and especially during hydration. This enabled the mortar to have a better troweling consistency in the wet state while improving hydration characteristics by providing a more even distribution of water throughout the microstructure.

The compatibility of cements and plasticizers can lead to frustrating bouts of iteration during development of cementitious materials. Spray dried powders of modified polycarboxylic ether were included as superplasticizers in this study. These materials seemed to work well with this CSA cement containing minor phase tri-calcium aluminate. Various combinations of this CSA cement and superplasticizers seem ideal for use with self-consolidating concretes, self-leveling underlayments or virtually any application requiring a low viscosity cementitious material for a short period of time with overwhelming potential for rapid strength gain. However, it must be noted that these materials demonstrated a significant amount of bleeding immediately after casting. Therefore, for most applications, it is recommended to include either HEMC or latex polymer to ensure a homogenous wet mix that is likely to yield improved mechanical property performance characteristics as a result of polymer addition.

4 REFERENCES:

- Anderberg, A., Wadso, L., 2010, Using a standard mix design to study properties of a flooring compound, Nordic Concrete Research Publications, 10; 21-32, NCR 40-3, ISSN: 0800-6377
- Baumann, R., Tarantul, K., Powell, C., Wichmann, A., Tepper, C., Perello, M., Heeringen, M., Kock, W., Griggs, P., Radler, M., 2007, Interaction of Cellulose Ethers and Redispersible Polymer Powders in Cement Based Tile Adhesives, The DOW Chemcial Company, Techline 3 For the Construction Industry, dccinfo@dow.com, www.dowcc.eu, 840-01201-032011
- Bensted, J., 1998, Lea's Chemistry of Cement and Concrete, 4th Edition, ISBN 0-340-56589-6
- Bishop, M., Barron, A., 2006, Cement Hydration Inhibition with Sucrose, Tartaric Acid, and Lignosulfonate: Analytical and Spectroscopic Study, Department of Chemistry and Department of Mechanical Engineering and Materials Science, Rice University, Houston TX 77005, Applied Chemistry, American Chemical Society, *Ind. Eng. Chem. Res.* 2006, *45*, 7042-7049
- Chandra, S., Ohama, Y., 1994, Polymers in Concrete, CRC Press, ISBN 0-8493-4815-3
- Gastaldi, D., Fulvio, C., Boccaleri, E.,2009, Ettringite and calcium sulfoaluminate cement: investigation of water content by near-infrared spectroscopy, Journal of Material Science, 44: 5788-5794, 2009
- Juenger, M., Winnefeld, F., Provis, J., Ideker, J., 2011, Alternative cementitious binders, Cement and Concrete Research 41 (2011) 1232-1243
- Marraccoli, M., Montagnaro, F., Pace, M.L., Telesca, A., Valenti, G.L., 2010, Synthesis of Calcium Sulfoaluminate Cements from Blends of Coal Combustion Ashes with Flue Gas Desulfurization Gypsum, Processes and Technologies for a Sustainable Energy, Ischia, June 17-30, 2010, PTSE 2010
- Pera, J., Ambroise, J., 2004, New applications of calcium sulfoaluminate cement, Cement and Concrete Research 34 (2004) 671-676
- Scrivener, K., Capmas, A., 1998, Calcium Aluminate Cements, Chapter 13, Lea's Chemistry of Cement and Concrete, 4th Edition, ISBN 0 340 56589 6
- Taylor, H., 1997, Cement Chemistry, Second Edition, ISBN 0 7277 2592 0
- Xu, Q., Stark, J., 2005, Early hydration of ordinary Portland cement with an alkaline shotcrete accelerator, Advances in Cement Research, 2005, 17, No. 1, January, 1-8

Chapter 5: Influence of Latex Polymer Addition on Mechanical Property Performance Characteristics of CSA Cement Mortar

Chapter 5 presents information discovered during the polymer modification step of the iterative process for developing dry mix mortar materials. The presented information provides new insight regarding the compatibility of vinyl acetate / ethylene based dispersible polymer powders with calcium sulfoaluminate cement containing minor phase tri-calcium aluminate. Chapter 5 consists of three studies assessing the influence of latex polymer addition on the strength characteristics of CSA cement mortars. The first study assesses the potential for latex polymer to improve the ductile performance of CSA cement mortars. The second study assesses the influence of curing conditions on the compressive strength behavior of polymer modified CSA cement mortars. The third study highlights latex polymer addition as being an effective means for mitigating ettringite decomposition in materials containing CSA cement cured at constant low humidity and 23^{o}C.

5.1 Method for Altering Ductile Behavior of Polymer Modified CSA Cement Mortars

INTRODUCTION

Over the past few decades, significant strides have been made in improving the ductile behavior of cementitious materials. One notable means is through introduction of "minimum defect" materials incorporating steel fibers (Vande Voot et al, 2008). A popular example of a "minimum defect" material is ultra high performance concrete (UHPC). Both the Federal Highway Administration (FHWA) and US Army Corps of Engineers (USACE) provide literature describing the performance behavior of "minimum defect" materials in specific applications (Graybeal, 2010, Graybeal, 2009, Oneil et al, 2004, Cargile et al, 2002). Although introduction of "minimum defect" materials is a viable means for improving the ductile behavior of cementitious materials, it is important to note that other methods exist.

It is well known that most latex-modified mortars and concretes provide larger deformation, ductility (or extensibility) and elasticity when compared with ordinary cement mortar and concrete (Ohama 1995). Scores of publications exist describing the performance of polymer modified cements and mortars (Medeiros et al, 2009, Afridi et al, 2003, Jenni et al, 2003, Routh et al, 1999, Ohama, 1995, Afridi et al, 1994 Chandra et al,

1994). Most available literature tends to focus on materials formulated with a majority of ordinary portland cement (OPC) or a combination of OPC and calcium aluminate cement (CAC) while having polymer / cement ratios up to 0.25. In former times, resources were seldom allocated for assessing the performance of materials with polymer / cement ratios exceeding 0.25 simply due to cost considerations for the finished product.

The present study assesses the mechanical property performance of mortars containing a combination of calcium sulfoaluminate (CSA) cement and vinyl acetate / ethylene (VAE) dispersible polymer powder (DPP). Marracolli et al, (2010), Pelletier et al, (2010), Renaudin et al, (2007) and Taylor (1997) provide valuable insight regarding the differences in hydration characteristics between CSA cement and OPC. Although literature exists describing the performance of CSA cement with styrene butadiene rubber (SBR) latex polymers (Sprinkel 2002), little is known about the combination of CSA cement and VAE DPP.

VAE polymers are film forming thermoplastics with the following origin. Vinyl acetate has a glass transition temperature of 30^{o}C (Blackley, 1997). Poly-vinyl acetate has a minimum film forming temperature of 20^{o}C (Blackley, 1997). These values of glass transition temperature and minimum film forming temperature make poly-vinyl acetate lattices unsuitable for many applications (Blackley, 1997). The minimum film forming temperature is too high for poly-vinyl acetate to be used effectively as a binder for pigments and fillers (Blackley, 1997). The glass transition temperature is too low for use as a rigid plastic. To make the polymer more suitable for application as a binder and an adhesive, it is useful to lower its glass transition temperature by plasticization (Blackley, 1997). Ethylene is an olefinic hydrocarbon used for plasticization of vinyl acetate (Blackley, 1997). Ethylene and vinyl acetate are combined in reactors under pressure to form liquid dispersions, known as vinyl acetate / ethylene or VAE dispersions. Often, these dispersions are stabilized using poly-vinyl alcohol as a protective colloid. Most VAE dispersions are milky white in appearance and are described as looking like Elmer's school glue. Vinyl acetate and ethylene ratios can be varied in the reactor to create VAE dispersions displaying different mechanical property performance upon film formation. Greater amounts of ethylene lead to greater flexibility and lower glass transition temperatures for films formed from the produced dispersions (Blackley, 1997). To form vinyl acetate / ethylene dispersible polymer powders (VAE DPP), VAE dispersions are diluted, mixed with protective colloids, mixed with other additives and spray dried into powder form (Ohama, 1995).

Originally, VAE DPP product portfolios were designed to provide a number of desirable characteristics to cementitious ceramic tile adhesives with examples being rheology modification, improved flexibility and improved bond strength to various substrates (Chandra et al, 1994). These VAE polymeric materials allowed the transition from thick bed mortar tile adhesives to thin bed mortar tile adhesives. Upon great success with ceramic tile adhesives, the whole dry mix mortar industry embraced these materials. Now, VAE dispersible polymer powders are widely used throughout the dry mix mortar industry to improve mechanical property performance of various cementitious systems. Aside from being used in tile adhesives, stuccos, underlayments and repair materials at somewhat low polymer / cement ratios, the use of VAE DPP for polymer modification of cementitious materials to be used in larger, civil engineering type applications is somewhat limited.

A few niche markets have begun to embrace the performance characteristics of cementitious materials with high polymer / cement ratios. An example of one such market is underground construction. Shotcrete and gunnite material suppliers are delivering high polymer / cement ratio materials to their respective market outlets for use as either a means of structural support or for creating waterproofing barriers. An example description for such materials is detailed in US Patent 6,869,987 B2, Cementitious Compositions and a Method of Their Use. Although significant experience exists within the underground construction marketplace regarding the use of high polymer / cement ratio materials, this knowledge is not easily transferred to the broader construction industry given the notable differences in common practices associated with both above ground and underground construction.

In the author's opinion, the use of VAE DPP in larger, civil engineering type applications should be pursued with more vigor, as this will allow the ductile behavior of the cementitious material to be precisely defined by specifying the material's polymer / cement ratio. The modulus of elasticity for the polymeric material is significantly less than the modulus of elasticity for cement hydrates (Ohama 1995). Therefore, increasing the polymer / cement ratio increases the quantity of low modulus of elasticity polymeric material within a specific volume of the cementitious material's microstructure thus improving the ductile performance of the system. Surpassing a polymer / cement ratio of 0.25 allows for development of interesting mechanical property performance

characteristics which may provide significant value for civil engineering applications. The presented information provides examples of polymer modified CSA cement mortars varying polymer / cement ratio.

MATERIALS

Cement

- CSA cement containing C_3A, tri-calcium aluminate, was utilized in this study. XRD analysis provides the following listing of constituent materials:

Yeelimite >> C_3A > Belite > Anhydrite (trace quantity)

Anhydrite

- Snow white filler with an average particle size of 7-9 microns sourced from United States Gypsum (USG) was utilized in this study (USG TDS)

Gypsum

- Terra Alba gypsum with an average particle size of 12-15 microns sourced from United States Gypsum (USG) was utilized in this study (USG TDS)

Aggregate

- ASTM finely graded sand from Ottawa Illinois was used in all formulations. A coarser, 20/30 sand was also used in all formulations

Polymer

- A vinyl acetate / ethylene dispersible polymer powder (VAE DPP) with Tg = -7^{o}C (19^{o}F) was utilized in this study

Experimental Program

Mechanical Property Testing

This study assessed split tensile strength, compressive strength, flexural strength and direct tensile strength for polymer modified CSA cement mortars at polymer / cement

ratios of 0.15, 0.3 and 0.45. An Instron universal testing machine was utilized for the mechanical property testing. Split tensile strength testing was performed in accordance with ASTM C496, Standard Test Method for Splitting Tensile Strength of Cylindrical Concrete Specimens. Compressive strength testing was performed in accordance with ASTM C109, Standard Test Method for Compressive Strength of Hydraulic Cement Mortars. Flexural strength testing was performed in accordance with ASTM C348, Standard Test Method for Flexural Strength of Hydraulic Cement Mortars. Direct tensile strength testing was performed in accordance with ASTM C307, Standard Test Method for Tensile Strength of Chemical-Resistant Mortar, Grouts and Monolithic Surfacings.

Scanning Electron Microscopy (SEM)

A Hitachi S4800 scanning electron microscope was utilized to view cement mortar surfaces after 21 days of hydration in a sealed plastic bag at ambient laboratory temperature of 23°C. SEM analysis specimens were obtained from broken direct tensile strength dog bone samples. SEM samples were prepared by placing the collected specimens in an oven at 45°C overnight. The sample specimens were then gold coated under a vacuum for viewing.

Mortars

Cement mortar 1 is considered to be a special base mortar formulation. In general terms, cement mortar 1 contains calcium sulfoaluminate (CSA) cement, anhydrite, gypsum, superplasticizer, aggregate and a few additional minor components. A soft VAE DPP with T_g = -7°C (19°F), also known as polymer 2, was added to cement mortar 1 such that three mortars could be tested at polymer / cement ratios of 0.15, 0.3 and 0.45. A water / cement ratio of 0.35 was utilized for the mortars with p/c = 0.15 and p/c = 0.3. In an effort to achieve a workable consistency, the water / cement ratio was increased to 0.38 for the mortar with p/c = 0.45.

To prepare the dry mix mortars, individual mortar components were weighed and placed into a plastic mixing bag. After all components were added, the bag was sealed and shaken vigorously by hand for approximately ninety seconds. This type of mixing is an industry proven simulation for blending operations in the manufacturing of dry mix mortar products containing minute quantities of additives such as accelerators and retarders.

Three test specimens were cast for each test series. During the first 24 hours of curing, each test specimen remained in the mold covered with plastic on the work bench. After this initial curing period,

test specimens were removed from their molds and placed in a sealed plastic bag at ambient laboratory temperature of 23°C until testing.

Table 5.1.1: CSA CEMENT MORTAR INFORMATION		
Cement Mortar 1	Cement Mortar 1	Cement Mortar 1
Polymer 2	Polymer 2	Polymer 2
p/c = 0.15	p/c = 0.3	p/c = 0.45
w/c = 0.35	w/c = 0.35	w/c = 0.38

Table 5.1.1: Polymer modified CSA cement mortars for mechanical property evaluation

RESULTS

Figure 5.1.1 displays indirect tensile strength values for the polymer modified mortars listed in Table 5.1.1 after curing for seven days in a sealed plastic bag at ambient laboratory temperature of 23°C (73°F). The split tensile strength values for mortars possessing polymer / cement ratios of 0.15, 0.3 and 0.45 are 727psi (5MPa), 647psi (4.5MPa) and 539psi (3.7MPa), respectively.

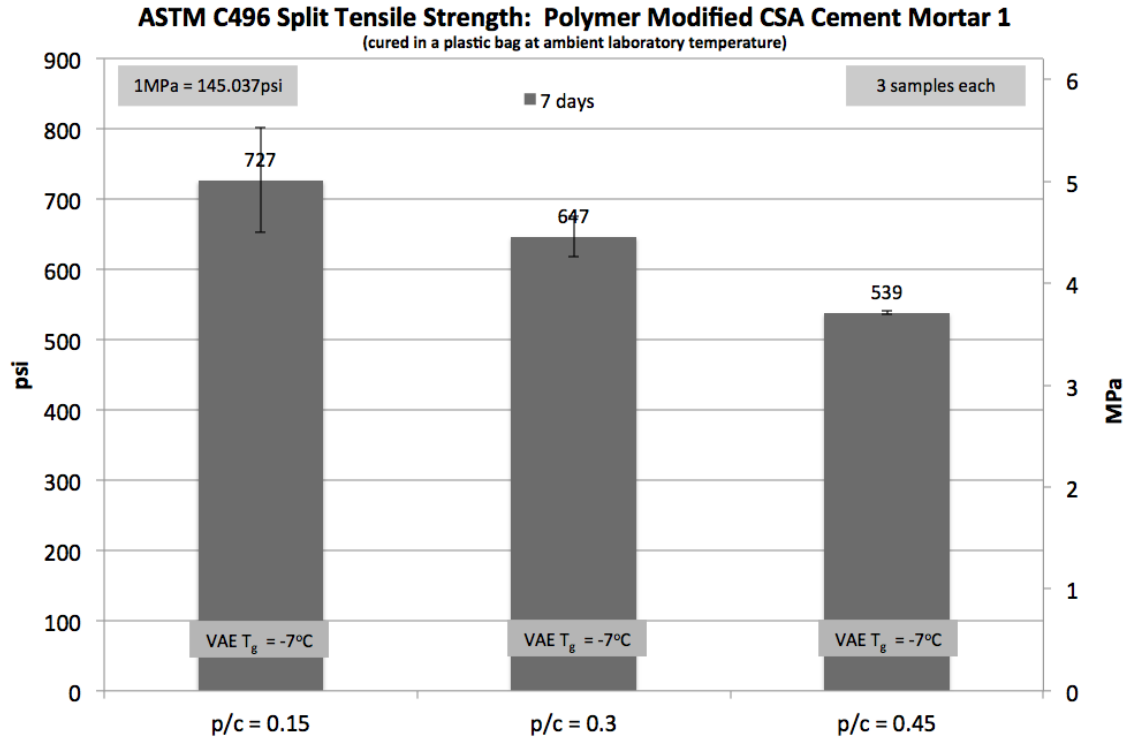

Figure 5.1.1: Split tensile strength of polymer modified CSA cement mortar at polymer / cement ratios of 0.15, 0.3 and 0.45

Figure 5.1.2 displays compressive strength values for the polymer modified mortars listed in Table 5.1.1 after curing for seven days in a sealed plastic bag at ambient laboratory temperature of 23°C (73°F). The trend displayed in Figure 5.1.2 agrees with compressive strength behavior of polymer modified mortars reported in literature (Ohama, 1995). The compressive strength values for mortars possessing polymer / cement ratios of 0.15, 0.3 and 0.45 are 3,684psi (25MPa), 3,239psi (22MPa) and 2,611psi (18MPa), respectively. As previously mentioned, literature reports tough, flexible polymer film occupies void space within the microstructure sometimes resulting in decreases in compressive strength with increases in polymer concentration (Ohama, 1995).

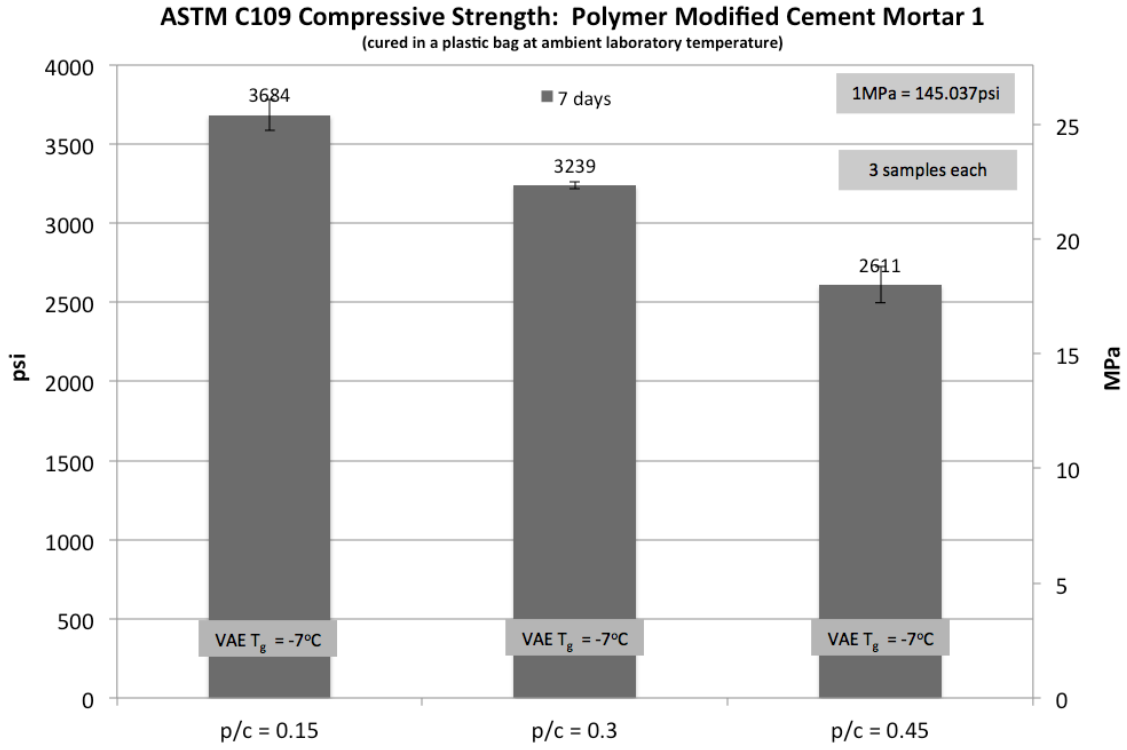

Figure 5.1.2: Compressive strength of polymer modified CSA cement mortar at polymer / cement ratios of 0.15, 0.3 and 0.45

Figure 5.1.3 displays flexural strength values for the polymer modified mortars listed in Table 5.1.1 after curing for seven days in a sealed plastic bag at ambient laboratory temperature of 23°C (73°F). The trend displayed in Figure 5.1.3 agrees with flexural strength behavior of polymer modified mortars reported in literature (Zurbriggen, 2004, Ohama, 1995). The flexural strength values for mortars possessing polymer / cement ratios of 0.15, 0.3 and 0.45 are 1,169psi (8MPa), 1,406psi (9.7MPa) and 1,596psi (11MPa),

respectively. As previously mentioned, literature reports tough, flexible polymer film occupying void space within the microstructure leading to increases in flexural strength until some optimum polymer / cement ratio is surpassed (Zurbriggen, 2004, Ohama, 1995). Once this optimum polymer / cement ratio is surpassed, further increases in polymer content result in decreases in flexural strength (Zurbriggen, 2004, Ohama, 1995).

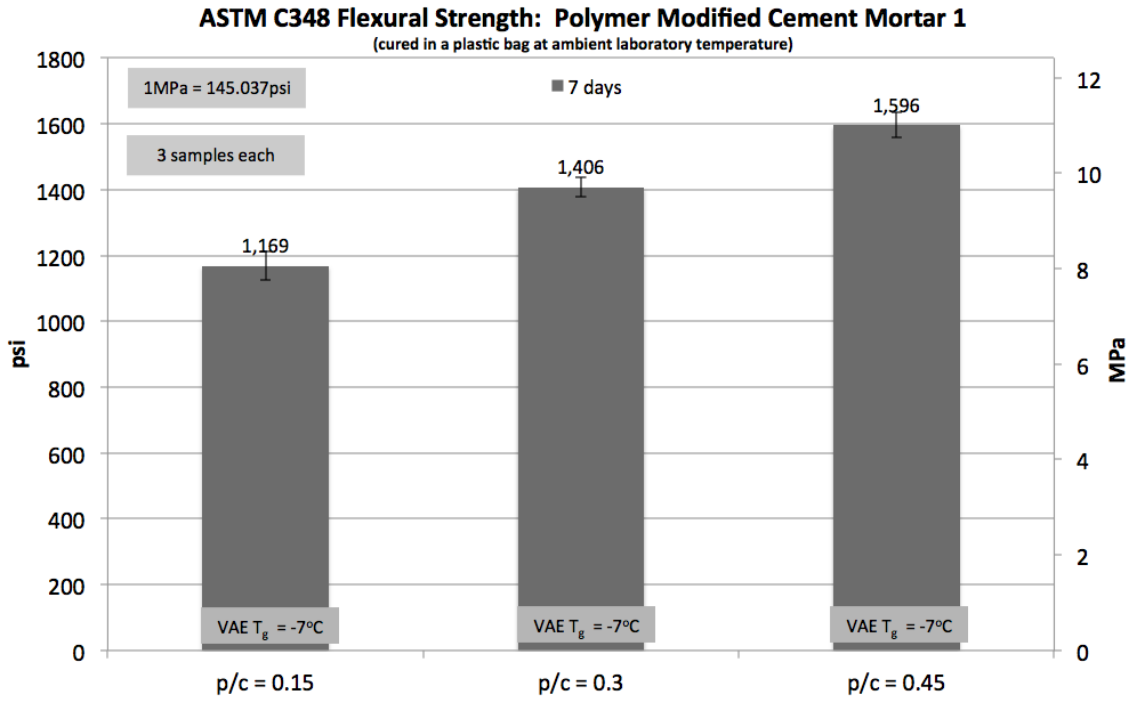

Figure 5.1.3: Flexural strength of polymer modified CSA cement mortar at polymer / cement ratios of 0.15, 0.3 and 0.45

Figure 5.1.4 displays direct tensile strength values for the polymer modified mortars listed in Table 5.1.1 after curing for seven days in a sealed plastic bag at ambient laboratory temperature of 23°C (73°F). The direct tensile strength values for mortars possessing polymer / cement ratios of 0.15, 0.3 and 0.45 are 692psi (4.8MPa), 775psi (5.3MPa) and 719psi (4.9MPa), respectively. The direct tensile strength information displayed in Figure 5.1.4 agrees with trends reported in literature for polymer modified ordinary portland cement based materials (Zurbriggen, 2004, Ohama, 1995).

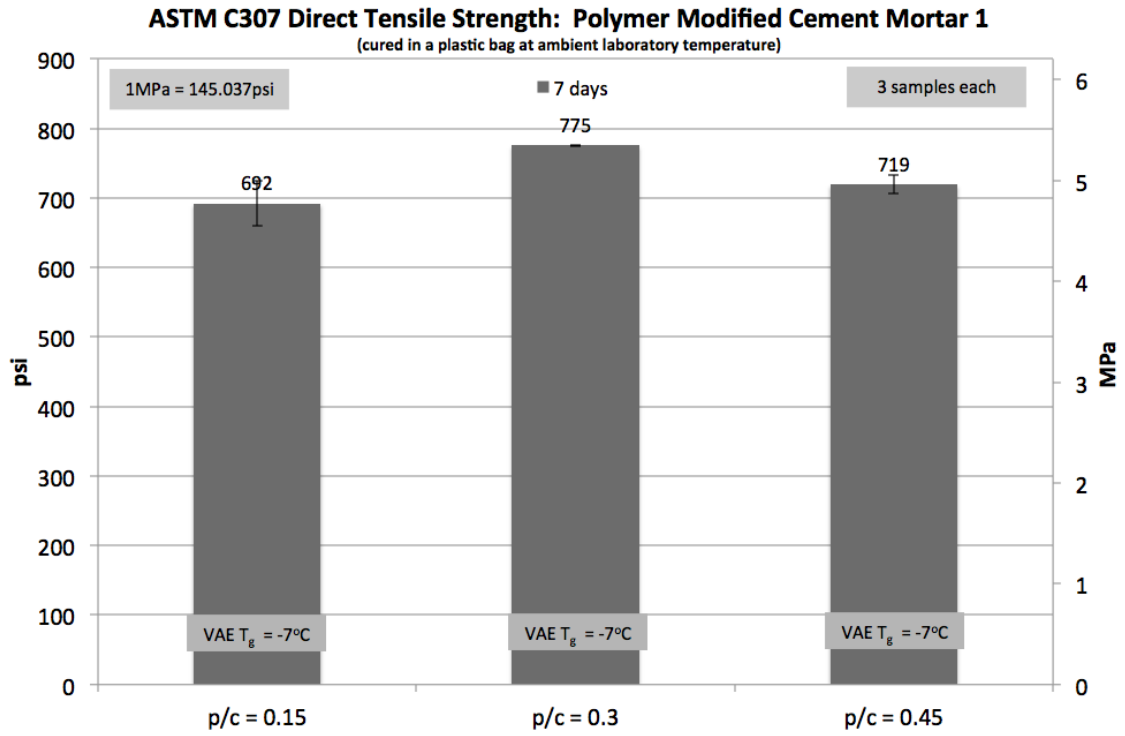

Figure 5.1.4: Direct tensile strength of polymer modified mortars at polymer / cement ratios of 0.15, 0.3 and 0.45

Figure 5.1.5 displays percent elongation at break as measured by the universal testing machine for the direct tensile strength information displayed in Figure 5.1.4. The average elongation at break values for direct tensile strength dog bone samples possessing polymer / cement ratios of 0.15, 0.3 and 0.45 are 4, 6 and 8 percent, respectively. The information displayed in both Figure 5.1.4 and Figure 5.1.5 illustrates a trend for increased ductile behavior with increases in polymer / cement ratio.

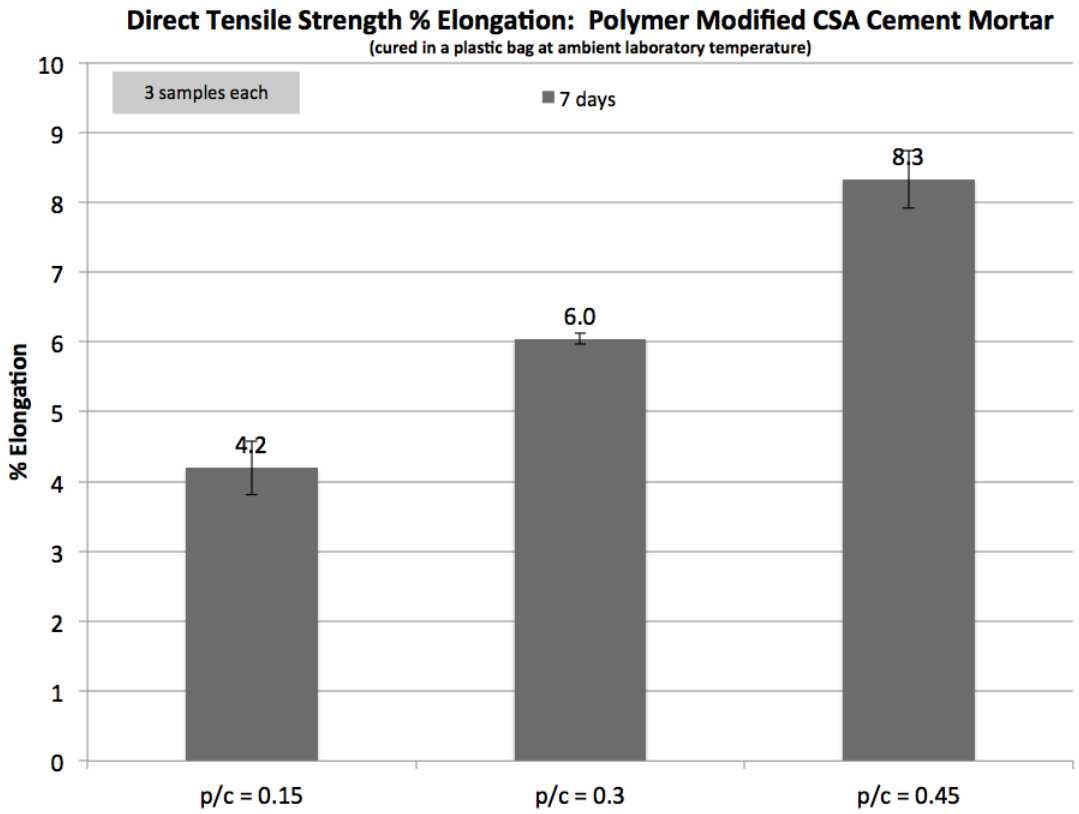

Figure 5.1.5: Percent elongation at break for direct tensile strength samples varying polymer / cement ratio

DISCUSSION

In latex polymer modified cementitious materials, the tough, flexible polymer film is dispersed somewhat uniformly throughout the material's microstructure (Chandra et al, 1994, Ohama, 1995). Increasing the polymer / cement ratio increases the quantity of tough, flexible material per unit volume allowing for improved ductile behavior without the necessity for inclusion of steel fibers or other traditional means of reinforcement. Figures 5.1.6, 5.1.7 and 5.1.8 display SEM images of each microstructure for each polymer modified mortar at polymer / cement ratios of 0.15, 0.3 and 0.45, respectively. Each image displays constituent materials and hydrated cement phases, a majority ettringite, surrounded by tough, elastic polymer film. From a visual perspective, it is interesting to note greater polymer concentration relative to other materials for mortars with increasing polymer / cement ratio. Figure 5.1.5 further illustrates the influence of greater concentrations of tough, elastic materials within the mortar microstructure as the percent elongation at break for direct tensile strength dog bone samples continually increases with increases in polymer / cement ratio.

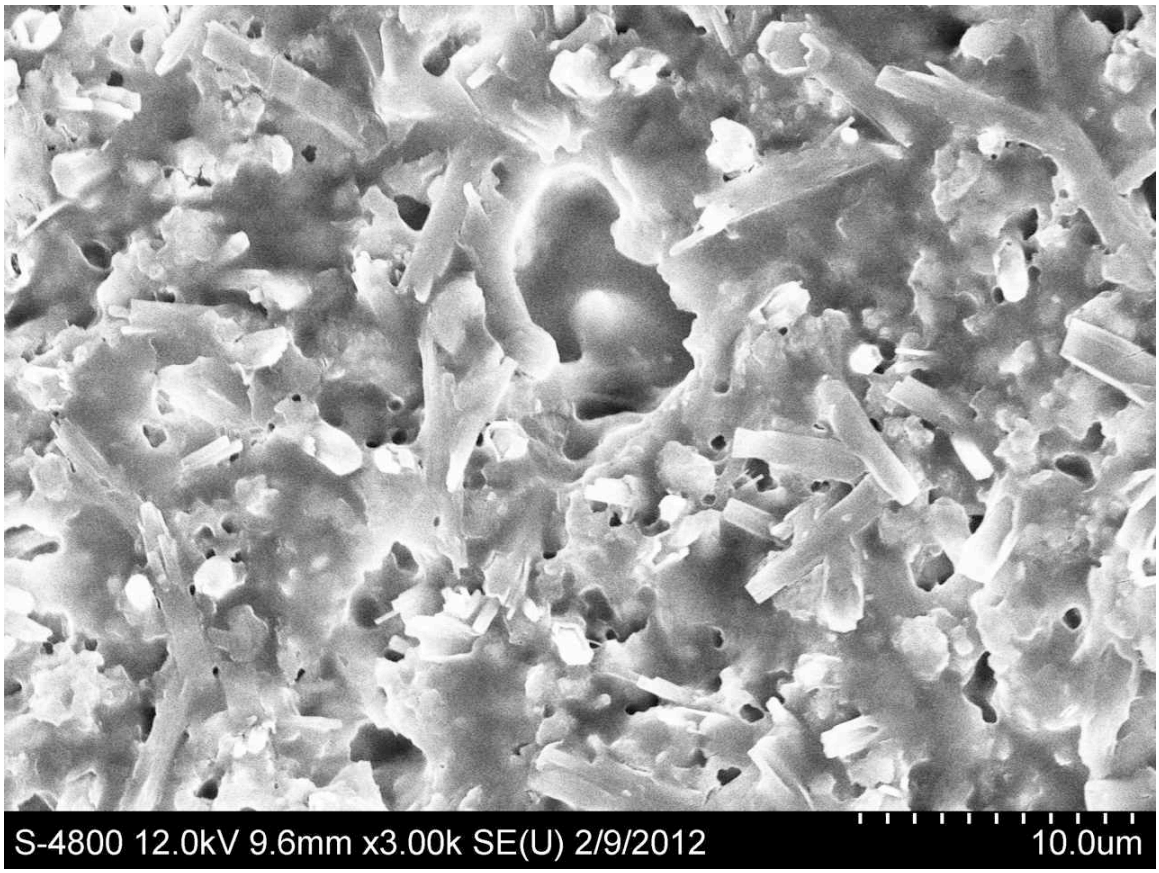

Figure 5.1.6: SEM image for polymer modified mortar with p/c = 0.15 after curing for 21days at ambient temperature sealed in a plastic bag

In polymer modified OPC based materials, both direct tensile strength and flexural strength increase to some optimum value before beginning a decreasing trend with increases in polymer / cement ratio (Bright et al, 1993, Ohama 1995). Figure 5.1.3 displays a continually increasing trend in flexural strength with increases in polymer / cement ratio for the tested CSA cement mortars. Flexural strength will inevitably begin to decrease once the optimum polymer / cement ratio is surpassed. Figure 5.1.4 displays direct tensile strength reaching an optimum value with a p/c = 0.3 before beginning its gradual decrease with increasing polymer / cement ratio. As seen in Figures 5.1.6, 5.1.7 and 5.1.8, these optimum strength values are dependent on both quantity and type of latex polymer incorporated within the material's microstructure, which agrees with literature (Zurbriggen, 2004). For example, VAE polymers with different glass transition temperatures may demonstrate different optimum strength characteristics at different polymer / cement ratios (Bright et al, 1993). The results of this study indicate CSA cement mortars follow reported flexural strength and direct tensile strength

trends for polymer modified mortars based upon hydraulic binders of different chemistry (Zurbriggen, 2004, Bright et al, 1993).

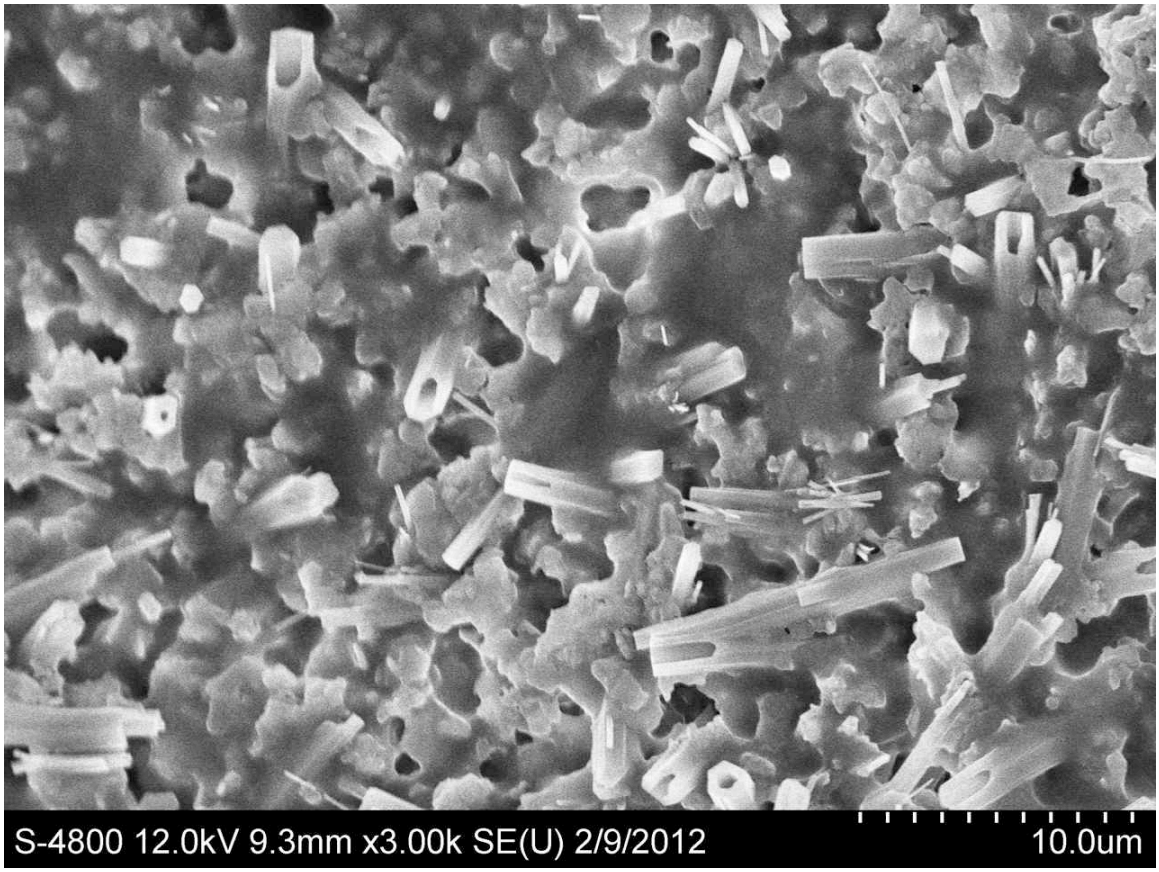

Figure 5.1.7: SEM image for polymer modified mortar with p/c = 0.3 after curing for 21d at ambient temperature sealed in a plastic bag

Compressive strengths of polymer modified cementitious materials are often lower than compressive strengths of traditional cementitious materials due to the presence of tough, flexible polymer film within the pore network of the polymer modified cementitious materials (Ohama 1995, Chandra et al, 1994, Bright et al, 1993). The polymer alone behaves as a rubber like material ultimately leading to decreases in compressive strength with increases in polymer dosage as displayed in Figure 5.1.2. This compressive strength behavior is further validated through visualization of increased polymer quantity per specific volume of microstructure with increases in polymer / cement ratio as displayed in Figures 5.1.6, 5.1.7 and 5.1.8.

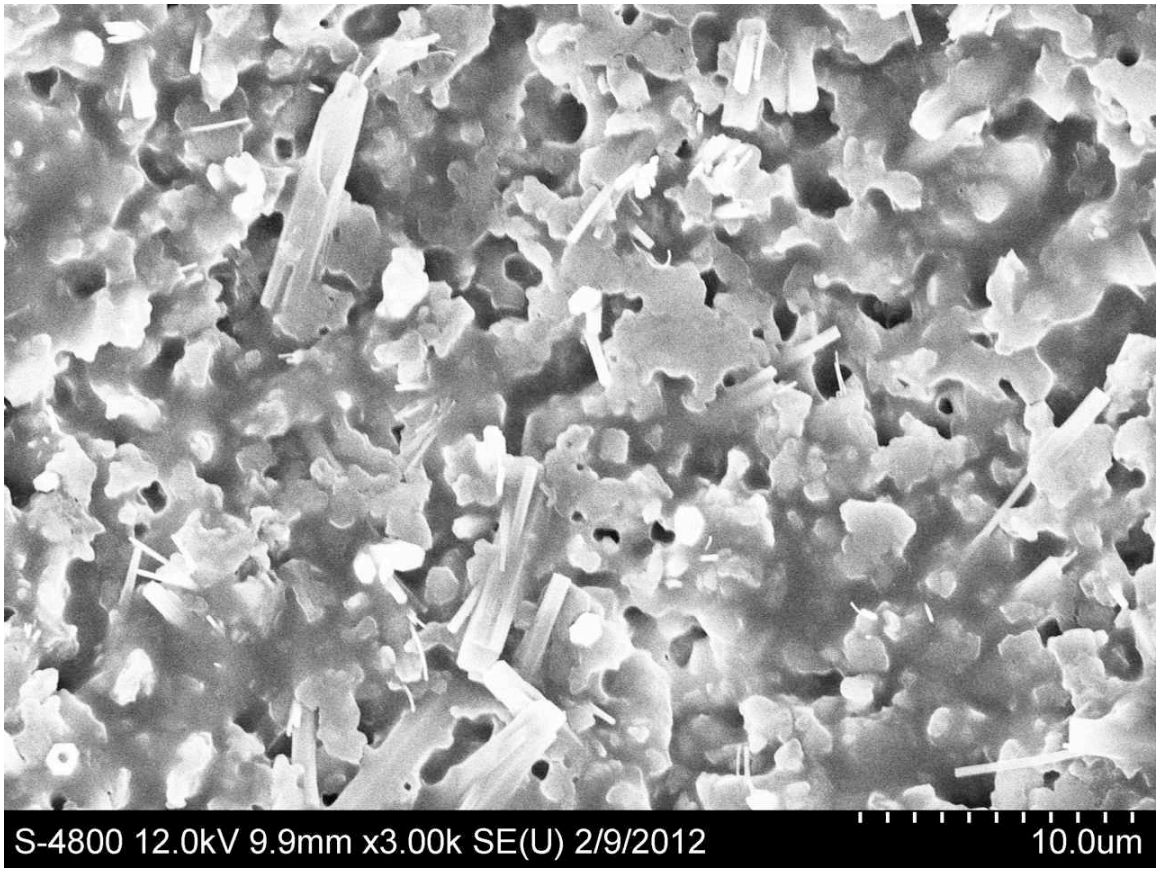

Figure 5.1.8: SEM image for polymer modified mortar with p/c = 0.45 after curing for 21d at ambient temperature sealed in a plastic bag

Literature reports very little information regarding correlations between indirect tensile strength and other mechanical property characteristics for polymer modified mortars and concretes. Nevertheless, literature reports increases in polymer concentration result in increases in flexibility for corresponding mortars (Zurbriggen, 2004). Furthermore, literature reports for ordinary portland cement based systems the relationship between polymer content and flexibility significantly changes at about 15 weight percent of polymer, where the influence of increases in polymer concentration on mortar flexibility is more pronounced above this threshold (Zurbriggen, 2004). For polymer modified OPC mortars, it seems the material properties are dominated by the mineral components at low polymer / cement ratios; whereas, the material properties seem to be more readily influenced by properties inherent to the polymeric material with higher polymer / cement ratios (Zurbriggen, 2004).

Literature reports numerous correlations between indirect tensile strength and other mechanical property characteristics for traditional, brittle concrete materials (Illston et al, 2007). For traditional, brittle concrete materials, Hassoun (1985), suggest the following predictive relationships for

indirect tensile strength, direct tensile strength and flexural strength as a function of compressive strength (f'_c):

$$\text{indirect tensile strength (psi)} = 6*(f'_c)^{1/2} \text{ to } 7*(f'_c)^{1/2} \quad (1)$$

$$\text{direct tensile strength} = 0.07*f'_c \text{ to } 0.11*f'_c \quad (2)$$

$$\text{flexural strength (psi)} = 7.5*(f'_c)^{1/2} \text{ to } 9.5*(f'_c)^{1/2} \quad (3)$$

It is important to note that predictive equations (1), (2) and (3) are for traditional concrete materials, not mortars.

Table 5.1.2 displays mechanical property average strength value ratios for the polymer modified CSA cement mortars specific to this study. It is interesting to note the differences in predictive equations (1), (2) and (3) from Hassoun (1985), when compared with the experimental values for the polymer modified mortars displayed in Table 5.1.2. This comparison suggests the developed polymer modified CSA cement mortars behave quite differently when compared with traditional concrete materials, and predictive equations (1), (2) and (3) should never be utilized for speculation regarding the behavior of polymer modified CSA cement mortars.

Table 5.1.2: MECHANICAL PROPERTY AVERAGE STRENGTH RATIOS				
Ratio	Curing Period	p/c = 0.15	p/c = 0.3	p/c = 0.45
direct tensile strength / compressive strength	7d	0.19	0.24	0.28
indirect tensile strength / compressive strength	7d	0.2	0.2	0.21
flexural strength / compressive strength	7d	0.32	0.43	0.61

Table 5.1.2: Mechanical property average strength value ratios for polymer modified CSA cement mortar at polymer / cement ratios of 0.15, 0.3 and 0.45 (3 samples each)

CONCLUSIONS

In conclusion, the mechanical property trends displayed in this work suggest that ductile behavior of polymer modified cementitious materials can be strictly controlled by specifying the material's polymer / cement ratio, ultimately specifying the quantity of tough, elastic polymer film incorporated within a specific volume of microstructure. Additionally, the experimental results suggest film forming thermoplastic materials in the form of vinyl acetate / ethylene (VAE) dispersible polymer powders (DPP) are indeed compatible with calcium sulfoaluminate (CSA) cement containing minor phase tri-calcium aluminate.

Furthermore, polymer modified CSA cement mortars follow reported literature trends for both direct tensile strength and flexural strength reaching some optimal value with increasing polymer / cement ratio before experiencing decreases in corresponding strength values once the optimum polymer / cement ratio is surpassed.

For the soft VAE DPP with T_g = -7°C (19°F) analyzed in this study, polymer modified CSA cement mortars experience decreases in both compressive strength and indirect tensile strength with increases in polymer / cement ratio. The compressive strength trend is in agreement with literature; whereas, literature is scarce regarding indirect tensile strength behavior of polymer modified CSA cement mortars.

Empirical relationships for predicting mechanical property performance behavior of contemporary, brittle cementitious materials should be extensively checked for applicability before employing their use for predicting mechanical property performance behavior of polymer modified cementitious materials with high polymer / cement ratios.

VAE polymer product portfolios offer a further advantage for fine tuning mechanical property performance of polymer modified cementitious materials, as VAE polymers are available with a wide range of glass transition temperatures thus enabling the mechanical property performance to be further tweaked after identifying an ideal polymer / cement ratio.

5.2 Assessing the Influence of Relative Humidity on Compressive Strength Behavior of Polymer Modified CSA Cement Mortar

INTRODUCTION

Calcium sulfoaluminate (CSA) cements provide interesting performance characteristics for use in patch and repair applications (Ambroise et al, 2009). Zhang and Glasser (2005), report the unique properties of CSA cements include rapid strength development even at low temperatures, good resistance to freezing during hydration and in service conditions, good corrosion resistance and excellent durability in aggressive water, e.g., sea water. Pelletier et al, (2010), Winnefeld et al, (2010) and Glasser and Zhang, (2001), provide interesting descriptions of hydration characteristics and accompanying performance behavior of various CSA cement systems.

Although calcium sulfoaluminate-based cements are increasingly being used in specialized applications where high early strengths and self-stressing or shrinkage compensation are required, their more general application to concrete is limited to China, where a wide range of $C_4A_3\bar{S}$ based cements has been developed and normalized under the name of the "Third Cement Series" (TCS) (Gartner 2004). When cured at constant high or low relative humidity, the long-term behavior of materials based upon CSA cement is not well documented. "Because it is so central to the formation and property development of cementitious systems, it is critical to understand the underlying mechanisms in order to progress; particularly on the most burning challenge facing the world today –the need to continually lower environmental impact, to do more with less." (Scrivener et al, 2011)

Vinyl acetate / ethylene based dispersible polymer powders (VAE DPP) are widely used for modification of mortars containing ordinary portland cement (OPC) or blends of calcium aluminate cement (CAC) and OPC. Numerous publications exist describing the interactions of these well known cementitious systems when cured under differing conditions (ACI 548.1R-09, ACI 503.5-R92, ACI 548.4-93, Ohama 1995, Chandra et al, 1994). Typically, polymer modified cementitious systems undergo dry curing for a specified period of time to ensure complete polymer film formation. After dry curing, polymer modified cementitious materials are often exposed to high humidity environments for extended periods of time. The family of latex polymers is quite large. Latex polymers of different chemistry behave differently when either exposed to high humidity environments or

immersed in water. Individuals formulating polymer modified CSA cement materials are encouraged to consult industry experts for polymer selection.

The purpose of this section is to evaluate three different mortar formulations based upon CSA cement and VAE DPP when cured under different relative humidity conditions. Three mortar formulations were tested with polymer / cement (p/c) ratios of 1/5, 2/5 and 3/5. Cube samples were cast according to ASTM C109, Standard Test Method for Compressive Strength of Hydraulic Cement Mortar. The cubes were tested after twenty eight days of curing at the following conditions: 28 days with 100% relative humidity, 28 days with 50% relative humidity, 7 days 100% relative humidity followed by 21 days 50% relative humidity, 7 days 50% relative humidity followed by 21 days 100% relative humidity.

MATERIALS

Cement

- Calcium sulfoaluminate (CSA) cement sourced from Buzzi Unicem was utilized in all formulations.

Aggregate

- ASTM finely graded sand from Ottawa Illinois was utilized in all formulations. A coarser, 20/30 sand, was also used in all formulations.

Polymer

- A vinyl acetate / ethylene based dispersible polymer powder (VAE DPP) with glass transition temperature (T_g) of -7°C (19°F) was included in all formulations.

EXPERIMENTAL PROGRAM

Mortars

Three mortar formulations were created with polymer / cement ratios of 1/5, 2/5 and 3/5 based upon mass of dry cementitious material and dry polymer. Cement mass remained constant across all formulations. Aggregate mass remained constant across all formulations. Individual mortar components (CSA cement, VAE DPP, ASTM graded sand and 20/30 sand) were weighed and placed into a plastic mixing bag. After all components were added, the bag was sealed and shaken vigorously by hand for approximately ninety

seconds. This type of mixing is an industry proven simulation for blending operations manufacturing dry mix mortar products containing minute quantities of additives such as accelerators and retarders. Table 5.2.1 lists mortar formulations analyzed in this experiment.

Table 5.2.1: CSA CEMENT MORTAR FORMULATIONS			
Materials (mass)	p/c = 1/5	p/c = 2/5	p/c = 3/5
CSA Cement (g)	500	500	500
VAE DPP (g)	100	200	300
Fine Sand (g)	1375	1375	1375
Coarse Sand (g)	125	125	125
Retarder (g)	2	2	2
Water (g)	200	200	300

Table 5.2.1: CSA cement mortar mix designs varying polymer / cement ratio for comparing the influence of curing conditions on compressive strength of polymer modified CSA cement mortars

Compressive Strength Test

Mortar cube specimens were cast in accordance to ASTM C109, Standard Test Method for Compressive Strength of Hydraulic Cement Mortars. Three mortar cubes were cast for each defined curing regimen. The cubes were tested after 28 days of curing at the following conditions: 28 days with 100% relative humidity, 28 days with 50% relative humidity, 7 days 100% relative humidity followed by 21 days 50% relative humidity, 7 days 50% relative humidity followed by 21 days 100% relative humidity.

RESULTS

Figure 5.2.1 displays average compressive strength values for the mortar formulation with p/c = 1/5 after curing with the following conditons: 28 days with 50% relative humidity, 28 days with 100% relative humidity, 7 days 50% relative humidity followed by 21 days 100% relative humidity, 7 days 100% relative humidity followed by 21 days 50% relative humidity.

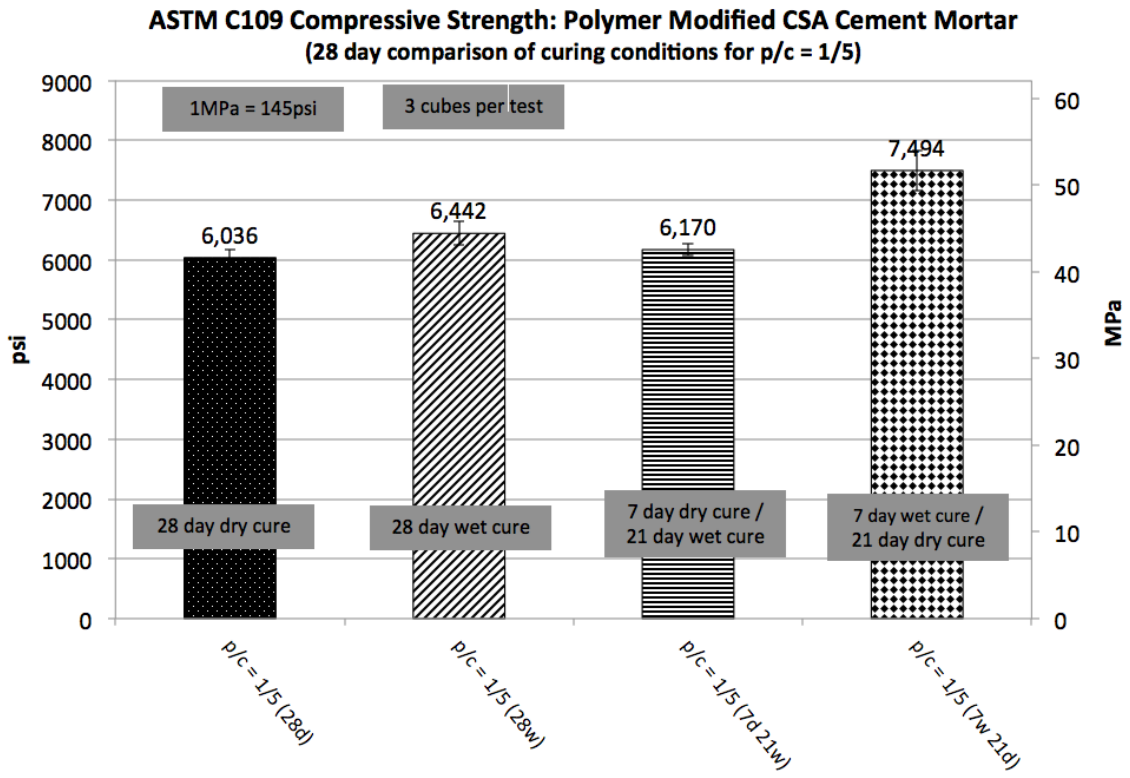

Figure 5.2.1: Compressive strength comparison of CSA cement mortar containing VAE DPP with p/c = 1/5 when cured under differing conditions (3 cubes per test)

As can be seen in Figure 5.2.1, the formulation with p/c = 1/5 displays the greatest compressive strength when cured at 100% relative humidity for seven days followed by a 21 day curing period at 50%relative humidity. This formulation experiences the second highest compressive strength values when cured at 100% relative humidity for 28 days. The formulation with p/c = 1/5 yields the third largest compressive strength value when cured at 50% relative humidity for seven days followed by a curing period of 100% relative humidity for twenty-one days. The formulation with p/c = 1/5 experiences the lowest compressive strength values when cured at 50% relative humidity for twenty-eight days.

Figure 5.2.2 displays average compressive strength values for the formulation with p/c =2/5 after curing with the following conditions: 28 days with 50% relative humidity, 28 days with 100% relative humidity, 7 days 50% relative humidity followed by 21 days 100% relative humidity, 7 days 100% relative humidity followed by 21 days 50% relative humidity.

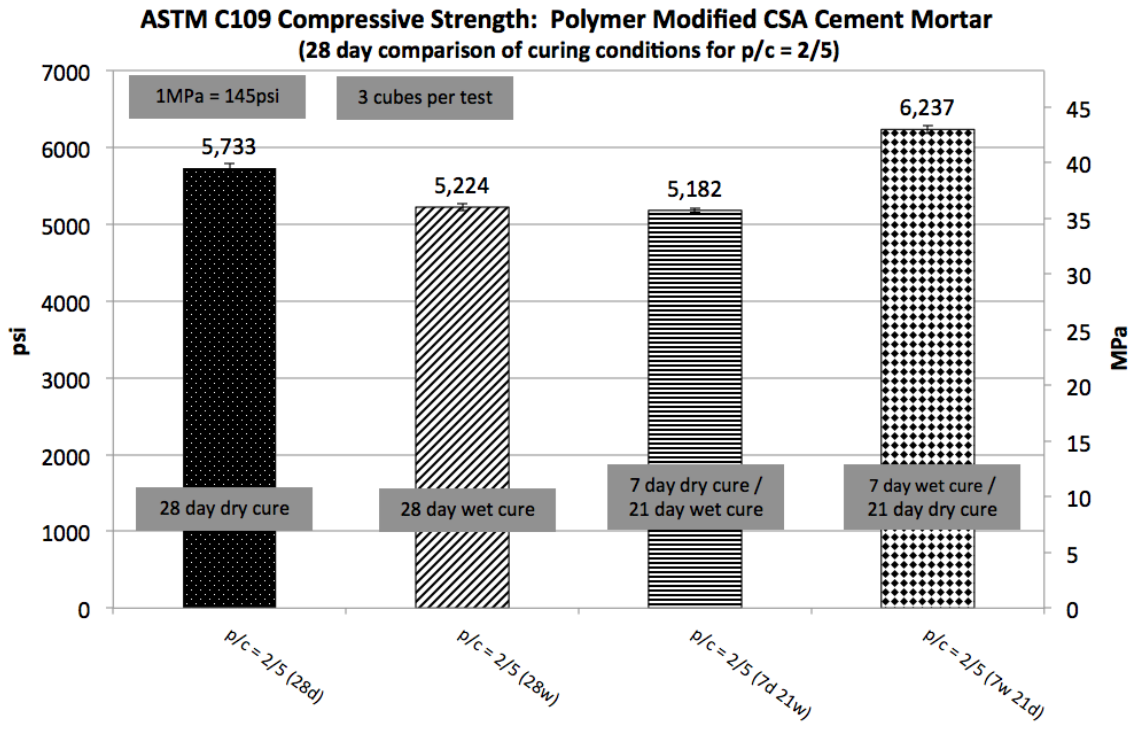

Figure 5.2.2: Compressive strength comparison of CSA cement mortar containing VAE DPP with p/c = 2/5 when cured under differing conditions (3 cubes per test)

As can be seen in Figure 5.2.2, the formulation with p/c = 2/5 displays the greatest compressive strength when cured at 100% relative humidity for seven days followed by a 21 day curing period at 50%relative humidity. This formulation experiences the second highest compressive strength values when cured at 50% relative humidity for 28 days. The formulation with p/c = 2/5 yields the third largest compressive strength value when cured at 100% relative humidity for 28 days. The formulation with p/c = 2/5 experiences the lowest compressive strength value when cured at 50% relative humidity for seven days followed by a curing period of 21 days at 100% relative humidity.

Figure 5.2.3 displays compressive strength values for the formulation with p/c = 3/5 after curing with the following conditions: 28 days with 50% relative humidity, 28 days with 100% relative humidity, 7 days 50% relative humidity followed by 21 days 100% relative humidity, 7 days 100% relative humidity followed by 21 days 50% relative humidity.

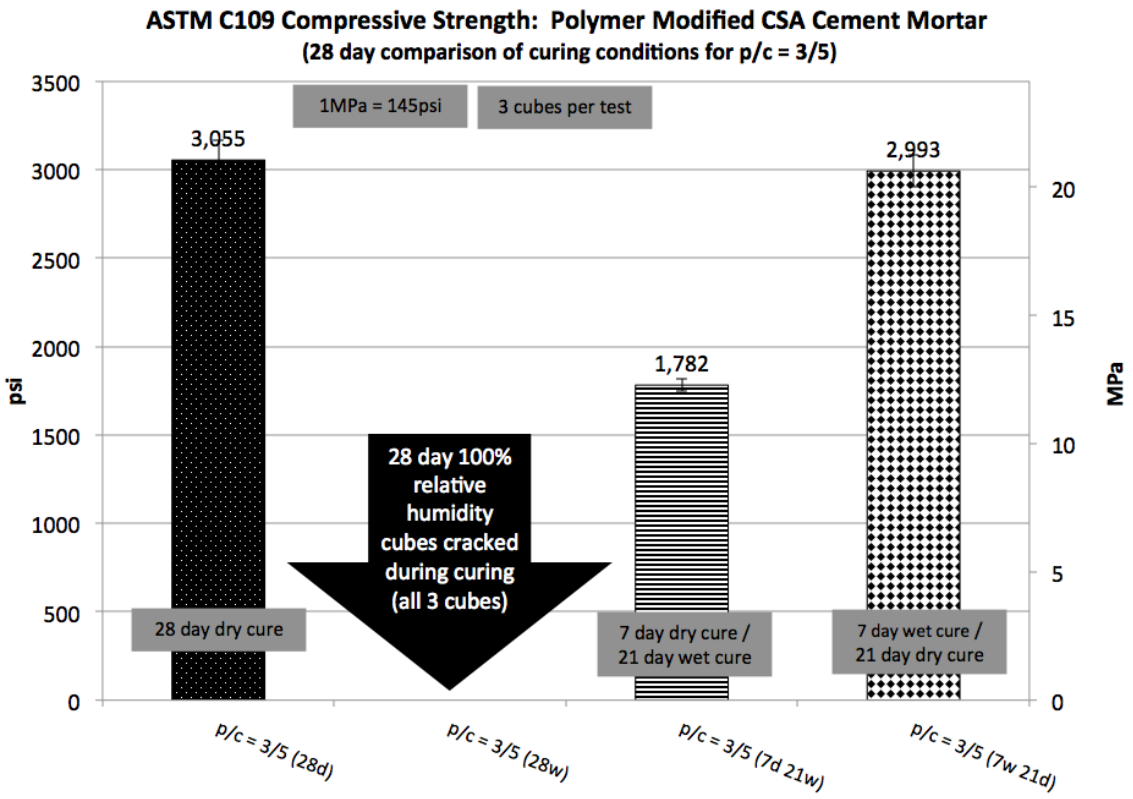

Figure 5.2.3: Compressive strength comparison of CSA cement mortar containing VAE DPP when cured under differing conditions (3 cubes per test)

As can be seen in Figure 5.2.3, the formulation with p/c = 3/5 displays similar compressive strength values for dry curing at 50% relative humidity and when cured at 100% relative humidity for seven days followed by a 21 day curing period at 50%relative humidity. All three cubes for the formulation with p/c = 3/5 experienced severe cracking when stored at 100% relative humidity for 28 days; therefore, compressive strength testing was not possible for this curing regimen. The cubes cured for 7 days at 50% relative humidity followed by 21 days at 100% relative humidity displayed the lowest compressive strength values.

The materials tested and displayed in Figure 5.2.1 were further examined to determine the influence of a short, two day drying period after being exposed to 100% relative humidity for 28 days. Figure 5.2.4 displays the information displayed in Figure 5.2.1 plus the additional 30 day testing samples –where the additional samples were cast from the same mortar batch as the materials displayed in Figure 5.2.1. The samples cured for 30 days at 50% relative humidity and 23°C displayed an average compressive strength value of 6,190psi (42.7MPa) while the samples cured for 28 days at 100% relative humidity

and two days at 50% relative humidity displayed an average compressive strength value of 7,266psi (50.1MPa). Comparing the 30 day samples with the 28 day samples in Figure 5.2.4 suggests the two day drying period allowed further drying of the polymer film, and perhaps a greater degree of hydration, resulting in improved compressive strength performance. The message of Figure 5.2.4 is polymer modified CSA cement materials rapidly desiccate while gaining strength, perhaps as a result of continued hydration, when transferred from a high humidity environment to a low humidity environment at constant temperature of 23°C.

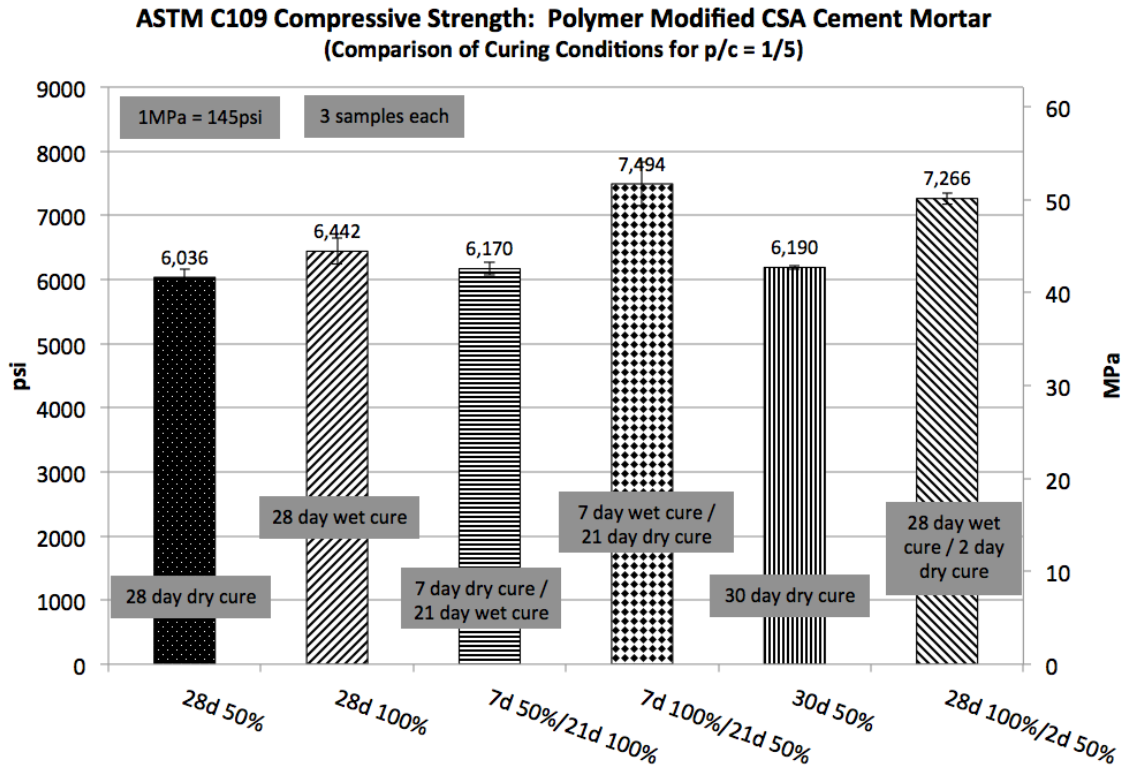

Figure 5.2.4: Polymer modified CSA cement mortar with p/c = 1/5 displayed in Figure 5.2.1 along with 30 day testing data demonstrating influence of wet curing plus a drying period for ensuring sufficient polymer film formation

DISCUSSION

The results presented in this section support the convention reported by Ohama, Chandra and others, which is quoted below. Please note that vinyl acetate / ethylene based polymer powders belong to a larger family known as "latex" polymeric materials.

> Latex modified mortar and concrete have a structure in which the larger pores can be filled with polymers or sealed with continuous polymer films. In general, the effect of polymer filling or sealing increases with a rise in polymer content or polymer / cement ratio. These features are reflected in reduced water absorption, water permeability, and water vapor transmission. As a result, the latex modified mortar and concrete have an improved waterproofness over ordinary mortar and concrete. On the other hand, they have a poorer water resistance so that their strength is decreased when exposed to water or high humidities. (Ohama 1995)

The thought of a material having "increased waterproofness but a poorer water resistance so that their strength is decreased when exposed to water or high humidities" could be interpreted as a contradiction. However, the data presented in Figures 5.2.2 and 5.2.3 support Ohama's statement. When exposed to water, the VAE polymer film becomes soft and flexible. As the polymer / cement ratio increases, the flexible influence of wet polymer film becomes more pronounced for cubes stored at 100% relative humidity before testing.

Considering the statements made above, it is important to remember the polymer being used in this experiment has a T_g = -7°C., which is a very flexible polymer. The nature of VAE dispersible polymer is to fill the voids within the cement matrix with a polymer film. As polymer / cement ratio increases, a higher percentage of flexible material exists within the defined volume of each mortar cube. This higher percentage of flexible material within the microstructure is apparent in the behavior displayed in Figures 5.2.1, 5.2.2 and 5.2.3.

Figure 5.2.1 displays information for a polymer modified CSA cement mortar with polymer / cement ratio of 1/5. Such a p/c is typical for general performance patch and repair materials, as the microstructure is more or less dominated by the mineral components. Such behavior is illustrated in Figure 5.2.1 as the 28 day sample cured at 100% relative humidity displays greater compressive strength when compared with the 28 day sample cured at 50% relative humidity. Specialized patch and repair materials typically have p/c ratios greater than 1/5 while often including a specialty polymer or blend of polymers to guarantee a certain performance. In higher p/c ratio materials, the greater the polymer concentration per specific material volume, the more the polymer begins to influence the microstructural behavior. The results displayed in Figure 5.2.3 clearly demonstrate the influence of higher p/c ratios on compressive strength behavior in different environments as all three cubes cured at 100% relative humidity experienced

severe cracking, while the material cured at 50% relative humidity did not demonstrate cracking.

Figures 5.2.5 and 5.2.6 display secondary ettringite formation as a root cause for cracking in a similar polymer modified mortar utilizing identical CSA cement, sand and polymer chemistry. The polymer modified mortar displayed in Figures 5.2.5 and 5.2.6 was dry cured for 14 days before being immersed in water. The author's experience suggests softening of the polymer film often requires time periods in excess of 150 days of water immersion for CSA cement mortars with p/c greater than 1/5; that is, if the mortar had been dry cured so as to completely form the polymer film before water immersion. For the case of a 100% humidity environment, the author has experience with cubes having p/c greater than 1/5 cracking at periods greater than 200 days if the polymer film had properly formed. It is quite important to note that the aforementioned experimental materials were poorly formulated, as the formulations contained no de-foaming, plasticizing or filling materials. Simply put, a properly formulated material based upon CSA cement and VAE polymer is likely to "weather" 100% humidity environments and water immersion tests for extended periods of time as the number of larger void spaces is more effectively controlled.

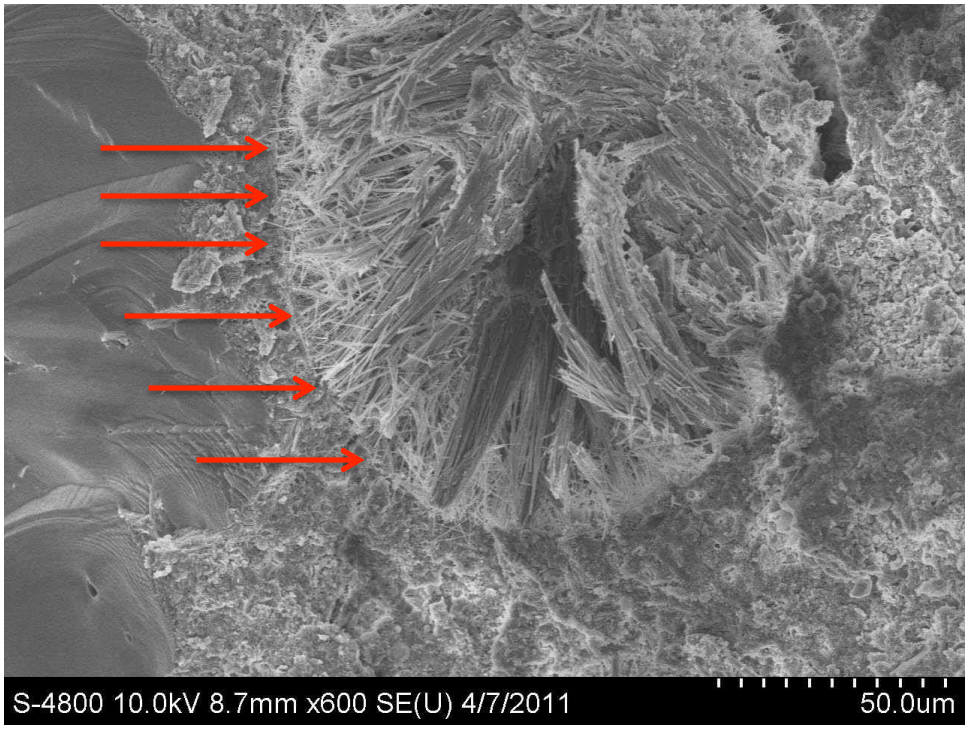

Figure 5.2.5: Display of long, slender ettringite crystals filling former void space as a result of secondary ettringite formation for polymer modified CSA cement mortar dry cured for 14 days then immersed in water at 23°C for > 150 days

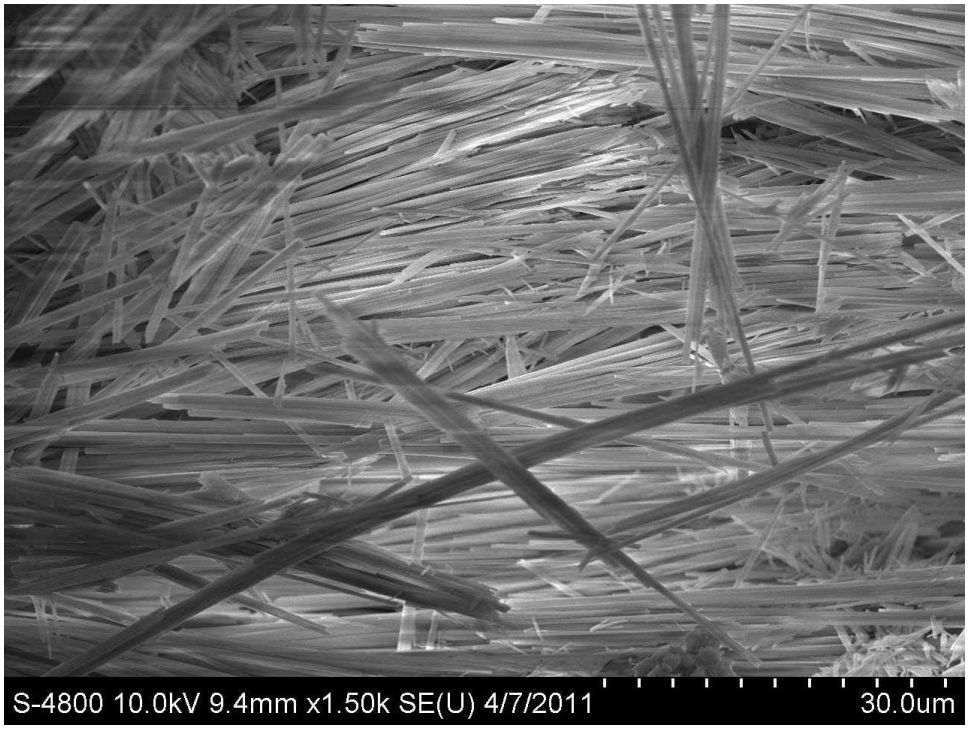

Figure 5.2.6: Display of ettringite crystals with needle like shape extending from adjacent crack faces as a result of secondary ettringite formation for polymer modified CSA cement mortar dry cured for 14 days then immersed in water at 23°C for > 150 days

CONCLUSION

In conclusion, the polymer modified calcium sulfoaluminate (CSA) cement mortars with polymer / cement ratios (p/c) of 1/5, 2/5 and 3/5 displayed unique compressive strength behavior when cured at constant 50% and 100% relative humidity or combinations thereof. All samples were cured at 23°C.

The CSA cement mortar with p/c of 1/5 demonstrated the greatest average compressive strength value after curing for 7 days at 100% relative humidity followed by 21 days at 50% relative humidity. The second highest compressive strength values belonged to cubes cured for 28 days at 100% relative humidity. The samples cured either at constant 50% relative humidity or those cured for 7 days at 50% relative humidity followed by 21 days at 100% relative humidity displayed the lowest compressive strength values.

The CSA cement mortar with p/c of 2/5 demonstrated the greatest average compressive strength value after curing for 7 days at 100% relative humidity followed by 21 days at 50% relative humidity. The second highest compressive strength values

belonged to cubes cured for 28 days at 50% relative humidity. The samples cured for 28 days at constant 100% relative humidity or samples cured for 7 days at 50% relative humidity followed by 21 days at 100% relative humidity displayed the lowest compressive strength values.

The CSA cement mortar with p/c of 3/5 demonstrated the greatest average compressive strength value after curing for 7 days at 100% relative humidity followed by 21 days at 50% relative humidity. The second highest compressive strength values belonged to cubes cured for 28 days at 50% relative humidity. The samples cured for 28 days at constant 100% relative humidity demonstrated severe cracking and could not be tested for compressive strength. The samples cured for 7 days at 50% relative humidity followed by 21 days at 100% relative humidity displayed the lowest compressive strength values.

The experimental results highlight the influence of both polymer concentration and relative humidity on compressive strength behavior of polymer modified CSA cement mortars. Materials with higher polymer / cement ratios experienced the greatest compressive strength differentials for samples cured in different humidity environments. Proper care should be taken when formulating polymer modified CSA cement materials for use in either high humidity environments or water immersion type applications.

5.3 Mitigating Carbonation Behavior of CSA Cement Mortars and Pastes

INTRODUCTION

The purpose of this study was to assess the influence of latex polymer addition on both ettringite decomposition behavior and direct tensile strength loss within calcium sulfoaluminate (CSA) cement pastes and mortars, respectively. CSA cement pastes were assessed from an analytical perspective at specific intervals while being cured at 23°C and 50% relative humidity. Analytical analysis included thermo-gravimetric analysis (TGA), X-Ray diffraction (XRD) along with visual phase confirmation through use of a scanning electron microscope (SEM). Mechanical property evaluation of CSA cement mortars included direct tensile strength, modulus of rupture and unconfined compressive strength testing for select specimens. The presented results strongly suggest latex polymer addition to be effective for mitigating ettringite decomposition behavior and direct tensile strength loss in materials based upon CSA cement cured at 23°C and 50% relative humidity for extended periods of time.

Table 5.3.1: CSA CEMENT MORTAR FORMULATIONS		
Materials	EF1-220 (Control)	HH9E (Polymer Modified)
CSA Cement	500	500
Anhydrite	160	160
VAE Polymer T_g = 20°C		100
Graded Sand	1375	1375
20/30 Sand	125	125
Tartaric Acid	2	2
Total Mass (g)	2162	2262
Deionized Water	220	220

Table 5.3.1: Listing of components by mass for polymer modified and non-polymer modified CSA cement mortars

RESULTS

Figure 5.3.1 displays direct tensile strength values for the control mix design containing solely anhydrite as a source of calcium sulfate listed in Table 5.3.1. For the tested samples, which were cured at 50% relative humidity and 23°C, the strength development trend increased from the point of initial hydration up through some period between 28 days and 56 days of hydration. As illustrated in Figure 5.3.1, the direct tensile strength results for 24 hours, 48 hours, 7 days and 28 days are 275psi (1.9MPa), 488psi

(3.4MPa), 493psi (3.4MPa) and 633psi (4.4MPa), respectively. Whereas, the direct tensile strength results for 28 days, 56 days and 109 days are 633psi (4.4MPa), 567psi (3.9MPa) and 539psi (3.7MPa), respectively. The period from initial hydration through 28 days is clearly a period of increasing direct tensile strength; whereas, the period from 28 days through 109 days of hydration is clearly a period of decreasing direct tensile strength.

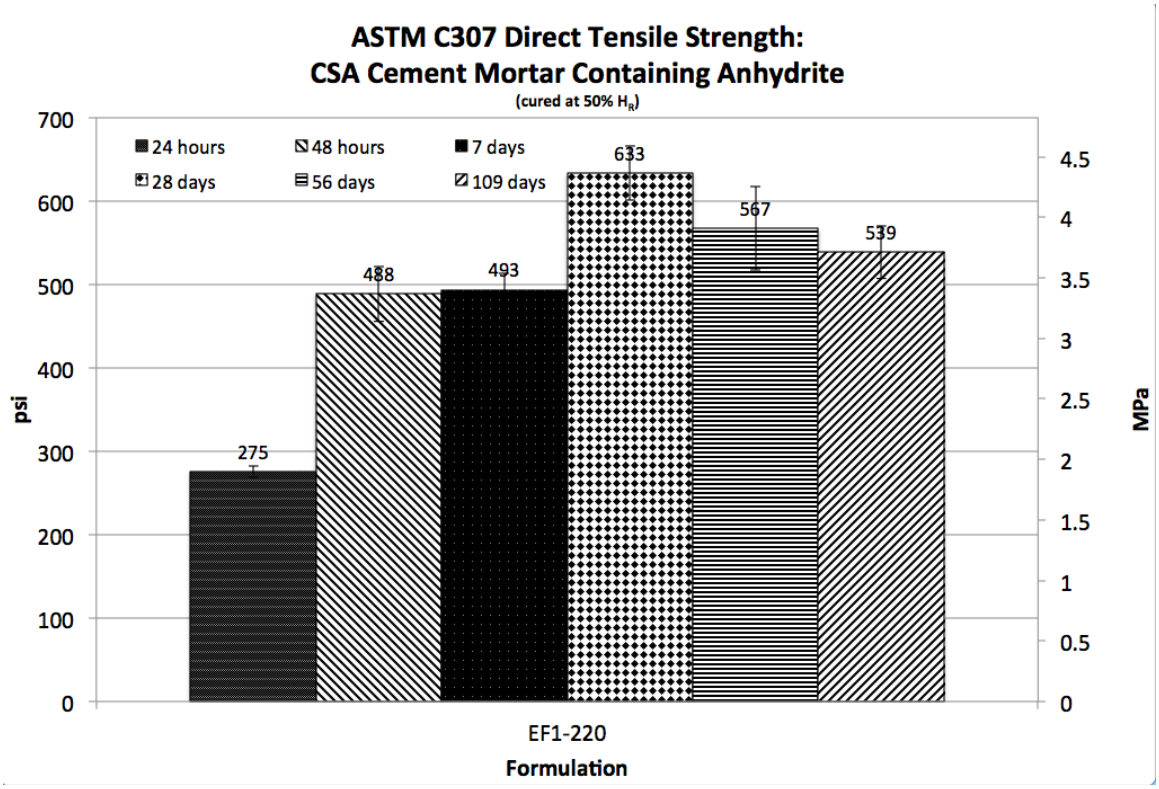

Figure 5.3.1: Direct tensile strength according to ASTM C307 for the CSA cement mortar control sample (EF1-220) displayed in Table 5.3.1 (3 dog bones each)

Figures 5.3.2, 5.3.3 and 5.3.4 display mechanical property performance information for the polymer modified CSA cement mortar mix design presented in Table 5.3.1 after curing for seven and 388 days at ambient laboratory temperature of 23°C and constant 50% relative humidity. Figure 5.3.2 displays the polymer modified CSA cement mortar presented in Table 5.3.1 having a direct tensile strength of 869psi (5.9MPa) and 1,051psi (7.2MPa), after hydrating for seven and 388 days, respectively. Figure 5.3.3 displays the polymer modified CSA cement mortar presented in Table 5.3.1 having a modulus of rupture, or flexural strength, of 1,635psi (11.3MPa) and 2,223psi (15.3MPa), after hydrating for seven and 388 days, respectively. Figure 5.3.4 displays the polymer modified CSA cement mortar presented in Table 5.3.1 having an unconfined compressive strength of 7,701psi

(53.1MPa) and 9,870psi (68.1MPa), for hydration periods of seven and 388 days, respectively. Samples yielding the results presented in Figures 5.3.2, 5.3.3 and 5.3.4 were cast from the same mortar batch --three dog bones, three flexural strength bars and two cubes. The results presented in Figures 5.3.2, 5.3.3 and 5.3.4 are astonishing considering no means of reinforcement, aside from polymer modification, exist within the CSA cement mortar mix designs. The results presented in Figures 5.3.2, 5.3.3 and 5.3.4 highlight latex polymer addition as a viable means for mitigating strength loss in cementitious materials based upon CSA cement when applied in low humidity environments.

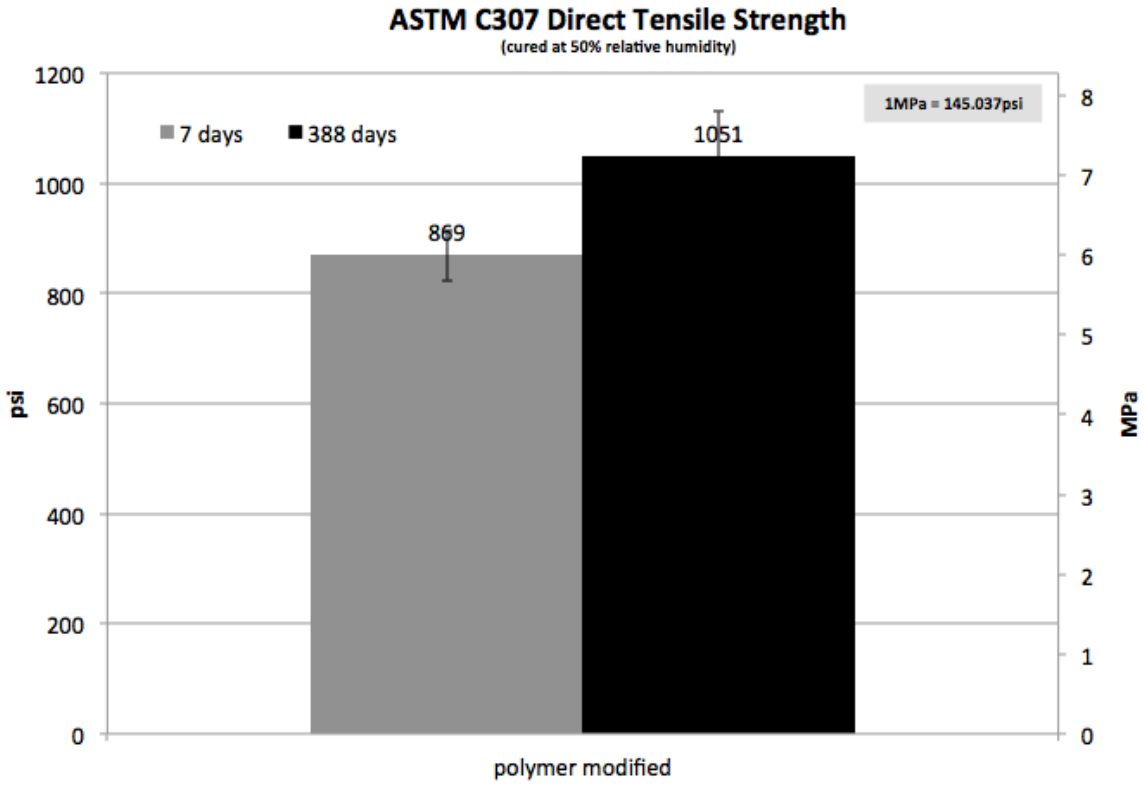

Figure 5.3.2: Direct tensile strength according to ASTM C307 for polymer modified CSA cement mortar (HH9E) containing solely anhydrite as a source of calcium sulfate displayed in Table 5.3.1 (3 dog bones)

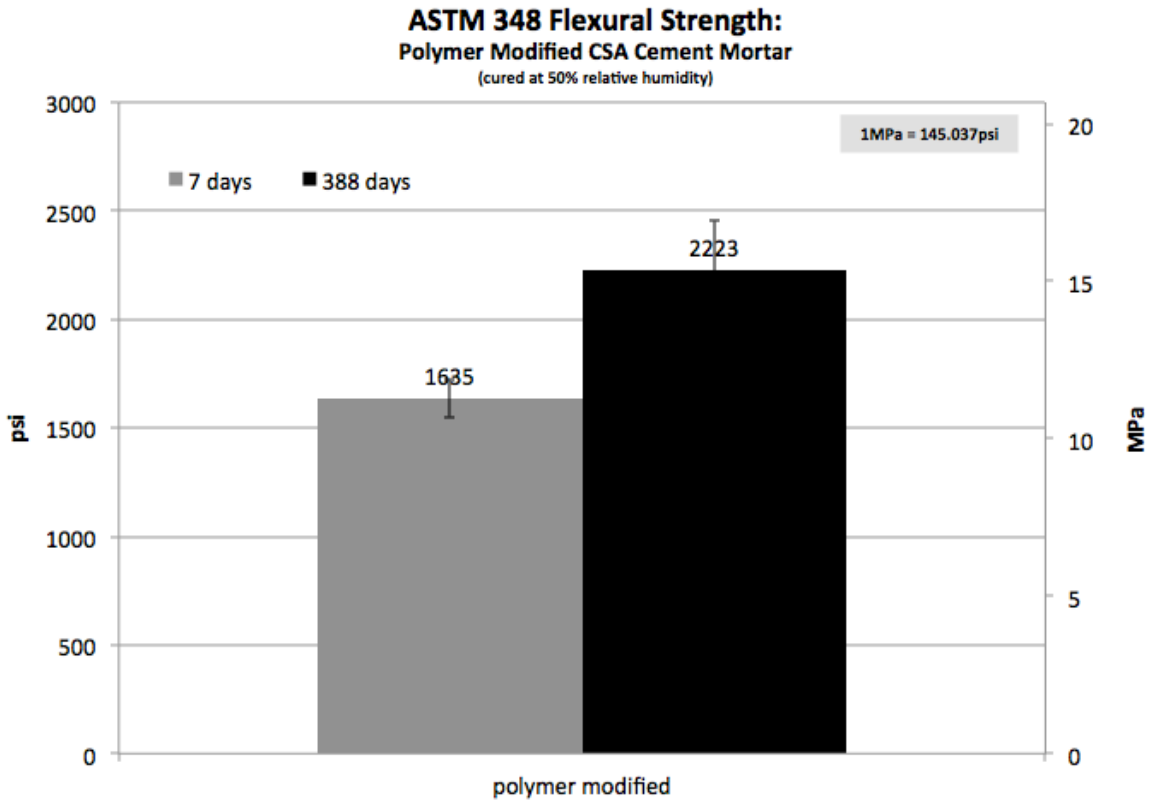

Figure 5.3.3: Flexural strength according to ASTM C348 for polymer modified CSA cement mortar (HH9E) containing solely anhydrite as a source of calcium sulfate displayed in Table 5.3.1 (3 flex bars)

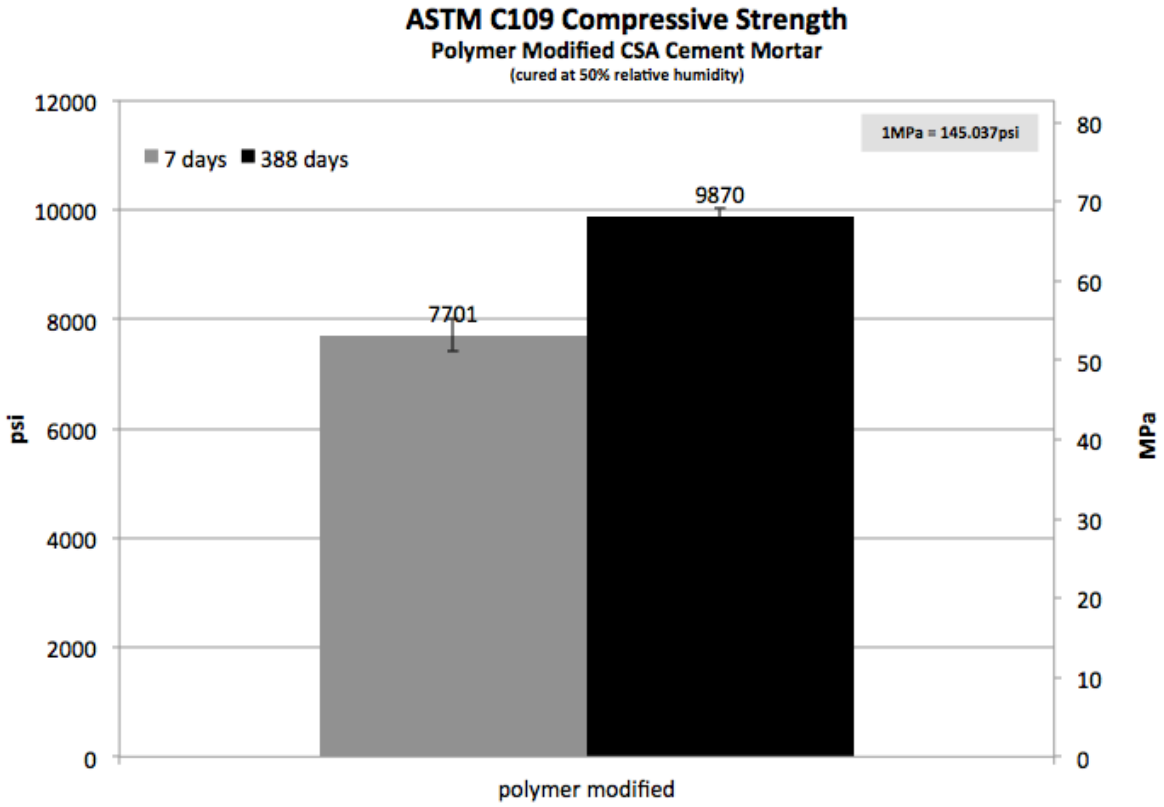

Figure 5.3.4: Compressive strength according to ASTM C109 for polymer modified CSA cement mortar (HH9E) containing solely anhydrite as a source of calcium sulfate displayed in Table 5.3.1 (2 cubes)

Table 5.3.2 displays CSA cement paste mix design information for TGA, XRD and calorimeter analyses. Table 5.3.2 lists components by mass. The CSA cement pastes are similar to the CSA cement mortars displayed in Table 5.3.1. The CSA cement pastes simply contain no sand. Sand was omitted in an effort to minimize contributions to experimental error during analytical analysis. The presented information related to Table 5.3.2 is important as it highlights differences in microstructural characteristics between polymer modified and non-polymer modified CSA cement pastes. Microstructural characteristics continually changed for both cement pastes throughout the duration of the study. The control CSA cement paste experienced decomposition of ettringite; whereas, the polymer modified CSA cement paste experienced growth in what is theorized to be monocarbonate while also maintaining a significant concentration of ettringite throughout the duration of the study. The results of the analytical analysis are presented in greater detail in the following pages.

Table 5.3.2: CSA CEMENT PASTE FORMULATIONS		
Materials	Control Cement Paste (CC7)	Polymer Modified Cement Paste (CC6)
CSA Cement	20	20
Anhydrite	6	6
VAE Polymer T_g = 20°C		4
Total Mass (g)	26	30
Deionized Water	8	8

Table 5.3.2: Listing of components by mass for polymer modified and non-polymer modified CSA cement pastes

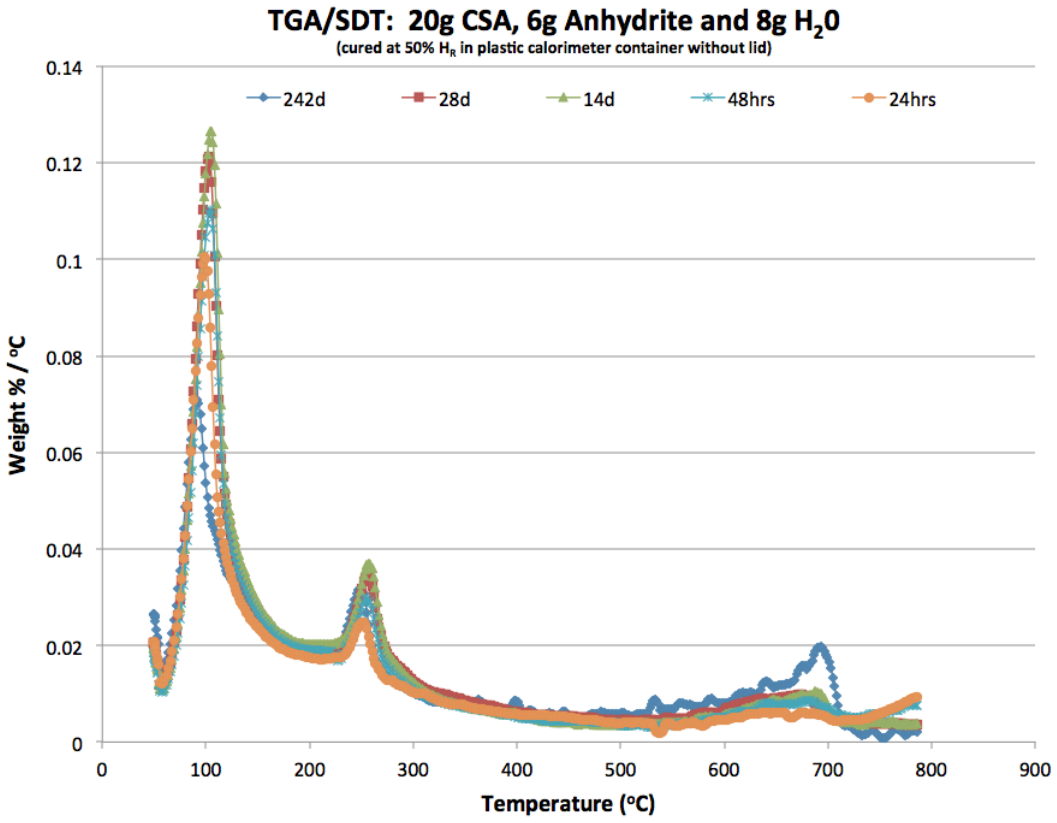

Figure 5.3.5: TGA/SDT analysis for CSA cement paste containing solely anhydrite as a source of calcium sulfate cured at constant 50% relative humidity

Figure 5.3.5 displays TGA/SDT analysis for control cement paste, CC7, in Table 5.3.2 after hydrating for 24 hours, 48 hours, 14 days and 28 days at 50% relative humidity and 23°C. The peak near 120°C represents the relative concentration of ettringite in each sample (Clark et al, 2006, Sherman et al, 1995). The curves suggest the concentration of ettringite increased from initial hydration through fourteen days. The concentration of

ettringite decreased from 14 days through 242 days of hydration at constant 50% relative humidity.

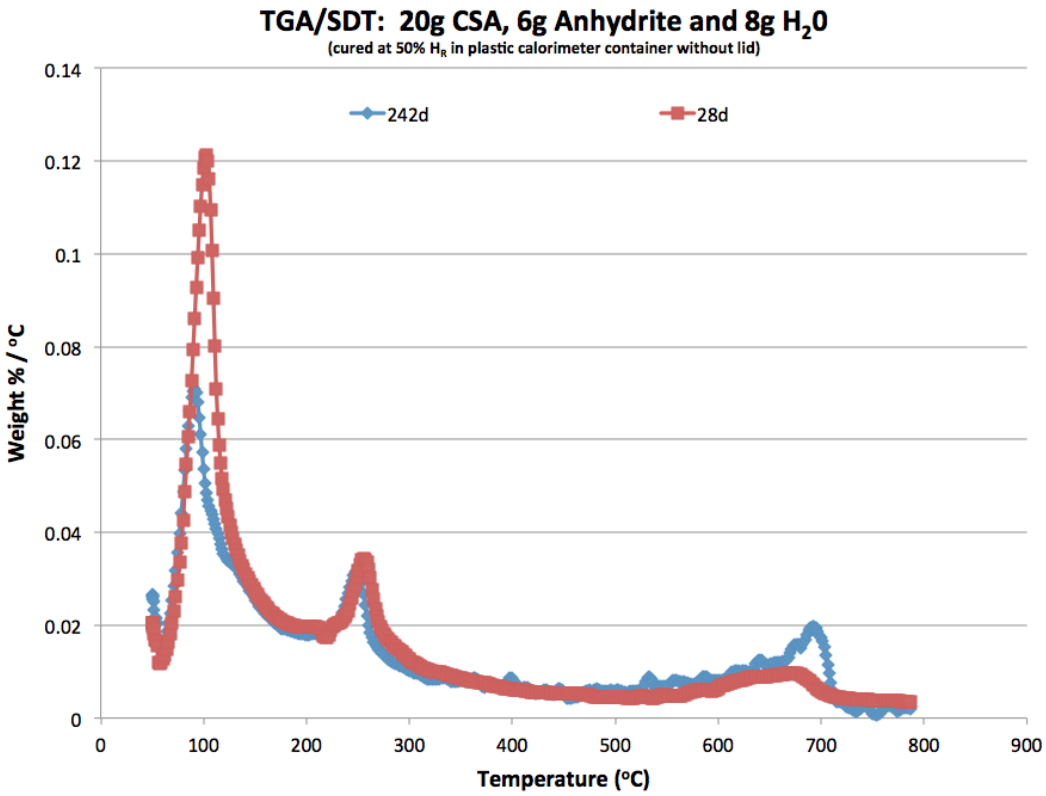

Figure 5.3.6: TGA/SDT analysis for CSA cement paste containing solely anhydrite as a source of calcium sulfate cured at constant 50% relative humidity

Figure 5.3.6 displays TGA/SDT analysis for the control cement paste, CC7, in Table 5.3.2 after hydrating for 28 days and 242 days at 50% relative humidity and 23°C. The important points to note are both the decrease in ettringite concentration represented by the peaks near 120°C and the increase in calcium carbaonte concentration. Such an increase in calcium carbonate concentration, with the peak at 700°C, at such a late stage in the hydration cycle suggests occurrence of ettringite decomposition (Sherman et al, 1995, Sato et al, 1992). Whether the ettringite decomposition is via carbonation type processes as explained by Sato et al, (1992), or some other mechanism due to low humidity environment is an excellent project for future research.

The relative concentrations of constituent materials according to XRD analysis for the control cement paste displayed in Table 5.3.2 after curing for 28 days at 50% relative humidity are listed below:

Yeelimite > Anhydrite >> Brownmillerite, $Ca_3Al_2O_6$ > Ettringite, Belite, alpha-Ca_2SiO_4

Similarly, the relative concentrations of constituent materials according to XRD analysis of the control cement paste listed in Table 5.3.2 after curing for 242 days at 50% relative humidity are listed below:

Yeelimite > Anhydrite >> Ettringite, $Ca_3Al_2O_6$ > Gamma Ca_2SiO_4, Belite

Comparing the XRD analysis supports other information suggesting the control CSA cement paste in Table 5.3.2 experienced changes in microstructural characterisitics between 28 days and 242 days of hydration at ambient laboratory temperature of 23°C and 50% relative humidity. The presented information further supports the decreases in direct tensile strength observed for the CSA cement mortar containing solely anhydrite displayed in Figure 5.3.1.

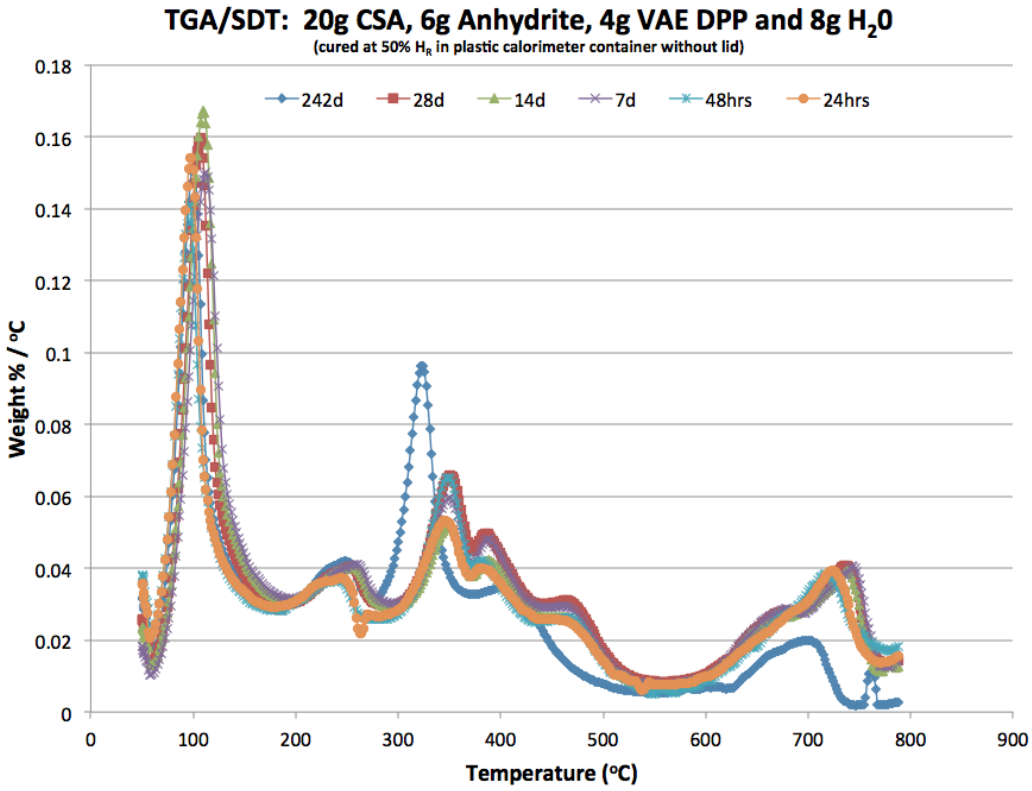

Figure 5.3.7: TGA/SDT analysis for polymer modified CSA cement paste in containing vinyl acetate / ethylene dispersible polymer powder displayed in Table 5.3.2 after curing for 24 hours, 48 hours, 7 days, 14 days, 28 days and 242 days at constant 50% relative humidity and ambient laboratory temperature of approximately 23°C.

Figure 5.3.7 displays TGA/SDT analysis of the CSA cement paste containing anhydrite and VAE dispersible polymer powder with T_g = 20°C after hydrating for periods of 24 hours, 48 hours, 7 days, 14 days, 28 days and 242 days at 50% relative humidity and 23°C. The interesting aspects of Figure 5.3.7 are the somewhat constant concentrations of ettringite, the increase in aluminum hydroxide concentration and the apparent decrease in calcium carbonate content at later ages. The peaks near 120°C suggest the concentration of ettringite remains relatively constant for hydration periods ranging from 24 hours to 242 days. The peaks near 250°C and 300°C suggest the concentration of aluminum hydroxide increased. Such aspects clearly suggest addition of latex polymer as an effective means for mitigating ettringite decomposition at later ages.

Additionally, and especially interesting for this polymer modified sample is a new peak seems to have emerged near 300°C. Before labeling this peak, it is important to note a number of items capable of influencing long term behavior. One important point to note is that VAE DPP includes anti-caking agents in the range of 10 to 15 percent by mass of the final product. Examples of typical anti-caking agents are calcium carbonate and kaolin clay. Winnefeld and Lothenbach, (2013), report the ternary system, yeelimite, calcium sulfate, calcium carbonate has potential to form either hemicarbonate or monocarbonate in addition to the primary hydration assemblages ettringite, monosulfate and aluminum hydroxide (Winnefeld and Lothenbach, 2013). Furthermore, it is suggested hemi-carbonate may initially form and coexist for some period of time, likely due to slow formation kinetics of moncarbonate as observed in ordinary portland cement, before reacting with yeelimite and calcite to form either ettringite or monocarbonate (Winnefeld and Lothenbach, 2013). Additionally, literature reports for CSA cements containing accessory phases, C-S-H, $C_2A\bar{S}H_8$ or calcium aluminate hydrates, mainly CAH_{10} or C_4AH_{13}, can be formed in addition to the aforementioned primary hydration assemblages (Pelletier-Chaignat et al, 2012). Before labeling the new late age peak at 300°C, consideration should also be given to reports stating for CSA cement containing belite as a constituent, belite reacts slower than yeelimite forming stratlingite at later ages (Romain et al, 2013). It is well known metastable aluminate hydrates, with examples being CAH_{10},C_4AH_{13} or $C_2A\bar{S}H_8$ may convert to C_3AH_6, hydrogarnet, at later ages (Taylor, 1997). Also of importance for labeling the peak is that literature reports thermal decomposition characteristics of monocarbonate, gamma aluminum hydroxide and hydrogarnet as being somewhat similar within temperature ranges, more specifically possessing similar peaks near 300°C (Chowaniec, 2012, Gameiro et

al, 2012, Gabrovsek et al, 2008, Scrivener and Capmas, 1998, Taylor, 1997). The size of the new peak at 300°C is also important for purposes of determination, as it displays a significant concentration relative to other materials. Given this information, the author theorizes the new peak near 300°C is associated with monocarbonate. The theory is further supported by the peaks near 450°C for the early age samples, likely representing hemicarbonate, which are not visible with analysis of the later age sample. The presence of hemicarbonate at early ages of hydration suggests the polymer modified CSA cement paste containing minor amounts of calcium carbonate hydrated to form ettringite, aluminum hydroxide, hemicarbonate and possibly monosulfate during the early ages, where the hemicarbonate converted to monocarbonate at later ages, which agrees with literature (Winnefeld and Lothenbach, 2013). In further support, Chowaniec, (2012), displays thermogravimetric analysis (TGA) charts for decomposition of both hemicarbonate and monocarbonate where the peak near 450°C is noted as a means for differentiating hemicarbonate from monocarbonate, as the peak does not appear during TGA analysis of monocarbonate. Additionally, the relatively constant concentrations of ettringite throughout the duration of all analyses together with the either constant or decreasing concentrations of calcium carbonate suggest latex polymer addition as an effective means for mitigating ettringite decomposition in the tested CSA cement pastes.

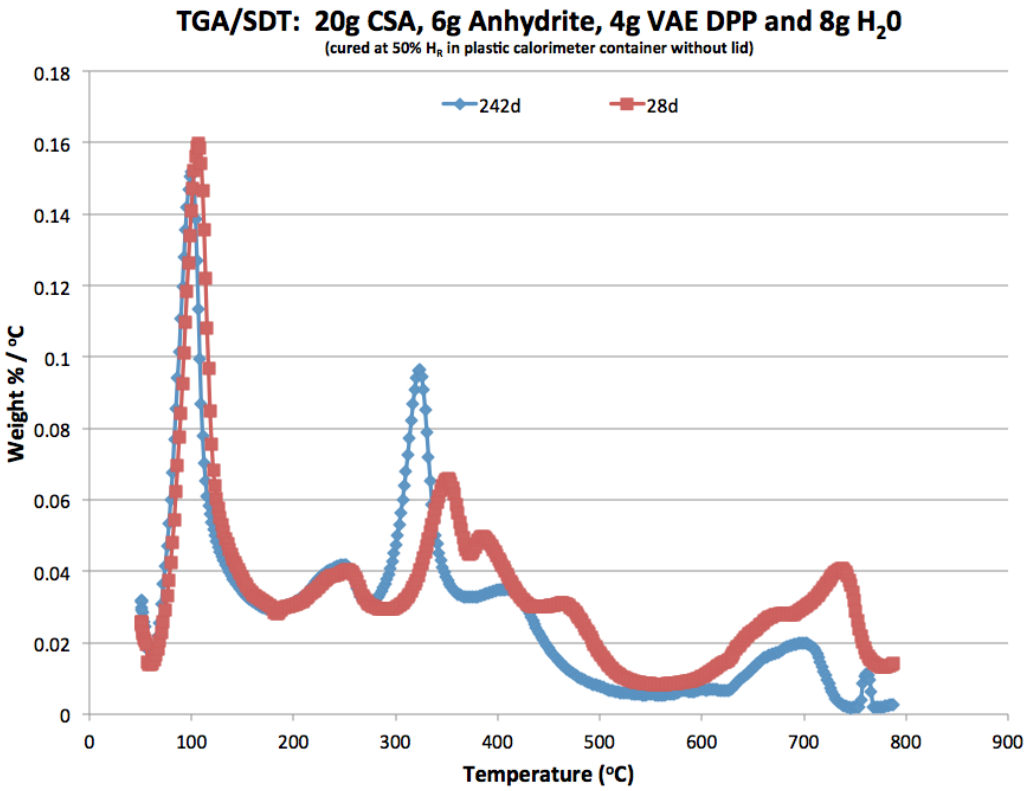

Figure 5.3.8: TGA analysis for polymer modified CSA cement paste containing vinyl acetate / ethylene dispersible polymer powder displayed in Table 5.3.2 after curing for 28 days and 242 days at constant 50% relative humidity and ambient laboratory temperature of approximately 23°C.

Furthermore, Figure 5.3.8 provides a focused look at theorized microstructural behavior. To reiterate points pertaining to monocarbonate formation, it is important to note the decrease in calcium carbonate concentration near 700°C, the decrease in hemi-carbonate concentration between 400 and 500°C and the increase in monocarbonate concentration near 300°C. Additionally, it is important to note the concentration of ettringite remains relatively constant for the later age samples, supporting the addition of VAE DPP as an effective means for mitigating ettringite decomposition in later age samples cured at constant 50% relative humidity and 23°C.

The relative concentration of constituent materials according to XRD analysis for the polymer modified CSA cement paste displayed in Table 5.3.2 after hydrating for 28 days at 50% relative humidity is listed below:

Yeelimite > Anhydrite >> Brownmillerite, Ettringite, $Ca_3Al_2O_6$ > Belite, alpha-Ca_2SiO_4

The concentration of ettringite in the XRD characterization relative to other constituent materials supports the TGA/SDT results displayed in Figure 5.3.8.

Similarly, the relative concentration of constituent materials for the polymer modified CSA cement paste displayed in Table 5.3.2 after hydrating for 242 days at 50% relative humidity is listed below:

$$\text{Yeelimite} > \text{Anhydrite} > \text{Ettringite} > Ca_3Al_2O_6 > \text{Belite}$$

The XRD analysis information further supports the presented information suggesting a change in microstructural characteristics occurred for the polymer modified CSA cement paste displayed in Table 5.3.2 after hydration periods of both 28 days and 242 days at 50% relative humidity and ambient laboratory temperature of 23°C. These analyses highlight the concentration of ettringite as being greater relative to other materials for the polymer modified CSA cement paste versus the control cement paste displayed in Table 5.3.2. This further supports the TGA/SDT information.

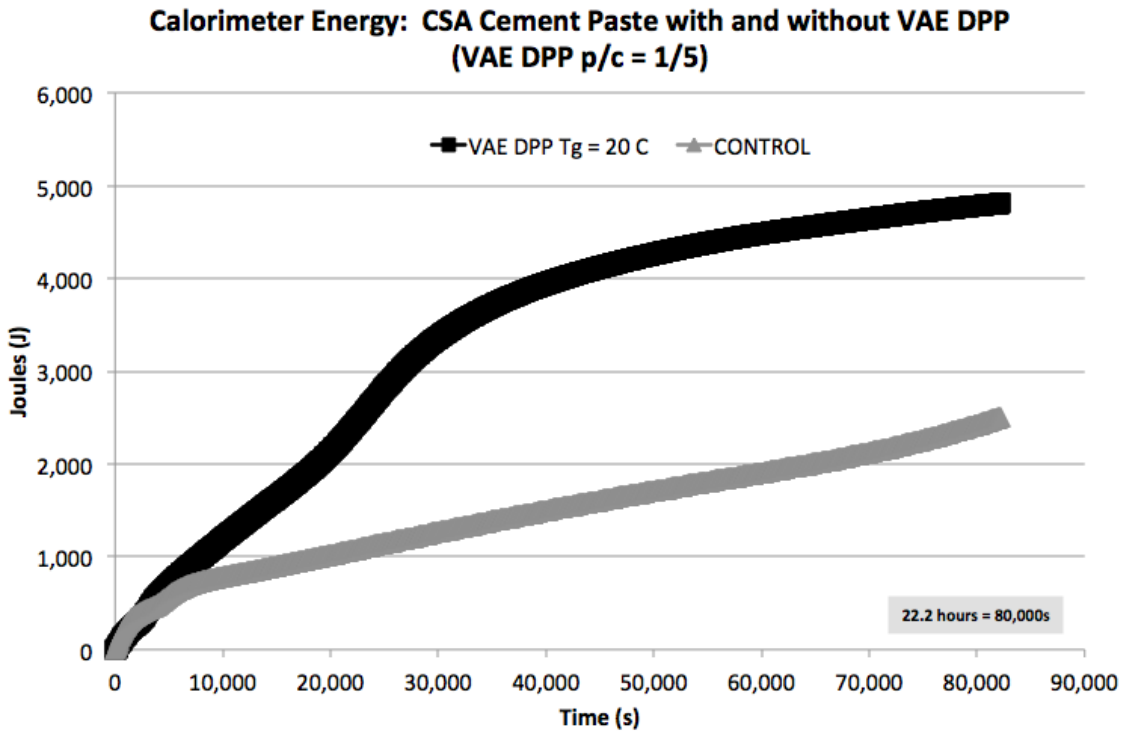

Figure 5.3.9: Early hydration period calorimeter analysis for both polymer modified and control CSA cement paste samples displayed in Table 5.3.2

Figure 5.3.9 displays energy released during the initial 22 hours of hydration for the CSA cement paste samples displayed in Table 5.3.3. It is interesting to note the influence of polymer modification on the energy released during the early hydration period considering all other variables remained constant –especially the water / cement ratio. It should be duly noted that the information presented in Figure 5.3.9 is based upon one sample, and is thus considered an observation. After 24 hours of hydration, TGA/SDT analysis for the cement pastes listed in Table 5.3.2 display ettringite concentrations being greater for the polymer modified versus control samples. The displayed calorimeter information suggests the microstructural behavior of polymer modified and non-polymer modified CSA cement pastes and mortars analyzed in this study differ from the point of initial hydration and continue to differ throughout the duration of the study.

The information related to the CSA cement mortar mix design displayed in Table 5.3.3 further supports the notion of latex polymer mitigating losses in direct tensile strength for CSA cement mortars. The mix design in Table 5.3.3 differs from the polymer modified mix design displayed in Table 5.3.1 in that the mix design displayed in Table 5.3.3 includes both superplasticizing and hydration accelerating admixtures. Use of such admixtures is commonplace within the cementitious materials industry; however, literature is scarce regarding the influence of said admixtures on the performance of CSA cement based materials. The CSA cement mortar mix design displayed in Table 5.3.3 performed nicely from a number of perspectives including workability, pot life and mechanical property performance. There were no signs of chemical incompatibility during hydration reactions associated with constituent materials throughout the duration of the study.

Table 5.3.3: CSA CEMENT MORTAR FORMULATION	
Materials	Polymer Modified CSA Cement Mortar (EF21-220)
CSA Cement	500
Anhydrite	160
VAE Polymer T_g = 20°C	100
Lithium Carbonate	2
Superplasticizer	1
Graded Sand	1375
20/30 Sand	125
Tartaric Acid	2
Total Mass (g)	2265
Deionized Water	220

Table 5.3.3: Rapid strength gain polymer modified CSA cement mortar mix design

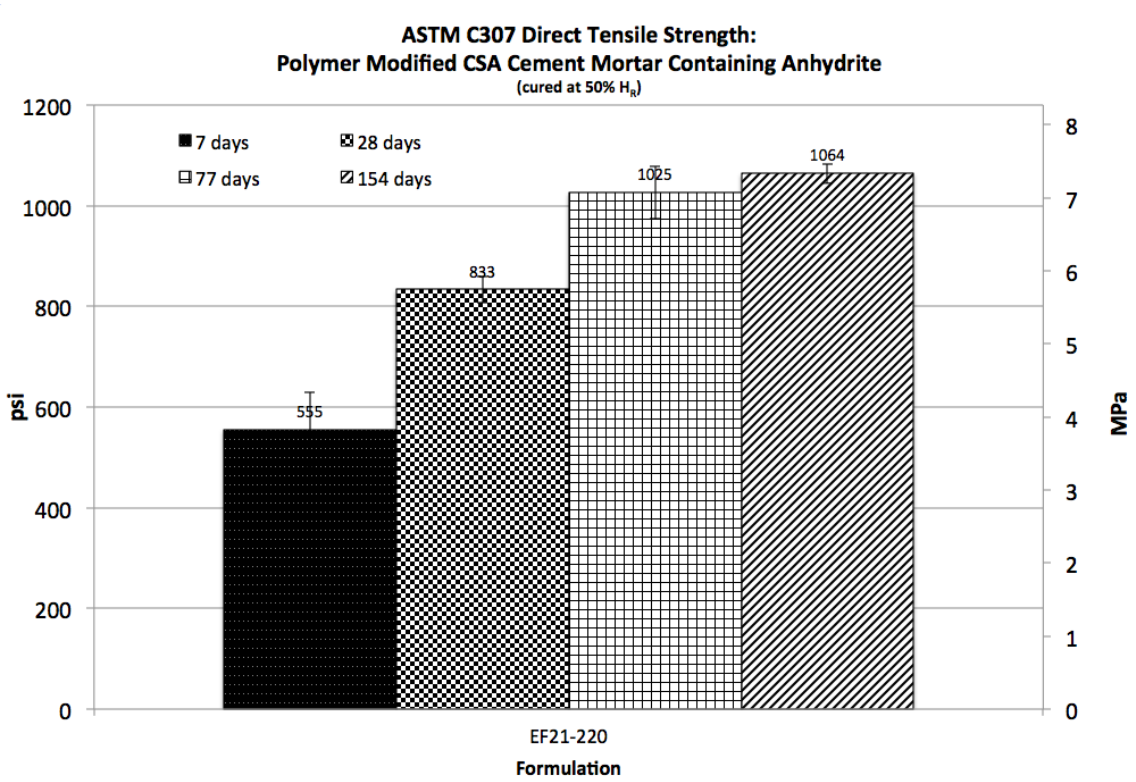

Figure 5.3.10: Direct tensile strength of rapid strength gain polymer modified CSA cement mortar displayed in Table 5.3.3 cured at constant low humidity (50% H_R)

Figure 5.3.10 displays ASTM C307 direct tensile strength values for the polymer modified CSA cement mortar mix design displayed in Table 5.3.3. After curing for seven days, 28 days, 77 days and 154 days at constant 50% relative humidity and ambient laboratory temperature of approximately 23°C, the direct tensile strength values are 555psi (3.8MPa), 833psi (5.7MPa), 1,025psi (7.1MPa) and 1,064psi (7.3MPa), respectively. The displayed information suggests direct tensile strength increases from the point of initial hydration through 77 days then remains somewhat constant from 77 days through 154 days. Through 154 days, the trend displayed in Figure 5.3.10 differs from the trend displayed in Figure 5.3.1 suggesting polymer modification of CSA cement mortars mitigates direct tensile strength loss when cured for extended periods of time at constant 50% relative humidity.

DISCUSSION

The following figures are SEM images for the control CSA cement paste listed in Table 5.3.2 after curing for 7 days, 14 days, 28 days and 251 days at 23°C and 50% relative humidity. SEM samples were taken in conjunction with TGA/SDT and XRD samples in an effort to visualize the microstructure as explained by TGA/SDT and XRD. Figures can be paired for comparison of polymer modified CSA cement paste and control CSA cement paste samples based upon hydration period. Figures 5.3.11 and 5.3.15 display a magnification of 2k after hydrating for seven days. Figures 5.3.12 and 5.3.16 display a magnification of 3k after hydrating for 14 days. Figures 5.3.13 and 5.3.17 display a magnification of 3k after hydrating for 28 days. Figures 5.3.14 and 5.3.18 display a magnification of 5k after hydrating for 251 days.

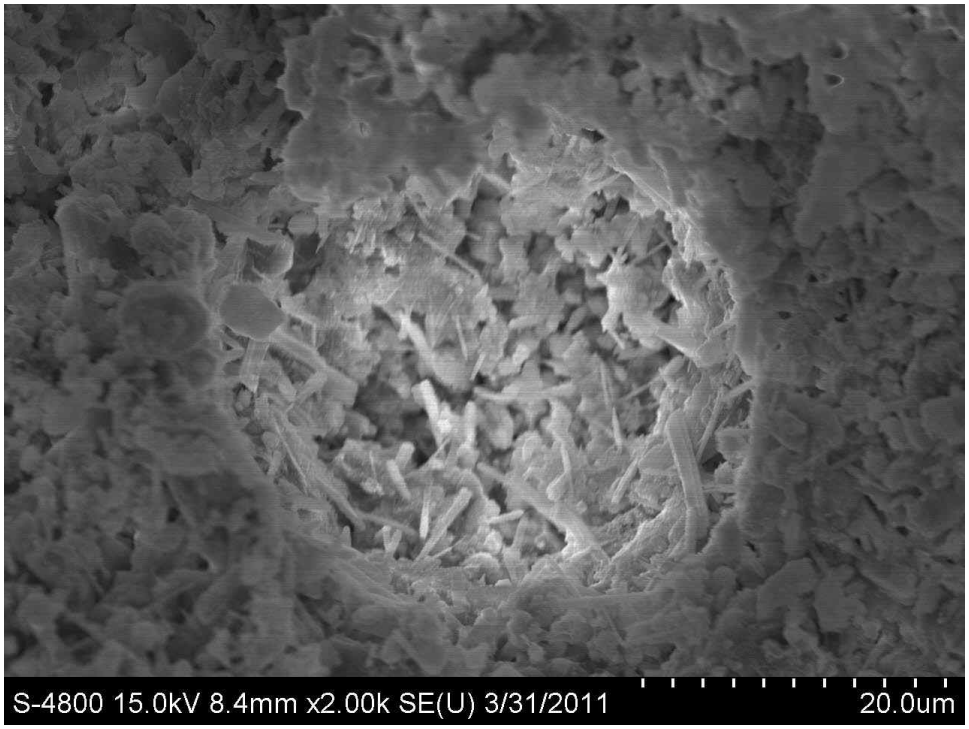

Figure 5.3.11: SEM image of control CSA cement paste listed in Table 5.3.2 after curing for 7 days at 50% relative humidity and 23°C

Figure 5.3.11 displays the control CSA cement paste displayed in Table 5.3.2 after hydrating for 7 days at 50% relative humidity and 23°C. As explained by analytical analysis, Figure 5.3.11 displays un-hydrated clinker, anhydrite, and long, slender ettringite crystals. When compared with Figure 5.3.15, it appears as though a greater amount of un-hydrated material can be seen in Figure 5.3.11.

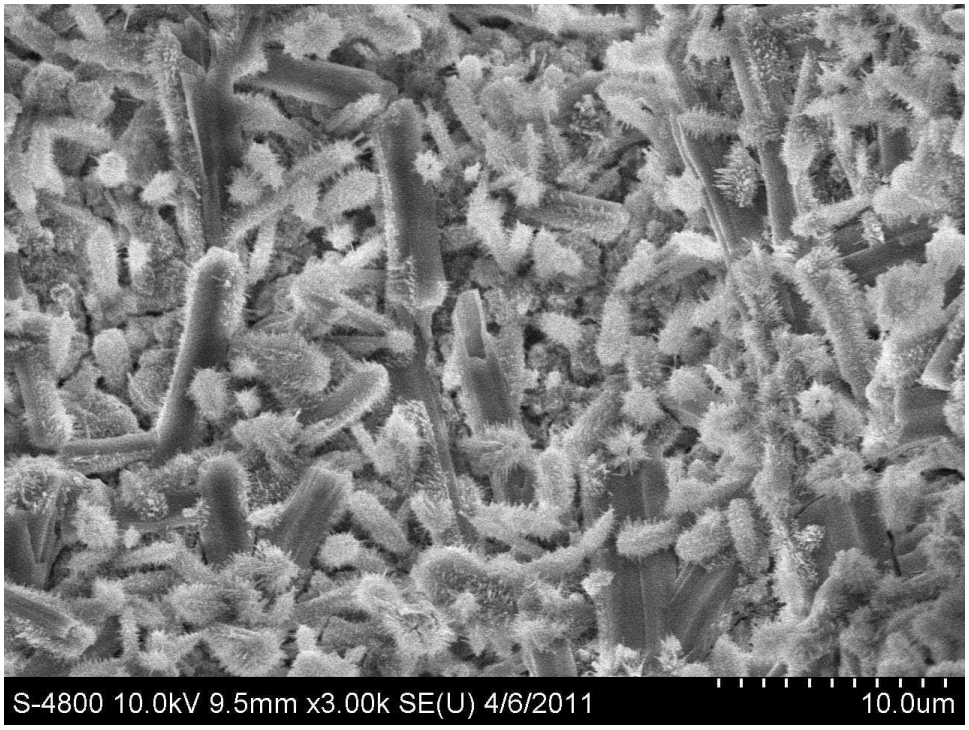

Figure 5.3.12: SEM image of control CSA cement paste listed in Table 5.3.2 after curing for 14 days at 50% relative humidity and 23°C

Figure 5.3.12 displays the control CSA cement paste displayed in Table 5.3.2 after curing for 14 days at 50% relative humidity and 23°C. As explained by analytical analysis, Figure 5.3.12 displays un-hydrated clinker, anhydrite, and long, slender ettringite crystals among other phases. The ettringite crystal growth is noteworthy, especially interesting is what appears to be smaller crystals on the surface of the larger crystals. When compared with Figure 5.3.16, it appears as though a greater amount of larger crystals with smaller crystals on the surface are displayed in Figure 5.3.12. It is theorized these smaller crystals may be associated with ettringite decomposition processes.

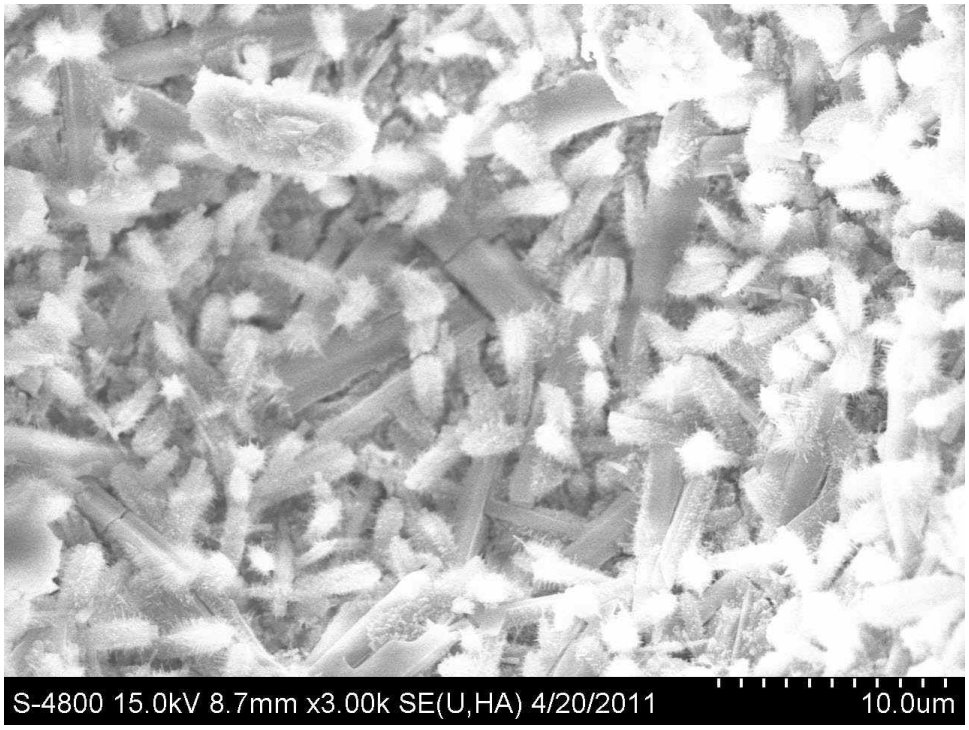

Figure 5.3.13: SEM image of control CSA cement paste listed in Table 5.3.2 after curing for 28 days at 50% relative humidity and 23°C

Figure 5.3.13 displays the control CSA cement paste displayed in Table 5.3.2 after hydrating for 28 days at 50% relative humidity and 23°C. As explained by XRD, Figure 5.3.13 displays the following phase concentrations:

Yeelimite > Anhydrite >> Brownmillerite, $Ca_3Al_2O_6$ > Ettringite, Belite, alpha-Ca_2SiO_4

When compared with Figure 5.3.17, it appears as though more cracked crystals are displayed in Figure 5.3.13. Also, Figure 5.3.13 seems to display a greater quantity of larger crystals with smaller crystals on the surface when compared with Figure 5.3.17. It is theorized Figure 5.3.13 displays ettringite decomposition processes associated with dehydration as explained by Skoblinskaya et al, (1975).

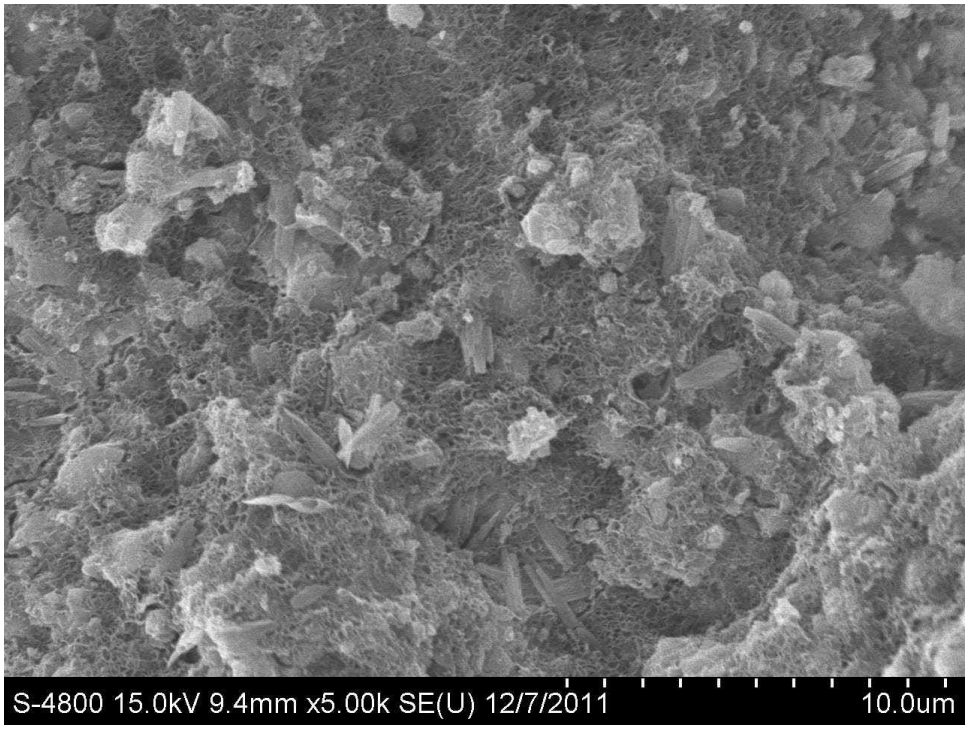

Figure 5.3.14: SEM image of control CSA cement paste listed in Table 5.3.2 after curing for 251 days at 50% relative humidity and 23°C

Figure 5.3.14 displays the control CSA cement paste displayed in Table 5.3.2 after hydrating for 251 days at 50% relative humidity and 23°C. As explained by XRD, Figure 5.3.14 displays the following phase concentrations:

Yeelimite > Anhydrite >> Ettringite, $Ca_3Al_2O_6$ > Gamma Ca_2SiO_4, Belite

When compared with Figure 5.3.18, it seems as though a large portion of ettringite crystals in Figure 5.3.14 have experienced some sort of decomposition process as they have a somewhat weathered appearance. Figure 5.3.14 also displays a large number of cracks throughout the microstructure which are theorized to be a result of ettringite decomposition as described by Skoblinskaya et al, (1975). Furthermore, such internal cracking of the microstructure supports the observed strength loss trends for the control CSA cement mortar displayed in Figure 5.3.1.

Latex polymers are known to occupy the pore structure within hydrating cementitious materials improving mechanical property performance and decreasing the rate of harmful ion ingress while mitigating carbonation behavior (Ohama 1995). Figures 5.3.15, 5.3.16, 5.3.17 and 5.3.18 display the polymer modified CSA cement paste displayed in Table 5.3.2 after hydrating for seven days, 14 days, 28 days and 251 days at 23°C and 50% relative humidity.

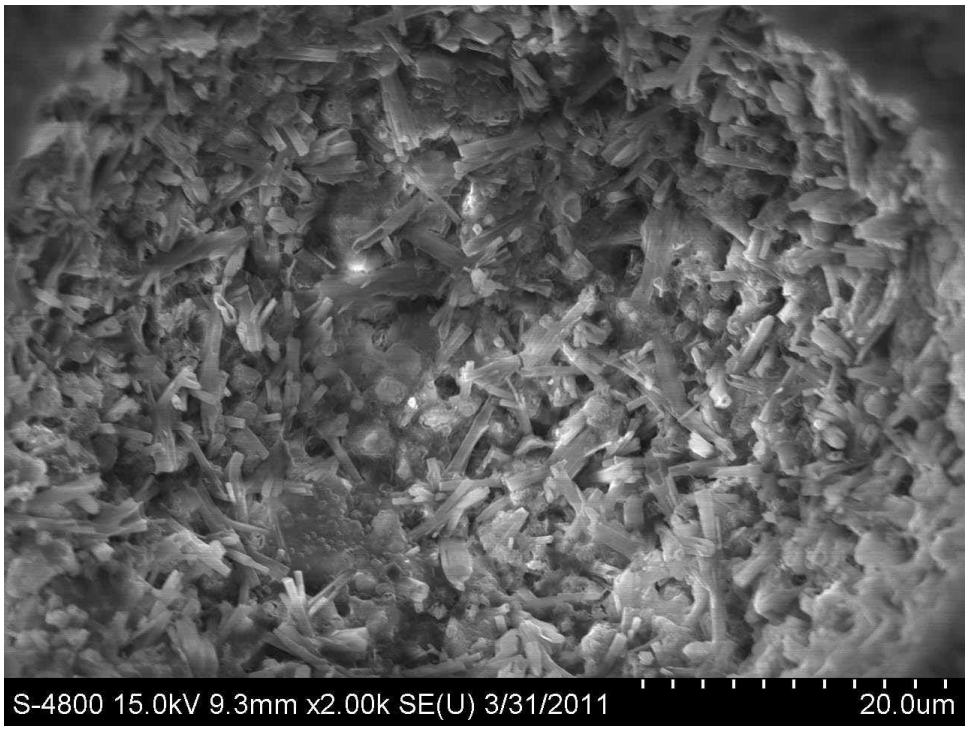

Figure 5.3.15: SEM image of polymer modified CSA cement paste listed in Table 5.3.2 after curing for 7 days at 50% relative humidity and 23°C

Figure 5.3.15 displays the polymer modified CSA cement paste displayed in Table 5.3.2 after hydrating for 7 days at 50% relative humidity and 23°C. As explained by analytical analysis, Figure 5.3.15 displays un-hydrated clinker, anhydrite, and long, slender ettringite crystals among other phases.

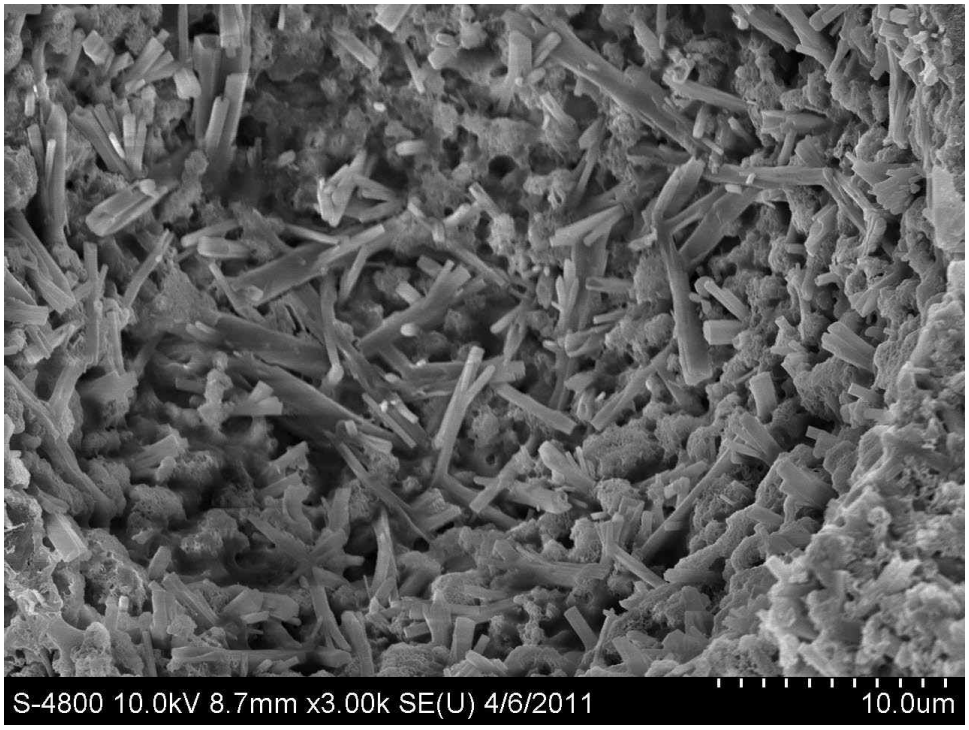

Figure 5.3.16: SEM image of polymer modified CSA cement paste listed in Table 5.3.2 after curing for 14 days at 50% relative humidity and 23°C

Figure 5.3.16 displays the polymer modified CSA cement paste displayed in Table 5.3.2 after hydrating for 14 days at 50% relative humidity and 23°C. As explained by analytical analysis, Figure 5.3.16 displays un-hydrated clinker, anhydrite, and long, slender ettringite crystals among other phases. It is interesting to note the polymer film in and amongst the ettringite cyrstals. The difference in ettringite crystal size when compared with Figure 5.3.12 is noteworthy. Also worthy of recognition is the lack of a "fuzzy" appearance on crystal surfaces when compared with Figure 5.3.12. It is theorized the "fuzzy" appearance is associated with ettringite decomposition processes, and the lack of such "fuzzy" crystal surfaces in Figure 5.3.16 suggests polymer modification as a viable means for mitigating ettringite decomposition for the tested CSA cement mortars.

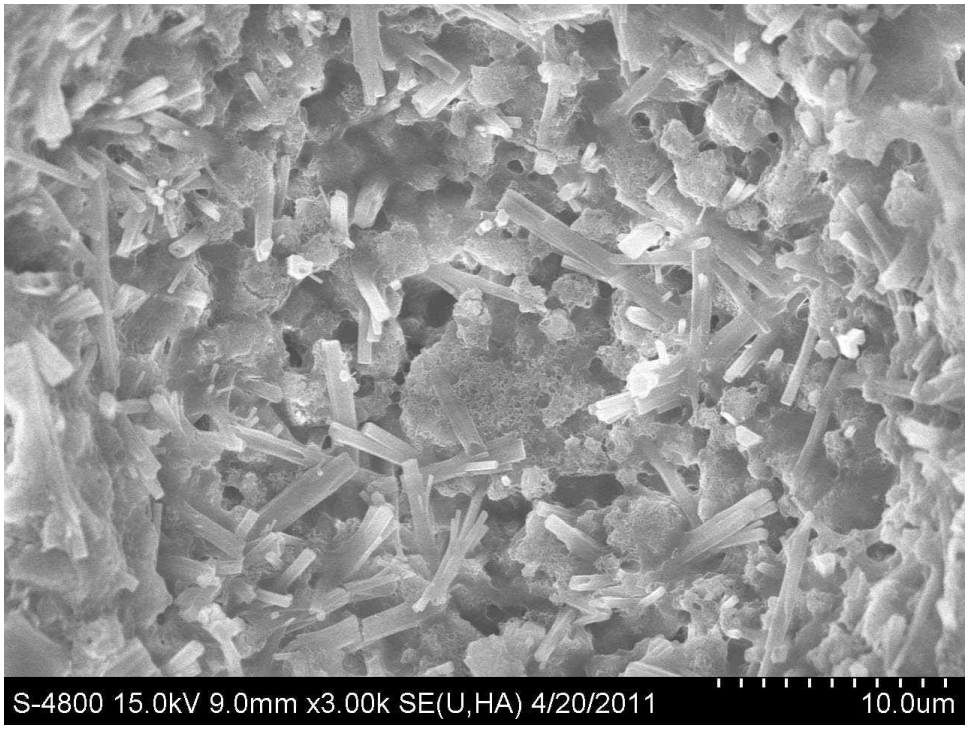

Figure 5.3.17: SEM image of polymer modified CSA cement paste listed in Table 5.3.2 after curing for 28 days at 50% relative humidity and 23°C

Figure 5.3.17 displays the polymer modified CSA cement paste displayed in Table 5.3.2 after curing for 28 days at 50% relative humidity and 23°C. According to XRD analysis, Figure 5.3.17 displays the following constituent concentrations:

Yeelimite > Anhydrite >> Brownmillerite, Ettringite, $Ca_3Al_2O_6$ > Belite, alpha-Ca_2SiO_4

A noticeable difference in ettringite crystal size appears when compared with that displayed in Figure 5.3.13. As previously discussed, when compared with Figure 5.3.13, both crystal size and surface appearance suggest polymer modification as a viable means of mitigating ettringite decomposition for the tested CSA cement materials.

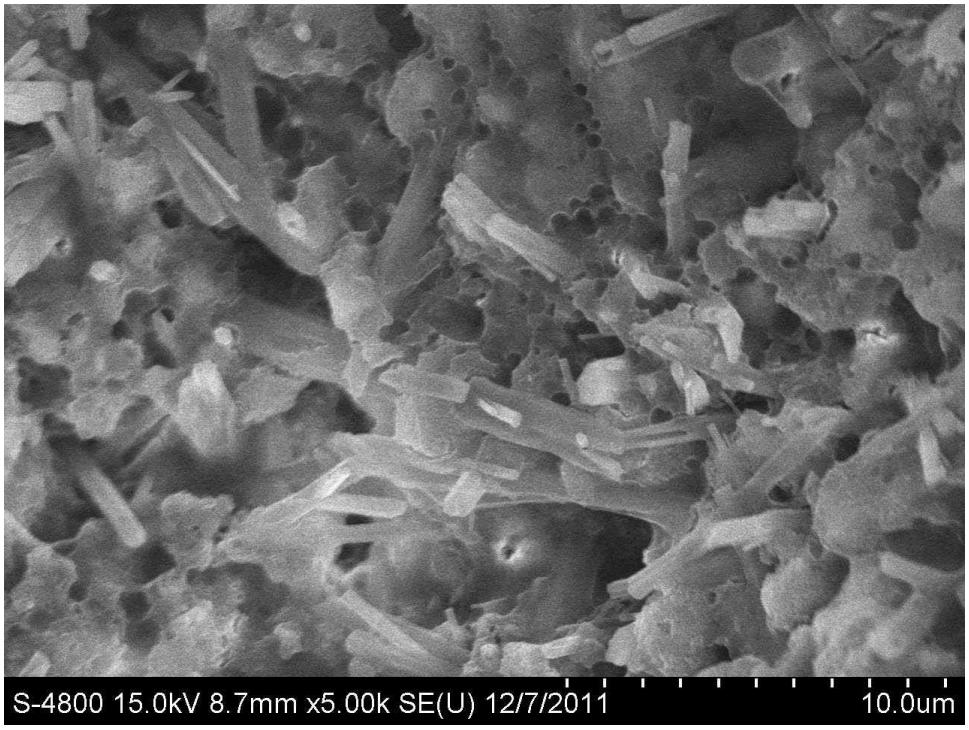

Figure 5.3.18: SEM image of polymer modified CSA cement paste listed in Table 5.3.2 after curing for 251 days at 50% relative humidity and 23°C

Figure 5.3.18 displays the polymer modified CSA cement paste displayed in Table 5.3.2 after hydrating for 251 days at 50% relative humidity and 23°C. According to XRD analysis, Figure 5.3.18 displays the following constituent concentrations:

Yeelimite > Anhydrite > Ettringite > $Ca_3Al_2O_6$ > Belite

It is also important to note the difference in ettringite crystal size when compared with that displayed in Figure 5.3.14. The number of visible ettringite crystals when compared with Figure 5.3.18 is also noteworthy. Comparison of Figures 5.3.14 and 5.3.18 further supports the notion of polymer modification being a viable means for mitigating ettringite decomposition in the tested CSA cement mortars.

CONCLUSION

The results presented in this study suggest latex polymer modification as a viable means for mitigating ettringite decomposition in CSA cement materials exposed to low humidity environments. Such a statement stems from analysis of mechanical property

performance characteristics coupled with analytical phase determination analyses for polymer modified and non-polymer modified CSA cement mortars.

Direct tensile strength testing for the control CSA cement mortar presents statistically significant trends of increasing direct tensile strength from initial hydration through 28 days followed by a period of decreasing direct tensile strength from 28 days to 109 days. TGA/SDT, XRD and SEM analysis confirm ettringite decomposition as a factor influencing strength loss in the tested mortars. These findings are in agreement with literature for ettringite containing systems.

Direct tensile strength testing, flexural strength testing and compressive strength testing suggests the polymer modified CSA cement mortars display excellent mechanical property performance after curing for extended periods of time at 50% relative humidity and 23^{o}C. TGA/SDT, XRD and SEM analyses confirm ettringite decomposition is far less severe in the tested polymer modified CSA cement mortars when compared with the CSA cement control samples.

The results of this study strongly suggest latex polymer addition to CSA cement mortar mitigates both ettringite decomposition behavior and accompanying strength loss for materials cured at 23^{o}C and 50% relative humidity for extended periods of time.

5 REFERENCES:

- ACI 548.1R-09, Guide for the Use of Polymers in Concrete, Reported by ACI Committee 548, American Concrete Institute
- ACI 503.5R-92, Guide for the Selection of Polymer Adhesives with Concrete, Reported by ACI Committee 503, American Concrete Institute
- ACI 548.4-93, Standard Specification for Latex Modified Concrete (LMC) Overlays, Reported by Committee 548, American Concrete Institute
- Afridi, M., Chaudhary, Z., Ohama, Y., Demura, K., 1994, Effects of polymer modification on the formation of high sulphoaluminate or ettringite type (Aft) crystals in polymer modified mortars, Cement and Concrete Research, Vol. 24, No. 8, 1492-1494, 1994
- Afridi, M., Chaudhary, Z., Ohama, Y., Katsunori, D., 1994, Strength and Elastic Properties of Powdered and Aqueous Polymer-Modified Mortars, Cement and Concrete Research, Vol 24, No. 7, pp. 1199-1213, 1994
- Afridi, M., Ohama, Y., Demura, K., Izbal, M.Z., 2003, Development of polymer films by the coalescence of polymer particles in powdered and aqueous polymer-modified mortars, Cement and Concrete Research, 33 (2003) 1715-1721
- Ambroise, J., Pera, J., 2009, Use of Calcium sulfoaluminate cement to improve strength of mortars at low temperature, Concrete Repair, Rehabilitation and Retrofitting II –Alexamder et al (eds), © 2009 Taylor and Francis Group, London, ISBN 978-0-415-46850-3
- Blackley, D.C., 1997, Polymer Latices Volume 2 and Volume 3, ISBN: 0412-62880-5 and ISBN 0412-62890-2
- Bright, R.P., Mraz, T.J., Vassallo, J.C., 1993, The Influence of Various Polymeric Materials on the Physical Properties of a Cementitious Patching Compound, Polymer Modified Hydraulic Cement Mixtures, American Society for Testing and Materials, STP 1176m, ASTM Publication Code Number 04-011760-07
- Cargile, J.D., Oneil, E.F., Neeley, B.D., 2002, Very High Strength Concretes for Use in Blast and Penetration Resistant Structures, US Army Corps of Engineers Engineer Research and Development Center, AMPTIAC Quarterly Volume 6, Number 4
- Chandra, S., Ohama, Y., 1994, Polymers in Concrete, CRC Press, ISBN 0-8493-4815-3

- Chowaniec, O., 2012, Limeston Addition in Cement, Thesis Number 5335, EPFL, Ecole Polytechnique Federale de Lausanne, www.epfl.ch
- Clark, S., Colas, B., Kunz, M., Speziale, S., Monteiro, P., 2006, Effect of pressure on the crystal structure of ettringite, Cement and Concrete Research 38 (2008) 19-26
- Gabrovsek, R., Vuk, T., Kaucic, V., 2008, The Preparation and Thermal Behavior of Calcium Monocarboaluminate, Acta Chim Slov, 2008, 55, 942-950
- Gameiro, A., Silva, A., Veiga, M., Velosa, A., 2012, Lime-Metakaoling Hydration Products: A Microscopy Analysis, Materials and Technology 46 (2012) 2, 145-148
- Gartner, E., 2004, Industrially interesting approaches to "low-CO_2" cements, Cement and Concrete Research 34 (2004) 1489-1498
- Glasser, F.P., Zhang, L., 2001, High-performance cement matrices based on calcium sulfoaluminate-belite compositions, Cement and Concrete Research 31 (2001) 1881-1886
- Graybeal, B., 2010, Behavior of Field Cast Ultra High Performance Concrete Bridge Deck Connections Under Cyclic and Static Structural Loading, November 2010, FHWA-HRT-11-023
- Graybeal, B., 2010, FHWA-HRT-11-022, Field Cast UHPC Connections for Modular Bridge Deck Components, November 2010, FHWA-HRT-11-022
- Graybeal, B., 2009, FHWA-HRT-09-069, Structural Behavior of a 2nd Generation UHPC Pi-Girder, October 2009, FHWA-HRT-09-069
- Hassoun, M.N., 1985, Design of Reinforced Concrete Structures, PWS Publishers, Boston, MA, ISBN 0-534-03759-3
- Illston, J.M., Domone, P.L.J., 2007, Construction Materials: Their Nature and Behaviour, Third Edition, Spon Press, ISBN 0-419-25860-4
- Jenni, A., Herwegh, M., Zurbriggen, R., Aberle, T. and Holzer, L., 2003, Quantitative micro-structure analysis of polymer modified mortars, Jounal of Microscopy, Vol 212, pgs 186-196
- Marraccoli, M., Montagnaro, F., Pace, M.L., Telesca, A., Valenti, G.L., 2010, Synthesis of Calcium Sulfoaluminate Cements from Blends of Coal Combustion Ashes with Flue Gas Desulfurization Gypsum, Processes and Technologies for a Sustainable Energy, Ischia, June 17-30, 2010, PTSE 2010

- Medeiros, M.H.F., Helene, P., Selmo, S., 2009, Influence of EVA and acrylate polymers on some mechanical properties of cementitious repair mortars, Construction and Building Materials 23 (2009) 2527-2533
- Ohama, Y., 1995, Handbook of Polymer Modified Concrete and Mortar, Noyes Publications, ISBN 0-8155-1358-5
- Oneil, E.F., Cummins, T.K., Durst, B.P., Kinnebrew, P.G., Boone, R.N., 2004, Development of Very High Strength and High Performance Concrete Materials for Improvement of Barriers Against Blast and Projectile Penetration, US Army Corps of Engineers, US Army Engineer Research and Development Center
- Pelletier-Chaignet, L., Winnefeld, F., Lothenbach, B., Muller, C., 2012, Beneficial use of limestone filler with calcium sulphoaluminate cement, Construction and Building Materials 26 (2012) 619-627
- Pelletier, L., Winnefeld, F., Lothenbach, B., 2010, The ternary system: Portland cement-calcium sulphoaluminate clinker-anhydrite: Hydration mechanism and mortar properties, Cement and Concrete Composites 32 (2010) 497-507
- Renaudin, G., Segni, R., Mentel, D., Nedelec, J., Leroux, F., Taviot-Gueho, C., 2007, A Raman Study of the Sulfated Cement Hydrates: Ettringite and Monosulfoaluminate, Journal of Advanced Concrete Technology, Vol. 5, No. 3, 299-312, October 2007
- Romain, T., Winnefeld, F., Mechling, J., Lecomte, A., Roux, A., LeRolland, B., 2013, Composition and Thermodynamic Modeling of Calcium Sulfoaluminate Cement and Ordinary Portland Cement Blends, Proceedings of the First International Conference on Sulphoaluminate Cement, Materials and Engineering Technology, Wuhan University of Technology, Wuhan, China, 23-25Oct2013
- Routh, A., Russel, W., 1999, A process model for latex film formation: limiting regimes for individual driving forces, Department of Chemical Engineering, Princeton University, Langmuir 1999, 15 7762-7773
- Sato, K., Takebe, T., 1992, Decomposition of Synthesized Ettringite by Carbonation, Cement and Concrete Research 22 (1992) 6-14
- Scrivener, K., Capmas, A., 1998, Calcium Aluminate Cements, Chapter 13, Lea's Chemistry of Cement and Concrete, 4th Edition, Arnold, John Wiley and Sons, New York, New York, ISBN 0-340-56589-6
- Scrivener, K.L., Nonat, A., 2011, Hydration of cementitious materials, present and future, Cement and Concrete Research 41 (2011) 651-665

- Sherman, N., Beretka, J., Santoro, L., Valenti, G., 1995, Long-Term Behaviour of Hydraulic Binders Based on Calcium Sulfoaluminate and Calcium Sulfosilicate, Cement and Concrete Research, Vol. 25, No. 1, pp. 113-126
- Skoblinskaya, N., Krasilnikov, K., 1975, Changes in Crystal Structure of Ettringite on Dehydration 1, Cement and Concrete Research, Vol. 5, pp. 381-394, 1975
- Skoblinskaya, N., Krasilnikov, K., Nikitina, L., Varlamov, V., 1975, Changes in Crystal Structure of Ettringite on Dehydration 2, Cement and Concrete Research, Vol. 5, pp. 419-432, 1975
- Sprinkel, M., 2002, Rapid Bridge Deck Rehabilitation Manual, SHRP Product 2035A, AASHTO Innovative Highway Technologies
- Taylor H.F.W., 1997, Cement Chemistry 2nd Edition, ISBN 0-7277-2592-0
- Vande Voort, T., Suleiman, M., Sritharan, S., 2008, Design and Performance Verification of Ultra-High Performance Concrete Piles for Deep Foundations, Iowa Highway Research Board, Iowa Department of Transportation, IHRB Project TR-558
- Winnefeld, F., Barlag, S., 2010, Calorimetric and thermogravimetric study on the influence of calcium sulfate on the hydration of yeelimite, Journal of Thermal Analysis and Calorimetry (2010) 101:949-957
- Winnefeld, F., Lothenbach, B., 2013, Thermodynamic modeling of hydration of calcium sulfoaluminate cements blended with mineral additions, Proceedings of the First International Conference on Sulphoaluminate Cement, Materials and Engineering Technology, Wuhan University of Technology, Wuhan, China, 23-25Oct2013
- Zhang, L., Glasser, F.P., 2005, Investigation of the microstructure and carbonation of CSA based concretes removed from service, Cement and Concrete Research 35 (2005) 2252-2260
- Zhou, Q., Glasser, F., 2001, Thermal stability and decomposition mechanisms of ettringite at <120°C, Cement and Concrete Research 31 (2001) 1333-1339
- Zhou, Q., Lachowski, E., Glasser, F., 2004, Metaettringite, a decomposition product of ettringite, Cement and Concrete Research 34 (2004) 703-710
- Zurbriggen, R., 2004, Influence of polymer glass transition temperature onto mortar flexibility, 6th International scientific and technical conference "Modern technologies of dry mixtures in building MixBUILD", Moscow, Russia, 23Nov2004 – 25Nov2004

Chapter 6: Influence of Polymer on Adhesion Characteristics of Mortars Containing CSA Cement

The information presented in Chapter 6 represents the task associated with testing developed materials in the iterative process for designing dry mix mortar products. The goal of the research was to develop mortars based upon calcium sulfoaluminate (CSA) cement which demonstrate excellent adhesion characteristics when applied to various substrate materials. Chapter 6 discusses the influence of polymer modification on the adhesion performance of materials containing CSA cement. Chapter 6 is significant as it illustrates the influence of polymer / cement ratio on adhesion performance of polymer modified CSA cement materials.

6.1 Assessing Adhesion Performance of Polymer Modified CSA Cement Mortar

INTRODUCTION

CSAC can lay claim to being a "high-performance" cement for three reasons (Glasser and Zhang, 2001):

- the low energy and low CO_2 emission associated with its production
- its ability to form cements, mortars and concretes with high early and final strengths
- its excellent durability, especially in saline marine environments, and the protection it affords to embedded mild steel

Although, CSA cements are considered high performance cements with regard to mechanical property characteristics, little is known about the adhesion performance of CSA cement based materials. CSA cements demonstrate different hydration characteristics when compared with OPC (Pelletier et al, 2010, Gastaldi et al, 2009, Glasser and Zhang, 2001). The chemical water demand (CWD) for complete hydration of clinker is characteristically higher for CSAC when compared with OPC (Glasser and Zhang, 2001). During early hydration, CSA cements demonstrate a tendency for somewhat rapid desiccation primarily as a result of ettringite formation (Glasser and Zhang, 2001). If not

managed properly during formulation, the desiccating nature of CSA cement hydration could be problematic for applications requiring both good adhesion characteristics and extended pot life.

Bond strength between mortar and existing concrete can be influenced by a number of factors including difference in shrinkage, elastic modulus and thermal movement (Vaysburd et al, 1999). Substrate porosity is also listed as an important factor when assessing adhesion characteristics for cementitious materials. Adhesion mechanisms for cementitious materials applied over various substrates are theorized to behave in similar fashion to the known behavior of cement paste and aggregate (Naderi 2008, Chandra et al, 2003). Lightweight aggregate is often more porous than traditional stone aggregate (Chandra et al, 2003). For lightweight aggregate, a portion of the paste bleed water moves into the aggregate's pore structure resulting in an overall decrease of the cement paste / aggregate interfacial zone (Chandra et al, 2003). Based upon this, existing cementitious substrate materials should allow movement of bleed water from the freshly applied mortar into the existing capillary pore structure of the substrate. For porous substrates, the author theorizes materials diffusing with the bleed water will set and harden in the substrate pore network thus forming a bonding mechanism for the adjacent materials. Therefore, it seems intuitive that reductions in bleed water quantity might lead to reduced adhesion performance in the absence of specialty chemicals for mitigating nuisances, i.e., self-desiccation, often encountered during the iterative product formulating process.

Literature review suggests addition of latex polymer could present a possibility for mitigating self-desiccating behavior while improving adhesion strength of CSA cement based materials. However, as shown in the following paragraph, the majority of available literature describes polymer modified systems based upon either OPC or a blend of OPC and calcium aluminate cement (CAC). It would not be wise to simply assume material compatibility based upon hydraulic binders of different chemistry; so, a great deal of testing is necessary to verify performance characteristics of polymer modified CSA cement materials.

Polymer modified OPC systems show higher water retention than traditional cement systems (Knapen et al, 2009, Knapen et al, 2005). Curing of polymer modified portland cement concrete (PPCC) is different from curing of portland cement concrete (PCC) in that extended moist curing is not required. In fact, moist curing beyond 24 to 48 hours is not recommended because it prevents the coalescence or formation of the polymer

film (ACI 548.1R-09). In latex modified mortar and concrete, both cement hydration and polymer phase formation by the coalescence of polymer particles proceed well to yield a monolithic matrix phase with a network structure in which the cement phase and polymer phase interpenetrate into each other, and aggregates are bound by such a comatrix phase (Chandra et al, 1994).

The present study assesses the adhesion characteristics of CSA cement mortars over concrete, wood, metal and glass substrate materials. It is often difficult to ascertain a great deal of information from pull-off tests for high performance mortar materials when cast over traditional porous concrete substrates as the failures predominantly occur in the substrate material. With this in mind, it is also important to ensure tested substrates are of consistent quality. Time constraints would not allow for concrete blocks to be cast and cured in the laboratory for use as porous cement based substrate materials. So, purchased blocks were utilized as substrate materials. Each block was sourced from the same shrink wrapped pallet in an effort to maintain some sort of quality control measures for the porous concrete substrate materials. Metal substrate materials were included to present a relatively non-porous material while eliminating the possibility for substrate failure. Glass was included as a relatively non-porous material with the possibility for substrate failure. Both metal and glass substrate materials provide valuable insight for the improved adhesion performance provided by increases in the polymer / cement ratio for polymer modified CSA cement mortars.

MATERIALS

Cements

- CSA cement containing C_3A, tri-calcium aluminate, was utilized in this study. XRD analysis provides the following listing of constituent materials:

Yeelimite >> C_3A > Belite > Anhydrite (trace quantity)

Anhydrite

- Snow white filler sourced from United States Gypsum (USG) was utilized in this study with average particle size in the range of 7 to 9 microns (USG TDS)

Gypsum

- Terra Alba gypsum sourced from United States Gypsum (USG) was utilized in this study with average particle size in the range of 12 to 15 microns (USG TDS)

Aggregate

- ASTM finely graded sand from Ottawa Illinois was used in all formulations. A coarser, 20/30 sand was also used in all formulations

Polymer

- A vinyl acetate / ethylene dispersible polymer powder (VAE DPP) with T_g = -7°C (19°F) was utilized in this study

Substrate Materials

- Ordinary portland cement based patio blocks sourced from Lowes were utilized as substrate materials.
- Commercial grade soft pine 2" x 6" (51mm x 152mm) boards were saw cut and utilized as wooden substrate materials.
- Rectangular pieces of glass with length of 4in (102mm), width of 2.5in (64mm) and thickness of 0.25in (6mm) were utilized as substrate materials.
- Rectangular metal plates with length of 6in (152mm), width of 4in (102mm) and thickness of 0.125in (3mm) were ground on the surface with a hand held grinder in an effort to create surface imperfections before being utilized as substrate materials. A previous experiment with similar mortars cast over similar metal substrates without surface imperfections did not provide good results.

EXPERIMENTAL PROGRAM

This study assessed both adhesion characteristics and direct tensile strength for CSA cement mortars with and without polymer. Direct tensile strength testing was performed according to ASTM C307, Standard Test Method for Tensile Strength of Chemical Resistant Mortars, Grouts and Monolithic Surface Coatings. Adhesion testing was performed using methods similar to those described in ASTM C1583, Standard Test Method for Tensile

Strength of Concrete Surfaces and the Bond Strength or Tensile Strength of Concrete Repair and Overlay Materials by Direct Tension (Pull-off Method).

Adhesion Analysis

As previously mentioned, adhesion testing was performed utilizing steps similar to those described in ASTM C1583, Standard Test Method for Tensile Strength of Concrete Surfaces and the Bond Strength or Tensile Strength of Concrete Repair and Overlay Materials by Direct Tension (Pull-off Method). An Instron universal testing machine outfitted with a special jig for pull-off testing was utilized during the presented study. This "pull off" testing scheme differs from the ASTM C1583 standard test method as provisions were necessary for maintaining a consistent testing protocol for all substrate materials as core drilling both metal and glass substrate materials was not practical. In response to this perceived issue, adhesion test specimens were cast by placing wet mortar into standard 1.5in (38mm) diameter PVC pipe couplings atop substrate materials immediately after mixing. Furthermore, after a series of failures between steel anchors and epoxy, another change was deemed necessary. Instead of using steel anchors and epoxy, standard, coarse thread bolts 3in (76mm) in length were placed into the center of wet mortar castings such that the bolt head was immediately adjacent to the substrate material. After the bolts were placed in the wet mortar, standard washers were gently slid down over the bolts such that the washers rested on the surface of the wet mortar in an effort to ensure the bolts remained perpendicular to the substrate material during the hydration process. This ad hoc set up worked well. Adhesion specimens were tested after curing on the bench top in ambient laboratory conditions at 23^{o}C for either 24 hours or 13 days, or both. Six adhesion samples were tested over each substrate material for each curing regimen. Figures 6.1.1 through 6.1.5 display adhesion test specimens cast over various substrate materials.

Figure 6.1.1: Adhesion test specimens cast over various substrate materials with concrete in the foreground while ground metal and wooden substrates can be seen in the background

Figure 6.1.2: This figure illustrates “pull off” testing in progress utilizing an Instron universal testing machine

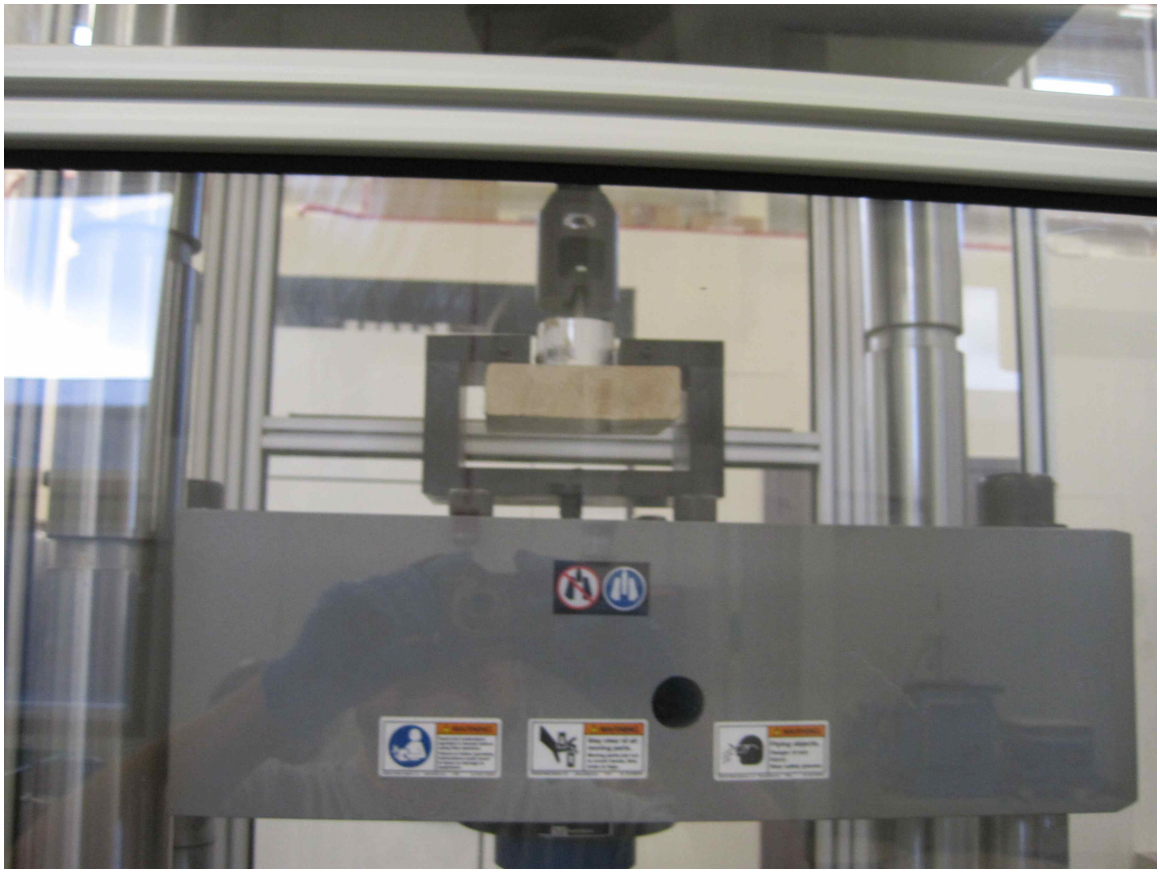

Figure 6.1.3: Illustration of "pull off" testing over a wooden substrate

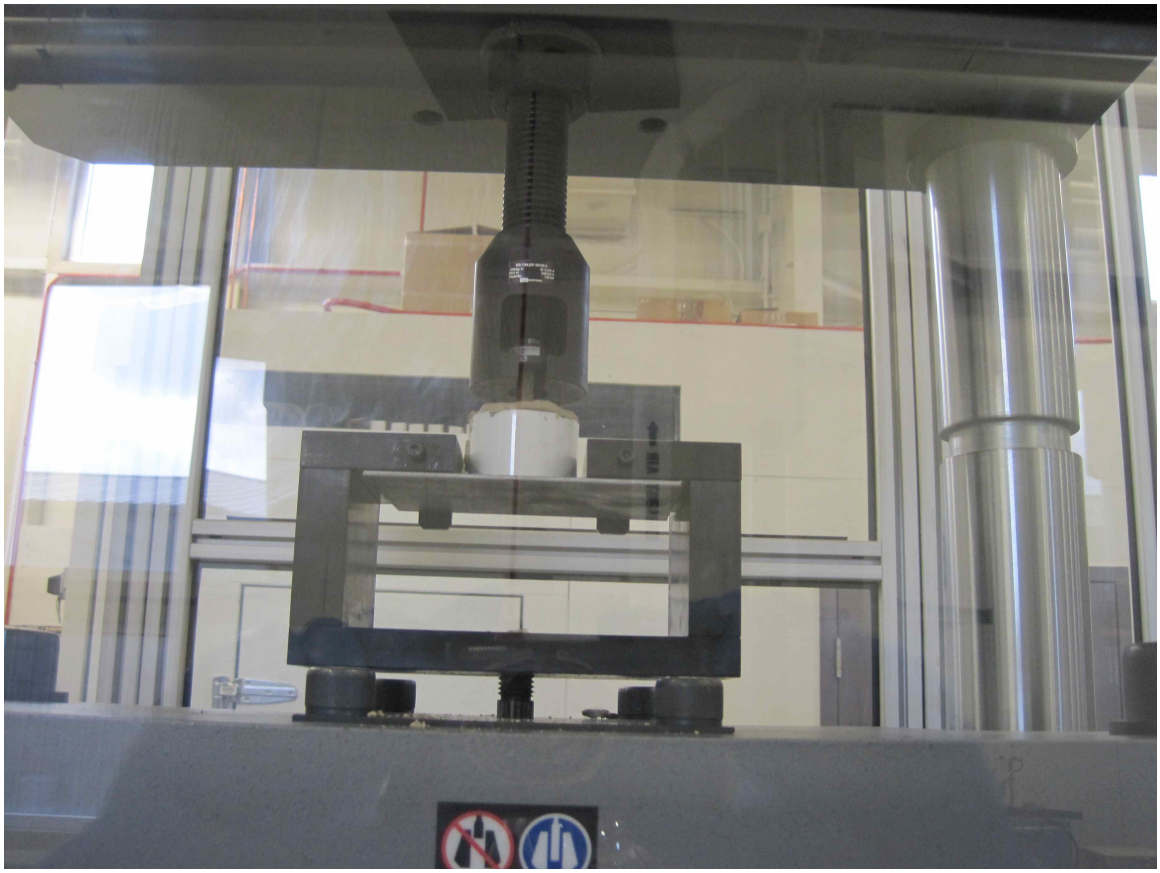

Figure 6.1.4: Illustration of “pull off” testing over a metal substrate

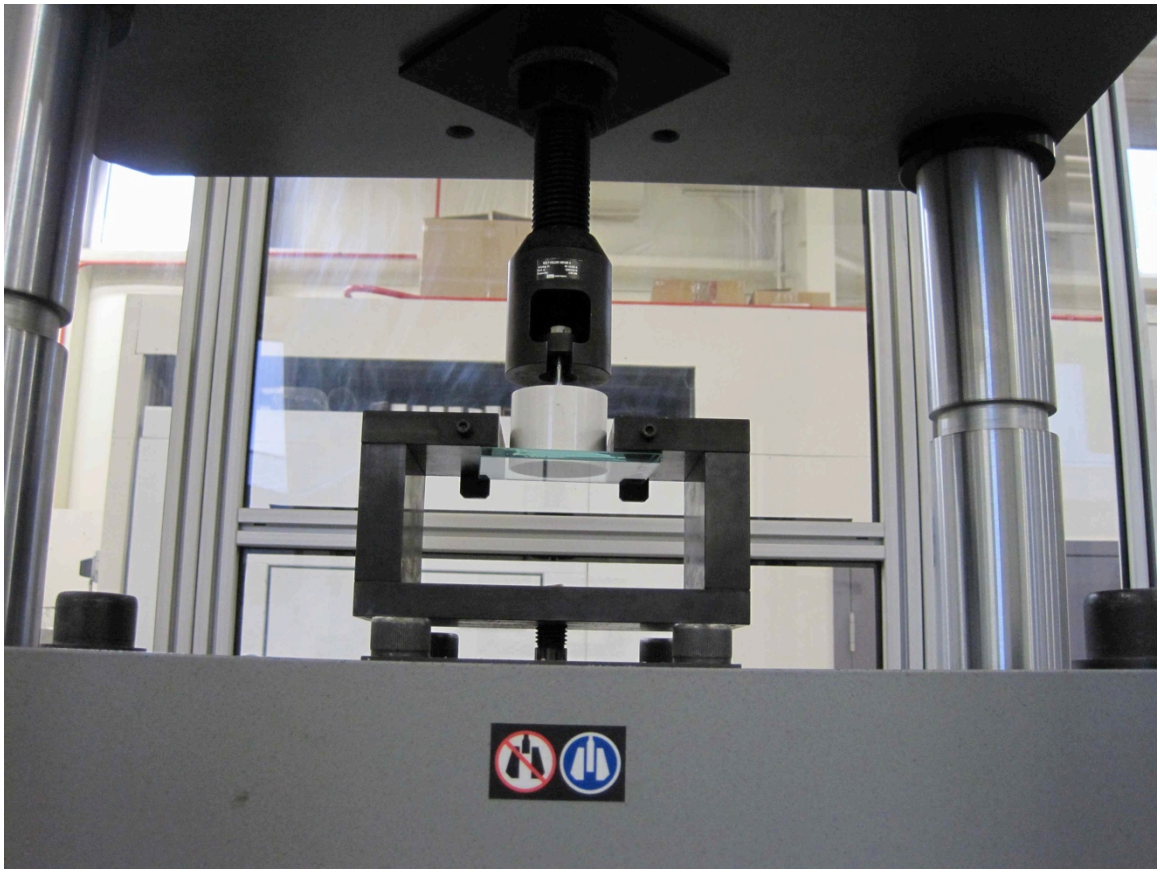

Figure 6.1.5: Illustration of "pull off" testing over a glass substrate

Mortars

Cement mortar 1 is considered to be a special base mortar formulation. In general terms, cement mortar 1 contains calcium sulfoaluminate (CSA) cement, anhydrite, gypsum, superplasticizer, aggregate and a few additional minor components. A hard VAE DPP with T_g = 18°C (64°F), also known as polymer 1, was added to cement mortar 1 at a p/c = 0.15. A soft VAE DPP with T_g = -7°C (19°F), also known as polymer 2, was added to cement mortar 1 such that three mortars could be tested at polymer / cement ratios of 0.15, 0.3 and 0.45. The specific polymers were selected to examine the influence of glass transition temperature on adhesion performance when cast over various substrate materials. Addtionally, the selected polymers are neutral rheology polymers without special additives that could potentially mask differences in behavior stemming from differences in glass transition temperatures. A water / cement ratio of 0.35 was utilized for all mortars with p/c = 0.15 and p/c = 0.3. In an effort to achieve a workable consistency, the water / cement ratio was increased to 0.38 for the mortar with p/c = 0.45.

To prepare the dry mix mortars, individual mortar components were weighed and placed into a plastic mixing bag. After all components were added, the bag was sealed and shaken vigorously by hand for approximately ninety seconds. This type of mixing is an industry proven simulation for blending operations in the manufacturing of dry mix mortar products containing minute quantities of additives such as accelerators and retarders.

For direct tensile strength testing, experimental specimens were cast according to ASTM C307. Three test specimens were cast for each test series. During the first 24 hours of curing, each test specimen remained in the mold covered with plastic on the work bench. After this initial curing period, test specimens were removed from their molds and placed in a sealed plastic bag at ambient laboratory temperature.

Table 6.1.1: CSA CEMENT MORTAR INFORMATION		
cement mortar 1	cement mortar 1	cement mortar 1
no polymer	polymer 1	polymer 2
	p/c = 0.15	p/c = 0.15
w/c = 0.35	w/c = 0.35	w/c = 0.35

Table 6.1.1: Polymer modified versus control mortars tested in the adhesion study

Table 6.1.2: POLYMER INFORMATION	
polymer 1	vinyl acetate / ethylene with T_g = 18°C (64°F)
polymer 2	vinyl acetate / ethylene with T_g = -7°C (19°F)

Table 6.1.2: Listing of polymer powders added to cement mortar 1 for the adhesion study

Table 6.1.3: CSA CEMENT MORTAR INFORMATION		
cement mortar 1	cement mortar 1	cement mortar 1
polymer 2	polymer 2	polymer 2
p/c = 0.15	p/c = 0.3	p/c = 0.45
w/c = 0.35	w/c = 0.35	w/c = 0.38

Table 6.1.3: Polymer modified CSA cement mortar varying polymer / cement ratio for adhesion testing

RESULTS

The results of this study compare and contrast mortar direct tensile strength with mortar pull off strength in an effort to truly understand the principles leading to failure in each pull off test. Typically, a cement mortar will fail through one of three possible mechanisms during pull off testing:

1. CF/A = cohesive failure within the adhesive
2. CF/S = cohesive failure within the substrate
3. AF/S = adhesive failure with the substrate

The CF/A failure mode results when the direct tensile strength of the mortar is less than both the bond strength between the mortar and substrate and the direct tensile strength of the substrate. The CF/S failure mode results when both the direct tensile strength of the mortar and the bond strength between the mortar and substrate is greater than the strength of the substrate. Dry mix mortars designed for use in patch and repair type applications should produce substrate failure, or CF/S type failure modes, during pull off testing when cast over traditional cement based substrate materials (Naderi, 2008). The AF/S failure mode results when the bond strength between the mortar and substrate is less than either the direct tensile strength of the mortar or the direct tensile strength of the substrate material.

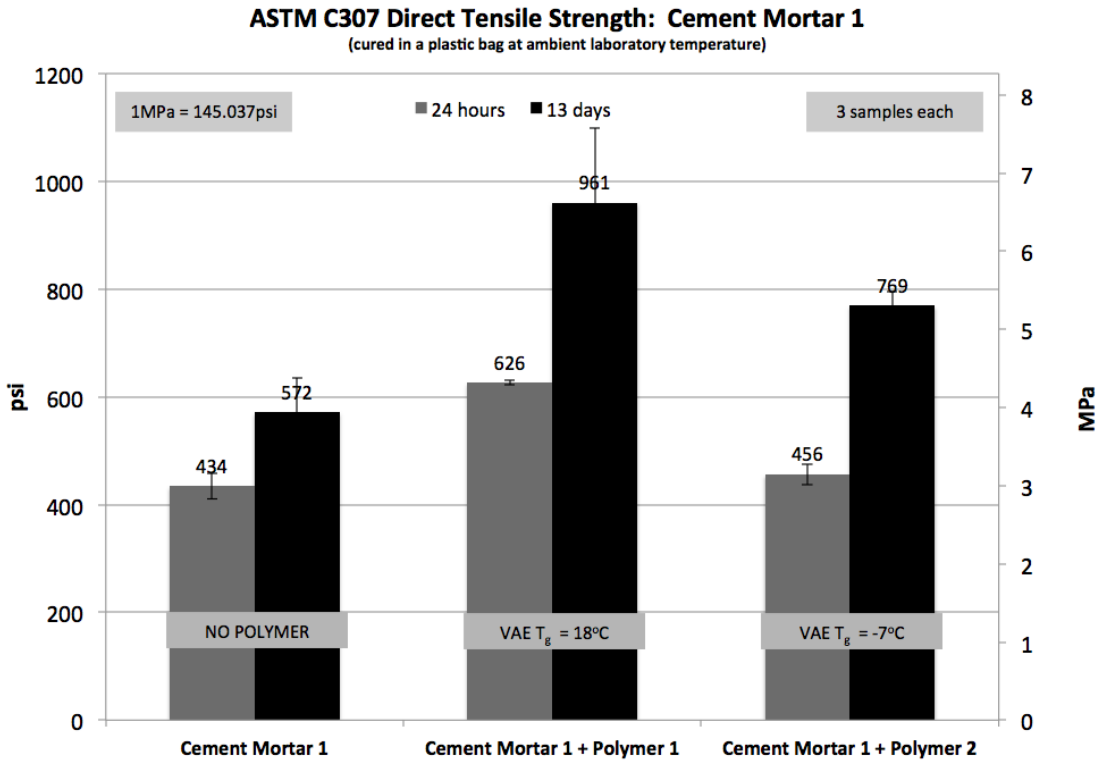

Figure 6.1.6: Direct tensile strength of polymer modified and non-polymer modified CSA cement mortar 1

Figure 6.1.6 displays direct tensile strength information for mortars displayed in Table 6.1.1 after curing for 24 hours and 13 days sealed in a plastic bag at ambient laboratory temperature. Cement mortar 1 displayed direct tensile strength values of 434psi (3MPa) and 572psi (3.9MPa) after curing for 24 hours and 13 days, respectively. Cement mortar 1 plus polymer 1 displayed direct tensile strength values of 626psi (4.3MPa) and 961psi (6.6MPa) after curing for 24 hours and 13 days, respectively. Cement mortar 1 plus polymer 2 displayed direct tensile strength values of 456psi (3.1MPa) and 769psi (5.3MPa) after curing for 24 hours and 13 days, respectively.

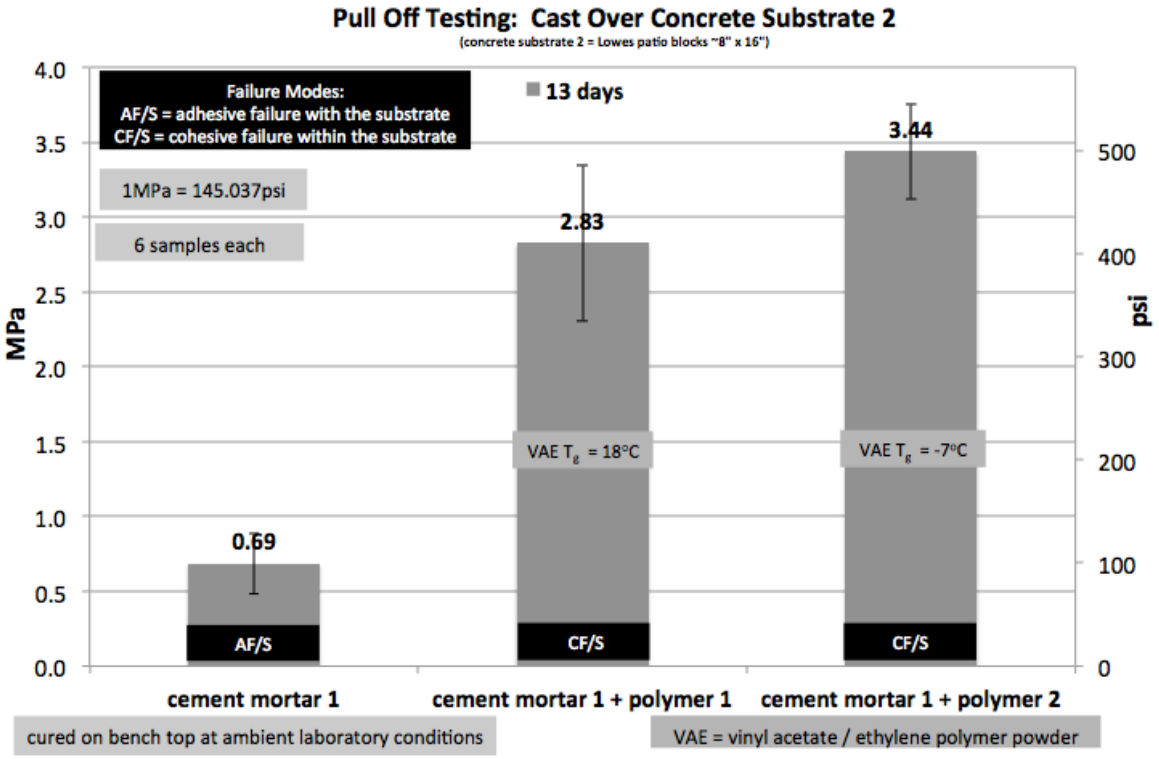

Figure 6.1.7: Polymer modified and non-polymer modified cement mortar 1 cast over concrete substrate 2 after 13 days of bench top curing at ambient laboratory conditions

Figure 6.1.7 displays pull-off test results for polymer modified and non-polymer modified cement mortar 1 cast over concrete substrate 2 after 13 days of bench top cure at ambient laboratory conditions. Cement mortar 1 displayed a pull-off strength value of 0.69MPa (100psi) with primary failure mode of AF/S, also known as failure at the bond line. Cement mortar 1 plus polymer 1 displayed a pull-off strength value of 2.83MPa (411psi) with primary failure mode of CF/S, also known as substrate failure. Cement mortar 1 plus polymer 2 displayed a pull-off strength value of 3.44MPa (499psi) with primary failure mode of CF/S.

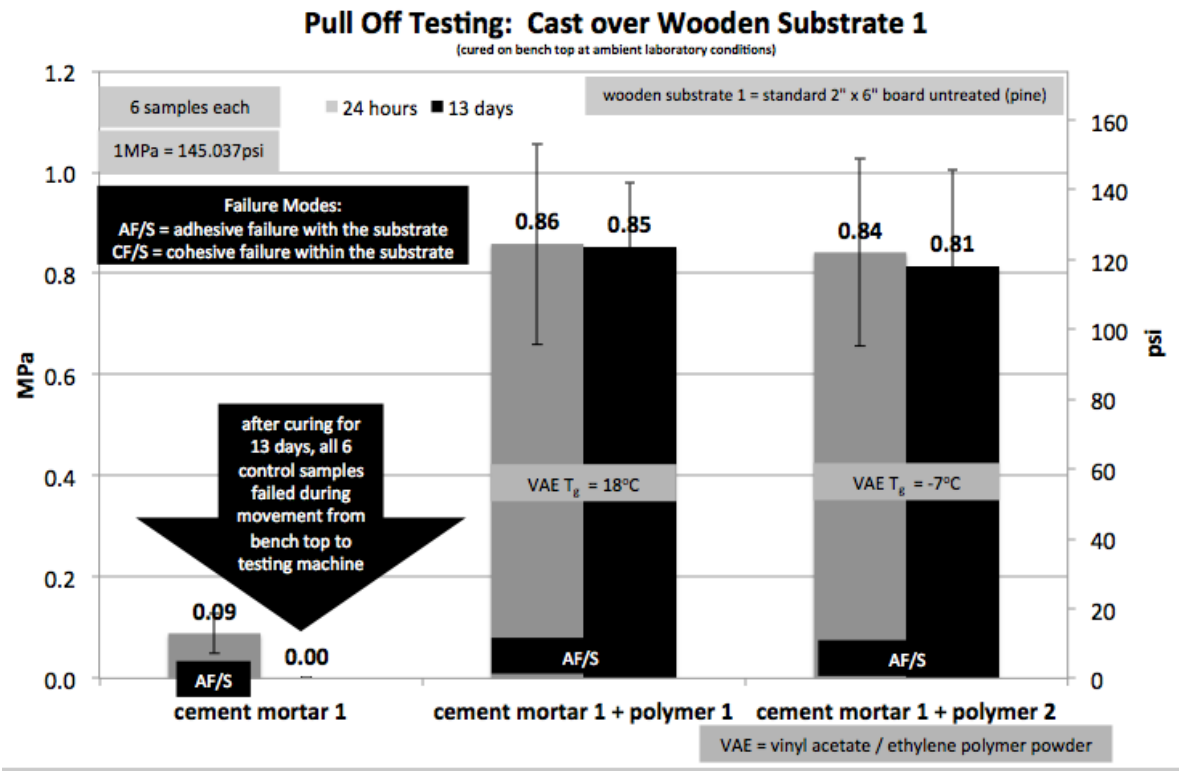

Figure 6.1.8: Polymer modified and non-polymer modified cement mortar 1 cast over wooden substrate 1 after both 24 hours and 13 days of bench top curing at ambient laboratory conditions

Figure 6.1.8 displays pull-off test results for polymer modified and non-polymer modified cement mortar 1 cast over wooden substrate 1 after both 24 hours and 13 days of bench top cure at ambient laboratory conditions. Cement mortar 1 displayed a pull-off strength value of 0.09MPa (13psi) after curing for 24 hours with primary failure mode of AF/S. After 13 days of curing, all six cement mortar 1 samples cast over wooden substrate failed during movement of samples from the curing area to the testing machine. The reason for such failures is not known with certainty. Various theories may include either the wood flexing thus destroying the bond, or perhaps strength loss associated with ettringite decomposition through dehydration type mechanisms weakened the bond. Cement mortar 1 plus polymer 1 displayed pull-off strength values of 0.86MPa (125psi) and 0.85MPa (123psi), both displaying primary failure mode of AF/S, after curing for 24hours and 13 days, respectively. Cement mortar 1 plus polymer 2 displayed pull-off strength values of 0.84MPa (122psi) and 0.81MPa (118psi), both with primary failure mode of AF/S, after curing for 24 hours and 13 days, respectively.

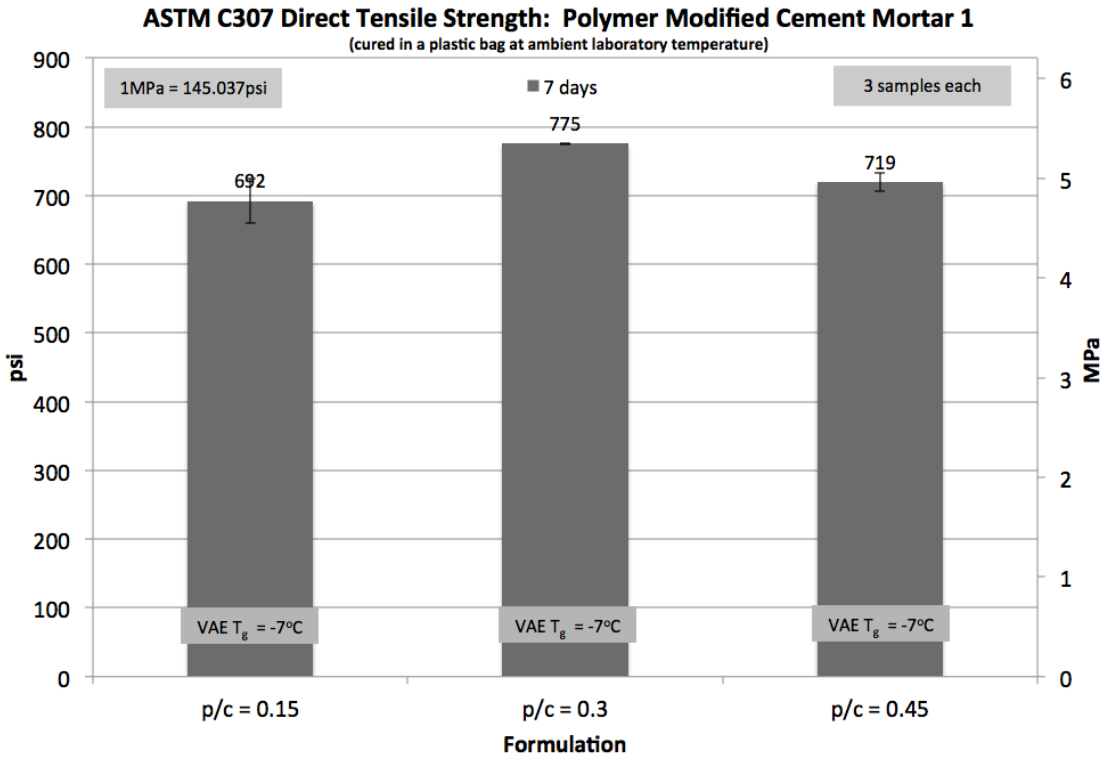

Figure 6.1.9: Direct tensile strength for polymer modified CSA cement mortar at polymer / cement ratios of 0.15, 0.3 and 0.45

Figure 6.1.9 displays average direct tensile strength values for the mortars displayed in Table 6.1.3 after curing for seven days in a sealed plastic bag at ambient laboratory conditions. The mortars displayed direct tensile strength values of 692psi (4.8MPa), 775psi (5.3MPa) and 719psi (5MPa) for polymer / cement ratios of 0.15, 0.3 and 0.45, respectively.

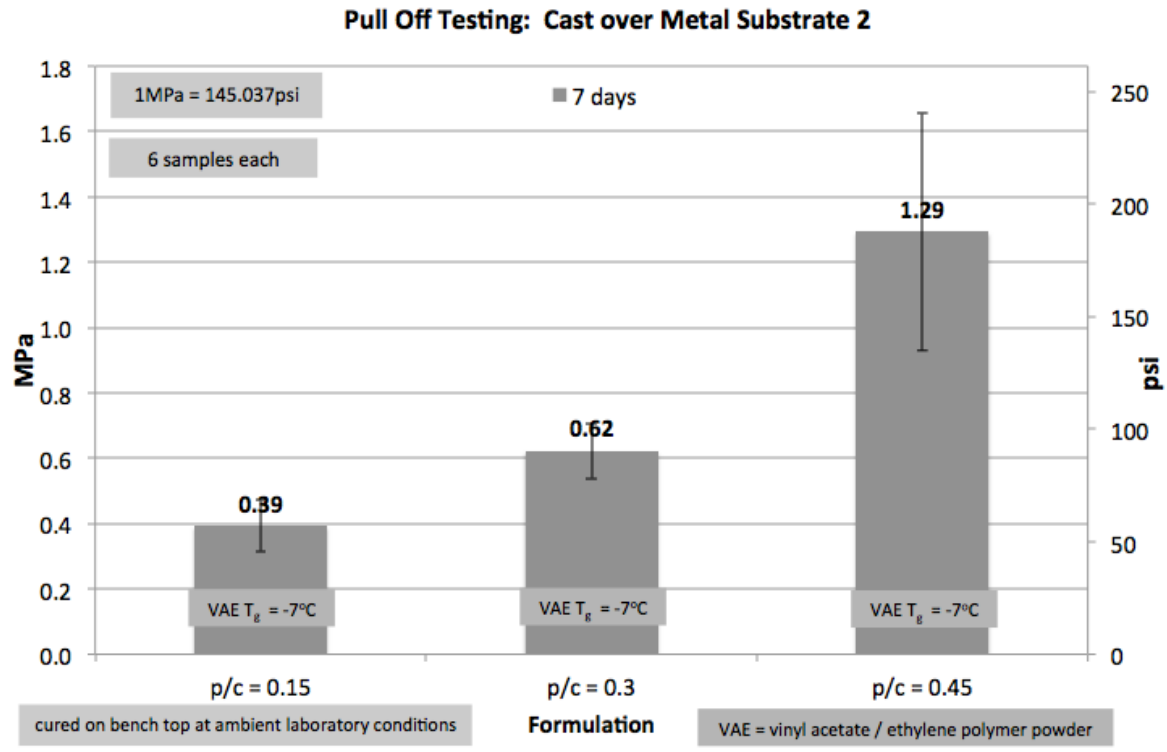

Figure 6.1.10: Polymer modified CSA cement mortar varying polymer / cement ratio cast over metal substrate 2 after 7 days of bench top curing at ambient laboratory conditions

Figure 6.1.10 displays adhesion strength values for the polymer modified CSA cement mortars in Table 6.1.3 cast over ground metal substrate after curing for seven days at ambient laboratory conditions. Mortars displayed pull-off strength values of 0.39MPa (57psi), 0.62MPa (90psi) and 1.29MPa (187psi) for polymer / cement ratios of 0.15, 0.3 and 0.45, respectively. All mortars displayed a majority failure mode of AF/S.

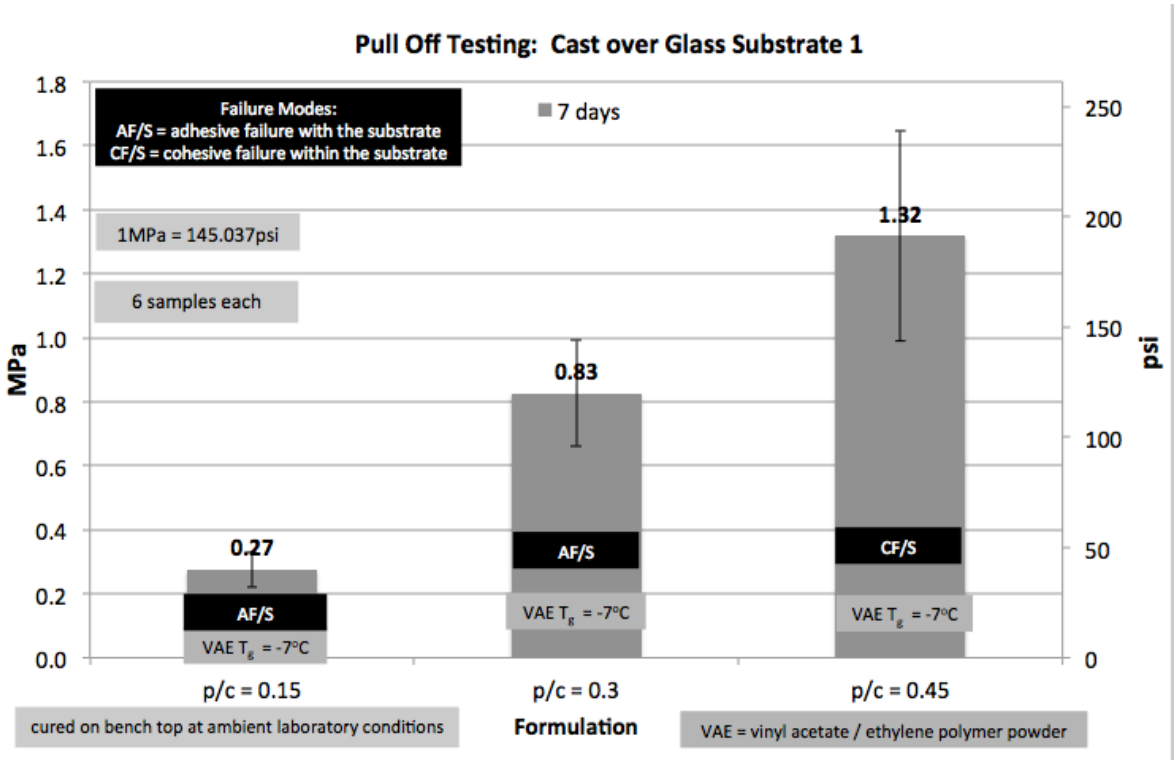

Figure 6.1.11: Polymer modified CSA cement mortar varying polymer / cement ratio cast over glass substrate 1 after 7 days of bench top curing at ambient laboratory conditions

Figure 6.1.11 displays cement mortar 1 plus polymer 2 cast over glass substrate after curing for seven days at ambient laboratory conditions. Mortars displayed pull-off strength values of 0.27MPa (39psi) and 0.83MPa (120psi) for polymer / cement ratios of 0.15 and 0.3. The mortar with p/c = 0.45 resulted in substrate failure or CF/S for all six samples at an average value of 1.32MPa (191psi). Mortars with p/c of 0.15 and 0.3 displayed a primary failure mode of AF/S; whereas, the mortar with p/c = 0.45 displayed a primary failure mode of CF/S, i.e., broken glass for all six samples.

DISCUSSION

For porous substrates, the nature of the polymer is of little consequence, because the bond is usually primarily mechanical in nature (Blackley 1997).

> The only technical requirements to be satisfied are that the latex particles should be able to enter the pores of the substrates, and subsequently to integrate to coherent films of adequate strength. Not only must the particles be sufficiently small to permit entrance into the substrate pores; impeding influences should be absent. One source of impedance in this respect is electrostatic repulsion between latex particles and pores, repulsions arising because the effective electric charge bound at the surface of the particles is of the same polarity as that bound at the interface presented by the pores (Blackley 1997).

For non-porous substrates, the nature of the polymer is sometimes significant. If non-porous surfaces are to be bonded, then the general principle which governs the selection of polymer is that of matched polarity, i.e. the polarity of the polymer should correspond as closely as possible to that of the adherends (Blackley 1997). When practicable, dry mix mortar materials designed for use in patch and repair type applications should possess strength characteristics such that substrate failure results during pull off testing.

The results displayed in Figure 6.1.7 are interesting as they clearly demonstrate the value of polymer modification for CSA cement mortars to be cast over porous substrate materials. Non-polymer modified CSA cement mortar 1 displayed impressive direct tensile strength values; however, all pull-off samples displayed a majority of AF/S or failure at the bond line as seen in Figure 6.1.12. Such adhesion performance is not acceptable for use in patch and repair applications. As previously mentioned, dry mix mortar materials designed for use in patch and repair type applications should result in a majority of substrate failure, or CF/S, during pull off testing when cast over traditional, porous cement based materials (Naderi, 2008).

Figure 6.1.12: CSA cement mortar 1 displaying failure mode AF/S following pull-off testing over concrete substrate 2 after curing for 13 days at ambient laboratory conditions

Both cement mortar 1 plus polymer 1 and cement mortar 1 plus polymer 2 displayed a primary failure mode of CF/S, or failure of the substrate for all samples during pull off testing. The tested samples are displayed in Figures 6.1.13 and 6.1.14. The difference in failure modes shown in Figures 6.1.12, 6.1.13 and 6.1.14 suggests addition of VAE DPP to CSA cement mortar leads to improvements in adhesion performance as described in relevant literature for polymer modified systems based upon OPC (Ohama, 1995). These results are quite encouraging given the self-desiccating nature of CSA cement hydration in the presence of sufficient amounts of calcium sulfate.

No statements can be made regarding adhesion performance of CSA cement mortar 1 plus polymer 1 versus CSA cement mortar 1 plus polymer 2 over concrete substrate as testing of both mortars resulted in substantial substrate failures. The substrate materials were weaker than both the bond strength and the direct tensile strength of the new mortar. Additional substrates must be tested to obtain more information regarding the adhesion characteristics specific to each polymer.

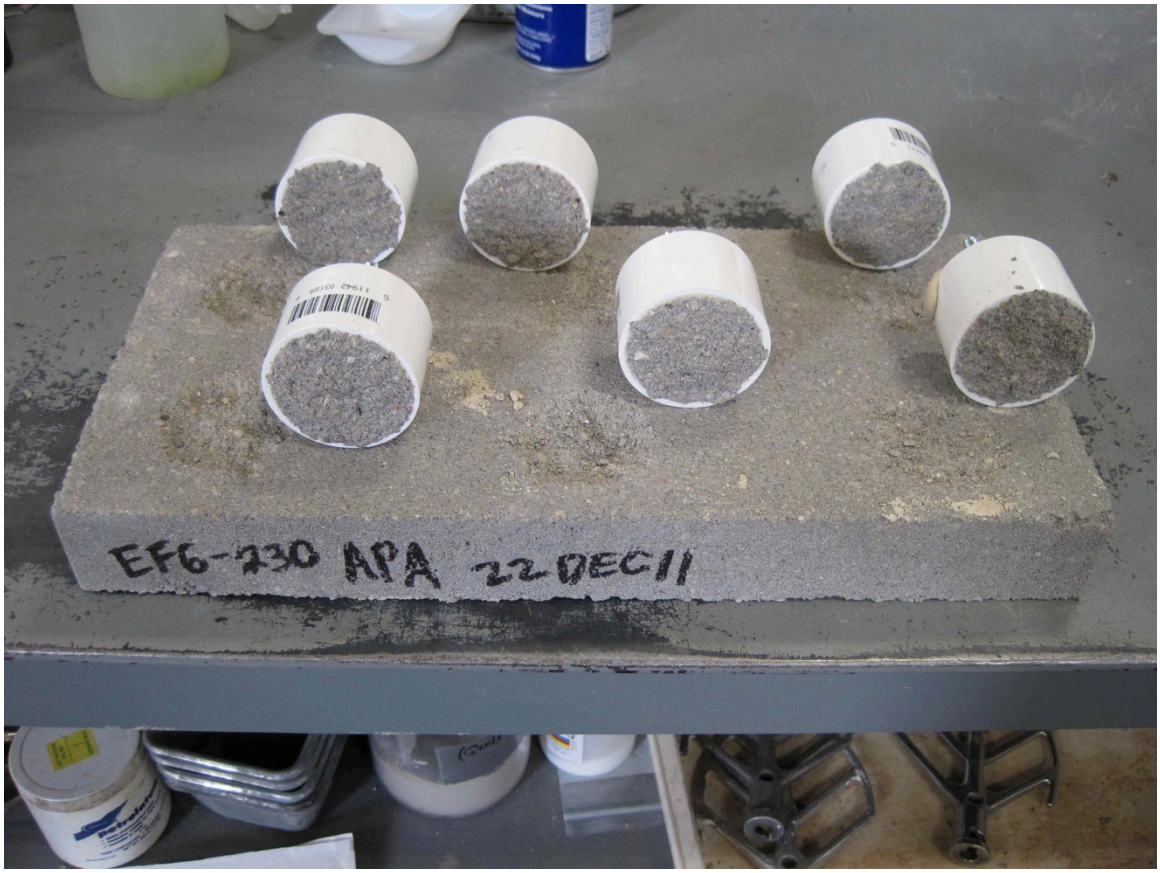

Figure 6.1.13: CSA cement mortar 1 plus polymer 1 displaying failure mode CF/S, substrate failure, following pull-off testing over concrete substrate 2 after curing for 13 days at ambient laboratory conditions

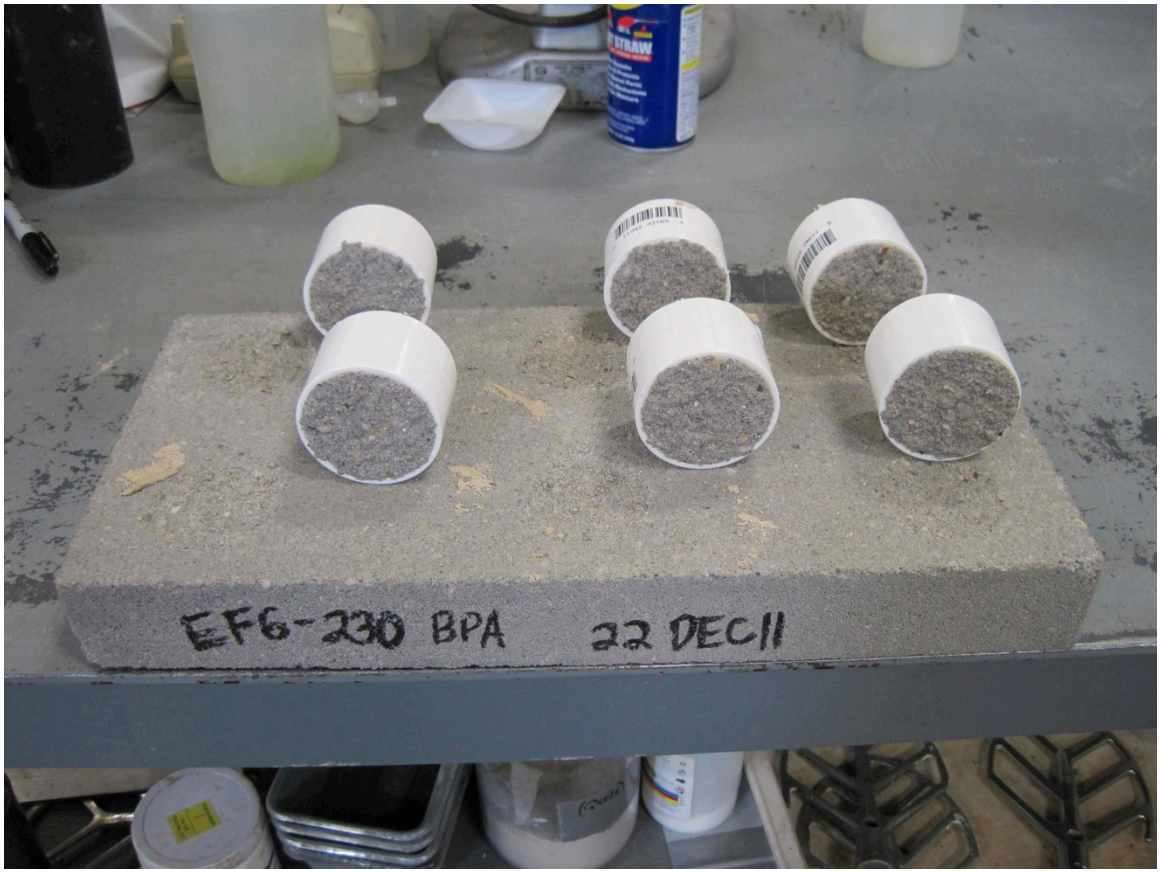

Figure 6.1.14: CSA cement mortar 1 plus polymer 2 displaying failure mode CF/S, substrate failure, following pull-off testing over concrete substrate 2 after curing for 13 days at ambient laboratory conditions

For the adhesion tests performed over wooden substrate 1 displayed in Figure 6.1.8, all samples showed a majority failure mode of adhesive failure with the substrate (AF/S). Therefore, direct statements can be made regarding adhesion performance for the mortar materials.

The results clearly indicate polymer modified CSA cement mortars demonstrate improved bonding strength to wooden substrates when compared with the control sample. Whether cured for 24 hours or 13 days, no difference in pull-off strength behavior over wooden substrate can be noted for cement mortar 1 plus polymer 1 versus cement mortar 1 plus polymer 2. Statistical analysis information is available in Appendix A. For both curing regimens, both cement mortar 1 plus polymer 1 and cement mortar 1 plus polymer 2 displayed significantly improved adhesion performance when compared with non-polymer modified cement mortar 1 cast over wooden substrate. For the 13 day control samples over wooden substrate, it is quite interesting that all six samples simply fell off the wooden

substrate either on the way to the universal testing machine or as the sample was being loaded into the machine. The wooden substrate is less porous when compared with the concrete substrate. After 13 days of hydration, the samples simply falling off the wooden substrate together with the results presented in Figure 6.1.12 suggest either dimensional stability, self-desiccation or both to be an issue for the non-polymer modified CSA cement mortar 1 in adhesion type applications. Certainly, this data is limited; however, it is statistically significant.

The information displayed in Figure 6.1.10 provides an illustration for improved adhesion performance with increases in polymer / cement ratio for mortars containing VAE DPP cast over non-porous substrates. Figure 6.1.10 displays cement mortar 1 plus polymer 2 at p/c of 0.15, 0.3 and 0.45 cast over ground metal substrate, metal substrate 2. For the adhesion tests performed in Figure 6.1.10, all samples displayed a majority failure mode of adhesive failure with the substrate (AF/S). Therefore, direct statements can be made regarding adhesion performance for the mortar materials. The results clearly indicate improved adhesion performance with increases in polymer content. The author theorizes increases in polymer concentration increase the number of polymer particles migrating with bleed water at the bond line. Such an increase in polymer particles in the wet state at the bond line allows for greater amounts of polymer film to be present for film formation and mechanical bonding as water is removed from the system during the hydration process.

In addition to the information displayed in Figure 6.1.11, the information displayed in Figures 6.1.15, 6.1.16 and 6.1.17 provides further illustration for improved adhesion performance with increases in polymer / cement ratio for mortars containing VAE DPP cast over glass substrate materials. For the adhesion tests performed over glass substrate displayed in Figures 6.1.15 and 6.1.16, cement mortar 1 plus polymer 2 at p/c =0.15 and p/c = 0.3 displayed majority failure modes of AF/S; whereas, cement mortar 1 plus polymer 2 at p/c = 0.45 displayed CF/S failure mode for all six samples as displayed in Figure 6.1.17.

Figure 6.1.15: CSA cement mortar 1 plus polymer 2 with p/c = 0.15 displaying failure mode AF/S, failure at bond line, following pull-off testing over glass substrate after curing for 7 days at ambient laboratory conditions

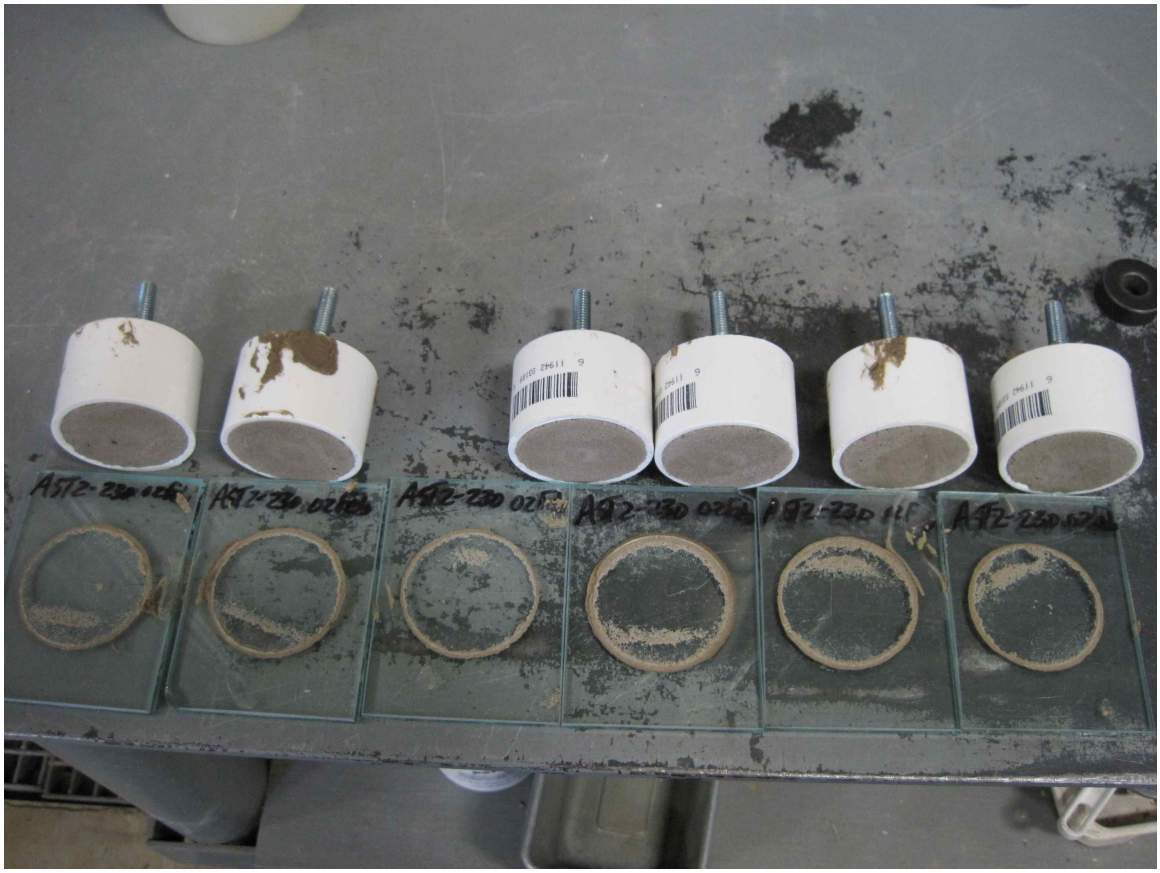

Figure 6.1.16: CSA cement mortar 1 plus polymer 2 with p/c = 0.3 displaying failure mode AF/S, failure at bond line, following pull-off testing over glass substrate after curing for 7 days at ambient laboratory conditions

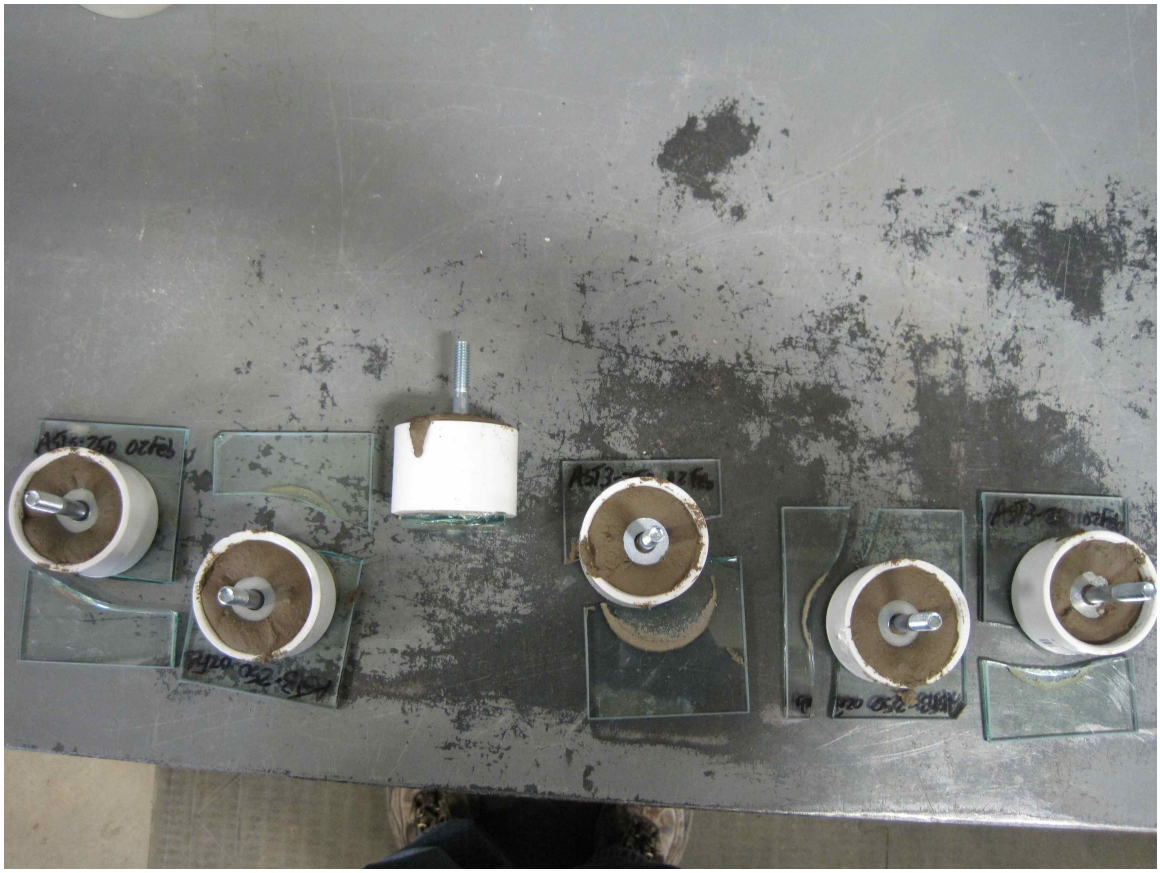

Figure 6.1.17: CSA cement mortar 1 plus polymer 2 with p/c = 0.45 displaying failure mode CF/S, substrate failure, following pull-off testing over glass substrate after curing for 7 days at ambient laboratory conditions.

As previously discussed, the information displayed in Figure 6.1.11 provides an illustration of improved adhesion performance with increases in polymer / cement ratio for mortars containing VAE DPP cast over non-porous substrates. Figure 6.1.11 displays cement mortar 1 plus polymer 2 at p/c of 0.15, 0.3 and 0.45 cast over glass substrate. For the adhesion tests displayed in Figure 6.1.11, all samples did not display the same majority failure mode; therefore, direct statements must be made in combination with the failure mode to eliminate confusion as the upper data point is an illustration of substrate strength; whereas, the lower two data points illustrate bond strength. Nevertheless, the author theorizes the same mechanism resulting in increased bond strength over metal substrate is plausible for like materials cast over glass substrates. Additionally, the mortar possessing the greatest polymer concentration created substrate failure, which is interesting as cementitious materials are not well known for demonstrating acceptable bond strengths to glass substrates, yet alone possess bond strength sufficient for breaking the glass substrate during pull off testing.

CONCLUSION

In conclusion, the results of this study indicate adhesion performance of calcium sulfoaluminate (CSA) cement mortars can be markedly improved through addition of vinyl acetate / ethylene (VAE) dispersible polymer powder (DPP) and even further improved through increases in the polymer / cement (p/c) ratio.

Bonding mechanisms for cementitious materials are reported as being primarily mechanical in nature. Literature reports a mechanical bond is formed as materials diffuse into the substrate pore network along with bleed water and subsequently set and harden. Polymer modified materials are reported to demonstrate like mechanical bond forming mechanisms, where migrating polymer particles coalesce to form polymer films as water is removed from the system.

When cast over traditional, porous concrete substrates, polymer modified CSA cement mortars displayed superior adhesion characteristics when compared with the CSA cement mortar without polymer. All polymer modified CSA cement mortars demonstrated failure modes within the concrete substrate material, or CF/S; whereas, the CSA cement mortar without polymer demonstrated adhesive failure with the substrate, or AF/S. A majority AF/S failure mode is unacceptable for cementitious patch and repair materials. The results presented in this study suggest latex polymer modification is a viable means for generating acceptable adhesion performance to concrete substrate materials for mortars based upon CSA cement.

When cast over wooden substrate materials, polymer modified CSA cement mortars also displayed significant improvements in adhesion characteristics when compared with the CSA cement mortar without polymer. All mortar samples displayed the same failure mode of AF/S. However, all polymer modified CSA cement mortars displayed average adhesion values much greater than the adhesion values displayed by the control sample. Noteworthy is that all control mortar samples over wooden substrates simply fell off the substrates during movement for testing after curing for 13 days at ambient laboratory conditions; whereas, similar control samples demonstrated weak bonding after curing for 24 hours.

Polymer modified CSA cement mortars demonstrated trends of increasing bond strength with increases in p/c when cast over non-porous substrate materials, glass and ground metal. The results presented in this study strongly suggest the adhesion

performance of polymer modified CSA cement mortars can be further improved by increasing the polymer to cement ratio. Furthermore, the presented results suggest the selected neutral rheology vinyl acetate / ethylene based dispersible polymer powders are compatible with the experimental calcium sulfoalumiante cement containing minor phase tri-calcium aluminate.

6 REFERENCES:

- ACI 548.1R-09, Guide for the Use of Polymers in Concrete, Reported by ACI Committee 548, American Concrete Institute
- Blackley, D.C., 1997, Polymer Latices, Science and Technology, 2nd Edition, ISBN 0412 62890 2
- Chandra, S., Berntsson, L., 2003, Lightweight Aggregate Concrete, Science, Technology and Applications, Noyes Publications, ISBN 0-8155-1486-7
- Chandra, S., Ohama, Y., 1994, Polymers in Concrete, CRC Press, ISBN 0-8493-4815-3
- Gastaldi, D., Fulvio, C., Boccaleri, E.,2009, Ettringite and calcium sulfoaluminate cement: investigation of water content by near-infrared spectroscopy, Journal of Material Science, 44: 5788-5794, 2009
- Glasser, F.P., Zhang, L., 2001, High-performance cement matrices based on calcium sulfoaluminate-belite compositions, Cement and Concrete Research 31 (2001) 1881-1886
- Knapen, E., Beeldens, A., Van Gemert, D., 2005, Water-soluble polymeric modifiers for cement mortar and concrete, ConMat'05 3rd Intern. Conference on Construction Materials: Performance, Innovation and Structural Implications, Vancouver, Canada, August 22-24, 2005
- Knapen, E., Gemert, D., 2009, Cement hydration and microstructure formation in the presence of water-soluble polymers, Cement and Concrete Research 39 (2009) 6-13
- Naderi, M., 2008, Adhesion of Different Concrete Repair Systems Exposed to Different Environments, The Journal of Adhesion, 84:78-104, 2008
- Ohama, Y., 1995, Handbook of Polymer Modified Concrete and Mortars, Noyes Publications, ISBN 0-8155-1358-5
- Pelletier, L., Winnefeld, F., Lothenbach, B., 2010, The ternary system Portland cement-calcium sulphoaluminate clinker-anhydrite: Hydration mechanism and mortar properties, Cement and Concrete Composites 32 (2010) 497-507
- Vaysburd, A., McDonald, J., 1999, An Evaluation of Equipment and Procedures for Tensile Bond Testing of Concrete Repairs, US Army Corps of Engineers, Technical Report REMR-CS-61, June 1999

Chapter 7: Concluding Remarks

CONCLUDING REMARKS

The information presented in this document is vital to formulating cementitious materials based upon a majority of calcium sulfoaluminate (CSA) cement containing minor phase tri-calcium aluminate. An abundance of literature exists describing the influence of various additives on performance behavior of ordinary portland cement (OPC) and calcium aluminate cement (CAC); however, the volume of literature describing the influence of various admixtures on performance behavior of CSA cements is comparatively small. This is likely related to CSA cements being used primarily as an expansive additive in cementitious systems for many decades, as opposed to the few recent decades when CSA cement has appeared attractive as a stand alone hydraulic binding agent. The research highlights the excellent mechanical property performance characteristics for polymer modified CSA cement materials. It raises questions regarding the long term viability of non-polymer modified CSA cement systems for use in constant low humidity environments. The following paragraphs summarize important findings.

The presented information relating to the cement analysis and design portion of the research is significant as it displayed the influence of relative humidity on hydration characteristics of CSA cement containing minor phase tri-calcium aluminate (C_3A) in the presence of different types of calcium sulfate. CSA cement mortars containing anhydrite and 50 weight % anhydrite and 50 weight % gypsum as sources of calcium sulfate displayed different direct tensile strength performance when cured at both 50% and 100% relative humidity. Furthermore, CSA cement mortars containing solely anhydrite, 50 weight % anhydrite and 50 weight % gypsum as a combined source of calcium sulfate and solely gypsum as sources of calcium sulfate displayed different direct tensile strength behaviors when cured at constant 50% relative humidity. When cured at constant 50% relative humidity and 23^{o}C, the formulation containing solely gypsum displayed significant direct tensile strength loss, followed by the formulation containing 50 weight % anhydrite and 50 weight % gypsum, while the formulation containing solely anhydrite was last to display significant direct tensile strength loss.

The presented information is of further significance as it showed latex polymer addition presents a viable means for mitigating ettringite decomposition behavior in CSA

cement materials cured at constant low humidity. CSA cement paste analysis containing anhydrite and VAE polymer displayed no significant decrease in ettringite concentration between hydration periods of 28 days and 242 days at constant 50% relative humidity and 23°C; whereas, the CSA cement paste formulation containing solely anhydrite displayed a decrease in ettringite concentration between hydration periods of 28 days and 242 days at constant 50% relative humidity and 23°C. In addition, polymer modified CSA cement mortars showed no decrease in long term tensile strength performance when cured at constant 50% relative humidity; whereas, CSA cement mortars without VAE polymer displayed decreases in direct tensile strength when cured at constant 50% relative humidity for extended periods of time.

The information regarding the use of accelerating and retarding admixtures in ettringite forming systems based upon calcium aluminate cement (CAC) is well documented. However, limited works exist describing the influence of commonly utilized admixtures on behavior of CSA cements, while information pertaining to combinations of admixtures with CSA cement containing minor phase tri-calcium aluminate is virtually non-existent. The most notable of such works is likely from Pera et al, (2004), where the combination of lithium carbonate and CSA cement is thoroughly discussed in regard to development of innovative materials based upon CSA cement. Therefore, information presented as a result of this research is significant as it further illustrates the potential for admixtures such as tartaric acid, hydroxyethyl methyl cellulose (HEMC), lithium carbonate and superplasticizer to be candidates for adjusting the hydration behavior of cementitious materials based upon CSA cement containing minor phase tri-calcium aluminate. Furthermore, tartaric acid served as a wonderful agent for retarding onset of hydration for the tested CSA cement. HEMC served as a terrific rheology modifier for the tested CSA cement materials. Lithium carbonate served as an excellent accelerating agent for hydration reactions of the tested CSA cement materials. Superplasticizing materials, spray dried powders of modified polycarboxylic ether, were successfully utilized as water reducing agents for the tested CSA cement materials.

The information associated with the polymer design phase of the research was significant as it demonstrated material compatibility between vinyl acetate / ethylene (VAE) based dispersible polymer powders (DPP) and CSA cement. Furthermore, the polymer design information illustrated a novel concept for varying polymer / cement (p/c) ratio within cementitious materials as a means for significantly improving ductile behavior

by increasing the concentration of tough, flexible polymer film per specific volume of material microstructure.

The information regarding adhesion characteristics of mortars containing a majority CSA cement was significant as it illustrated the improved adhesion performance of polymer modified CSA cement mortars when compared with non-polymer modified CSA cement mortars when cast over tradition concrete substrate materials. Additionally, polymer modified mortars containing CSA cement demonstrated impressive bond strengths to wood, ground metal and glass substrate materials. For the specific case of pull off testing over glass substrate materials, the mortar with p/c = 0.45 resulted in failure of the glass substrate materials suggesting the developed materials demonstrated excellent adhesion characteristics to relatively non-porous substrates. Therefore, the developed polymer modified mortars should be viewed as ideal candidates for use with new generations of cementitious materials known for possessing fewer microstructural type defects, with an example being macro defect free (MDF) cementitious materials.

FURTHER RESEARCH

The presented information creates a need for further research in an effort to truly understand the long-term performance behavior of calcium sulfoalumiante (CSA) cement materials. With regard to ettringite decomposition, based upon comments from Taylor (1997), future research should focus on specimen size and its relation to observed strength loss versus time for materials based upon CSA cement cured at constant low humidity. Future research should also focus on the influence of calcium sulfate type on onset of strength loss and microstructural changes within CSA cement based materials –a number of materials from different suppliers with different particle size distributions should be tested. Future research should focus on defining acceptable levels of strength loss within CSA cement materials as a function of constituent materials comprising the microstructure. For example, perhaps anhydrite should be the only type of calcium sulfate for development of patch and repair materials for use with cantilevered balconies.

Additional research should focus on developing methods for choosing strength criteria for use with design equations for structural concrete elements based upon CSA cement. For example, given the information presented in this study, non-polymer modified CSA cement mortars demonstrated different tensile strength behavior for like samples

cured at either constant 50% relative humidity or constant 100% relative humidity and ambient laboratory temperature of 23°C.

The topic of utilizing the polymer to cement ratio as a means for specifying ductile behavior of cementitious materials is deemed worthy of further exploration. Before implementing high polymer / cement ratio materials on a large scale within the broad construction industry, more research is necessary to develop a fundamental understanding of these materials. For example, little is known about the creep behavior of high polymer / cement ratio materials in structural applications. In addition to creep behavior, different families of latex polymers demonstrate different behaviors when exposed to high humidity environments. The research community would benefit from studies describing the influence of environment on the performance behavior of materials possessing high polymer / cement ratios while varying polymer chemistry. Last but not least, modeling the behavior of polymer modified concretes and mortars at various polymer / cement ratios would constitute a wonderful project for ANSYS enthusiasts. If successful, ANSYS modeling would allow development of a protocol for truly "engineering" the ductile behavior of polymer modified cement based materials.

Appendix A: Analysis of Variance

Minitab statistical software was utilized for both analysis of variance testing and post hoc comparisons. Analysis of variance is particularly useful when the basic differences between the groups cannot be stated quantitatively (Bethea et al, 1975). One-way analysis of variance is used to test the equality of J population means. The procedure is based on assumptions that each of J groups of observations is a random sample from a normal distribution and that the population variance $s^2_x = s^2$ is constant among the groups (Bethea et al, 1975). Pooled variances were used for the analyses.

The Tukey comparison method is an example of a post hoc method, that is, it can be used after the analyst looks at the data (Mickey et al, 2004). Hypothesis tests performed using Tukey's Honestly Significant Difference comparison method tend to have greater power than those performed using either Bonferroni's or Scheffe's method (Mickey et al, 2004). Tukey's Honestly Significant Difference (HSD) method tests all pairs against:

$$W_k = q_{k,u,1-a}*(s^2/n)^{1/2}$$

Where $q_{k,u,1}$ is the 100(1-a)th percentile of the distribution of the Studentized range of k means with u d.f. (Fisher's LSD = W_2) (ESS Vol. 8).

Fisher's protected least significant difference method is identical with the Student's t-test, except that it requires a significant F-test for the equality of all k means before individual paired differences may be tested (ESS Vol. 8). None of the other STPs and SMCPs have this prerequisite (ESS Vol. 8). Two sample means y_i and y_j will be declared to be significantly different at the 100a% level if their absolute difference exceeds

$$LSD = t_{u,1-(a/2)}*((s^2*(n_i^{-1} + n_j^{-1}))^{1/2}$$

Where tu,g is the (100g)th percentile of Student's t-distribution with u degrees of freedom (d.f.) and s^2 (with u d.f.) is the pooled estimate of s^2 (ESS Vol.8).
ANOVA reporting for this study presents an observed F-value written with convention F(degrees of freedom between / degrees of freedom within) = value, a significance level p-value, the pooled standard deviation and a value for R^2.

Boxplot
The boxplot is to serve as an aid for understanding the distribution of data. The boxplot consists of horizontal and vertical lines. Three horizontal lines are arranged to form an interquartile range box representing the middle 50% of the data as follows:

- Top line – Q3 (third quartile) such that 75% of the data are less than or equal to this value
- Middle line – Q2 (median) such that 50% of the data are less than or equal to this value
- Bottom line – Q1 (first quartile) such that 25% of the data are less than or equal to this value

Vertical lines represent upper and lower whiskers. The upper whisker extends to the maximum data point within 1.5 box heights from the uppermost portion of the box. Likewise, the lower whisker extends to the minimum data point within 1.5 box heights from the lower most portion of the box. Outliers are listed as asterisks outside the range of the upper or lower whiskers.

Histogram

The histogram is to serve as an aid for analyzing the shape and spread of the data set. The statistical software divides sample values into many intervals called bins. Bars represent the frequency of observations falling within bins.

Individual Value Plots

Individual value plots serve as an aid for assessing the assumption of equal variances for data sets.

Normal Probability Plots

The normal probability plots use an alpha value of 0.05. In the normal probability plot of standard effects, points that do not lie near the line signify important effects which are typically larger and generally further from the fitted line in comparison with unimportant effects. Unimportant effects are typically smaller and centered around zero.

Adhesion Statistical Analysis Summary

Experiment 1: Adhesion of Polymer Modified CSA Cement to Glass Substrates

mortar = cement mortar 1 plus polymer 2

curing regimen = 24 hours ambient laboratory conditions

Protocoal similar to that described in ASTM C1583 was followed for data collection. Six samples were cast and tested for each mortar formulation. Samples were stored at ambient laboratory temperature and humidity from the time of casting to the time of testing. Tested mortar formulations differed in polymer concentration. Mortars with polymer / cement ratios of 0.15, 0.3 and 0.45 were tested.

p/c = 0.15 7d glass	p/c = 0.3 7d glass	p/c = 0.45 7d glass
0.2447	0.9359	1.3052
0.1991	0.5394	1.4323
0.3526	0.8736	1.8586
0.2614	0.9526	0.8859
0.2763	0.9447	1.3288
0.3131	0.7140	1.1008

Table A1: Adhesion pull off test data for polymer modified CSA cement cast over glass substrates

H_o: Polymer concentration (polymer / cement ratio (p/c)) does not effect the average bond strength for polymer modified mortar cast over glass substrate materials ($u_i = u_j$)

H_a: Polymer concentration (polymer / cement ratio (p/c)) effects the average bond strength for polymer modified mortar cast over glass substrate materials (u_i does not equal u_j)

One-way ANOVA was used to test the equality of the population means for 24 hour adhesion testing of cement mortar 1 plus polymer 2 at p/c = 0.15, p/c = 0.3 and p/c = 0.45 cast over glass substrate. Results from ANOVA are: $F(2/15) = 35.43$, $p < 0.001$, pooled standard deviation = 0.2149 and $R^2 = 82.53\%$. Based upon the F value of 35.43 and corresponding p-value < 0.001, if an alpha value of 0.05 is chosen, it is safe to reject the null hypothesis and ultimately conclude that at least two means differ from one another, and this inequality is highly unlikely due to chance. Further "post hoc" statistical analysis utilizing Tukey's Honestly Significant Difference Test assigned cement mortar 1 plus polymer 2 at p/c = 0.45 to "A" substrate strength classification, while cement mortar 1 plus polymer 2 with p/c = 0.3 was assigned to "B" adhesion strength classification and cement mortar 1 plus polymer 2 with p/c = 0.15 was assigned to "C" adhesion strength classification. For the Tukey comparison method, mortars that do not share the same letter strength classification are significantly different. However, it must be duly noted that the mortar with p/c = 0.45 experienced a CF/S failure mode; whereas, mortars with p/c = 0.15 and p/c = 0.3 displayed AF/S failure mode. With CF/S failure mode, the recorded values are related to the strength of the substrate material, and these recorded values are likely less than the true bond strength values.

One-way ANOVA: p/c = 0.15 7d glass, p/c = 0.3 7d glass, p/c = 0.45 7d glass

Source DF SS MS F P
Factor 2 3.2739 1.6369 35.43 0.000
Error 15 0.6930 0.0462
Total 17 3.9668

S = 0.2149 R-Sq = 82.53% R-Sq(adj) = 80.20%

Level N Mean StDev
p/c = 0.15 7d glass 6 0.2745 0.0535
p/c = 0.3 7d glass 6 0.8267 0.1668
p/c = 0.45 7d glass 6 1.3186 0.3285

Individual 95% CIs For Mean Based on
Pooled StDev
Level --------+---------+---------+---------+-
p/c = 0.15 7d glass (----*----)
p/c = 0.3 7d glass (----*---)
p/c = 0.45 7d glass (----*----)
--------+---------+---------+---------+-
0.40 0.80 1.20 1.60

Pooled StDev = 0.2149

Grouping Information Using Tukey Method

N Mean Grouping
p/c = 0.45 7d glass 6 1.3186 A
p/c = 0.3 7d glass 6 0.8267 B
p/c = 0.15 7d glass 6 0.2745 C

Means that do not share a letter are significantly different.

Tukey 95% Simultaneous Confidence Intervals
All Pairwise Comparisons

Individual confidence level = 97.97%

p/c = 0.15 7d glass subtracted from:

Lower Center Upper
p/c = 0.3 7d glass 0.2301 0.5522 0.8742
p/c = 0.45 7d glass 0.7220 1.0441 1.3661

----+---------+---------+---------+-----
p/c = 0.3 7d glass (----*-----)

```
p/c = 0.45 7d glass                    (----*-----)
               ----+---------+---------+---------+-----
                -0.60     0.00     0.60     1.20
```

p/c = 0.3 7d glass subtracted from:

	Lower	Center	Upper
p/c = 0.45 7d glass	0.1699	0.4919	0.8139

```
               ----+---------+---------+---------+-----
p/c = 0.45 7d glass              (----*-----)
               ----+---------+---------+---------+-----
                -0.60     0.00     0.60     1.20
```

Grouping Information Using Fisher Method

	N	Mean	Grouping
p/c = 0.45 7d glass	6	1.3186	A
p/c = 0.3 7d glass	6	0.8267	B
p/c = 0.15 7d glass	6	0.2745	C

Means that do not share a letter are significantly different.
Fisher 95% Individual Confidence Intervals
All Pairwise Comparisons

Simultaneous confidence level = 88.31%

p/c = 0.15 7d glass subtracted from:

	Lower	Center	Upper
p/c = 0.3 7d glass	0.2877	0.5522	0.8167
p/c = 0.45 7d glass	0.7796	1.0441	1.3086

```
               ---+---------+---------+---------+------
p/c = 0.3 7d glass               (---*----)
p/c = 0.45 7d glass                    (---*----)
               ---+---------+---------+---------+------
               -0.60     0.00     0.60     1.20
```

p/c = 0.3 7d glass subtracted from:

	Lower	Center	Upper
p/c = 0.45 7d glass	0.2274	0.4919	0.7564

```
               ---+---------+---------+---------+------
p/c = 0.45 7d glass              (---*----)
```

```
---+---------+---------+---------+------
-0.60      0.00      0.60      1.20
```

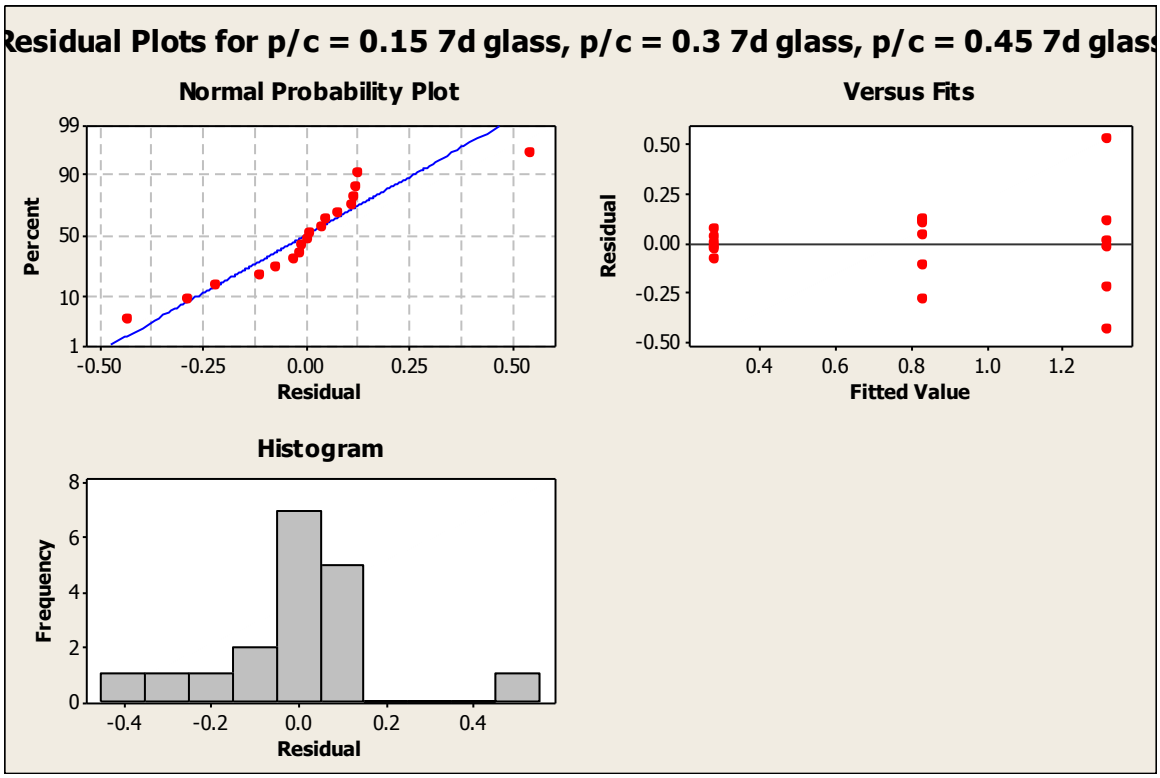

Figure A1: Minitab statistical software generated normal probability plot, plot of residuals and histogram for adhesion bond strengths of cement mortar 1 plus polymer 2 varying polymer / cement ratio cast over glass substrates

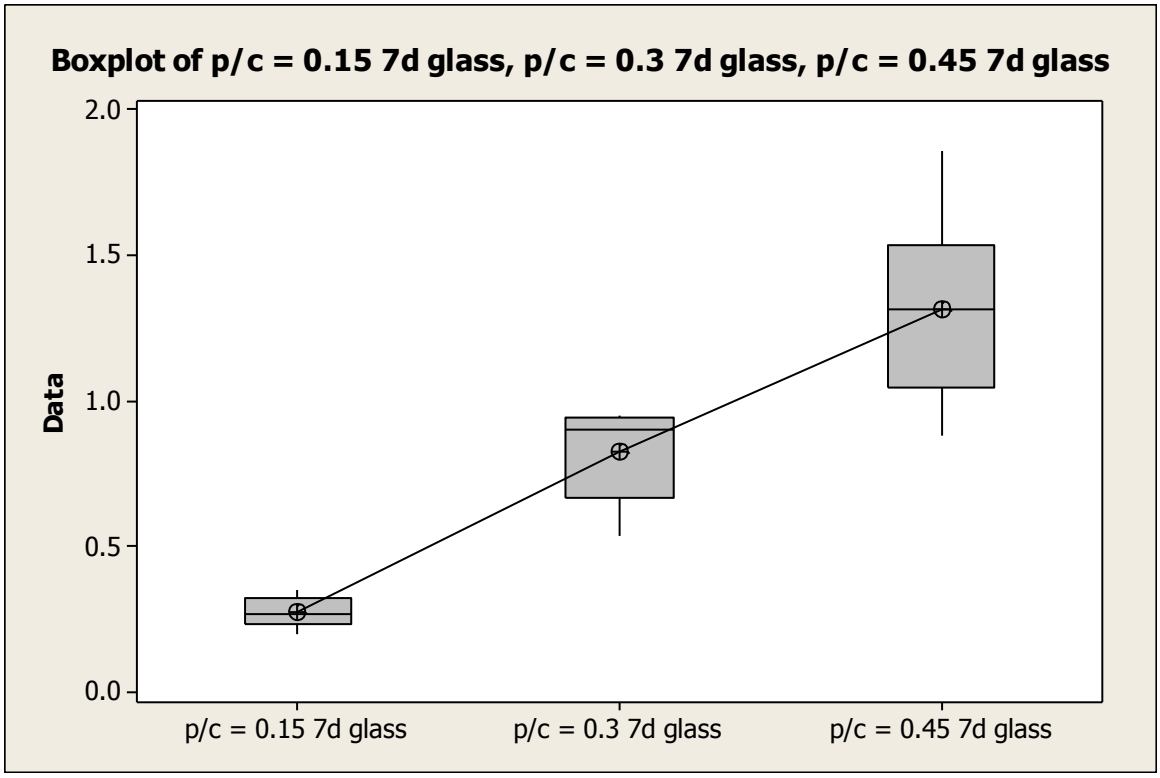

Figure A2: Minitab statistical software generated boxplot for adhesion bond strengths of cement mortar 1 plus polymer 2 varying polymer / cement ratio cast over glass substrates

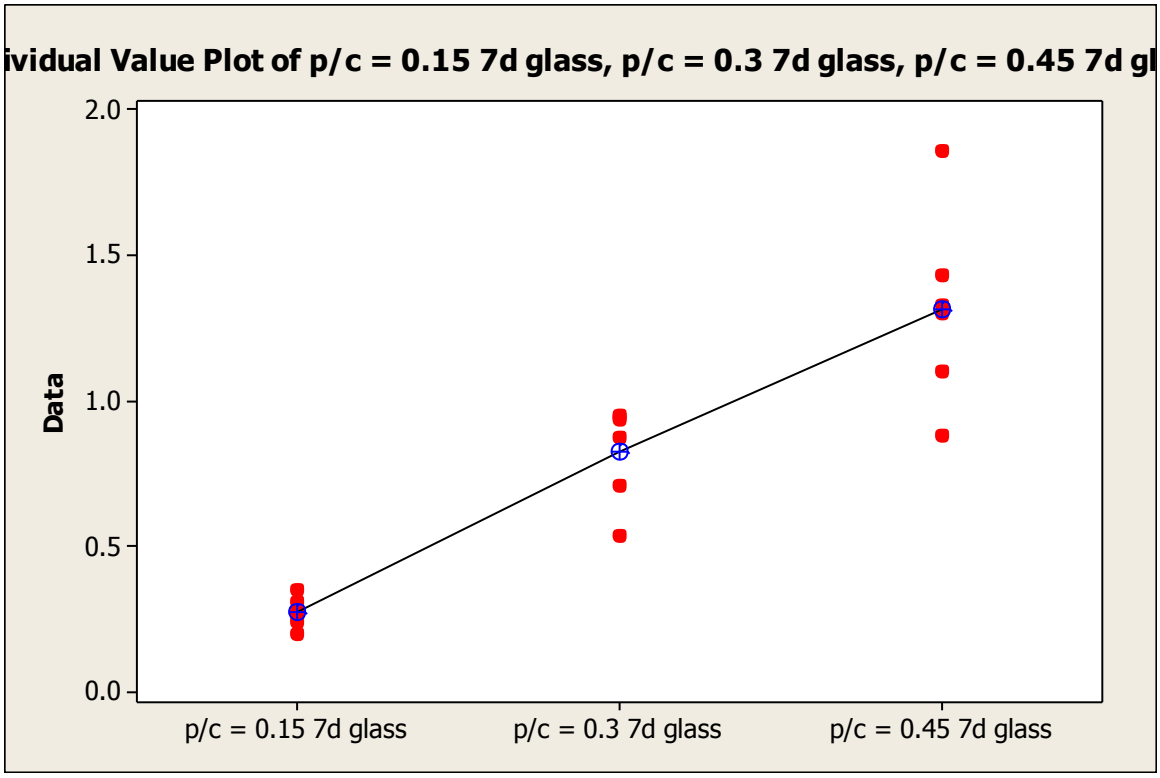

Figure A3: Minitab statistical software generated individual value plot for adhesion bond strengths of cement mortar 1 plus polymer 2 varying polymer / cement ratio cast over glass substrates

Experiment 2: Adhesion of Polymer Modified CSA Cement to Metal Substrates

mortar = cement mortar 1 plus polymer 2

curing regimen = 24 hours ambient laboratory conditions

Protocoal similar to that described in ASTM C1583 was followed for data collection. Six samples were cast and tested for each mortar formulation. Samples were stored at ambient laboratory temperature and humidity from the time of casting to the time of testing. Tested mortar formulations differed in polymer concentration. Mortars with polymer / cement ratios of 0.15, 0.3 and 0.45 were tested.

p/c = 0.15 7d metal2	p/c = 0.3 7d metal 2	p/c = 0.45 7d metal2
0.4859	0.5938	1.0587
0.3333	0.6833	1.0789
0.3596	0.7254	1.1771
0.5017	0.5631	0.9508
0.3272	0.4965	1.6595
0.3465	0.6684	1.8376

Table A2: Adhesion pull off test data for polymer modified CSA cement cast over metal substrates

H_o: Polymer concentration (polymer / cement ratio (p/c)) does not effect the average bond strength for polymer modified mortar cast over metal substrate materials ($u_i = u_j$)

H_a: Polymer concentration (polymer / cement ratio (p/c)) effects the average bond strength for polymer modified mortar cast over metal substrate materials (u_i does not equal u_j)

One-way ANOVA was used to test the equality of the population means for 24 hour adhesion testing of cement mortar 1 plus polymer 2 at p/c = 0.15, p/c = 0.3 and p/c = 0.45 cast over metal substrate. Results from ANOVA are: $F(2/15) = 27.04$, $p < 0.001$, pooled standard deviation = 0.2207 and $R^2 = 78.29\%$. Based upon the F value of 27.04 and corresponding p-value < 0.001, if an alpha value of 0.05 is chosen, it is safe to reject the null hypothesis and ultimately conclude that at least two means differ from one another, and this inequality is highly unlikely due to chance. Further "post hoc" statistical analysis utilizing Tukey's Honestly Significant Difference Test assigned cement mortar 1 plus polymer 2 at p/c = 0.45 to "A" substrate strength classification, while cement mortar 1 plus polymer 2 with p/c = 0.3 was assigned to "B" adhesion strength classification and cement mortar 1 plus polymer 2 with p/c = 0.15 was also assigned to "B" adhesion strength classification. For the Tukey comparison method, mortars that do not share the same letter strength classification are significantly different.

One-way ANOVA: p/c = 0.15 7d metal2, p/c = 0.3 7d metal 2, p/c = 0.45 7d metal2

Source DF SS MS F P
Factor 2 2.6335 1.3167 27.04 0.000
Error 15 0.7304 0.0487
Total 17 3.3639

S = 0.2207 R-Sq = 78.29% R-Sq(adj) = 75.39%

Level N Mean StDev
p/c = 0.15 7d metal2 6 0.3924 0.0795
p/c = 0.3 7d metal 2 6 0.6218 0.0856
p/c = 0.45 7d metal2 6 1.2938 0.3639

Individual 95% CIs For Mean Based on
Pooled StDev

```
Level            ----+---------+---------+---------+-----
p/c = 0.15 7d metal2  (----*-----)
p/c = 0.3 7d metal 2       (-----*----)
p/c = 0.45 7d metal2                    (-----*----)
                 ----+---------+---------+---------+-----
                  0.35      0.70      1.05      1.40
```

Pooled StDev = 0.2207

Grouping Information Using Tukey Method

N Mean Grouping
p/c = 0.45 7d metal2 6 1.2938 A
p/c = 0.3 7d metal 2 6 0.6218 B
p/c = 0.15 7d metal2 6 0.3924 B

Means that do not share a letter are significantly different.

Tukey 95% Simultaneous Confidence Intervals
All Pairwise Comparisons

Individual confidence level = 97.97%

p/c = 0.15 7d metal2 subtracted from:

Lower Center Upper
p/c = 0.3 7d metal 2 -0.1012 0.2294 0.5600
p/c = 0.45 7d metal2 0.5708 0.9014 1.2320

```
                -------+---------+---------+---------+--
p/c = 0.3 7d metal 2            (-----*----)
p/c = 0.45 7d metal2                    (----*-----)
                -------+---------+---------+---------+--
                  -0.60     0.00     0.60     1.20
```

p/c = 0.3 7d metal 2 subtracted from:

```
                 Lower  Center   Upper
p/c = 0.45 7d metal2  0.3414  0.6720  1.0026

                -------+---------+---------+---------+--
p/c = 0.45 7d metal2                  (----*-----)
                -------+---------+---------+---------+--
                  -0.60     0.00     0.60     1.20
```

Grouping Information Using Fisher Method

```
                N    Mean  Grouping
p/c = 0.45 7d metal2  6  1.2938  A
p/c = 0.3 7d metal 2  6  0.6218    B
p/c = 0.15 7d metal2  6  0.3924    B
```

Means that do not share a letter are significantly different.

Fisher 95% Individual Confidence Intervals
All Pairwise Comparisons

Simultaneous confidence level = 88.31%

p/c = 0.15 7d metal2 subtracted from:

```
                 Lower  Center   Upper
p/c = 0.3 7d metal 2  -0.0422  0.2294  0.5009
p/c = 0.45 7d metal2   0.6298  0.9014  1.1730

                -------+---------+---------+---------+---
p/c = 0.3 7d metal 2            (----*---)
p/c = 0.45 7d metal2                    (----*----)
                -------+---------+---------+---------+---
                  -0.60     0.00     0.60     1.20
```

p/c = 0.3 7d metal 2 subtracted from:

```
                Lower  Center   Upper
p/c = 0.45 7d metal2  0.4005  0.6720  0.9436

                ------+---------+---------+---------+---
p/c = 0.45 7d metal2                  (---*----)
                ------+---------+---------+---------+---
```

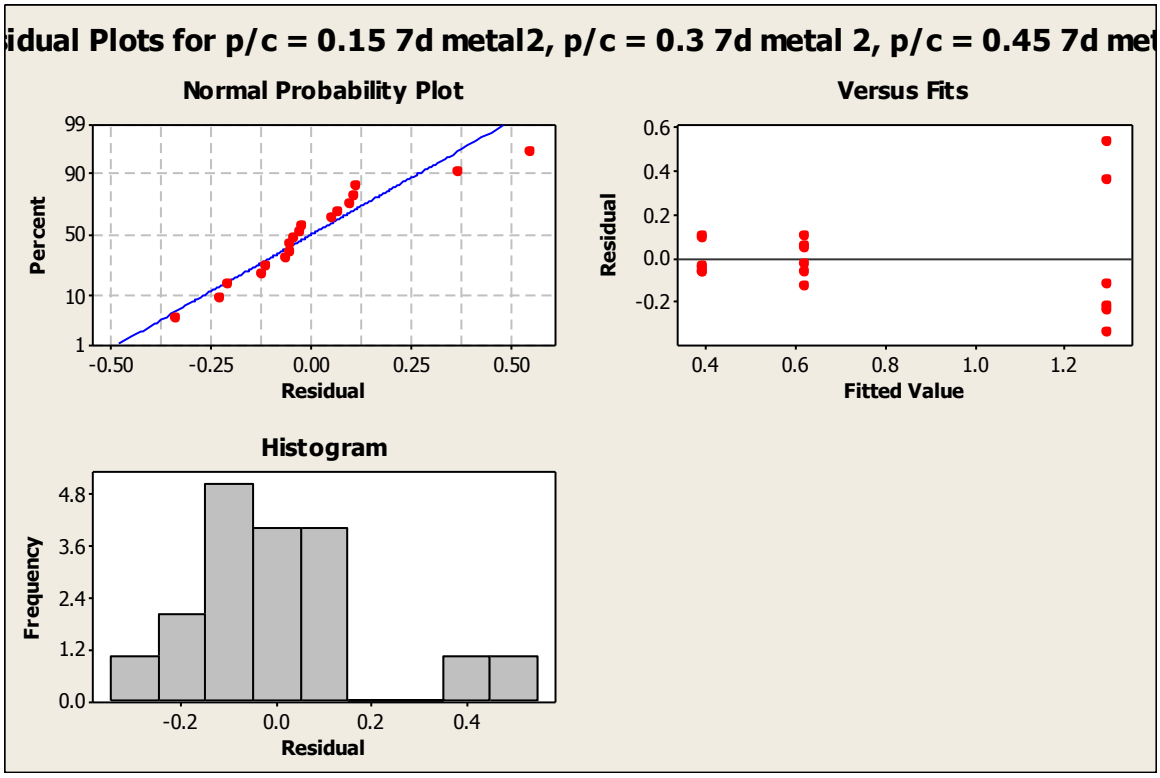

Figure A4: Minitab statistical software generated normal probability plot, plot of residuals and histogram for adhesion bond strengths of cement mortar 1 plus polymer 2 varying polymer / cement ratio cast over metal substrates

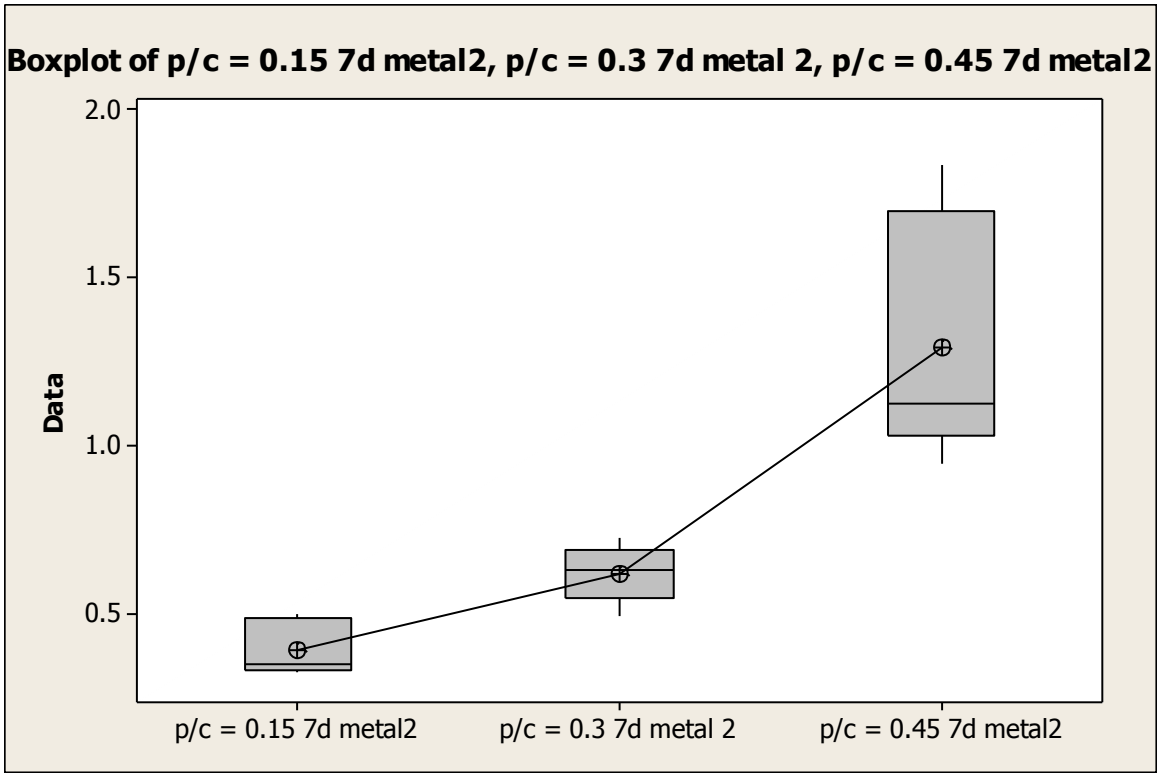

Figure A5: Minitab statistical software generated boxplot for adhesion bond strengths of cement mortar 1 plus polymer 2 varying polymer / cement ratio cast over metal substrates

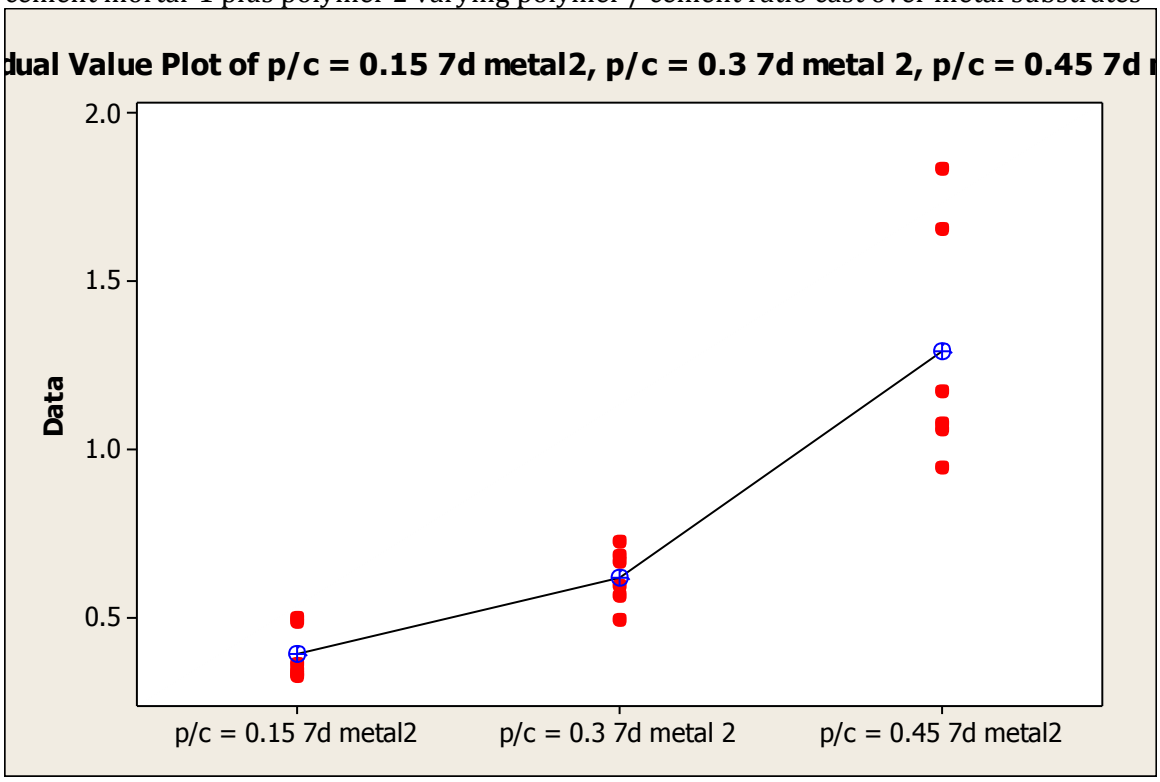

Figure A6: Minitab statistical software generated individual value plot for adhesion bond strengths of cement mortar 1 plus polymer 2 varying polymer / cement ratio cast over metal substrate

Experiment 3: Adhesion of CSA Cement Mortar to Wooden Substrates

mortars = cement mortar 1, cement mortar 1 plus polymer 1, cement mortar 1 plus polymer 2

curing regimen = 24 hours ambient laboratory conditions

A variant of ASTM C1583 was followed for data collection. Six samples were cast and tested for each mortar formulation. Samples were stored at ambient laboratory temperature and humidity from the time of casting to the time of testing. Tested mortar formulations included a control formulation cement mortar 1, a polymer modified formulation cement mortar 1 plus polymer 1 and another polymer modified formulation cement mortar 1 plus polymer 2. Polymer modified mortar formulations contained polymer mass amounts such that the polymer / cement ratios were 0.15.

Control 24hr wood	Polymer 1 24hr wood	Polymer 2 24hr wood
0.1053	0.5850	0.7368
0.0000	0.8315	1.0385
0.1281	1.1964	0.7605
0.0851	0.9052	0.9341
0.0360	0.7850	1.0148
0.0000	0.8482	0.5657

Table A3: Adhesion pull off test data for CSA cement mortars cast over wooden substrates

H_o: Latex polymer addition does not effect the average bond strength for CSA cement mortar cast over wooden substrate materials ($u_i = u_j$)

H_a: Latex polymer addition effects the average bond strength for CSA cement mortar cast over wooden substrate materials (u_i does not equal u_j)

One-way ANOVA was used to test the equality of the population means for 24 hour adhesion testing of cement mortar 1, cement mortar 1 plus polymer 1 and cement mortar 1 plus polymer 2 cast over wooden substrate. Results from ANOVA are: $F(2/15) = 48.97$, $p < 0.001$, pooled standard deviation = 0.1599 and $R^2 = 86.72\%$. Based upon the F value of 48.97 and corresponding p-value < 0.001, if an alpha value of 0.05 is chosen, it is safe to reject the null hypothesis and ultimately conclude that at least two means differ from one another, and this inequality is highly unlikely due to chance. Further "post hoc" statistical analysis utilizing Tukey's Honestly Significant Difference Test assigned both cement mortar 1 plus polymer 1 and cement mortar 1 plus polymer 2 to "A" bond strength classification, while cement mortar 1, the control sample, was assigned to "B" adhesion bond strength classification. For the Tukey comparison method, mortars that do not share the same letter strength classification are significantly different.

One-way ANOVA: Control 24hr wood, Polymer 1 24hr wood, Polymer 2 24hr wood

Source DF SS MS F P
Factor 2 2.5039 1.2520 48.97 0.000
Error 15 0.3835 0.0256
Total 17 2.8874

S = 0.1599 R-Sq = 86.72% R-Sq(adj) = 84.95%

Level N Mean StDev
Control 24hr wood 6 0.0591 0.0549
Polymer 1 24hr wood 6 0.8586 0.1987
Polymer 2 24hr wood 6 0.8417 0.1849

Individual 95% CIs For Mean Based on
Pooled StDev
Level ---+---------+---------+---------+------
Control 24hr wood (----*----)
Polymer 1 24hr wood (----*---)
Polymer 2 24hr wood (----*----)
---+---------+---------+---------+------
0.00 0.30 0.60 0.90

Pooled StDev = 0.1599

Grouping Information Using Tukey Method

N Mean Grouping
Polymer 1 24hr wood 6 0.8586 A
Polymer 2 24hr wood 6 0.8417 A
Control 24hr wood 6 0.0591 B

Means that do not share a letter are significantly different.

Tukey 95% Simultaneous Confidence Intervals
All Pairwise Comparisons

Individual confidence level = 97.97%

Control 24hr wood subtracted from:

Lower Center Upper
Polymer 1 24hr wood 0.5599 0.7995 1.0390
Polymer 2 24hr wood 0.5431 0.7826 1.0222

```
                -------+---------+---------+---------+--
Polymer 1 24hr wood                    (------*------)
Polymer 2 24hr wood                    (-----*------)
                -------+---------+---------+---------+--
                   0.00     0.35     0.70     1.05
```

Polymer 1 24hr wood subtracted from:

	Lower	Center	Upper
Polymer 2 24hr wood	-0.2564	-0.0168	0.2227

```
                -------+---------+---------+---------+--
Polymer 2 24hr wood  (------*-----)
                -------+---------+---------+---------+--
                   0.00     0.35     0.70     1.05
```

Grouping Information Using Fisher Method

	N	Mean	Grouping
Polymer 1 24hr wood	6	0.8586	A
Polymer 2 24hr wood	6	0.8417	A
Control 24hr wood	6	0.0591	B

Means that do not share a letter are significantly different.

Fisher 95% Individual Confidence Intervals
All Pairwise Comparisons

Simultaneous confidence level = 88.31%

Control 24hr wood subtracted from:

	Lower	Center	Upper
Polymer 1 24hr wood	0.6027	0.7995	0.9962
Polymer 2 24hr wood	0.5859	0.7826	0.9794

```
                ------+---------+---------+---------+---
Polymer 1 24hr wood                    (-----*----)
Polymer 2 24hr wood                    (----*-----)
                ------+---------+---------+---------+---
                   0.00     0.35     0.70     1.05
```

Polymer 1 24hr wood subtracted from:

	Lower	Center	Upper

Polymer 2 24hr wood -0.2136 -0.0168 0.1799

```
                 ------+---------+---------+---------+---
Polymer 2 24hr wood  (-----*----)
                 ------+---------+---------+---------+---
```

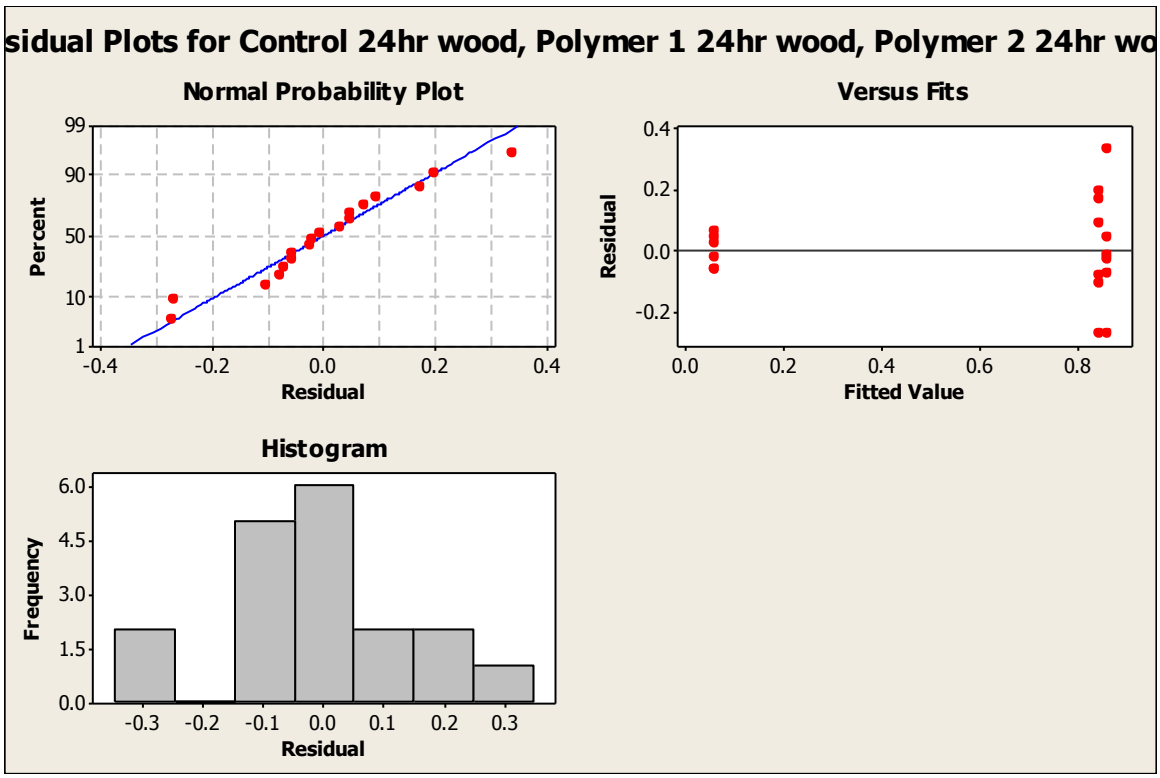

Figure A7: Minitab statistical software generated normal probability plot, plot of residuals and histogram for adhesion bond strengths of cement mortar 1, cement mortar 1 plus polymer 1 and cement mortar 1 plus polymer 2 cast over wooden substrates

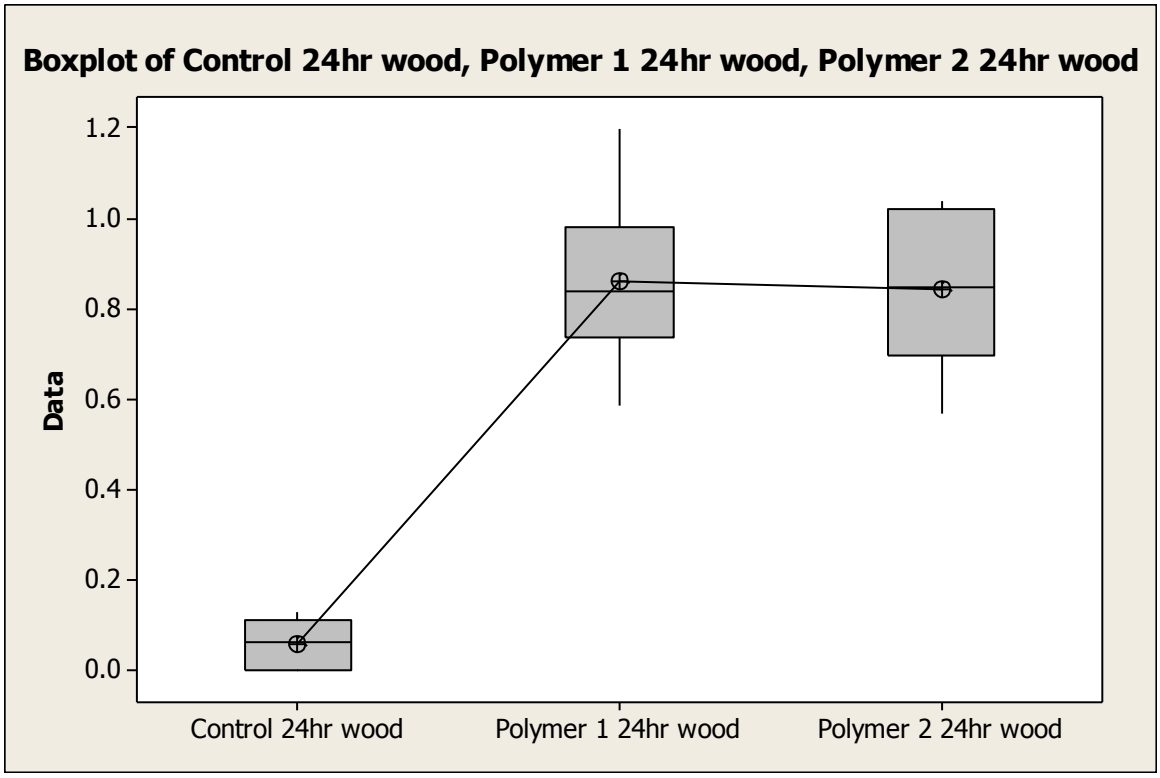

Figure A8: Minitab statistical software generated boxplot for adhesion bond strengths of cement mortar 1, cement mortar 1 plus polymer 1 and cement mortar 1 plus polymer 2 cast over wooden substrates

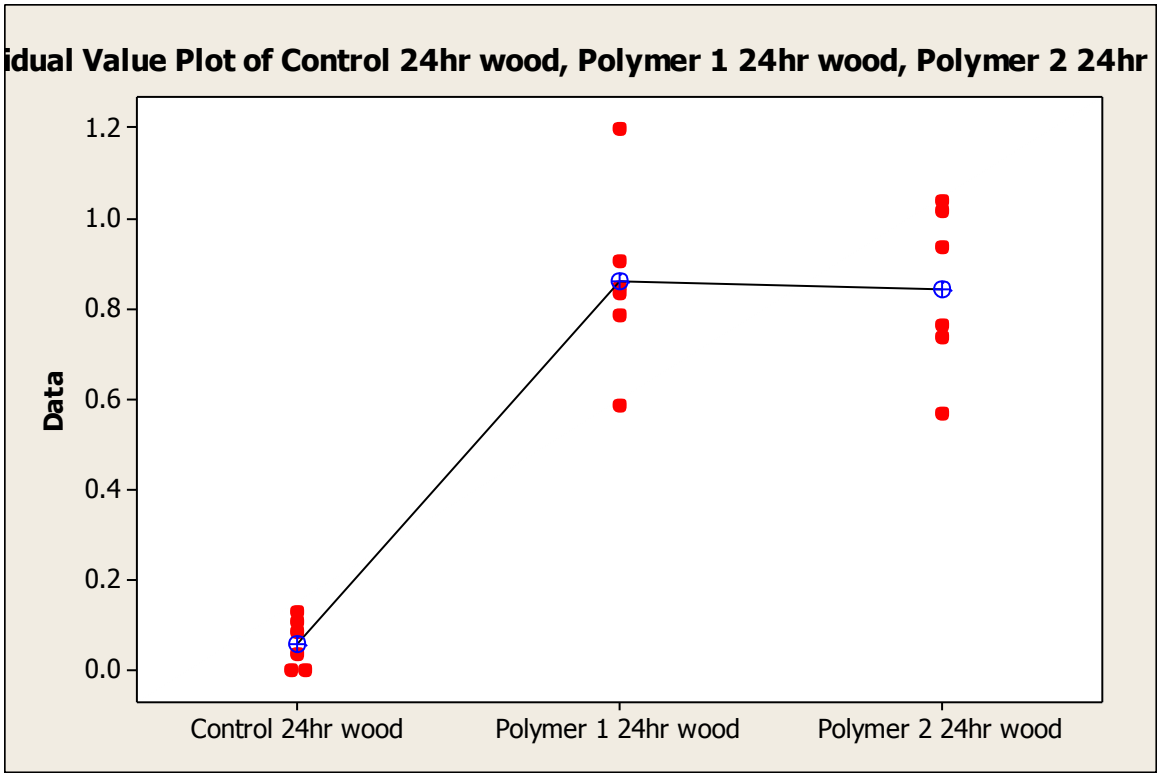

Figure A9: Minitab statistical software generated individual value plot for adhesion bond strengths of cement mortar 1, cement mortar 1 plus polymer 1 and cement mortar 1 plus polymer 2 cast over wooden substrates

Experiment 4: Adhesion of CSA Cement Mortar to Wooden Substrates

mortars = cement mortar 1, cement mortar 1 plus polymer 1, cement mortar 1 plus polymer 2

curing regimen = 13 days ambient laboratory conditions

remarks: control samples simply fell off the wooden substrates either during transport to the testing machine or during set up of the sample to be tested

Protocoal similar to that described in ASTM C1583 was followed for data collection. Six samples were cast and tested for each mortar formulation. Samples were stored at ambient laboratory temperature and humidity from the time of casting to the time of testing. Tested mortar formulations included a control formulation cement mortar 1, a polymer modified formulation cement mortar 1 plus polymer 1 and another polymer modified formulation cement mortar 1 plus polymer 2. Polymer modified mortar formulations contained polymer mass amounts such that the polymer / cement ratios were 0.15.

control 13d wood	polymer 1 13d wood	polymer 2 13d wood
0.0000	0.9148	0.8569
0.0000	0.7113	0.7780
0.0000	0.9034	0.9780
0.0000	0.6789	0.4929
0.0000	0.9657	0.7508
0.0000	0.9455	1.0280

Table A4: Adhesion pull off test data for CSA cement mortars cast over wooden substrates

H_o: Latex polymer addition does not effect the average bond strength for CSA cement mortar cast over wooden substrate materials ($u_i = u_j$)

H_a: Latex polymer addition effects the average bond strength for CSA cement mortar cast over wooden substrate materials (u_i does not equal u_j)

One-way ANOVA was used to test the equality of the population means for 13 day adhesion testing of cement mortar 1, cement mortar 1 plus polymer 1 and cement mortar 1 plus polymer 2 cast over wooden substrate. Results from ANOVA are: $F(2/15) = 80.04$, $p < 0.001$, pooled standard deviation = 0.1319 and $R^2 = 91.43\%$. Based upon the F value of 80.04 and corresponding p-value < 0.001, if an alpha value of 0.05 is chosen, it is safe to reject the null hypothesis and ultimately conclude that at least two means differ from one another, and this inequality is highly unlikely due to chance. Further "post hoc" statistical analysis utilizing Tukey's Honestly Significant Difference Test assigned both cement mortar 1 plus polymer 1 and cement mortar 1 plus polymer 2 to "A" bond strength classification, while cement mortar 1, the control sample, was assigned to "B" adhesion bond strength classification. For the Tukey comparison method, mortars that do not share the same letter strength classification are significantly different.

One-way ANOVA: control 13d wood, polymer 1 13d wood, polymer 2 13d wood

Source DF SS MS F P
Factor 2 2.7847 1.3924 80.04 0.000
Error 15 0.2609 0.0174
Total 17 3.0456

S = 0.1319 R-Sq = 91.43% R-Sq(adj) = 90.29%

Individual 95% CIs For Mean Based on Pooled StDev

Level	N	Mean	StDev	----+---------+---------+---------+-----
control 13d wood	6	0.0000	0.0000	(---*---)
polymer 1 13d wood	6	0.8533	0.1249	(--*---)
polymer 2 13d wood	6	0.8141	0.1913	(---*---)

----+---------+---------+---------+-----
0.00 0.30 0.60 0.90

Pooled StDev = 0.1319

Grouping Information Using Tukey Method

	N	Mean	Grouping
polymer 1 13d wood	6	0.8533	A
polymer 2 13d wood	6	0.8141	A
control 13d wood	6	0.0000	B

Means that do not share a letter are significantly different.

Tukey 95% Simultaneous Confidence Intervals
All Pairwise Comparisons

Individual confidence level = 97.97%

control 13d wood subtracted from:

	Lower	Center	Upper
polymer 1 13d wood	0.6557	0.8533	1.0509
polymer 2 13d wood	0.6165	0.8141	1.0117

-------+---------+---------+---------+--
polymer 1 13d wood (----*-----)
polymer 2 13d wood (----*-----)
-------+---------+---------+---------+--
0.00 0.35 0.70 1.05

polymer 1 13d wood subtracted from:

	Lower	Center	Upper
polymer 2 13d wood	-0.2368	-0.0392	0.1584

```
                -------+---------+---------+---------+--
polymer 2 13d wood  (-----*-----)
                -------+---------+---------+---------+--
                   0.00      0.35      0.70      1.05
```

Grouping Information Using Fisher Method

	N	Mean	Grouping
polymer 1 13d wood	6	0.8533	A
polymer 2 13d wood	6	0.8141	A
control 13d wood	6	0.0000	B

Means that do not share a letter are significantly different.

Fisher 95% Individual Confidence Intervals
All Pairwise Comparisons

Simultaneous confidence level = 88.31%

control 13d wood subtracted from:

	Lower	Center	Upper
polymer 1 13d wood	0.6910	0.8533	1.0156
polymer 2 13d wood	0.6518	0.8141	0.9764

```
                ------+---------+---------+---------+---
polymer 1 13d wood                    (---*----)
polymer 2 13d wood                   (---*----)
                ------+---------+---------+---------+---
                  0.00      0.35      0.70      1.05
```

polymer 1 13d wood subtracted from:

	Lower	Center	Upper
polymer 2 13d wood	-0.2015	-0.0392	0.1231

```
                ------+---------+---------+---------+---
polymer 2 13d wood  (----*----)
                ------+---------+---------+---------+---
                  0.00      0.35      0.70      1.05
```

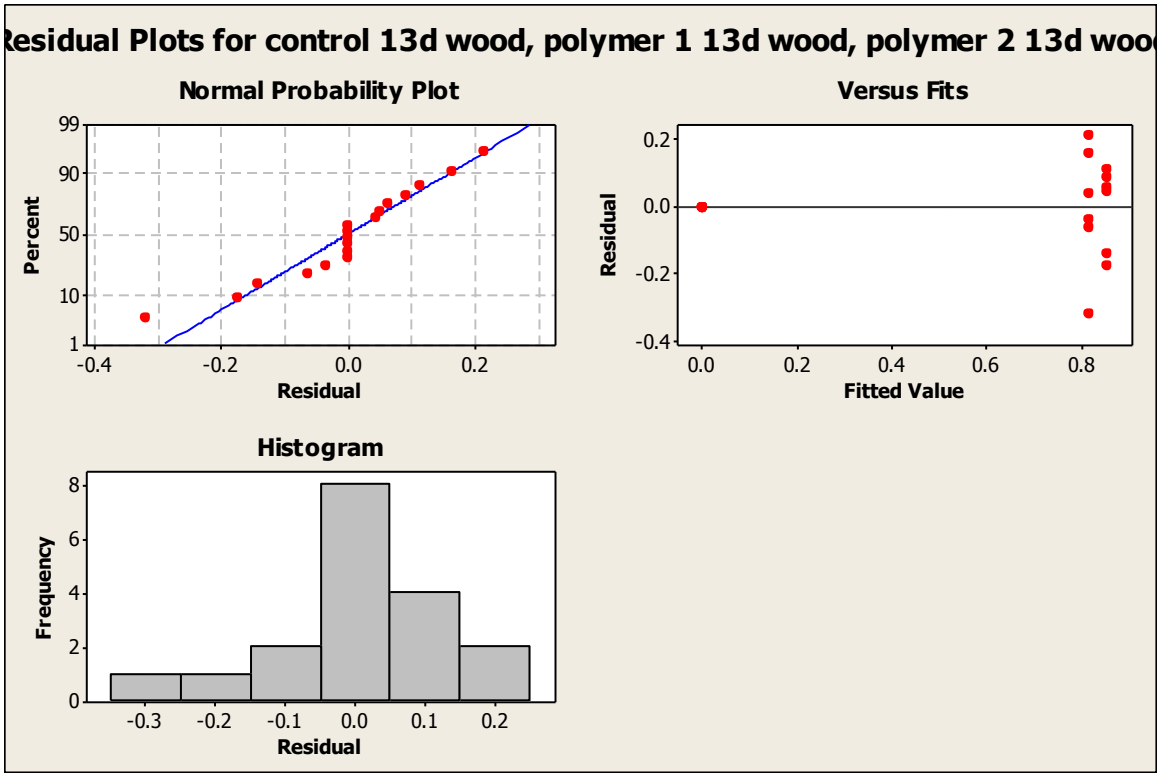

Figure A10: Minitab statistical software generated normal probability plot, plot of residuals and histogram for adhesion bond strengths of cement mortar 1, cement mortar 1 plus polymer 1 and cement mortar 1 plus polymer 2 cast over wooden substrates

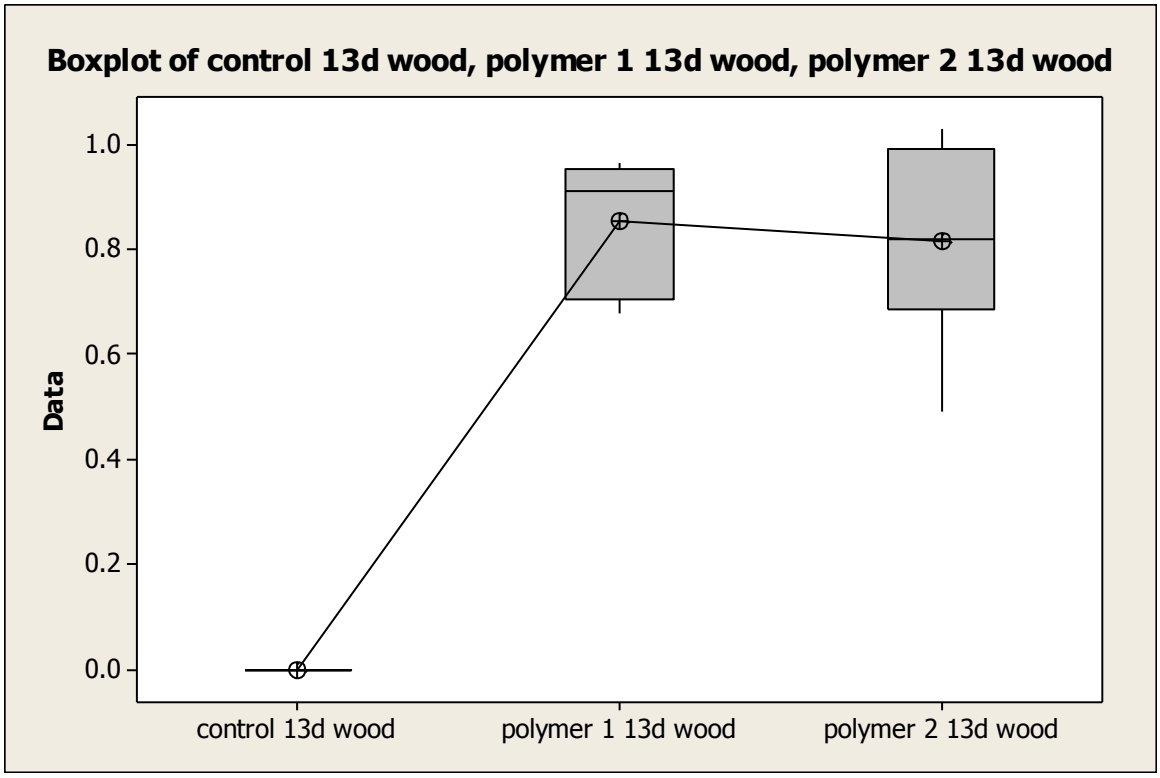

Figure A11: Minitab statistical software generated boxplot for adhesion bond strengths of cement mortar 1, cement mortar 1 plus polymer 1 and cement mortar 1 plus polymer 2 cast over wooden substrates

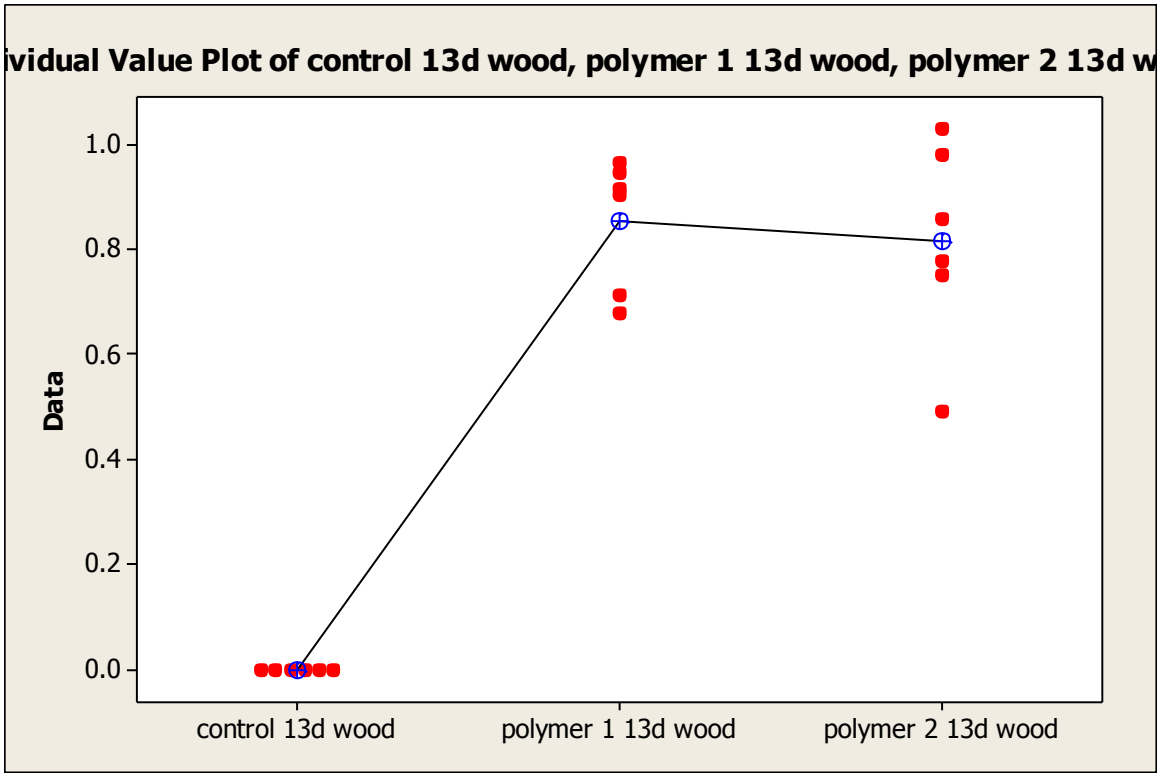

Figure A12: Minitab statistical software generated individual value plot for adhesion bond strengths of cement mortar 1, cement mortar 1 plus polymer 1 and cement mortar 1 plus polymer 2 cast over wooden substrates

Experiment 5: Adhesion of CSA Cement Mortar to Wooden Substrates

mortars = cement mortar 2 plus polymer 2, cement mortar 2 plus polymer 3, cement mortar 2 plus polymer 4, cement mortar 2 plus polymer 5

curing regimen = 13 days ambient laboratory conditions

Protocoal similar to that described in ASTM C1583 was followed for data collection. Six samples were cast and tested for each mortar formulation. Samples were stored at ambient laboratory temperature and humidity from the time of casting to the time of testing. Tested mortar formulations included cement mortar 2 plus polymer 2, cement mortar 2 plus polymer 3, cement mortar 2 plus polymer 4 and cement mortar 2 plus polymer 5. Polymer modified mortar formulations contained polymer mass amounts such that the polymer / cement ratios were 0.15.

Polymer 2 13d wood	Polymer 3 13d wood	Polymer 4 13d wood	Polymer 5 13d wood
1.2403	1.1262	0.3158	1.4850
2.1042	1.0543	0.5114	1.5508
1.0534	1.1350	0.6894	1.9990
0.8420	1.3420	0.2684	2.4963
1.3499	1.3034	0.3228	1.4718
0.4456	0.8973	0.3649	1.1648

Table A5: Adhesion pull off test data for polymer modified CSA cement mortars varying polymer type with polymer / cement ratio of 0.15 cast over wooden substrates

H_o: Latex polymer type does not effect the average bond strength for CSA cement mortar cast over wooden substrate materials ($u_i = u_j$)

H_a: Latex polymer type effects the average bond strength for CSA cement mortar cast over wooden substrate materials (u_i does not equal u_j)

One-way ANOVA was used to test the equality of the population means for 13 day adhesion testing of polymer modified mortars containing polymer 2, polymer 3, polymer 4 and polymer 5 cast over wooden substrate. Results from ANOVA are: $F(3/20) = 11.32$, $p < 0.001$, pooled standard deviation = 0.3839 and $R^2 = 62.93\%$. Based upon the F value of 11.32 and corresponding p-value < 0.001, if an alpha value of 0.05 is chosen, it is safe to reject the null hypothesis and ultimately conclude that at least two means differ from one another, and this inequality is highly unlikely due to chance. Further "post hoc" statistical analysis utilizing Tukey's Honestly Significant Difference Test assigned the mortars containing polymers 2, 3 and 5 to "A" adhesion strength classification while the mortar containing polymer 4 was assigned to "B" adhesion strength classification. For the Tukey comparison method, mortars that do not share the same letter strength classification are significantly different.

One-way ANOVA: Polymer 2 13, Polymer 3 13, Polymer 4 13, Polymer 5 13

Source DF SS MS F P
Factor 3 5.002 1.667 11.32 0.000
Error 20 2.947 0.147
Total 23 7.950

S = 0.3839 R-Sq = 62.93% R-Sq(adj) = 57.37%

Individual 95% CIs For Mean Based on Pooled StDev

Level	N	Mean	StDev	--------+---------+---------+---------+-
Polymer 2 13d wood	6	1.1726	0.5578	(-----*------)
Polymer 3 13d wood	6	1.1430	0.1637	(------*-----)
Polymer 4 13d wood	6	0.4121	0.1593	(-----*------)
Polymer 5 13d wood	6	1.6946	0.4755	(------*-----)

--------+---------+---------+---------+-
0.50 1.00 1.50 2.00

Pooled StDev = 0.3839

Grouping Information Using Tukey Method

	N	Mean	Grouping
Polymer 5 13d wood	6	1.6946	A
Polymer 2 13d wood	6	1.1726	A
Polymer 3 13d wood	6	1.1430	A
Polymer 4 13d wood	6	0.4121	B

Means that do not share a letter are significantly different.

Tukey 95% Simultaneous Confidence Intervals
All Pairwise Comparisons

Individual confidence level = 98.89%

Polymer 2 13d wood subtracted from:

	Lower	Center	Upper
Polymer 3 13d wood	-0.6501	-0.0295	0.5910
Polymer 4 13d wood	-1.3810	-0.7604	-0.1399
Polymer 5 13d wood	-0.0985	0.5221	1.1426

---------+---------+---------+---------+
Polymer 3 13d wood (------*-----)
Polymer 4 13d wood (-----*------)

```
Polymer 5 13d wood               (-----*-----)
                ---------+---------+---------+---------+
                   -1.0      0.0      1.0      2.0
```

Polymer 3 13d wood subtracted from:

```
                 Lower   Center    Upper
Polymer 4 13d wood  -1.3515  -0.7309  -0.1103
Polymer 5 13d wood  -0.0690   0.5516   1.1722

                ---------+---------+---------+---------+
Polymer 4 13d wood      (------*-----)
Polymer 5 13d wood               (------*-----)
                ---------+---------+---------+---------+
                   -1.0      0.0      1.0      2.0
```

Polymer 4 13d wood subtracted from:

```
                 Lower  Center   Upper
Polymer 5 13d wood  0.6619  1.2825  1.9031

                ---------+---------+---------+---------+
Polymer 5 13d wood                    (-----*-----)
                ---------+---------+---------+---------+
                   -1.0      0.0      1.0      2.0
```

Grouping Information Using Fisher Method

```
                N    Mean  Grouping
Polymer 5 13d wood  6  1.6946  A
Polymer 2 13d wood  6  1.1726    B
Polymer 3 13d wood  6  1.1430    B
Polymer 4 13d wood  6  0.4121      C
```

Means that do not share a letter are significantly different.

Fisher 95% Individual Confidence Intervals
All Pairwise Comparisons

Simultaneous confidence level = 80.83%

Polymer 2 13d wood subtracted from:

```
                 Lower   Center    Upper
Polymer 3 13d wood  -0.4918  -0.0295   0.4328
```

```
Polymer 4 13d wood  -1.2228  -0.7604  -0.2981
Polymer 5 13d wood   0.0597   0.5221   0.9844

                 -------+---------+---------+---------+--
Polymer 3 13d wood              (----*---)
Polymer 4 13d wood        (---*----)
Polymer 5 13d wood                  (---*----)
                 -------+---------+---------+---------+--
                   -1.0      0.0      1.0      2.0
```

Polymer 3 13d wood subtracted from:

```
                  Lower   Center    Upper
Polymer 4 13d wood  -1.1932  -0.7309  -0.2686
Polymer 5 13d wood   0.0893   0.5516   1.0139

                 -------+---------+---------+---------+--
Polymer 4 13d wood      (----*---)
Polymer 5 13d wood                  (----*---)
                 -------+---------+---------+---------+--
                   -1.0      0.0      1.0      2.0
```

Polymer 4 13d wood subtracted from:

```
                  Lower  Center   Upper
Polymer 5 13d wood  0.8202  1.2825  1.7448

                 -------+---------+---------+---------+--
Polymer 5 13d wood                      (----*---)
                 -------+---------+---------+---------+--
                   -1.0      0.0      1.0      2.0
```

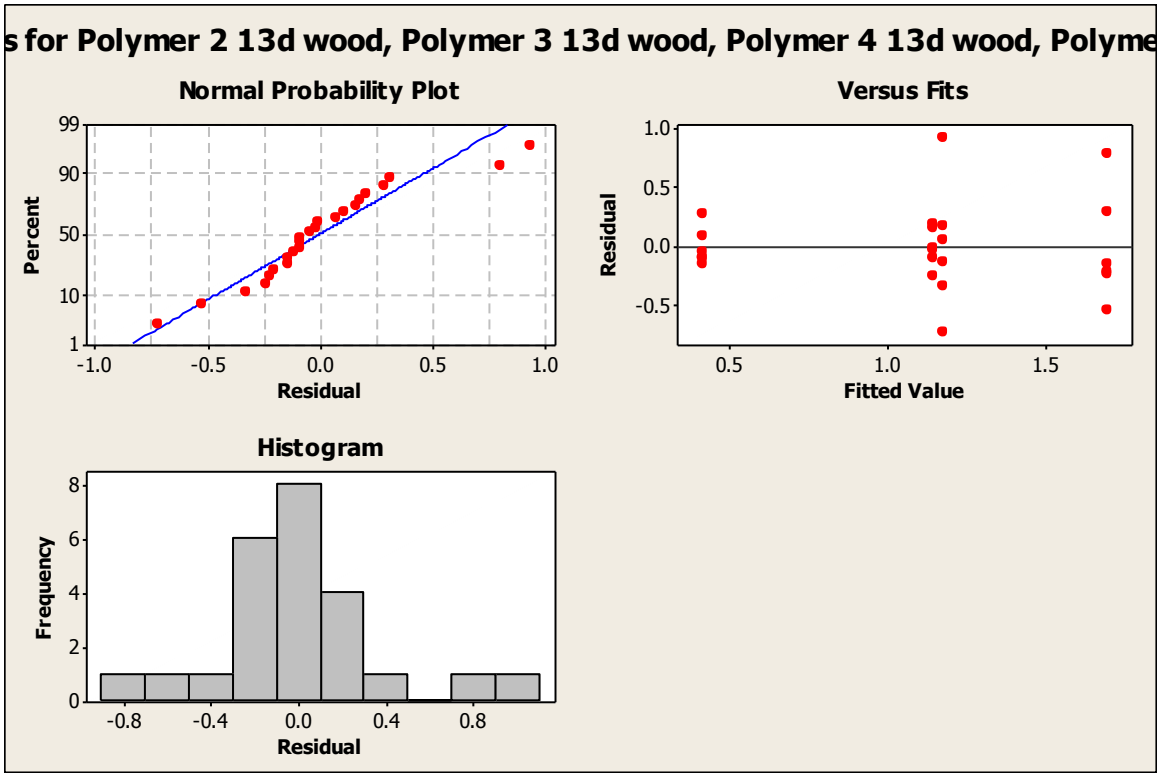

Figure A13: Minitab statistical software generated normal probability plot, plot of residuals and histogram for adhesion bond strengths of cement mortar 2 plus polymer 2, cement mortar 2 plus polymer 3, cement mortar 2 plus polymer 4 and cement mortar 2 plus polymer 5 cast over wooden substrates

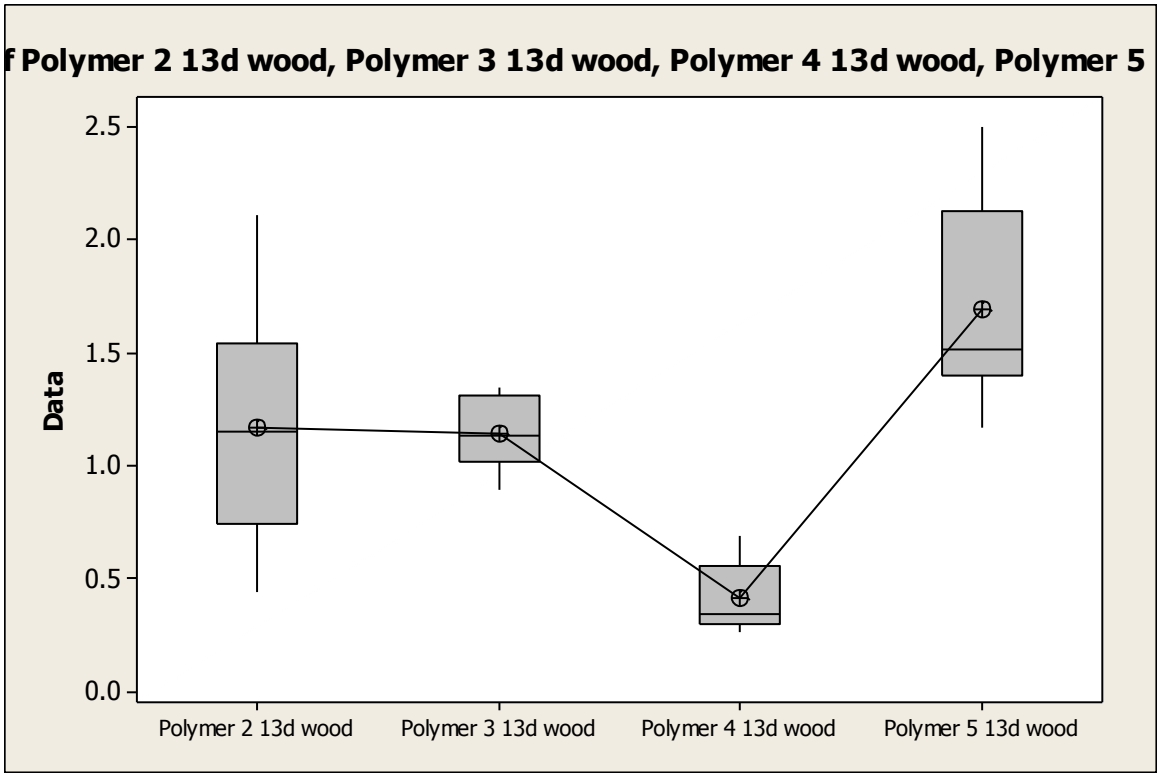

Figure A14: Minitab statistical software generated boxplot for adhesion bond strengths of cement mortar 2 plus polymer 2, cement mortar 2 plus polymer 3, cement mortar 2 plus polymer 4 and cement mortar 2 plus polymer 5 cast over wooden substrates

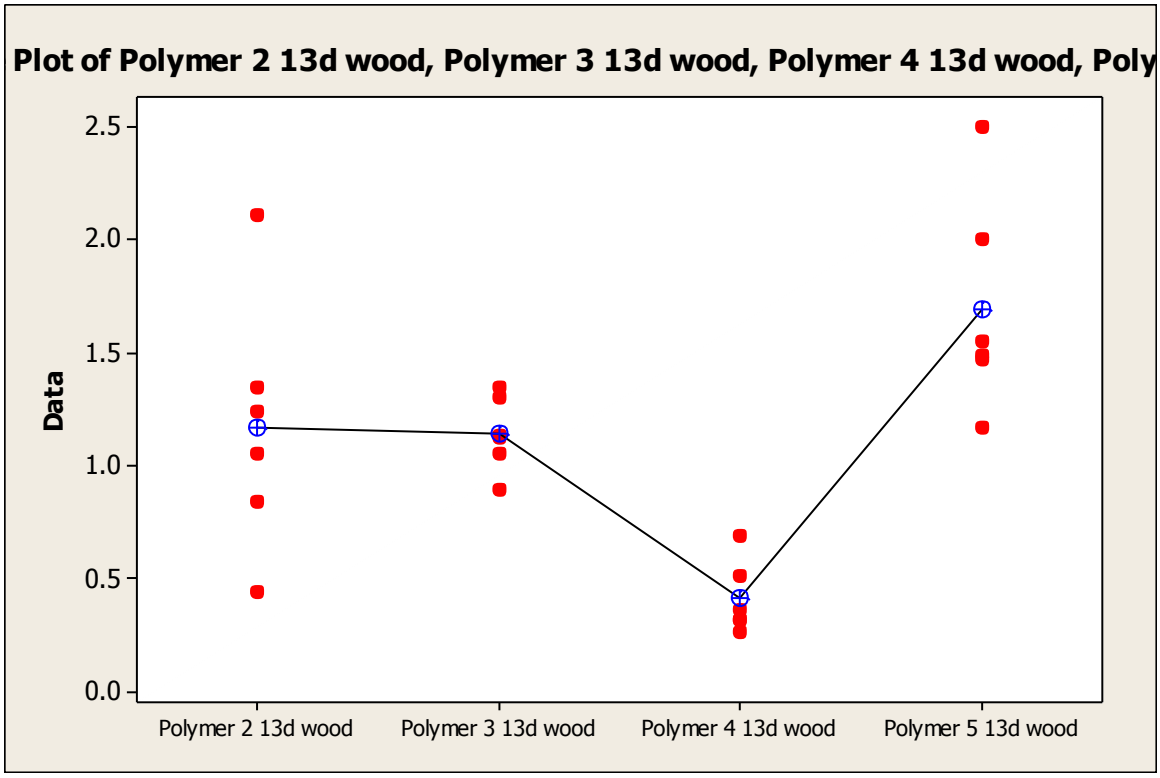

Figure A15: Minitab statistical software generated individual value plot for adhesion bond strengths of cement mortar 2 plus polymer 2, cement mortar 2 plus polymer 3, cement mortar 2 plus polymer 4 and cement mortar 2 plus polymer 5 cast over wooden substrates

Experiment 6: Adhesion of Polymer Modified CSA Cement Mortar to Glass Substrates

mortars = cement mortar 2 plus polymer 2, cement mortar 2 plus polymer 3, cement mortar 2 plus polymer 4, cement mortar 2 plus polymer 5

curing regimen = 24 hours ambient laboratory conditions

Protocoal similar to that described in ASTM C1583 was followed for data collection. Six samples were cast and tested for each mortar formulation. Samples were stored at ambient laboratory temperature and humidity from the time of casting to the time of testing. Tested mortar formulations included cement mortar 2 plus polymer 2, cement mortar 2 plus polymer 3, cement mortar 2 plus polymer 4 and cement mortar 2 plus polymer 5. Polymer modified mortar formulations contained polymer mass amounts such that the polymer / cement ratios were 0.15.

Polymer 2 24hr glass	Polymer 3 24hr glass	Polymer 4 24hr glass	Polymer 5 24hr glass
0.6710	0.5245	0.1140	0.5140
0.6320	0.5105	0.1254	0.4815
0.5833	0.2333	0.1403	0.5254
0.4552	0.3842	0.0202	0.4684
0.5614	0.3649	0.1360	0.4842
0.7192	0.4631	0.1684	0.4745

Table A6: Adhesion pull off test data for polymer modified CSA cement mortars varying polymer type with polymer / cement ratio of 0.15 cast over glass substrates

H_o: Latex polymer type does not effect the average bond strength for CSA cement mortar cast over glass substrate materials ($u_i = u_j$)

H_a: Latex polymer type effects the average bond strength for CSA cement mortar cast over glass substrate materials (u_i does not equal u_j)

One-way ANOVA was used to test the equality of the population means for 24 hour adhesion testing of polymer modified mortars containing polymer 2, polymer 3, polymer 4 and polymer 5 cast over glass substrate. Results from ANOVA are: $F(3/20) = 42.85$, $p < 0.001$, pooled standard deviation = 0.079 and $R^2 = 86.54\%$. Based upon the F value of 42.85 and corresponding p-value < 0.001, if an alpha value of 0.05 is chosen, it is safe to reject the null hypothesis and ultimately conclude that at least two means differ from one another, and this inequality is highly unlikely due to chance. Further "post hoc" statistical analysis utilizing Tukey's Honestly Significant Difference Test assigned the mortars containing polymers 2 and 5 to "A" adhesion strength classification. The mortars containing polymers 5 and 3 were assigned to "B" adhesion strength classification, while the mortar containing polymer 4 was assigned to "C" adhesion strength classification. This test allows for overlapping of strength classifications. For the Tukey comparison method, mortars that do not share the same letter strength classification are significantly different.

One-way ANOVA: Polymer 2 24, Polymer 3 24, Polymer 4 24, Polymer 5 24

Source DF SS MS F P
Factor 3 0.80240 0.26747 42.85 0.000
Error 20 0.12483 0.00624
Total 23 0.92724

S = 0.07900 R-Sq = 86.54% R-Sq(adj) = 84.52%

Level N Mean StDev
Polymer 2 24hr glass 6 0.61368 0.09932
Polymer 3 24hr glass 6 0.41342 0.10944
Polymer 4 24hr glass 6 0.11738 0.05098
Polymer 5 24hr glass 6 0.49133 0.02294

Individual 95% CIs For Mean Based on Pooled StDev

```
Level                 -------+---------+---------+---------+--
Polymer 2 24hr glass                          (---*----)
Polymer 3 24hr glass                  (---*---)
Polymer 4 24hr glass  (---*----)
Polymer 5 24hr glass                      (---*---)
                      -------+---------+---------+---------+--
                         0.16      0.32      0.48      0.64
```

Pooled StDev = 0.07900

Grouping Information Using Tukey Method

	N	Mean	Grouping
Polymer 2 24hr glass	6	0.61368	A
Polymer 5 24hr glass	6	0.49133	A B
Polymer 3 24hr glass	6	0.41342	B
Polymer 4 24hr glass	6	0.11738	C

Means that do not share a letter are significantly different.

Tukey 95% Simultaneous Confidence Intervals
All Pairwise Comparisons

Individual confidence level = 98.89%

Polymer 2 24hr glass subtracted from:

Lower Center Upper

Polymer 3 24hr glass -0.32799 -0.20027 -0.07254
Polymer 4 24hr glass -0.62402 -0.49630 -0.36858
Polymer 5 24hr glass -0.25007 -0.12235   0.00537

```
                  -+---------+---------+---------+--------
Polymer 3 24hr glass           (---*----)
Polymer 4 24hr glass    (---*----)
Polymer 5 24hr glass             (---*---)
                  -+---------+---------+---------+--------
                -0.60     -0.30      0.00      0.30
```

Polymer 3 24hr glass subtracted from:

	Lower	Center	Upper
Polymer 4 24hr glass	-0.42376	-0.29603	-0.16831
Polymer 5 24hr glass	-0.04981	0.07792	0.20564

```
                  -+---------+---------+---------+--------
Polymer 4 24hr glass         (---*---)
Polymer 5 24hr glass                   (----*---)
                  -+---------+---------+---------+--------
                -0.60     -0.30      0.00      0.30
```

Polymer 4 24hr glass subtracted from:

	Lower	Center	Upper
Polymer 5 24hr glass	0.24623	0.37395	0.50167

```
                  -+---------+---------+---------+--------
Polymer 5 24hr glass                         (---*----)
                  -+---------+---------+---------+--------
                -0.60     -0.30      0.00      0.30
```

Grouping Information Using Fisher Method

	N	Mean	Grouping
Polymer 2 24hr glass	6	0.61368	A
Polymer 5 24hr glass	6	0.49133	B
Polymer 3 24hr glass	6	0.41342	B
Polymer 4 24hr glass	6	0.11738	C

Means that do not share a letter are significantly different.

Fisher 95% Individual Confidence Intervals
All Pairwise Comparisons

Simultaneous confidence level = 80.83%

Polymer 2 24hr glass subtracted from:

	Lower	Center	Upper
Polymer 3 24hr glass	-0.29541	-0.20027	-0.10512
Polymer 4 24hr glass	-0.59145	-0.49630	-0.40115
Polymer 5 24hr glass	-0.21750	-0.12235	-0.02720

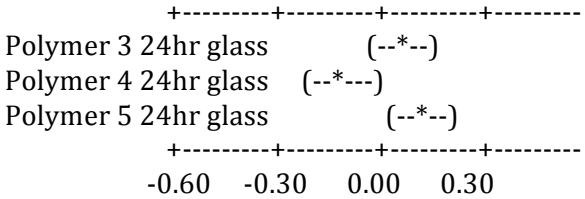

Polymer 3 24hr glass subtracted from:

	Lower	Center	Upper
Polymer 4 24hr glass	-0.39118	-0.29603	-0.20089
Polymer 5 24hr glass	-0.01723	0.07792	0.17306

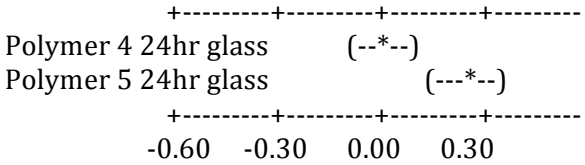

Polymer 4 24hr glass subtracted from:

	Lower	Center	Upper
Polymer 5 24hr glass	0.27880	0.37395	0.46910

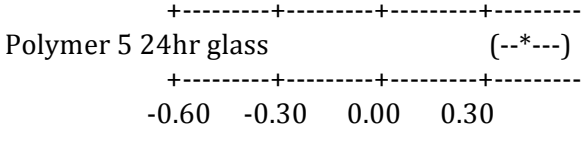

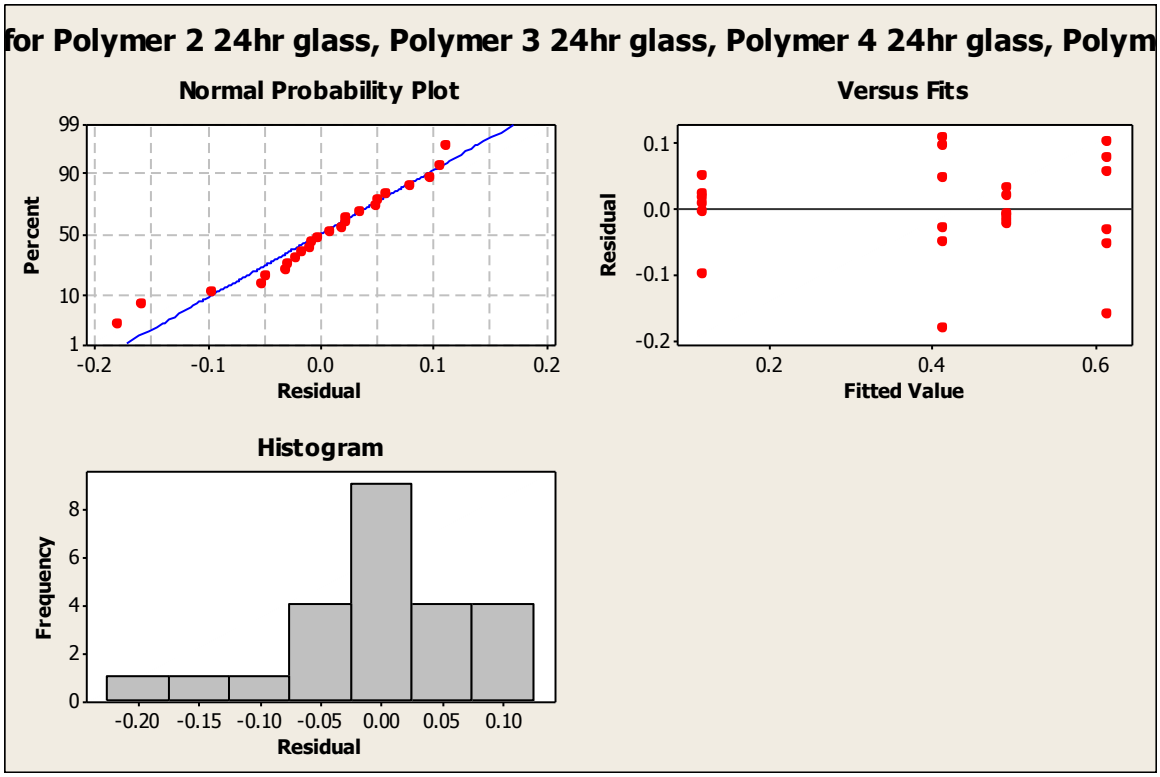

Figure A16: Minitab statistical software generated normal probability plot, plot of residuals and histogram for adhesion bond strengths of cement mortar 2 plus polymer 2, cement mortar 2 plus polymer 3, cement mortar 2 plus polymer 4 and cement mortar 2 plus polymer 5 cast over glass substrates

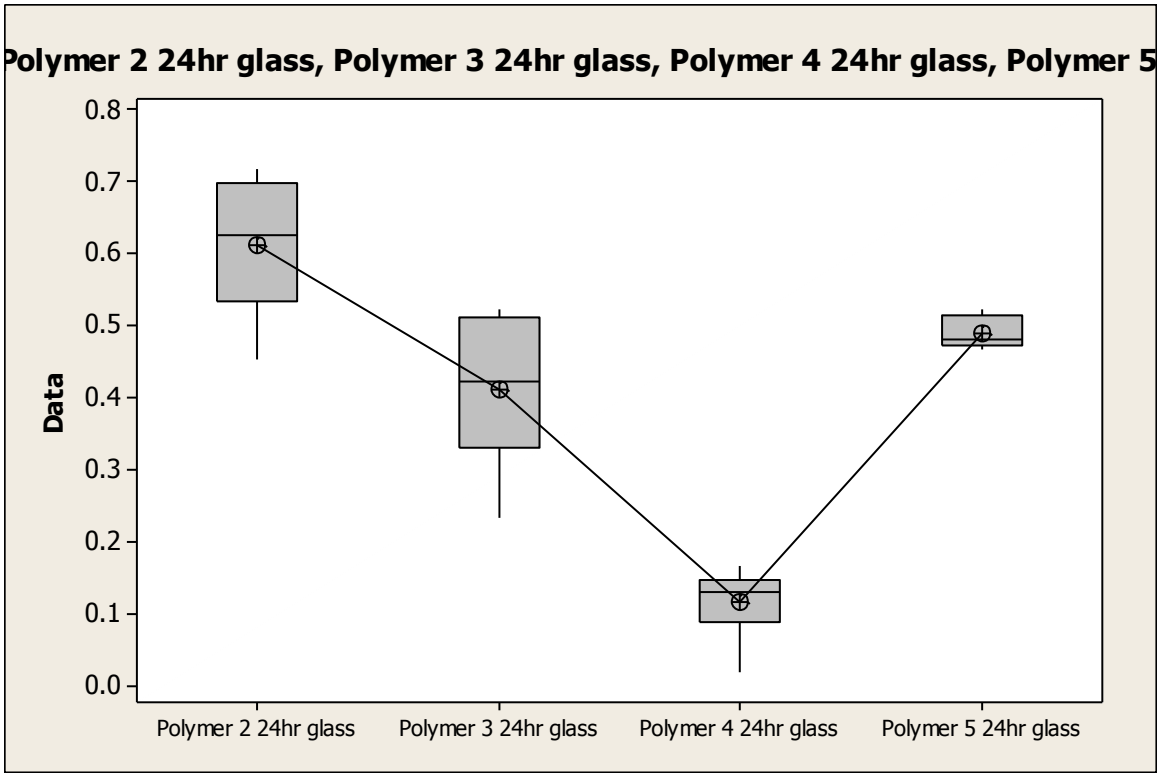

Figure A17: Minitab statistical software generated boxplot for adhesion bond strengths of cement mortar 2 plus polymer 2, cement mortar 2 plus polymer 3, cement mortar 2 plus polymer 4 and cement mortar 2 plus polymer 5 cast over glass substrates

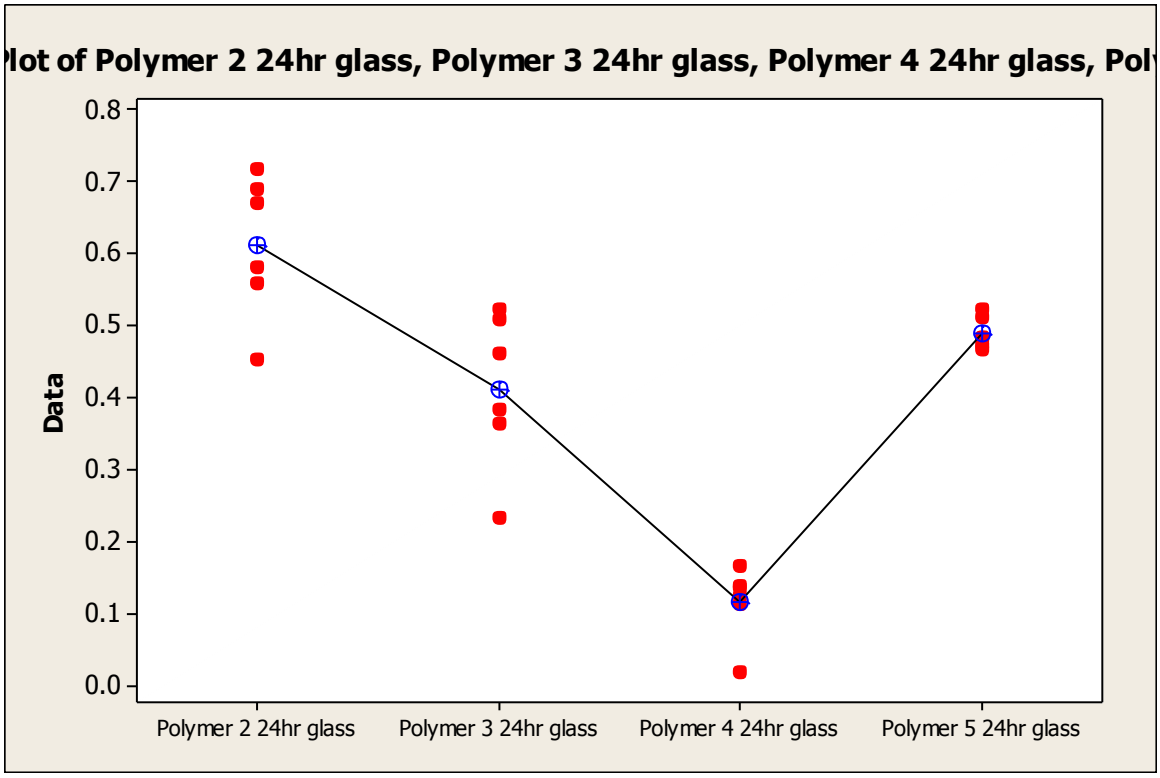

Figure A18: Minitab statistical software generated individual value plot for adhesion bond strengths of cement mortar 2 plus polymer 2, cement mortar 2 plus polymer 3, cement mortar 2 plus polymer 4 and cement mortar 2 plus polymer 5 cast over glass substrates

Experiment 7: Adhesion of Polymer Modified CSA Cement Mortar to Metal Substrates

mortars = cement mortar 2 plus polymer 2, cement mortar 2 plus polymer 3, cement mortar 2 plus polymer 4, cement mortar 2 plus polymer 5

curing regimen = 24 hours ambient laboratory conditions

Protocoal similar to that described in ASTM C1583 was followed for data collection. Six samples were cast and tested for each mortar formulation. Samples were stored at ambient laboratory temperature and humidity from the time of casting to the time of testing. Tested mortar formulations included cement mortar 2 plus polymer 2, cement mortar 2 plus polymer 3, cement mortar 2 plus polymer 4 and cement mortar 2 plus polymer 5. Polymer modified mortar formulations contained polymer mass amounts such that the polymer / cement ratios were 0.15.

Polymer 2 24hr metal	Polymer 3 24hr metal	Polymer 4 24hr metal	Polymer 5 24hr metal
0.1886	0.2579	0.0939	0.1807
0.3877	0.2114	0.0526	0.2166
0.4386	0.2535	0.0447	0.3631
0.2517	0.2228	0.0482	0.1219
0.2500	0.1982	0.1017	0.3403
0.2482	0.3009	0.0351	0.3842

Table A7: Adhesion pull off test data for polymer modified CSA cement mortars varying polymer type with polymer / cement ratio of 0.15 cast over metal substrates

H_o: Latex polymer type does not effect the average bond strength for CSA cement mortar cast over wooden substrate materials ($u_i = u_j$)

H_a: Latex polymer type effects the average bond strength for CSA cement mortar cast over wooden substrate materials (u_i does not equal u_j)

One-way ANOVA was used to test the equality of the population means for 24 hour adhesion testing of polymer modified mortars containing polymer 2, polymer 3, polymer 4 and polymer 5 cast over metal substrate. Results from ANOVA are: $F(3/20) = 11.25$, $p < 0.001$, pooled standard deviation = 0.07647 and $R^2 = 62.8\%$. Based upon the F value of 11.25 and corresponding p-value < 0.001, if an alpha value of 0.05 is chosen, it is safe to reject the null hypothesis and ultimately conclude that at least two means differ from one another, and this inequality is highly unlikely due to chance. Further "post hoc" statistical analysis utilizing Tukey's Honestly Significant Difference Test assigned the mortars containing polymers 2, 3 and 5 to "A" adhesion strength classification while the mortar containing polymer 4 was assigned to "B" adhesion strength classification. For the Tukey comparison method, mortars that do not share the same letter strength classification are significantly different.

One-way ANOVA: Polymer 2 24, Polymer 3 24, Polymer 4 24, Polymer 5 24

Source	DF	SS	MS	F	P
Factor	3	0.19742	0.06581	11.25	0.000

Error 20 0.11696 0.00585
Total 23 0.31438

S = 0.07647 R-Sq = 62.80% R-Sq(adj) = 57.21%

Level N Mean StDev
Polymer 2 24hr metal 6 0.29413 0.09656
Polymer 3 24hr metal 6 0.24078 0.03760
Polymer 4 24hr metal 6 0.06270 0.02790
Polymer 5 24hr metal 6 0.26780 0.10898

Individual 95% CIs For Mean Based on Pooled StDev

```
Level              +---------+---------+---------+---------
Polymer 2 24hr metal                     (-----*------)
Polymer 3 24hr metal                  (-----*------)
Polymer 4 24hr metal    (-----*------)
Polymer 5 24hr metal                   (------*-----)
                  +---------+---------+---------+---------
                 0.00      0.10      0.20      0.30
```

Pooled StDev = 0.07647

Grouping Information Using Tukey Method

	N	Mean	Grouping
Polymer 2 24hr metal	6	0.29413	A
Polymer 5 24hr metal	6	0.26780	A
Polymer 3 24hr metal	6	0.24078	A
Polymer 4 24hr metal	6	0.06270	B

Means that do not share a letter are significantly different.

Tukey 95% Simultaneous Confidence Intervals
All Pairwise Comparisons

Individual confidence level = 98.89%

Polymer 2 24hr metal subtracted from:

	Lower	Center	Upper
Polymer 3 24hr metal	-0.17698	-0.05335	0.07028
Polymer 4 24hr metal	-0.35507	-0.23143	-0.10780
Polymer 5 24hr metal	-0.14997	-0.02633	0.09730

```
                --------+---------+---------+---------+-
Polymer 3 24hr metal          (-----*------)
```

```
Polymer 4 24hr metal  (-----*------)
Polymer 5 24hr metal          (-----*-----)
                --------+---------+---------+---------+-
                  -0.20     0.00     0.20     0.40
```

Polymer 3 24hr metal subtracted from:

```
                  Lower    Center     Upper
Polymer 4 24hr metal  -0.30172  -0.17808  -0.05445
Polymer 5 24hr metal  -0.09662   0.02702   0.15065

                --------+---------+---------+---------+-
Polymer 4 24hr metal    (-----*-----)
Polymer 5 24hr metal          (-----*------)
                --------+---------+---------+---------+-
                  -0.20     0.00     0.20     0.40
```

Polymer 4 24hr metal subtracted from:

```
                  Lower   Center    Upper
Polymer 5 24hr metal  0.08147  0.20510  0.32873

                --------+---------+---------+---------+-
Polymer 5 24hr metal                  (-----*-----)
                --------+---------+---------+---------+-
                  -0.20     0.00     0.20     0.40
```

Grouping Information Using Fisher Method

```
                N     Mean  Grouping
Polymer 2 24hr metal  6  0.29413  A
Polymer 5 24hr metal  6  0.26780  A
Polymer 3 24hr metal  6  0.24078  A
Polymer 4 24hr metal  6  0.06270    B
```

Means that do not share a letter are significantly different.

Fisher 95% Individual Confidence Intervals
All Pairwise Comparisons

Simultaneous confidence level = 80.83%

Polymer 2 24hr metal subtracted from:

```
                  Lower    Center     Upper
```

```
Polymer 3 24hr metal  -0.14545  -0.05335   0.03875
Polymer 4 24hr metal  -0.32353  -0.23143  -0.13933
Polymer 5 24hr metal  -0.11843  -0.02633   0.06577

                   +---------+---------+---------+---------
Polymer 3 24hr metal             (-----*----)
Polymer 4 24hr metal     (-----*----)
Polymer 5 24hr metal               (----*-----)
                   +---------+---------+---------+---------
                 -0.32     -0.16      0.00      0.16
```

Polymer 3 24hr metal subtracted from:

```
                   Lower    Center     Upper
Polymer 4 24hr metal  -0.27018  -0.17808  -0.08598
Polymer 5 24hr metal  -0.06508   0.02702   0.11912

                   +---------+---------+---------+---------
Polymer 4 24hr metal       (-----*-----)
Polymer 5 24hr metal                 (-----*----)
                   +---------+---------+---------+---------
                 -0.32     -0.16      0.00      0.16
```

Polymer 4 24hr metal subtracted from:

```
                  Lower   Center    Upper
Polymer 5 24hr metal  0.11300  0.20510  0.29720

                   +---------+---------+---------+---------
Polymer 5 24hr metal                         (-----*-----)
                   +---------+---------+---------+---------
                 -0.32     -0.16      0.00      0.16
```

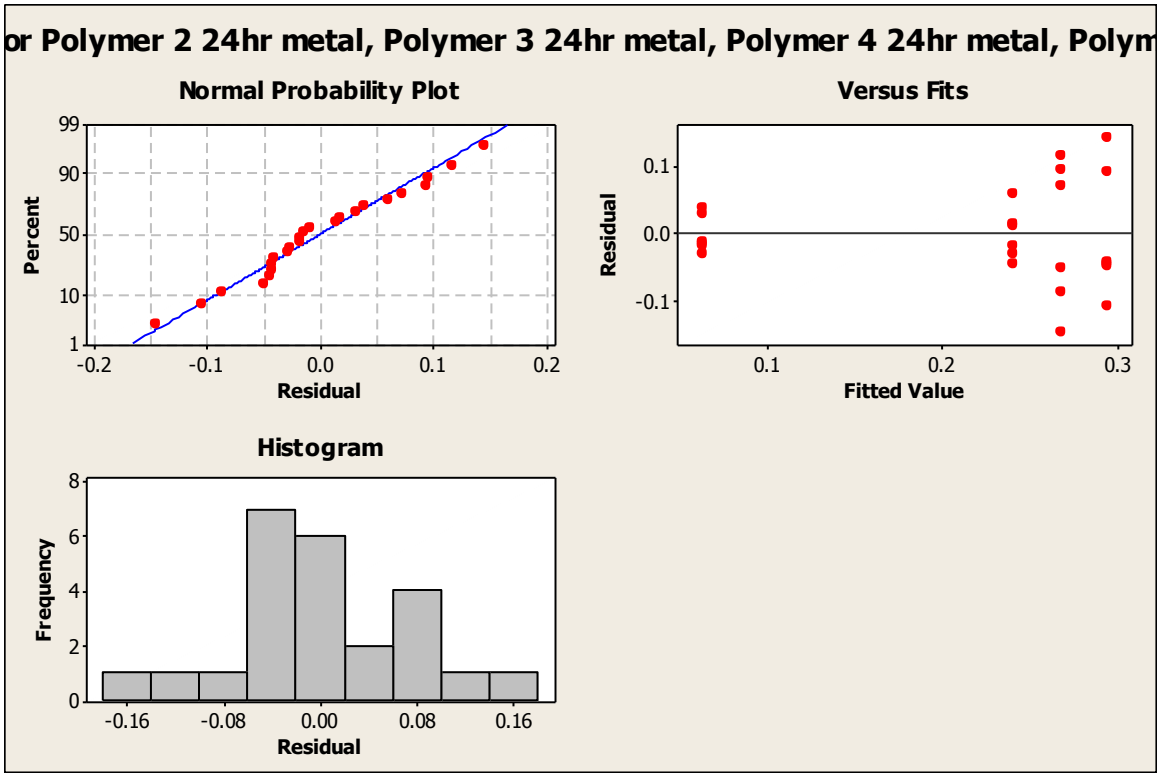

Figure A19: Minitab statistical software generated normal probability plot, plot of residuals and histogram for adhesion bond strengths of cement mortar 2 plus polymer 2, cement mortar 2 plus polymer 3, cement mortar 2 plus polymer 4 and cement mortar 2 plus polymer 5 cast over metal substrates

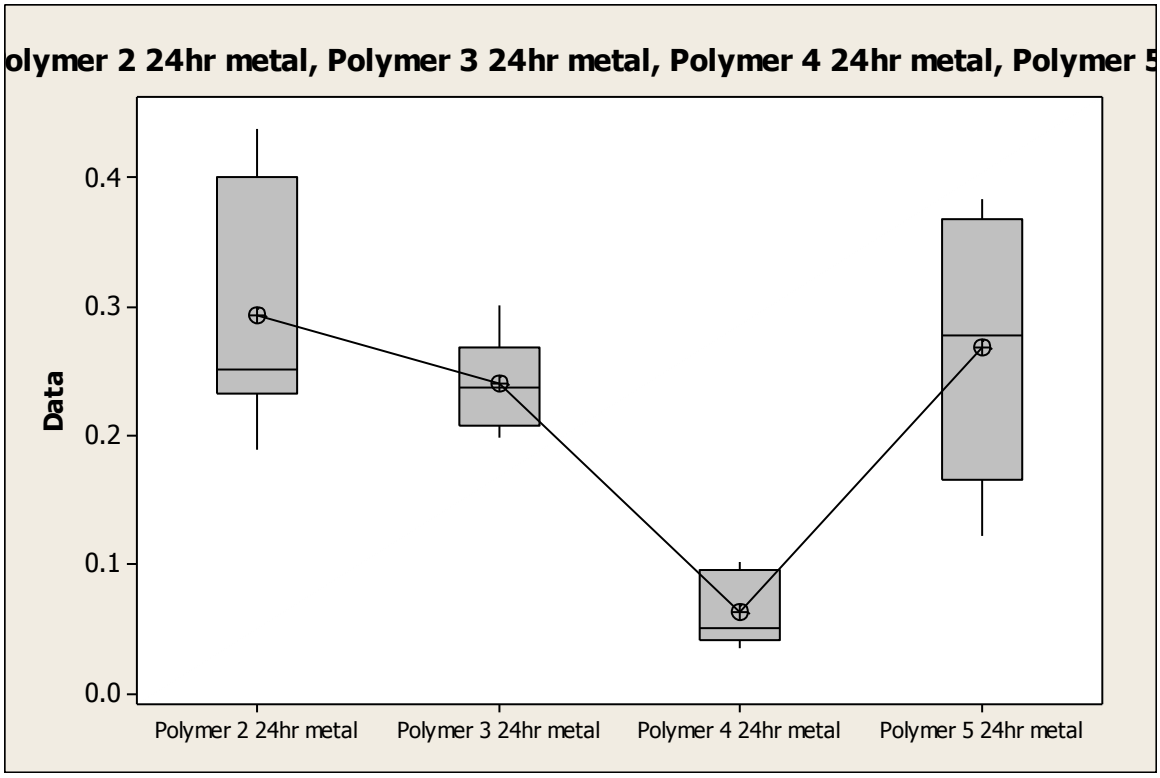

Figure A20: Minitab statistical software generated boxplot for adhesion bond strengths of cement mortar 2 plus polymer 2, cement mortar 2 plus polymer 3, cement mortar 2 plus polymer 4 and cement mortar 2 plus polymer 5 cast over metal substrates

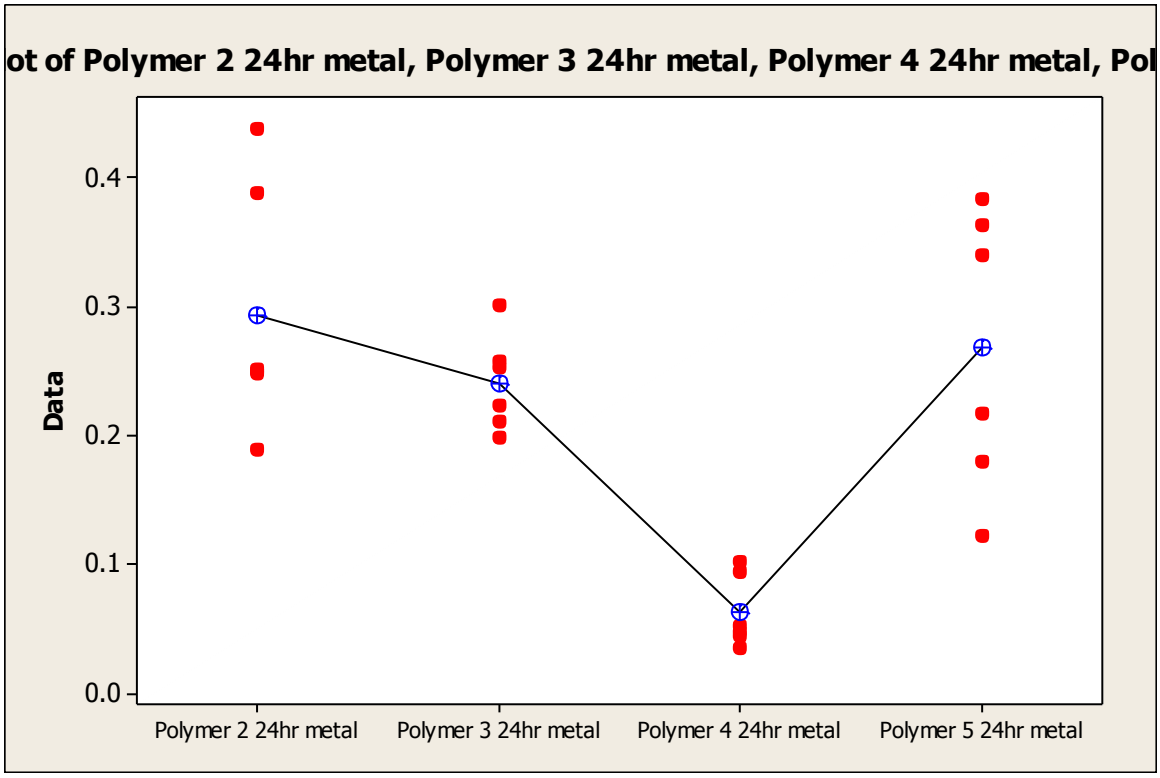

Figure A21: Minitab statistical software generated individual value plot for adhesion bond strengths of cement mortar 2 plus polymer 2, cement mortar 2 plus polymer 3, cement mortar 2 plus polymer 4 and cement mortar 2 plus polymer 5 cast over metal substrates

Experiment 8: Adhesion of Polymer Modified CSA Cement Mortar to Wooden Substrates

mortars = cement mortar 2 plus polymer 2, cement mortar 2 plus polymer 3, cement mortar 2 plus polymer 4, cement mortar 2 plus polymer 5

curing regimen = 24 hours ambient laboratory conditions

Protocoal similar to that described in ASTM C1583 was followed for data collection. Six samples were cast and tested for each mortar formulation. Samples were stored at ambient laboratory temperature and humidity from the time of casting to the time of testing. Tested mortar formulations included cement mortar 2 plus polymer 2, cement mortar 2 plus polymer 3, cement mortar 2 plus polymer 4 and cement mortar 2 plus polymer 5. Polymer modified mortar formulations contained polymer mass amounts such that the polymer / cement ratios were 0.15.

Polymer 2 24hr wood	Polymer 3 24hr wood	Polymer 4 24hr wood	Polymer 5 24hr wood
1.0069	0.8754	0.4526	1.1499
1.0024	1.0718	0.1772	1.4902
1.2025	0.6798	0.3824	1.7937
0.6333	0.8306	0.3166	1.2964
0.8306	0.9017	0.2272	1.5315
0.9219	0.8429	0.3044	1.3525

Table A8: Adhesion pull off test data for polymer modified CSA cement mortars varying polymer type with polymer / cement ratio of 0.15 cast over wooden substrates

H_o: Latex polymer type does not effect the average bond strength for CSA cement mortar cast over wooden substrate materials ($u_i = u_j$)

H_a: Latex polymer type effects the average bond strength for CSA cement mortar cast over wooden substrate materials (u_i does not equal u_j)

One-way ANOVA was used to test the equality of the population means for 24 hour adhesion testing of polymer modified mortars containing polymer 2, polymer 3, polymer 4 and polymer 5 cast over wooden substrate. Results from ANOVA are: $F(3/20) = 45.3$, $p < 0.001$, pooled standard deviation = 0.1676 and $R^2 = 87.17\%$. Based upon the F value of 45.3 and corresponding p-value < 0.001, if an alpha value of 0.05 is chosen, it is safe to reject the null hypothesis and ultimately conclude that at least two means differ from one another, and this inequality is highly unlikely due to chance. Further "post hoc" statistical analysis utilizing Tukey's Honestly Significant Difference Test assigned the mortar containing polymer 5 to "A" adhesion strength classification, the mortar containing polymer 2 to "B" adhesion strength classification, the mortar containing polymer 3 to "B" adhesion strength classification while the mortar containing polymer 4 was assigned to "C" adhesion strength classification. For the Tukey comparison method, mortars that do not share the same letter strength classification are significantly different.

One-way ANOVA: Polymer 2 24, Polymer 3 24, Polymer 4 24, Polymer 5 24

Source DF SS MS F P
Factor 3 3.8186 1.2729 45.30 0.000
Error 20 0.5620 0.0281
Total 23 4.3806

S = 0.1676 R-Sq = 87.17% R-Sq(adj) = 85.25%

Level N Mean StDev
Polymer 2 24hr wood 6 0.9329 0.1915
Polymer 3 24hr wood 6 0.8670 0.1266
Polymer 4 24hr wood 6 0.3101 0.1001
Polymer 5 24hr wood 6 1.4357 0.2229

Individual 95% CIs For Mean Based on
Pooled StDev
Level ------+---------+---------+---------+---
Polymer 2 24hr wood (--*---)
Polymer 3 24hr wood (---*--)
Polymer 4 24hr wood (---*--)
Polymer 5 24hr wood (---*--)
------+---------+---------+---------+---
0.40 0.80 1.20 1.60

Pooled StDev = 0.1676

Grouping Information Using Tukey Method

N Mean Grouping
Polymer 5 24hr wood 6 1.4357 A
Polymer 2 24hr wood 6 0.9329 B
Polymer 3 24hr wood 6 0.8670 B
Polymer 4 24hr wood 6 0.3101 C

Means that do not share a letter are significantly different.

Tukey 95% Simultaneous Confidence Intervals
All Pairwise Comparisons

Individual confidence level = 98.89%

Polymer 2 24hr wood subtracted from:

Lower Center Upper
Polymer 3 24hr wood -0.3369 -0.0659 0.2051
Polymer 4 24hr wood -0.8939 -0.6229 -0.3519
Polymer 5 24hr wood 0.2318 0.5028 0.7738

```
                +---------+---------+---------+---------
Polymer 3 24hr wood             (---*---)
Polymer 4 24hr wood         (---*---)
Polymer 5 24hr wood                 (---*---)
                +---------+---------+---------+---------
              -1.40     -0.70     0.00      0.70
```

Polymer 3 24hr wood subtracted from:

```
                Lower   Center    Upper
Polymer 4 24hr wood  -0.8280  -0.5570  -0.2860
Polymer 5 24hr wood   0.2977   0.5687   0.8397
```

```
                +---------+---------+---------+---------
Polymer 4 24hr wood         (---*---)
Polymer 5 24hr wood                 (---*---)
                +---------+---------+---------+---------
              -1.40     -0.70     0.00      0.70
```

Polymer 4 24hr wood subtracted from:

```
                Lower  Center   Upper
Polymer 5 24hr wood  0.8546  1.1256  1.3966
```

```
                +---------+---------+---------+---------
Polymer 5 24hr wood                         (---*---)
                +---------+---------+---------+---------
              -1.40     -0.70     0.00      0.70
```

Grouping Information Using Fisher Method

```
                N    Mean  Grouping
Polymer 5 24hr wood  6  1.4357  A
Polymer 2 24hr wood  6  0.9329    B
Polymer 3 24hr wood  6  0.8670    B
Polymer 4 24hr wood  6  0.3101      C
```

Means that do not share a letter are significantly different.

Fisher 95% Individual Confidence Intervals
All Pairwise Comparisons

Simultaneous confidence level = 80.83%

Polymer 2 24hr wood subtracted from:

	Lower	Center	Upper
Polymer 3 24hr wood	-0.2678	-0.0659	0.1360
Polymer 4 24hr wood	-0.8247	-0.6229	-0.4210
Polymer 5 24hr wood	0.3009	0.5028	0.7046

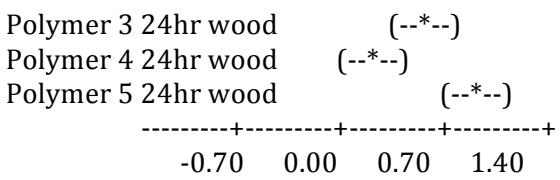

Polymer 3 24hr wood subtracted from:

	Lower	Center	Upper
Polymer 4 24hr wood	-0.7588	-0.5570	-0.3551
Polymer 5 24hr wood	0.3668	0.5687	0.7705

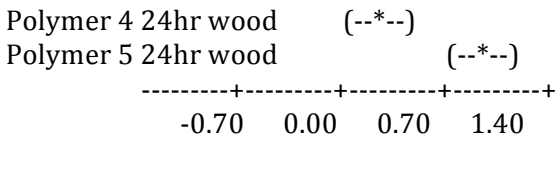

Polymer 4 24hr wood subtracted from:

	Lower	Center	Upper
Polymer 5 24hr wood	0.9238	1.1256	1.3275

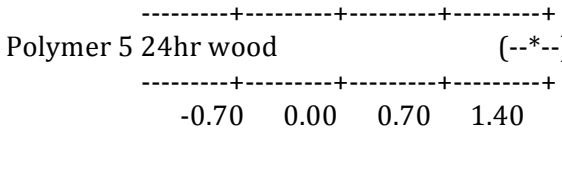

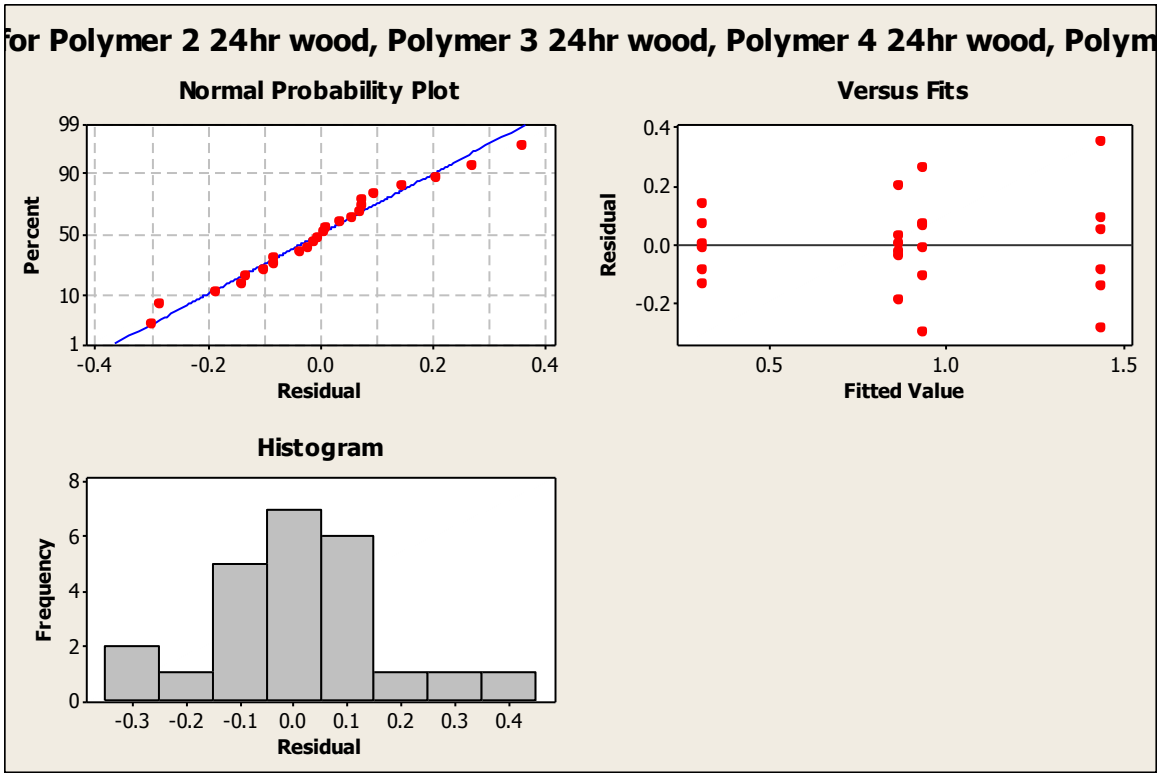

Figure A22: Minitab statistical software generated normal probability plot, plot of residuals and histogram for adhesion bond strengths of cement mortar 2 plus polymer 2, cement mortar 2 plus polymer 3, cement mortar 2 plus polymer 4 and cement mortar 2 plus polymer 5 cast over wooden substrates

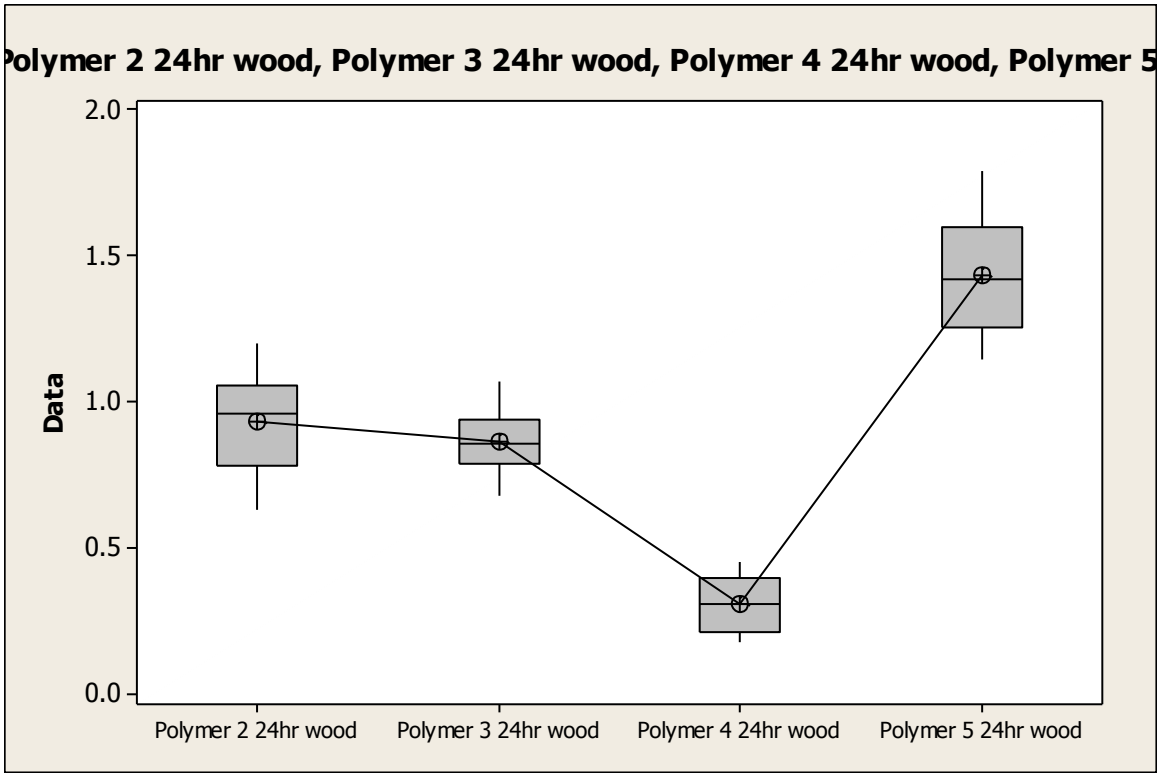

Figure A23: Minitab statistical software generated boxplot for adhesion bond strengths of cement mortar 2 plus polymer 2, cement mortar 2 plus polymer 3, cement mortar 2 plus polymer 4 and cement mortar 2 plus polymer 5 cast over wooden substrates

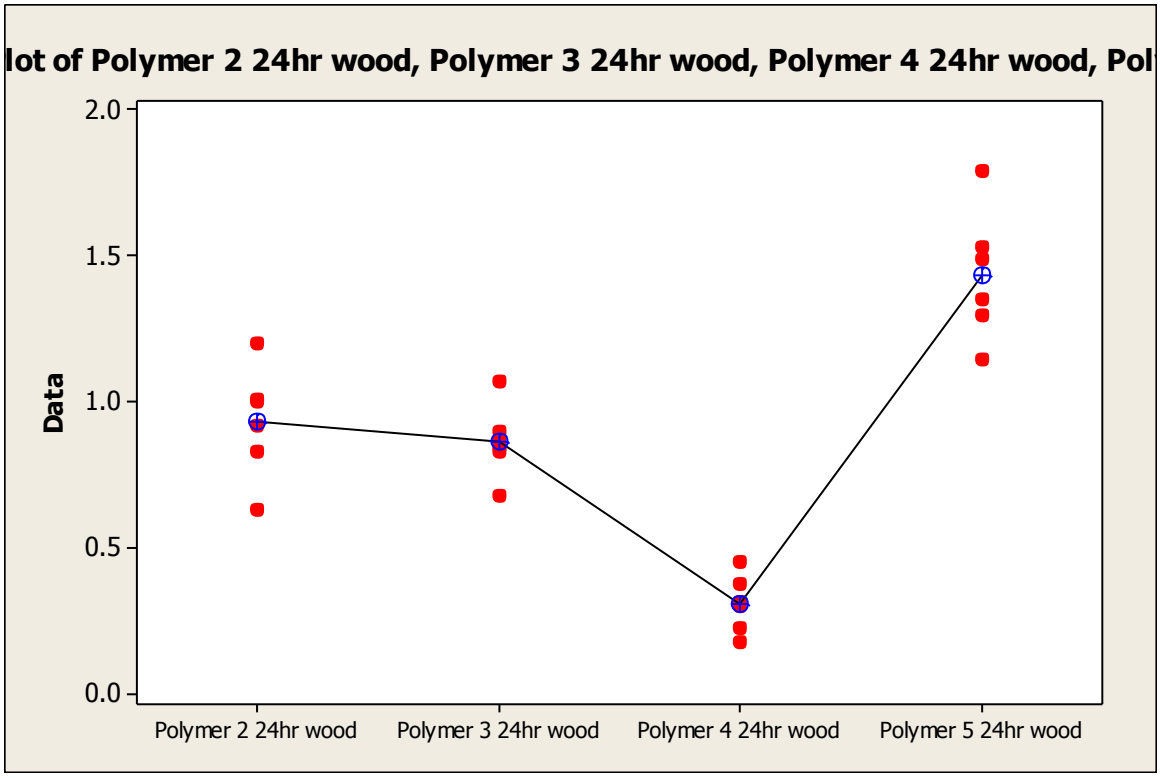

Figure A24: Minitab statistical software generated individual value plot for adhesion bond strengths of cement mortar 2 plus polymer 2, cement mortar 2 plus polymer 3, cement mortar 2 plus polymer 4 and cement mortar 2 plus polymer 5 cast over wooden substrates

Strength Loss Statistical Analysis Summary

Experiment 1: Direct Tensile Strength Behavior of CSA Cement Mortar Containing Anhydrite as a Source of Calcium Sulfate

mortar = CSA cement mortar containing solely anhydrite

curing regimen = 24hrs, 48hrs, 7d, 28d, 56d and 109d at ambient laboratory temperature and constant 50% relative humidity

Test method ASTM C307 was followed for data collection. Three samples were cast and tested for each mortar formulation. Samples were stored at ambient laboratory temperature and constant 50% relative humidity from the time of removal from molds to the time of testing. A CSA cement mortar containing solely anhydrite as a source of calcium sulfate was tested after curing at constant low humidity for various durations in an effort to assess direct tensile strength behavior versus time.

Anh 24hr	Anh 48hr	Anh 7d	Anh 28d	Anh 56d	Anh 109d
270	453	516	628	543	502
283	494	487	603	533	557
273	518	477	668	624	557

Table A9 : Direct tensile strength testing data (psi) for CSA cement mortar containing anhydrite as a source of calcium sulfate cured at constant 50% relative humidity

H_o: Curing at ambient laboratory temperature and constant 50% relative humidity does not effect the average direct tensile strength for CSA cement mortar containing solely anhydrite as a source of calcium sulfate ($u_i = u_j$)

H_a: Curing at ambient laboratory temperature and constant 50% relative humidity effects the average direct tensile strength for CSA cement mortar containing solely anhydrite as a source of calcium sulfate (u_i does not equal u_j)

One-way ANOVA was used to test the equality of the population means for direct tensile strength testing of the CSA cement mortar containing solely anhydrite when cured for 24 hours, 48 hours, 7, 28, 56 and 109 days at ambient laboratory temperature and constant 50% relative humidity. Results from ANOVA are: $F(5/12) = 43.76$, $p < 0.001$, pooled standard deviation = 31.91 and $R^2 = 94.8\%$. Based upon the F value of 43.76 and corresponding p-value < 0.001, if an alpha value of 0.05 is chosen, it is safe to reject the null hypothesis and ultimately conclude that at least two means differ from one another, and this inequality is highly unlikely due to chance. Further statistical comparison methods utilizing Tukey's Honestly Significant Difference test along with Fisher's test can be seen in Table A10. In Table A10, average direct tensile strength values for specific curing regimens not sharing the same letter strength classification are significantly different. Therefore, direct tensile strength loss versus time for the CSA cement mortar containing anhydrite is statistically significant for the period from 28 days to 109 days.

Post Hoc Statistical Analysis	Tukey	Fisher
24 hour	C	D
48 hour	B	C
7 days	B	C
28 days	A	A
56 days	A B	B
109 days	B	B C

Table A10: Direct tensile strength classifications as assigned by statistical comparison methods for the CSA cement mortar containing solely anhydrite in Table 1. Direct tensile strength results for specific curing regimens not sharing the same letter are significantly different.

One-way ANOVA: Anh 24hr, Anh 48hr, Anh 7d, Anh 28d, Anh 56d, Anh 109d

Source DF SS MS F P
Factor 5 222842 44568 43.76 0.000
Error 12 12221 1018
Total 17 235063

S = 31.91 R-Sq = 94.80% R-Sq(adj) = 92.63%

Individual 95% CIs For Mean Based on Pooled StDev

```
Level    N   Mean  StDev   +---------+---------+---------+---------
Anh 24hr 3  275.33   6.81   (--*--)
Anh 48hr 3  488.33  32.87             (---*--)
Anh 7d   3  493.33  20.26            (--*--)
Anh 28d  3  633.00  32.79                    (---*--)
Anh 56d  3  566.67  49.90                 (--*---)
Anh 109d 3  538.67  31.75                 (--*--)
                  +---------+---------+---------+---------
                 240       360       480       600
```

Pooled StDev = 31.91

Grouping Information Using Tukey Method

	N	Mean	Grouping
Anh 28d	3	633.00	A
Anh 56d	3	566.67	A B
Anh 109d	3	538.67	B
Anh 7d	3	493.33	B
Anh 48hr	3	488.33	B
Anh 24hr	3	275.33	C

Means that do not share a letter are significantly different.

Tukey 95% Simultaneous Confidence Intervals
All Pairwise Comparisons

Individual confidence level = 99.43%

Anh 24hr subtracted from:

```
          Lower  Center  Upper  --+---------+---------+---------+-------
Anh 48hr  125.48  213.00  300.52              (----*---)
Anh 7d    130.48  218.00  305.52             (---*---)
Anh 28d   270.15  357.67  445.19                   (---*---)
Anh 56d   203.81  291.33  378.85                (----*---)
Anh 109d  175.81  263.33  350.85                (---*----)
                    --+---------+---------+---------+-------
                   -200       0      200     400
```

Anh 48hr subtracted from:

```
          Lower  Center  Upper  --+---------+---------+---------+-------
Anh 7d    -82.52   5.00  92.52        (---*----)
Anh 28d    57.15  144.67  232.19            (---*----)
Anh 56d    -9.19   78.33  165.85          (---*---)
Anh 109d  -37.19   50.33  137.85          (----*---)
                    --+---------+---------+---------+-------
                   -200       0      200     400
```

Anh 7d subtracted from:

```
          Lower  Center  Upper  --+---------+---------+---------+-------
Anh 28d    52.15  139.67  227.19            (---*---)
Anh 56d   -14.19   73.33  160.85          (----*---)
Anh 109d  -42.19   45.33  132.85          (---*----)
                    --+---------+---------+---------+-------
                   -200       0      200     400
```

Anh 28d subtracted from:

```
          Lower  Center  Upper  --+---------+---------+---------+-------
Anh 56d   -153.85  -66.33  21.19      (----*---)
Anh 109d  -181.85  -94.33  -6.81      (---*----)
                    --+---------+---------+---------+-------
                   -200       0      200     400
```

Anh 56d subtracted from:

```
        Lower  Center  Upper  --+---------+---------+---------+-------
Anh 109d  -115.52  -28.00  59.52       (----*---)
                    --+---------+---------+---------+-------
                   -200       0      200     400
```

Grouping Information Using Fisher Method

```
       N   Mean  Grouping
Anh 28d   3  633.00  A
Anh 56d   3  566.67   B
Anh 109d  3  538.67   B C
Anh 7d    3  493.33     C
Anh 48hr  3  488.33     C
Anh 24hr  3  275.33       D
```

Means that do not share a letter are significantly different.

Fisher 95% Individual Confidence Intervals
All Pairwise Comparisons

Simultaneous confidence level = 68.63%

Anh 24hr subtracted from:

```
       Lower  Center  Upper ---+---------+---------+---------+------
Anh 48hr  156.23  213.00  269.77                 (--*---)
Anh 7d    161.23  218.00  274.77                (---*--)
Anh 28d   300.89  357.67  414.44                       (--*---)
Anh 56d   234.56  291.33  348.11                    (--*---)
Anh 109d  206.56  263.33  320.11                    (--*---)
                  ---+---------+---------+---------+------
                  -160       0      160     320
```

Anh 48hr subtracted from:

```
       Lower  Center  Upper ---+---------+---------+---------+------
Anh 7d   -51.77   5.00  61.77         (--*---)
Anh 28d   87.89  144.67  201.44              (---*---)
Anh 56d   21.56   78.33  135.11           (---*--)
Anh 109d  -6.44   50.33  107.11           (--*---)
                  ---+---------+---------+---------+------
                  -160       0      160     320
```

Anh 7d subtracted from:

```
        Lower  Center  Upper ---+---------+---------+---------+------
Anh 28d   82.89  139.67  196.44             (---*--)
Anh 56d   16.56   73.33  130.11          (---*--)
Anh 109d -11.44   45.33  102.11          (---*--)
                   ---+---------+---------+---------+------
                   -160       0     160     320
```

Anh 28d subtracted from:

```
        Lower  Center  Upper ---+---------+---------+---------+------
Anh 56d  -123.11 -66.33  -9.56     (---*--)
Anh 109d -151.11 -94.33 -37.56     (--*---)
                   ---+---------+---------+---------+------
                   -160       0     160     320
```

Anh 56d subtracted from:

```
        Lower  Center  Upper ---+---------+---------+---------+------
Anh 109d -84.77 -28.00  28.77       (--*---)
                   ---+---------+---------+---------+------
                   -160       0     160     320
```

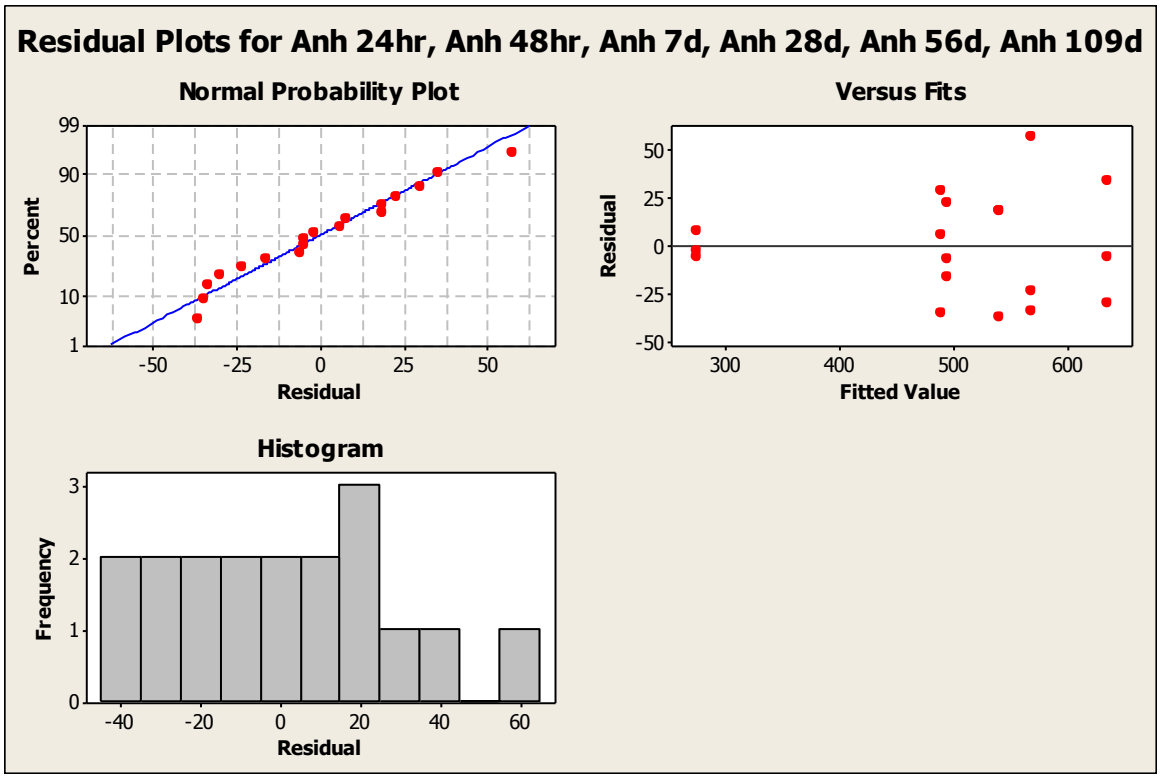

Figure A25: Minitab statistical software generated normal probability plot, plot of residuals and histogram for assessing direct tensile strength behavior of CSA cement containing anhydrite as a source of calcium sulfate cured at constant 50% relative humidity and ambient laboratory temperature

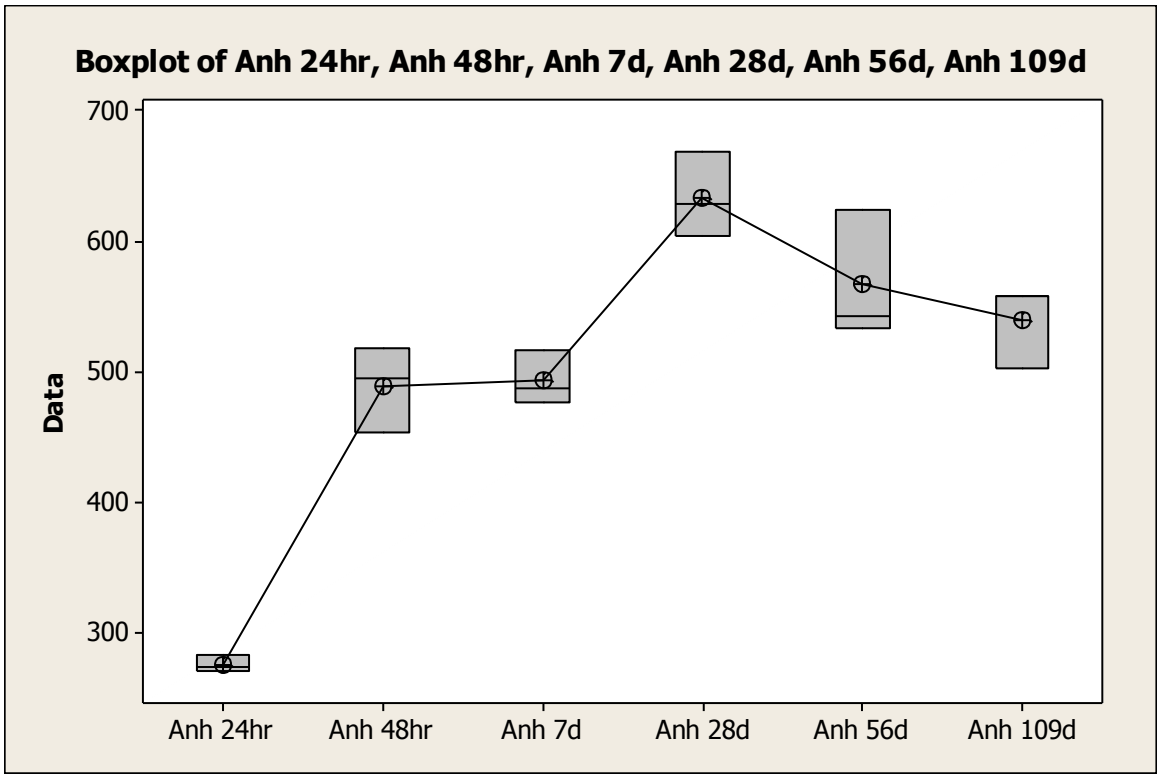

Figure A26: Minitab statistical software generated boxplot for assessing direct tensile strength behavior of CSA cement containing anhydrite as a source of calcium sulfate cured at constant 50% relative humidity and ambient laboratory temperature

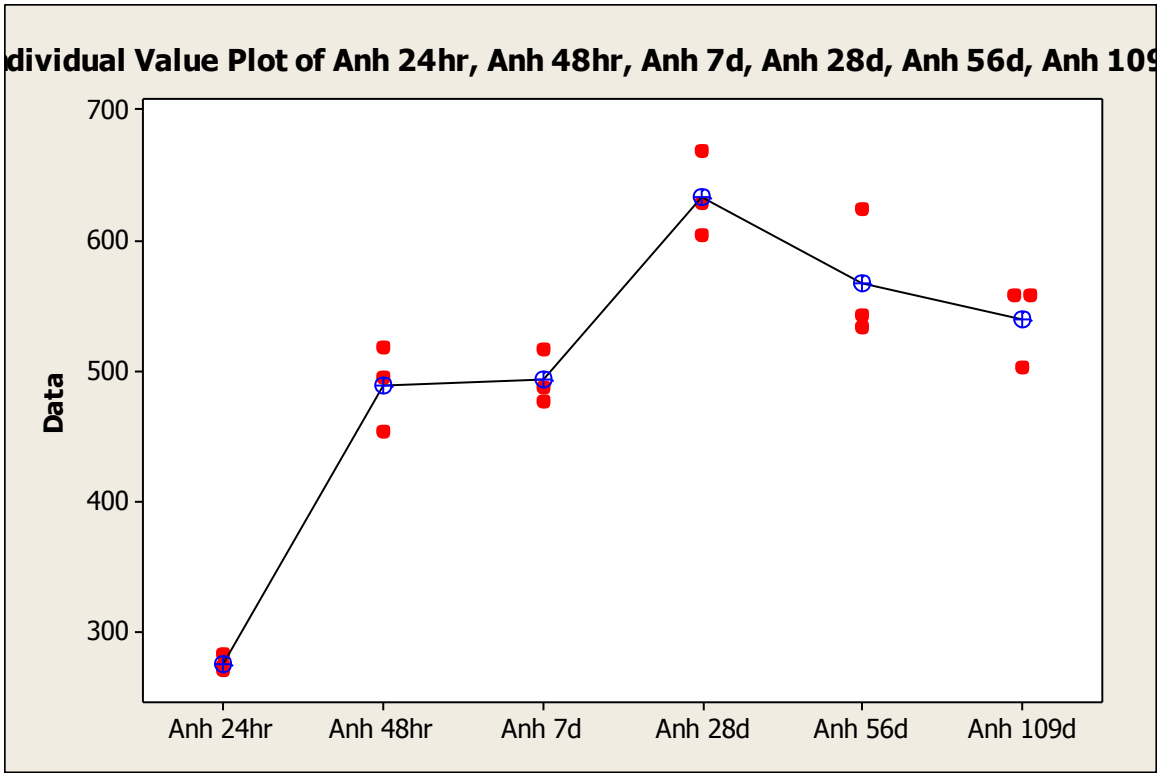

Figure A27: Minitab statistical software generated individual value plot for assessing direct tensile strength behavior of CSA cement containing anhydrite as a source of calcium sulfate cured at constant 50% relative humidity and ambient laboratory temperature

Experiment 2: Direct Tensile Strength Behavior of CSA Cement Mortar Containing Gypsum as a Source of Calcium Sulfate

mortar = CSA cement mortar containing solely gypsum

curing regimen = 24hrs, 48hrs, 7d and 28d at ambient laboratory temperature and constant 50% relative humidity

Test method ASTM C307 was followed for data collection. Three samples were cast and tested for each mortar formulation. Samples were stored at ambient laboratory temperature and constant 50% relative humidity from the time of removal from molds to the time of testing. A CSA cement mortar containing solely gypsum as a source of calcium sulfate was tested after curing at constant low humidity for various durations in an effort to assess direct tensile strength behavior versus time.

Gyp 24hr	Gyp 48hr	Gyp 7d	Gyp 28d
369	301	417	333
341	409	506	354
329	404	467	342

Table A11: Direct tensile strength testing data (psi) for CSA cement mortar containing gypsum as a source of calcium sulfate cured at constant 50% relative humidity

H_o: Curing at ambient laboratory temperature and constant 50% relative humidity does not effect the average direct tensile strength for CSA cement mortar containing solely gypsum as a source of calcium sulfate ($u_i = u_j$)

H_a: Curing at ambient laboratory temperature and constant 50% relative humidity effects the average direct tensile strength for CSA cement mortar containing solely gypsum as a source of calcium sulfate (u_i does not equal u_j)

One-way ANOVA was used to test the equality of the population means for direct tensile strength testing of the CSA cement mortar containing gypsum when cured for 24 hours, 48 hours, 7 days and 28 days at ambient laboratory temperature and constant 50% relative humidity. Results from ANOVA are: $F(3/8) = 6.1$, $p = 0.018$, pooled standard deviation = 39.49 and $R^2 = 69.59\%$. Based upon the F value of 6.1 and corresponding p-value = 0.018, if an alpha value of 0.05 is chosen, it is safe to reject the null hypothesis and ultimately conclude that at least two means differ from one another, and this inequality is highly unlikely due to chance. Further statistical comparison methods utilizing Tukey's Honestly Significant Difference test along with Fisher's test can be seen in Table A12. In Table A12, average direct tensile strength values for specific curing regimens not sharing the same letter strength classification are significantly different. Therefore, direct tensile strength loss versus time for the CSA cement mortar containing solely gypsum is statistically significant for the period from 7 days to 28 days.

Post Hoc Statistical Analysis	Tukey	Fisher
24 hour	B	B
48 hour	A B	B
7 days	A	A
28 days	B	B

Table A12: Direct tensile strength classifications as assigned by statistical comparison methods for the CSA cement mortar containing solely gypsum in Table 1. Direct tensile strength results for specific curing regimens not sharing the same letter are significantly different.

One-way ANOVA: Gyp 24hr, Gyp 48hr, Gyp 7d, Gyp 28d

Source DF SS MS F P
Factor 3 28554 9518 6.10 0.018
Error 8 12478 1560
Total 11 41032

S = 39.49 R-Sq = 69.59% R-Sq(adj) = 58.19%

Individual 95% CIs For Mean Based on Pooled StDev

Level	N	Mean	StDev	--+---------+---------+---------+-------
Gyp 24hr	3	346.33	20.53	(--------*-------)
Gyp 48hr	3	371.33	60.96	(--------*--------)
Gyp 7d	3	463.33	44.61	(--------*--------)
Gyp 28d	3	343.00	10.54	(--------*--------)

--+---------+---------+---------+-------
300 360 420 480

Pooled StDev = 39.49

Grouping Information Using Tukey Method

	N	Mean	Grouping
Gyp 7d	3	463.33	A
Gyp 48hr	3	371.33	A B
Gyp 24hr	3	346.33	B
Gyp 28d	3	343.00	B

Means that do not share a letter are significantly different.

Tukey 95% Simultaneous Confidence Intervals
All Pairwise Comparisons

Individual confidence level = 98.74%

Gyp 24hr subtracted from:

```
          Lower  Center   Upper ----------+---------+---------+---------+
Gyp 48hr   -78.29   25.00  128.29          (---------*---------)
Gyp 7d      13.71  117.00  220.29                   (---------*--------)
Gyp 28d   -106.62   -3.33   99.96         (---------*--------)
                    ----------+---------+---------+---------+
                       -120       0      120      240
```

Gyp 48hr subtracted from:

```
          Lower  Center   Upper ----------+---------+---------+---------+
Gyp 7d    -11.29   92.00  195.29                (---------*--------)
Gyp 28d  -131.62  -28.33   74.96        (---------*--------)
                    ----------+---------+---------+---------+
                       -120       0      120      240
```

Gyp 7d subtracted from:

```
          Lower  Center   Upper ----------+---------+---------+---------+
Gyp 28d  -223.62  -120.33  -17.04  (---------*---------)
                    ----------+---------+---------+---------+
                       -120       0      120      240
```

Grouping Information Using Fisher Method

```
          N   Mean  Grouping
Gyp 7d    3  463.33  A
Gyp 48hr  3  371.33    B
Gyp 24hr  3  346.33    B
Gyp 28d   3  343.00    B
```

Means that do not share a letter are significantly different.

Fisher 95% Individual Confidence Intervals
All Pairwise Comparisons

Simultaneous confidence level = 82.43%

Gyp 24hr subtracted from:

```
          Lower  Center   Upper ----------+---------+---------+---------+
Gyp 48hr  -49.36   25.00   99.36           (--------*-------)
Gyp 7d     42.64  117.00  191.36                   (--------*-------)
Gyp 28d   -77.69   -3.33   71.03          (--------*-------)
```

```
                  ---------+---------+---------+---------+
                      -100       0     100     200
```

Gyp 48hr subtracted from:

```
          Lower  Center  Upper ---------+---------+---------+---------+
Gyp 7d    17.64  92.00 166.36                (------*-------)
Gyp 28d -102.69 -28.33  46.03        (------*-------)
                  ---------+---------+---------+---------+
                      -100       0     100     200
```

Gyp 7d subtracted from:

```
          Lower   Center   Upper ---------+---------+---------+---------+
Gyp 28d -194.69 -120.33 -45.97  (------*------)
                  ---------+---------+---------+---------+
                      -100       0     100     200
```

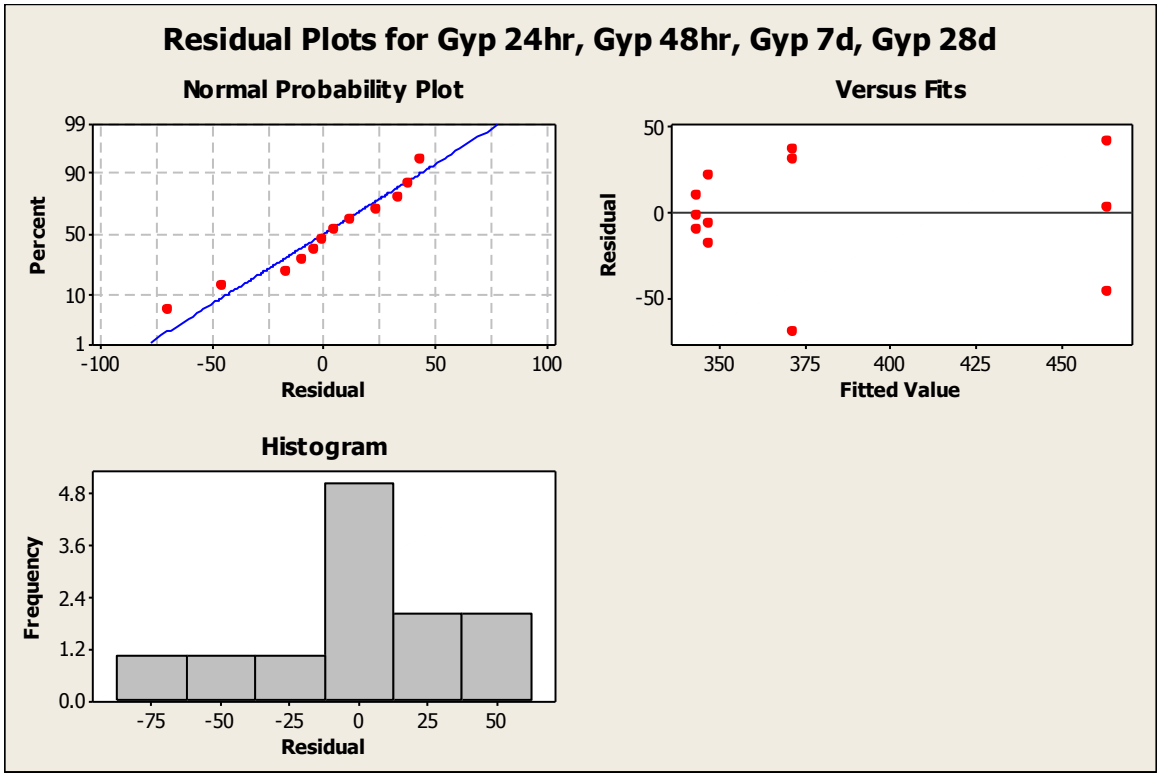

Figure A28: Minitab statistical software generated normal probability plot, plot of residuals and histogram for assessing direct tensile strength behavior of CSA cement containing gypsum as a source of calcium sulfate cured at constant 50% relative humidity and ambient laboratory temperature

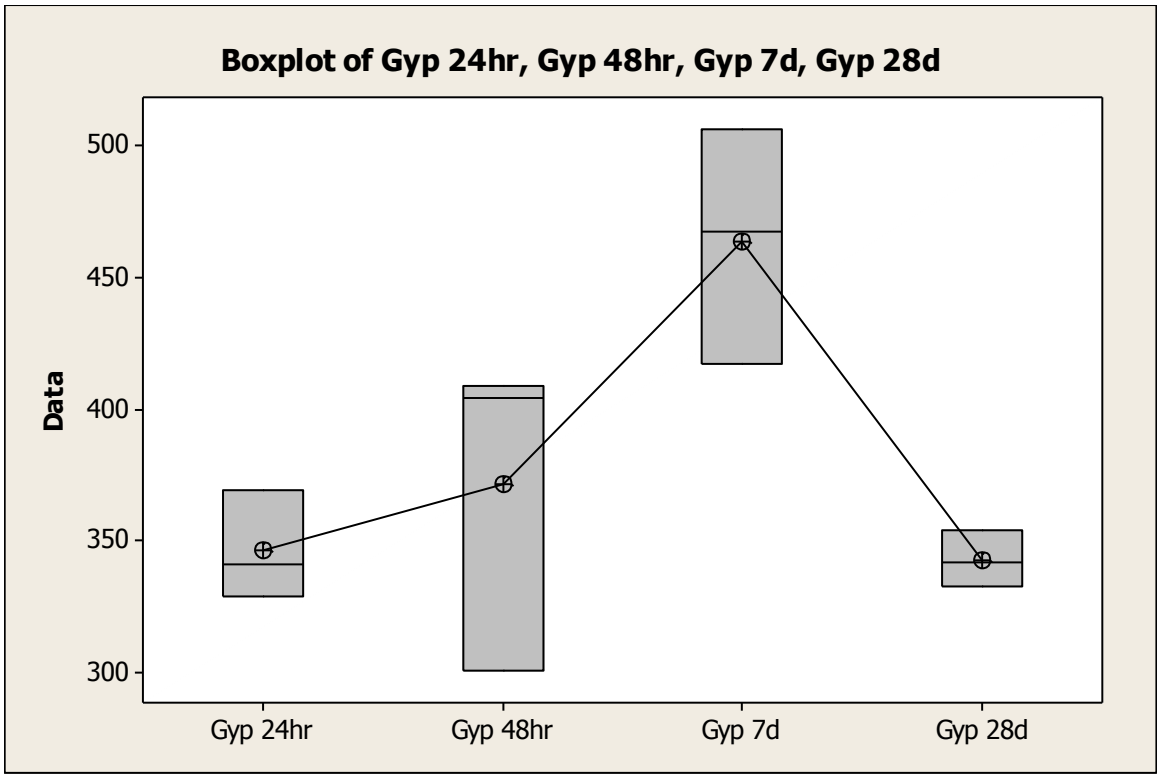

Figure A29: Minitab statistical software generated boxplot for assessing direct tensile strength behavior of CSA cement containing gypsum as a source of calcium sulfate cured at constant 50% relative humidity and ambient laboratory temperature

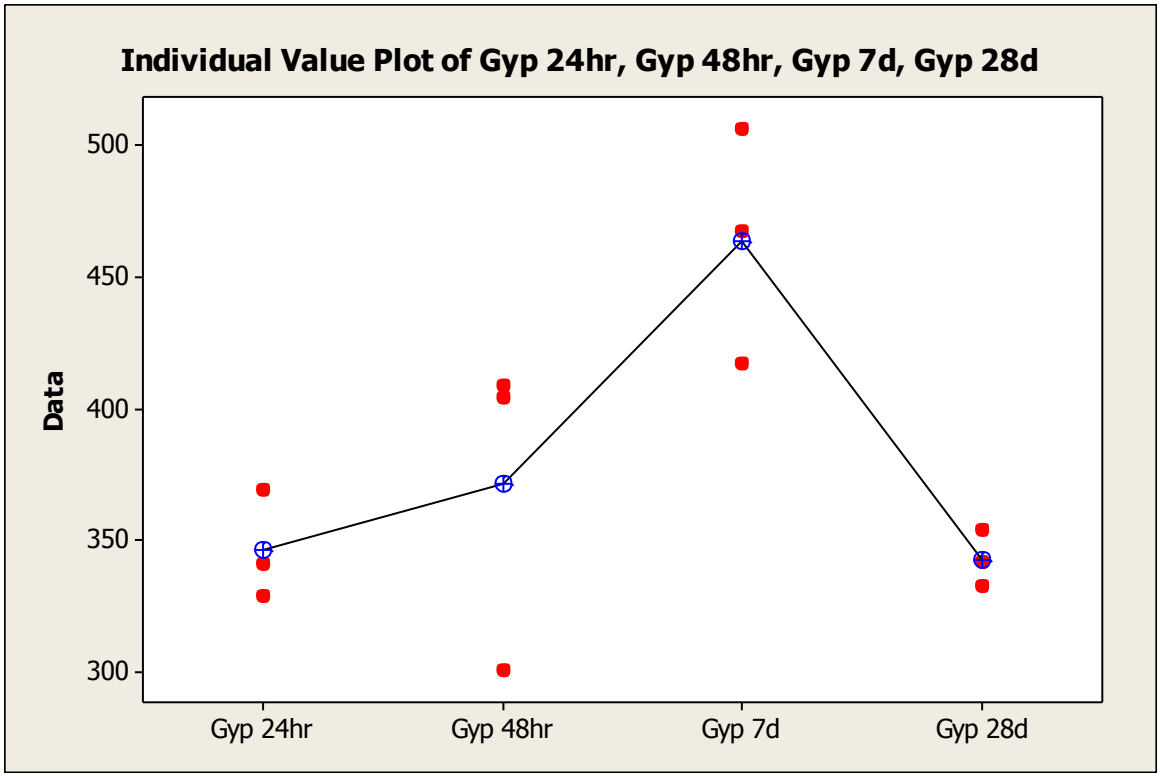

Figure A30: Minitab statistical software generated individual value plot for assessing direct tensile strength behavior of CSA cement containing gypsum as a source of calcium sulfate cured at constant 50% relative humidity and ambient laboratory temperature

Experiment 3: Direct Tensile Strength Behavior of CSA Cement Mortar containing 50% Anhydrite and 50% Gypsum as a Source of Calcium Sulfate

mortar = CSA cement mortar containing 50% anhydrite and 50% gypsum

curing regimen = 24hrs, 48hrs, 7d, 28d and 56d at ambient laboratory temperature and constant 50% relative humidity

Test method ASTM C307 was followed for data collection. Three samples were cast and tested for each mortar formulation. Samples were stored at ambient laboratory temperature and constant 50% relative humidity from the time of removal from molds to the time of testing. A CSA cement mortar containing 50 weight % anhydrite and 50 weight % gypsum as a source of calcium sulfate was tested after curing at constant low humidity for various durations in an effort to assess direct tensile strength behavior versus time.

50% Anh 50% Gyp 24hr	50% Anh 50% Gyp 48hr	50% Anh 50% Gyp 7d	50% Anh 50% Gyp 28d	50% Anh 50% Gyp 56d
337	529	492	669	308
407	456	451	537	305
418	490	530	585	327

Table A13: Direct tensile strength testing data (psi) for CSA cement mortar containing half anhydrite and half gypsum as a source of calcium sulfate cured at constant 50% relative humidity

H_o: Curing at ambient laboratory temperature and constant 50% relative humidity does not effect the average direct tensile strength of CSA cement mortar containing 50 weight % anhydrite and 50 weight % gypsum as a source of calcium sulfate ($u_i = u_j$)

H_a: Curing at ambient laboratory temperature and constant 50% relative humidity effects the average direct tensile strength of CSA cement mortar containing 50 weight % anhydrite and 50 weight % gypsum as a source of calcium sulfate (u_i does not equal u_j)

One-way ANOVA was used to test the equality of the population means for direct tensile strength testing of the CSA cement mortar containing half anhydrite and half gypsum when cured for 24 hours, 48 hours, 7, 28, and 56 days at ambient laboratory temperature and constant 50% relative humidity. Results from ANOVA are: $F(4/10) = 18.86$, $p < 0.001$, pooled standard deviation = 43.43 and $R^2 = 88.3\%$. Based upon the F value of 18.86 and corresponding p-value < 0.001, if an alpha value of 0.05 is chosen, it is safe to reject the null hypothesis and ultimately conclude that at least two means differ from one another, and this inequality is highly unlikely due to chance. Further statistical comparison methods utilizing Tukey's Honestly Significant Difference test along with Fisher's test can be seen in Table A14. In Table A14, average direct tensile strength values for specific curing regimens not sharing the same letter strength classification are significantly different. Therefore, direct tensile strength loss versus time for the CSA cement mortar containing half anhydrite and half gypsum is statistically significant for the period from 28 days to 56 days.

Post Hoc Statistical Analysis	Tukey	Fisher
24 hour	B C	C
48 hour	A B	B
7 days	A B	B
28 days	A	A
56 days	C	C

Table A14: Direct tensile strength classifications as assigned by statistical comparison methods for the CSA cement mortar containing half anhydrite and half gypsum in Table 1. Direct tensile strength results for specific curing regimens not sharing the same letter are significantly different.

One-way ANOVA: 50% Anh 50% , 50% Anh 50% , 50% Anh 50% , 50% Anh 50% , ...

Source DF SS MS F P
Factor 4 142341 35585 18.86 0.000
Error 10 18864 1886
Total 14 161205

S = 43.43 R-Sq = 88.30% R-Sq(adj) = 83.62%

Level N Mean StDev
50% Anh 50% Gyp 24hr 3 387.33 43.94
50% Anh 50% Gyp 48hr 3 491.67 36.53
50% Anh 50% Gyp 7d 3 491.00 39.51
50% Anh 50% Gyp 28d 3 597.00 66.81
50% Anh 50% Gyp 56d 3 313.33 11.93

Individual 95% CIs For Mean Based on Pooled StDev

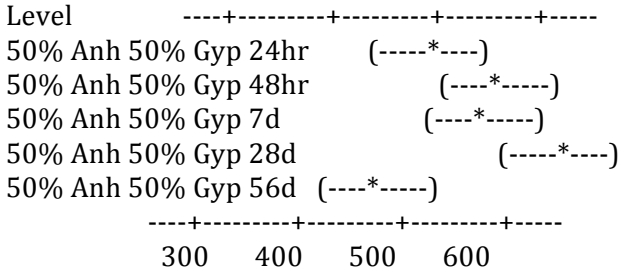

Pooled StDev = 43.43

Grouping Information Using Tukey Method

	N	Mean	Grouping
50% Anh 50% Gyp 28d	3	597.00	A
50% Anh 50% Gyp 48hr	3	491.67	A B
50% Anh 50% Gyp 7d	3	491.00	A B
50% Anh 50% Gyp 24hr	3	387.33	B C
50% Anh 50% Gyp 56d	3	313.33	C

Means that do not share a letter are significantly different.

Tukey 95% Simultaneous Confidence Intervals
All Pairwise Comparisons

Individual confidence level = 99.18%

50% Anh 50% Gyp 24hr subtracted from:

	Lower	Center	Upper
50% Anh 50% Gyp 48hr	-12.27	104.33	220.94
50% Anh 50% Gyp 7d	-12.94	103.67	220.27
50% Anh 50% Gyp 28d	93.06	209.67	326.27
50% Anh 50% Gyp 56d	-190.60	-74.00	42.60

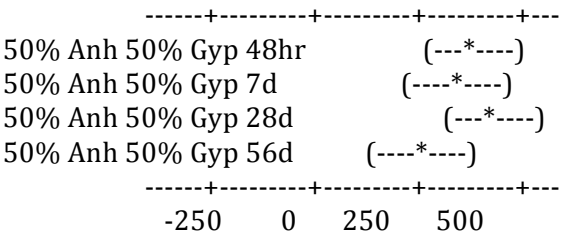

50% Anh 50% Gyp 48hr subtracted from:

	Lower	Center	Upper
50% Anh 50% Gyp 7d	-117.27	-0.67	115.94
50% Anh 50% Gyp 28d	-11.27	105.33	221.94
50% Anh 50% Gyp 56d	-294.94	-178.33	-61.73

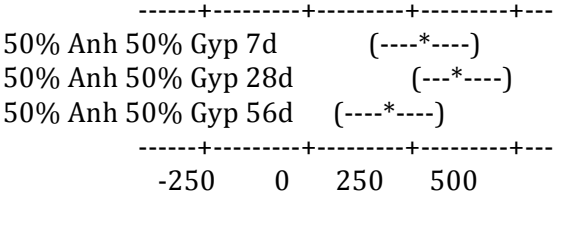

50% Anh 50% Gyp 7d subtracted from:

	Lower	Center	Upper
50% Anh 50% Gyp 28d	-10.60	106.00	222.60
50% Anh 50% Gyp 56d	-294.27	-177.67	-61.06

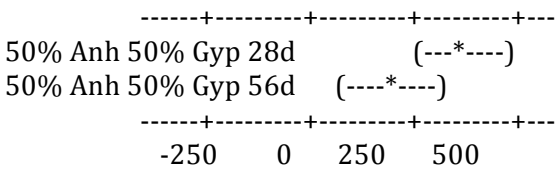

50% Anh 50% Gyp 28d subtracted from:

	Lower	Center	Upper
50% Anh 50% Gyp 56d	-400.27	-283.67	-167.06

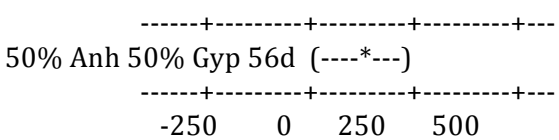

Grouping Information Using Fisher Method

	N	Mean	Grouping
50% Anh 50% Gyp 28d	3	597.00	A
50% Anh 50% Gyp 48hr	3	491.67	B
50% Anh 50% Gyp 7d	3	491.00	B
50% Anh 50% Gyp 24hr	3	387.33	C
50% Anh 50% Gyp 56d	3	313.33	C

Means that do not share a letter are significantly different.

Fisher 95% Individual Confidence Intervals
All Pairwise Comparisons

Simultaneous confidence level = 75.51%

50% Anh 50% Gyp 24hr subtracted from:

	Lower	Center	Upper
50% Anh 50% Gyp 48hr	25.32	104.33	183.35
50% Anh 50% Gyp 7d	24.65	103.67	182.68
50% Anh 50% Gyp 28d	130.65	209.67	288.68
50% Anh 50% Gyp 56d	-153.02	-74.00	5.02

```
                --------+---------+---------+---------+-
50% Anh 50% Gyp 48hr                  (---*---)
50% Anh 50% Gyp 7d                  (---*---)
50% Anh 50% Gyp 28d                       (--*---)
50% Anh 50% Gyp 56d           (---*---)
                --------+---------+---------+---------+-
                   -200       0      200      400
```

50% Anh 50% Gyp 48hr subtracted from:

```
                 Lower   Center   Upper
50% Anh 50% Gyp 7d    -79.68    -0.67   78.35
50% Anh 50% Gyp 28d    26.32   105.33  184.35
50% Anh 50% Gyp 56d  -257.35  -178.33  -99.32

                --------+---------+---------+---------+-
50% Anh 50% Gyp 7d              (---*---)
50% Anh 50% Gyp 28d                   (---*---)
50% Anh 50% Gyp 56d      (---*---)
                --------+---------+---------+---------+-
                   -200       0      200      400
```

50% Anh 50% Gyp 7d subtracted from:

```
                 Lower   Center   Upper
50% Anh 50% Gyp 28d    26.98   106.00  185.02
50% Anh 50% Gyp 56d  -256.68  -177.67  -98.65

                --------+---------+---------+---------+-
50% Anh 50% Gyp 28d                   (---*---)
50% Anh 50% Gyp 56d      (---*---)
                --------+---------+---------+---------+-
                   -200       0      200      400
```

50% Anh 50% Gyp 28d subtracted from:

```
                 Lower   Center    Upper
50% Anh 50% Gyp 56d  -362.68  -283.67  -204.65

                --------+---------+---------+---------+-
50% Anh 50% Gyp 56d  (---*---)
                --------+---------+---------+---------+-
                   -200       0      200      400
```

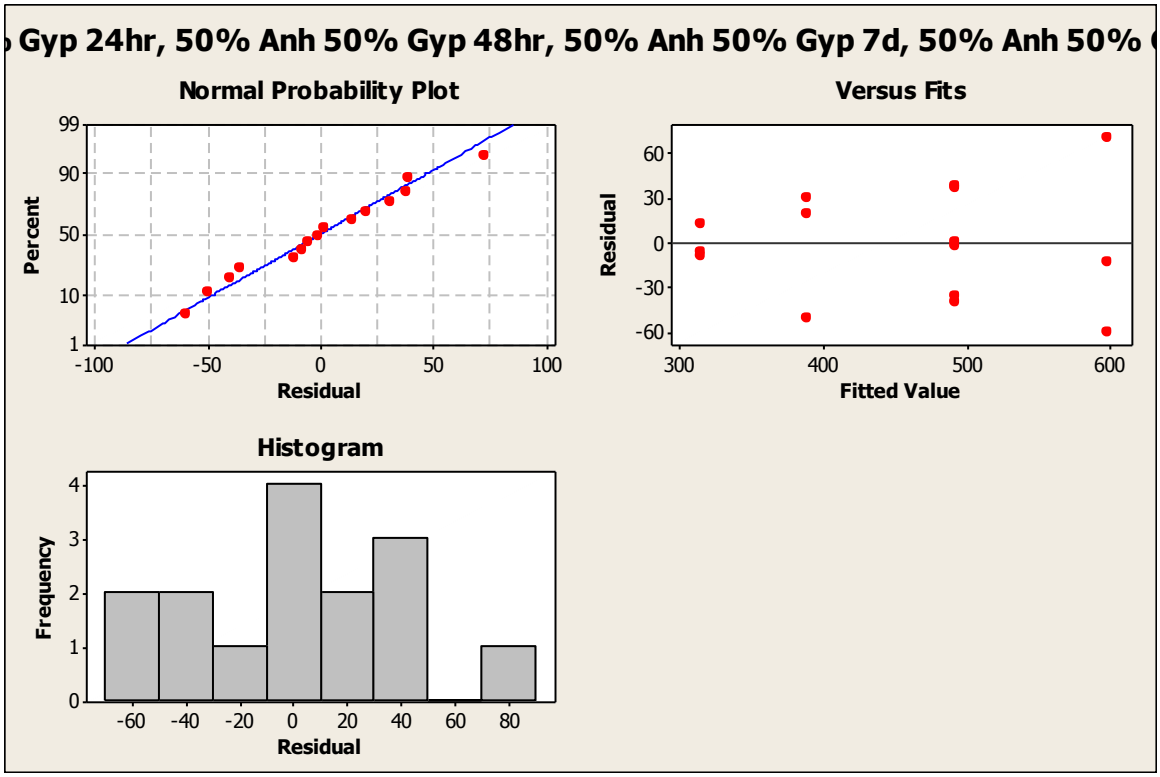

Figure A31: Minitab statistical software generated normal probability plot, plot of residuals and histogram for assessing direct tensile strength behavior of CSA cement containing 50 weight % anhydrite and 50 weight % gypsum as a source of calcium sulfate cured at constant 50% relative humidity and ambient laboratory temperature

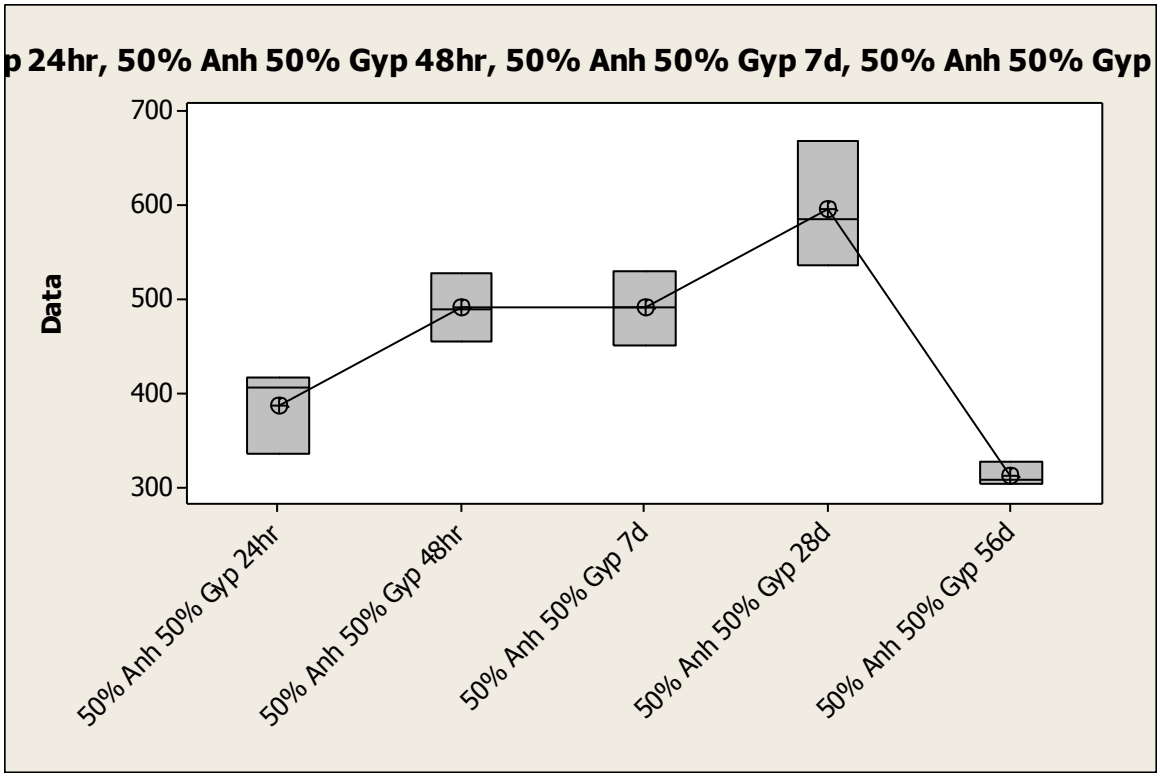

Figure A32: Minitab statistical software generated boxplot for assessing direct tensile strength behavior of CSA cement containing 50 weight % anhydrite and 50 weight % gypsum as a source of calcium sulfate cured at constant 50% relative humidity and ambient laboratory temperature

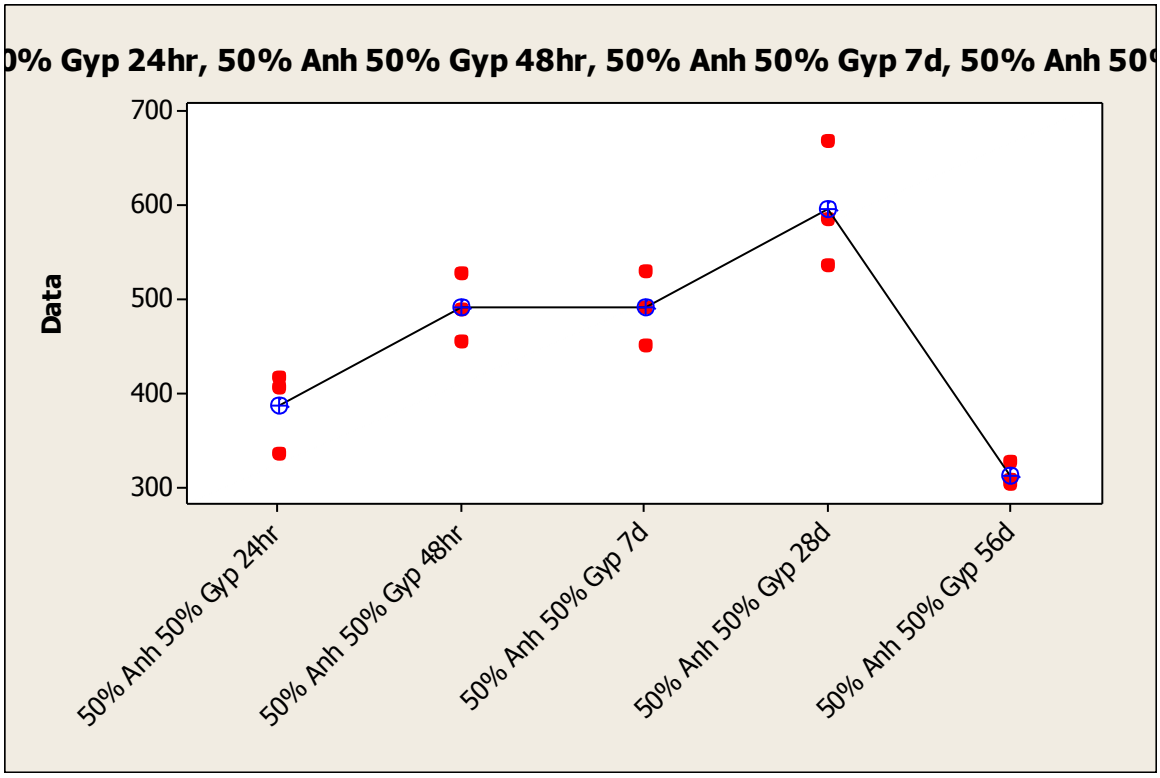

Figure A33: Minitab statistical software generated individual value plot for assessing direct tensile strength behavior of CSA cement containing 50 weight % anhydrite and 50 weight % gypsum as a source of calcium sulfate cured at constant 50% relative humidity and ambient laboratory temperature

Experiment 4: Compressive Strength Behavior of CSA Cement Mortar Containing Half Anhydrite and Half Gypsum as a Source of Calcium Sulfate

mortar = CSA cement mortar containing 50% anhydrite and 50% gypsum

curing regimen = 24hrs, 48hrs, 7d, 461d and 537d at ambient laboratory temperature and constant 50% relative humidity

Test method ASTM C109 was followed for data collection. Three samples were cast and tested for each mortar formulation. Samples were stored at ambient laboratory temperature and constant 50% relative humidity from the time of removal from molds to the time of testing. A CSA cement mortar containing 50 weight % anhydrite and 50 weight % gypsum as a source of calcium sulfate was tested after curing at constant low humidity for various durations in an effort to assess compressive strength behavior versus time.

160g Anh 160g Gyp 24hr 50Hr	160g Anh 160g Gyp 48hr 50Hr	160g Anh 160g Gyp 7d 50Hr	160g Anh 160g Gyp 461d 50Hr	160g Anh 160g Gyp 537d 50Hr
6231	9332	12169	12647	9776
6029	9912	12087	11937	10776
5876	9369	12292	12633	9848

Table A15: Compressive strength testing data (psi) for CSA cement mortar containing half anhydrite and half gypsum as a source of calcium sulfate cured at constant 50% relative humidity

H_o: Curing at ambient laboratory temperature and constant 50% relative humidity does not effect the average compressive strength of CSA cement mortar containing 50 weight % anhydrite and 50 weight % gypsum as a source of calcium sulfate ($u_i = u_j$)

H_a: Curing at ambient laboratory temperature and constant 50% relative humidity effects the average compressive strength of CSA cement mortar containing 50 weight % anhydrite and 50 weight % gypsum as a source of calcium sulfate (u_i does not equal u_j)

One-way ANOVA was used to test the equality of the population means for compressive strength testing of the CSA cement mortar containing half anhydrite and half gypsum when cured for 24 hours, 48 hours, 7 days, 461 days and 537 days at ambient laboratory temperature and constant 50% relative humidity. Results from ANOVA are: $F(4/10) = 158.77$, $p < 0.001$, pooled standard deviation = 353.2 and $R^2 = 98.45\%$. Based upon the F value of 158.77 and corresponding p-value < 0.001, if an alpha value of 0.05 is chosen, it is safe to reject the null hypothesis and ultimately conclude that at least two means differ from one another, and this inequality is highly unlikely due to chance. Further statistical comparison methods utilizing Tukey's Honestly Significant Difference test along with Fisher's test can be seen in Table A16. In Table A16, average compressive strength values for specific curing regimens not sharing the same letter strength classification are significantly different. Therefore, compressive strength loss versus time for the CSA cement mortar containing 50 weight % anhydrite and 50 weight % gypsum is statistically significant for the period from 461 days to 537 days.

Post Hoc Statistical Analysis	Tukey	Fisher
24 hour	C	C
48 hour	B	B
7 days	A	A
461 days	A	A
537 days	B	B

Table A16: Compressive strength classifications as assigned by statistical comparison methods for the CSA cement mortar containing half anhydrite and half gypsum in Table 2. Compressive strength results for specific curing regimens not sharing the same letter are significantly different.

One-way ANOVA: 160g Anh 160, 160g Anh 160, 160g Anh 160, 160g Anh 160, ...

Source DF SS MS F P
Factor 4 79210860 19802715 158.77 0.000
Error 10 1247271 124727
Total 14 80458131

S = 353.2 R-Sq = 98.45% R-Sq(adj) = 97.83%

Level N Mean StDev
160g Anh 160g Gyp 24hr 5 3 6045 178
160g Anh 160g Gyp 48hr 5 3 9538 325
160g Anh 160g Gyp 7d 50H 3 12183 103
160g Anh 160g Gyp 461d 5 3 12406 406
160g Anh 160g Gyp 537d 5 3 10133 558

Individual 95% CIs For Mean Based on Pooled StDev

```
Level                --+---------+---------+---------+-------
160g Anh 160g Gyp 24hr 5   (-*-)
160g Anh 160g Gyp 48hr 5               (--*-)
160g Anh 160g Gyp 7d 50H                        (-*-)
160g Anh 160g Gyp 461d 5                        (-*-)
160g Anh 160g Gyp 537d 5                 (--*-)
                   --+---------+---------+---------+-------
                   6000      8000      10000     12000
```

Pooled StDev = 353

Grouping Information Using Tukey Method

	N	Mean	Grouping
160g Anh 160g Gyp 461d 50Hr	3	12405.7	A
160g Anh 160g Gyp 7d 50Hr	3	12182.7	A

160g Anh 160g Gyp 537d 50Hr 3 10133.3   B
160g Anh 160g Gyp 48hr 50Hr 3   9537.7   B
160g Anh 160g Gyp 24hr 50Hr 3   6045.3   C

Means that do not share a letter are significantly different.

Tukey 95% Simultaneous Confidence Intervals
All Pairwise Comparisons

Individual confidence level = 99.18%

160g Anh 160g Gyp 24hr 50Hr subtracted from:

	Lower	Center	Upper
160g Anh 160g Gyp 48hr 5	2544.2	3492.3	4440.5
160g Anh 160g Gyp 7d 50H	5189.2	6137.3	7085.5
160g Anh 160g Gyp 461d 5	5412.2	6360.3	7308.5
160g Anh 160g Gyp 537d 5	3139.9	4088.0	5036.1

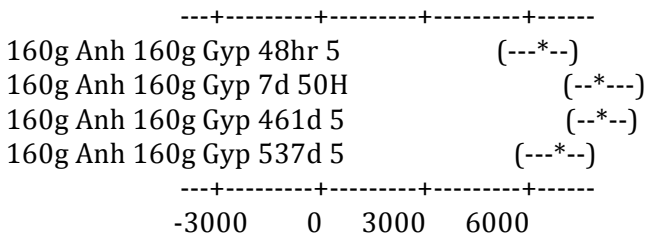

160g Anh 160g Gyp 48hr 50Hr subtracted from:

	Lower	Center	Upper
160g Anh 160g Gyp 7d 50H	1696.9	2645.0	3593.1
160g Anh 160g Gyp 461d 5	1919.9	2868.0	3816.1
160g Anh 160g Gyp 537d 5	-352.5	595.7	1543.8

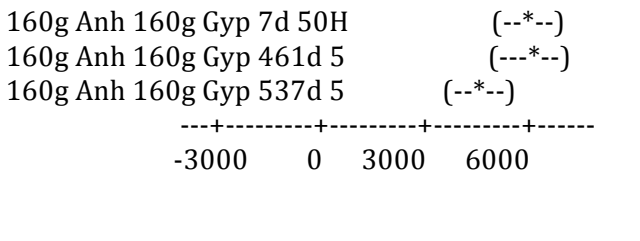

160g Anh 160g Gyp 7d 50Hr subtracted from:

	Lower	Center	Upper
160g Anh 160g Gyp 461d 5	-725.1	223.0	1171.1
160g Anh 160g Gyp 537d 5	-2997.5	-2049.3	-1101.2

```
                  ---+---------+---------+---------+------
160g Anh 160g Gyp 461d 5            (--*--)
160g Anh 160g Gyp 537d 5      (--*--)
                  ---+---------+---------+---------+------
                 -3000       0     3000     6000
```

160g Anh 160g Gyp 461d 50Hr subtracted from:

	Lower	Center	Upper
160g Anh 160g Gyp 537d 5	-3220.5	-2272.3	-1324.2

```
                  ---+---------+---------+---------+------
160g Anh 160g Gyp 537d 5     (--*---)
                  ---+---------+---------+---------+------
                 -3000       0     3000     6000
```

Grouping Information Using Fisher Method

	N	Mean	Grouping
160g Anh 160g Gyp 461d 50Hr	3	12405.7	A
160g Anh 160g Gyp 7d 50Hr	3	12182.7	A
160g Anh 160g Gyp 537d 50Hr	3	10133.3	B
160g Anh 160g Gyp 48hr 50Hr	3	9537.7	B
160g Anh 160g Gyp 24hr 50Hr	3	6045.3	C

Means that do not share a letter are significantly different.

Fisher 95% Individual Confidence Intervals
All Pairwise Comparisons

Simultaneous confidence level = 75.51%

160g Anh 160g Gyp 24hr 50Hr subtracted from:

	Lower	Center	Upper
160g Anh 160g Gyp 48hr 5	2849.8	3492.3	4134.8
160g Anh 160g Gyp 7d 50H	5494.8	6137.3	6779.8
160g Anh 160g Gyp 461d 5	5717.8	6360.3	7002.8
160g Anh 160g Gyp 537d 5	3445.5	4088.0	4730.5

```
                  --+---------+---------+---------+-------
160g Anh 160g Gyp 48hr 5                (--*-)
160g Anh 160g Gyp 7d 50H                      (-*--)
160g Anh 160g Gyp 461d 5                      (-*-)
160g Anh 160g Gyp 537d 5                 (--*-)
                  --+---------+---------+---------+-------
                 -3000       0     3000     6000
```

160g Anh 160g Gyp 48hr 50Hr subtracted from:

	Lower	Center	Upper
160g Anh 160g Gyp 7d 50H	2002.5	2645.0	3287.5
160g Anh 160g Gyp 461d 5	2225.5	2868.0	3510.5
160g Anh 160g Gyp 537d 5	-46.8	595.7	1238.2

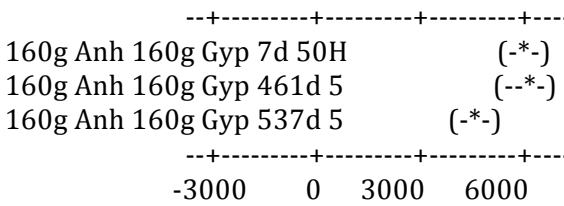

160g Anh 160g Gyp 7d 50Hr subtracted from:

	Lower	Center	Upper
160g Anh 160g Gyp 461d 5	-419.5	223.0	865.5
160g Anh 160g Gyp 537d 5	-2691.8	-2049.3	-1406.8

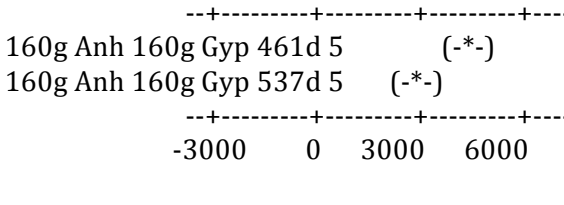

160g Anh 160g Gyp 461d 50Hr subtracted from:

	Lower	Center	Upper
160g Anh 160g Gyp 537d 5	-2914.8	-2272.3	-1629.8

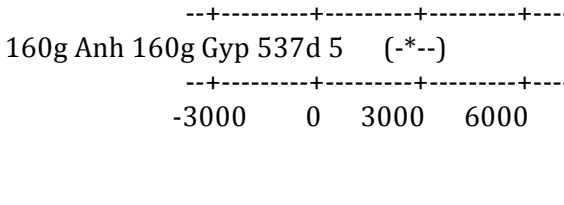

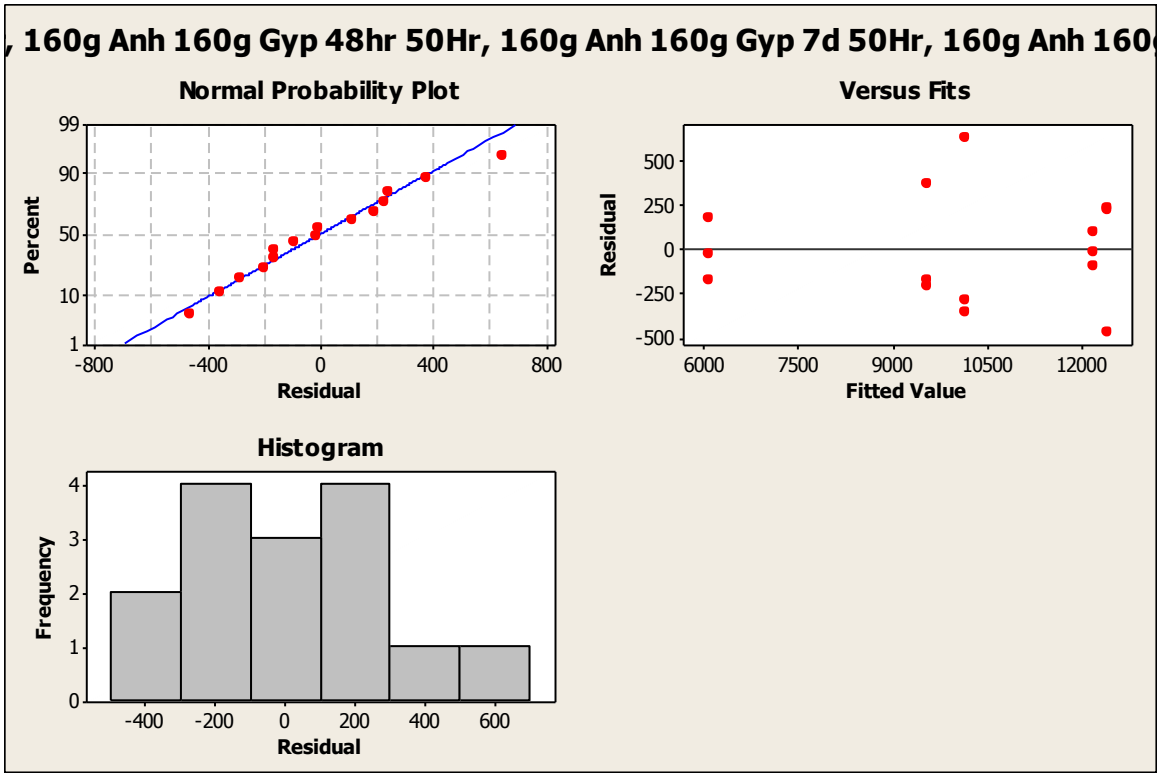

Figure A34: Minitab statistical software generated normal probability plot, plot of residuals and histogram for assessing compressive strength behavior of CSA cement containing 50 weight % anhydrite and 50 weight % gypsum as a source of calcium sulfate cured at constant 50% relative humidity and ambient laboratory temperature

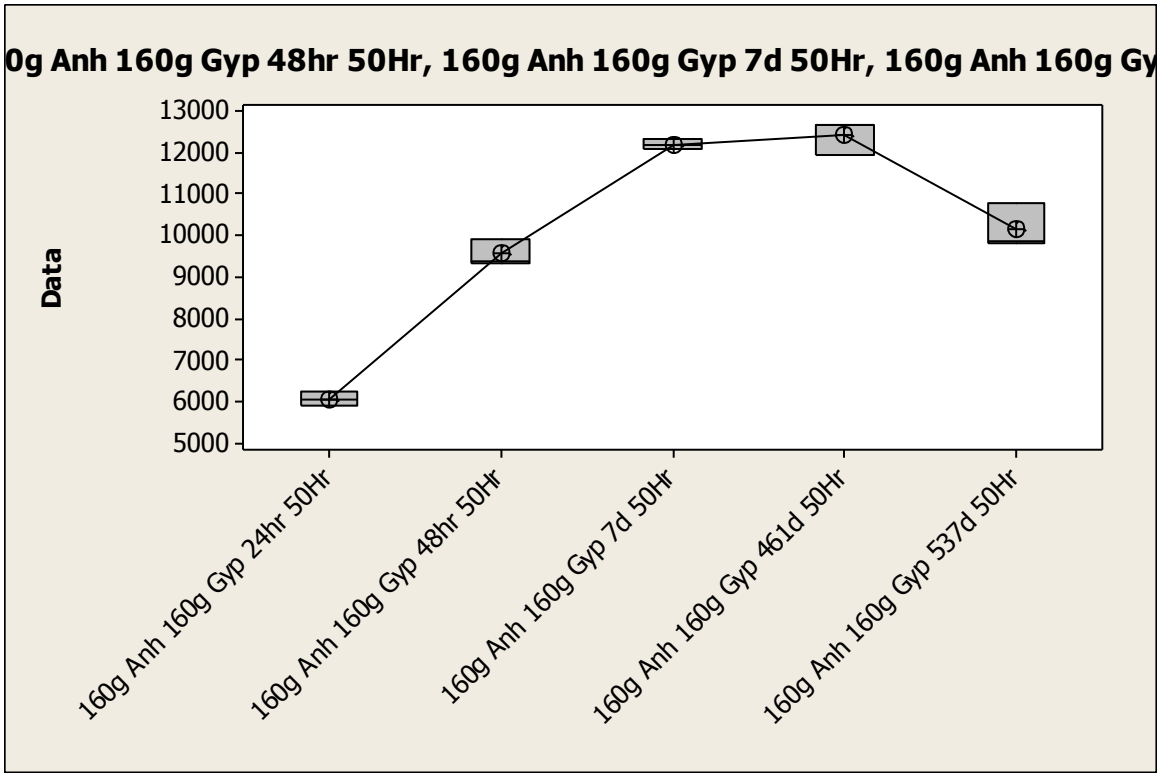

Figure A35: Minitab statistical software generated boxplot for assessing compressive strength behavior of CSA cement containing 50 weight % anhydrite and 50 weight % gypsum as a source of calcium sulfate cured at constant 50% relative humidity and ambient laboratory temperature

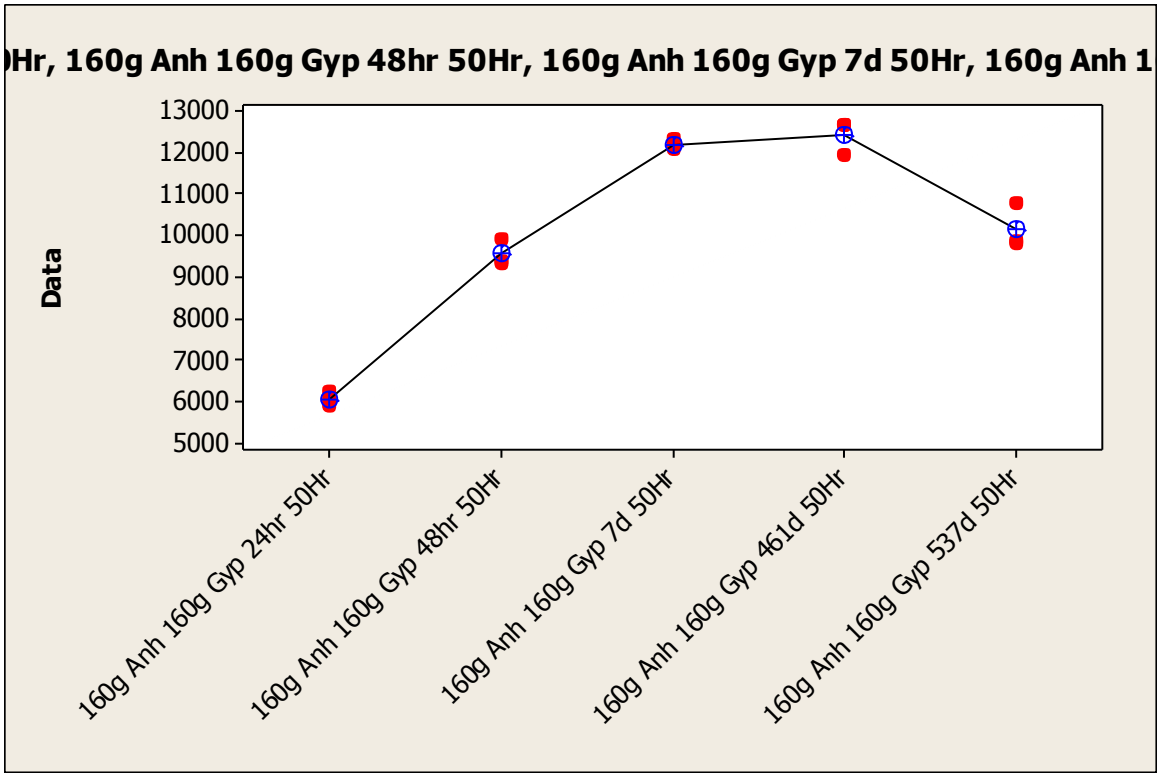

Figure A36: Minitab statistical software generated individual value plot for assessing compressive strength behavior of CSA cement containing 50 weight % anhydrite and 50 weight % gypsum as a source of calcium sulfate cured at constant 50% relative humidity and ambient laboratory temperature

Experiment 5: Compressive Strength Behavior of CSA Cement Mortar Containing Gypsum as a Source of Calcium Sulfate

mortar = CSA cement mortar containing gypsum

curing regimen = 24hrs, 48hrs, 7d, 460d and 537d at ambient laboratory temperature and constant 50% relative humidity

Test method ASTM C109 was followed for data collection. Three samples were cast and tested for each mortar formulation. Samples were stored at ambient laboratory temperature and constant 50% relative humidity from the time of removal from molds to the time of testing. A CSA cement mortar containing solely gypsum as a source of calcium sulfate was tested after curing at constant low humidity for various durations in an effort to assess compressive strength behavior versus time.

160g Gyp 24hr 50Hr	160g Gyp 48hr 50Hr	160g Gyp 7d 50Hr	160g Gyp 460d 50Hr	160g Gyp 537d 50Hr
6364	9994	11824	9863	6802
6040	9457	11116	9485	6599
6011	9485	12330	9398	7150

Table A17: Compressive strength testing data (psi) for CSA cement mortar containing gypsum as a source of calcium sulfate cured at constant 50% relative humidity

H_o: Curing at ambient laboratory temperature and constant 50% relative humidity does not effect the average compressive strength of CSA cement mortar containing gypsum as a source of calcium sulfate ($u_i = u_j$)

H_a: Curing at ambient laboratory temperature and constant 50% relative humidity effects the average compressive strength of CSA cement mortar containing gypsum as a source of calcium sulfate (u_i does not equal u_j)

One-way ANOVA was used to test the equality of the population means for compressive strength testing of the CSA cement mortar containing solely gypsum when cured for 24 hours, 48 hours, 7 days, 460 days and 537 days at ambient laboratory temperature and constant 50% relative humidity. Results from ANOVA are: $F(4/10) = 122.7$, $p < 0.001$, pooled standard deviation = 357.9 and $R^2 = 98\%$. Based upon the F value of 122.7 and corresponding p-value < 0.001, if an alpha value of 0.05 is chosen, it is safe to reject the null hypothesis and ultimately conclude that at least two means differ from one another, and this inequality is highly unlikely due to chance. Further statistical comparison methods utilizing Tukey's Honestly Significant Difference test along with Fisher's test can be seen in Table A18. In Table A18, average compressive strength values for specific curing regimens not sharing the same letter strength classification are significantly different. Therefore, compressive strength loss versus time for the CSA cement mortar containing solely gypsum is statistically significant for the period from 7 days to 537 days.

Post Hoc Statistical Analysis	Tukey	Fisher
24 hour	C	D
48 hour	B	B
7 days	A	A
460 days	B	B
537 days	C	C

Table A18: Compressive strength classifications as assigned by statistical comparison methods for the CSA cement mortar containing solely gypsum in Table 2. Compressive strength results for specific curing regimens not sharing the same letter are significantly different.

One-way ANOVA: 160g Gyp 24h, 160g Gyp 48h, 160g Gyp 7d , 160g Gyp 460, ...

Source DF SS MS F P
Factor 4 62860531 15715133 122.70 0.000
Error 10 1280783 128078
Total 14 64141314

S = 357.9 R-Sq = 98.00% R-Sq(adj) = 97.20%

Individual 95% CIs For Mean Based on Pooled StDev

```
Level              N   Mean  StDev  --+---------+---------+---------+-------
160g Gyp 24hr 50Hr 3   6138    196  (--*-)
160g Gyp 48hr 50Hr 3   9645    302            (-*--)
160g Gyp 7d 50Hr   3  11757    610                  (--*-)
160g Gyp 460d 50Hr 3   9582    247             (-*-)
160g Gyp 537d 50Hr 3   6850    279     (-*--)
                      --+---------+---------+---------+-------
                      6000     8000    10000    12000
```

Pooled StDev = 358

Grouping Information Using Tukey Method

```
                   N     Mean  Grouping
160g Gyp 7d 50Hr   3  11756.7  A
160g Gyp 48hr 50Hr 3   9645.3    B
160g Gyp 460d 50Hr 3   9582.0    B
160g Gyp 537d 50Hr 3   6850.3     C
160g Gyp 24hr 50Hr 3   6138.3     C
```

Means that do not share a letter are significantly different.

Tukey 95% Simultaneous Confidence Intervals
All Pairwise Comparisons

Individual confidence level = 99.18%

160g Gyp 24hr 50Hr subtracted from:

	Lower	Center	Upper
160g Gyp 48hr 50Hr	2546.2	3507.0	4467.8
160g Gyp 7d 50Hr	4657.5	5618.3	6579.1
160g Gyp 460d 50Hr	2482.9	3443.7	4404.5
160g Gyp 537d 50Hr	-248.8	712.0	1672.8

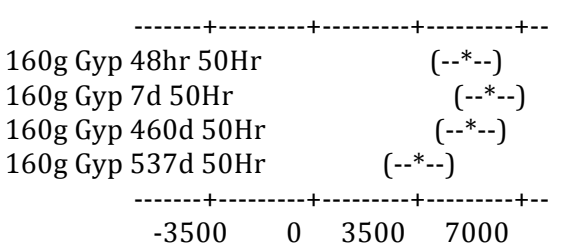

160g Gyp 48hr 50Hr subtracted from:

	Lower	Center	Upper
160g Gyp 7d 50Hr	1150.5	2111.3	3072.1
160g Gyp 460d 50Hr	-1024.1	-63.3	897.5
160g Gyp 537d 50Hr	-3755.8	-2795.0	-1834.2

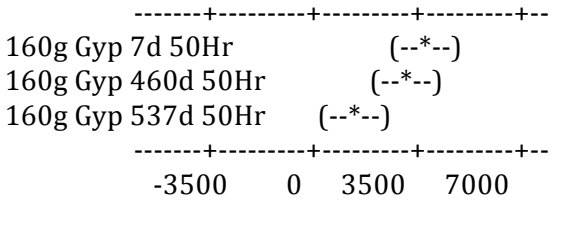

160g Gyp 7d 50Hr subtracted from:

	Lower	Center	Upper
160g Gyp 460d 50Hr	-3135.5	-2174.7	-1213.9
160g Gyp 537d 50Hr	-5867.1	-4906.3	-3945.5

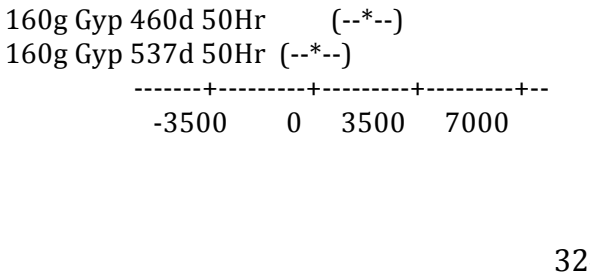

160g Gyp 460d 50Hr subtracted from:

	Lower	Center	Upper
160g Gyp 537d 50Hr	-3692.5	-2731.7	-1770.9

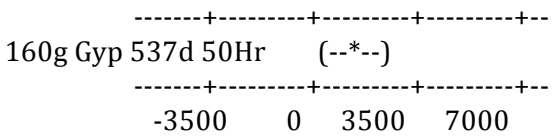

Grouping Information Using Fisher Method

	N	Mean	Grouping
160g Gyp 7d 50Hr	3	11756.7	A
160g Gyp 48hr 50Hr	3	9645.3	B
160g Gyp 460d 50Hr	3	9582.0	B
160g Gyp 537d 50Hr	3	6850.3	C
160g Gyp 24hr 50Hr	3	6138.3	D

Means that do not share a letter are significantly different.

Fisher 95% Individual Confidence Intervals
All Pairwise Comparisons

Simultaneous confidence level = 75.51%

160g Gyp 24hr 50Hr subtracted from:

	Lower	Center	Upper
160g Gyp 48hr 50Hr	2855.9	3507.0	4158.1
160g Gyp 7d 50Hr	4967.3	5618.3	6269.4
160g Gyp 460d 50Hr	2792.6	3443.7	4094.7
160g Gyp 537d 50Hr	60.9	712.0	1363.1

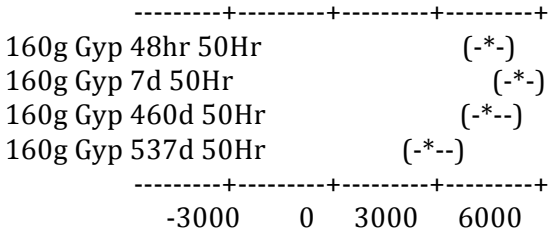

160g Gyp 48hr 50Hr subtracted from:

	Lower	Center	Upper

```
160g Gyp 7d 50Hr    1460.3   2111.3   2762.4
160g Gyp 460d 50Hr  -714.4    -63.3    587.7
160g Gyp 537d 50Hr -3446.1  -2795.0  -2143.9

             ---------+---------+---------+---------+
160g Gyp 7d 50Hr                       (-*-)
160g Gyp 460d 50Hr                  (-*-)
160g Gyp 537d 50Hr           (-*-)
             ---------+---------+---------+---------+
               -3000       0     3000     6000
```

160g Gyp 7d 50Hr subtracted from:

```
              Lower   Center    Upper
160g Gyp 460d 50Hr  -2825.7  -2174.7  -1523.6
160g Gyp 537d 50Hr  -5557.4  -4906.3  -4255.3

             ---------+---------+---------+---------+
160g Gyp 460d 50Hr            (-*-)
160g Gyp 537d 50Hr  (--*-)
             ---------+---------+---------+---------+
               -3000       0     3000     6000
```

160g Gyp 460d 50Hr subtracted from:

```
              Lower   Center    Upper
160g Gyp 537d 50Hr  -3382.7  -2731.7  -2080.6

             ---------+---------+---------+---------+
160g Gyp 537d 50Hr           (-*-)
             ---------+---------+---------+---------+
               -3000       0     3000     6000
```

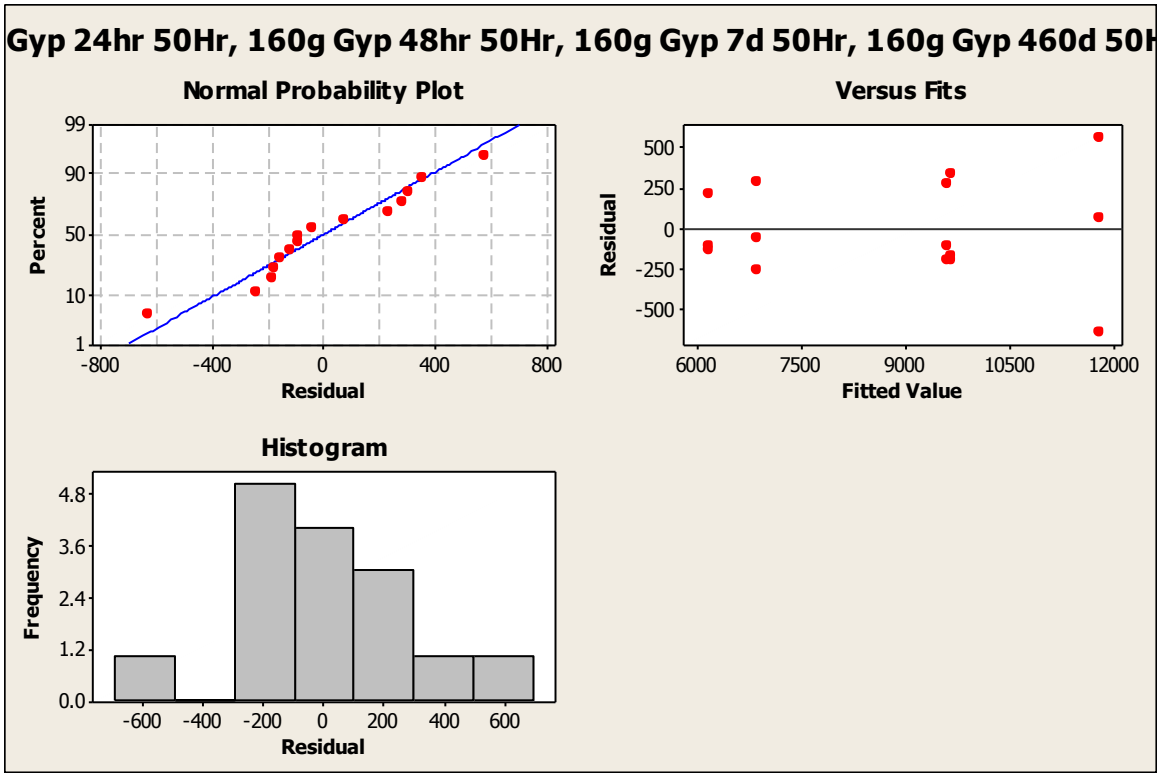

Figure A37: Minitab statistical software generated normal probability plot, plot of residuals and histogram for assessing compressive strength behavior of CSA cement containing gypsum as a source of calcium sulfate cured at constant 50% relative humidity and ambient laboratory temperature

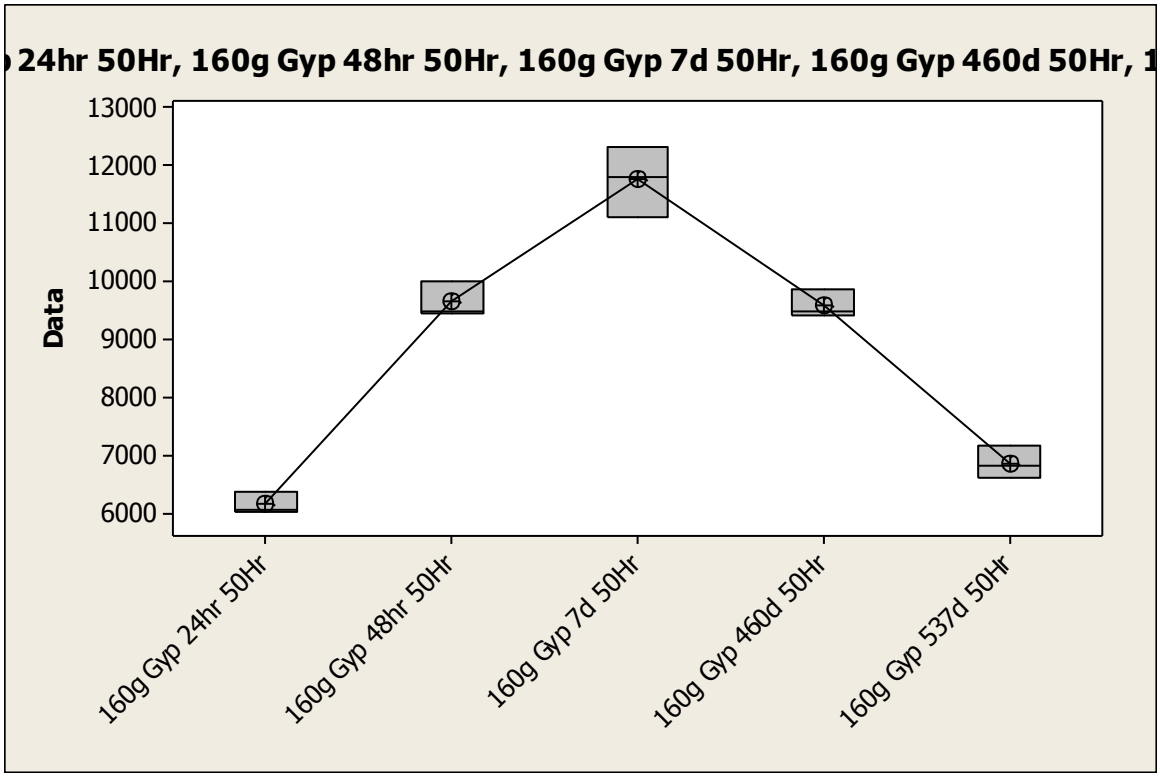

Figure A38: Minitab statistical software generated boxplot for assessing compressive strength behavior of CSA cement containing gypsum as a source of calcium sulfate cured at constant 50% relative humidity and ambient laboratory temperature

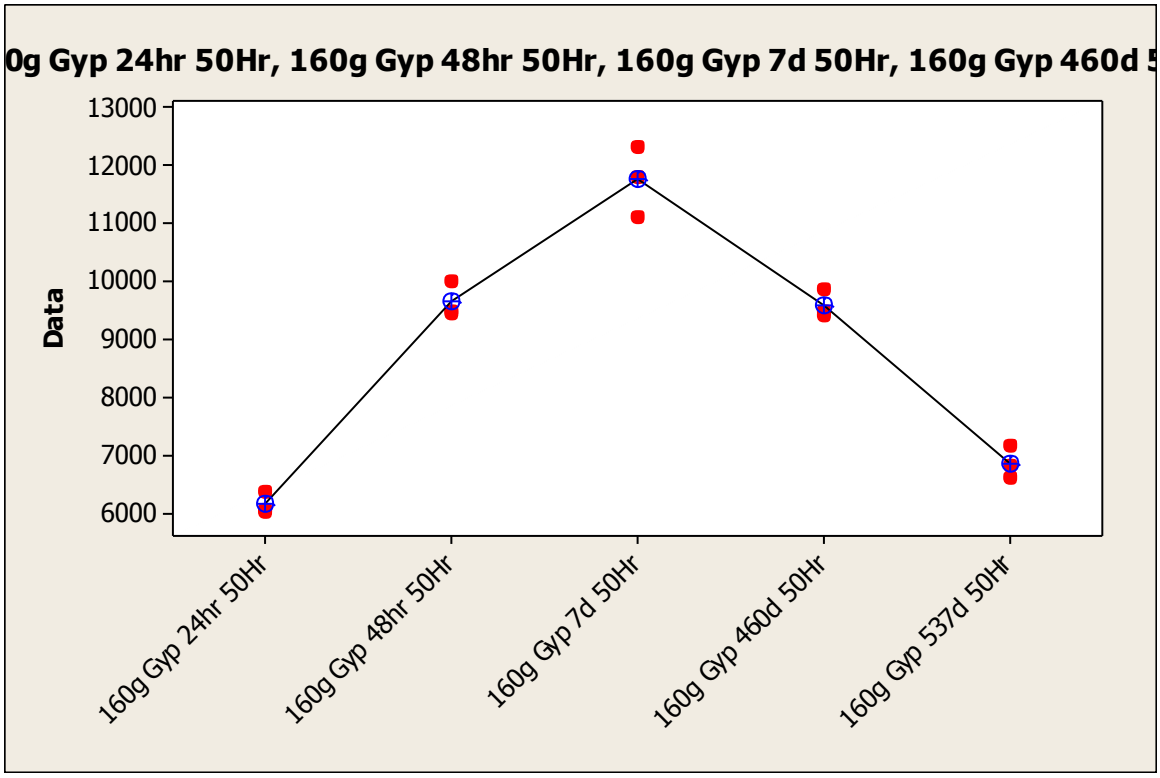

Figure A39: Minitab statistical software generated individual value plot for assessing compressive strength behavior of CSA cement containing gypsum as a source of calcium sulfate cured at constant 50% relative humidity and ambient laboratory temperature

Appendix B: Curve Fitting

Curve fitting is known as a statistical procedure whose purpose is to define a relatively smooth curve that describes the behavior of the response variable usually without any reference to a meaningful model (Freund et al, 2006). A very popular and easily implemented method for curve fitting is the use of a polynomial model, which is readily handled by ordinary linear regression methods (Freund et al, 2006). Though many applications exist for curve fitting, it seems the most frequently applied is fitting time series data (Freund et al, 2006).

A recommended first step in the process of curve fitting is generation of a scatter plot (DeLurgio, 1998, Freund et al, 2006, Riggs, 1994). The scatter plot shape can be utilized for selecting an appropriate polynomial equation for curve fitting. An example of a polynomial model with one independent variable, x, is written below (Freund et al, 2006):

$$y = B_o + B_1x + B_2x^2 + B_3x^3 + \ldots + B_mx^m + e$$

where,

y is the response variable,

x is the independent variable,

B_i, i = 0,1,2,…,m, are the coefficients for the i^{th} power of x,

e is the random error, defined as usual.

The model as written is referred to as an "m^{th} order polynomial", where m can be any value; however, values of m less than 4 are most commonly used in practice (Freund et al, 2006). The model utilizes sequential sums of squares (Freund et al, 2006). The method for determining sequential sums of squares for the quadratic equation is that obtained by adding that term to the model containing the intercept and linear term, and so forth (Freund et al, 2006). It is important to note polynomial models are simply a curve fitting process and normally do not correspond to some physical model; therefore, the fitted curve should not be used for extrapolation purposes (Freund et al, 2006).

The F value is used to measure the overall statistical significance of the relationship (DeLurgio, 1998). Typically, but not always, higher F-values represent more significant relationships (DeLurgio, 1998). The significance level denotes the probability that the calculated F-value would be this high, or higher, if no relationship existed between the dependent and independent variables (DeLurgio, 1998). The sum of squared errors is literally that, which is also the value to be minimized through selection of model parameters (DeLurgio, 1998). The standard error of the estimate, S_{yx}, the standard deviation of y given x values, measures the scatter of actual y values about the regression line (DeLurgio, 1998). The standard error of the estimate is an absolute measure of the fit of a model because its value is dependent on the scale of y (DeLurgio, 1998). The adjusted coefficient of determination, $\bar{R}^2$, compares S^2_{yx} to total variance (S^2_y) (DeLurgio, 1998). The adjusted coefficient of determination equals the proportion of the variance in the dependent variable y that is explained or eliminated through the relationship with the independent variable x (DeLurgio, 1998).

Total Variance = Explained Variance + Unexplained Variance

S^2_y = Explained Variance + S^2_{yx}

The adjusted $\bar{R}^2$ is referred to as being adjusted because the denominator of S_{yx} is adjusted for model complexity as measured by the degrees of freedom (DeLurgio, 1998). The unadjusted R^2 is not adjusted for model complexity while neither the numerator nor the denominator is adjusted for the loss of degrees of freedom (DeLurgio, 1998). As a result, the unadjusted R^2 may become larger and larger as more variables are added to a model while the adjusted $\bar{R}^2$ may be decreasing because of the degrees of freedom related term, (n-k) (DeLurgio, 1998). Therefore, the adjusted $\bar{R}^2$ is typically the better statistic (DeLurgio, 1998). The standard error of regression coefficient measures how much individual b_i's vary about individual means, b (DeLurgio, 1998). The question of statistical significance is answered by comparing the coefficient b value to its standard error, s_b, where b/s_b is known as the t-value (DeLurgio, 1998).

In regression analysis, the total sum of squares equals the summation of regression sum of squares and error sum of squares (DeLurgio, 1998). Explained variation equals the regression sum of squares (RSS) (DeLurgio, 1998). Unexplained variation equals the error sum of squares (ESS). The overall significance of a regression relationship can be tested with the ratio of explained variation to unexplained variation (DeLurgio, 1998). Such a variance ratio follows an F-distribution with (k-1) and (n-k) degrees of freedom in the numerator and denominator, respectively (DeLurgio, 1998). As previously mentioned, a high F-value is often an indicator of differences between two variances (DeLurgio, 1998).

The plot of residuals offers an opportunity to visualize the scatter of individual data points about the regression line. Typically, residual plots associated with good curve fits display data points somewhat evenly and randomly distributed about the regression line. Checking the residual plots is an important step for determining model validity as certain fitted polynomials may display a high R^2 while also demonstrating unbalanced distribution of data points with respect to the regression line. Even though the curve possesses a high R^2 value, the unbalanced distribution of data points with respect to the regression line as displayed in the plot of residuals may suggest the relationship is not nearly as significant as the unadjusted coefficient of determination suggests.

Experiment 1: Direct Tensile Strength Behavior of CSA Cement Mortar Containing Anhydrite as a Source of Calcium Sulfate

mortar = CSA cement mortar containing solely anhydrite as a source of calcium sulfate

curing regimen = 24hrs, 48hrs, 7d, 28d, 56d and 109d at ambient laboratory temperature and constant 50% relative humidity

Test method ASTM C307 was followed for data collection. Three samples were cast and tested for each mortar formulation. Samples were stored at ambient laboratory temperature and constant 50% relative humidity from the time of removal from molds to the time of testing. A CSA cement mortar containing solely anhydrite as a source of calcium sulfate was tested after curing at constant low humidity for various durations in an effort to assess direct tensile strength behavior versus time.

The scatter plot displayed in Figure B1 suggests the relationship between direct tensile strength and time is quadratic. Both Minitab and SAS statistical software were utilized to fit a quadratic equation to the data set displayed in Table B1. The resulting regression equation is below:

Tensile Strength (psi) = 401.8 + 7.263 Time (days) - 0.05615 Time (days)**2

The coefficient of determination, R^2, equals 50.6%. The adjusted coefficient of determination, adjusted ~~R~~^{2}, equals 44%. The standard error of the regression equals 87.96. The standard error of one way ANOVA for the same data set equals 31.91. The plot of residuals suggests the data points are not somewhat evenly distributed about the fitted regression line. The low values for both R^2 and adjusted ~~R~~^{2} suggest the fitted quadratic equation is not a good predictor of tensile strength behavior versus time for the range of data. Additionally, the plot of residuals suggests the fitted equation is not completely ideal for describing the relationship between direct tensile strength versus time for the CSA cement mortar containing anhydrite cured at 23^{o}C and 50% relative humidity. Furthermore, the broad range between confidence interval lines in relation to the fitted line of Figure B2 further suggests the model is deficient for predicting tensile strength behavior within the range of data. The author theorizes a better relationship between fitted polynomial equations and experimental observations may be obtained for future experiments by increasing both testing frequency and sample size.

x = time (days)	y = strength (psi)
1	270
1	283
1	273
2	453
2	494
2	518
7	516
7	487
7	477
28	628
28	603
28	668
56	543
56	533
56	624
109	502
109	557
109	557

Table B1: Direct tensile strength testing data versus time for CSA cement mortar containing anhydrite as a source of calcium sulfate when cured at 23°C and 50% relative humidity

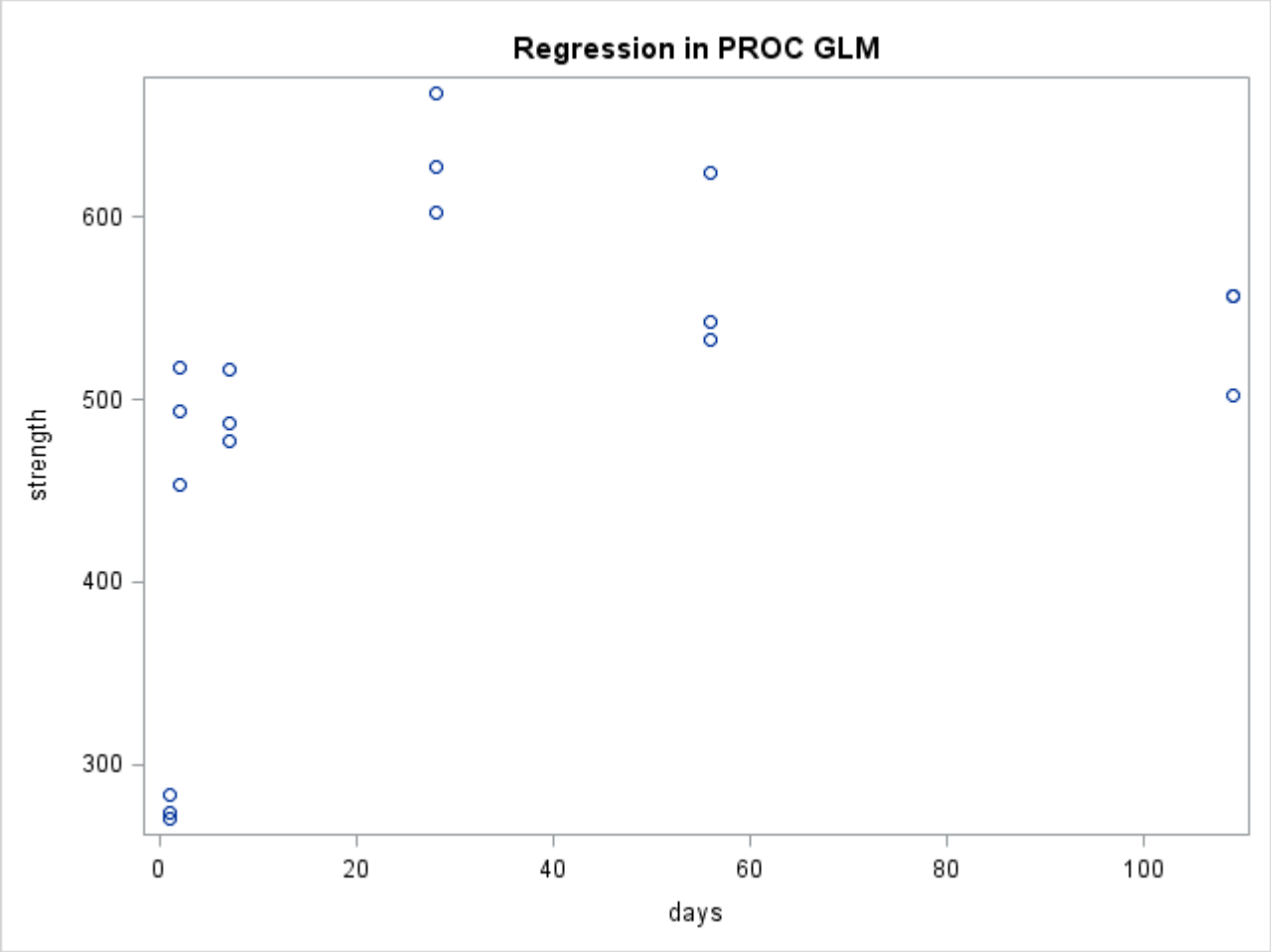

Figure B1: SAS statistical software scatter plot of direct tensile strength (psi) versus time (days) testing for CSA cement mortar containing anhydrite as source of calcium sulfate cured at 23°C and 50% relative humidity

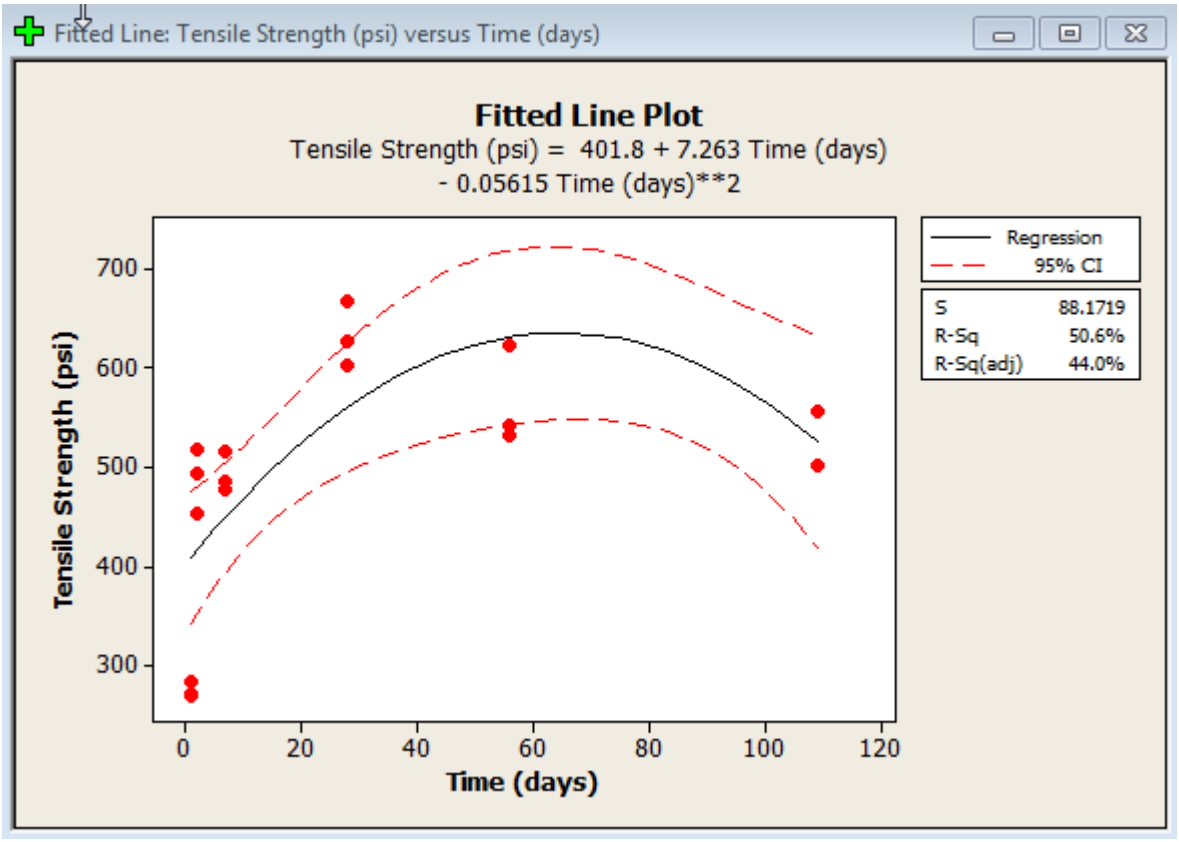

Figure B2: Minitab statistical software generated fitted polynomial curve with tensile strength as dependent variable and time as independent variable for the CSA cement mortar containing anhydrite cured at 23°C and 50% relative humidity

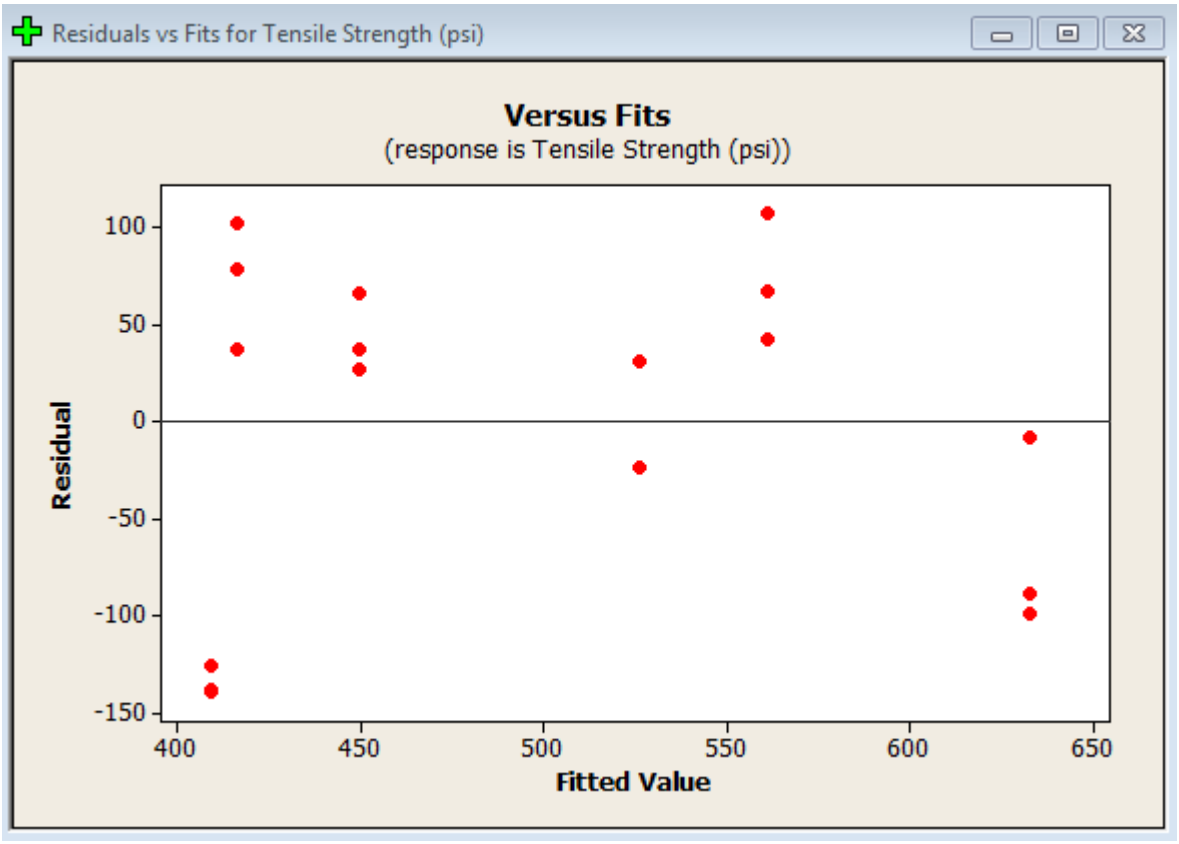

Figure B3: Minitab generated plots of residuals for CSA cement mortar containing anhydrite as source of calcium sulfate tensile strength versus time data for samples cured at 23°C and 50% relative humidity

Minitab Polynomial Regression Analysis: Tensile Strength (psi) versus Time (days)

The regression equation is
Tensile Strength (psi) = 401.8 + 7.263 Time (days) - 0.05615 Time (days)**2

S = 88.1719 R-Sq = 50.6% R-Sq(adj) = 44.0%

Analysis of Variance

Source	DF	SS	MS	F	P
Regression	2	119357	59678.7	7.68	0.005
Error	15	116614	7774.3		
Total	17	235972			

Sequential Analysis of Variance

Source	DF	SS	F	P
Linear	1	44587.5	3.73	0.071
Quadratic	1	74770.0	9.62	0.007

SAS Statistical Software Polynomial Fit Regression Information

Regression in PROC GLM

The GLM Procedure

Number of Observations Read	18
Number of Observations Used	18

Regression in PROC GLM

The GLM Procedure

Dependent Variable: strength

Source	DF	Sum of Squares	Mean Square	F Value	Pr > F
Model	2	118997.2286	59498.6143	7.69	0.0050
Error	15	116065.8825	7737.7255		
Corrected Total	17	235063.1111			

R-Square	Coeff Var	Root MSE	strength Mean
0.506235	17.62028	87.96434	499.2222

Source	DF	Type I SS	Mean Square	F Value	Pr > F
Days	1	44418.76692	44418.76692	5.74	0.0301
days*days	1	74578.46173	74578.46173	9.64	0.0072

Source	DF	Type III SS	Mean Square	F Value	Pr > F
Days	1	102169.8149	102169.8149	13.20	0.0025
days*days	1	74578.4617	74578.4617	9.64	0.0072

Parameter	Estimate	Standard Error	t Value	Pr > |t|
Intercept	402.0381300	32.53039090	12.36	<.0001
Days	7.2524345	1.99585585	3.63	0.0025
days*days	-0.0560794	0.01806357	-3.10	0.0072

Experiment 2: Direct Tensile Strength Behavior of CSA Cement Mortar Containing Gypsum as a Source of Calcium Sulfate

mortar = CSA cement mortar containing solely gypsum

curing regimen = 24hrs, 48hrs, 7d and 28d at ambient laboratory temperature and constant 50% relative humidity

Test method ASTM C307 was followed for data collection. Three samples were cast and tested for each mortar formulation. Samples were stored at ambient laboratory temperature and constant 50% relative humidity from the time of removal from molds to the time of testing. A CSA cement mortar containing solely gypsum as a source of calcium sulfate was tested after curing at constant low humidity for various durations in an effort to assess direct tensile strength behavior versus time.
The scatter plot displayed in Figure B4 suggests the relationship between direct tensile strength and time is quadratic. Both Minitab and SAS statistical software were utilized to fit a quadratic equation to the data set displayed in Table B2. The resulting regression equation is below:

Tensile Strength (psi) = 320.7 + 26.91 Time (days) - 0.9328 Time (days)**2

The coefficient of determination, R^2, equals 69.6%. The adjusted coefficient of determination, adjusted $\cancel{R}^2$, equals 62.8%. The standard error of the regression equals 37.24. The standard error of one way ANOVA for the same data set equals 39.49. The plot of residuals suggests the data points are more or less evenly distributed about the fitted regression line. The values for both R^2 and adjusted $\cancel{R}^2$ suggest the fitted quadratic equation is a decent predictor of tensile strength behavior versus time for the range of data. Additionally, the plot of residuals suggests the fitted equation is somewhat reliable for describing the relationship between direct tensile strength versus time for the CSA cement mortar containing gypsum cured at 23°C and 50% relative humidity. However, the broad range between confidence interval lines in relation to the fitted line of Figure B5 suggests the model is deficient for predicting tensile strength behavior within a large portion of the data range. The author theorizes a better relationship between fitted polynomial equations and experimental observations may be obtained for future experiments by increasing both testing frequency and sample size.

x = time (days)	y = strength (psi)
1	369
1	341
1	329
2	301
2	409
2	404
7	417
7	506
7	467
28	333
28	354
28	342

Table B2: Direct tensile strength testing data versus time for CSA cement mortar containing gypsum as a source of calcium sulfate when cured at 23°C and 50% relative humidity

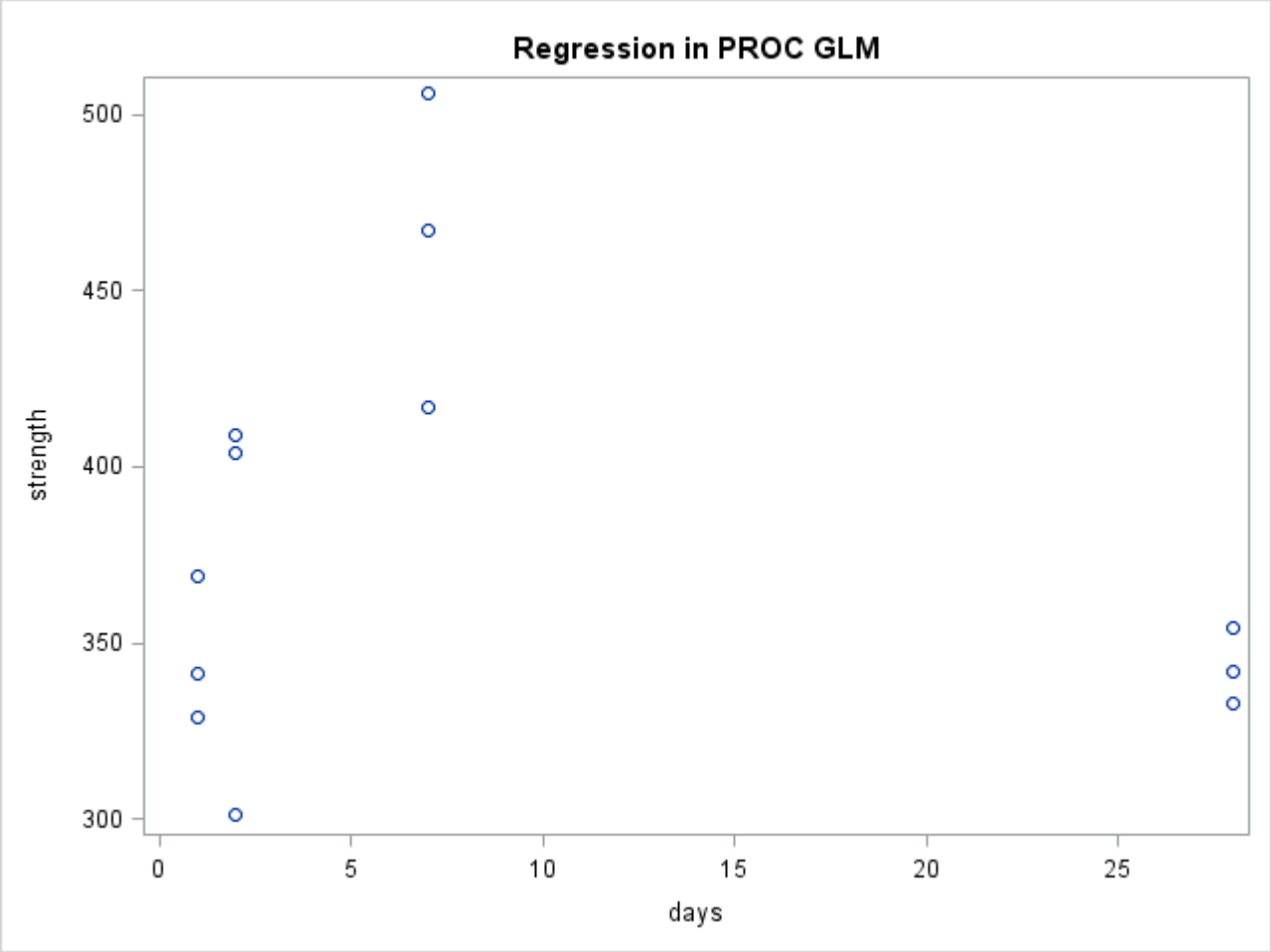

Figure B4: SAS statistical software scatter plot of direct tensile strength (psi) versus time (days) testing for CSA cement mortar containing gypsum as source of calcium sulfate cured at 23°C and 50% relative humidity

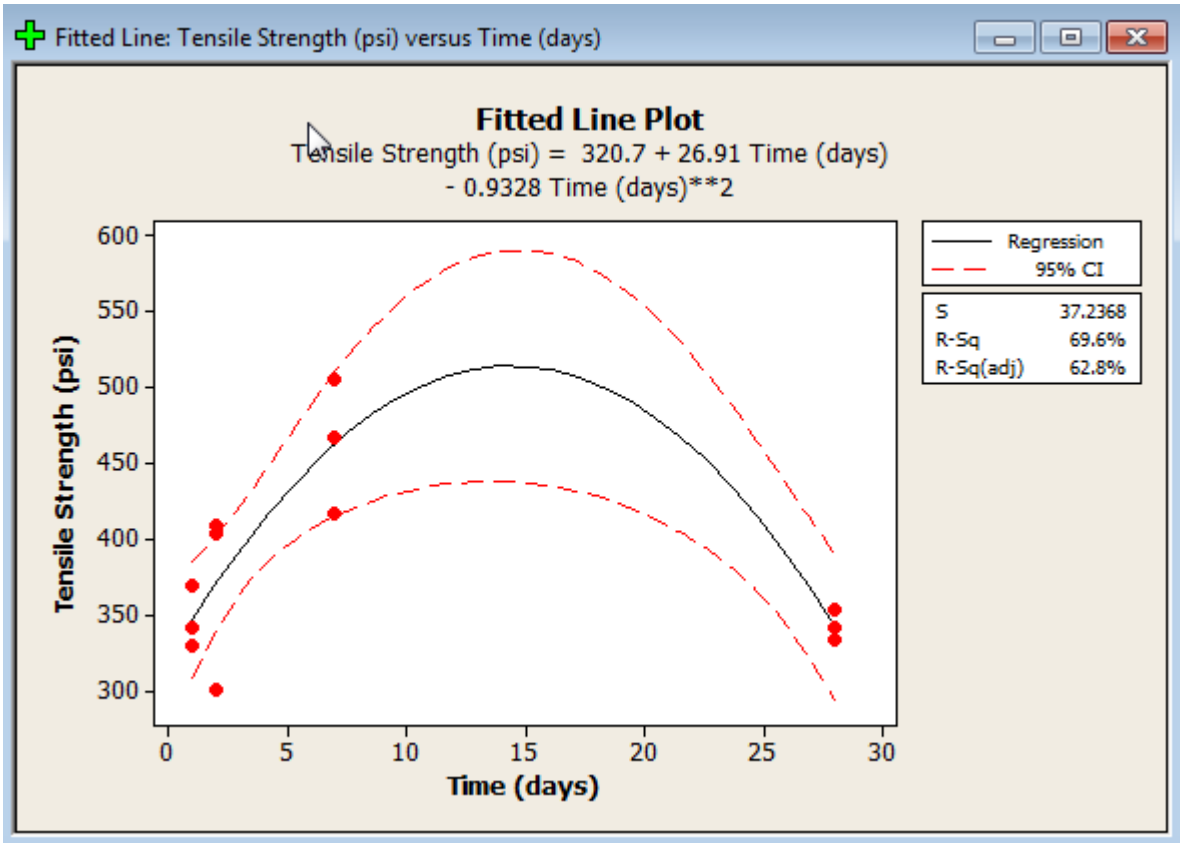

Figure B5: Minitab statistical software generated fitted polynomial curve with tensile strength as dependent variable and time as independent variable for the CSA cement mortar containing gypsum cured at 23°C and 50% relative humidity

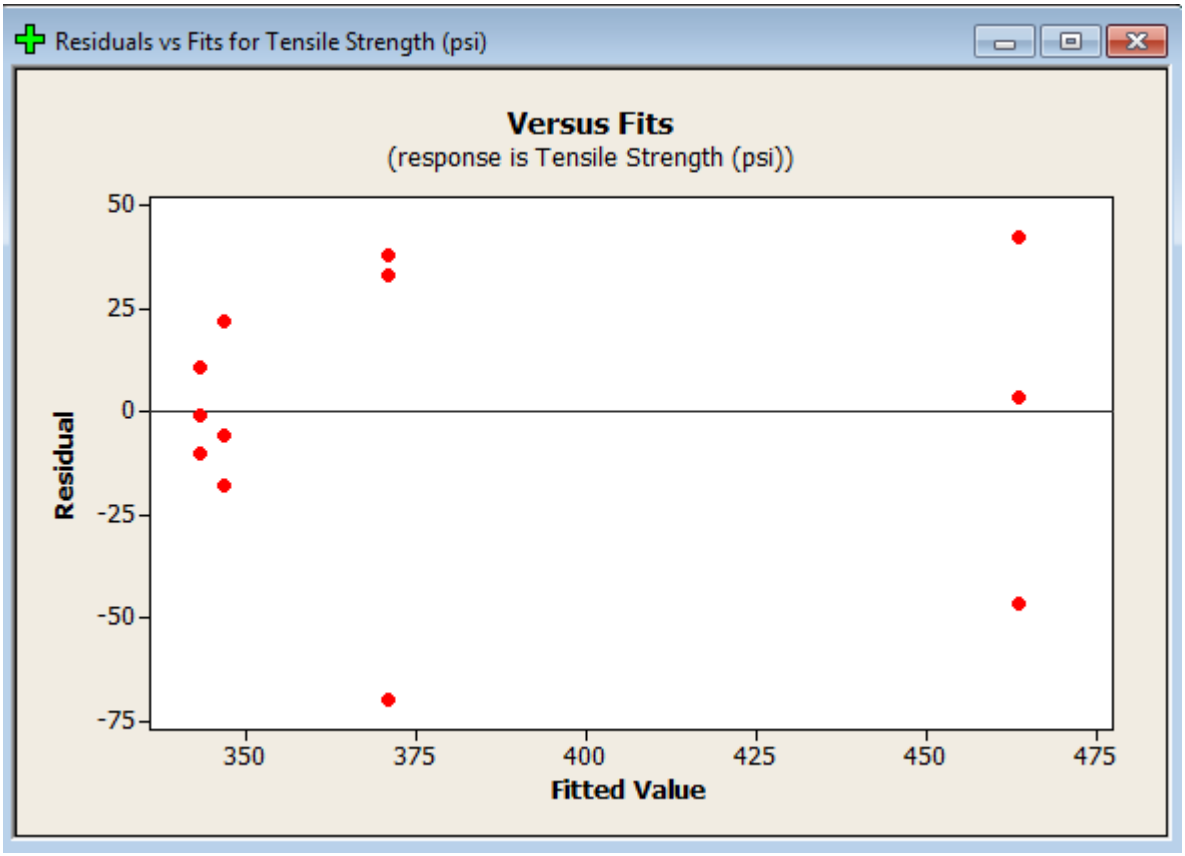

Figure B6: Minitab generated plots of residuals for CSA cement mortar containing anhydrite as source of calcium sulfate tensile strength versus time data for samples cured at 23°C and 50% relative humidity

The regression equation is

Tensile Strength (psi) = 320.7 + 26.91 Time (days) - 0.9328 Time (days)**2

S = 37.2368 R-Sq = 69.6% R-Sq(adj) = 62.8%

Analysis of Variance

Source	DF	SS	MS	F	P
Regression	2	28552.8	14276.4	10.30	0.005
Error	9	12479.2	1386.6		
Total	11	41032.0			

Sequential Analysis of Variance

Source	DF	SS	F	P
Linear	1	1845.3	0.47	0.508
Quadratic	1	26707.5	19.26	0.002

SAS Statistical Software Polynomial Fit Regression Information

Regression in PROC GLM

The GLM Procedure

Number of Observations Read 12

Number of Observations Used 12

The GLM Procedure

Dependent Variable: strength

Source	DF	Sum of Squares	Mean Square	F Value	Pr > F
Model	2	28552.78129	14276.39064	10.30	0.0047
Error	9	12479.21871	1386.57986		
Corrected Total	11	41032.00000			

R-Square	Coeff Var	Root MSE	strength Mean
0.695866	9.773440	37.23681	381.0000

Source	DF	Type I SS	Mean Square	F Value	Pr > F
days	1	1845.30049	1845.30049	1.33	0.2784
days*days	1	26707.48080	26707.48080	19.26	0.0017

Source	DF	Type III SS	Mean Square	F Value	Pr > F
days	1	24019.00384	24019.00384	17.32	0.0024
days*days	1	26707.48080	26707.48080	19.26	0.0017

Parameter	Estimate	Standard Error	t Value	Pr > |t|
Intercept	320.7461109	21.56432510	14.87	<.0001
days	26.9138849	6.46653063	4.16	0.0024
days*days	-0.9328306	0.21254886	-4.39	0.0017

Experiment 3: Direct Tensile Strength Behavior of CSA Cement Mortar containing 50% Anhydrite and 50% Gypsum as a Source of Calcium Sulfate

mortar = CSA cement mortar containing 50% anhydrite and 50% gypsum

curing regimen = 24hrs, 48hrs, 7d, 28d and 56d at ambient laboratory temperature and constant 50% relative humidity

Test method ASTM C307 was followed for data collection. Three samples were cast and tested for each mortar formulation. Samples were stored at ambient laboratory temperature and constant 50% relative humidity from the time of removal from molds to the time of testing. A CSA cement mortar containing 50 weight % anhydrite and 50 weight % gypsum as a source of calcium sulfate was tested after curing at constant low humidity for various durations in an effort to assess direct tensile strength behavior versus time. The scatter plot displayed in Figure B7 suggests the relationship between direct tensile strength and time is quadratic. Both Minitab and SAS statistical software were utilized to fit a quadratic equation to the data set displayed in Table B3. The resulting regression equation is below:

Tensile strength (psi) = 412.6 + 14.89 time(days) - 0.2975 time(days)**2

The coefficient of determination, R^2, equals 80.4%. The adjusted coefficient of determination, adjusted $\cancel{R}^2$, equals 77.1%. The standard error of the regression equals 51.36. The standard error of one way ANOVA for the same data set equals 43.43. The plot of residuals suggests the data points are more or less evenly distributed about the fitted regression line. The values for both R^2 and adjusted $\cancel{R}^2$ suggest the fitted quadratic equation is a good predictor of tensile strength behavior versus time for the range of data. Additionally, the plot of residuals suggests the fitted equation is somewhat reliable for describing the relationship between direct tensile strength versus time for the CSA cement mortar containing half anhydrite and half gypsum by mass as a combined source of calcium sulfate when cured at 23^{o}C and 50% relative humidity. Furthermore, the narrow range between confidence interval lines in relation to the fitted line of Figure B8 suggests the model is efficient for predicting tensile strength behavior within a large portion of the data range. The author theorizes an even better relationship between fitted polynomial equations and experimental observations may be obtained for future experiments by increasing both testing frequency and sample size.

x = time (days)	y = strength (psi)
1	337
1	407
1	418
2	529
2	456
2	490
7	492
7	451
7	530
28	669
28	537
28	585
56	308
56	305
56	327

Table B3: Direct tensile strength testing data versus time for CSA cement mortar containing half anhydrite and half gypsum by mass as a combined source of calcium sulfate when cured at 23°C and 50% relative humidity

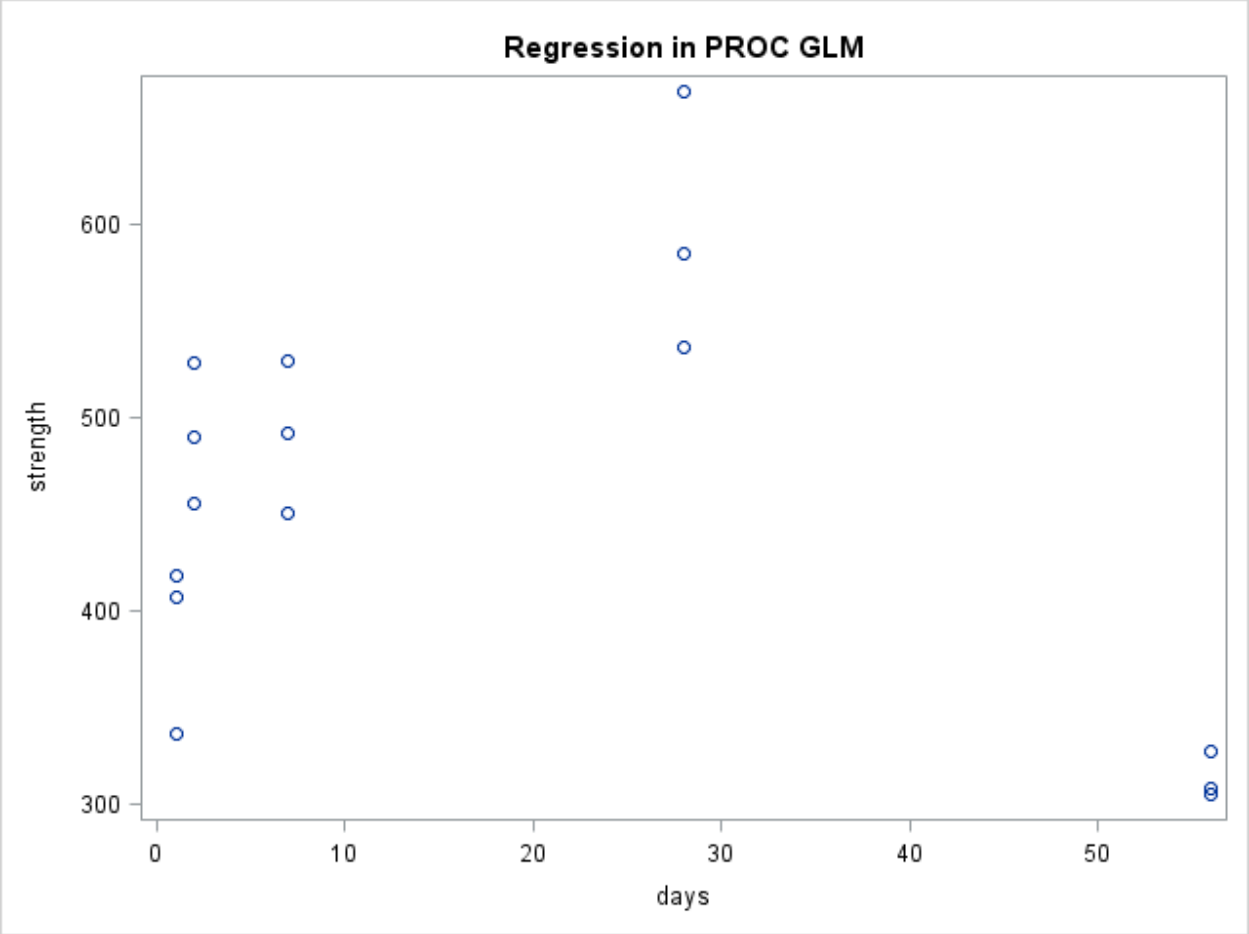

Figure B7: SAS generated scatter plot of test results for CSA cement mortar containing half anhydrite and half gypsum by mass as a combined source of calcium sulfate when cured at 23°C at 50% relative humidity

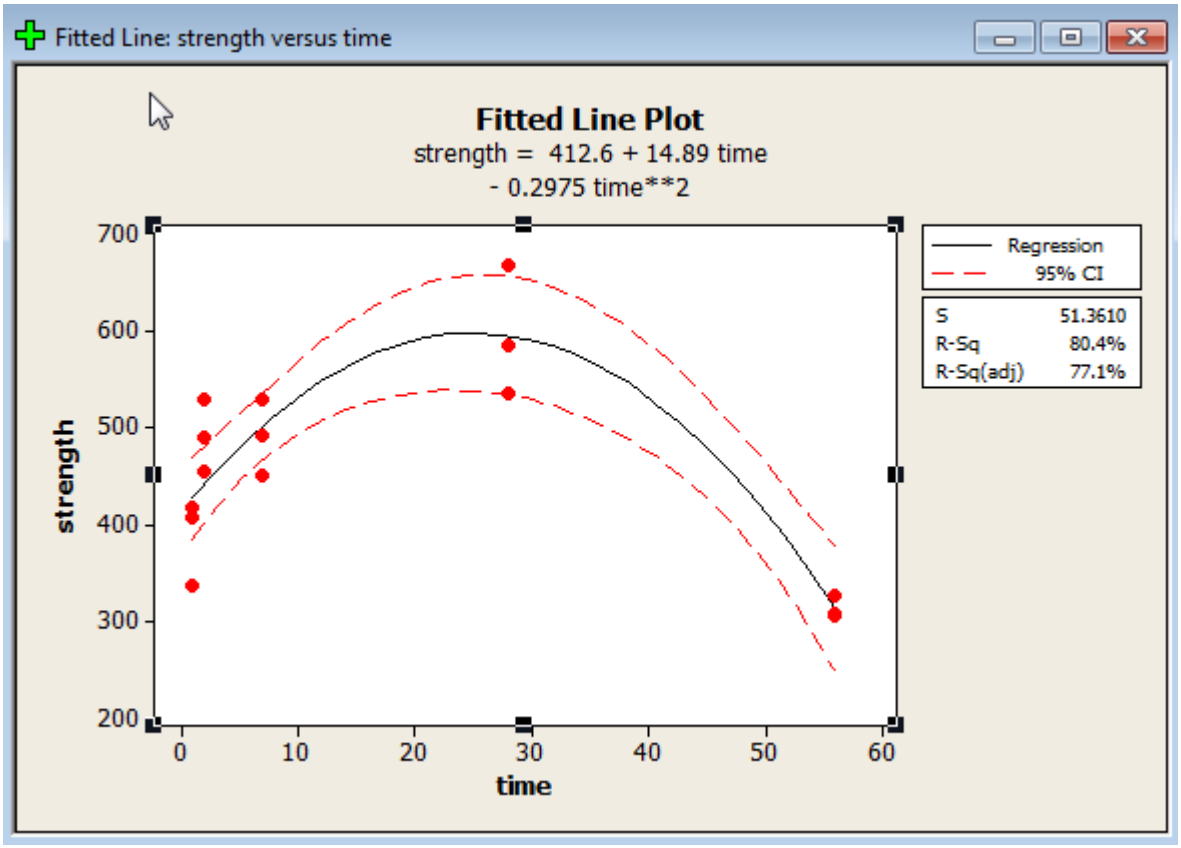

Figure B8: Minitab generated fitted line plot for direct tensile strength testing of CSA cement mortar containing half anhydrite and half gypsum by mass as a combined source of calcium sulfate when cured at 23°C and 50% relative humidity

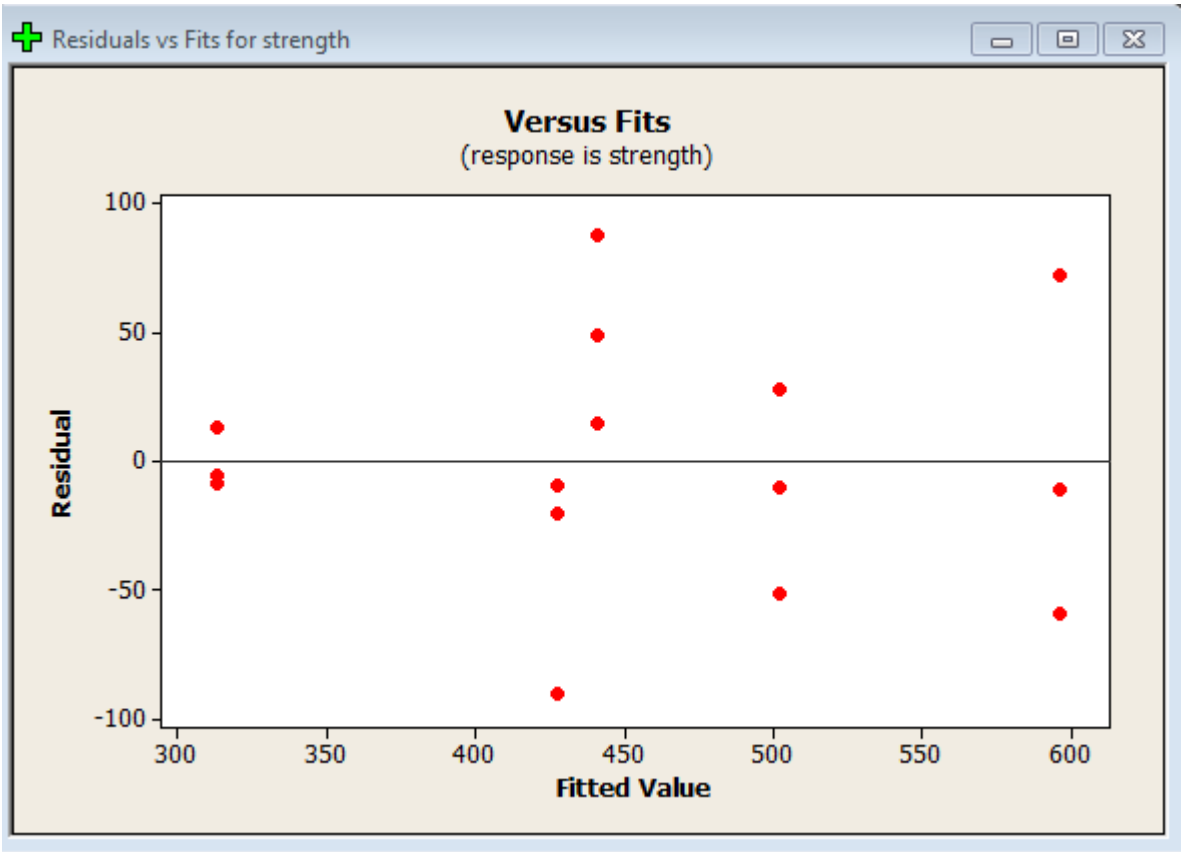

Figure B9: Minitab generated residual plots for direct tensile strength testing of CSA cement mortar containing half anhydrite and half gypsum by mass as a combined source of calcium sulfate cured at 23°C and 50% relative humidity

Polynomial Regression Analysis: strength versus time

The regression equation is
strength = 412.6 + 14.89 time - 0.2975 time**2

S = 51.3610 R-Sq = 80.4% R-Sq(adj) = 77.1%

Analysis of Variance

Source	DF	SS	MS	F	P
Regression	2	129550	64774.8	24.55	0.000
Error	12	31655	2637.9		
Total	14	161205			

Sequential Analysis of Variance

Source	DF	SS	F	P
Linear	1	19630	1.80	0.202
Quadratic	1	109920	41.67	0.000

SAS Statistical Software Polynomial Fit Regression Information

Regression in PROC GLM

The GLM Procedure

Number of Observations Read	15
Number of Observations Used	15

Regression in PROC GLM

The GLM Procedure

Dependent Variable: strength

Source	DF	Sum of Squares	Mean Square	F Value	Pr > F
Model	2	129549.5495	64774.7748	24.55	<.0001
Error	12	31655.3838	2637.9487		
Corrected Total	14	161204.9333			

R-Square	Coeff Var	Root MSE	strength Mean
0.803633	11.26172	51.36096	456.0667

Source	DF	Type I SS	Mean Square	F Value	Pr > F
days	1	19629.5450	19629.5450	7.44	0.0183
days*days	1	109920.0045	109920.0045	41.67	<.0001

Source	DF	Type III SS	Mean Square	F Value	Pr > F
days	1	83293.3762	83293.3762	31.58	0.0001
days*days	1	109920.0045	109920.0045	41.67	<.0001

Parameter	Estimate	Standard Error	t Value	Pr > |t|
Intercept	412.6384048	21.32097312	19.35	<.0001
days	14.8853388	2.64902868	5.62	0.0001
days*days	-0.2974536	0.04608016	-6.46	<.0001

Experiment 4: Compressive Strength Behavior of CSA Cement Mortar Containing Half Anhydrite and Half Gypsum as a Source of Calcium Sulfate

mortar = CSA cement mortar containing 50% anhydrite and 50% gypsum

curing regimen = 24hrs, 48hrs, 7d, 461d and 537d at ambient laboratory temperature and constant 50% relative humidity

Test method ASTM C109 was followed for data collection. Three samples were cast and tested for each mortar formulation. Samples were stored at ambient laboratory temperature and constant 50% relative humidity from the time of removal from molds to the time of testing. A CSA cement mortar containing 50 weight % anhydrite and 50 weight % gypsum as a source of calcium sulfate was tested after curing at constant low humidity for various durations in an effort to assess compressive strength behavior versus time. The scatter plot displayed in Figure B10 suggests the relationship between compressive strength and time is quadratic. Both Minitab and SAS statistical software were utilized to fit a quadratic equation to the data set displayed in Table B4. The resulting fitted equation is below:

Compressive Strength (psi) = 9083 + 45.18 Time (days) - 0.08116 Time (days)**2

The coefficient of determination, R^2, equals 33.2%. The adjusted coefficient of determination, adjusted R^2, equals 22%. The standard error of the regression equals 2116. The standard error of one way ANOVA for the same data set equals 353. The plot of residuals suggests the data points are not evenly distributed about the fitted regression line. The low values for both R^2 and adjusted R^2 suggest the fitted quadratic equation is not a good predictor of compressive strength behavior versus time for the range of data. Additionally, the plot of residuals suggests the fitted equation is not at all ideal for describing the relationship between compressive strength versus time for the CSA cement mortar containing half anhydrite and half gypsum by mass as a combined source of calcium sulfate when cured at 23°C and 50% relative humidity. Furthermore, the broad range between confidence interval lines in relation to the fitted line of Figure B11 further suggests the model is deficient for predicting compressive strength behavior within the range of data. The author theorizes a better relationship between fitted polynomial equations and experimental observations may be obtained for future experiments by increasing both testing frequency and sample size.

x = time (days)	y = strength (psi)
1	6231
1	6029
1	5876
2	9332
2	9912
2	9369
7	12169
7	12087
7	12292
461	12647
461	11937
461	12633
537	9776
537	10776
537	9848

Table B4: Compressive strength testing data versus time for CSA cement mortar containing half anhydrite and half gypsum by mass as a combined source of calcium sulfate when cured at 23°C and 50% relative humidity

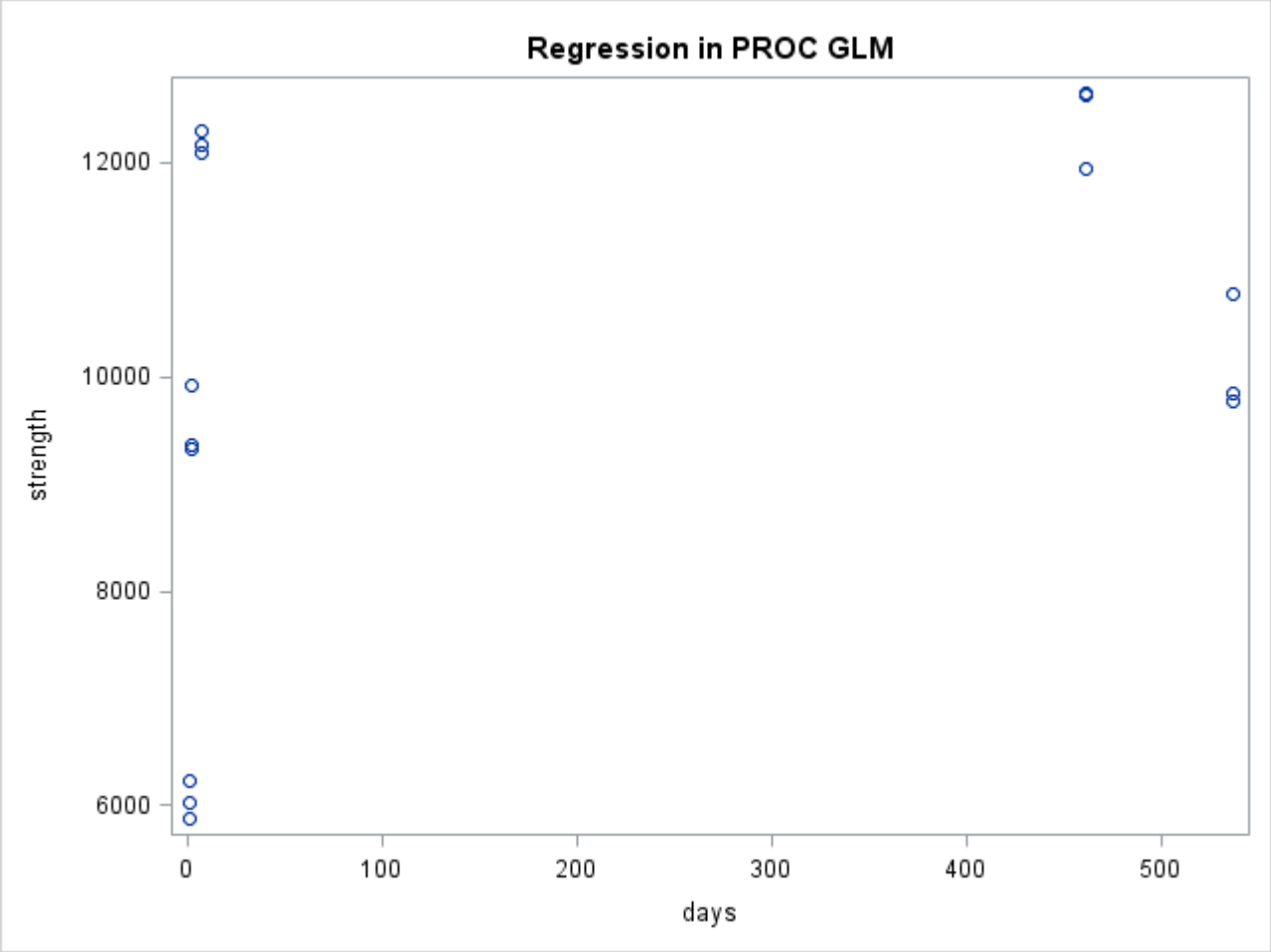

Figure B10: SAS generated scatter plot of compressive strength versus time testing data for CSA cement mortar containing half anhydrite and half gypsum by mass as a combined source of calcium sulfate when cured at 23°C and 50% relative humidity

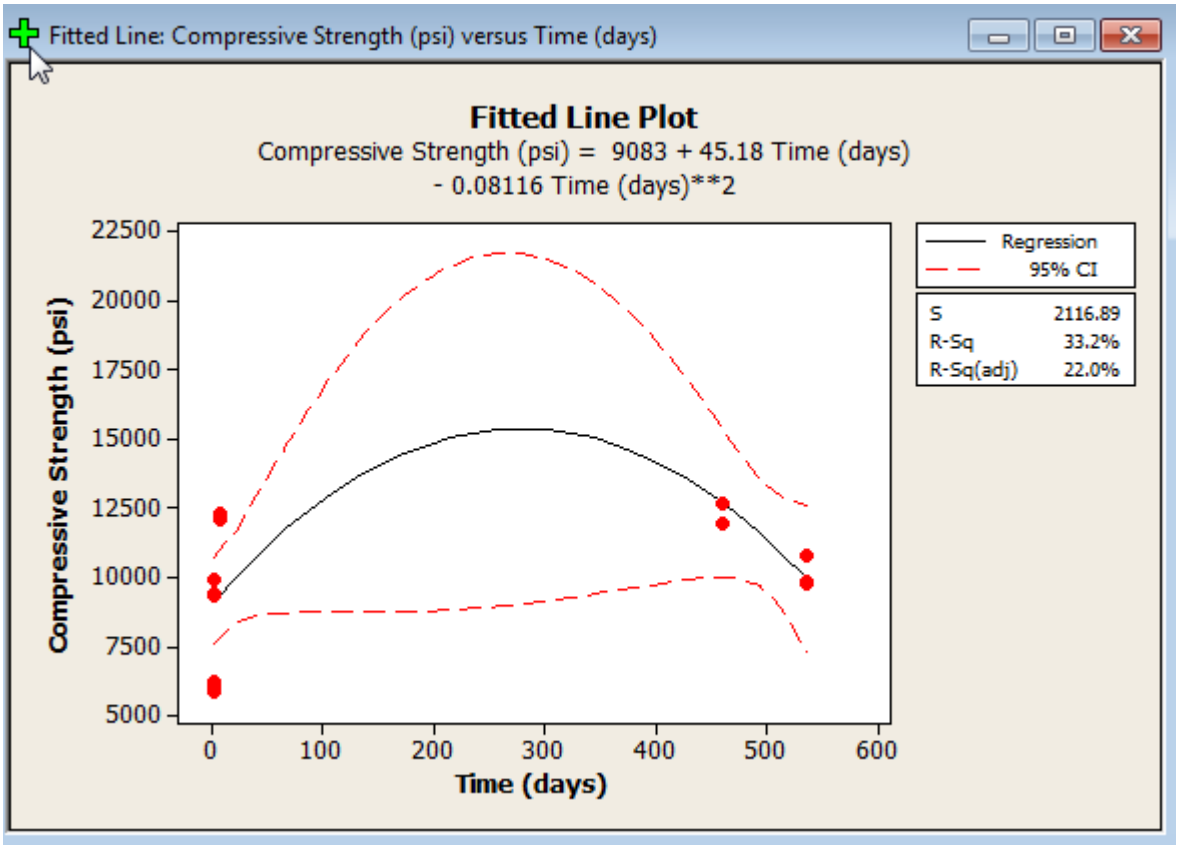

Figure B11: Minitab generated fitted polynomial equation displaying compressive strength versus time testing data for CSA cement mortar containing half anhydrite and half gypsum by mass as a combined source of calcium sulfate when cured at 23°C and 50% relative humidity

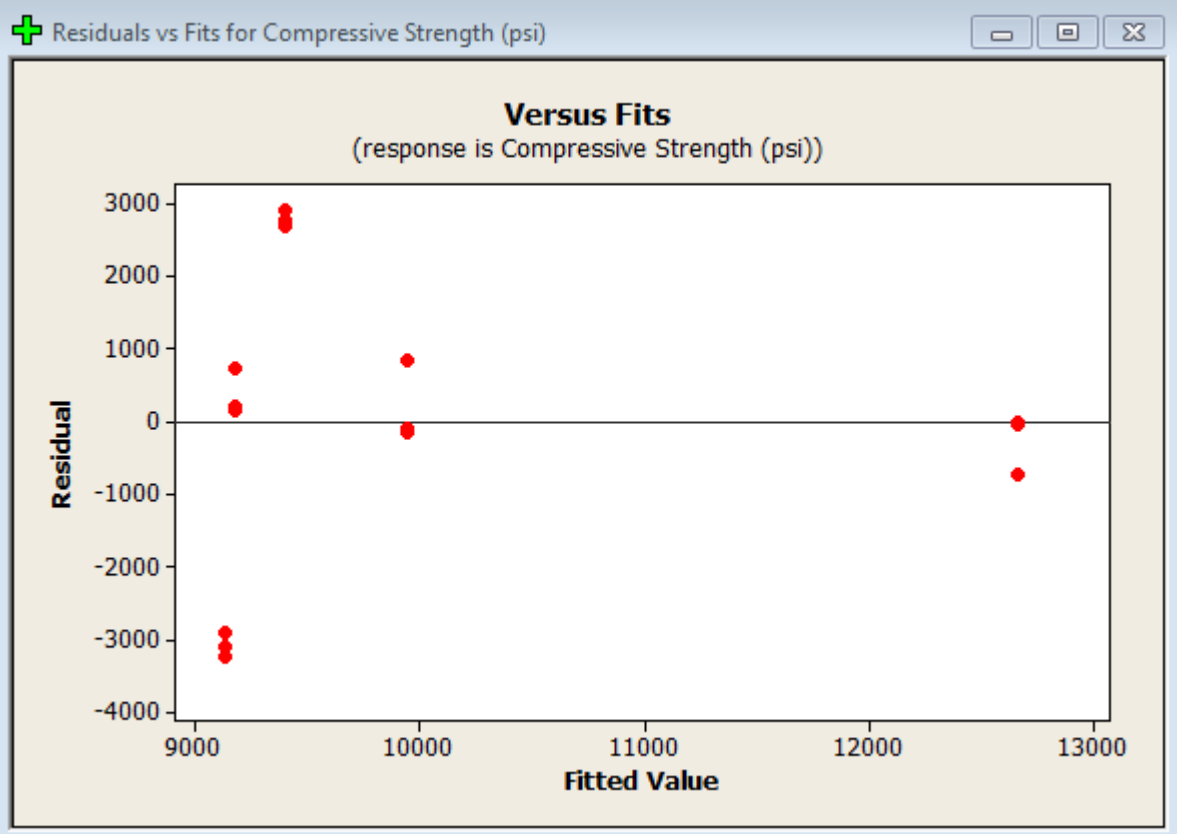

Figure B12: Minitab generated plot of residuals for compressive strength testing data for CSA cement mortar containing half anhydrite and half gypsum by mass as a combined source of calcium sulfate when cured at 23°C and 50% relative humidity

Polynomial Regression Analysis: Compressive Strength (psi) versus Time (days)

The regression equation is
Compressive Strength (psi) = 9083 + 45.18 Time (days) - 0.08116 Time (days)**2

S = 2116.89 R-Sq = 33.2% R-Sq(adj) = 22.0%

Analysis of Variance

Source	DF	SS	MS	F	P
Regression	2	26683452	13341726	2.98	0.089
Error	12	53774679	4481223		
Total	14	80458131			

Sequential Analysis of Variance

Source	DF	SS	F	P
Linear	1	12856988	2.47	0.140
Quadratic	1	13826464	3.09	0.104

SAS Statistical Software Polynomial Fit Regression Information

Regression in PROC GLM

The GLM Procedure

Number of Observations Read 15

Number of Observations Used 15

Regression in PROC GLM

The GLM Procedure

Dependent Variable: strength

Source	DF	Sum of Squares	Mean Square	F Value	Pr > F
Model	2	26683452.22	13341726.11	2.98	0.0891
Error	12	53774678.72	4481223.23		
Corrected Total	14	80458130.93			

R-Square	Coeff Var	Root MSE	strength Mean
0.331644	21.04069	2116.890	10060.93

Source	DF	Type I SS	Mean Square	F Value	Pr > F
days	1	12856988.38	12856988.38	2.87	0.1161
days*days	1	13826463.84	13826463.84	3.09	0.1045

Source	DF	Type III SS	Mean Square	F Value	Pr > F
days	1	16329836.83	16329836.83	3.64	0.0805
days*days	1	13826463.84	13826463.84	3.09	0.1045

Parameter	Estimate	Standard Error	t Value	Pr > |t|
Intercept	9083.195133	719.2644520	12.63	<.0001
days	45.184658	23.6700059	1.91	0.0805
days*days	-0.081162	0.0462055	-1.76	0.1045

Experiment 5: Compressive Strength Behavior of CSA Cement Mortar Containing Gypsum as a Source of Calcium Sulfate

mortar = CSA cement mortar containing gypsum

curing regimen = 24hrs, 48hrs, 7d, 460d and 537d at ambient laboratory temperature and constant 50% relative humidity

Test method ASTM C109 was followed for data collection. Three samples were cast and tested for each mortar formulation. Samples were stored at ambient laboratory temperature and constant 50% relative humidity from the time of removal from molds to the time of testing. A CSA cement mortar containing solely gypsum as a source of calcium sulfate was tested after curing at constant low humidity for various durations in an effort to assess compressive strength behavior versus time.

The scatter plot displayed in Figure B13 suggests the relationship between compressive strength and time is quadratic. Both Minitab and SAS statistical software were utilized to fit a quadratic equation to the data set displayed in Table B5. The resulting fitted equation is below:

Compressive Strength (psi) = 9035 + 37.95 Time (days) - 0.07882 Time (days)**2

The coefficient of determination, R^2, equals 27.7%. The adjusted coefficient of determination, adjusted $\bar{R}^2$, equals 15.7%. The standard error of the regression equals 1965. The standard error of one way ANOVA for the same data set equals 358. The plot of residuals suggests the data points are not evenly distributed about the fitted regression line. The low values for both R^2 and adjusted $\bar{R}^2$ suggest the fitted quadratic equation is not a good predictor of compressive strength behavior versus time for the range of data. Additionally, the plot of residuals suggests the fitted equation is not at all ideal for describing the relationship between compressive strength versus time for the CSA cement mortar containing gypsum as a source of calcium sulfate when cured at 23°C and 50% relative humidity. Furthermore, the broad range between confidence interval lines in relation to the fitted line of Figure B14 further suggests the model is deficient for predicting compressive strength behavior within the range of data. The author theorizes a better relationship between fitted polynomial equations and experimental observations may be obtained for future experiments by increasing both testing frequency and sample size.

x = time (days)	y = strength (psi)
1	6364
1	6040
1	6011
2	9994
2	9457
2	9485
7	11824
7	11116
7	12330
460	9863
460	9485
460	9398
537	6802
537	6599
537	7150

Table B5: Compressive strength testing data versus time for CSA cement mortar containing gypsum as a source of calcium sulfate when cured at 23°C and 50% relative humidity

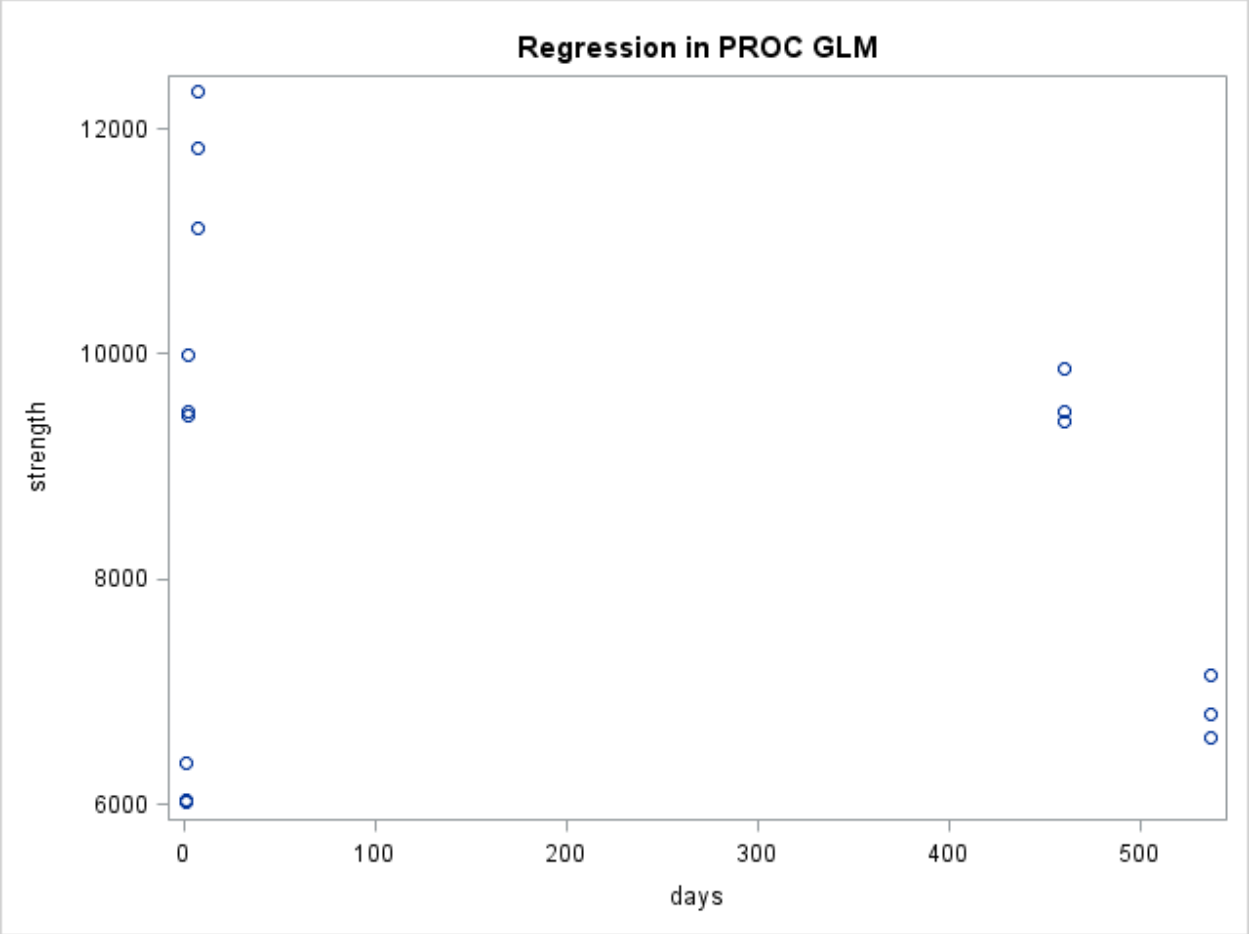

Figure B13: SAS generated scatter plot for compressive strength versus time testing of CSA cement mortar containing gypsum as a source of calcium sulfate when cured at 23°C and 50% relative humidity

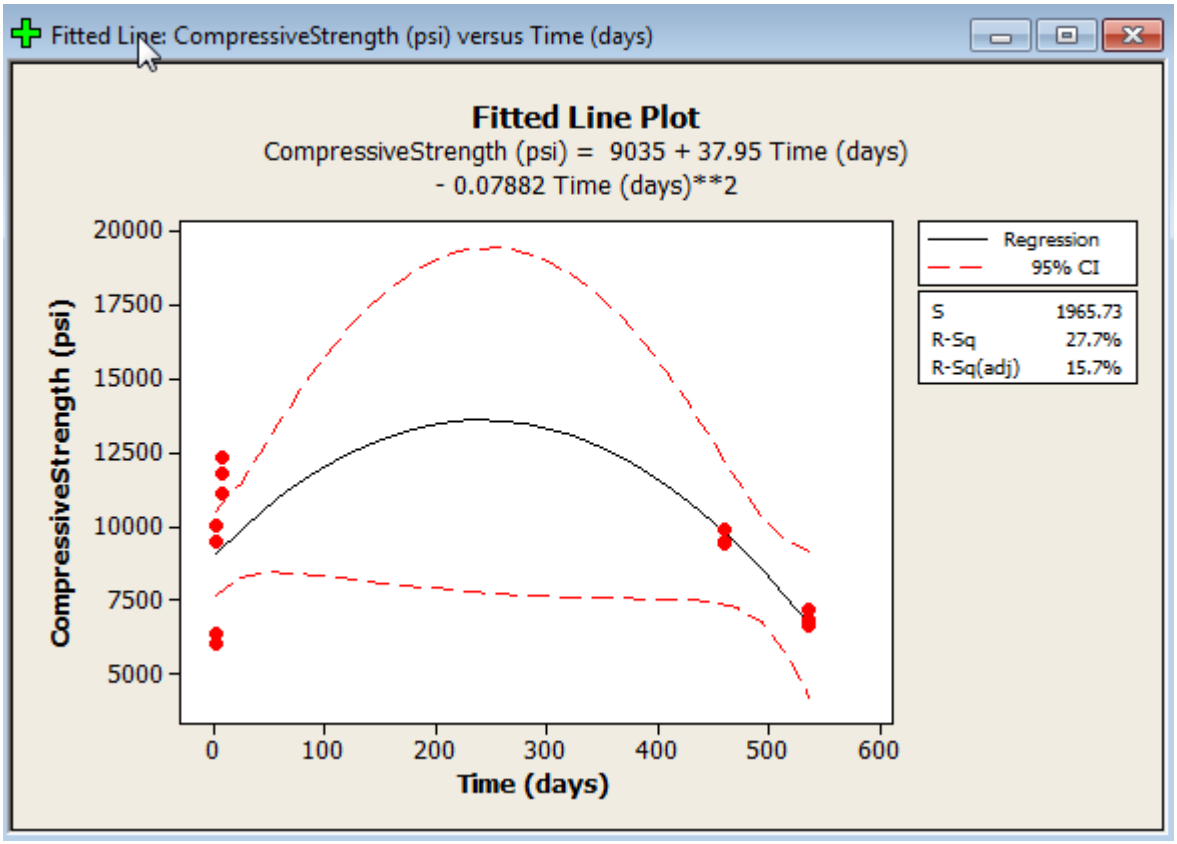

Figure B14: Minitab generated fitted polynomial equation displaying compressive strength versus time testing data for CSA cement mortar containing gypsum as a source of calcium sulfate when cured at 23°C and 50% relative humidity

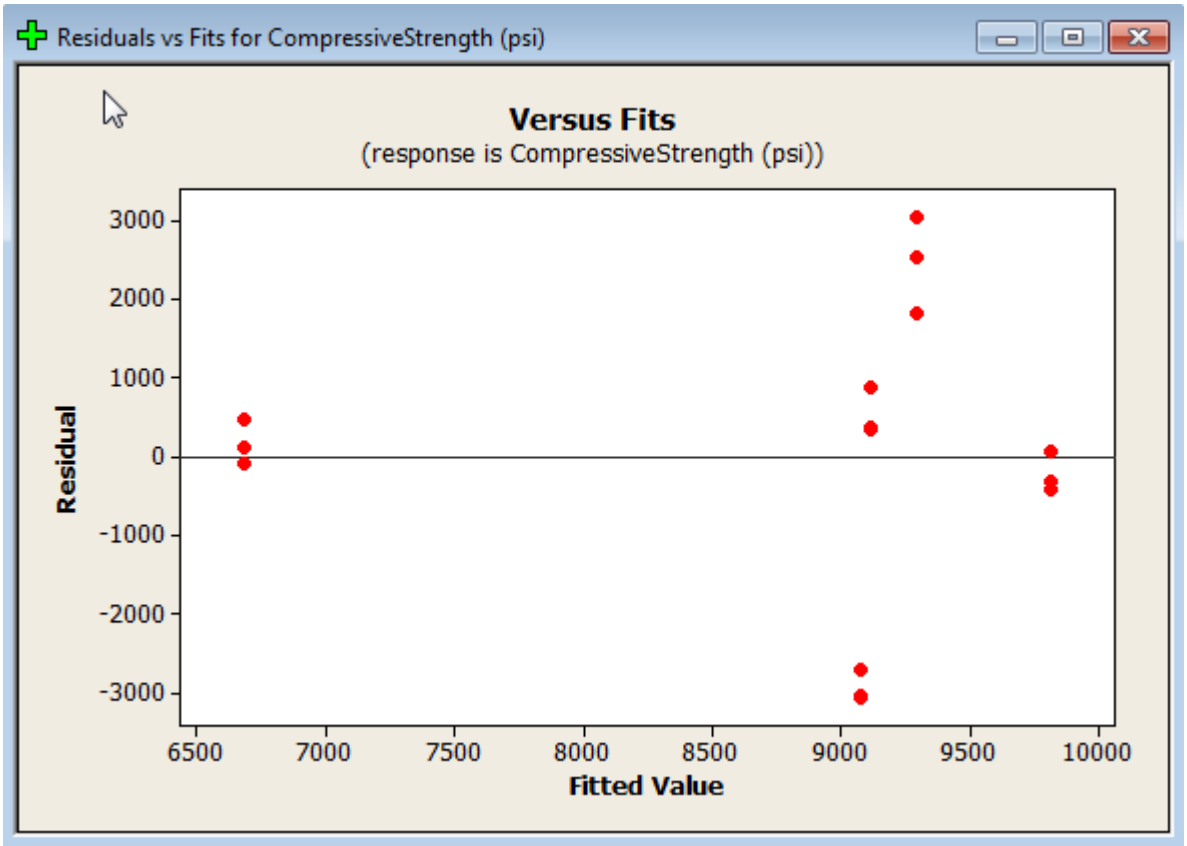

Figure B15: Minitab generated plot of residuals for compressive strength testing data for CSA cement mortar containing gypsum as a source of calcium sulfate when cured at 23°C and 50% relative humidity

Polynomial Regression Analysis: CompressiveStrength (psi) versus Time (days)

The regression equation is
Compressive Strength (psi) = 9035 + 37.95 Time (days) - 0.07882 Time (days)**2

S = 1965.73 R-Sq = 27.7% R-Sq(adj) = 15.7%

Analysis of Variance

Source	DF	SS	MS	F	P
Regression	2	17772013	8886006	2.30	0.143
Error	12	46369301	3864108		
Total	14	64141314			

Sequential Analysis of Variance

Source	DF	SS	F	P
Linear	1	4423804	0.96	0.344
Quadratic	1	13348208	3.45	0.088

SAS Statistical Software Polynomial Fit Regression Information

Regression in PROC GLM

The GLM Procedure

Number of Observations Read	15
Number of Observations Used	15

Regression in PROC GLM

The GLM Procedure

Dependent Variable: strength

Source	DF	Sum of Squares	Mean Square	F Value	Pr > F
Model	2	17772012.79	8886006.40	2.30	0.1427
Error	12	46369300.94	3864108.41		
Corrected Total	14	64141313.73			

R-Square	Coeff Var	Root MSE	strength Mean
0.277076	22.35177	1965.734	8794.533

Source	DF	Type I SS	Mean Square	F Value	Pr > F
days	1	4423804.29	4423804.29	1.14	0.3057
days*days	1	13348208.50	13348208.50	3.45	0.0878

Source	DF	Type III SS	Mean Square	F Value	Pr > F
days	1	11799623.74	11799623.74	3.05	0.1061
days*days	1	13348208.50	13348208.50	3.45	0.0878

Parameter	Estimate	Standard Error	t Value	Pr > |t|
Intercept	9034.539575	667.8228573	13.53	<.0001
days	37.946554	21.7151543	1.75	0.1061
days*days	-0.078821	0.0424086	-1.86	0.0878

BIBLIOGRAPHY

- ACI 548.1R-09, Guide for the Use of Polymers in Concrete, Reported by ACI Committee 548, American Concrete Institute
- ACI 503.5R-92, Guide for the Selection of Polymer Adhesives with Concrete, Reported by ACI Committee 503, American Concrete Institute
- ACI 548.4-93, Standard Specification for Latex Modified Concrete (LMC) Overlays, Reported by Committee 548, American Concrete Institute
- ASTM C109, Standard Test Method for Compressive Strength of Hydraulic Cement Mortars, ASTM International
- ASTM C307, Standard Test Method for Tensile Strength of Chemical Resistant Mortars, Grouts and Monolithic Surface Coatings, ASTM International
- ASTM C348, Standard Test Method for Flexural Strength of Hydraulic Cement Mortars, ASTM International
- ASTM C496, Standard Test Method for Splitting Tensile Strength of Cylindrical Concrete Specimens, ASTM International
- ASTM C1583, Standard Test Method for Tensile Strength of Concrete Surfaces and the Bond Strength or Tensile Strength of Concrete Repair and Overlay, ASTM International
- Afridi, M., Chaudhary, Z., Ohama, Y., Demura, K., 1994, Effects of polymer modification on the formation of high sulphoaluminate or ettringite type (Aft) crystals in polymer modified mortars, Cement and Concrete Research, Vol. 24, No. 8, 1492-1494, 1994
- Afridi, M., Chaudhary, Z., Ohama, Y., Katsunori, D., 1994, Strength and Elastic Properties of Powdered and Aqueous Polymer-Modified Mortars, Cement and Concrete Research, Vol 24, No. 7, pp. 1199-1213, 1994
- Afridi, M., Ohama, Y., Demura, K., Izbal, M.Z., 2003, Development of polymer films by the coalescence of polymer particles in powdered and aqueous polymer-modified mortars, Cement and Concrete Research, 33 (2003) 1715-1721
- Ambroise, J., Pera, J., 2009, Use of Calcium sulfoaluminate cement to improve strength of mortars at low temperature, Concrete Repair, Rehabilitation and Retrofitting II –Alexamder et al (eds), © 2009 Taylor and Francis Group, London, ISBN 978-0-415-46850-3

- Anderberg, A., Wadso, L., 2010, Using a standard mix design to study properties of a flooring compound, Nordic Concrete Research Publications, 10; 21-32, NCR 40-3, ISSN: 0800-6377
- Atkins, P., 1997, The Elements of Physical Chemistry, Oxford University Press, ISBN 0-7167-3077-4
- Baumann, R., Tarantul, K., Powell, C., Wichmann, A., Tepper, C., Perello, M., Heeringen, M., Kock, W., Griggs, P., Radler, M., 2007, Interaction of Cellulose Ethers and Redispersible Polymer Powders in Cement Based Tile Adhesives, The DOW Chemcial Company, Techline 3 For the Construction Industry, dccinfo@dow.com, www.dowcc.eu, 840-01201-032011
- Bensted, J., 1998, Lea's Chemistry of Cement and Concrete, 4th Edition, ISBN 0-340-56589-6
- Beretka, J., Marroccoli, M., Sherman, N., Valenti, G., 1996, The Influence of C4A3S Content and W/S Ratio on the Performance of Calcium Sulfoaluminate Based Cements, Cement and Concrete Research, Vol. 26, No. 11, pp 1673-1681, 1996
- Beretka, J., Vito, B., Santoro, L., Sherman, N., Valenti, G., 1993, Hydraulic Behavior of Calcium Sulfoaluminate Based Cements Derived from Industrial Process Wastes, Cement and Concrete Research, Vol 23 pp. 1205-1214
- Bethea, R.M., Duran, B.S., Boullion, T.L.,1975, Statistical Method for Engineers and Scientists, ISBN 0-8247-6217-7, UK Call Number QA276.B425
- Bishop, M., Barron, A., 2006, Cement Hydration Inhibition with Sucrose, Tartaric Acid, and Lignosulfonate: Analytical and Spectroscopic Study, Department of Chemistry and Department of Mechanical Engineering and Materials Science, Rice University, Houston TX 77005, Applied Chemistry, American Chemical Society, *Ind. Eng. Chem. Res.* 2006, *45*, 7042-7049
- Blackley, D.C., 1997, Polymer Latices, Science and Technology, 2nd Edition, ISBN 0412 62890 2
- Blount, C., 1973, Gypsum-Anhydrite Equilibria in Systems CaSO4-H2O and CaCO4-NaCL-H2O, American Mineralogist, Volume 58, pages 323-333, 1973
- Bright, R.P., Mraz, T.J., Vassallo, J.C., 1993, The Influence of Various Polymeric Materials on the Physical Properties of a Cementitious Patching Compound, Polymer Modified Hydraulic Cement Mixtures, American Society for Testing and Materials, STP 1176m, ASTM Publication Code Number 04-011760-07

- Candela, L., Perlmutter, D., 1986, Pore Structure and Kinetics of Thermal Decomposition of $Al(OH)_3$, AIChe Journal, September 1986, Vol. 32, No. 9
- Cargile, J.D., Oneil, E.F., Neeley, B.D., 2002, Very High Strength Concretes for Use in Blast and Penetration Resistant Structures, US Army Corps of Engineers Engineer Research and Development Center, AMPTIAC Quarterly Volume 6, Number 4
- Chandra, S., Berntsson, L., 2003, Lightweight Aggregate Concrete, Science, Technology and Applications, Building Materials Series ISBN 0-8155-1486-7
- Chandra, S., Ohama, Y., 1994, Polymers in Concrete, CRC Press, ISBN 0-8493-4815-3
- Chowaniec, O., 2012, Limeston Addition in Cement, Thesis Number 5335, EPFL, Ecole Polytechnique Federale de Lausanne, www.epfl.ch
- Christensen, A., Olesen, M., Cerenius, Y., Jensen, T., 2008, Formation and Transformation of Five Different Phases in the CaSO4-H2O System: Crystal Structure of the Subhydrate beta-CaSO4*0.5H2O and Soluble Anhydrite CaSO4, Chem. Mater. 2008, 20, 2124-2132, 2008 American Chemical Society
- Clark, S., Colas, B., Kunz, M., Speziale, S., Monteiro, P., 2006, Effect of pressure on the crystal structure of ettringite, Cement and Concrete Research 38 (2008) 19-26
- CRC Handbook of Chemistry and Physics, 68th Edition, CRC press, 1987-1988
- DeLurgio, S.A., 1998, Forecasting Principles and Applications, 1st Edition, Irwin McGraw Hill, Boston, ISBN 0-256-13433-2
- ESS, Volume 8, Encyclopedia of Statistical Sciences, Second Edition, Volume 8, John Wiley and Sons, Inc, ISBN: 0 471 74374 7
- Freund, R.J., Wilson, W.J., Sa, P., 2006, Regression Analysis, Statistical Modeling of a Response Variable, 2nd Edition, Elsevier, Boston, ISBN: 978-0-12-088597-8
- Gabrovsek, R., Vuk, T., Kaucic, V., 2008, The Preparation and Thermal Behavior of Calcium Monocarboaluminate, Acta Chim Slov, 2008, 55, 942-950
- Gameiro, A., Silva, A., Veiga, M., Velosa, A., 2012, Lime-Metakaoling Hydration Products: A Microscopy Analysis, Materials and Technology 46 (2012) 2, 145-148
- Garnter, E., 2004, Industrially Interesting Approaches to "low-CO_2" Cements, Cement and Concrete Research 34 (2004) 1489-1498
- Gastaldi, D., Fulvio, C., Boccaleri, E.,2009, Ettringite and calcium sulfoaluminate cement: investigation of water content by near-infrared spectroscopy, Journal of Material Science, 44: 5788-5794, 2009

- Glasser, F., Zhang, L., 2001, High-performance cement matrices based on calcium sulfo-aluminate-belite compositions, Cement and Concrete Research 31 (2001) 1881-1886
- Graybeal, B., 2010, Behavior of Field Cast Ultra High Performance Concrete Bridge Deck Connections Under Cyclic and Static Structural Loading, November 2010, FHWA-HRT-11-023
- Graybeal, B., 2010, FHWA-HRT-11-022, Field Cast UHPC Connections for Modular Bridge Deck Components, November 2010, FHWA-HRT-11-022
- Graybeal, B., 2009, FHWA-HRT-09-069, Structural Behavior of a 2nd Generation UHPC Pi-Girder, October 2009, FHWA-HRT-09-069
- Grounds, T., Midgley, H., Nowell, D., 1988, Carbonation of Ettringite by Atmospheric Carbon Dioxide, Thermochimica Acta, 135 (1988) 347-352
- Hardie, L., 1967, The Gypsum-Anhydrite Equilibrium at One Atmosphere Pressure, The American Mineralogist, Volume 52, January-February, 1967
- Hassoun, M.N., 1985, Design of Reinforced Concrete Structures, PWS Publishers, Boston, MA, ISBN 0-534-03759-3
- Hull, T., Price, D., Liu, Y., Wills, C., Brady, J., 2003, An investigation into the decomposition and burning behaviour of Ethylene-vinyl acetate copolymer nanocomposite materials, Polymer Degradation and Stability 82 (2003) 365-371
- Illston, J.M., Domone, P.L.J., 2007, Construction Materials: Their Nature and Behaviour, Third Edition, Spon Press, ISBN 0-419-25860-4
- Jenni, A., Herwegh, M., Zurbriggen, R., Aberle, T. and Holzer, L., 2003, Quantitative micro-structure analysis of polymer modified mortars, Jounal of Microscopy, Vol 212, pgs 186-196
- Jewell, R., Rathbone, R., Robl, T., Henke, K., 2009, Fabrication and Testing of CSAB Cements in Mortar and Concrete that Utilize Circulating Fluidized Bed Combustion Byproducts, 2009 World of Coal Ash (WOCA) Conference, 4-7May2009, Lexington, KY, USA, http://www.flyash.info
- Juenger, M., Winnefeld, F., Provis, J., Ideker, J., 2011, Alternative cementitious binders, Cement and Concrete Research 41 (2011) 1232-1243
- Kalousek, G.L., 1973, Klein's Symposium on Expansive Cement Concretes, ACI Special Publication, SP-38, Library of Congress Catalog Number 73-77948

- Knapen, E., Beeldens, A., Van Gemert, D., 2005, Water-soluble polymeric modifiers for cement mortar and concrete, ConMat'05 3rd Intern. Conference on Construction Materials: Performance, Innovation and Structural Implications, Vancouver, Canada, August 22-24, 2005
- Knapen, E., Gemert, D., 2009, Cement hydration and microstructure formation in the presence of water-soluble polymers, Cement and Concrete Research 39 (2009) 6-13
- Lawrence, C.D., Hewlett, P., 1998, Production of Low Energy Cements, Chapter 9, Lea's Chemistry of Cement and Concrete, 4th Edition, Arnold, John Wiley and Sons, New York, New York, ISBN 0-340-56589-6
- Lide, D.R., 1997, CRC Handbook of Chemistry and Physics, 78th Edition, CRC Press, New York, New York, Boca Raton, FL, ISBN 0-07-016197-6
- Majling, J., Znasik, P., Gabrisova, A., Svetik, S., 1985, The Influence of Anhydrite Activity upon the Hydration of Calcium Sulphoaluminate Cement Clinker, Thermochimica Acta, 92 (1985) 349-352, Elsevier Science Publishers B.V., Amsterdam
- Maurin, M., Dittert, L., Hussain, A., 1991, Thermogravimetric analysis of ethylene-vinyl acetate copolymers with Fourier transform infrared analysis of the pyrolysis products, Thermochimica Acta, 186 (1991) 97-102
- Meredith, P., Donald, A., Meller, N., Hall, C., 2004, Tricalcium aluminate hydration: microstructural observations by in-situ electron microscopy, Jounal of Materials Science 39 (2004) 997-1005
- Mickey, R.M., Dunn, O.,J., Clark, V.A.,2004, Applied Statistics, Analysis of Variance and Regression, Third Edition, Wiley Series in Probability and Statistics, ISBN 0-471-37038-X
- Marroccoli, M., Lucia Pace, M., Telesca, A., Lorenzo Valenti, G., 2010, Synthesis of Calcium Sulfoaluminate Cements From Al2O3 Rich By-products from Aluminum Manufacture, Second International Conference on Sustainable Construction Materials and Technologies, June 28-30 2010, Main Proceedings ISBN 978-1-4507-1490-7, www.claisse.info/proceedings.htm
- Marroccoli, M., Montagnaro, F., Telesca, A., Valenti, G., 2010, Environmental Implications of the Manufacture of Calcium Sulfoaluminate-Based Cements, Second International Conference on Sustainable Construction Materials and Technologies, Ancona, Italy, Main Proceedings, ISBN 978-1-4507-1490-7

- Medeiros, M.H.F., Helene, P., Selmo, S., 2009, Influence of EVA and acrylate polymers on some mechanical properties of cementitious repair mortars, Construction and Building Materials 23 (2009) 2527-2533
- Mertz, D., Rehm, K., Beal, D., 2005, Grand Challenges: A Strategic Plan for Bridge Engineering, AASHTO Highway Subcommittee on Bridges and Structures, June 2005
- Mickey, R.M., Dunn, O.,J., Clark, V.A.,2004, Applied Statistics, Analysis of Variance and Regression, Third Edition, Wiley Series in Probability and Statistics, ISBN 0-471-37038-X
- Naderi, M., 2008, Adhesion of Different Concrete Repair Systems Exposed to Different Environments, The Journal of Adhesion, 84:78-104, 2008
- NOAA, National Weather Service, www.noaa.gov, relative humidity = www.erh.noaa.gov/er/gyx/climo/avgrh.html
- Ohama, Y., 1995, Handbook of Polymer-Modified Concrete and Mortars, Noyes Publications, ISBN 0-8155-1358-8
- Oneil, E.F., Cummins, T.K., Durst, B.P., Kinnebrew, P.G., Boone, R.N., 2004, Development of Very High Strength and High Performance Concrete Materials for Improvement of Barriers Against Blast and Projectile Penetration, US Army Corps of Engineers, US Army Engineer Research and Development Center
- Patnaik, P., 2003, Handbook of Inorganic Chemicals, The McGraw Hill Companies, ISBN 0-07-049439-8
- Pelletier-Chaignet, L., Winnefeld, F., Lothenbach, B., Muller, C., 2012, Beneficial use of limestone filler with calcium sulphoaluminate cement, Construction and Building Materials 26 (2012) 619-627
- Pelletier, L., Winnefeld, F., Lothenbach, B., 2010, The ternary system Portland cement – calcium sulphoaluminate clinker – anhydrite: Hydration mechanism and mortar properties, Cement and Concrete Composites, 32 (2010) 497-507
- Pera, J., Ambroise, J., 2004, New applications of calcium sulfoaluminate cement, Cement and Concrete Research 34 (2004) 671-676
- Perry, D., 1995, Handbook of Inorganic Compounds, CRC Press, New York, New York, Boca Raton, FL, ISBN 0-8493-8671-3
- Perry, R., Green, D., 1997, Perry's Chemical Engineers Handbook, 7th Edition, McGraw Hill, ISBN 0-07-049841-5

- Pourchet, S., Regnaud, L., Perez, J., Nonat, A., 2009, Early C3A hydration in the presence of different kinds of calcium sulfate, Cement and Concrete Research 39 (2009) 989-996
- Ramachandran, X., Chun-Mei, Z., 1986, Hydration kinetics and microstructural development in the 3CaO.Al2O3-CaSO4.2H2O-CaCO3-H2O system, Division of Building Research, National Research Council of Canada
- Renaudin, G., Segni, R., Mentel, D., Nedelec, J., Leroux, F., Taviot-Gueho, C., 2007, A Raman Study of the Sulfated Cement Hydrates: Ettringite and Monosulfoaluminate, Journal of Advanced Concrete Technology, Vol. 5, No. 3, 299-312, October 2007
- Riggs, J.B., 1994, An Introduction to Numerical Methods for Chemical Engineers Texas Tech University Press, 2nd Edition, ISBN: 0-89672-334-8
- Romain, T., Winnefeld, F., Mechling, J., Lecomte, A., Roux, A., LeRolland, B., 2013, Composition and Thermodynamic Modeling of Calcium Sulfoaluminate Cement and Ordinary Portland Cement Blends, Proceedings of the First International Conference on Sulphoaluminate Cement, Materials and Engineering Technology, Wuhan University of Technology, Wuhan, China, 23-25Oct2013
- Routh, A., Russel, W., 1999, A process model for latex film formation: limiting regimes for individual driving forces, Department of Chemical Engineering, Princeton University, Langmuir 1999, 15 7762-7773
- Sahu, S., Havlica, J., Tomkova, V., Majling, J., 1991, Hydration Behaviour of Sulphoaluminate Belite Cement in the Presence of Various Calcium Sulphates, Thermochimica Acta, 175 (1991) 45-52, Elsevier Science Publications B.V., Amsterdam
- Sato, T., 1985, Thermal Decomposition of Aluminum Hydroxides to Aluminas, Thermochimica Acta, 88 (1985) 69-84
- Sato, K., Takebe, T., 1992, Decomposition of Synthesized Ettringite by Carbonation, Cement and Concrete Research 22 (1992) 6-14
- Schneider, M., Romer, M., Tschudin, M., Bolio, H., 2011, Sustainable cement production –present and future, Cement and Concrete Research 41 (2011) 642-650
- Scrivener, K., Capmas, A., 1998, Calcium Aluminate Cements, Chapter 13, Lea's Chemistry of Cement and Concrete, 4th Edition, Arnold Publishers, ISBN 0 340 56589 6

- Scrivener, K., Nonat, A., 2011, Hydration of cementitious materials, present and future, Cement and Concrete Research 41 (2011) 651-665
- Sherman, N., Beretka, J., Santoro, L., Valenti, G., 1995, Long-Term Behaviour of Hydraulic Binders Based on Calcium Sulfoaluminate and Calcium Sulfosilicate, Cement and Concrete Research, Vol. 25, No. 1, pp. 113-126
- Silva, D., Monteiro, P., 2007, Early Formation of Ettringite in Tricalcium Aluminate – Calcium Hydroxide – Gypsum Dispersions, Journal of American Ceramic Society 90(2) 614-617
- Skoblinskaya, N., Krasilnikov, K., 1975, Changes in Crystal Structure of Ettringite on Dehydration 1, Cement and Concrete Research, Vol. 5, pp. 381-394, 1975
- Skoblinskaya, N., Krasilnikov, K., Nikitina, L., Varlamov, V., 1975, Changes in Crystal Structure of Ettringite on Dehydration 2, Cement and Concrete Research, Vol. 5, pp. 419-432, 1975
- Sprinkel, M., 2002, Rapid Bridge Deck Rehabilitation Manual, SHRP Product 2035A, AASHTO Innovative Highway Technologies
- Taylor, H., 1997, Cement Chemistry, Second Edition, Thomas Telford Publishing, 1997, ISBN 0 7277 2592 0
- Telesca, A.,.Marroccoli, M., Tomasulo, M., Valenti, G., Allevi, S., Marchi, M., 2013, Microstructural Features and Technical Properties of Calcium Sulfoaluminate Based Cements, Proceedings of The First International Conference on Sulphoaluminate Cement: Materials and Engineering Technology, Wuhan, China, October, 2013
- Tossavainen, M., Engstrom, F., Yang, Q., Nourreddine, M., Lidstrom, M., Bjorkman, B., 2007, Characteristics of Steel Slag Under Different Cooling Conditions, Waste Management (2007), Vol 27, p 1335-1344
- Vande Voort, T., Suleiman, M., Sritharan, S., 2008, Design and Performance Verification of Ultra-High Performance Concrete Piles for Deep Foundations, Iowa Highway Research Board, Iowa Department of Transportation, IHRB Project TR-558
- Vaysburd, A., McDonald, J., 1999, An Evaluation of Equipment and Procedures for Tensile Bond Testing of Concrete Repairs, US Army Corps of Engineers, Technical Report REMR-CS-61, June 1999
- Winnefeld, F., Barlag, S., 2010, Calorimetric and thermogravimetric study on the influence of calcium sulfate on the hydration of yeelimite, Journal of Thermal Analysis and Calorimetry (2010) 101:949-957

- Winnefeld, F., Lothenbach, B., 2013, Thermodynamic modeling of hydration of calcium sulfoaluminate cements blended with mineral additions, Proceedings of the First International Conference on Sulphoaluminate Cement, Materials and Engineering Technology, Wuhan University of Technology, Wuhan, China, 23-25Oct2013
- Winnefeld, F., Lothenbach, B., 2010, Hydration of calcium sulfoaluminate cements – Experimental findings and thermodynamic modeling, Cement and Concrete Research 40 (2010) 1239-1247
- World Business Council for Sustainable Development, http://www.wbcsd.org
- Xu, Q., Stark, J., 2005, Early hydration of ordinary Portland cement with an alkaline shotcrete accelerator, Advances in Cement Research, 2005, 17, No. 1, January, 1-8
- Yu, Q.L., Brouwers, H.J.H., 2010, Gypsum: an investigation of microstructure and mechanical properties, Department of Architecture, Building and Planning, Eindhoven University of Technology, the Netherlands, 8th fib PhD Symposium in Kgs. Lyngby, Denmark, June 20-23, 2010
- Zhang, L., Glasser, F., 2005, Investigation of the microstructure and carbonation of CSA based concretes removed from service, Cement and Concrete Research 35 (2005) 2252-2260
- Zhou, Q., Glasser, F., 2001, Thermal stability and decomposition mechanisms of ettringite at <120^{o}C, Cement and Concrete Research 31 (2001) 1333-1339
- Zhou, Q., Lachowski, E., Glasser, F., 2004, Metaettringite, a decomposition product of ettringite, Cement and Concrete Research 34 (2004) 703-710
- Zurbriggen, R., 2004, Influence of polymer glass transition temperature onto mortar flexibility, 6th International scientific and technical conference "Modern technologies of dry mixtures in building MixBUILD", Moscow, Russia, 23Nov2004 – 25Nov2004

Vita

Joshua V Brien
Birthplace: Paducah, Kentucky

Educational Institutions
University of Kentucky

- Masters Business Administration, December 1999
- BS Chemical Engineering, May 1998

Professional Positions Held
Wacker Chemical Corporation

- Plant Manager 2008-2009
- Supply Chain Manager 2003-2008
- Senior Application Specialist 2002-2003
- Production Engineer 2000-2002

Academic Publications

- Brien, J.V., Mahboub, K.C., 2013, Influence of Polymer Type on Adhesion Performance of a Blended Cement Mortar, International Journal of Adhesion and Adhesives, http://www.sciencedirect.com/science/article/pii/S0143749613000080
- Brien, J.V., Mahboub, K.C., Robl, T.L., 2013, Mechanical Property Performance of Polymer Modified CSA Cement Mortar Systems, ASTM Advances in Civil Engineering Materials Journal http://www.astm.org/DIGITAL_LIBRARY/JOURNALS/ACEM/PAGES/ACEM20120036.htm
- Brien, J.V., Henke, K.R., Mahboub, K.C., 2013, Observations on Peak Strength Behavior of Calcium Sulfoaluminate (CSA) Cement Mortars, Journal of Green Building, published in V8 N3
- Brien, J.V., Henke, K.R., Mahboub, K.C., 2013, Influence of Latex Polymer Addition on the Behavior of Materials Containing CSA Cement Cured at Low Humidity, Journal of Green Building, published in V8 N4

_____Joshua V Brien_____
Student Signature

_____08May2014_____
Date